16-19 September 2026
Hamburg, Germany

PHYSIOLOGY WITH FLOW: SET SAIL!

© Daniel Fröhlich by stock.adobe.com

Abstract Booklet

PHYSIOLOGY in FOCUS 2026

The joint ANNUAL MEETING OF THE GERMAN PHYSIOLOGICAL SOCIETY and the SCANDINAVIAN PHYSIOLOGICAL SOCIETY

www.dpg-congress.de

DPG DEUTSCHE PHYSIOLOGISCHE GESELLSCHAFT

UKE HAMBURG

Table of Content

Oral Sessions....4

OC-01 FLOW of Motion: Skeletal Muscle function in physiology & disease....4
OC-02 FLOW of Air: Pulmonary function, oxygen metabolism, hypoxia....10
OC-03 FLOW of Urine: Glomerula function....17
OC-04 FLOW of Blood: Blood & Immune system....23
OC-05 FLOW of Urine: Transport function....31
OC-06 FLOW of Ions: Ion channels Structure & Function....37
OC-07 FLOW of Ions: Ion channels pathophysiology....43
OC-08 FLOW of Signals: Hard core cell signaling....49
OC-09 FLOW of Blood: Cardiac physiology....56
OC-10 FLOW of Connections: Neurophysiology....62
OC-11 FLOW of Blood: Vascular physiology....68
OC-12 FLOW of Signals: & Pathophysiology....74
OC-13 FLOW of Urine: Kidney disease....81
OC-14 FLOW of Blood: Systemic cardiovascular physiology....87
OC-15 FLOW of Knowledge: Methods and teaching in Physiology....93

Poster Sessions....99

P01: Renal Vascular & Glomerular Function....99
P02: Vascular Smooth Muscle Physiology....113
P03: Vascular Disease....126
P04: Transcriptional & epigenetic reviving of disease....140
P05: Renal Tubular Disease....150
P06: Hypoxia & pulmonary functions....160
P07: Neuoscience & Behavior....170
P08: In vivo nevrophysiology & connectivity....182
P09: Cation & non-selective channels....196
P10: Skeletal Muscle....211
P11: New & old hormones....221
P12: Cardiac electrophysiology ECG....236
P13: Diastolic Function - a matter of relaxation....246

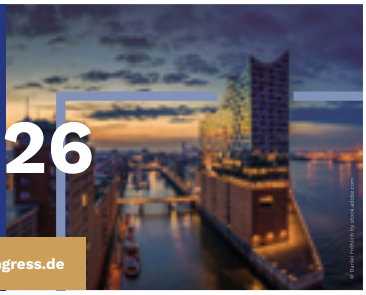

Table of Content

P14: Capturing Calcium Connections....254
P15: Hypoxia & pulmonary functions (applications, preclinical models)....265
P16: Endothelial biology & Systemic Vascular Physiology....275
P17: Metabolism in Physioloy....286
P18: K-Channels....299
P19: Synaptic Signalling....313
P20: Knowledge - Methods and teaching in Physiology....329
P21: Urine - Renal disease - inflammation....333
P22: Urine - Tubular transport....343
P23: The heart of the matter - drilling into genes & function....358
P24: Chloride Channels & Transporters....367
P25: Cardiac Function - essential knowledge....380
P26: Renal disease - oxygen/metabolism....390

List of authors....402

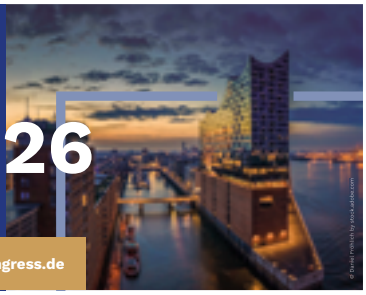

OC01 FLOW of Motion: Skeletal Muscle function in physiology & disease

OC0101
Respiratory impairment in severe cancer cachexia: a comprehensive characterisation of the novel KPP model of pancreatic ductal adenocarcinoma

Ben Murphy; Anthony Marullo; Ken O´Halloran
Department of Physiology, University College Cork, Cork, Ireland;

Objective: Cancer cachexia is hypothesised to be responsible for 2030% of cancerrelated deaths. Notwithstanding the contribution of respiratory failure toward cancer mortality, there remains a dearth of respiratoryfocussed research in this condition. The objective of the current study was to investigate the respiratory phenotype of the novel KPP model of pancreatic cancer cachexia.
Method: Experimental (KPP) and control mice were entered into procedures subsequent to phenotype induction and progression. Maximal inspiratory pressure was measured *invivo* with contemporaneous electromyogram activity of 8 respiratory muscles during airway occlusion. Ventilatory capacity during chemoactivation was determined via wholebody plethysmography. Diaphragm contractile performance was assessed *exvivo*. Structural and molecular analyses are ongoing.
Results: KPP animals lost 23.4% bodyweight. Whole diaphragm muscle mass was reduced by 43%. Diaphragm absolute isometric force was significantly reduced ($P < 0.0001$), however, specific force was equivalent between groups, indicating preservation of intrinsic function. KPP isotonic maximum shortening velocity was reduced ($P = 0.0035$), contributing toward a 10% deficit in peak power. Ventilatory equivalents were unchanged during hypercapnichypoxic exposure, indicating maintenance of ventilatory capacity in KPP mice. Impaired respiratory performance was evident in reduced peak inspiratory pressure ($P = 0.0177$), alongside decreased peak diaphragm electromyographic activity ($P = 0.0029$).
Conclusion: Severely cachectic KPP animals retained sufficient ventilatory capacity to meet metabolic demand. Altered contractile kinetics suggest a compensatory mechanism may have preserved diaphragm force production at the expense of shortening velocity, ultimately contributing to dysfunction revealed in peak power production. Despite preservation of intrinsic force production, maximal respiratory performance is decreased due to loss of diaphragm mass. Our study revealed respiratory dysfunction in a translational model of cancer cachexia. We will employ a multiomic approach to delineate molecular mechanisms contributing to diaphragm dysfunction.

16-19 September 2026 — Hamburg, Germany

Physiology with Flow: Set Sail!

PHYSIOLOGY in FOCUS 2026

The joint ANNUAL MEETING OF THE GERMAN PHYSIOLOGICAL SOCIETY
and the SCANDINAVIAN PHYSIOLOGICAL SOCIETY

www.dpg-congress.de

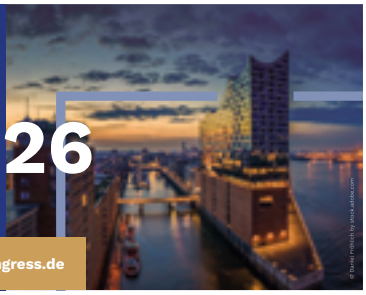

OC 01 FLOW of Motion: Skeletal Muscle function in physiology & disease

OC0102

Cancers reprogram SUMO landscape in striated muscle cells: atypical link between ubiquitinlike proteins, polycomb repressors and muscle atrophy

Luis Gand; Mugeng Li; Katharina Brandt; Baoyu Zhou; Amel NasserGrioua; Julien Gondin [1]; Edgar Becker; Andreas Pich [2]; Theresia Kraft; Mamta AmruteNayak; Arnab Nayak Institute of Molecular and Cell Physiology, Hannover Medical School, Hannover, Germany; [1] INSERM U1315, Lyon, Lyon, France; [2] Institute of Toxicology, Hannover Medical School, Hannover, Germany;

Objective: Cachexia is a debilitating musclewasting disorder associated with 80% of cancer patients, with mortality in 30% of patients. The molecular mechanisms underlying cancerinduced cachexia (CIC) remain poorly understood. Cells use the SUMO (Small Ubiquitinlike Modifier) posttranslational protein modification machinery to respond rapidly to external challenges, particularly during the stress response. As cancer triggers oxidative stress, we hypothesize in favor of unknown links between SUMO and CIC.
Method: By using muscle tissues from C26 cancer cachexia mice, progenitor myoblastderived differented muscle cells and neonatal rat cardiomyocytes**,** we performed endogenous SUMO proteomics, checked sarcomere organization and followed intracellular Ca^{2+} transient. By pacing experiments, we checked muscle cell contractile properties. By combining siRNAmediated knockdown and RNAseq assays, we measured global transcriptional changes in CIC. We checked epigenetic signaling on musclespecific gene promoters by ChIP (chromatin immunoprecipitation) assays. Finally, by endogenous coimmunoprecipitation assays, we tested protein complex composition in CIC.
Results: Here, we observed that CIC triggered an increased SUMOylation of global nuclearsoluble and chromatinbound proteins in skeletal and cardiac muscle cells. CIC altered stability of various SUMO machinery components, including SUMO isopeptidases. Quantitative mass spectrometry revealed that SUMOylation of the noncanonical polycomb repressor protein L3MBTL2 was enhanced in CIC. Contrary to previous notions, we found that L3MBTL2 activates musclespecific gene expression program. Mechanistically, L3MBTL2 interacts with Ash2L, a component of the SET1/MLL histone methyltransferase epigenetic complex. Increased SUMO modification of L3MBTL2 in CIC led to partitioning of Ash2L from its target genes including *myosin heavy chain* (*Myh1*) and *Atp2a1* (protein- SERCA1). At cellular level, this resulted in sarcomere disorganization and impaired calciumhandling i.e, a prolonged time constant (τ) for Ca^{2+} reuptake into the sarcoplasmic reticulum. Altogether, it significantly impeded muscle contraction. Interestingly, depleted L3MBTL2 level phenocopied CIC and SUMOsite mutant L3MBTL2 partially rescued musclespecific gene expression.
Conclusion: Collectively, Our findings revealed an atypical connection of SUMO with CIC, a paradoxical SUMOassociated transcriptional activator function of L3MBTL2 repressor protein and hold promise toward new therapeutic strategies to improve CIC.

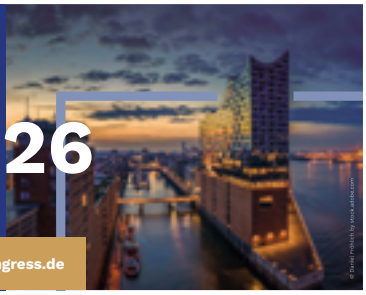

OC 01 FLOW of Motion: Skeletal Muscle function in physiology & disease

OC0103

Exercise as a potential diseasemodifying therapy in multiple sclerosis

Sina Cathérine Rosenkranz; Joana F. da Rocha [1]; Luis Moreira [1]; Pius Schlachter [1]; Jasmina Bier; Kaela Haley [1]; Daniela Neves Silva; Mohammed Ariff Iqbal [1]; Marjan Gharagozloo [2]; Yueyue Xiong [3]; Matthew A. Murphy [3]; Helena C. Lichtenfeld; Lukas Raich; Michaela Schweizer [4]; Asude Ertas [1]; Marcel S. Woo; Vanessa Vieira; Samuel E. Honeycutt [5]; James P. White [5]; Gregory A. Wyant [1]; Manuel A. Friese [6]; Peter A. Calabresi [2]; Ruxandra F. Sîrbulescu [3]; Christiane D. Wrann [1]
INIMS, UKE, Hamburg, Germany; [1] Cardiovascular Research Center, Massachusetts General Hospital, Boston, United States; [2] Department of Neurology, Johns Hopkins University, School of Medicine, Baltimore, United States; [3] Vaccine and Immunotherapy Center, Massachusetts General Hospital, Boston, United States; [4] Zentrum für Molekulare Neurobiologie, Universitätsklinikum HamburgEppendorf, Hamburg, Germany; [5] Department of Medicine, Duke University School of Medicine, Durham, Germany; [6] Institute of Neuroimmunology and Multiple Sclerosis, Universitätsklinikum HamburgEppendorf, Hamburg, Germany;

Objective: Aerobic exercise is a diseasemodifying intervention in multiple sclerosis (MS) that ameliorates several progressive neurological symptoms, yet the underlying mechanisms remain incompletely understood. The muscle–brain signaling axis involving induction of the exercise hormone irisin may play an important role in enhancing neuronal resilience in MS.
Method: Using the experimental autoimmune encephalomyelitis (EAE) mouse model of MS, the effects of voluntary wheel running and peripheral irisin administration were assessed. Gain- and lossoffunction approaches were used to determine the role of *Fndc5*/irisin in inflammationinduced neurodegeneration. Clinical outcomes, neuronal loss, immune responses, synaptic integrity, mitochondrial activity, and neuronal gene expression in spinal cord neurons were analyzed.
Results: Voluntary exercise reduced inflammationinduced neurodegeneration in EAE, whereas these effects were lost in *Fndc5*/irisindeficient mice. Peripheral irisin administration increased circulating irisin plasma levels and reduced clinical severity and neuronal loss. Irisin did not substantially alter peripheral or central immune responses but instead induced a neuroprotective gene program in spinal neurons, preserved synapses, and enhanced mitochondrial activity, likely through direct interaction with motor neurons.
Conclusion: These findings identify irisin may represent one piece of the puzzle in explaining how exercise promotes neuronal survival in inflammatory neurodegeneration.

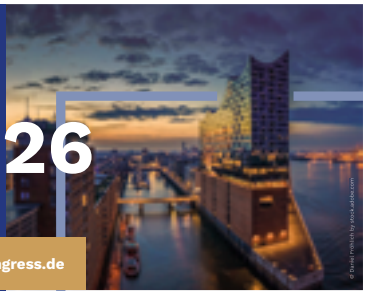

OC 01 FLOW of Motion: Skeletal Muscle function in physiology & disease

OC0104

Sex- and fiber typespecific remodeling of the muscle proteome implicates CSRP3 in resistance traininginduced hypertrophy

Lukas Moesgaard; Roger MorenoJusticia [1]; Johann Schmalbruch [2]; Soeren Jessen [2]; Ben Stocks [3]; Nicoline R. Andersen [4]; Jens J. Nielsen [2]; Caio Y. Yonamine [1]; Jonas T. Treebak [1]; Jens Bangsbo [2]; Clara Prats [5]; Lykke Sylow [6]; Atul S. Deshmukh [1]; Morten Hostrup [2] Department of Physiology and Pharmacology, Karolinska Institutet, Stockholm, Sweden; [1] Novo Nordisk Foundation Center for Basic Metabolic Research, University of Copenhagen, Copenhagen, Denmark; [2] The August Krogh Section for Human and Molecular Physiology, Department of Nutrition, Exercise and Sports, University of Copenhagen, Copenhagen, Denmark; [3] Department of Physiology and Pharmacology, Karolinska Institutet, Stockholm, Sweden; [4] Health and Medical Sciences, University of Copenhagen, Copenhagen, Denmark; [5] The Core Facility for Integrated Microscopy, Faculty of Health and Medical Sciences, University of Copenhagen, Copenhagen, Denmark; [6] Department of Biomedical Sciences, University of Copenhagen, Copenhagen, Denmark;

Objective: Skeletal muscle hypertrophy is a hallmark of resistance training that improves health and longevity. However, despite physiological differences between sexes and fiber types, the underlying proteome changes with resistance training have not been studied in a sex- and fiber typespecific manner. In this study, we applied our recently developed muscle fiber proteomics workflow to investigate sex- and fiber typespecific adaptations to resistance training.
Method: Twelve females and 12 males who did not engage in resistance training prior to the intervention completed 8 weeks of supervised resistance training performed 3 times a week, with muscle biopsies sampled from *m. vastus lateralis* before and 3 days after the last training bout. After freezedrying the muscle biopsies, single fibers were dissected and typified using dot blotting with antibodies against MYH7 (type I) and MYH2 (type II). Fibers were then pooled by participant and time point, resulting in pools of 18 ± 6 (mean ± SD) type I and 18 ± 5 type II fibers in females, and 14 ± 6 type I and 23 ± 6 type II fibers in males that were analyzed by liquid chromatography tandem mass spectrometrybased proteomics (LCMS/MS).
Results: Following 8 weeks of resistance training, remodeling of the human skeletal muscle proteome occurred in a sex- and fiber typespecific manner. Notably, type II fibers exhibited much greater adaptations across both sexes, whereas the main sexdifference was a greater remodeling of intermediate filaments in females. Of proteins that were specifically upregulated in type II fibers by resistance training in both males and females, overexpression of the mechanosensitive protein CSRP3 induced muscle hypertrophy in mice, indicating a role of fiber typespecific upregulation of CSRP3 in muscle hypertrophy. In addition, baseline abundance of proteins involved in translation correlated highly with fiber hypertrophy, and differed between sexes and fiber types.
Conclusion: These findings demonstrate key aspects of sex- and fiber type differences in muscle physiology and their contributions to resistance traininginduced adaptions, and implicate CSRP3 as a mediator of resistance traininginduced muscle hypertrophy.

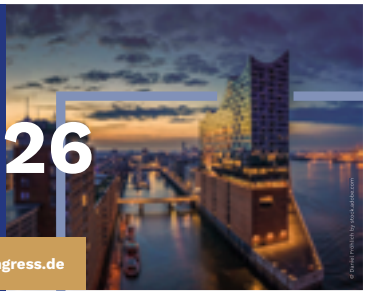

OC01 FLOW of Motion: Skeletal Muscle function in physiology & disease

OC0105

Genetic deletion of the cation channel TRPV4 attenuates fibrosis in dystrophic *mdx* mouse muscle, but has only minor protective effects on dystrophindeficient muscle fibers

Ruth S. Eller; Alexander Möller; Mirjam Krautwald; Yaxin Zhang; Heinrich Brinkmeier [1] Institute of Pathophysiology, University Medicine Greifswald, Greifswald, Germany; [1] Institute of Physiology, University Medicine Greifswald, Greifswald, Germany;

Objective: Gene mutations causing loss of the cytoskeletal protein dystrophin lead to the severe muscle disease Duchenne muscular dystrophy (DMD). The phenotype of DMD is widely reproduced in the murine model *mdx* and characterized by Ca^{2+} induced damage of muscle fibers and fibrosis, leading to progressive muscle weakness. The mechanosensitive cation channel TRPV4 is one putative ion channel, relevant in the pathomechanism of dystrophindeficient muscle. It could function in two ways: first, as a dysregulated Ca²? influx channel that causes abnormal force and Ca^{2+} dependent stress responses in muscle fibers; and second, as a Ca^{2+} channel in fibroblasts promoting fibroblast activation and proliferation, and thus fibrosis.
Method: We investigated whether TRPV4 gene deletion in *mdx* mice improves contractile muscle function and histomorphological architecture of muscles. Muscles of four genotypes were studied, the wildtype (WT), TRPV4 deficient mice, *mdx* mice and double mutants lacking both proteins, dystrophin and TRPV4. Experiments were performed with muscles from 100 d and 180day old male mice (background: C57BL/6J strain).
Results: Initially, EDL muscles were studied under isometric conditions. Specific muscle force of twitches and responses to repetitive stimulation (120 Hz, 600 ms) of both *mdx* genotypes was about 3039% lower than those of WT and TRPV4 deficient mice (180 d). The differences were significant, $p < 0.01$, n=8 for each group. Kinetics of twitches and tetani were similar in all four strains. When muscles of *mdx* and *mdx/trpv4*$^{-/-}$ mice were subjected to eccentric stimulation (7 x 600 ms, 10% stretch between 200 and 300 ms) drop of force was even more pronounced: in WT muscles 57 ± 11% of the initial force remained, but only 40 ± 12 % in *mdx* and 41 ± 12 % in *mdx/trpv4*$^{-/-}$. Interestingly, TRPV4 deficient muscles were rather resistant to the challenge showing 72 ± 5 % of initial force. In contrast to the results of the contraction experiments, histomorphological analyses of EDL, soleus, tibialis anterior and diaphragm muscles showed an improved structure in *mdx/trpv4*$^{-/-}$ mice compared to *mdx*. Cross sections of muscles displayed typical signs of muscular dystrophy, both for *mdx* and *mdx/trpv4*$^{-/-}$ mice. However, the fraction of centralized nuclei, the Sirius Red stained area, indicating collagen deposits and fibrosis and the fast to slow shift of muscle fiber types were significantly attenuated in double mutants vs. *mdx*.
Conclusion: We conclude that deletion of the TRPV4 channel does not influence force characteristics of *mdx* EDL muscles, i.e. reduction of specific force and reduced resistance to eccentric contractions. However, histological analyses indicate reduced degeneration/regeneration cycles of muscle fibers and reduced fibrosis. The findings support the hypothesis that TRPV4mediated Ca^{2+} influx may contribute to the dystrophic pathology and that inhibition of TRPV4 channels could improve histopathological features of DMD.

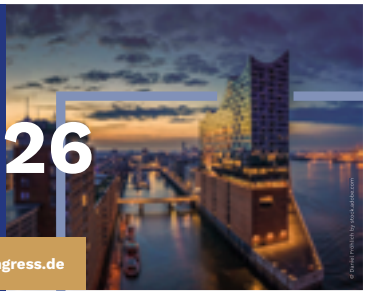

OC01 FLOW of Motion: Skeletal Muscle function in physiology & disease

OC0106

SingleNucleus Transcriptomics Uncovers CellTypeSpecific Remodelling in Gastrocnemius and Vastus Lateralis Muscles in Peripheral Artery Disease

Emily Shorter; Tina Gorsek Sparove; Thomas Gustafsson [1]; Carl Magnus Wahlgren [2]; Gustaw Eriksson [3]; Björn Alkner [4]; Ferdinand von Walden [5]; Elisabet StenerVictorin [3]; Johanna Lanner Department of Physiology, Nutrition and Biomechanics, Swedish School of Sport and Health Sciences, Stockholm, Sweden; [1] Department of Laboratory Medicine, Swedish School of Sport and Health Sciences, Stockholm, Sweden; [2] Department of Molecular Medicine and Surgery, Swedish School of Sport and Health Sciences, Stockholm, Sweden; [3] Department of Physiology & Pharmacology, Swedish School of Sport and Health Sciences, Stockholm, Sweden; [4] Department of Orthopaedic Surgery, Swedish School of Sport and Health Sciences, Eksjö, Sweden; [5] Department of Women's and Children's Health, Karolinska Institutet, Stockholm, Sweden;

Objective: Comorbidities of type II diabetes (T2D), including peripheral artery disease (PAD), are major global health concerns. PAD involves reduced blood flow to the lower limbs, causing muscle ischemia, dysfunction, and weakness that can progress to necrosis if untreated. Current interventions, such as bypass surgery and endovascular procedures, restore blood flow but often fail to correct skeletal muscle abnormalities. Despite this, the molecular mechanisms underlying intramuscular dysfunction in PAD remain poorly understood.
Method: To define cellular and transcriptional alterations in PAD muscle, we generated singlenucleus RNAsequencing data from approximately 100,000 nuclei isolated from paired gastrocnemius and vastus lateralis biopsies obtained from 6 patients with PAD and 6 healthy controls.
Results: Our analysis identified marked cell typespecific changes in PAD muscle. Fibroadipogenic progenitor cells had an increased proportion in both muscles of PAD patients, indicating broad remodelling of the stromal niche. The ischemic gastrocnemius showed a higher proportion of immune cells, consistent with an altered inflammatory landscape. At the myofiber level, type I fibers exhibited downregulation of mitochondrial pathways, implicating mitochondrial dysfunction in PADassociated muscle pathology.
Conclusion: Together, these data establish a singlenucleus transcriptomic atlas of human skeletal muscle in PAD, strengthened by paired distal and proximal sampling alongside controls, providing a foundation for mechanistic insight into PADassociated myopathy.

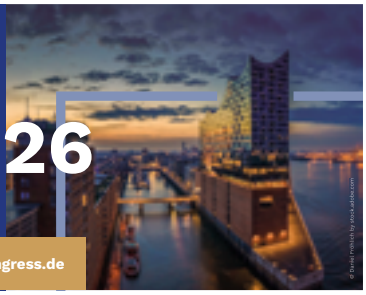

OC 02 FLOW of Air: Pulmonary function, oxygen metabolism, hypoxia

OC0201
Lung microvascular rarefaction impairs pulmonary gas exchange and exacerbates heart failure with preserved ejection fraction

Ceren Kocana; Lara Jaeschke; Alexandra Maria Chitroceanu [1]; Qi Zhang; Niklas Hegemann; Pengchao Sang; Qiuhua Li; Mariya M. Kucherenko [2]; Kristin Kraeker [3]; Kristina Franz [4]; Alexandr Melnikov; David Faidel; Leonardo A. von der Ohe; PaulLennard Perret; Jonathan L. Gillan; Annika Winkler; Edwardo [5 4 4 4 4]Reynolds ; Andreas Kind ; Lucie Kretzler ; Daniela Zurkan ; Veronika Zach ; Samuel Mathew Tharakan [6]; Mohammad Amiruddin Hashmi [6]; Bakhrom K. Berdiev [7]; Saba Al Heialy [7]; Mohammed Uddin [7]; Frank Edelmann [8]; Ralf Dechend [9]; Gabriele G. Schiattarella [10]; Szandor Simmons; Christina Brandenberger [11]; Jana Grune; Wolfgang Kübler Institut für Physiologie, Campus Charité Mitte, Charité - Universitätsmedizin Berlin, Berlin, Germany; [1] Department of Cardiology, Angiology and Intensive Care Medicine, Deutsches Herzzentrum der Charite; Charite´ – Universita¨tsmedizin Berlin, Berlin, Germany; [2] Deutsches Herzzentrum der Charité, Berlin, Germany; [3] Experimental and Clinical Research Center (ECRC), a joint cooperation between Max Delbru¨ck Center for Molecular Medicine and Charite´ – Universita¨tsmedizin Berlin; DZHK (German Centre for Cardiovascular Research), Berlin, Germany; [4] Department of Cardiology, Angiology and Intensive Care Medicine, Deutsches Herzzentrum der Charite´, Berlin, Germany; [5] Department of Cardiothoracic and Vascular Surgery, Deutsches Herzzentrum der Charite´, Berlin, Germany; [6] Center for Applied and Translational Genomics (CATG), Mohammed Bin Rashid University of Medicine and Health Sciences (MBRU), Dubai, Saudi Arabia; [7] College of Medicine, Mohammed Bin Rashid University of Medicine and Health Sciences (MBRU), Dubai, Saudi Arabia; [8] Medizinische Klinik mit Schwerpunkt Kardiologie, Campus VirchowKlinikum, Charité - Universitätsmedizin Berlin, Berlin, Germany; [9] ECRCKooperation von MDC und Charité, Experimental and Clinical Research Center, Berlin, Germany; [10] Department of Cardiology, Angiology and Intensive Care Medicine, Deutsches Herzzentrum der Charite´, Berlin, Germany; [11] Institut für Funktionelle Anatomie, Charité - Universitätsmedizin Berlin, Berlin, Germany;

Objective: HFpEF is characterized by dyspnea and hypoxemia at rest and during exercise. Yet, the molecular and structural changes underlying impaired pulmonary gas exchange in HFpEF are not understood. Here, we hypothesized that HFpEF induces lung microvascular rarefaction causing hypoxemia that worsens biventricular dysfunction in a detrimental feedback loop.

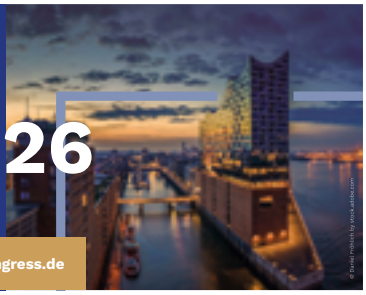

OC0201

Lung microvascular rarefaction impairs pulmonary gas exchange and exacerbates heart failure with preserved ejection fraction

Results: In 234 HFpEF patients, advancing New York Heart Association class was associated with reduced arterial oxygen saturation at rest and during exercise and reduced lung diffusing capacity that correlated with indices of left ventricular (LV) diastolic dysfunction. Lung microvascular rarefaction was assessed in three animal models of LV diastolic dysfunction, namely male ZSF1 obese rats treated with SU5416, C57BL/6J mice of both sexes on highfat diet plus LNAME, and male Sprague‐Dawley rats subjected to aortic banding (AoB). Echocardiographic analyses demonstrated characteristics of LV diastolic dysfunction (decreased global longitudinal strain, increased E/e´) with ejection fration >50% in all models. Microcomputed tomography revealed decreased vascular volume in microvessels <250 µm in diameter in all models. Stereological assessment confirmed reduced capillary number in AoB rats and HFpEF mice, and reduced capillary volume density in ZSF1 rats. Flow cytometry showed time‐dependent loss of lung microvascular endothelial cells exceeding 50% after 12 weeks of HFpEF in mice. Single‐cell transcriptomics identified upregulation of autophagy and regulated cell death genes in capillary endothelial cells in HFpEF, with subsequent confirmation of increased endothelial autophagic flux and apoptosis by flow cytometry, electron microscopy and immunohistology. HFpEF mice with an endothelial‐specific loss of the essential autophagy gene *Atg7* (*Atg7*^{ENKO}) had preserved capillary numbers, restored normoxemia and improved LV diastolic function relative to wild‐type controls. Hypoxic exposure (10% O2) worsened whereas moderate hyperoxia (40% O2) normalized echocardiographic signs of LV diastolic dysfunction.
Conclusion: Our findings identify autophagy‐driven lung capillary rarefaction as a novel pathomechanism in HFpEF causing hypoxemia and exacerbating LV dysfunction. Targeting endothelial autophagy or restoring oxygenation protects cardiac function, highlighting novel promising therapeutic avenues in HFpEF.
Supported by the Deutsche Forschungsgemeinschaft, CRC1470, subproject A04 to WMK and JG.

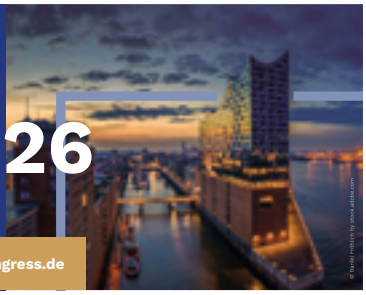

OC 02 FLOW of Air: Pulmonary function, oxygen metabolism, hypoxia

OC0202

Endothelial Hspa1a is Required for Hypoxia Tolerance in the Pulmonary Vasculature

Alia Ablieh; Laban Hebatullah; Tom Kretzschmar; Markus Hecker; Thomas Korff Department of Cardiovascular Physiology, Institute of Physiology and Pathophysiologygie, Heidelberg university, Heidelberg, Germany;

Objective: Hypoxia requires rapid and coordinated adaptation of lung endothelial cells (ECs) to maintain vascular homeostasis. In this context, *in vitro* analyses revealed that hypoxiaexposed murine lung endothelial cells (MLEC) activate nuclear factor of activated Tcells 5 (NFAT5/TonEBP) - a transcription factor that adjusts the cellular transcriptome to cope with multiple environmental stressors. *In vivo*, targeted ablation of *Nfat5* in endothelial cells did not evoke phenotypic abnormalities in normoxiaexposed mice. However, *Nfat5*deficient MLEC reinforced energy- and proteinmetabolismassociated gene expression under normobaric hypoxia (10% O_2) for seven days as evidenced by microarray- and scRNAseqbased analyses.
Method: We identified *Hspa1a* and *Hspa1b* as transcriptional targets of NFAT5 in hypoxic MLEC encoding subunits of heat shock protein 70 (HSP70). Considering the important role of HSP70 protein, we assumed that shortage of HSP70 as observed in *Nfat5*deficient MLEC impairs their capability to adequately cope with hypoxia. Chromatin accessibility profiling further demonstrates that the *Hspa1a* promoter is selectively activated under hypoxia, in contrast to *Hspa1b*, and is enriched for multiple HIF1α binding sites, indicating hypoxiaspecific regulation.
Results: To directly evaluate the functional role of *Hspa1a*, we generated endothelialspecific *Hspa1a* knockout model. Loss of *Hspa1a* resulted in impaired endothelial adaptation to hypoxia, characterized by suppression of protein synthesis, translational dysregulation and irregular cell cycle progression. Functionally, loss of *Hspa1a* promoted senescence like phenotype, evidenced by upregulation of senescenceassociated genes including *Cdkn2a*, *Tert1*, and *H2afx* (vs. control), suggesting a disrupted stress response pathway under these conditions. Moreover, besides senescenceassociated morphological features, βgalactosidase activity was significantly elevated *in Hspa1a*deficient MLEC.
Conclusion: Collectively, our data support a model in which NFAT5dependent induction of *Hspa1a* is required to enable adequate protein synthesis and chaperonemediated folding capacity under hypoxic stress. Disruption of this axis drives endothelial dysfunction and premature senescence. Together, our findings demonstrate that *Hspa1a acts as a critical determinant of* pulmonary endothelial resilience during hypoxic stress.

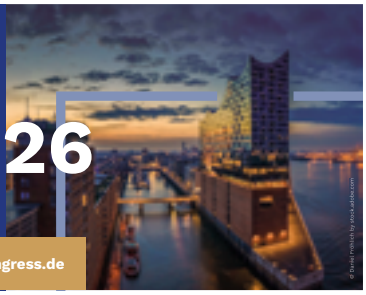

OC 02 FLOW of Air: Pulmonary function, oxygen metabolism, hypoxia

OC0203

Longlasting effects of hypoxic priming on macrophage biology and function

Brenda Krishnacoumar; Joachim Fandrey
Abteilung Physiologie, Universitätsklinikum Essen, Essen, Germany;

Objective: Cyclic hypoxia is a hallmark of chronic inflammatory conditions such as rheumatoid arthritis (RA) and also occurs during ischemia–reperfusion following organ transplantation. In these settings, tissueresident macrophages are exposed to transient hypoxia followed by reoxygenation. Although hypoxia is known to modulate macrophage function, the longterm effects of hypoxic priming on macrophage physiology remain poorly understood.
Method: To investigate the longlasting effects of hypoxic priming, murine bone marrowderived macrophages (BMDMs) were exposed to 1% O2 for 24 h followed by reoxygenation at 21% O2 for 3 days. Inflammatory responses were assessed by quantifying IL1β secretion using ELISA. Mitochondrial morphology was analyzed by TOM20 immunostaining, and metabolic alterations were characterized using Seahorse extracellular flux analysis.
Results: Our findings demonstrate that hypoxic priming reduces the release of proinflammatory cytokines. Furthermore, hypoxiaprimed macrophages exhibited persistent alterations in mitochondrial morphology, characterized by increased branching and a more elongated, thinner mitochondrial network. Seahorse extracellular flux analysis revealed reduced glycolytic capacity and glycolytic reserve following hypoxic priming, indicating longlasting metabolic adaptation in macrophages.
Conclusion: Our findings demonstrate that transient hypoxic exposure induces persistent changes in macrophage function, mitochondrial architecture, and metabolic programming. These adaptations may contribute to altered macrophage responses in chronic inflammatory and ischemia–reperfusionassociated conditions.

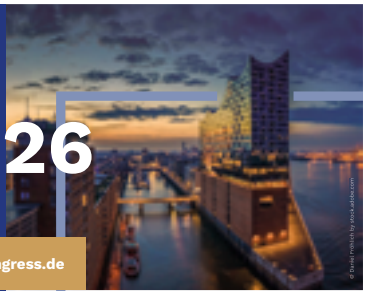

OC 02 FLOW of Air: Pulmonary function, oxygen metabolism, hypoxia

OC0204

The oxygen sensor FIH regulates proinflammatory signaling in THP1 monocytes and macrophages

Marleen Silke Oswald; Karla Märtin; Carsten C. Scholz
Institute of Physiology, University Medicine Greifswald, Greifswald, Germany;

Objective: During inflammatory processes, reduced local tissue oxygen availability (hypoxia) occurs due to damaged blood vessels and/or increased local oxygen consumption. The asparagine hydroxylase factor inhibiting HIF (FIH) is a key oxygen sensor that enables cells to detect and adapt to hypoxia. FIH has previously been linked to the regulation of inflammatory responses *in vitro* and *in vivo*, however, the underlying molecular mechanism(s) remain poorly understood. Here, we investigated whether FIH modulates inflammatory signaling in monocytes and macrophages. The cytokines TNFα and, IL1β as well as the bacterial product LPS stimulate signaling pathways in mammalian cells, leading to the activation of the transcription factor NFκB. In the absence of a signal, the protein IκBα keeps NFκB in the cytosol, inhibiting its activity. Upon stimulation, IκBα is phosphorylated and subsequently degraded, allowing NFκBmediated transcription.
Method: To examine the role of FIH in monocyte and macrophagedependent inflammation, FIH expression was reduced using stable shRNAmediated knockdown (KD) or inhibited using the pharmacologic compound DMNOFD in the human monocytic cell line THP1. Proinflammatory signaling pathway and NFκB activity were assessed by investigating total and phosphorylated IκBα (pIκBα), an activating phosphorylation of the NFκB subunit p65 (pp65) as well as NFκB target gene expression.
Results: FIH KD in monocytes resulted in decreased TNFα- and IL1βinduced pIκBα and pp65. TNFα and IL1βmediated expression of the NFκB target gene COX2 was also diminished, overall demonstrating a decreased NFκB activity following FIH KD. In THP1derived macrophages, TNFαdependent pIκBα level was also reduced by FIH KD. Interestingly, FIH KD had no effect on LPSinduced pIκBα and pp65 but led to increased COX2 protein levels in monocytes and macrophages. Pharmacologic FIH inhibition by DMNOFD resulted in a similar reduction in TNFαinduced pIκBα similar to the observed effect of FIH KD.
Conclusion: Our results identify FIH as an important regulator of TNFα- and IL1βmediated NFκB activity in monocytes and macrophages and indicate that pharmacologic FIH inhibition represents a potential novel antiinflammatory treatment option.

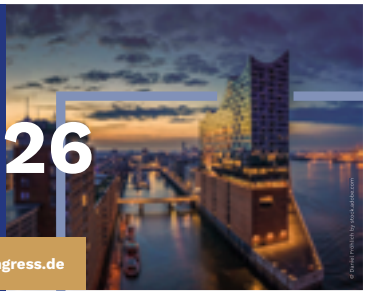

OC 02 FLOW of Air: Pulmonary function, oxygen metabolism, hypoxia

OC0205

Transcriptomic adaptation to hypoxia in neuroblastoma: HIF and beyond

Xheni Meçi; Helena Landstorfer; Simon Kelterborn; Holger Scholz Institut für Translatioinal Physiologie, Campus Charité Mitte, Charité - Universitätsmedizin Berlin, Berlin, Germany;

Objective: Neuroblastoma is a malignant pediatric tumor originating from the peripheral sympathetic nervous system affecting 1:100.000 children worldwide. In addition to genetic drivers, local tissue hypoxia has been reported to promote aggressive tumor growth. Cellular adaptation to reduced oxygen availability is primarily mediated by hypoxiainducible factors (HIFs). Yet, the respective roles of HIF1α and HIF2α in neuroblastoma biology and patient outcome remain controversial.
The goal of this study is to analyze the transcriptional response of neuroblastoma cells to hypoxia. Particularly, we aim to delineate HIF1α and HIF2α target genes in neuroblastoma cells and correlate their expression with clinical outcome.
Method: CRISPR/Cas9 gene editing was used to delete HIF1α, HIF2α, or their shared βsubunit in *MYCN*amplified Kelly neuroblastoma. Wildtype and HIFdeficient cells were exposed to either normoxia (21% O_2) or hypoxia (0.5% O_2, 16 h), followed by transcriptomic profiling using bulk RNAsequencing. Additionally, HIF binding sites were mapped in the genome of DMOGtreated Kelly cells by CUT&RUNsequencing.
Results: A total of 360 transcripts were identified as HIF1αdependent, including previously known targets such as CA9, BNIP3 and PFKFB3. A substantially larger set of 1387 transcripts, including EPO, PDGFB and FLT1 was classified as HIF2αdependent. Fortynine genes, including MMP9 and BIRC3, were coregulated by both HIF1α and HIF2α. Functional enrichment analysis showed that HIF1α target genes were mainly associated with immune regulation and cytotoxicity, while HIF2αdependent genes were linked to developmental and nervous system processes. Analysis of microarray data from 478 neuroblastoma patients revealed significantly reduced survival rates in patients with elevated expression of HIF1α candidate target genes, an effect that was further exacerbated in *MYCN*amplified tumors. In contrast, HIF2αdependent transcripts did not closely correlate with patient survival.
Conclusion: CRISPR/Cas9 editing followed by bulk RNAsequencing provides a powerful approach to distinguish between HIF1α and HIF2αdependent genes in neuroblastoma cells. Combination with bioinformatic analyses suggests an unfavorable role of role HIF1α in these tumors.

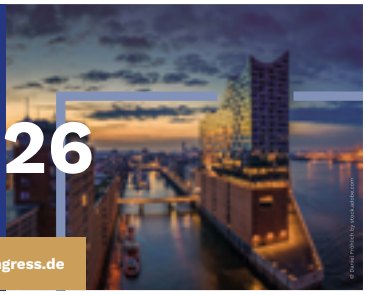

OC 02 FLOW of Air: Pulmonary function, oxygen metabolism, hypoxia

OC0206

Primary cilium elongation by lithium rescues pathological cellular phenotype *in vitro* and attenuates pulmonary hypertension in chronic hypoxic mice *in vivo*

Alexandr Melnikov; Philip D. Solymosi; PaulLennard Perret; Szandor Simmons; Wolfgang Kübler Institut für Physiologie, Campus Charité Mitte, Charité - Universitätsmedizin Berlin, Berlin, Germany;

Objective: The primary cilium (PC) is a hairlike structure protruding from the cell membrane and acting as a signaling hub. We recently identified PC loss and shortening as both hallmark and driver of the pathological vascular phenotype in pulmonary hypertension (PH) as i) PC were found to be shorter and less frequent in pulmonary artery smooth muscle (PASMC) and endothelial cells (PAEC) from PAH patients, ii) PC loss by siRNAmediated *IFT88* knockdown increased migration and proliferation in PASMC and PAEC *in vitro* and iii) *ift88*deficient mice developed aggravated PH in hypoxia *in vivo*. We therefore hypothesized that lithium, a known PC elongator, may alleviate the proproliferative and promigratory phenotype of pulmonary vascular cells from PAH patients *in vitro* as well as attenuate the development of PH in chronic hypoxic mice *in vivo*.
Method: PASMC and PAEC were treated with LiCl (50 mM). PC length was measured by acetylatedαtubulin immunofluorescence. Cell migration and proliferation were assessed by wound healing and BrdU incorporation assays. Male C57BL/6J mice were kept under hypoxia (10% O_2) or normoxia for 5 weeks. Mice were fed chow containing 0.2% Li_2CO_3 for five weeks in the “prophylactic”, or for the last 2 weeks in the “therapeutic” treatment groups. After 5 weeks, PH was evaluated by echocardiographic assessment of tricuspid annular plane systolic excursion (TAPSE) and measurement of right ventricular systolic pressure (RVSP) via right heart catheterization. Pulmonary vessel wall thickness was determined in H&Estained lung sections.
Results: *In vitro*, lithium elongated the PC and reduced lung vascular cell migration and proliferation. *In vivo*, mice exposed to 5 weeks of hypoxia developed characteristic signs of PH, including an increase in mean RVSP (51.9 ± 12.2 mmHg), a decrease in mean TAPSE (0.70 ± 0.15 mm), and histological evidence of pulmonary vascular wall thickening vs. normoxia. Prophylactic lithium treatment largely normalized these changes. Therapeutic lithium proved less effective but still resulted in reduced vessel wall thickness, a 20.2% decrease in RVSP and a 39.4% increase in TAPSE relative to hypoxic controls.
Conclusion: These data demonstrate that lithiummediated restoration of PC length attenuates the pathological phenotype of PAH vascular cells *in vitro* and alleviates PH development and pulmonary vascular remodeling in chronic hypoxic mice *in vivo*, identifying PC elongation as a novel therapeutic strategy for PH.

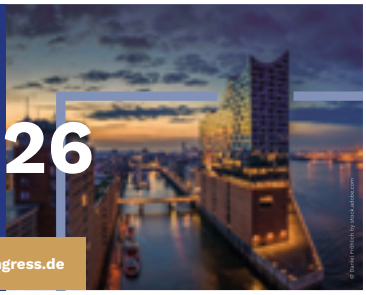

OC 03 FLOW of Urine: Glomerula function

OC0301

Influence of SGLT2 treatment on renal micro vessels in the db/db mouse model

Cem Erdogan; Minze Xu; FalkBach Lichtenberger; Lingyan Fei [1]; Julia Sophie Schröter Bonk; Robert Labes; Vera Anna Kulow; Michael Fähling; Andreas Patzak; Pratik Hemant Khedkar
Institut für Translatioinal Physiologie, Campus Charité Mitte, Charité - Universitätsmedizin Berlin, Berlin, Germany; [1] Department of Nephrology, Center of Kidney and Urology, The Seventh Affiliated Hospital, Shen Zhen, China;

Objective: Diabetic nephropathy is a leading cause of chronic kidney disease. While SGLT2 inhibitors are known to stabilize glomerular filtration rate (GFR), the underlying mechanism remain elusive. We proposed that SGLT2 inhibition restores glomerular microvascular function by correcting altered vasoreactivity of afferent and efferent arterioles, thereby limiting hyperfiltration.
Method: Db/db mice and nondiabetic db/+ littermates were assigned randomly to four experimental groups (± SGLT2 inhibitor; empagliflozin (EMPA)) and observed for 8 weeks. Serum glucose, body weight and kidney histology were assessed. Vasodilatory responses of isolated renal afferent and efferent arterioles were examined using microperfusion with acetylcholine and the NO donor SnitrosoNacetylpenicillamine (SNAP). In addition, RNA sequencing was performed to identify differentially regulated pathways.
Results: Untreated db/db mice showed markedly elevated glucose levels, which were significantly reduced by EMPA. Body weight was increased in diabetic animals, but did not differ within the same genotype. Afferent arterioles from untreated db/db mice exhibited enhanced acetylcholineinduced vasodilation compared to controls; this effect was attenuated by EMPA treatment. In contrast, efferent arterioles of untreated db/db mice displayed impaired vasodilation following NO synthase inhibition and reduced responsiveness to SNAP, both of which improved under EMPA treatment. RNA sequencing demonstrated upregulation of oxidative stressassociated pathways in untreated diabetic mice along with alterations in pathways related to blood circulation. No relevant structural differences were observed in kidney histology.
Conclusion: SGLT2 inhibition with EMPA lowered hyperglycemia and partially restored dysregulated vasoactivity in glomerular microvessels, particularly sGCdependent responses in efferent arterioles. The observed normalization of oxidative stressrelated and circulation associated pathways suggests a molecular basis for improved microvascular function. These results support the idea that restoration of glomerular vascular function contributes to the protective effects of SGLT2 inhibitors on the kidney.

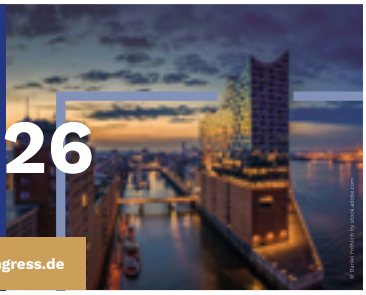

OC 03 FLOW of Urine: Glomerula function

OC0302

Secretin signaling and the reninangiotensinaldosterone system

Jesper Frank Andersen; Laura Woidemann Trans; Jens Georg Leipziger; Peder Matzen Berg Department of Biomedicine, Aarhus University, Aarhus, Denmark;

Objective: The reninangiotensinaldosterone system is activated through several different pathways in response to loss of circulatory volume. Activation increases renal electrolyte and water reabsorption along with bicarbonate excretion mediated through the Cl/HCO_3 antiporter pendrin.
Secretin, a hormone typically associated with the gastrointestinal system, also increases pendrindependent base excretion. Additional evidence suggests that secretin signaling affects both AVP and aldosterone release and that the secretin receptor (SCTR) and angiotensin II receptor interact functionally.
This study aimed to investigate how loss of secretin signaling alters the activation of the reninangiotensinaldosterone system and the cardiovascular and renal consequences hereof.
Method: Following cardiovascular and renal phenotyping, SCTR WT and KO mice (10+10, C57BL/6 background) were subjected to continuous angiotensin II infusion via miniosmotic pumps (750 ng/kg/min) for 28 days. At termination, similar phenotyping was repeated. The mice were then anesthetized (i.p. ketamine/xylazine) and kidney tissue and plasma harvested. Western blots for relevant transporters were performed on kidney lysates. Additionally, fibrosis staining and immunohistochemistry were performed on the harvested tissue.
Results: Angiotensin II induced marked hypertension in both KO and WT mice and decreased GFR. WTs developed significantly more albuminuria. Urinary pH increased significantly in WTs while no effect was seen in the KOs. WTs had significantly higher fractional sodium excretion than KOs. Furthermore, WTs had a greater upregulation of both ENaC and pendrin protein levels compared with KOs, while both genotypes exhibited increased NCC activation. Further analyses of aldosterone levels and ADH activation are pending.
Conclusion: Defective secretin signaling in SCTR KO mice blunts the systemic and renal effects of angiotensin II. Together, these data expand on the importance of functional secretin signaling in the activation of the reninangiotensinaldosterone system.

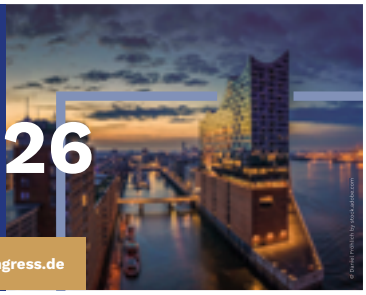

OC 03 FLOW of Urine: Glomerula function

OC0303

Nephrocyte Injury Triggers ImmuneMediated Gut Barrier Dysfunction

Paris HazeltonCavill; Berk Cantutan; Moritz Lassé; Tobias B. Huber; Philipp Antczak [1]; Sybille Köhler
Nephrologie/Rheumatologie und Endokrinologie/Diabetologie, III. Medizinische Klinik, Universitätsklinikum HamburgEppendorf, Hamburg, Germany; [1] Zentrum für Molekulare Medizin, CECAD, Uniklinik Köln, Klinik II für Innere Medizin, Universität zu Köln, Köln, Germany;

Objective: Drosophila nephrocytes are homologous to kidney podocytes, sharing striking morphological and molecular features, and have been defined as clearance cells that filter the haemolymph. They form membrane invaginations, which are spanned by the nephrocyte diaphragm, a filtration barrier and signaling hub. Recent work suggests that nephrocytes may also secrete factors, indicating an active role in systemic homeostasis. Moreover, emerging data point to a contribution of nephrocytes to immune signalling: transcriptomic profiles reveal a pronounced immune signature, and nephrocytes take up gutderived peptidoglycan to help maintain haemolymph homeostasis and support fly lifespan. However, whether nephrocytes function as active players in the immune response remains unresolved.
Method: We combined morphological and functional analyses of nephrocytes and gut with transcriptomic and proteomic profiling.
Results: Our preliminary data show that nephrocyte injury induced by loss of filtration barrier components or complete nephrocyte ablation triggers a leaky gut phenotype characterized by disruption of the epithelial barrier and premature death. Although our data clearly demonstrate crosstalk between nephrocytes and the gut, the molecular mechanisms driving this interorgan communication are still unresolved. To dissect these pathways, we conducted transcriptomic and proteomic profiling of haemolymph and gut tissue, aiming to identify dysregulated soluble factors that may serve as ligands for gut epithelial receptors, thereby initiating injury signalling cascades culminating in barrier dysfunction. Early gut injury (days 1–5) features acute damage and regeneration, and by days 14 – 30 immune signalling, together with adhesion, ECM, and cytoskeletal programs, promotes epithelial stabilization. By day 37, however, a lateonset leaky gut emerges despite preserved structural integrity, implicating chronic or dysregulated immune signalling and persistent microbial interaction in failed junctional stabilization. Haemolymph profiling highlights immune and metabolic pathway upregulation, with the immune effector Bombardier (Bbd) consistently elevated in all nephrocyteinjury models. Bbd depletion in the gut improves survival, positioning immune signalling as a central axis linking nephrocyte dysfunction to gut pathology.
Conclusion: Ongoing work examines whether nephrocyte injury drives fatbodyderived Bbd release and Toll pathway activation that underlie leaky gut development.

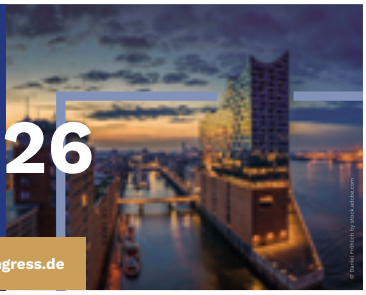

OC 03 FLOW of Urine: Glomerula function

OC0304

Generation of Monoclonal Antibodies Targeting AutoImmunoglobulinTriggered Extracellular Vesicles in Membranous Nephropathy

LenaMarie Reimers; Karen Lahme; Philipp Raabe; Björn Rissiek [1]; Friedrich KochNolte [1]; Catherine MeyerSchwesinger
Institut für Zelluläre und Integrative Physiologie, Zentrum für Experimentelle Medizin, Universitätsklinikum HamburgEppendorf, Hamburg, Germany; [1] Institut für Immunologie, Universitätsklinikum Hamburg
Eppendorf, Hamburg, Germany;

Objective: AutoImmunoglobulinTriggered Extracellular Vesicles (AITEVs) have recently been described as a novel podocytederived vesicle population released upon autoantibody binding to podocyte surface antigens in membranous nephropathy (MN). These vesicles contain autoantibodies, their cognate antigens, and markers of cellular stress, yet remain incompletely characterized and lack specific detection tools. We therefore immunized rats with patient AITEVs and explored the potential of monoclonal anti–AITEV antibodies for diagnostic applications.
Method: Two rats were immunized with AITEVs isolated from urine of MN patients. Successful immunization was confirmed at week 10 by flow cytometric analysis. Lymph node and splenic B cells were subsequently fused with mouse myeloma cells using hybridoma technology. Primary hybridoma clones were screened, selected, cryopreserved, and later subcloned to establish monoclonal cultures based on their reactivity toward MNderived or control AITEVs, as determined by ELISA. Monoclonal antibodies were further characterized by flow cytometry and Western blot analysis targeting AITEVassociated components.
Results: A total of 180 primary clones were screened by ELISA, of which 71 demonstrated reactivity toward AITEVs. Among these, 52 clones exhibited at least a twofold higher reactivity toward MNderived AITEVs compared to control AITEVs. Notably, a subset of clones (n=34) exhibited approximately fourfold higher reactivity toward MNderived AITEVs, while a small number of clones (n=3) showed the opposite pattern, indicating differential and heterogeneous antigen recognition across vesicle populations. Following subcloning, six subclones were generated per primary clone. Reactivity was confirmed by ELISA, and subsequent analyses by flow cytometry and Western blot consistently validated specific binding of selected clones to surface proteins of MNderived AITEVs.
Conclusion: AITEVs derived from the urine of MN patients are highly immunogenic and enable the generation of monoclonal antibodies with selective reactivity toward diseaseassociated vesicles, indicating the presence of diseasespecific and differentially accessible antigens. Overall, this approach provides a novel platform for the detection and molecular characterization of diseasespecific extracellular vesicles, with strong potential for biomarker development and precision medicine in kidney disease.

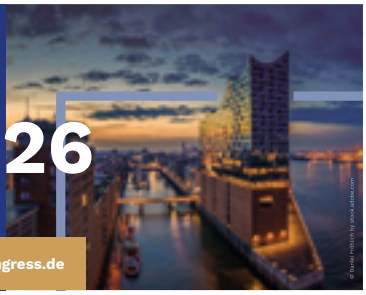

OC 03 FLOW of Urine: Glomerula function

OC0305

The intracellular form of renin as a potential new client of the PAQosome

Till Sommer; Stefanie Reuter; Kristina Herold; Nadine Reiher; Mario Müller [1]; Jonas Marx [1]; Yue Yang [1]; Felix Schneidmadel [1]; Florian MeierRosar [1]; Ralf Mrowka
Experimentelle Nephrologie, Klinik für Innere Medizin III, FriedrichSchillerUniversität Jena, Jena, Germany; [1] Funktionelle Proteomanalyse, Universitätsklinkum, FriedrichSchillerUniversität Jena, Jena, Germany;

Objective: Renin (secreted renin, sRen) is an aspartyl protease secreted by cells of the juxtaglomerular apparatus in response to reduced blood pressure, thereby initiating the reninangiotensinaldosterone system (RAS). There is, however, also an intracellular form (icRen), whose function, localisation and regulation in human cells remain poorly understood. Therefore, the goal of this study was to identify candidate interaction partners of human icRen as they might help elucidate the cellular roles of icRen.
Method: Proximity labelling coupled to mass spectrometry was used to identify candidate interaction partners of icRen. Both renin isoforms were fused to the biotin ligase BioID2, which biotinylates proteins in close proximity, and stable transfected into HEK293T cell lines. Expression of the fusion constructs was validated by qPCR. Biotinylated proteins were enriched using streptavidincoated beads and enrichment was assessed using HRPstreptavidin blotting. Onbead digestion of biotinylated proteins was performed and the resulting peptides were identified by liquid chromatographytandem mass spectrometry. Using AlphaFoldMultimer direct interaction prediction with candidate proteins was carried out.
Results: As expected, sRen was associated with the secretory pathway. icRen interacted with the prefoldin and R2TP/PAQosome cochaperone system, which assembles large protein complexes and regulatory networks in humans, suggesting that icRen is incorporated into an as yet uncharacterised protein complex. AlphaFoldMultimer predictions further supported a potenital direct interaction of icRen with components of the PAQosome. Interestingly, no RAS components were enriched among icRen interactors, suggesting that renin functions intracellularly independently of the RAS.
Conclusion: A proximity labellingbased workflow was established to identify intracellular interaction partners of renin. In HEK293T cells, icRen appears to function independently of the classical RAS and may be assembled into a so far uncharacterised protein complex by the PAQosome cochaperone system.

OC 03 FLOW of Urine: Glomerula function

OC0306

C5aC5aR1 Signaling as a Regulator of PericyteMediated Vasa Recta Tone in Acute Kidney Injury

Minze Xu; Yipeng Chen; Pontus B. Persson; Karin Michaela Kirschner
Institut für Translatioinal Physiologie, Campus Charité Mitte, Charité - Universitätsmedizin Berlin, Berlin, Germany;

Objective: Acute kidney injury (AKI) following ischemia–reperfusion injury (IRI) is frequently associated with persistent renal microcirculatory impairment. Sustained constriction of the descending vasa recta contributes to the renal medullary “noreflow” phenomenon and subsequent tissue hypoxia. Since pericytes are key regulators of vasa recta tone, this study aimed to investigate whether complement activation, particularly C5a–C5aR1 signaling, directly enhances pericytedependent vasoconstriction and sensitizes descending vasa recta to angiotensin II (Ang II). In addition, we assessed whether pharmacological inhibition of C5aR1 with Avacopan could prevent or reverse C5ainduced microvascular dysfunction.
Method: Descending vasa recta were isolated from the renal outer medulla and perfused ex vivo in a chamber using handmade glass pipettes under isobaric conditions at 10 mmHg. To comply with 3R principles, multiple vessels were harvested from each animal and assigned to distinct experimental protocols. Luminal diameter was continuously monitored by video microscopy and quantified using ImageJ at sites showing maximal pericytemediated constriction.
Results: C5a pretreatment markedly enhanced the sensitivity of descending vasa recta to Ang IIinduced vasoconstriction. Compared with baseline control vessels, C5atreated vessels responded to lower Ang II concentrations, indicating that C5a lowered the threshold required to induce measurable luminal narrowing. This suggests that C5a–C5aR1 signaling sensitizes pericytecontrolled renal microvessels to vasoconstrictive stimulation.
Coadministration of Avacopan with C5a normalized Ang II responsiveness to control levels, demonstrating effective prevention of C5amediated vascular sensitization through C5aR1 inhibition. Notably, Avacopan applied after Ang IIinduced preconstriction partially reversed vasoconstriction in both C5atreated and untreated vessels. This indicates that Avacopan may exert not only a preventive antiinflammatory effect but also a direct vasoregulatory effect on renal microvascular tone.
Conclusion: These findings provide direct functional evidence that C5a enhances Ang IIinduced, pericytedependent vasoconstriction in descending vasa recta, thereby potentially contributing to renal medullary noreflow after ischemia–reperfusion injury. Pharmacological inhibition of C5aR1 with Avacopan effectively prevents C5ainduced sensitization and can partially reverse established vasoconstriction, identifying C5aR1 signaling as a promising therapeutic target for renal microvascular dysfunction.

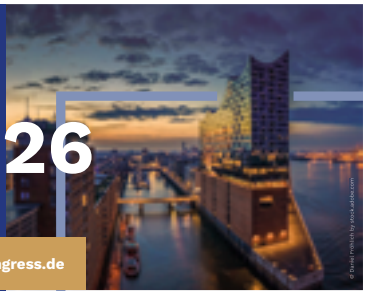

OC 04 FLOW of Blood: Blood & Immune system

OC0401

VPS18 controls vesicle dynamics and is essential for neutrophil development

Jincheng Gao; Almke Bader; Monika I. Linder [1]; Jingyuan Cheng [2]; Mathis Richter [3]; Raul da Costa [4]; Annette Zehrer; Karl Mitt; Bastian Popper [5]; Felix Meissner [2]; Xiang Wei; Enrique de Vega Gomez; Megumi Tatematsu [1]; Meino Rohlfs [6]; Stephanie FrenzWiessner [1]; Mehmet Kiziltug [1]; Ido Somekh [7]; Joanne Yacobovich [8]; Orna SteinbergShemer [8]; Raz Somech [7]; Oliver Soehnlein [3]; Bettina Schmid [9]; Christoph Klein [1]; Barbara Walzog; Daniela MaierBegandt [10] Institute of Cardiovascular Physiology and Pathophysiology, LudwigMaximiliansUniversität München, PlaneggMartinsried, Germany; [1] Department of Pediatrics, Dr. von Hauner Children's Hospital, LudwigMaximiliansUniversität München, München, Germany; [2] MaxPlanck Institute for Biochemistry, PlaneggMartinsried, Germany; [3] Institute of Experimental Pathology (ExPat), Center for Molecular Biology of Inflammation (ZMBE), University of Münster, Münster, Germany; [4] Institute of Experimental Pathology (ExPat), Center for Molecular Biology of Inflammation (ZMBE) and Münster Flow Cytometry Facility (MFlow), University of Münster, Münster, Germany; [5] Institut für Anatomie und Zellbiologie, LudwigMaximiliansUniversität München, München, Germany; [6] Department of Pediatrics, Dr. von Hauner Children's Hospital, University Hospital, LMU München, Munich, Germany; [7] Pediatric Department A and the Immunology Service, Jeffrey Modell Foundation Center, Edmond and Lily Safra Children's Hospital, Sheba Medical Center, affiliated to the Faculty of Medicine, Tel Aviv University, Ramat Gan, Israel; [8] Department of Pediatric Hematology Oncology, Schneider Children's Medical Center of Israel, affiliated to the Faculty of Medicine, Tel Aviv University, Petah Tikva, Israel; [9] Fish Core Unit, German Center for Neurodegenerative Diseases (DZNE), München, Germany; [10] Institute of Cardiovascular Physiology and Pathophysiology, LudwigMaximiliansUniversität München, München, Germany;

Objective: Neutrophils are the most prevalent type of leukocytes in the blood and are vital for defense against pathogens. Continuous production in the bone marrow is absolutely essential and patients with neutropenia suffer from lifethreatening recurrent bacterial and fungal infections. During neutrophil development, processes such as up- and downregulation of cell surface proteins, production of granules and metabolism strongly depend on vesicle dynamics. Vacuolar protein sortingassociated protein 18 homolog (VPS18), as part of the tethering factors CORVET and HOPS, mediates the fusion between early endosomes and of autophagosomes with late endosomes or lysosomes. In this project, we investigated the role of VPS18 for neutrophil development.

Method: We generated heterozygous *Vps18* knockout (KO) Hoxb8 cells using CRISPR/Cas9 technique and used Western blot technique, flow cytometric analyses, mass spectrometry and transmission electron microscopy to characterize the role of VPS18 for neutrophil development. To verify our findings in a human cell system, we generated human induced pluripotent stem (iPS) cells with mutations in *VPS18* using CRISPR/Cas9. As an *in vivo* model, we used the zebrafish and induced mutations in *vps18* using CRISPR/Cas9.

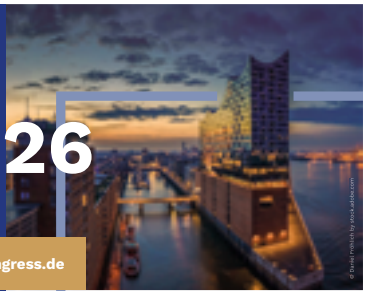

OC0401
VPS18 controls vesicle dynamics and is essential for neutrophil development

Results: We found that heterozygous *Vps18* KO Hoxb8 cells have a late maturation defect resulting in increased apoptotic cell death in heterozygous *Vps18* KO Hoxb8 cells compared to *Vps18* control Hoxb8 cells. On a molecular level, reduced expression of VPS18 induced an increased number in and size of autophagosomes accompanied by irregularly shaped vesicles. Impaired vesicle dynamics interfered with cellular metabolism and induced cell stress. Additionally, we described a patient with a heterozygous stopgain mutation (Arg234*) in *VPS18* suffering from recurrent infections and neutropenia. Further, a full KO of *VPS18* in iPS cells resulted in almost complete abrogation of developing neutrophils whereas heterozygous as well as the patientspecific *VPS18* mutations in iPS cells caused a significant reduction in developing neutrophils. Heterozygous *vps18* KO zebrafish larvae were characterized by a significantly reduced number of neutrophils compared to wildtype zebrafish larvae.
Conclusion: With this study, we found VPS18 to be essential for vesicle dynamics during neutrophil development and identified mutations in *VPS18* as a novel underlying cause of congenital neutropenia. Gao et al., 2026, Cell Death Dis, DOI: 10.1038/s4141902508338w.

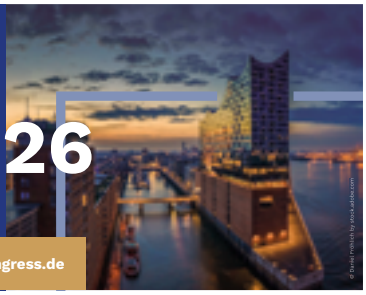

OC 04 FLOW of Blood: Blood & Immune system

OC0402

Maternal circulating neutrophils act as a survival niche for *Listeria monocytogenes* infection of the placenta and fetus

Nikita Raj; Myriam Ripphahn; Hellen IshikawaAnkerhold 1; Zhouyi Rong 2; Bastian Popper 3; Bianca Portugal Tavares de Moraes; Xia Li; Ying Chen 2; Roland Immler; Lou Martha Wackerbarth; Dominic van den Heuvel 4; Barbara Schmidinger 5; Rainer Haas 5; Udo Jeschke 6; Anne Loesslein 7; Steffen Massberg 8; Farida Hellal 2; Ali Ertürk 2; Markus Sperandio 9 Institute of Cardiovascular Physiology and Pathophysiology, Biomedical Center, LudwigMaximiliansUniversität München, München, Germany; 1 Medical Clinic and Polyclinic I, WalterBrendelCentre of Experimental Medicine, LMU Klinikum, München, Germany; 2 Institute for Tissue Engineering and Regenerative Medicine, Helmholtz Munich, Neuherberg, Germany; 3 Institut für Anatomie und Zellbiologie, LudwigMaximiliansUniversität München, München, Germany; 4 Medical Clinic and Polyclinic I, WalterBrendelCentre of Experimental Medicine, LudwigMaximiliansUniversität München, Munich, Germany; 5 Medical Microbiology and Hospital Epidemiology, Max von Pettenkofer Institute, LudwigMaximiliansUniversität München, Munich, Germany; 6 Dept. of Obstetrics and Gynecology, Universitätsklinikum Augsburg, Augsburg, Germany; 7 Institute for Infection Prevention and Control, University Hospital Freiburg, Freiburg, Germany; 8 Medizinische Klink I, Campus Großhadern, LudwigMaximiliansUniversität München, München, Germany; 9 Institut für Kardiovaskuläre Physiologie und Pathophysiologie, Biomedizinisches Centrum München, LudwigMaximiliansUniversität München, Munich, Germany;

Objective: *Listeria monocytogenes* (Lm) is a foodborne pathogen that poses a major global health risk during pregnancy, often resulting in severe complications such as preterm labor and fetal mortality. However, the cellular and molecular mechanisms by which circulating Lm breaches the maternalfetal barrier and causes placental and fetal infections remain poorly understood. Here, we investigate the role of maternal peripheral blood neutrophils in facilitating Lm dissemination to the placenta and fetus.
Method: Ex vivo human blood infection assays, in vitro human placental trophoblast infection models, and in vivo placental infection studies using pregnant humanized Ecadherin and C57BL/6 mouse models (E13.515.5), were used to investigate the role of maternal neutrophils in Lm dissemination, intracellular localization, and trophoblast susceptibility during infection. Cytoplasmic localization of Lm was confirmed by transmission electron and confocal microscopy. The transfer of neutrophilassociated Lm to placenta was clarified using tissueclearing microscopy and intravital placental imaging. Statistical significance was assessed using Student's ttest or oneway ANOVA depending on experimental groups, with $p<0.05$ considered significant. Animal experiments and use of human samples were ethically approved by local authorities.

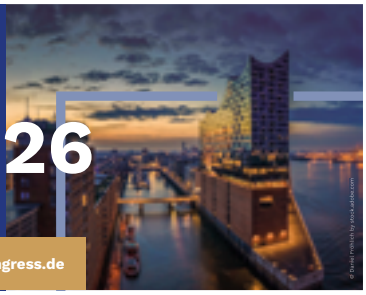

OC0402

Maternal circulating neutrophils act as a survival niche for *Listeria monocytogenes* infection of the placenta and fetus

Results: We identify maternal peripheral blood neutrophils as key facilitators of Lm dissemination to the placenta and fetus. Neutrophils provide an intravascular survival niche for Lm during bloodborne infection. This is supported by a threefold increase in cytoplasmic localization of Lm within human and mouse blood neutrophils, indicating vacuolar escape-mediated survival. Infection of human trophoblast cells revealed differential susceptibility of trophoblast subtypes depending on their activation status. Notably, TLR2stimulated HTR8/SVneo extravillous trophoblasts exhibited a fourfold increase in susceptibility and an eightyfold increase in intracellular survival of neutrophildelivered Lm. Tissueclearing analyses of infected mouse placentas demonstrated sporadic colocalization of neutrophils and Lm, while neutrophil depletion or adhesion inhibition significantly reduced placental and fetal infection threefold in vivo.

Conclusion: Collectively, our findings highlight maternal circulating neutrophils as “Trojan horses” for Lm, enabling immune evasion within the circulation and promoting bloodborne invasion of Lm to the placenta and fetus. These findings advance our understanding of maternalfetal immune regulation during infection and suggest potential therapeutic strategies for mitigating fetal listeriosis. (Supported by the German Research Foundation DFG, TRR359, SFB914).

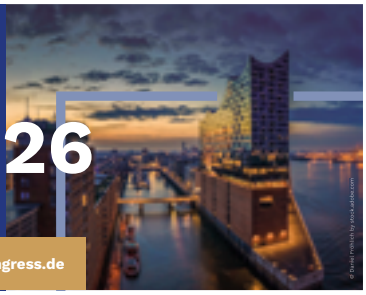

OC 04 FLOW of Blood: Blood & Immune system

OC0403

SCAMP3 is a novel regulator of granule formation and function in neutrophils

Almke Bader; Jincheng Gao; Nina Reiter; Devon Siemes [1]; Annette Zehrer; Xiang Wei; Ingrid Hepper; Enrique de Vega Gómez; Bettina Schmid [2]; Ignasi Forné [3]; Daniel Robert Engel [4]; Barbara Walzog; Daniela MaierBegandt
Institute of Cardiovascular Physiology and Pathophysiology, LudwigMaximiliansUniversität München, PlaneggMartinsried, Germany; [1] Department of Immunodynamics, Institute for Experimental Immunology and Imaging, University DuisburgEssen, Essen, Germany; [2] Fish Core Unit, German Center for Neurodegenerative Diseases (DZNE), München, Germany; [3] Protein Analysis Unit, Biomedical Center, LudwigMaximiliansUniversität München, PlaneggMartinsried, Germany; [4] Immundynamik, Institut für Experimentelle Immunologie und Bildgebung, Universität DuisburgEssen, Essen, Germany;

Objective: Neutrophils are the first leukocytes recruited to sites of inflammation, where they combat infections by killing pathogens through multiple effector functions, including phagocytosis, production of reactive oxygen species, and release of microbicidal proteins from intracellular granules into phagosomes or the extracellular space. During granulopoiesis, primary, secondary, and tertiary granules are generated in a sequential manner, and defective granule production can impair pathogen clearance, leading to persistent bacterial and fungal infections. In this study, we analysed the role of secretory carrier associated membrane protein 3 (SCAMP3) for neutrophil defence functions.
Method: We generated stable *Scamp3* knockout (KO) Hoxb8 cells using CRISPR/Cas9 technique and applied Western blot technique, flow cytometry, mass spectrometry, ELISA, and bacterial killing assays to characterize the role of SCAMP3 for neutrophil defence functions. Furthermore, we generated Scamp3deficient zebrafish in the Tg(*fli1:gfp;lyz:dsred*) background using CRISPR/Cas9 technique to study the role of SCAMP3 in neutrophils *in vivo*.
Results: Differentiation of *Scamp3* KO Hoxb8 cells into neutrophils (dHoxb8 cells) was unaffected. However, *Scamp3* KO dHoxb8 cells exhibited a strongly impaired killing of *Escherichia coli* K12 as compared to control dHoxb8 cells. Whole proteome mass spectrometric analyses revealed a significant reduction in primary, secondary, and tertiary granule proteins in *Scamp3* KO dHoxb8 cells compared to control dHoxb8 cells, resulting in an overall reduced granularity of *Scamp3* KO dHoxb8 cells. Consistently, degranulation of primary, secondary, and tertiary granule proteins was significantly diminished in *Scamp3* KO dHoxb8 cells. Similarly, neutrophils from *scamp3* KO zebrafish had a reduced granularity as compared to wildtype zebrafish. However, neutrophil migration towards sites of *E. coli* injection as well as bacterial clearance was normal in absence of Scamp3, indicating that other defence mechanisms remained functional in this *in vivo* model.
Conclusion: In summary, we identified SCAMP3 as a novel regulator of neutrophil granule formation, thereby modulating neutrophil defence functions. The absence of SCAMP3 resulted in disarmed neutrophils.
(Bader et al., J Leukoc Biol. 2025 117(12):qiaf153. doi: 10.1093/jleuko/qiaf153)

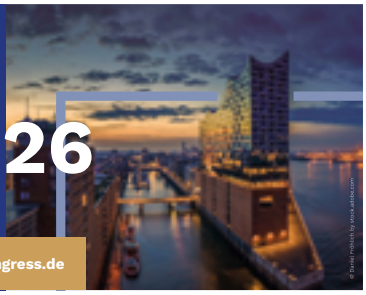

OC 04 FLOW of Blood: Blood & Immune system

OC0404

Postnatal maturation of circadian leukocyte dynamics and immune clock organization in mice

Xia Li; Andrew Kwon [1]; Zeynep Melis Gül [2]; Miho Sato [3]; Paula Rothämel [4]; Florian Seytter [5]; Lou Martha Wackerbarth [6]; Sarah KimHellmuth [4]; Claudia Nussbaum [7]; Shaon Sengupta [8]; Markus Sperandio [9]; Christoph Scheiermann [2]
Institute for Cardiovascular Physiology and Pathophysiology , LudwigMaximiliansUniversität München, Munich, Germany; [1] Department of Neuroscience, University of Pennsylvania, Philadelphia, United States; [2] Department of Pathology and Immunology, University of Geneva, Geneva, Switzerland; [3] Institute of Pharmacology and Toxicology, University of Zurich, Zurich, Switzerland; [4] Department of Pediatrics, Dr. von Hauner Children's Hospital, University Hospital LMU Munich, Munich, Germany; [5] Institute for Cardiovascular Physiology and Pathophysiology, Biomedical Center, LudwigMaximiliansUniversität München, Munich, Germany; [6] Institute of Cardiovascular Physiology and Pathophysiology, Biomedical Center, LudwigMaximiliansUniversität München, Munich, Germany; [7] Pädiatrische Nephrologie, Dr. von Haunersches Kinderspital, LudwigMaximiliansUniversität München, München, Germany; [8] The Children's Hospital of Philadelphia, Philadelphia, United States; [9] Institut für Kardiovaskuläre Physiologie und Pathophysiologie, Biomedizinisches Centrum München, LudwigMaximiliansUniversität München, Munich, Germany;

Objective: Circadian rhythms regulate leukocyte trafficking in the adult immune system, but when these temporal programs are established after birth remains unclear. We aimed to define how leukocyte rhythmicity, promigratory marker expression and peripheral clock gene oscillations develop during postnatal life.
Method: To assess postnatal circadian immune development, C57BL/6 mice were sampled from postnatal day 1 to 60 (P1–P60) at four zeitgeber times (ZT0 = lights on; n = 2–8 per age/time point). Leukocyte and subset counts were quantified by haematology analysis and flow cytometry. Migration- and adhesionrelated marker expression was assessed by multicolour flow cytometry, and clock gene expression in blood leukocytes and peripheral tissues was measured by RTqPCR. Rhythmicity was tested by 24h cosinor analysis, with $p < 0.05$ considered rhythmic.
Results: Circadian leukocyte rhythms were not fully established immediately after birth. Most major leukocyte populations acquired significant daily rhythmicity around P17, with peak abundance preferentially aligned to the light phase, corresponding to the resting phase in mice. Promigratory factor rhythms showed marked heterogeneity across markers, leukocyte subsets and postnatal ages. However, migration- and adhesionrelated marker profiles became progressively more synchronized during development, with peak phases increasingly organized around the light–dark transition. Peripheral clock gene expression showed parallel maturation across blood leukocytes and multiple peripheral organs. Several clock genes acquired stronger oscillations and more coherent systemic phase organization during postnatal development, although the timing of maturation remained tissue- and genedependent.
Conclusion: Together, these findings indicate that circadian immune organization in mice emerges after birth through coordinated maturation of leukocyte abundance rhythms, promigratory programs and peripheral clock networks. This postnatal temporal organization may represent an additional layer of immune system maturation.

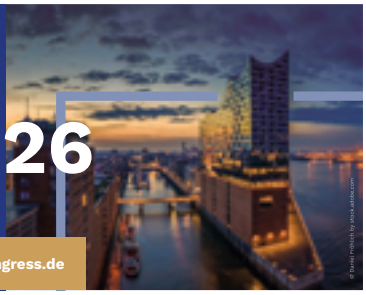

OC 04 FLOW of Blood: Blood & Immune system

OC0405

Immunoproteasomedependent regulation of endothelial antigen presentation and IgG trafficking

Rebecca Braun; Hayato Yuuto Kakinuma; Lukas Blume; Elke Krüger [1]; Catherine MeyerSchwesinger; Katrin Neumann
Institut für Zelluläre und Integrative Physiologie, Zentrum für Experimentelle Medizin, Universitätsklinikum HamburgEppendorf, Hamburg, Germany; [1] Institut für Medizinische Biochemie und Molekularbiologie, Universitätsmedizin Greifswald, Greifswald, Germany;

Objective: The proteasome is a multicatalytic protein complex crucial for intracellular protein degradation to maintain cellular homeostasis. The immunoproteasome is one proteasome subtype particularly involved in major histocompatibility complex classI (MHCI)mediated antigen presentation. It is constitutively expressed in immune cells and can be induced in other cell types during inflammation. Interestingly, our data demonstrate that murine and human endothelial cells (EnCs) express the immunoproteasome under homeostatic conditions. This project aims to uncover previously unrecognized cellintrinsic functions of the immunoproteasome in endothelial homeostasis.

Method: *Psmb8*$^{flox/flox}$ x *C*^{dh5}CreERT2 mice lacking expression of the immunoproteasomespecific catalytic subunit low molecular mass protein 7 (Lmp7) in EnCs were used for endothelial phenotype analysis by flow cytometry, western blot and immunofluorescence. Human EA.hy926 cells deficient in LMP7 expression were employed for functional studies by performing live cell imaging and pulsechase experiments.

Results: Murine Lmp7$^{-/-}$EnCs from kidney, liver, lung, and heart, as well as LMP7$^{-/-}$EA.hy926 cells, upregulated expression of β5c, the catalytic counterpart of Lmp7 (β5i) in the constitutive proteasome, compared to wildtype controls. However, surface levels of MHCI were reduced in all murine Lmp7$^{-/-}$ EnC populations and in LMP7$^{-/-}$ EA.hy926 cells. Moreover, murine glomerular EnCs exhibited intracellular IgG accumulation, indicative of altered antibody trafficking and vesicular transport. In line with this, LMP7$^{-/-}$ EA.hy926 cells showed reduced expression of Rab5 and Rab11, associated with early and recycling endosomes, respectively, whereas Rab7, linked to late endosomes, was increased. Reexpression of LMP7 in LMP7$^{-/-}$ EA.hy926 cells increased Rab5 and Rab11 expression and decreased Rab7 expression. In addition, surface levels of the neonatal Fc receptor (FcRn), which mediates IgG recycling, were decreased in LMP7$^{-/-}$EA.hy926 cells, while total FcRn expression remained unchanged.

Conclusion: LMP7 deficiency was associated with impaired endothelial MHCI surface expression and altered FcRn trafficking, accompanied by changes in Rab5/Rab7/Rab11 expression. These findings suggest a potential role for the immunoproteasome in the regulation of endothelial antigen presentation and IgG trafficking.

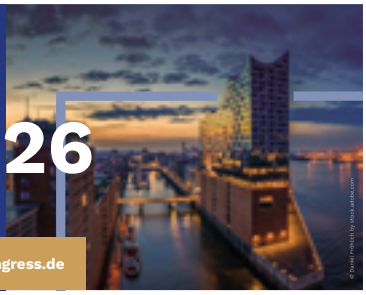

OC 04 FLOW of Blood: Blood & Immune system

OC0406

Dietary MediumChain Triacylglycerol Induces Erythropoietin and initiation af erythropoeisis

Josephine Maria Kanta; Kasper S Jørgensen; Casper M. Sigvardsen [1]; Nicoline R. Andersen [2]; Pernille Andersen [1]; Bente Kiens [1]; Andreas M Fritzen [1]
Biomedical Sciences, University of Copenhagen, Copenhagen, Denmark; [1] University of Copenhagen, Copenhagen, Denmark; [2] Health and Medical Sciences, University of Copenhagen, Copenhagen, Denmark;

Objective: Erythropoietin (EPO) stimulates erythropoiesis. Beyond hypoxia, exogenous administration of the ketone body, betahydroxybutyrate (BHB), was recently shown to increase circulating EPO levels. We recently demonstrated that a modest, nutritionally induced endogenous rise in BHB via mediumchain triacylglycerol (MCT) intake elevated circulating EPO by 38% within 8 days in humans. We investigated whether acute and chronic MCT intake regulates EPO and induces erythropoietic and hematological adaptations in mice. We further assessed if MCT mediates these effects using liverspecific 3hydroxy3methylglutarylCoA synthase 2 knockout (LiKO) mice, incapable of producing BHB.
Method: C57Bl/6JRj wildtype (WT) or LiKO mice were subjected to either an acute oral gavage with MCT oil, longchain triacylglycerol (LCT) oil, or water as control, or 6 weeks intake of MCT- or LCTenriched highfat diets. Blood and tissues were collected to assess hematological effects, circulating BHB and EPO levels, and tissue signaling.
Results: Acute MCT increased circulating BHB levels by 706% (MCT: 2.5±0.2mmol/l vs. LCT: 0.3±0.0, $p<0.001$) vs LCT, and a 113% higher renal *Epo* mRNA after 2 hours ($p=0.045$), vs placebo.
Chronic MCT intake increased basal circulating BHB by 62% ($p<0.001$) and EPO by 37% ($p=0.008$) compared with LCT, with a positive correlation between BHB and EPO levels ($r=0.66$, $p=0.001$). This was accompanied by 31% higher phosphoSTAT5 in bone marrow ($p=0.015$). MCT fed mice showed higher reticulocyte count (13%, $p=0.0216$), immature reticulocyte fraction (26%, $p=0.060$), and mean corpuscular volume (3%, $p<0.001$), with lower red cell distribution width (9%, $p<0.001$). LiKO mice did not increase BHB with MCT, however, LiKO MCTfed mice had higher reticulocyte count (18%, $p=0.021$), immature reticulocytes (30%, $p<0.001$), mean corpuscular volume (2%, $p=0.026$), but also red cell distribution width (3%, $p=0.044$) than WT mice.
Conclusion: MCT intake increases circulating EPO and initiates erythropoiesis, with the kidney as a key site of transcriptional induction. This is accompanied by enhanced bone marrow signaling and production of younger and more uniform erythrocytes. Notably, mice incapable of hepatic ketogenesis show an even greater erythropoietic response, indicating that the effect of MCT is partly independent of ketone bodies. This suggests that mediumchain fatty acids, rather than ketones alone, may drive this regulatory axis of erythropoiesis.

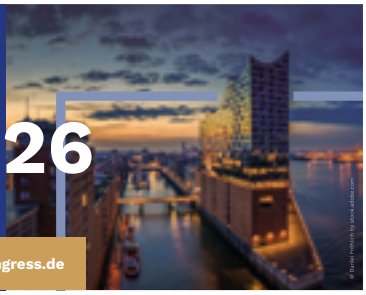

OC 05 FLOW of Urine: Transport function

OC0501

Renal NHE3 is required to limit hypokalemia and metabolic acidosis during dietary K^+ deficiency

Jennifer Nogueira Coelho; Natalie Hayslip; Rebecca Zoe Halter; Sima AlMasri; Adriana C. C. Girardi [1]; Maryam Tahmasbi [2]; Jessica A. Dominguez Rieg; Timo Rieg [3] Molecular Pharmacology and Physiology, University of South Florida, Tampa, United States; [1] Departamento de Cardiopneumologia, Faculdade de Medicina, Laboratório de Fisiologia Renal e Cardiometabolismo, Universidade de São Paulo, São Paulo, Brazil; [2] James A. Haley Veterans' Hospital, Tampa, United States; [3] Molecular Pharmacology and Physiology, University of South Florida, Tampa, United States;

Objective: The sodiumhydrogen exchanger isoform 3 (NHE3) is a critical mediator of proximal tubule and thick ascending limb Na^+ reabsorption and H^+/NH_4^+ secretion, yet the physiological implications of its upregulation during low K^+ intake remain poorly understood.
Method: To test this, we utilized kidneyspecific NHE3 knockout ($NHE3^{KSKO}$) mice. Control and $NHE3^{KSKO}$ mice were monitored during a baseline period on a 1% K^+ diet and then switched to a K^+deficient diet for 10 days to track metabolic and physiological parameters. Renal function was determined longitudinally via transdermal FITCsinistrin clearance at baseline and day 9, complemented by blood gas and urinary electrolyte , osmolality, and pH measurements. On day 10, kidneys were harvested for downstream tissue analysis, combining immunoblotting, quantitative realtime polymerase chain reaction for transport and metabolic markers in combination with blinded histopathological and quantitative fluorescent microscopy analysis.
Results: Following 10 days of a K^+deficient diet (<30 ppm), $NHE3^{KSKO}$ mice exhibited exacerbated hypokalemia compared to control mice, despite near complete elimination of urinary K^+ excretion and comparable levels of ROMK and BKα protein abundance in both genotypes. Control and $NHE3^{KSKO}$ mice developed hypernatremia secondary to a urinary concentrating defect; however, this was associated with a ~2fold greater fluid intake in $NHE3^{KSKO}$ mice. These effects occurred without changes in glomerular filtration rate. Both genotypes developed metabolic acidosis, which was significantly more severe in $NHE3^{KSKO}$ mice. This exacerbated acidosis correlated with a ~60% lower mRNA expression of glutamine synthetase and a lower urinary NH_4^+/creatinine ratio. Furthermore, early histopathological signs of hypokalemic nephropathy were observed exclusively in some of the $NHE3^{KSKO}$ mice.
Conclusion: Our findings demonstrate that renal NHE3 attenuates the severity of hypokalemia and metabolic acidosis during K^+ restriction, possibly via NH_4^+ formation/transport, which might accelerate the development of hypokalemic nephropathy.

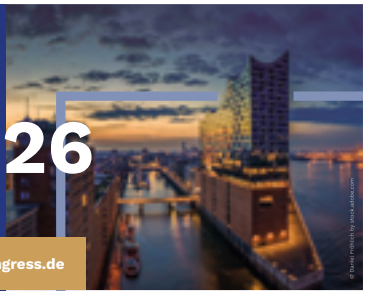

OC 05 FLOW of Urine: Transport function

OC0502

Impaired calcineurin signaling in the thick ascending limb of Henle's loop provokes increased NKCC2 phosphorylation and hyperkalemia

Wouter van Megen; Bo Peusen; Anna Moser; Monique Carrel; Dominique Loffing; Johannes Loffing
Institute of Anatomy, University of Zurich, Zurich, Switzerland;

Objective: Calcineurin inhibitors (CNIs) are cornerstone immunosuppressants used to prevent graft rejection after organ transplantation. However, their use is often associated with adverse effects such as hypertension and hyperkalemia, which have been linked to increased activity of the sodium chloride cotransporter (NCC) in the distal convoluted tubule (DCT). Yet, targeted deletion of the regulatory calcineurin subunit CnB1 in the DCT did not alter blood pressure or plasma potassium levels, implying that additional nephron segments may be involved. In this study, we investigated a potential role of the thick ascending limb of Henle's loop (TAL) in these CNIinduced adverse effects.
Method: TALspecific CnB1 knockout mice were generated by crossing $CnB1^{flox}$ mice with $_{flox}$ a novel NKCC2CreERT2 mouse line. Tamoxifen (2 mg/animal/day) was administered orally for five consecutive days to induce Cre recombination. Four weeks postinduction, mice were placed in metabolic cages for 24hour urine collection, followed by blood and kidney sampling for further analysis.
Results: While urinary sodium, potassium, ammonium excretion and urinary osmolarity were unchanged, both male and female TALspecific CnB1 knockout mice displayed significantly elevated plasma potassium levels compared to control animals (males: 4.1 *vs.* 3.6 mM, females: 4.0 *vs.* 3.4 mM). Additionally, TALspecific CnB1 knockout mice displayed lower blood pH values than controls (males: 7.41 *vs.* 7.45; females: 7.34 *vs.* 7.40). Immunoblot analysis demonstrated increased phosphorylation of the sodiumpotassiumchloride cotransporter 2 (NKCC2) in both sexes, whereas total NKCC2 abundance at the mRNA and protein levels remained unchanged between genotypes. Similarly, the expression of other major TAL proteins involved in ion transport (e.g., ROMK; NHE3) was unaltered. Moreover, neither the abundance nor the phosphorylation of NCC in DCT, nor the expression of the epithelial sodium channel (ENaC) in the collecting system, differed between genotypes. Renin mRNA expression and urinary uromodulin excretion were also comparable between groups.
Conclusion: Calcineurin signaling in the TAL plays a significant role in potassium homeostasis, potentially through regulation of NKCC2 activity. Disruption of calcineurin function in the TAL may therefore contribute to the hyperkalemia commonly observed in transplant recipients receiving CNIs.

OC 05 FLOW of Urine: Transport function

OC0503

Volumetric Nanoscale Quantification of VasopressinRegulated Renal AQP2 Vesicle Networks

Benjamin B. Green; Frédéric H. Login; Lene Niemann Nejsum; Vibeke S. Dam; Chad Hobson [1]; Rachel Lee [1]
Department of Clinical Medicine, Aarhus University, Aarhus, Denmark; [1] Advanced Imaging Center, Janelia Research Campus, Ashburn, United States;

Objective: Nanoscale transport vesicles reside below the diffraction limit of conventional light microscopy, limiting quantitative threedimensional analysis of vesicle organization in intact epithelial systems. We aimed to establish an expansion microscopy (ExM)based workflow for volumetric nanoscale quantification of vesicle populations in cultured epithelial cells and renal tissue.
Method: A 4.5× ExM workflow combining confocal imaging, deconvolution, and objectbased 3D segmentation was developed for quantitative analysis of vesicle organization. The method enables extraction of populationlevel metrics including vesicle size, intervesicle spacing, membrane association, and spatial distribution along the apicalbasal axis. The workflow was applied to vasopressinregulated aquaporin2 (AQP2) trafficking in epithelial monolayers and rat kidney collecting duct following cAMP elevation in vitro and vasopressin V2 receptor activation in vivo. Ongoing studies combine ExM with lattice light sheet microscopy for volumetric imaging of extended tubular segments.
Results: ExM resolved stimulationdependent nanoscale reorganization of AQP2 vesicle populations in both cultured cells and native tissue. Vasopressin stimulation induced increased subapical intervesicle spacing, reduced vesicle size, and redistribution of vesicles toward the apical membrane. In addition, phosphorylation of AQP2 at serine 256 (pS256) showed compartmentspecific differences between systems, with phosphorylated AQP2 associated with larger intracellular structures in cultured epithelial cells but not in native renal tissue. Combination of ExM with lattice light sheet microscopy further improved volumetric imaging of large tissue regions and enabled spatial mapping of total AQP2 and pS256AQP2 across intact collecting duct architecture.
Conclusion: This workflow enables quantitative volumetric nanoscale analysis of transport vesicle organization in intact epithelial systems and provides new insight into vasopressinregulated AQP2 trafficking. The approach establishes a scalable framework for spatial analysis of regulated membrane trafficking in complex tissues using advanced optical imaging strategies.

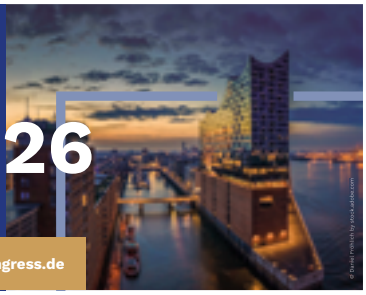

OC 05 FLOW of Urine: Transport function

OC0504

Effect of Camostat Mesylate, a serine protease inhibitor, on sodium excretion, extracellular volume, and blood pressure in patients with chronic kidney disease and healthy controls

Mette Boye Boes; Per Svenningsen; Gitte R. Hinrichs; Yaseelan Palarasah; Mads Kjølby [1]; Boye Lagerbon Jensen; Claus Bistrup
Cardiovascular & Renal Research, Department of Molecular Medicin, University of Southern Denmark, Odense, Denmark; [1] Department of Clinical Pharmacology, Aarhus University Hospital, Aarhus, Denmark;

Objective: In patients with albuminuric chronic kidney disease (CKD), aberrantly filtered serine proteases may activate the epithelial sodium channel (ENaC), driving sodium retention, extracellular volume expansion, and hypertension. We hypothesized that camostat mesylate, an oral serine protease inhibitor, would promote natriuresis, reduce extracellular water (ECW), and lower blood pressure in patients with albuminuric CKD. Healthy controls were included as a physiological comparator.
Method: This singlecenter, openlabel study (Department of Nephrology, Odense University Hospital, Denmark) enrolled 20 patients with CKD (eGFR ≥ 30 mL/min/1.73 m^2; urine albumintocreatinine ratio ≥ 300 mg/g) and 20 healthy controls. All followed a fixed 150 mmol sodium/day diet for 8 days; camostat 200 mg three times daily was given on days 58. Primary outcomes were withinperson changes in 24h urine sodium (UNa), body weight, ECW, total body water (TBW), and blood pressure. Secondary outcomes included plasma aldosterone, potassium, creatinine, and urinary camostat metabolites. Ethical approval and written informed consent were obtained (EUCT 20235085163400).
Results: Urinary GBPA (the active metabolite of camostat) confirmed drug exposure in both groups (CKD: 0.46±0.59 µg/mL; controls: 1.26±1.30 µg/mL). *In CKD*, body weight decreased (0.6% [95% CI 1.1 to 0.2], p=0.010) and plasma albumin increased (1.7 % [95% CI 0.3 to 3], p=0.018), while 24h UNa, FENa, UNa/Kratio, blood pressure, albuminuria, aldosterone, plasma potassium, and creatinine were unchanged. *In controls*, body weight (0.8% [95% CI 1.3 to 0.4], p=0.001), TBW (1.3% [95% CI 2.3 to 0.2], p=0.022), and ECW (1.9% [95% CI 3.3 to 0.5], p=0.012) all decreased. Aldosterone increased (28.2% [95% CI 16.4 to 40.1], p<0.001), UNa/Kratio decreased (0.88 [95% CI 0.78 to 1], p=0.043), and creatinine increased slightly (3.1 % [95% CI 0.3 to 5.9], p=0.030); UNa, FENa, blood pressure, plasma albumin, and potassium remained unchanged.
Conclusion: The active metabolite of camostat, GBPA, reached urinary concentrations previously shown to inhibit serine proteases in vitro and promoted modest fluid loss in both groups, without sustained natriuresis or blood pressure reduction. The rise in aldosterone in healthy controls indicates compensatory volume regulation. Ongoing analyses will determine whether these effects coincide with reduced urinary protease activity and altered ENaC cleavage.

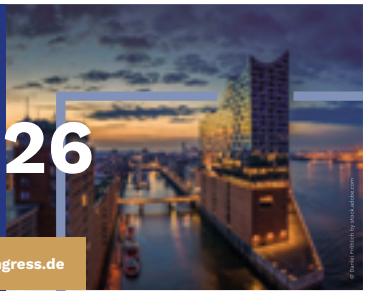

OC 05 FLOW of Urine: Transport function

OC0505
AE4 sustains βintercalated cellmediated bicarbonate excretion during respiratory alkalosis

Benedikte Skjoldborg; Laura Woidemann Trans; Jens Georg Leipziger; Peder Matzen Berg; Helga Vitzthum [1]
Department of Biomedicine, Aarhus University, Aarhus, Denmark; [1] Institut für Zelluläre und Integrative Physiologie, Zentrum für Experimentelle Medizin, Universitätsklinikum HamburgEppendorf, Hamburg, Germany;

Objective: Hyperventilation lowers arterial pCO_2, causing respiratory alkalosis and triggering renal bicarbonate excretion to restore blood pH. Unpublished own data show that this renal response is fast (onsetting after ~10 min) and mediated by βintercalated cells (βIC) via pendrindependent apical Cl/HCO_3 exchange. Sustained secretion requires base uptake for substrate availability. The basolateral anion exchanger 4 (AE4) is highly and specifically expressed in βIC and a proposed mediator of this flux. However, AE4's functional contribution to renal base excretion during respiratory alkalosis remains unknown. Defining its role is essential for understanding how the kidney sustains bicarbonate excretion to support systemic pH recovery during acute hypocapnia.
Method: AE4 function was examined in anesthetized (ketamine 100 mg/kg and xylazine 10 mg/kg, i.p.), mechanically ventilated C57BL/6 AE4 WT and KO mice. After 30 minutes of normoventilation (endtidal CO_2 ~3,78%), respiratory alkalosis was induced by controlled hyperventilation (endtidal CO_2 <2% for 60 minutes). Arterial blood gas analysis confirmed pCO_2levels ~20 mmHg. Urinary pH was continuously monitored via micro pH electrodes in a bladder catheter and urine was collected every 5 minutes for further analysis.
Results: After correction for genotypematched timecontrol drift, WT mice showed a hyperventilationinduced ΔpH of 0.257 ± 0.076, whereas AE4 KO mice showed a smaller response of 0.076 ± 0.150 (mean ± SEM, n=3 hyperventilated mice per genotype), corresponding to a 0.181 pH unit difference and approximately 3.4fold larger response in WT mice.
Conclusion: These preliminary data suggest that AE4 contributes to the rapid urinary alkalinization response during acute respiratory alkalosis, with additional experiments ongoing to increase group sizes. The impaired response in AE4 KO mice supports a role for AE-4mediated basolateral bicarbonate uptake in sustaining pendrindependent βIC bicarbonate secretion, thereby enabling effective urinary alkalinization and systemic pH recovery.

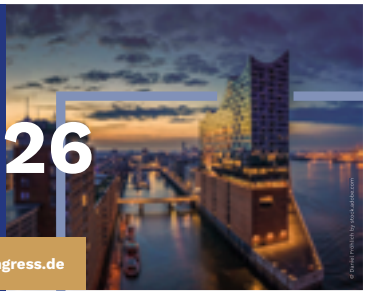

OC 05 FLOW of Urine: Transport function

OC0506

GlucagonLike Peptide1 receptor (GLP1R) blockade elicits saltdependent blood pressure responses and impairs renal adaptation to high salt intake

Gabriela Catão D. Braga; Flavia L. Martins [1]; Érika F. Jesus [1]; Renato O. Crajoinas [1]; Fatih Demir; Markus M. Rinschen; Adriana C. C. Girardi [1]
Department of Biomedicine, Aarhus University, Aarhus, Denmark; [1] Department of Cardiology, University of Sao Paulo, Sao Paulo, Brazil;

Objective: Glucagonlike peptide1 receptor (GLP1R) signalling exerts a tonic natriuretic effect, contributing to sodium balance regulation and may modulate blood pressure (BP) responses. This study tested the hypothesis that GLP1R blockade induces saltdependent BP responses and impairs renal adaptive mechanisms to variations in dietary sodium intake.
Method: Male Wistar rats were fed lowsalt (LS; 0.03% NaCl), normalsalt (NS; 0.3% NaCl), or highsalt (HS; 4% NaCl) diet for 21 days and treated with the GLP1R antagonist exendin9 (Ex9; 100 µg/kg/day, i.p.) or saline as control (Veh). Animals were allocated into six groups (Veh+LS, Veh+NS, Veh+HS, Ex9+LS, Ex9+NS, Ex9+HS). BP was monitored longitudinally by tailcuff plethysmography and confirmed by direct carotid cannulation at the end of the protocol.
Results: Salinetreated rats exhibited similar BP across all diets, consistent with a saltresistant phenotype. In contrast, GLP1R blockade induced saltdependent increases in BP, with Ex9+HS rats displaying higher BP compared with Ex9+NS (140±1 vs. 133±1 mmHg, p<0.0001) and Ex9+LS (140±1 vs. 128±0.4 mmHg, p<0.0001). Direct BP measurements confirmed elevated systolic and diastolic pressures in Ex9+HS vs. Ex9+LS rats. Renal sodium handling was assessed by acute salt- loading challenge. Control rats exhibited a graded natriuretic response to dietary salt, with greater sodium excretion in HSfed animals compared with NS and LSfed groups. This adaptive natriuretic response was blunted under GLP- 1R blockade, with differences observed between Ex9+HS and Ex9+LS groups, suggesting impaired renal adaptation to sodium overload. At the molecular level, dietary salt intake induced expected changes in sodium transporter regulation in control rats, as increased inhibitory phosphorylation of NHE3 (Ser552) and reduced phosphorylation of NCC (Thr53) in HSfed animals, while GLP1R blockade blunted these dietdependent responses, abolishing salt- induced differences in NHE3 phosphorylation and attenuating NCC phosphorylation across dietary sodium conditions. Additionally, proteomics data showed that GLP1R blockade in NSfed rats decreases Nos1 expression, which could be connected to the modifications in natriuretic response and BP.
Conclusion: In conclusion, GLP1R signalling contributes to renal and molecular adaptation to dietary sodium intake. GLP1R blockade impairs sodium transporter remodelling and attenuates natriuretic responses to high salt intake, predisposing to saltdependent elevations in BP.

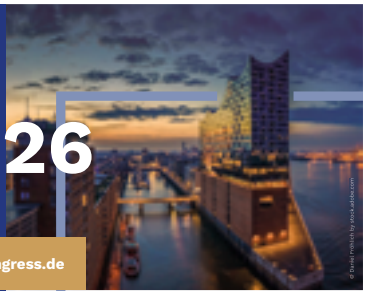

OC 06 FLOW of Ions: Ion channels Structure & Function

OC0601

Targeting the central cavity of TASK1 K2P channels: A novel mechanism for direct activation with therapeutic drugs

Thomas Baukrowitz
Physiologisches Institut, Christian
Albrechts
Universität Kiel, Kiel, Germany;

Objective: The TWIKrelated acidsensitive K2P channel TASK1 is implicated in neurodevelopmental, respiratory and cardiovascular diseases, including pulmonary arterial hypertension (PAH), where reduced TASK1 activity enhances vascular tone. Pharmacological activation of TASK1 has therefore been proposed as a therapeutic strategy. The phospholipase A inhibitor ONORS082 was previously reported to activate TASK1 and attenuate PAH in animal models, yet its mechanism of action has remained unclear and is investigated here.
Method: Here, we combined structural, electrophysiological, computational and pharmacological approaches to define the mechanism of ONORS082 action on human TASK1 channels and to assess its therapeutic potential for PAH.
Results: Here, we demonstrate that ONORS082 does not act through phospholipase A inhibition, but instead functions as a direct agonist of TASK1 and heteromeric TASK1/TASK3 channels. Structural and functional analyses identified a binding site for ONORS082 within the inner pore beneath the selectivity filter, where it stabilizes the open state by preventing Xgate closure. Furthermore, the strong dependence of channel activation on extracellular K^+ suggests an additional contribution of the selectivity filter to the activation mechanism.
Conclusion: Together, these findings establish porecavity binding as a previously unrecognized mechanism of TASK1 activation and demonstrate that diseaseassociated channel variants can be pharmacologically rescued by smallmolecule agonists. Our work broadens the therapeutic scope of TASK channel pharmacology and provides a mechanistic framework for

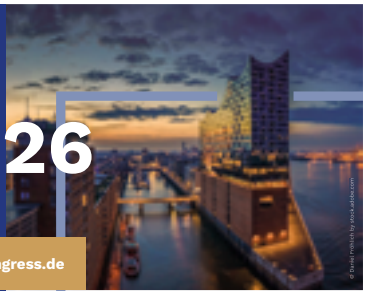

OC 06 FLOW of Ions: Ion channels Structure & Function

OC0602

Singlechannel activity of two K⁺selective channelrhodopsins at femtosiemens resolution

Klaus Benndorf; Ralf Schmauder; Peter Hegemann [1]
Institute of Physiology II, University Hospital Jena, Jena, Germany; [1] Institute of Biology, Experimental Biophysics, HumboldtUniversität zu Berlin, Berlin, Germany;

Objective: The analysis of how sensation, cognition, and behavior arise from neuronal activity has been enormously facilitated by optogenetics, using the expression of algaederived light sensitive channelrhodopsins, ChRs, in brain cells. Among ChRs, K⁺selective ChRs have great potential as inhibitory optogenetic tools. At the singlechannel level, their basic functional properties, as ionconductance and channel gating, are still unknown.
Method: We performed a detailed singlechannel analysis of two K⁺selective ChRs, KCR1 and WiChR1, at femtosiemens resolution.
Results: We show that both channels open in bursts with a continuum of conductance levels in the range of 0.3 to 3.0 pS among which a large conductance level is prevalent. The preferential level of WiChR1 is about 1.5 times larger than the corresponding level of KCR1. Kinetically, a burst of WiChR1 has a four times longer lifetime and contains three times more openings than a burst of KCR1. The unitary events explain all typical features of macroscopic currents, including inward rectification by a voltagedependent flicker as well as the differences between both channels in activation and deactivation speed and degree of desensitization. In the context of the photocycle, our data show that the closedopen gating is orthogonal to photoactivation.
Conclusion: Our data provide unprecedented insight into the molecular function of two K⁺selective ChRs which opens the door for tailoring specific new tools for optogenetic control of neurons in brain networks.

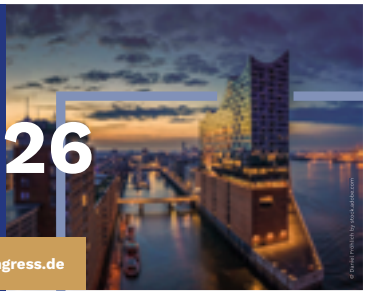

OC 06 FLOW of Ions: Ion channels Structure & Function

OC0603

Modulation of gating in an autonomous K^+ channel selectivity filter

Nils Drexler; Lena Diederich; UlfPeter Hansen [1]; Indra Schroeder Physiology II, University Hospital Jena, FriedrichSchiller University Jena, Jena, Germany; [1] Department of Structural Biology, ChristianAlbrechtsUniversität Kiel, Kiel, Germany;

Objective: Potassium (K^+) channels are involved in countless physiological and pathological processes. Despite their diversity in sensing (voltage, Ca^{2+}, ATP, neurotransmitters, temperature, etc.) and function (open probability, conductance), the K^+ channels in all domains of life, even in some viruses, share an identical selectivity filter (SF) structure, which discriminates cations. In some channels (e.g., hERG, K2P), it acts as a physiological gate regulated by external signals and is therefore regulated by physiological signals via e.g. voltage sensing or ligandbinding domains. Beneath this regulation lies direct modulation of SF gating by permeating ions and the surrounding protein scaffold, which also transmits physiological signals to the SF.
Method: To study the autonomous SF, we use minimal viral Kcv channels, lacking regulatory domains. Proteins are expressed *in vitro*, reconstituted into planar lipid bilayers, and analyzed via singlechannel recordings. From the current traces, we determine the open probability and the openchannel current with standard methods, and the gating kinetics of the SF in the microsecond range with extended beta distribution analysis.
Results: Analysis of >40 Kcv_{NTS} mutants revealed an interaction network between residue T45 (near a K? binding site in the SF) and several residues on transmembrane helix 2 (TM2). Most mutations here cause severe loss of function, suggesting that these residues anchor the SF to TM2. Further mutational studies suggest a predominantly hydrophobic nature of this interaction as opposed to a directed bond between two or more residues. A similar network exists in the same position in KcsA and other channels, but with different amino acids involved and with the additional function to couple the SF in this channel to the activation state of the cytosolic gate. This implies evolutionary functional adaptation.
The modulation of SF gating by the ion flow is especially interesting, because the voltagedependent ion movement and occupation of the K^+ binding sites in the SF confers a voltage dependence to SF gating, as we have shown previously (doi: 10.1038/s4159801828751w). Substituting K^+ with Tl^+ preserves voltagedependent gating, confirming similar SF binding. However, Tl^+ alters opening/closing kinetics, suggesting voltageindependent forces on the protein, likely affecting signal transfer (doi: 10.1080/19336950.2026.2623375). This aligns with structural data showing Tl^+ occupies the same SF sites as K^+.
Conclusion: In summary, Kcv channels are the simplest available model of the SF of mammalian and human K^+ channels, therefore the basic principles we discover in this model system are in principle also transferrable to those more complex channels.

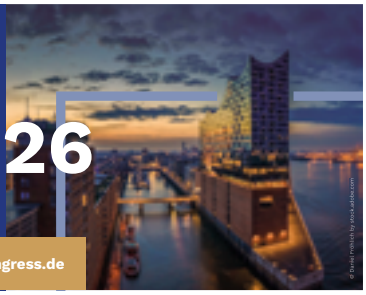

OC 06 FLOW of Ions: Ion channels Structure & Function

OC0604

Mechanisms of volumeregulated anion channel (VRAC) activation: the LRRC8A intracellular subdomain couples conformational dynamics to pore opening

Sara Bertelli; Lu Wang [1]; Malte Klüssendorf [2]; Michael Pusch; Raimund Dutzler [1]; Tobias Stauber [3]
Biophysics Institute, National Research Council, Genova, Italy; [1] Department of Biochemistry, University of Zurich, Zürich, Switzerland; [2] Stauber Lab, Institute for Molecular Medicine, MSH Medical School Hamburg, Hamburg, Germany; [3] Institute for Molecular Medicine, MSH Medical School Hamburg, Hamburg, Germany;

Objective: Volumeregulated anion channels (VRACs), formed by LRRC8 proteins, are widely expressed and contribute not only to cell volume regulation but also to diverse physiological processes including epithelial transport, cell survival, immune signaling, glianeuron communication, and stress responses. Importantly, LRRC8/VRAC activity is regulated by multiple cellular inputs beyond osmotic swelling, yet the molecular principles integrating these signals into channel gating remain unclear. Here, we investigated how a cytosolic region of the essential LRRC8A subunit functions as a regulatory element controlling VRAC activation.
Method: We combined sitedirected mutagenesis of LRRC8A with electrophysiological recordings, livecell Förster resonance energy transfer (FRET) measurements, and cryoelectron microscopy (cryoEM) to link channel function with conformational dynamics of cytosolic domains.
Results: A single amino acid substitution within an intracellular hydrophobic pocket of LRRC8A (L402W) converted VRAC into a constitutively active state in homomeric assemblies, independent of osmotic stimulation or pharmacological modulation. A second mutation in a nearby position (W168L) also enhanced channel activity, whereas the combined mutant partially reduced the hyperactive phenotype of L402W. FRET measurements revealed increased flexibility of cytosolic leucinerich repeat domains in L402W, which was normalized in the double mutant and upon inhibition by a sybody. CryoEM structures showed that L402W induces pronounced rearrangements in the intracellular subdomain accompanied by outward movement of cytosolic domains, consistent with channel opening. The double mutant adopted an intermediate conformation correlating with reduced channel activity.
Conclusion: Our findings identify a cytosolic regulatory hub in LRRC8A that integrates conformational dynamics to control VRAC activation and pore opening. This provides a mechanistic framework for how VRAC activity can be modulated by intracellular signals beyond cell volume changes, supporting its broader physiological roles.

OC 06 FLOW of Ions: Ion channels Structure & Function

OC0605

Optogenetic control of RyR2 combined with automatic cell segmentation and analysis enables highcontent screening of RyR2modulating compounds in HEK293 cells

Wanchana Jangsangthong; Jan V. Otte [1]; Judith Sofie Langen; Miroslav Dura [2]; Housen Li [1]; Martina Krüger [3]; Alexander Gottschalk [4]; Stephan E. Lehnart [2]; Axel Munk [1]; Philipp Sasse Institute of Physiology I, University Bonn, Bonn, Germany; [1] Institute for Mathematical Stochastics, University of Göttingen, Göttingen, Germany; [2] Department of Cardiology and Pneumology, Cellular Biophysics and Translational Cardiology Section, Heart Research Center Göttingen, University Medical Center Göttingen, Göttingen, Germany; [3] HerzKreislaufPhysiologie, Heinrich Heine Universität Düsseldorf, Düsseldorf, Germany; [4] Institute of Biochemistry, Johann Wolfgang GoetheUniversity Frankfurt, Frankfurt a. M., Germany;

Objective: In cardiomyocytes, the ryanodine receptor type 2 (RyR2) mediates Ca^{2+} release from the sarcoplasmic reticulum by the Ca^{2+}induced Ca^{2+} release mechanism. Pathological Ca^{2+} leak through RyR2 can initiate lethal cardiac arrhythmias.
Method: To establish a cellular platform for screening RyR2modulating compounds, we developed a lightgated OptoRyR2 by fusing a Ca^{2+}permeable Channelrhodopsin2 variant (CatChUP) with EYFP and a 157 Å linker to the Nterminus of human RyR2.
Results: OptoRyR2 expression in HEK293 cells showed correct intracellular localization by STED superresolution imaging, absence of leaky membrane photocurrents as well as the predicted size of OptoRyR2 fusion protein of ~640 kDa by Western blot analysis. Singlechannel recording of OptoRyR2 in planar lipid bilayers revealed a transient increase of open probability only when light (470 nm) was applied. Ca^{2+} imaging with XRhod1 showed Ca^{2+} release events after illumination and after application of the RyR2agonist Caffeine in stably expressing OptoRyR2HEK293 cells, whereas wildtype cells showed no comparable response, suggesting lightinduced Ca^{2+} release and preserved RyR2 function.
To test RyR2 modulators, a screening system was established in 96well plates by recording and automatically analyzing Ca^{2+} release events in single HEK293 cells. For analyzing Ca^{2+} imaging data, we developed the opensource *bcells* pipeline, available on GitHub, which includes automated cell segmentation, local background correction, baseline detection, temporal trace denoising and peak analysis across multiple recordings. The software quantified Ca^{2+} release events per cell using parameters such as peak height, time to peak, drifts in baseline activity, area under the curve and other eventspecific metrics.
In OptoRyR2 expressing cells, illumination led to a Ca^{2+} transient height of 1.43 ± 0.02 (F/F_0, n=1864 cells) over baseline which was significantly larger than spontaneous activity without light (F/F_0: 1.22 ± 0.01, n=1114, p<0.0001, unpaired ttest) resulting in a relative light effect (difference to spontaneous activity) of 21%. Light had a significantly smaller effect on wildtype cells (relative light effect of 8.4%, n=650795, p=0.0003). Importantly, application of the RyR2 blocker TMDJ035 significantly reduced the relative light effect to 7.7% in OptoRyR2 expressing cells (n=11141407, p<0.0001) but had no significant effect in wildtype cells (n=469795, p=0.27).
Conclusion: Thus, light activation of the CatChUP domain in OptoRyR2 triggers Ca^{2+} release from the sarcoplasmic reticulum, which subsequently activates RyR2 through its physiological gating mechanism. We propose that OptoRyR2 represents a powerful new tool for highcontent screening of RyR2modulating compounds and for investigating mechanisms of pathological Ca^{2+} release.

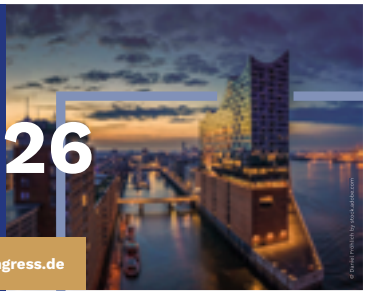

OC 06 FLOW of Ions: Ion channels Structure & Function

OC0606

SubMillivolt Voltage Imaging Reveals Gap JunctionMediated Bioelectric Contact Inhibition

Philipp Rühl; Rama Hussein; Stefanie Reuter [1]; Konrad S. Frahnert; Anagha G. Nair; Ralf Mrowka [1]; Roland Schönherr; Stefan H. Heinemann
Biophysics, Center for Molecular Biomedicine, Friedrich Schiller University Jena and Jena University Hospital, Jena, Germany; [1] Experimentelle Nephrologie, Klinik für Innere Medizin III, FriedrichSchillerUniversität Jena, Jena, Germany;

Objective: Membrane potential (V_m) dynamics in nonexcitable cells are emerging as potential regulators of proliferation and tumorigenesis. While upregulation of Ca^{2+}activated oncochannels (ANO1, $K_{Ca}3.1$) and loss of connexinbased gap junctions are established signs of cancer, their collective biophysical consequences for multicellular V_m behavior remain poorly understood. A central barrier has been the lack of imaging tools with sufficient sensitivity to resolve submillivolt V_m fluctuations in nonexcitable cells.
Method: We developed rEstus2s, a nextgeneration genetically encoded voltage indicator providing submillivolt sensitivity across the full physiological V_m range (100 to 0 mV), representing a twofold improvement in sensitivity over its precursor rEstus. Combined with the Ca^{2+} indicator KGECO1, we investigated V_m and Ca^{2+} dynamics in HEK293T networks. CRISPRCas9 knockout of connexins 43/45 and heterologous overexpression of ANO1/$K_{Ca}3.1$ were used to dissect oncochannel and gap junction contributions. Experiments were extended to cancerous (MCF7, A375, PANC1) and noncancerous (HaCaT) cell lines.
Results: V_m fluctuations were strongly correlated between connected cell pairs (r^2 = 0.894 ± 0.016, n = 45), whereas Ca^{2+} dynamics remained spatially confined (r^2 = 0.125 ± 0.020), even in the presence of open gap junctions. The magnitude of V_m fluctuations decreased markedly from isolated cells (11.6 ± 0.4%, n = 144) to confluent layers (1.358 ± 0.023%, n = 200), whereas Ca^{2+} fluctuations were unaffected by cell density (isolated: 3.63 ± 0.23%; confluent: 3.45 ± 0.13%). The timedependent variance of V_m scaled inversely with the number of cells (n) in a network, following a $1/n$ relationship, a phenomenon we term bioelectric contact inhibition (BCI). Connexin 43/45 knockout attenuated BCI, restoring high V_m volatility in confluent layers (isolated: 15.8 ± 0.8%, n = 70; confluent: 12.0 ± 0.3%, n = 188). Although expression of the oncochannels ANO1 (19.4 ± 1.5%, n = 71) and $K_{Ca}3.1$ (21.5 ± 1.2%, n = 124) markedly increased volatility relative to control HEK293T cells (13.9 ± 0.8%, n = 80) in isolated cells, electrically coupled wildtype networks suppressed this effect through BCI, whereas connexinknockout networks did not. Across all cell lines tested, strong gapjunction coupling consistently correlated with robust BCI.
Conclusion: BCI constitutes a fundamental biophysical principle by which gap junctionmediated coupling passively stabilizes V_m in multicellular networks, acting as an electrical lowpass filter. Loss of connexin expression in cancer may unleash V_m volatility, establishing a potential mechanistic framework linking electrical dysregulation to tumorigenesis.

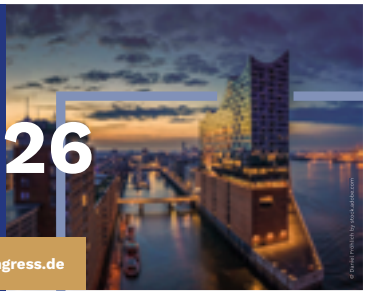

OC 07 FLOW of Ions: Ion channels pathophysiology

OC0701

THIK makes Sick: New Insights in Regulation, Pathophysiology and Pharmacology of THIK1 K_{2P} Channels

Marcus Schewe
Physiologisches Institut, Christian
Albrechts
Universität zu Kiel, Kiel, Germany;

Objective: THIK1 (TWIKrelated halothaneinhibited K^+ channel, *KCNK13*) is a lipidregulated twopore domain K^+ (K_{2P}) channel predominantly expressed in microglia and increasingly recognized as a key regulator of neuroinflammatory signaling. Dysregulation of THIK1 activity has been implicated in neurodegenerative disorders including Alzheimer's disease and amyotrophic lateral sclerosis (ALS). Despite its emerging physiological relevance, the molecular mechanisms underlying THIK1 gating, pharmacology, and functional regulation remain poorly understood.
Method: Here, we combined structural, electrophysiological and computational approaches to characterize the overall architecture and structural determinants for gating of human THIK1 channels. Structures were determined by singleparticle cryoelectron microscopy (CryoEM) in the absence and presence of small molecule modulators. Functional characterization was performed using wholecell and excised patchclamp electrophysiology. Systematic cysteine/alanine scanning mutagenesis was used to investigate critical residues involved in gating and ligand interactions. Statedependent inhibitor binding was examined under conditions associated with apoptotic signaling and caspase8 regulation.
Results: We determined CryoEM structures of human THIK1 revealing several previously unrecognized features that define channel gating and modulation. In particular, a tyrosine residue in M4 (Y273) that forms a lower intracellular "Ygate" controlling ion permeation in addition to the selectivity filter (SF). Functional studies demonstrated that activation by anionic lipids such as oleoylCoA and PIP_2 induces opening of the Ygate, whereas halothane stabilizes a closed conformation. Extending these initial findings, we performed an expanded pharmacological characterization of THIK1 channels and identified and characterized highly potent inhibitors with nanomolar efficacy. Interestingly, these compounds exhibit pronounced statedependent kinetics and inhibitor binding kinetics correlated with THIK1 channel activity. These properties establish the compounds not only as promising lead structures for therapeutic targeting of neuroinflammatory pathways, but also as reporter molecules capable of probing THIK1 channel state transitions such as by caspase8 cleavage in living cells.
Conclusion: Collectively, our combined structural and functional analyses provide important mechanistic insights into THIK1 gating, lipid regulation, and anesthetic inhibition. The identification of a Ygate as a central regulatory element together with the discovery of potent statedependent inhibitors substantially advances the understanding of THIK1 physiology and pharmacology. These findings highlight THIK1 as a promising therapeutic target in neuroinflammatory and neurodegenerative diseases and establish novel pharmacological tools for monitoring channel conformational dynamics during cellular stress and apoptosis.

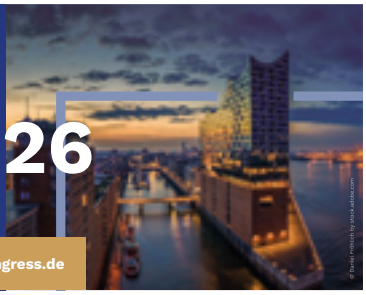

OC 07 FLOW of Ions: Ion channels pathophysiology

OC0702

Mechanistic Insights into the Na^+dependent HCO_3 Transport by NBCn2 (SLC4A10)

Lasse Messell Desdorf; Amanda Dyrholm Stange; Helle Hasager Damkier [1]; Birgit Schiøtt; Jeppe Praetorius [1]; Anna Louise Duncan
Department of Chemistry, Aarhus University, Aarhus, Denmark; [1] Department of Biomedicine, Aarhus University, Aarhus, Denmark;

Objective: The SLC4A protein family regulates the transport of bicarbonate (HCO_3) across cell membranes. The SLC4A10 protein, also known as NBCn2/Ncbe, is highly expressed in the choroid plexus epithelium and is thought to be involved in cerebrospinal fluid secretion. Dysregulation of NBCn2 has been associated with conditions featuring elevated intracranial pressure, such as stroke. Determining how NBCn2 binds and subsequently transports its substrate into the cell is key to understanding how it regulates intra- and extracellular pH in the choroid plexus epithelium, as well as sustaining cerebrospinal fluid production.
Method: AlphaFold2 was employed, using relevant structural information and MSA depth tuning, to generate models of NBCn2. Molecular dynamics simulations were used to study the structure and stability of ions in the binding sites. The accelerated weighted histogram method was used to obtain the binding energetics of each ion. Intracellular pH and Na^+ concentrations were measured in NIH3T3 mouse SLC4A10 (NBCn2/Ncbe) fibroblasts using fluorescence microscopy.
Results: We identified key bindingsite residues using proteinion fingerprint analysis. This revealed similar key residues compared with other Na^+dependent HCO_3^- transporters in the SLC4A family. Ion stability analysis showed that HCO_3^- depends on the prior binding of Na^+, whereas Na^+ can remain bound in the absence of HCO_3. Measurements of intracellular pH and Na^+ concentration also displayed a clear Na^+dependence, only increasing when Na^+ was present in the solution. Energy calculations based on enhanced sampling simulations showed a clear sequential pattern for ion binding. HCO_3^- is only thermodynamically favoured in the binding site in the presence of Na^+. The energy profile for Na^+, however, is largely unaffected by the presence or absence of HCO_3.
Conclusion: Based on our results, we conclude that NBCn2 has a sequential binding mechanism in which Na^+ binds first, followed by HCO_3. The initial binding of Na^+ is locked by the subsequent binding of HCO_3, thereby kinetically trapping Na^+ in the binding site and stabilising it. This is achieved by the thermodynamically favoured binding of HCO_3.

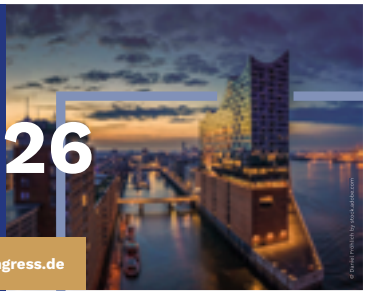

OC 07 FLOW of Ions: Ion channels pathophysiology

OC0703

Shared Structure and Mechanisms of the Human SLC26 Family of Anion Transporters

Bassam George Haddad; Piersilvio Longo; Felix Niklas GroßEsser; Dominik Oliver [1]; JanPhilipp Machtens
Institute of Neurophysiology, Medizinische Hochschule Hannover, Hannover, Germany; [1] Department of Neurophysiology, Institute of Physiology and Pathophysiology, Philipps University Marburg, Marburg, Germany;

Objective: The human solute carrier 26 (SLC26) family of anion transporters are expressed throughout the body, with aberrant mutations leading to a myriad of diseases. SLC26 isoforms can act as exchangers, channels, a combination thereof and in one particular case, as the voltageactivated membrane motor. Recent elucidation of human SLC26 family members showed a high degree of structural conservation, despite vast differences in their transport mode, mechanism, and physiological functions. However, the structural basis of the functional specialiasation of the SLC26 family members, which underlies their physiological role, remains largely unclear.
Method: Here we utilized extensive AIbased protein structure prediction in combination with allatom moleculardynamics simulations to probe for the unifying mechanistic principles of the human SLC26 family
Results: Analysis of the combined protein family reveals a conserved elevatortransport mechanism, with functional diversity arising from isoformspecific size and electrostatic potential of the anionbinding pocket.
Conclusion: Our work provides a framework for understanding functional diversity of whole families of transport proteins.

OC 07 FLOW of Ions: Ion channels pathophysiology

OC0704

Probing the limits of TRPM8 agonist efficacy and selectivity

Tudor Selescu; VioletaMaria Caragea; Alexandra Manolache; Edward T. Wei [1]; Alexandru Babes
Department of Anatomy, Animal Physiology and Biophysics, Faculty of Biology, University of Bucharest, Bucharest, Romania; [1] School of Public Health, University of California, Berkeley, Berkeley, United States;

Objective: The TRPM8 ion channel is the main coolinggated channel expressed in the somatosensory systems of animals ranging from amphibians to mammals. Here we describe a strategy of testing the efficacy of TRPM8 agonists while making use of the channel's thermal and chemical modalities. Identifying efficacious and selective TRPM8 agonists is important as these molecules find novel therapeutic roles.
Method: Wholecell currents were recorded in HEK293T cells expressing mammalian (rat and human) or avian (chicken) TRPM8 orthologs, while superfusing the cells with solutions of the TRP channel agonists WS12 (acoltremon) and Cryosim1. During chemical challenges, the extracellular temperature was gradually decreased (60 s ramps from ~32 to 18 °C). Primary dorsal root ganglia (DRG) cultures from adult Wistar rats, C57BL/6 mice (wildtype and *Trpm8/*) and Plymouth Rock chickens were investigated using calcium imaging while challenged with TRP channel agonists. Calcium transients were also measured in HEK293T cells expressing TRPV1 orthologs (mouse and rat) stimulated with WS12, Cryosim1, capsaicin and AMG9810.
Results: In TRPM8expressing HEK293T cells, voltage clamped at 80 mV and superfused with Cryosim1 (10 μM) or WS12 (10 μM), cooling evoked inward currents displaying a local minimum at the minimum of the temperature ramp. The Q_{10} coefficients for the decreasing currents ranged from 1.2 to 1.3 in all TRPM8 orthologs, similar to values found in nontemperaturegated ion channels. This allowed selecting the most efficacious TRPM8 agonists, namely the agonists that elicited current decreases at the highest temperatures during descending temperature ramps. For the agonistortholog pairs tested, Cryosim1 was the most efficacious at the chicken ortholog, while WS12 at the mammalian TRPM8 orthologs.
In DRG neurons from rat and chicken, the sensitivities to WS12 (5 μM) and Cryosim1 (10 or 100 μM) overlapped to a large degree, while in mouse neurons we identified a substantial population of cells (6.6% from total) sensitive to WS12 while insensitive to Cryosim1. A similar population (5.2%) was found responding to WS12 in DRG neurons from *Trpm8/* mice. The responsiveness to capsaicin (1 μM) found in most of these neurons (87% for wild-type and 78% for *Trpm8/*) suggested that WS12 is activating mouse TRPV1. In HEK293T cells expressing mouse TRPV1, WS12 (5 μM) evoked robust calcium transients that were abolished by the selective TRPV1 antagonist AMG9810 (1 μM).
Conclusion: These results show that at TRPM8's maximum open probability, as a result of simultaneous agonist and cold stimulation, further cooling decreases the currents in a diffusionlimited manner and this property can be exploited for finding efficacious TRPM8 agonists. In mouse DRG neurons, Cryosim1 shows a higher TRPM8 selectivity than WS12, as the latter can also activate mouse TRPV1.

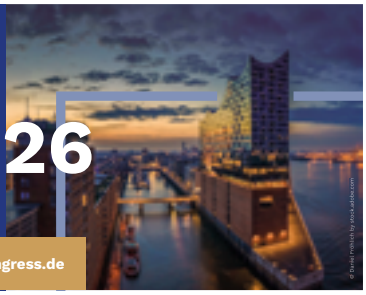

OC 07 FLOW of Ions: Ion channels pathophysiology

OC0705

The cystic fibrosis transmembrane conductance regulator (CFTR) potentiator ivacaftor stabilizes endothelial CFTR in lung infection

Caihong Li; Lasti Erfinanda; Wolfgang M. Kuebler
Institute of Physiology, Charité
–
Universitätsmedizin Berlin, Berlin, Germany;

Objective: Pneumonia remains one of the leading causes of mortality worldwide. We recently demonstrated that loss of CFTR in pulmonary endothelial cells drives lung barrier failure in *Streptococcus pneumoniae* infection, whereas the CFTR potentiator ivacaftor prevents CFTR downregulation and the development of lung edema (Erfinanda et al., Sci Transl Med 2022). However, the mechanisms by which ivacaftor stabilizes CFTR remain unclear. Here, we hypothesized that ivacaftor inhibits CFTR degradation by modulating the ubiquitination/deubiquitination pathway.
Method: Human pulmonary microvascular endothelial cells (human PMEC) and precisioncut lung slices (PCLS) from male C57BL/6 mice were pretreated with ivacaftor (VX770) and stimulated with pneumolysin (PLY), a virulence factor of *Streptococcus pneumoniae*. Proteasomal and lysosomal degradation were inhibited using MG132 and bafilomycin A1, respectively. Protein expression and ubiquitination were analyzed by qPCR, Western blot, immunoprecipitation (IP), and cycloheximide chase assay. The role of ubiquitin specific peptidase 10 (USP10) was assessed by deubiquitinase (DUB) activity assay, pharmacological inhibition (spautin1) or siRNAmediated knockdown (siUSP10).
Results: PLY induced K48- and K63linked CFTR polyubiquitination and increased global protein ubiquitination in human PMEC. PLYinduced CFTR loss was similarly prevented by MG132 or BafA1, respectively, suggesting that PLY induces CFTR degradation via both proteasomal and lysosomal pathways. PLY upregulated the E3 ligases HRD1 and RFFL while downregulating the CFTR deubiquitinase USP10. Ivacaftor increased general DUB and USP10specific activity and restored the expression of CFTR and other USP10 targets by reducing their polyubiquitination. USP10 inhibition abolished the protective effects of ivacaftor, as ivacaftor no longer stabilized CFTR in CHX chase assays nor reduced PLYinduced CFTR polyubiquitination in the presence of spautin1. Ivacaftor also rescued the PLYinduced reduction of USP13, a DUB that cooperates with USP10 in CFTR regulation, in human PMECs.
Conclusion: Lung infection causes CFTR loss in lung endothelial cells via ubiquitination and proteasomal/lysosomal degradation. Ivacaftor counteracts CFTR polyubiquitination by enhancing DUB activity, particularly USP10, thereby stabilizing CFTR. Supported by grants from the Deutsche Forschungsgemeinschaft (DFG) to WMK.

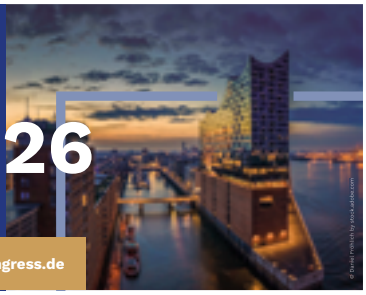

OC 07 FLOW of Ions: Ion channels pathophysiology

OC0706

Inhibiting transmembrane serine protease 2 (TMPRSS2) reduces transepithelial sodium absorption mediated by the epithelial sodium channel (ENaC) in murine cortical collecting duct cells

Florian Sure; Franziska Schreiber; Yaman Anan; Marko Bertog; Christoph Korbmacher; Alexandr V. Ilyaskin
Institut für Zelluläre und Molekulare Physiologie, FriedrichAlexanderUniversität ErlangenNürnberg, Erlangen, Germany;

Objective: Distal tubular sodium absorption via the epithelial sodium channel (ENaC) plays a crucial role in sodium homeostasis and longterm blood pressure control. A unique feature of ENaC is its activation by proteases. We demonstrated that transmembrane serine protease 2 (TMPRSS2) contributes to proteolytic ENaC activation in the kidney (Sure et al. *J Am Soc Nephrol*. 2025;36(3):420434). Here, we explored the potential of pharmacologically blocking TMPRSS2 to reduce ENaCmediated transepithelial sodium absorption.
Method: We applied the TMPRSS2 inhibitor N0385 and the inactive control compound N0385(OH) (100 nM; Shapira et al. *Nature.* 2022;605(7909):340348; provided by P.L. Boudreault and R. Leduc, Université de Sherbrooke, Canada) to murine cortical collecting duct cells ($mCCD_{cl1}$) during short circuit current (I_{SC}) measurements.
Results: In native $mCCD_{cl1}$ cells, apical application of N0385 significantly decreased ENaCmediated I_{SC} (−3.3±0.5 with N0385 vs. −0.2±0.4 µA/cm² with N0385(OH); n=1420; p<0.001, Student's *t*test). Subsequent application of the prototypical protease chymotrypsin increased I_{SC} in N0385 treated cells (+4.8±0.5) but not in N0385(OH) treated controls (−0.3±0.5 µA/cm²; p<0.001). In contrast, N0385 had no effect on TMPRSS2deficient $mCCD_{cl1}$ cells (−0.1±0.2 µA/cm²; n=16) or when administered basolaterally (+0.0±0.2 µA/cm²; n=10). These findings suggest that the effect of N0385 is due to specific TMPRSS2 inhibition resulting in impaired proteolytic ENaC activation at the apical membrane. Moreover, N0385 reduced the stimulatory effects of aldosterone (from +34.5±3.9 to +24.3±2.2 µA/cm²; n=1415; p<0.05) or vasopressin (from +57.2±2.9 to +33.6±0.7 µA/cm²; n=9; p<0.001) on ENaCmediated I_{SC}.
Conclusion: In conclusion, pharmacological inhibition of TMPRSS2 reduced proteolytic ENaC activation. Thus, TMPRSS2 inhibition may be a promising therapeutic strategy to decrease renal sodium reabsorption.

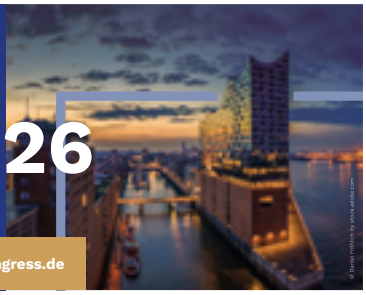

OC 08 FLOW of Signals: Hard core cell signaling

OC0801

The protonsensing GPR68GβγPI3KβAKT axis orchestrates acidinduced migration in glioblastoma stemlike cell spheres

Xiaochen Niu; Wangming Zeng; Stefan Gründer
Institut of physiology, RWTH Aachen University, Aachen, Germany;

Objective: The aggressive dissemination of glioblastoma (GBM) is significantly promoted by the acidic tumor microenvironment, a metabolic hallmark arising from the Warburg effect wherein lactate accumulation lowers extracellular pH. While acidosis is known to drive malignant progression, the specific molecular mechanism translating extracellular proton signals into enhanced migration are incompletely understood. This study aims to elucidate the transduction pathway by acidosis induces motility in GBM.
Method: To simulate the migration niche, we utilized a 2.5D migration assay. Glioblastoma stemlike cell (GSC) spheres were seeded onto culture plates coated with PolyDLysine (PDL) and laminin to facilitate adherence and migration. Migratory capacity was assessed by quantifying the cumulative emigration of single cells from the sphere core under varying pH conditions (pH 6.6 vs pH 7.4). A comprehensive pharmacological strategy using specific smallmolecule drugs was employed to analyze the downstream signaling cascade.
Results: Extracellular acidosis robustly enhanced the migration ability of GSCs. Pharmacological investigation identified the protonsensing G proteincoupled receptor, GPR68, as an upstream sensing molecule: the GPR68 agonist Ogerin further promoted the migration ability under both normal and acidic conditions, while the inhibitor of GPR68 (Ogremorphin1) weakened this ability. While the Gα inhibitor YM254890 failed to alter the acidinduced response, the Gβγ inhibitor Gallein significantly suppressed it. Subsequent profiling using isoformselective phosphoinositide3kinase (PI3K) inhibitors (alpelisib for PI3Kα; GSK2636771 for PI3Kβ) and the panPI3K inhibitor wortmannin demonstrated that blockade of either isoform abolished migratory enhancement, indicating the recruitment of both PI3K subtypes. Finally, inhibition of the downstream effector AKT similarly inhibited the migratory response.
Conclusion: Our findings reveal a novel GPR68GβγPI3KβAKT signaling axis linking metabolic acidosis to GSCs migration. This suggests that targeting GPR68 could effectively impede GBM dissemination within the acidic tumor environment.

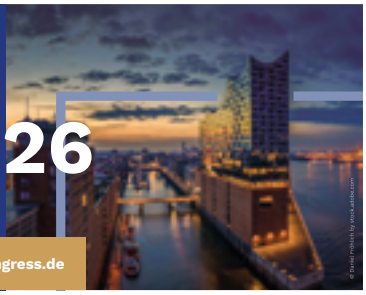

OC 08 FLOW of Signals: Hard core cell signaling

OC0802
Combined loss of *Pak1* and *Pak2* enhances macrophage motility while preserving chemotaxis

Markus Horsthemke; Julie Drieu La Rochelle 1; Jonathan Chernoff 2; Matthew Fuszard 3; Ulla G. Knaus 1; Peter Hanley 4
Faculty of Medicine, Institute for Molecular Medicine, Health and Medical University Potsdam, Potsdam, Germany; 1 School of Medicine, University College Dublin, Dublin, Ireland; 2 Philadelphia, United States; 3 Halle (Saale), Germany; 4 Münster, Germany;

Objective: Macrophages navigate along chemoattractant gradients by producing membrane protrusions toward higher concentrations and coordinately retracting of the trailing end. In line with the canonical dendritic actin nucleation model of membrane protrusion and cell motility, chemoattractant receptor signaling activates the Rho GTPases Rac1, Rac2, and Cdc42 at the leading edge, thereby promoting barbedend actin polymerization through actinnucleating factors such as the Arp2/3 complex. Simultaneously, these Rho GTPases activate p21activated kinases (PAKs), which inhibit ADF/cofilinmediated actin severing and depolymerization at pointed ends through LIM kinase activation. Here, we investigated whether PAKs are required for cell motility and chemotactic navigation.
Method: Resident peritoneal macrophages isolated from myeloidrestricted *Pak2* conditional knockout (cKO), *Pak1*/*Pak2* double knockout (dKO), and *Pak1* knockout (*Pak1*$^{-/-}$) mice were analyzed in realtime chemotaxis assays.
Results: *Pak1*deficient macrophages were largely indistinguishable from control cells, whereas *Pak2* cKO macrophages frequently adopted a dendritic morphology and exhibited modestly impaired chemotaxis and reduced cell velocity. In contrast, *Pak1*/*Pak2* dKO macrophages exhibited robust chemotaxis and markedly increased cell velocity. Strikingly, *Pak1*/*Pak2* dKO cells adopted a distinct, chemoattractantinduced rounded morphology characterized by extensive ruffling at the leading edge and a compact trailing end, although these cells intermittently transitioned to slower, partially spread or elongated morphologies.
Conclusion: In summary, whereas loss of *Pak2* alone modestly impairs chemotaxis, combined deletion of *Pak1* and *Pak2* preserves directional navigation while enhancing cell motility, potentially through increased ADF/cofilinmediated severing at pointed ends and increased actin treadmilling at the leading edge.

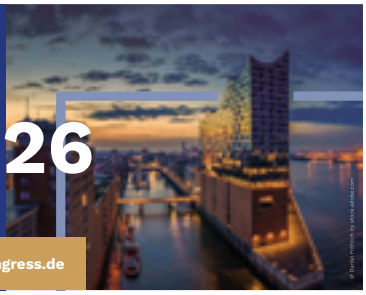

OC 08 FLOW of Signals: Hard core cell signaling

OC0803

Muscle Rac1 deficiency reduces mitochondrial respiratory capacity and impairs fatty acid metabolism, leading to muscle wasting

Lisbeth Liliendal Valbjørn Møller; Steffen H. Raun; Emma Frank; Andreas B. Jordy [1]; Nicoline R. Andersen [2]; Anders Gudiksen [3]; Zakarias Ogueboule; T. C. Phung Pham; Jessica L. Braun; Esben Nyborg; Jeffrey Molendijk [4]; Anders Karlsen [5]; Jakob Agergaard [5]; Sean A. Newsom [6]; Bryan C. Bergman [7]; Niels Ørtenblad [8]; Michael Kjær [5]; Henriette Pilegaard [3]; Bente Kiens [1]; David E. James [9]; Benjamin L. Parker [4]; Joachim Nielsen [8]; Steen Larsen; Erik A. Richter [1]; Lykke Sylow Department of Biomedical Sciences, University of Copenhagen, Copenhagen, Denmark; [1] Department of Nutrition, Exercise and Sports, University of Copenhagen, Copenhagen, Denmark; [2] Health and Medical Sciences, University of Copenhagen, Copenhagen, Denmark; [3] Department of Biology, University of Copenhagen, Copenhagen, Denmark; [4] Department of Anatomy & Physiology, The University of Melbourne, Parkville, Australia; [5] Department of Orthopedic Surgery, University of Copenhagen, Copenhagen, Denmark; [6] School of Exercise, Sport, and Health Sciences, Oregon State University, Corvallis, United States; [7] School of Medicine, University of Colorado Anschutz, Aurora, United States; [8] Department of Sports Science and Clinical Biomechanics, University of Southern Denmark, Odense, Denmark; [9] The University of Sydney, Camperdown, Australia;

Objective: Agerelated progressive decline in skeletal muscle function is characterised by perturbed mitochondrial quality control and fatty acid metabolism, contributing to frailty and increased mortality. The actin cytoskeleton has been implicated in mitochondrial anchoring and dynamics. Yet, the role of actinregulators such as the Rho GTPase Rac1 in mitochondrial function and ageassociated metabolic and functional muscle deterioration remains undefined.
Method: Skeletal muscle from anaesthetised (6 mg pentobarbital sodium 100 g^{-1} body weight i.p.) mice with inducible musclespecific deletion of Rac1 (Rac1 imKO) underwent unbiased mass spectrometrybased proteomic profiling. Mitochondrial morphology was assessed by transmission electron microscopy, and physiological parameters, including muscle mass and contractionstimulated palmitate oxidation in isolated muscle, were evaluated. Mitochondrial respiratory capacity was determined by highresolution respirometry in permeabilised skeletal muscle fibre bundles. In muscle biopsies from healthy, young (2030 years) and sarcopenic, old (8394 years) men, Rac1 and mitochondrial respiratory protein abundances were measured. A complementary human genetic association analysis was performed using the FinnGen dataset.

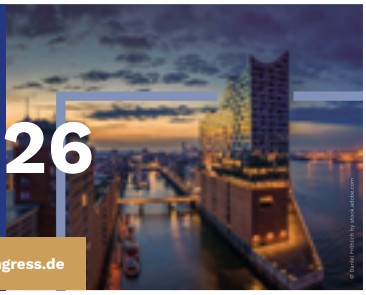

OC0803

Muscle Rac1 deficiency reduces mitochondrial respiratory capacity and impairs fatty acid metabolism, leading to muscle wasting

Results: Rac1 deficiency triggered muscle wasting in middleaged mice (Gastrocnemius: 10%, Quadriceps: 7%; n=8/15 [Control/Rac1 imKO], mixed model, $p<0.01$). Preceding muscle wasting, gene set enrichment analysis identified enrichment of fatty acid metabolism and oxidative phosphorylation pathways, consistent with increased mitochondrial volume density in Rac1 imKO muscle (subsarcolemmal: +467%, intermyofibrillar: +166%, n=4/5, ttest, $p<0.01$). Despite mitochondrial expansion at this stage, Rac1 deficiency attenuated the increase in palmitate oxidation with contraction (62%; n=14/9, ttest, $p<0.05$). At the stage of muscle atrophy, Rac1 imKO muscle exhibited reduced mitochondrial respiratory capacity (2532%; n=8/14, ANOVA, $p<0.01$). In humans, Rac1 muscle protein content was increased in old, sarcopenic subjects compared to young (+41%; n=10/9 [Young/Old], ttest, $p<0.05$), and negatively correlated with quadriceps crosssectional area (CSA) ($r=0.475$, Pearson's correlation, $p<0.05$) and type II fibre CSA ($r=0.466$, Pearson's correlation, $p=0.051$). In old, sarcopenic muscle, Rac1 protein content correlated negatively with protein content of multiple mitochondrial respiratory complexes (CI: $r=0.690$, CIV: $r=0.938$, CV: $r=0.704$; Pearson's correlation, $p<0.05$). GWAS further identified associations between Rac1 SNP variants and lipid metabolic (OR: 2.92, $p=3.00\times10^{4}$) and musclewasting diseases (OR: 4.44, $p=1.00\times10^{5}$).
Conclusion: Muscle Rac1 deficiency reduces mitochondrial respiratory capacity and metabolic flexibility through impaired fatty acid metabolism, leading to muscle wasting and highlighting a potential therapeutic target in agerelated functional decline.

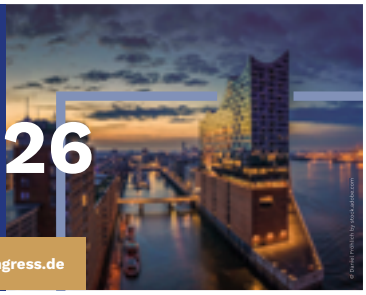

OC 08 FLOW of Signals: Hard core cell signaling

OC 08 04

Cigarette smokeinduced suppression of mTORC1 signaling disrupts mitochondrial respiration of RPE cells and the retina

Annika Schubert; Katrin Willbrand; Gesa Weißenberg; GinaEva Görtz [1]; Johann Matschke [2]; Joachim Fandrey; Yoshiyuki Henning
Institut für Physiologie, Universitätsklinikum Essen AöR, Essen, Germany; [1] Department of Ophthalmology, Orbital Diseases Science Lab, University Hospital Essen, Essen, Germany; [2] Institute of Cell Biology (Cancer Research), University Hospital Essen, Essen, Germany;

Objective: Agerelated macular degeneration (AMD) is the leading cause of irreversible vision loss in the elderly population, characterized by progressive degeneration of photoreceptors in the macula. Still, the molecular mechanisms underlying AMD pathophysiology remain incompletely understood. Mitochondrial dysfunction in retinal pigment epithelium (RPE) cells has been proposed as an early driver of disease progression, as RPE cells and photoreceptors function as a metabolic unit. Cigarette smoking, the strongest modifiable risk factor for AMD, is associated with mitochondrial dysfunction, although the underlying signaling pathways remain unclear. Therefore, this study investigated the metabolic effects of cigarette smoke and related signaling pathways to identify mechanisms contributing to AMD pathophysiology.
Method: For this purpose, we exposed a human RPE cell line and porcine retinal explant cultures derived from pig eyes obtained from a slaughterhouse to cigarette smoke extract (CSE) and analyzed CSE effects on mitochondrial respiration and mTOR signaling pathways.
Results: CSE exposure severely impaired mitochondrial respiration in both, RPE cells and retinal explant cultures. Given the central role of mTOR in cellular metabolism, we investigated whether CSE exposure is associated with altered signaling of the mTOR complexes mTORC1 and mTORC2. We found that downstream signaling of mTORC1 was significantly impaired, whereas mTORC2 activity was upregulated. Consistently, the downregulation of mTORC1 was accompanied by an increase in autophagic flux. Finally, we confirmed a causal link between mTORC1 suppression and mitochondrial dysfunction, as restoring mTORC1 activity with fetal bovine serum rescued the metabolic phenotype in RPE cells.
Conclusion: Collectively, these data identify mTORC1 signaling as a critical metabolic checkpoint in cigarette smokeassociated metabolic dysregulation and highlight its potential as a therapeutic target for early prevention strategies.

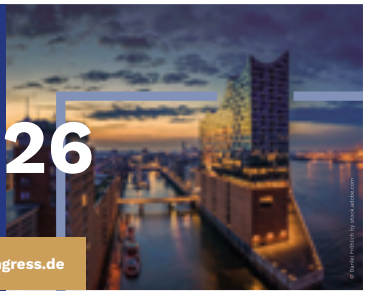

OC 08 FLOW of Signals: Hard core cell signaling

OC0805

Role of Regulator of Gprotein signaling 4 in renal erythropoietin regulation under hypoxic and fibrotic conditions in mice

Bettina Katharina Mariana Firmke; AnnaLena Forst [1]; Katharina AnnaElisabeth Broeker Lehrstuhl Physiologie I, Institut für Physiologie, Universität Regensburg, Regensburg, Germany; [1] Lehrstuhl für Medizinische Zellbiologie, Institut für Physiologie, Universität Regensburg, Regensburg, Germany;

Objective: Erythropoietin (EPO) is produced by interstitial PDGFRβ? fibroblasts in mice. Under hypoxic conditions, additional fibroblasts are recruited via the HIF2 pathway to produce EPO, whereas chronic kidney disease (CKD) leads to reduced EPO expression. Previously, we demonstrated that regulator of Gprotein signaling 4 (RGS4) is coexpressed with EPO in a HIF2dependent manner under normoxia and hypoxia. Furthermore, recent publications suggest that RGS4, similar to HIF2, is regulated by oxygen availability. Therefore, we investigated whether RGS4 contributes to renal EPO regulation under (patho)physiological conditions.
Method: *Rgs4* expression was examined in wildtype mouse kidneys under normoxic, hypoxic, and fibrotic conditions using RNAscope and RTqPCR. Anemia was induced as a hypoxic stimulus by phlebotomy of the vena facialis, reducing hematocrit to 25%, while administration of roxadustat acted as a pharmacological hypoxic stimulus by stabilizing HIF2. The functional role of RGS4 was assessed using an inducible PDGFRβ cellspecific RGS4 knockout mouse model (RGS4KO).
Results: Under normoxic, anemic, and roxadustattreated conditions, *Rgs4* expression was consistently colocalized with EPO in interstitial fibroblasts. In fibrotic lesions, *Rgs4* was detected in tubular cells and, more prominently, in interstitial fibroblasts. RGS4 deletion reduced *Rgs4* expression to ~10% of control levels and significantly increased *Epo* mRNA and plasma EPO concentrations under normoxic and hypoxic conditions (Student's ttest, $n \geq 5$/group, $p < 0.05$).
Conclusion: In summary, we identified RGS4 as a negative regulator of renal *Epo* expression, and its upregulation in fibrosis suggests a role in *Epo* suppression during CKD. Future studies will clarify whether targeting RGS4 could restore *Epo* expression in CKD.

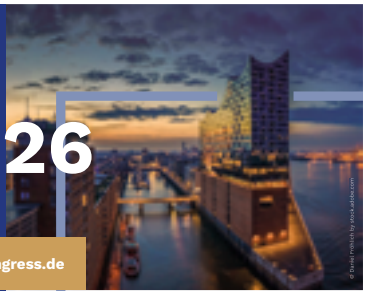

OC 08 FLOW of Signals: Hard core cell signaling

OC0806

Distinct roles of NEDD41 and NEDD42 in aSynuclein regulation and dopaminergic neuron survival

James Conway; Helia Weiberlen [1]; Aayushi Kaira [2]; Hiroshi Kawabe [3]; Edgar Kramer [4] UK Dementia Research Institute, University College London, London, United Kingdom; [1] Center for Molecular Neurobiology, University Medical Center HamburgEppendorf, Hamburg, Germany; [2] Medical School, University of Plymouth, Plymouth, United Kingdom; [3] Department of Biochemistry and Molecular Biology, Kobe University Graduate School of Medicine, Kobe, Japan; [4] Health and Medical University, Potsdam, Germany;

Objective: We want to investigate the in vivo function of the E3 ubiquitin protein ligases NEDD41 and NEDD42 in the midbrain dopaminergic system. αSynuclein aggregation and progressive nigrostriatal degeneration are the defining features of Parkinson's disease and other Lewy body disorders, but the E3 ubiquitin ligases that govern αSynuclein homeostasis *in vivo* are not known and the mechanisms of nigrostriatal dopaminergic neuron death is not well understood. Currently, there are only transient symptomatic treatments available for these devastating diseases.
Method: Using two independent conditional mouse lines lacking NEDD41 and NEDD42, or both ligases in dopaminergic neurons, we show that the two paralogues perform nonredundant functions. These mice were also combined with mice overexpressing human αSynuclein. We analyzed the behavioral, biochemical and histological phenotypes in these mice during adulthood and ageing, In addition, we investigated the expression of NEDD41 and NEDD42 in human brain tissue from healthy controls and Parkinson#s disease patients. All procedures on mice and human tissue were accorded with current EU/UK legislation.
Results: Loss of NEDD41 raises endogenous αSynuclein levels in substantia nigra dopaminergic neurons but does not cause neurodegeneration. Loss of NEDD42, by contrast, drives a selective, progressive, dyingback loss of nigrostriatal neurons with reactive gliosis and proinflammatory microglial activation, independently of αSynuclein levels. Combined deletion of both ligases in mice expressing human A53T αSynuclein further exacerbates αSynuclein aggregation and nigrostriatal degeneration.
Against previous published reports we did not find significant expression of NEDD41 and NEDD42 in human dopaminergic neurons but only in cortical neurons raising the question about the difference between mice and men.
Conclusion: NEDD41 and NEDD42 seem to act through dissociable pathways, one controlling αSynuclein abundance, the other controlling dopaminergic neuronal survival, that converge to determine vulnerability in Parkinson's disease and other Lewy body disorders. Inducing expression of NEDD41 and NEDD42 in dopaminergic neurons of these patients and directing the ubiquitination activty to relevant NEDD41 and NEDD42 substrates is an exciting novel approach that could be beneficial for these patients.

OC 09 FLOW of Blood: Cardiac physiology

OC 09 01

Geometric remodelling overrides reduced myocardial stiffness following in vivo titin cleavage to increase diastolic pressure

Annika J. Klotz; Kimberley Stein 1; Johanna Freundt; Susanne Hille 2; Oliver J. Müller 2; Daniela Wenzel 1; Wolfgang Linke
Institut für Physiologie II, Universitätsklinikum, Westfälische Wilhelms-Universität Münster, Münster, Germany; 1 Systemphysiologie, Institut für Physiologie, Ruhr-Universität Bochum, Bochum, Germany; 2 Translationale kardiovaskuläre Forschung, Klinik für Innere Medizin III, Universitätsklinikum Schleswig-Holstein, Kiel, Germany;

Objective: Increased titinbased myocardial stiffness is a recognised driver of diastolic dysfunction in HFpEF, and titin softening is being explored therapeutically. However, the acute consequences of titin softening on ventricular pressure remain unclear. We therefore investigated the haemodynamic effects of in vivo titin cleavage in titincleavage (TC) mice using a Laplacebased framework to distinguish myocardial stiffness from geometric determinants of left ventricular (LV) pressure.

Method: Selective titin cleavage was induced in homozygous TC mice (C57BL/6) carrying a TEV site within elastic Iband titin via AAV9mediated TEV protease expression; AAV9GFP served as control (n=8/group). LV pressurevolume analyses were performed under 11.5% isoflurane 6 days postinjection. Titin cleavage was quantified by SDSPAGE, passive mechanics assessed in permeabilized trabeculae, and cardiac MRI data (Freundt et al., Nat. Cardiovasc. Res. 2026: In press) reanalysed for LV geometry. Statistical analyses used unpaired ttests and MannWhitney U tests.

Results: TEVtreated hearts exhibited robust titin cleavage (38.5±4.2%) and markedly reduced passive elastic stress (p=0.0009) without changes in viscous stress (p=0.9746). Despite reduced myocardial stiffness, in vivo analyses revealed diastolic dysfunction with a smallvolume, highpressure phenotype, including reduced enddiastolic (p=0.0020) and stroke (p=0.0008) volumes, ~150% elevated enddiastolic pressure (p=0.0003), prolonged tau (p=0.0039), and increased EDPVR (p=0.0006) and ESPVR (p=0.0110). Preload responsiveness was impaired, with a reduced FrankStarling slope (p=0.0222) and delayed preload adaptation (p=0.0003). MRI showed reduced LV radius (p=2.1×105) and increased wall thickness (p=4.6×106) without changes in LV mass/tibia length (p=0.9927). Laplace decomposition revealed that geometric remodelling increased enddiastolic and endsystolic pressure by 89% (p=2.3×105) and 181% (p=1.5×105), respectively.

Conclusion: Loss of titinbased elasticity induces diastolic dysfunction with elevated enddiastolic pressure predominantly through geometric remodelling. These findings challenge the prevailing paradigm that diastolic dysfunction is primarily driven by increased myocardial stiffness and raise important considerations regarding the safety of titintargeting therapeutic strategies in HFpEF.

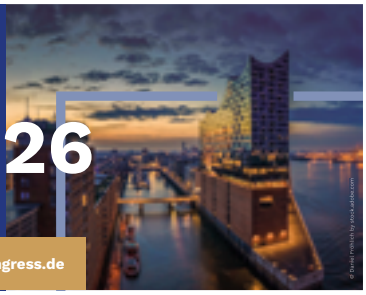

OC 09 FLOW of Blood: Cardiac physiology

OC0902

Induction of fibrosis and myocardial dysfunction by inflammatory signals in an exvivo model of beating rabbit and human myocardium

Hena Jasarevic; Pooja Joshi; Katy A. Trampel [1]; Binjie Li [1]; Igor Efimov [1]; Tilmann Volk; Thomas Seidel
Institut für Zelluläre und Molekulare Physiologie, FriedrichAlexanderUniversität ErlangenNürnberg, Erlangen, Germany; [1] Department of Biomedical Engineering, Northwestern University, Chicago, United States;

Objective: Cardiac fibrosis causes extracellular matrix (ECM) accumulation by myofibroblasts leading to myocardial stiffness and impaired contractility. An exvivo fibrosis model will advance insight into cardiac remodeling and enable therapeutic studies. Here, we established such model by exposing beating rabbit and human myocardium to cytokines (TGFβ, TNFα, IL1β) known to be upregulated during cardiac remodeling.
Method: Human cardiac samples were obtained from heart transplant patients after informed consent and from healthy donor hearts not suitable for transplantation. Rabbit hearts were obtained after lethal sodium phenobarbital injection. A circular lesion (0.79mm^2) was created in leftventricular cardiac slices with a 1mm biopsy punch, mimicking tissue loss. Scar healing was assessed by measuring lesion area postculture by confocal microscopy (rabbit: n=79/6, human: n=56/3). Functional parameters (contraction force, CF, contraction duration, CD, time-topeak, TTP, timetorelaxation, TTR) were measured in rabbit (n=1827/7) and human (n=89/3) cardiac slices cultured under continuous electrical stimulation (0.5Hz), while treated with TGFβ, TGFβ+TNFα, TGFβ+TNFα+IL1β. Western blots of fibrotic and ECM markers (αSMA, vimentin, periostin, fibronectin) were performed (rabbit: n=35/5, human: n=1/2).
Results: CF decreased by 41%±47% after 4d of TGFβ treatment vs control in rabbit cardiac slices ($p<0.05$). TGFβ prolonged parameters of myocardial relaxation, CD (1.2fold), TTR (1.4fold) at $p<0.05$ while no significant changes were seen in control. Contraction velocity parameter, TTP, was unchanged. No additional changes were observed with TNFα or IL1β. In human cardiac slices, a CF decrease (70%±23%) and increase in CD (1.7fold) and TTR (1.6hold) was found after 14d of TGFβ exposure ($p<0.05$). These effects were consistent in healthy and failing human cardiac slices. TGFβtreated slices showed a smaller lesion area (rabbit: 0.29±0.44mm^2, human: 0.30±0.34mm^2) against control (rabbit: 1.67±0.96mm^2, human: 1.21±0.61mm^2, $p<0.05$). Western blot analysis revealed enhanced αSMA (log_2fold change: 4.8fold), vimentin (1.0fold), periostin (1.1fold), fibronectin (3.5fold) protein levels with TGFβ exposure in rabbit cardiac slices ($p<0.05$). Data was analyzed via oneway ANOVA and post hoc multiple comparison correction.
Conclusion: Exposing beating rabbit and human myocardium to TGFβ induces myofibroblast differentiation, ECM remodeling and reduced contractility (CF, CD, TTR). This suggests a feasible exvivo tissue model that replicates key fibrotic effects, including elevated myocardial stiffness and dysfunction.

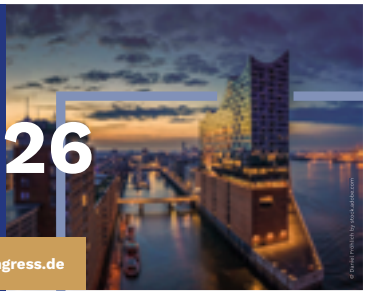

OC 09 FLOW of Blood: Cardiac physiology

OC0903

Transient Inhibition of the NLRP3 inflammasome improves cardiac pump function long-term via improved cardiomyocyte survival after myocardial infarction in mice

Esther Carls; Pia Leineweber [1]; Miriam Schiffer; Timo Mohr; Bernd K. Fleischmann [1]; Wilhelm Röll
Cardiac Surgery, University Hospital Bonn, Bonn, Germany; [1] Institute of Physiology I, University Hospital Bonn, Bonn, Germany;

Objective: Cardiovascular diseases, particularly myocardial infarction (MI), are the world's leading cause of death. Coronary artery occlusion causes ischaemia, followed by cardiomyocyte (CM) death and their replacement with a noncontractile scar impairing cardiac function. Acute ischaemia triggers NLRP3 inflammasome activation eliciting IL1βmediated inflammation and Gasdermin Dmediated pyroptosis. Thus, pharmacologic NLRP3 inhibition may attenuate postischaemic inflammation and cell death, and therby preserve cardiac pump function.
Method: MI was induced by permanent ligation of the left anterior descending (LAD) coronary artery in C57 Bl/6J mice (10 - 12 weeks old). Surgery was performed under inhalative Isoflurane anaesthesia (5% for induction, 1.52% for maintenance). Mice received the NLRP3 inhibitor MCC950 (20 mg/kg i.p.) intraoperatively and thereafter every other day until d14 postMI. Animals were euthanized 1, 3, or 7 days postMI for histological analyses of the immune response. After 2 and 8 weeks, left ventricular function was assessed via echocardiography and pressurevolume loop measurements, followed by tissue collection for histological analyses.
Results: Immunofluorescent staining of cardiac sections showed strong infiltration of $CD45^+$ leukocytes into the infarction area of LAD control mice peaking 3d postMI, which was significantly attenuated in MCC950treated mice. Expression of NLRP3 and cleaved IL1β were significantly reduced in LAD+MCC950 hearts compared to LAD controls 3d postMI. Although infarct scar volume did not differ between groups 2 or 8 weeks postMI, strikingly, LAD+MCC950 mice exhibited no transmural scars after 2 weeks. Functional assessment demonstrated significantly greater fractional shortening (24.56% *vs.* 20.58%) and anterior wall motion by echocardiography, as well as increased stroke volume by pressurevolume analysis in LAD+MCC950 mice 2 weeks postMI. Eight weeks postMI, ejection fraction was also significantly improved in MCC950treated animals (62.57% *vs.* 36.78%). Strikingly, TUNEL staining, which indicates dying cells, revealed a 3fold higher proportion of $TUNEL^+$ nuclei in LAD control hearts (49%) compared to inhibitortreated mice (15%) 1d postMI.
Conclusion: Transient (14day) pharmacological inhibition of NLRP3 with MCC950 attenuates early postischaemic inflammation and cell death, resulting in longterm improvement of cardiac function following MI. These findings identify NLRP3 as a promising therapeutic target to mitigate adverse cardiac remodelling and preserve cardiac function after ischaemic injury.

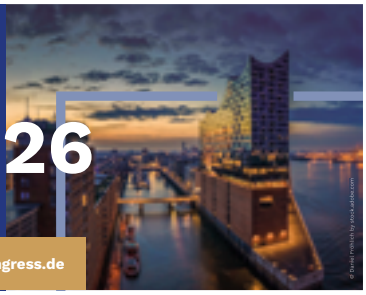

OC 09 FLOW of Blood: Cardiac physiology

OC 09 04
Neurocardiac interactions using hiPSC derived cardiomyocytes and sympathetic neurones from CPVT patients

Yoon Young Choi; Ni Li; Dan Li; David J. Paterson
Department of Physiology, Anatomy and Genetics, University of Oxford, Oxford, United Kingdom;

Objective: Catecholaminergic polymorphic ventricular tachycardia (CPVT) is a lifethreatening inherited arrhythmia caused by mutations in the cardiac ryanodine receptor2 (RYR2), although the contribution of sympathetic neurones (SNs) to disease pathophysiology remains incompletely understood. We therefore tested whether CPVT SNs contribute directly to the arrhythmic phenotype using human induced pluripotent stem cell (hiPSC)derived cardiomyocytes (CMs) and SNs in 2D and 3D neurocardiac coculture models.
Method: Patientderived and control hiPSCs were differentiated into CMs and SNs. Electrophysiology was assessed by multielectrode arrays, calcium handling by Fura2AM imaging and cAMP by FRET. 3D microtissues were generated by dropletbased bioprinting and calcium transients were analysed using optical mapping. All hiPSC lines were obtained with appropriate ethical approval.
Results: CPVT CMs exhibited spontaneous arrhythmic activity at baseline (47% vs 0% in controls; n>20), shorter RR intervals (0.441±0.025 vs 0.564±0.049s, $p<0.05$) and field potential durations (0.184±0.015 vs 0.341±0.041s, $p<0.01$), with isoprenaline inducing arrhythmias only in CPVT CMs. CPVT CMs also had larger Ca^{2+} transients, more spontaneous Ca^{2+} discharges (77.4% vs 10%), and greater cAMP responses ($p<0.0001$).
CPVT SNs demonstrated increased Ca^{2+} transients and exaggerated cAMP responses following nicotine stimulation. In neurocardiac coculture, neuronal activation increased CM beating rate, confirming functional coupling. Upon high K^{+} (50mM) stimulation, calcium release in CPVT SNs remained greater than in controls irrespective of the CM genotype ($p<0.0001$), supporting intrinsic neuronal hyperactivity. Notably, control CMs cocultured with CPVT SNs exhibited greater RR shortening than those with control SNs ($p<0.05$).
These findings were recapitulated in 3D microtissue models. CPVT cardiac microtissues displayed irregular, oscillatory Ca^{2+} waveforms and prolonged Ca^{2+} transient duration.
Coculture of control CMs with CPVT SNs resulted in irregular Ca^{2+} waveforms, multipeaked transients and prolonged CaTD70 compared with control SNs ($p<0.05$).
Conclusion: CPVT hiPSCCMs show expected electrophysiological and calciumhandling abnormalities, while CPVT hiPSCSNs display intrinsic hyperexcitability that drives CM dysfunction via neurocardiac crosstalk. As such, CPVT should be considered a neurocardiac disorder, supporting sympathetic targeting as a therapeutic strategy.

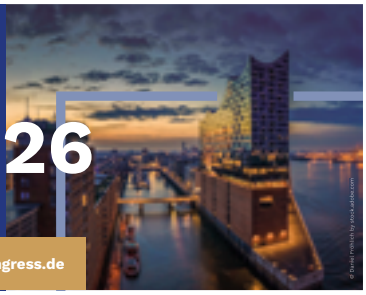

OC 09 FLOW of Blood: Cardiac physiology

OC0905

Embryonic electrophysiology of the pulmonary veinmyocardium reveals early arrhythmogenic triggers

Megan McKie; Emma Meibom; Luca Soattin; Bo Bentzen
Department of Biomedical Sciences, Faculty of Health and Medical Sciences, Universtiy of Copenhagen, Copenhagen, Denmark;

Objective: In the adult heart, cardiomyocytes populate the pulmonary veinsleeve myocardium and spontaneously generate intermittent action potentials that can initiate atrial fibrillation. Using landscape transcriptomics, we found that besides smooth muscle cells, endothelial cells, fibroblasts, macrophages and Tcells, pulmonary veins house three subtypes of cardiomyocytes: *atriallike*, *transitional* and *pacemakerlike* cells, respectively, which in turn give rise to six different action potential waveforms detected by customised machine learning technology. We therefore hypothesised that specialised cardiomyocyte subtypes with arrhythmogenic potential may already emerge during embryonic development and display a distinct molecular signature predictive of future electrical trigger activity.
Method: Pulmonary veins were freshly isolated from IGSWistar rat embryos at embryonic day 18 (corresponding to *Carnegie Stage XXIII* in humans). Electrophysiological activity was assessed using a dualcamera optical mapping system enabling simultaneous recordings of spontaneous action potentials and intracellular calcium transients. Immunofluorescence imaging and 3Dlightsheet microscopy were performed to characterise the cellular composition and cell organisation of embryonic pulmonary vein tissue. In parallel, gene expression analyses were conducted to investigate the molecular profile of pulmonary veinresident cardiomyocytes, with particular focus on pacemakerassociated transcripts and developmental transcription factors.
Results: Optical mapping experiments demonstrated that embryonic pulmonary veins exhibit spontaneous electrical activity and calcium transients. Immunofluorescence imaging and 3Dreconstruction revealed a dense population of cardiac cells, heterogeneously distributed within the pulmonary vein tissue. Gene expression analysis showed that pulmonary veinresident cardiomyocytes express HCN4 transcripts, consistent with a pacemakerlike phenotype. Furthermore, chamberrepressing transcription factors, including TBX3, were found to be overexpressed in pulmonary vein cardiomyocytes, supporting the presence of a specialised electrophysiological phenotype in the embryonic pulmonary veinmyocardium.
Conclusion: Taken together, these data suggest that cardiac cells generating arrhythmogenic spontaneous triggers do not only infiltrate *de novo* from the nearby left atrium but might migrate from different regions of the splanchnic mesoderm during development. Understanding the specification and migration processes of cardiac progenitors in the pulmonary veins might unveil which molecular and electrophysiological mechanisms underly the onset of atrial fibrillation.

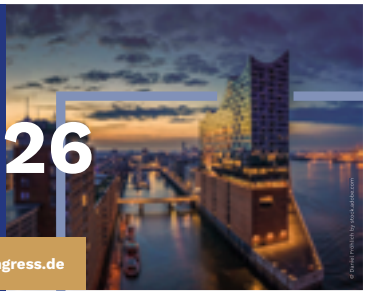

OC 09 FLOW of Blood: Cardiac physiology

OC0906

Heartspecific inactivation of the transcriptional regulator PR domain 16, *Prdm16* induces severe cardiac dysfunction in mice

Simon Theisen; Josephine Brendel [1]; Franz Kürstein [2]; Benedikt Obermayer [3]; Dieter Beule [3]; Arnd Heuser [4]; Norbert Hubner [4]; Olaf Grisk [2]; Sabine Klaassen [4]; Jirko Kühnisch [2]
VincentiusDiakonissenKliniken, Karlsruhe, Germany; [1] Charité - Universitätsmedizin Berlin, Berlin, Germany; [2] Institute of Physiology, Medical School of Brandenburg, Brandenburg, Germany; [3] Berlin Institute of Health (BIH), Charité - Universitätsmedizin Berlin, Berlin, Germany; [4] Experimental and Clinical Research Center (ECRC), Max Delbrück Center and Charité - Universitätsmedizin Berlin, Berlin, Germany;

Objective: Genetic variants in the transcriptional regulator PR domain 16 (*PRDM16*) gene may cause cardiomyopathy. Recently, early pathological events associated with the *PRDM16* cardiomyopathy were uncovered in heterozygous cleft secondary palate 1 mice ($Prdm16^{csp1/wt}$). Here, we analyze the cardiac phenotype of heartspecific heterozygous and homozygous *Prdm16*deficient mice.
Method: Heartspecific *Prdm16* inactivation was achieved with the Cre/loxPsystem using the Crerecombinase under control of the Nkx2.5 promoter. Cardiac function of heterozygous and homozygous male and female $Nkx2.5Cre;Prdm16^{flox/flox}$ mice was characterized by transthoracic echocardiography. Analysis of cardiac tissue was performed by RNA sequencing and by histological examination of picrosirius redstained sections. All animal experiments conformed to the German animal protection act.
Results: Homozygous $Nkx2.5Cre;Prdm16^{flox/flox}$ mice developed hypoplastic hearts at postnatal day 5, and approximately 40% died spontaneously within two months after birth. Echocardiography revealed significantly diminished cardiac output, stroke volume, and ejection fraction in female homozygous $Nkx2.5Cre;Prdm16^{flox/flox}$ mice at four months of age compared to wildtype controls. Relative total heart and left ventricle weights were increased in $Nkx2.5;Prdm16^{flox/flox}$ mice compared to wildtype animals suggesting cardiac hypertrophy. Heart tissue of $Nkx2.5;Prdm16^{flox/flox}$ mice showed fibrosis. Expression analysis of natriuretic peptide A (*Nppa*), a marker of cardiac stress and indicator of heart failure, demonstrated marked *Nppa* upregulation in the left ventricle myocardium of $Nkx2.5;Prdm16^{flox/flox}$ mice.
Conclusion: Homozygous heartspecific *Prdm16* inactivation in mice induces severe cardiac dysfunction. Loss of *Prdm16* causes cardiac hypoplasia during development, which converts to cardiac hypertrophy in young adulthood.

OC 10 FLOW of Connections: Neurophysiology

OC1001

Neocortical expansion gives rise to dense synaptic connectivity onto extratelencephalic projection neurons in human layer 5

Franz Xaver Mittermaier; Sabine Grosser [1]; Emilia Thoma; Henrik Alle; Jörg Rolf Paul Geiger Institut für Neurophysiologie, Charité - Universitätsmedizin Berlin, Berlin, Germany; [1] Institut für integrative Neuroanatomie, Charité - Universitätsmedizin Berlin, Berlin, Germany;

Objective: The human neocortex is considerably expanded compared to that of the mouse – the primary model species in neuroscience. This raises the question of how synaptic circuit rules identified in the mouse scale to the human neocortex. Here, we addressed this in layer 5 (L5), one of the most extensively studied microcircuits in rodents. We examined how neocortical expansion alters this microcircuit and whether the canonical directional connectivity from intratelencephalic (L5IT) onto extratelencephalic (L5ET) pyramidal neurons is preserved in humans.
Method: We performed multineuron patchclamp recordings in acute brain slices obtained during neurosurgeries. A total of 221 pyramidal neurons were recorded and classified as L5IT or L5ET celltypes using transcriptomicinformed electrophysiological features. Synaptic connectivity, dendritic morphology, spine density, and secondorder network motifs were analyzed and compared with rodent data.
Results: The strong directional connectivity from L5IT onto L5ET neurons, observed in rodents, is perserved in humans. Human L5IT neurons connect onto L5ET neurons with a high connection probability of 22.4%, whereas connectivity in the reverse direction is sparse with less than 3%. Due to the disproportionate expansion of the L5IT population in humans, individual L5ET neurons integrate substantially more L5IT inputs compared to their rodent counterparts. Human L5ET neurons exhibited elongated dendrites and markedly increased spine numbers, supporting enhanced synaptic convergence. Network analyses further demonstrated enriched convergent and directed connectivity motifs within the human L5 circuit.
Conclusion: The canonical feedforward IT→ET wiring rule is conserved in the human L5 microcircuit. The disproportionate expansion of the human L5IT population gives rise to increased synaptic convergence onto L5ET neurons. Therefore human L5ET neurons are “giant integrators”, which may support enhanced combinatorial processing and contribute to advanced human cognitive abilities.

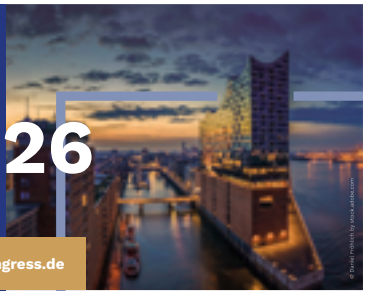

OC 10 FLOW of Connections: Neurophysiology

OC1002

Weak evidence for functional division into medial and lateral pain system from correlating EEG with psychophysical data

Ulf Baumgaertner; Pauline Kraus; Dominika Sulcova; Edoardo Arcuri
ICAN Institute of Affective and Cognitive Neuroscience, MSH Medical School Hamburg, Hamburg, Germany;

Objective: Pain is a multimodal sensation that includes both sensory and affective components. The brain regions activated by nociceptive stimuli include parts of the socalled lateral system and the medial system, which are believed to be primarily responsible for processing these two components. This study uses EEG source analysis to investigate whether the brain activation of lateral parts of the system (S1, operculoininsular cortex) triggered by pain stimulation correlates more strongly with subjective sensory pain assessment, and whether the activation of medial structures (mid cingulate gyrus) correlates more strongly with the affective pain component.
Method: In an exploratory crosssectional study, 30 participants were stimulated with nociceptive laser stimuli on the back of the hand (2 sets of 30 stimuli per hand), while the resulting brain activity was continuously recorded using a 64channel EEG. Participants rated their subjective pain sensation on the Sensory and Affective Pain Scale (SES), which includes a list of sensory and affective pain components; their ratings yielded a sensory and an affective pain score. In addition, participants were asked to provide an overall rating of overall pain intensity. The laserevoked potentials (LEPs) were averaged and fed into the source analysis (BESA). A 4source model was created based on the grand mean (one source in S1, two bilateral operculoinsular sources, one source in the middle cingulate gyrus), and the individual source potential curves were then correlated with the SES scores (sensory and affective) and the global intensity score.
Results: Laser stimuli were painful in all cases (25.8 ±11.4 out of 100, mean ± SD). The 4source model had a high goodness of fit (87% variance explained) and was therefore suitable for further analysis. The overall subjective pain intensity was correlated with the overall EEGsurface activity (GFP; Spearman's rho 0.36, $p = 0.05$). No significant correlation between source activity in the lateral system (S1 activity) with sensory scores, while a trend was detected between mid cingulate activity and affective scores (Spearman's rho 0.34, $p = 0.09$), not sensory scores.
Conclusion: As a nonspecific measure, the LEP global field power reflects subjective pain intensity. Apart from a weak association of one (medial) region's activity with affective ratings, no clear functional division into lateral and medial system could be shown.

OC 10 FLOW of Connections: Neurophysiology

OC1003

Close but Not Ready: Unexpected Ultrastructural Correlates of Synaptic Release Probability

Maximilian Zettner; Robert Jacobi; Martin Pauli; Christian Stigloher [1]; AnnaLeena Sirén; Manfred Heckmann; Kristina Lippmann [2]
Neurophysiology, Institute of Physiology, University of Würzburg, Würzburg, Germany; [1] Biocenter, University of Würzburg, Würzburg, Germany; [2] Carl Ludwig Institute for Physiology, University of Leipzig, Leipzig, Germany;

Objective: The release probability (pr) of synaptic vesicles (SVs) close to the Active Zone (AZ) membrane (<30 nm) determines synaptic responsiveness and strength, influencing presynaptic plasticity and behavior. Yet what determines pr ultrastructurally remains unclear. We compared the Parallel Fiber (PF)–Purkinje cell (PC) synapse, which exhibits moderate pr and shortterm facilitation, with the Climbing Fiber (CF)–PC synapse, which shows very high pr and shortterm depression - differences that have long puzzled neuroscientists and whose ultrastructural basis a prior serial scanning electron microscopy study failed to resolve.
Method: Using focusedion beam milling and serial liftout with cryogenic electron tomography (cryoET) of highpressurefrozen acute mouse brain slices, we analyzed both synapse types in a nearnative state at unprecedented resolution. Structural information was extracted using a semiautomated pipeline combining machinelearning and thresholdbased segmentation.
Results: We found that SVs in PFPC synapses are positioned closer to the AZ membrane (8.0 nm) than in CFPC synapses (9.9 nm) — counterintuitively, given the higher pr of CF synapses. However, SVs in CF synapses are bound by smaller tethering complexes oriented more directly beneath the SVs, rather than around them, suggesting an ultrastructural correlate for their higher pr. Additionally, CF SVs are located closer to the AZ center (see also contribution by Jacobi et al.).
Conclusion: Our findings highlight how the ultrastructural organization of the fusion machinery and SVs within the AZ together determine p_r, with implications for synaptic plasticity and synaptopathies.

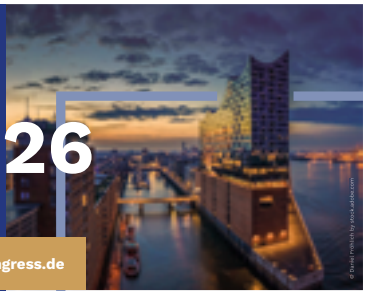

OC 10 FLOW of Connections: Neurophysiology

OC1004

Noiseinduced cochlear synaptopathy and synaptic plasticity in a gainoffunction mouse model for the $Ca_V1.3$ Ca^{2+} channel in inner hair cells

Jutta Engel; Kerstin Blum; Philipp Fischer; Simone Kurt
Biophysics, CIPMM, Saarland University, Homburg, Germany;

Objective: Voltageactivated $Ca_V1.3$ Ca^{2+} channels mediate Ca^{2+} influx for synaptic transmission in cochlear inner hair cells (IHC) after soundinduced depolarization. Information is transmitted by the ~18 ribbon presynapses of an IHC each of which is connected to a spiral ganglion neuron. Noiseinduced cochlear synaptopathy is characterized by irreversible loss of synapses between inner hair cells (IHC) and spiral ganglion neurons, which may occur even without an increase in hearing thresholds. To unravel mechanisms of synapse death, we studied 'HA' mice $Ca_V1.3DCRD^{HA/HA}$ with a modified $Ca_V1.3$ channel, which carries a 30 % larger peak Ca^{2+} current into IHCs. We hypothesized that increased Ca^{2+} influx per se would cause damage at IHC synapses in HA mice, and that a noise trauma would aggravate this process.
Method: Eightweekold C57BL/6N wildtype (WT) and HA mice were exposed to 816 kHz noise at 106 dB SPL for 2 h. Auditory brainstem responses (ABR) were assessed before, directly after and 28 days post trauma. At this endpoint, number, size, and pairing of IHC presynaptic (CtBP2positive) ribbons and postsynaptic AMPA receptor scaffold (Homer-1positive) clusters were analyzed along the cochlea. Nonexposed control groups of WT and HA mice served as controls.
Results: Without trauma, IHCs of HA mice showed normal numbers of ribbons yet a 30% reduction in size in the apical, medial and midbasal region compared to WT. In the basal region, ~8 ribbons/IHC were missing.
Four weeks after a trauma, both genotypes showed a permanent threshold shift (PTS) from 8 kHz to 45 kHz and reduced ABR wave I amplitudes, which indicates loss of functional IHC synaptic connections. Numbers of ribbons and postsynapses were reduced similarly as in WT mice in the medial and midbasal region, with up to 50 % ribbon loss. Surviving ribbons of HA mice were enlarged and paired with a postsynapse. Noise trauma left up to 46 orphan postsynapses per IHC (midbasal in either genotype indicating that postsynapses were more stable than ribbons.
Conclusion: These data confirm the susceptibility of ribbon synapses and ABR wave I amplitudes to a noise trauma of 106 dB SPL. In both WT and HA mice, IHC postsynapses were more resistant than ribbons to the noise trauma applied, see Blum et al., Front Cell Neurosci 2024. Reduction of ribbons sizes before and normalization of sizes after the trauma in HA mice demonstrates plastic changes in ribbon structure. The degeneration of a subset of ribbons in basal IHCs of HA mice without any acoustic trauma plus the fact that a trauma did not further reduce ribbon numbers suggests that a subset of ribbons had degenerated by Ca^{2+} excitotoxicity before.

Supported by DFG SFB 894.

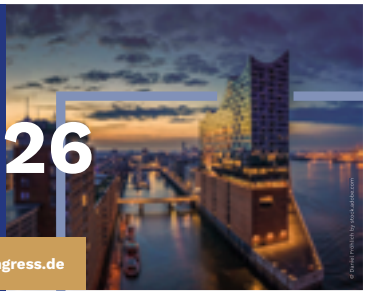

OC 10 FLOW of Connections: Neurophysiology

OC1005

Cortical extracellular pH shifts dynamically across brain states in mice

Verena Untiet
Division of Astrocyte Driven Ionostasis, Center for Translational Neuromedicine, Universtiy of Copenhagen, Copenhagen, Denmark;

Objective: Extracellular brain pH (pH) is tightly regulated, yet whether it varies across natural behavioural states and contributes to cortical activity is unclear. We asked how pH changes across sleepwake cycles and how these dynamics relate to autonomic physiology and cortical state transitions.
Method: All procedures conformed to European Directive 2010/63/EU and were approved by the Danish Animal Inspectorate (Dyreforsøgstilsynet). Adult male and female C57BL/6JRj and heterozygous TH::Cre mice were used. Surgeries on 710 weekold mice were performed under isoflurane (induction 4%, maintenance 1.5% in O2; buprenorphine 0.05 mg/kg i.p., lidocaine 2 mg/kg s.c., carprofen 5 mg/kg s.c. for analgesia). pH? was recorded in somatosensory cortex by fiber photometry of an extracellularly targeted, astrocyteexpressed pH sensor (AAV2GFAPILP.pHuji.PTD) calibrated to absolute pH using H?selective microelectrodes during graded hypercapnia. EEG/EMG were recorded simultaneously for vigilancestate scoring. Respiration was monitored with a nasal thermocouple; blood pH was imaged in vivo with i.v. FITCdextran (2000 kDa, pHsensitive) corrected by Oregon Greendextran (70 kDa). Data are mean ± SEM; paired/Wilcoxon tests for two conditions, repeatedmeasures ANOVA with Šídak correction for multifactor designs, Pearson's r for correlations; significance at $p<0.05$.
Results: Cortical pH was statedependent, highest in wake and lowest in REM (microelectrode: 7.27±0.18 wake, 7.26±0.18 NREM, 7.21±0.20 REM; n=6 mice; matched by photometry in n=16 mice; $p<0.05$). pH correlated positively with pupil diameter across transitions ($R^2=0.68$, $p=0.0003$). Across NREM→wake transitions, ΔpH correlated negatively with the change in delta power ($r=–0.703$, $p=8.78\times10$; 51 transitions, n=5 mice). Arousalassociated state transitions were accompanied by rapid cortical alkalinisation, accelerated breathing, and elevations in arterial blood pH. Respiratory and bloodpH dynamics were temporally correlated across trials (Pearson $r=0.66$, $p<0.001$; 24 trials, n=5 mice).
Conclusion: Cortical pH shifts dynamically across behavioural states and closely tracks changes in respiration, blood pH, and cortical activity. These findings identify extracellular pH as a physiological signal linking autonomic state transitions to cortical network dynamics and brainstatedependent activity.

OC 10 FLOW of Connections: Neurophysiology

OC1006

Lateral hypothalamic neurotensinexpressing neurons regulate the prioritization of drinking, feeding and socializing

Chantal Wissing; Anne Petzold [1]; Hanna van den Munkhof; Ilia Komoltsev; Tatiana Korotkova Institute for Systems Physiology, University of Cologne, Köln, Germany; [1] European Neuroscience Institute, A Joint Initiative of the University Medical Center Göttingen and the Max Plank Institute for Multidisciplinary Sciences, Göttingen, Germany;

Neuronal populations within the lateral hypothalamus (LH) play essential roles in coordinating motivational drives and guiding adaptive behaviors. Neurotensinexpressing LH (NtsLH) neurons have emerged as important integrators of internal state signals and external sensory cues. Here, we combined in vivo calcium imaging, circuit mapping, and optogenetic manipulations to investigate how NtsLH neurons regulate competing behaviors related to feeding, drinking, and social interaction.

NtsLH neurons displayed distinct activity patterns during approach and consumption of food and water, and their responses dynamically shifted with hunger state, indicating a role in balancing hydration and energy needs under metabolic pressure. Activation of NtsLH neurons promoted water intake and modestly increased feeding, biasing behavior toward hydration when animals were hungry. These neurons also encoded socially relevant stimuli, responding preferentially to unfamiliar conspecifics, and their activation reduced social exploration, suggesting contextdependent modulation of social behavior.

Anterograde tracing and optogenetic stimulation revealed that NtsLH projections to anterior thalamic regions support the integration of motivational drive with spatially directed foraging. Stimulation of this pathway enhanced responsiveness to foodpredictive cues, navigation toward food sources, and influenced the prioritization of social versus feeding behaviors depending on internal state and resource availability.

Together, these findings demonstrate that NtsLH neurons form a multifunctional circuit that coordinates survivalrelated behaviors by integrating hunger, hydration, and social context. This work provides a unifying framework for understanding how the LH contributes to adaptive decisionmaking when animals face competing motivational demands.

We gratefully acknowledge support by the ERC consolidator grant HypFeedNet, DFGCRC1451 (to TK, AP) and EXC2030CECAD.

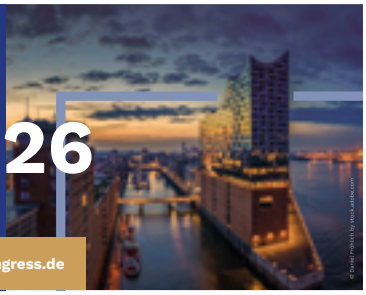

OC 11 FLOW of Blood: Vascular physiology

OC1101

p90 Ribosomal S6 kinase (RSK) differentially contributes to agonistinduced vasoconstriction in human resistance arteries

Jirko Kühnisch; Simon JasinskiBergner; Sabine Summer; Lubomir Lubomirov [1]; Thomas Kalinski [2]; Hendrik Borgmann [3]; Roland Becker [4]; Svetlana Tschaikovski [5]; René Mantke [6]; Olaf Grisk Institute of Physiology, Medical School of Brandenburg, Brandenburg, Germany; [1] Biomedical Center for Education and Research (ZBAF), Institute of Physiology and Pathophysiology, Witten/Herdecke University, Witten, Germany; [2] Institute of Pathology, Medical School of Brandenburg, Brandenburg, Germany; [3] Institute of Urology, Medical School of Brandenburg, Brandenburg, Germany; [4] Alterstraumatologie, Zentrum für Orthopädie/Unfallchirurgie, Universitätsklinikum Brandenburg, Brandenburg, Germany; [5] Institute of Obstetrics and Gynecology, Medical School of Brandenburg, Brandenburg, Germany; [6] General and Visceral Surgery, Medical School of Brandenburg, Brandenburg, Germany;

Objective: RSKs modify cell functions including motility in response to extracellular signals. RSK2 phosphorylates smooth muscle myosin regulatory light chain at Ser19, activates nitric oxide synthase (NOS)3 and inhibits NOS1. We tested if pharmacological RSK inhibition blunts agonistinduced human resistance artery constriction.
Method: Small arteries from human kidney, skeletal muscle, uterus and mesentery elective surgery samples were investigated by small vessel myography according to the World Medical Association Declaration on principles of biomedical research involving humans. The effects of the RSK2specific inhibitor LJI308 and the panRSK inhibitor BID1870 on phenylephrine (PE)- and endothelin1 (ET1)induced vasoconstriction were tested.
Results: LJI308 did not affect PEinduced intrarenal artery constriction. Endothelial function was preserved. PanNOS inhibition did not alter the responses to RSK2 inhibition. In skeletal muscle arteries, LJI308 shifted the PE concentration response curve to the right (logEC50 6.49 ± 0.15 mol/l in controls vs. 6.0 ± 0.13 mol/l in LJI308treated, $p < 0.05$, $n = 1213$ vessels, 8 patients). PE induced weak and variable vasoconstrictions in uterine and mesenteric arteries while ET1 potently constricted these vessels. BID1870 did not affect ET1induced uterine artery constriction but reduced the area under the ET1 concentration response curves of mesenteric arteries by 24 percent vs. controls ($p < 0.05$, $n = 1920$ vessels, 10 patients).
Conclusion: In the human vasculature, the intensity of $\alpha_1$adrenoceptormediated vasoconstriction and the sensitivity of agonistinduced vasoconstriction to RSK inhibition depend on the vascular bed. The findings support that in humans, smooth muscle phenotype varies between resistance arteries of different vascular beds and that RSKs contribute to arterial tone regulation in a tissuedependent manner.

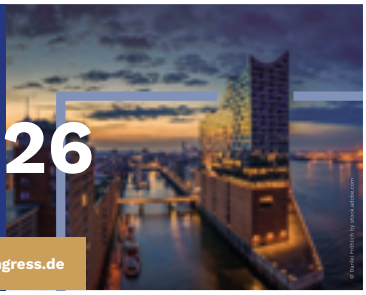

OC 11 FLOW of Blood: Vascular physiology

OC1102

Mechanisms of Piezo1 dependent relaxation in mouse tail artery

Alina Maslakova; Peggy Becker; Birgit Zatschler; Stephan Speier; Michael Mederos y Schnitzler [1]; Irakli Kopaliani; Andreas Deußen
Institut für Physiologie, Universitätsklinikum Carl Gustav Carus, Technische Universität Dresden, Dresden, Germany; [1] Pharmacology and Toxicology, LMU München, München, Germany;

Objective: Piezo1 is a mechanosensitive cation channel implied in diverse physiological processes, including regulation of vascular function. However, the mechanism of Piezo1 in regulation of vascular tone is poorly understood.
Method: Caudal artery segments isolated from C57BL/6JOlaHsd (Harlan) mice and preconstricted with phenylephrine or U46619 were studied in a Mulvany myograph. Immunohistochemistry staining of frozen 7 µm thick caudal artery sections was done following the three major steps: tissue preparation and PFAbased fixation, tissue sectioning, and fluorescent staining.
Results: Pharmacological activation of Piezo1 with Yoda1 (10?7–10?5 mol/L) induced concentrationdependent relaxations (max. relaxation ~30%, n=95). This response was significantly ($p<0.0001$) attenuated after endothelial removal or inhibition of Piezo1 channel with tubeimoside. Acetylcholine and sodium nitroprusside were used as control stimuli for endotheliumdependent and endotheliumindependent relaxations, respectively. Experiments revealed that Yoda1induced relaxation was unaffected by the eNOS inhibitor LNMMA. Further pharmacological inhibition studies demonstrated a functional interplay between Piezo1 and CYP450, Cx43, TRPV4, K_{ATP}, and largeconductance $K_{Ca}1.1$ channels. Yoda1induced relaxation was significantly attenuated following inhibition of above mentioned downstream signaling components, including the CYP450 inhibitor sulfaphenazole (max. relaxation ~18%, n=18, $p<0.0001$), the Cx43 inhibitor carbenoxolone (max. relaxation ~20%, n=22, $p<0.0001$), the TRPV4 inhibitor RN1734 (max. relaxation ~20%, n=3, $p<0.01$), the K_{ATP}channel inhibitor glibenclamide (max. relaxation ~14%, n=5, $p<0.0001$), and largeconductance $K_{Ca}1.1$ channel inhibitors iberiotoxin and charybdotoxin (max. relaxation ~17%, n=15 and n=13, respectively, $p<0.0001$). Immunohistochemical analysis of mouse tail artery sections further demonstrated close spatial localization of Piezo1 and TRPV4 channels, alongside endothelialspecific expression of K_{ATP}channels, thereby supporting our functional findings.
Conclusion: Pharmacological activation of Piezo1 by Yoda1 in mouse tail artery elicits an endotheliumdependent but NOindependent vasorelaxation, which involves coordinated functional interactions of Piezo1 with endothelial TRPV4, CYP450, as well as K_{ATP}channels and, via gap junction Cx43, activation of smooth muscle $K_{Ca}1.1$ channels.

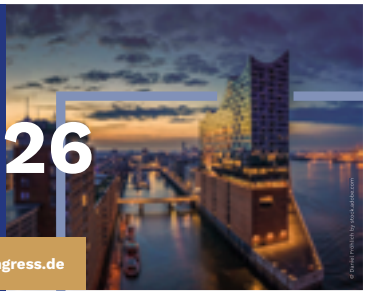

OC 11 FLOW of Blood: Vascular physiology

OC1103

Targeting SGLT2 in SaltSensitive Hypertension

Olha Kravtsova; Timo Rieg; Alexander Staruschenko
Molecular Pharmacology and Physiology, University of South Florida, Tampa, United States;

Objective: Sodiumglucose cotransporter 2 inhibitors (SGLT2i), initially developed for glycemic control in type 2 diabetes, have since been shown to provide substantial cardiovascular and renal protection. However, the specific effects and mechanisms of SGLT2i on saltsensitive hypertension (SS HTN) remain poorly understood. This study aimed to determine the effects of SGLT inhibition on SS HTN and to identify the underlying renal and systemic mechanisms involved.
Method: Eightweekold male and female Dahl saltsensitive (SS) rats were treated with dapagliflozin (Dapa; 2 mg/kg/day) or sotagliflozin (Sota; 30 mg/kg/day) for 3 weeks while maintained on a highsalt diet (4% NaCl). In addition, an SGLT2 knockout strain was generated on the Dahl SS background ($SS^{SGLT2/}$). Blood pressure was continuously monitored by radiotelemetry. Comprehensive transcriptomic, proteomic, and lipidomic analyses were performed on renal tissues and biological fluids to identify molecular mechanisms associated with SGLT inhibition.
Results: Our previous studies demonstrated that dapagliflozin (Dapa) prevented the development of saltsensitive hypertension (SS HTN) in both male and female Dahl SS rats without altering sodium channel expression or the reninangiotensinaldosterone system. When administered therapeutically after hypertension was established, Dapa still lowered blood pressure, although the effect was less pronounced. Compared with selective SGLT2 inhibition, dual SGLT1/2 inhibition produced a greater reduction in mean arterial pressure (MAP; Sota vs. vehicle: 126 ± 2 vs. 157 ± 5 mmHg in males and 126 ± 3 vs. 167 ± 10 mmHg in females), while heart rate remained unchanged. Under a normalsalt diet (0.4% NaCl), Sota had no effect on MAP or heart rate. Relative to Dapa, Sota reduced body weight, increased urinary Na^+ and Clexcretion, and produced greater fractional glucose excretion. $SS^{SGLT2/}$rats showed markedly greater diuresis (17 ± 1 vs 10 ± 1 ml/24h) and ~25% higher kidney weight. On the HS diet, $SS^{SGLT2/-}$ rats exhibited a significant attenuation of hypertension, with lower MAP on day 28 (156 ± 5 vs 174 ± 8 mmHg, p=0.01). $SS^{SGLT2/-}$ animals showed elevated urinary glucose and calcium excretion, while sodium, potassium, and chloride remained $SS^{SGLT2/}$ unchanged. GFR was not significantly different between WT and . Multiomics analyses of kidneys from SGLT inhibitortreated animals revealed enrichment of lipid metabolism and inflammatory pathways.
Conclusion: Both genetic and pharmacological inhibition of SGLT2 significantly attenuated saltsensitive hypertension. Dual SGLT1/2 inhibition provided greater protection against SS HTN and renal injury compared with selective SGLT2 inhibition alone. These findings suggest distinct and additive mechanisms of SGLT inhibition and support further investigation into the underlying molecular pathways.

OC 11 FLOW of Blood: Vascular physiology

OC1104

Reduced βadrenoceptor function in parenchymal arterioles from glioblastoma in comparison with healthy human brain

Ruofei Ning; Elizaveta Melnikova; Ask Andersen; Christian Stæhr; Line Mathilde Brostrup Hansen; Mads Rasmussen [1]; Anders Rosendal Korshø [1]; Vladimir V. Matchkov Department of Biomedicine, Aarhus University, Aarhus, Denmark; [1] Department of Clinical Medicine, Aarhus University, Aarhus, Denmark;

Objective: Noradrenaline is widely used during neurosurgical anesthesia to maintain systemic blood pressure, but its effects on cerebral arteries remain debated. Human cerebral arteries express both α- and βadrenergic receptors, mediating vasoconstriction and vasorelaxation. The vascular responses to noradrenaline within the central nervous system have been reported to be variable. Adrenergic regulation of human brain parenchymal arteries has not been characterized in detail. Moreover, vascular remodeling and receptor imbalance in glioblastoma may further modify adrenergic signaling, potentially affecting local cerebral perfusion. The study aims to examine adrenergic vascular responses in glioblastomainfiltrated versus healthy human parenchymal arteries.
Method: Parenchymal arteries were isolated from surgical cortical biopsies obtained from glioblastoma patients. Cerebrovascular function was assessed ex vivo using isometric myography. Concentration–response curves to noradrenaline and the thromboxane A2 analog U46619 were generated with and without the βadrenoceptor inhibitor, propranolol (1 μM). Adrenergic receptor expression was analyzed by qPCR, and arterial wall structure was characterized immunohistochemically.
Results: Arteries from glioblastoma tissue exhibited smaller inner diameters compared with arteries from healthy brain tissue(HE) (P=0.026, n=48). Under control conditions, noradrenalineinduced contraction was greater in glioblastoma arteries than in HE (P=0.0001, extra sumofsquares Ftest). Maximal contractile responses were 0.36±0.01 mN/mm and 0.09±0.08 mN/mm in glioblastoma and HE, respectively (P=0.025). Despite the enhanced maximal response, the glioblastoma arteries were less sensitive to noradrenaline than HE ($logEC_{50}$: 6.60±1.4 vs. 7.27±0.14, respectively; P=0.017). βadrenoceptor inhibition with propranolol significantly potentiated noradrenalininduced contraction in HE (P=0.0005), increasing the maximal contractile response to 0.44±0.18 mN/mm without affecting noradrenaline sensitivity ($logEC_{50}$: 7.15±0.22). In contrast, propranolol had no effect on glioblastoma arteries. Gene expression analysis with qPCR demonstrated upregulation of the α1adrenoreceptor subtypes ADRA1B and ADRA1D in glioblastoma arteries compared with HE($P < 0.05$). Conversely, expression of the βadrenoreceptors ADRB1 and ADRB2 was reduced in glioblastoma arteries ($P < 0.05$), suggesting a shift toward enhanced vasocontractile signaling in glioblastomaassociated arteries.
Conclusion: Adrenergic regulation of human cerebral arteries is altered in glioblastoma, with increased αadrenergic and reduced βadrenoceptor contributions at both functional and transcriptional levels. These alterations may have important implications for noradrenaline as a vasopressor during neurosurgical anesthesia and for the management of cerebral perfusion in patients undergoing brain tumor surgery.

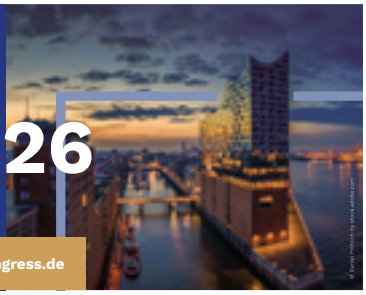

OC 11 FLOW of Blood: Vascular physiology

OC1105

Beta arrestin 1 is required for nitric oxidedependent vasorelaxation in pulmonary arteries in health and disease

Alexander Seidinger; Leonard F Lebender [1]; Michaela Matthey; Birte Dyck [2]; Evi Kostenis [3]; Volkmar Gieselmann [4]; Michael Adamzik [2]; Björn Koos [2]; Bernd K Fleischmann [1]; Daniela Wenzel Department of Systems Physiology, Institute of Physiology, Ruhr University Bochum, Bochum, Germany; [1] Institute of Physiology I, University of Bonn, Bonn, Germany; [2] Department of Anesthesiology, Intensive Care Medicine and Pain Therapy, Knappschaft Kliniken University Hospital Bochum, Bochum, Germany; [3] Molecular, Cellular, and Pharmacobiology Section, Institute of Pharmaceutical Biology, University of Bonn, Bonn, Germany; [4] Institute of Biochemistry and Molecular Biology, University of Bonn, Bonn, Germany;

Objective: Pulmonary hypertension (PH) is a severe disease characterized by increased pulmonary blood pressure due to sustained vasoconstriction and remodeling. The nitric oxide (NO)–soluble guanylate cyclase (sGC)–cGMP signaling pathway is central to vascular tone regulation and promotes smooth muscle relaxation. This study aims to identify the role of beta arrestin 1 (bArr1) as a potential modulator of NOsGC signaling in pulmonary arteries (PAs).
Method: We analyzed PA tone regulation in C57BL/6 (WT), bArr1/- and bArr2/- mice using isometric force measurements ex vivo. We examined cGMP production in isolated WT and bArr1/- PA smooth muscle cells (PASMCs) using ELISA and performed protein interaction assays in HEK cells and mouse intrapulmonary PAs. Finally, we analyzed typical PH parameters in WT, bArr1/- and smooth muscle specific bArr1 KO (SMA bArr1 KO) mice (carprofen 5 mg/kg s.c., 1.5 % isoflurane) in vivo.
Results: Isometric force measurements revealed impaired sodium nitroprusside (SNP)/NO-induced relaxation of PAs in bArr1/- mice compared to controls (pEC50: WT: 7.9±0.06, n=7; bArr1−/−: 7.3±0.08, n=7; bArr2−/−: 7.8±0.16, n=5; $p<0.01$ WT vs. bArr1−/−; oneway ANOVA). This was confirmed by reduced SNPdependent relaxation in functional lung slices of bArr1/ mice, as well as diminished cGMP production in bArr1/- PASMCs. The rightward shift of SNP doseresponse curves in bArr1/- PAs was unaffected by the PDE5inhibitor Sildenafil or the sGC stimulator BAY582667, but it disappeared after sGC activator BAY582667 treatment, highlighting the role of bArr1 in protecting sGC oxidation. Coimmunoprecipitation and pull-downassays in HEK cells (each n=3), as well as a proximity ligation assay in murine lung slices, revealed a direct interaction between bArr1, the sGC b1 subunit, and the sGC heme reductase Cyb5r3. Finally, the lack of bArr1 led to an increased right ventricular (RV) systolic pressure (WT: 21.2±0.1 mmHg, n=9; bArr1−/−: 23.7±0.6 mmHg, n=7; $p<0.01$; unpaired ttest), PA wall thickness, and RV hypertrophy. Similar results were obtained in SMA bArr1 KO mice, demonstrating the importance of bArr1 in PAs.
Conclusion: We identified bArr1 as a key molecular regulator of the NO–sGC–cGMP pathway and pulmonary vascular function. By linking scaffoldmediated protein interactions to the redox regulation of sGC, we provide a novel mechanism underlying vascular tone control.

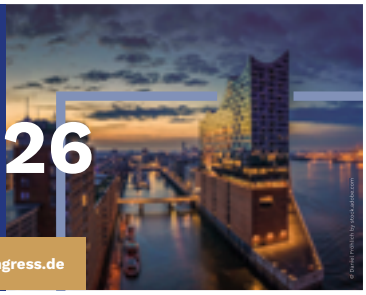

OC 11 FLOW of Blood: Vascular physiology

OC1106

The role of Perivascular Adipose Tissue and Endothelium in regulating the vascular tone activity: focusing on SIRT1

Yujiao Zhan; Shing Hei Darren Chan; Peichun Wang; Beijia Zhang; Yu Xu; Yu Li; Yu Wang Dept. of Pharmacology and Pharmacy, LKS Faculty of Medicine, University of Hong Kong, Pok Fu Lam, Hong Kong;

Objective: This study investigated the distinct regulatory roles of endothelial and adipose SIRT1 in vasodilatation and arterial stiffness modulation in a female mouse model of heart failure with preserved ejection fraction (HFpEF).
Method: Female wildtype (WT) mice and transgenic mice with endothelial (ECH363Y) or adipose tissue (AdiposeH363Y) specific overexpression of dominantnegative human SIRT1 mutant H363Y received 30 weeks of highfat diet (45 kcal% fat) plus LNAME (1 g/L) treatment to induce HFpEF. WT mice fed a standard chow diet served as controls. Cardiac diastolic function and aortic stiffness were evaluated via echocardiography and Doppler flow velocimetry. Endotheliumdependent vasodilatation of isolated aortae with or without perivascular adipose tissue (PVAT) was assessed using a Halpern–Mulvany myograph system.
Results: HFpEFchallenged WT mice displayed significantly higher pulse wave velocity than chowfed controls (4.76 ± 0.79 m/s vs. 3.16 ± 0.09 m/s, n=3–5, *P*=0.015). In aortic rings precontracted with 10^{8} M U46619, cumulative acetylcholine (10^{9} to M)induced$_{10^{4.5}}$ vasodilatation was impaired in all HFpEF groups versus controls. PVAT presence effectively rescued AChmediated vasodilatation in ECH363Y arteries. In contrast, PVAT failed to restore vascular function in AdiposeH363Y mice, which exhibited the most severe endotheliumdependent vasodilatation impairment among all groups, with a higher logEC50 value (4.8±1.3, n=3) of the vasodilatation curves than WT (6.3±0.08, n=3) and ECH363Y mice (6.3±0.27, n=3).
Conclusion: PVAT confers protective arterial regulatory effects and compensates for vascular dysfunction caused by endothelial SIRT1 deficiency in HFpEF. Adipose SIRT1 dysfunction impairs endotheliumdependent vasodilatation and abolishes the vascular regulatory activity of PVAT.

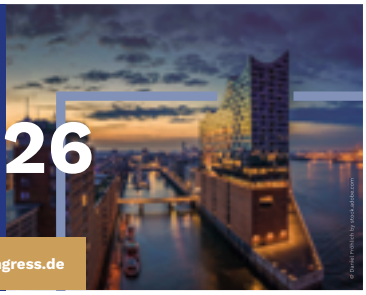

OC 12 FLOW of Signals: & Pathophysiology

OC1201

Cadmium Triggers Lysosomal Exocytosis via the Endo/Lysosomal Ion Channel TRPML1 in Renal Pathophysiology

Kaya Elisa Witte; Moritz Spallek; WingKee Lee
Physiology and Pathophysiology of Cells and Membranes, Medical School OWL, Bielefeld University, Bielefeld, Germany;

Objective: Cadmium (Cd) exposure remains a global health concern due to its accumulation in the kidney, its role in nephrotoxicity and carcinogenesis. The renal proximal tubule is particularly vulnerable due to intensive turnover of macromolecules and ions, which is tightly regulated by endo- and exocytic pathways. The endolysosomal cation channel TRPML1 (*MCOLN1*) is a key regulator of exocytosis, yet its response to Cd is unknown. This study investigates whether Cd activates TRPML1 and thereby promotes lysosomal exocytosis as an early adaptive stress response.
Method: Human proximal convoluted tubule cells were exposed to $CdCl_2$ under serumfree conditions, while TRPML1overexpression (OE) was established by transient transfection with HA/YFPtagged human *MCOLN1* in pcDNA3.1. Lysosomal dynamics were assessed by immunocytochemistry, livecell imaging, and AIbased software for vesicle tracking. Plasma membrane (PM) localization of TRPML1 and lysosomeassociated membrane glycoprotein 1 (LAMP1) was analyzed by biotinylation and immunoblotting. Cellular stress responses were evaluated via trypan blue exclusion and protein expression.
Results: Cd exposure induced lysosomal scattering and increased lysosome–nucleus distance (13.5µm vs 12.0µm) in parallel to rapid, transient upregulation of lysosomal biogenesis transcription factor EB (TFEB) and TRPML1. In Cdtreated TRPML1OE, lysosomal spreading was augmented and the number of dead cells ($2.3x10^4$ vs $3.6x10^4$) was reduced compared to vector controls ($2.8x10^4$ vs $5.1x10^4$). Furthermore, Cd transiently increased TRPML1/LAMP1 localization at PM (45.7% vs 33.6%), peaking after 5min of treatment and returning to controllike distribution by 60min. Surface biotinylation assay confirmed higher PM TRPML1/LAMP1 abundance, comparable to the TRPML1 agonist MLSA5 and consistent with enhanced lysosomal exocytosis. Considering TRPML1 can be activated by reactive oxygen species and Cd is known to elicit oxidative stress, the impact of the ROS scavenger Tempol was examined. In the presence of Tempol, cell viabilities decreased after 24h of Cd even in TRPML1OE (Cd 89.5% vs Cd/Tempol 70.6%), suggesting a modulatory role of ROS in the TRPML1mediated lysosomal response to Cd.
Conclusion: These findings indicate that Cd transiently enhances lysosomal biogenesis and exocytosis in renal cells. We propose that Cdtriggered TRPML1 activation contributes to an early adaptive response, potentially influencing the progression of Cdinduced nephrotoxicity.

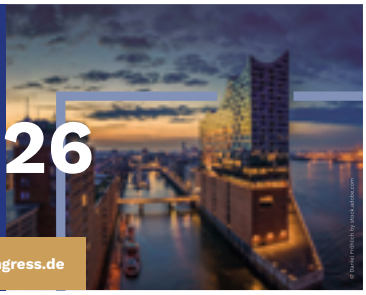

OC 12 FLOW of Signals: Signalling & Pathophysiology

OC1202

A prion proteintargeting antibody with an unparalleled dual effect against neurodegenerative protein misfolding diseases

JosephineElisabeth Pippi; Feizhi Song [1]; Behnam Mohammadi [1]; Mohsin Shafiq [1]; Edda Thies [1]; Julia Bär [2]; Lars Röttger [1]; Andreu Matamoros Angles [1]; Hela Uplegger [3]; Björn Rissiek [4]; Alexander Schwarz [5]; Michaela Schweizer [6]; Emiliano Biasini [7]; Melissa Graewert [8]; Clement Blanchet [8]; Janine Kamps [9]; Valerija Kovac [10]; Vladka Curin Serbec [10]; Berta Puig [3]; Katarzyna Grochowska [11]; Marcel S. Woo [12]; Marina Mikhaylova [2]; Jörg Tatzelt [9]; Adriano Aguzzi [13]; Markus Glatzel [1]; Hermann Clemens Altmeppen [1]

Center for Diagnostics, Neuropathology, University Medical Center HamburgEppendorf (UKE), Hamburg, Germany; [1] Center for Diagnostics, Institute of Neuropathology, University Medical Center HamburgEppendorf (UKE), Hamburg, Germany; [2] Institute of Biology, Humboldt University Berlin, Berlin, Germany; [3] Department of Neurology, ERSI group, University Medical Center HamburgEppendorf (UKE), Hamburg, Germany; [4] Institut für Immunologie, Universitätsklinikum HamburgEppendorf, Hamburg, Germany; [5] Chemistry Department / MINT Faculty, Institute of Nanostructure and Solid State Physics, University Hamburg, Hamburg, Germany; [6] Zentrum für Molekulare Neurobiologie, Universitätsklinikum HamburgEppendorf, Hamburg, Germany; [7] CIBIO, Dulbecco Telethon Laboratory of Prions and Amyloids, University of Trento, Trento, Italy; [8] European Molecular Biology Laboratory (EMBL), Hamburg, Germany; [9] Department Biochemistry of Neurodegenerative Diseases, Institute of Biochemistry and Pathobiochemistry, Ruhr University Bochum, Bochum, Germany; [10] Blood Transfusion Center of Slovenia, Ljubljana, Slovenia; [11] Center for Molecular Neurobiology Hamburg (ZMNH), University Medical Center HamburgEppendorf (UKE), Hamburg, Germany; [12] INIMS, UKE, Hamburg, Germany; [13] Institute of Neuropathology, University of Zurich, Zürich, Switzerland;

Objective: The prion protein (PrP) is mostly known for its key role in transmissible prion diseases in humans and other mammals. It also is a high affinity neuronal receptor for harmful protein species excessively generated in more common neurodegenerative proteinopathies such as Alzheimer's (AD) and Parkinson's disease. These progressive diseases remain inevitably fatal as causative cures are still lacking to date. Novel targets/approaches enabling effective therapies are thus urgently required.
Reducing PrP levels is considered a promising approach and intensively investigated by various means. We showed that several PrPdirected antibodies increase its proteolytic cell surface release ('shedding') by the metalloprotease ADAM10, whereas one particular IgG induces large PrP:antibody clusters at the membrane, which are rapidly endocytosed and send for lysosomal degradation. We now identified a unique antibody combining both aspects and aim at an indepth characterization of its mode(s) of action and therapeutic potential.

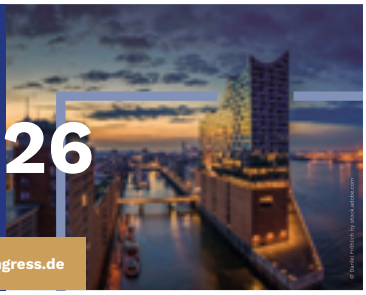

OC1202

A prion proteintargeting antibody with an unparalleled dual effect against neurodegenerative protein misfolding diseases

Method: combined with results (see below)**Results:** The dual effect of (i) elevated proteolytic PrP shedding and (ii) pronounced surface cluster formation, uptake and degradation was confirmed by western blot in several human and mouse cell lines, rodent primary cells and brain slice cultures (BSC). We performed qPCR and a battery of toxicity/viability assays to exclude potential transcriptional and adverse effects, respectively. We found no altered cellular PrP release via extracellular vesicles (EVs) using stateoftheart EV isolation and nanoparticle tracking analyses. Live fluorescent, immunoelectron, and atomic force microscopy, as well as protein aggregation (liquidliquid phase separation [LLPS] assay) and structural studies (e.g., size exclusion chromatographycoupled smallangle Xray scattering) were employed to yield mechanistic insight. Evidence for beneficial effects of the candidate against ADassociated Aβ toxicity was so far found in a phosphoCREB nuclear translocation assay in rat neurons and by increased microglia cell bodies in murine BSC. We also found reduced formation of resistant and infectious prion particles in chronically prioninfected neuronal cells.
Conclusion: Our candidate's dual effect is unique among several PrPdirected antibodies we have tested thus far. It is conserved in several models and first data support (neuro)protective effects. Future functional assays in diseaserelevant models (human organoids and mouse models) will reveal whether it really holds treatment potential.

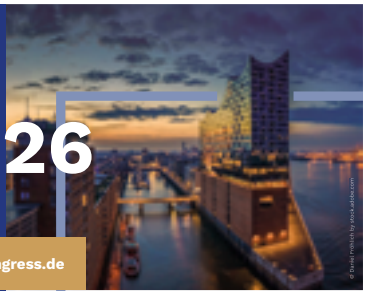

OC 12 FLOW of Signals: Signalling & Pathophysiology

OC1203

ANP/cyclic GMPmediated heartadrenal connection prevents us getting salty

Zihou Liu; Franziska Werner; Julia Sudnitsyna; Tamara Potapenko; Marco Abeßer; Viacheslav O. Nikolaev [1]; Michaela Kuhn
Physiology, Julius Maximilian University Würzburg, Würzburg, Germany; [1] Institute of Experimental Cardiovascular Research, University Medical Center HamburgEppendorf, Hamburg, Germany;

Objective: Cardiac atrial natriuretic peptide (ANP) maintains intravascular volume homeostasis through coordinated endothelial and renal effects. In cultured bovine adrenal cells ANP inhibits acute ACTHstimulated cAMP levels and aldosterone release through activating the guanylyl cyclaseA (GCA)/cGMP pathway and the cAMPdegrading cGMPstimulated phosphodiesterase (PDE)2A. To dissect the physiological relevance, we generated mice with deleted (KO) GCA receptor or downstream PDE2A in zona glomerulosa (ZG) cells. **Results:** Already under normalsalt diet ZGGCAKO mice had expanded ZG, more aldosterone synthaseexpressing cells, elevated plasma aldosterone and mild hypokalemia. ZG hyperplasia was associated with activated MAPK ERK and p38 signaling. In control mice, highsalt diet reduced ZG area and aldosterone production. In ZG GCA KO littermates, these responses were blunted, provoking hypervolemic hypertension. Surprisingly, ZG PDE2A KO mice did not exhibit such alterations. In cultured human adrenal cells ANP prevented Angiotensin IIinduced MAPK activation, proliferation, and aldosterone synthase expression through activating cGMPdependent protein kinase I.
Conclusion: We conclude that ANPmediated heartadrenal communication adapts ZG cell growth and aldosterone release to dietary salt/volume load. In human aldosteroneproducing adenomas, GCA expression is reduced, which may contribute to excessive cell growth and aldosterone production. Reinforcing ANP/GCA signaling with recently developed GCA agonists can benefit patients with hyperaldosteronism and therapyresistant hypertension.

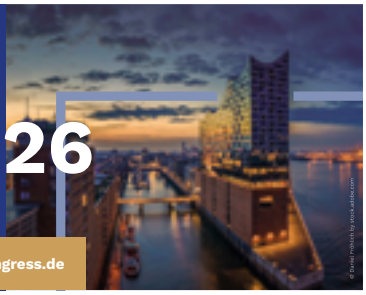

OC 12 FLOW of Signals: Signalling & Pathophysiology

OC1204
Occludin and tricellulin confer complementary epithelial barrier protection during DSSinduced colitis

Franziska Janus; InFah M. Lee; Anja Fromm; Fabian Guendel [1]; Andreas Diefenbach [1]; Michael Fromm; JörgDieter Schulzke; Susanne Krug
Klinische Physiologie, Campus Benjamin Franklin, Charité - Universitätsmedizin Berlin, Berlin, Germany; [1] Institut für Mirkobiologie und Infektionsimmunologie, Campus Benjamin Franklin, Charité - Universitätsmedizin Berlin, Berlin, Germany;

Objective: Intestinal epithelial tight junctions regulate both ion transport and macromolecular antigen access, but whether distinct tight junction proteins control separable barrierimmune axes during inflammation remains unclear. Occludin and tricellulin are both affected in inflammatory bowel disease and have been implicated in different aspects of epithelial barrier regulation. We therefore hypothesized that intestinal epithelial overexpression of occludin or tricellulin may protect against colitisassociated barrier dysfunction through complementary, rather than redundant, mechanisms.
Method: To study this, we investigated mice with intestinal epithelial overexpression of occludin (OclnOE) or tricellulin (TricOE) and wildtype littermates during dextran sodium sulfate (DSS)induced colitis. All animal procedures complied with German/EU legislation and were approved by the responsible authority (G0059/13, G0143/18). Colitis severity was assessed by disease activity index, epithelial ion barrier function by Ussing chamber electrophysiology, macromolecule permeability by 4kDa FITCdextran flux, and immune composition by compartmentresolved flow cytometry of epithelial and lamina propria fractions. In addition, in HT29/B6 monolayers, shRNAmediated tricellulin knockdown was used to quantify and visualize lipopolysaccharide (LPS) passage as an immunerelevant macromolecular permeability readout.
Results: DSS increased disease activity in wildtype (wt) mice to 7.9±0.6 (SEM; n=21), whereas both OclnOE and TricOE mice showed reduced disease activity (OclnOE 6.3±0.7; n=16, $p<0.001$ and TricOE 5.7±0.5; n=13; $p<0.0001$). Barrier analyses revealed divergent protection: OclnOE preserved ion barrier function, for example reflected by a stable transepithelial resistance in the DSStreated animals in contrast to wt and TricOE, whereas TricOE selectively limited macromolecule permeability, possesing lower DSSinduced FITCdextran permeabilty than wt and OclnOE from. Immune profiling showed that this macromolecule barrier protection was accompanied by reduced lamina propria inflammation due to lower immune cell infiltration, including dendritic cells and their tolerogenic and inflammatory subsets.
Complementary experiments in HT29/B6 with a tricellulin knockdown to 50%, levels seen in ulcerative colitis, doubled LPS passage ($p<0.05$), which was detectable at tricellular contacts, and enhanced macrophage activation in coculture, supporting a causal link between tricellular sealing and immune stimulation.
Conclusion: Thus, occludin and tricellulin confer complementary epithelial barrierprotective effects during colitis: occludin primarily stabilizes ion barrier properties, whereas tricellulin restricts macromolecular antigen access and downstream mucosal immune activation. These findings identify tricellular junctional sealing as a physiologically relevant control point linking epithelial barrier function to intestinal inflammation.

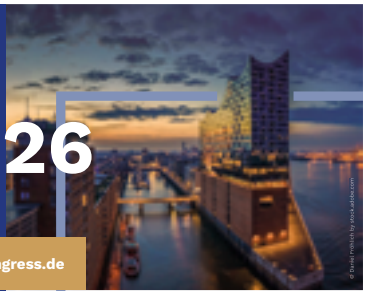

OC 12 FLOW of Signals: Signalling & Pathophysiology

OC1205

Colontargeted nutrient delivery stimulates prolonged GLP1 secretion and reduces weight gain in high fat diet fed mice

Nalini Sodum; Ghulam Shere Raza [1]; VesaPekka Lehto [2]; Jaroslaw Walkowiak [3]; KarlHeinz Herzig [1]
Physiology, Research institute of Biomedicine and Internal Medicine, University of Oulu, Oulu, Finland; [1] Department of Physiology, Institute of Biomedicine and Internal Medicine, University of Oulu, Oulu, Finland; [2] Department of Technical Physics, Faculty of Science, Forestry and Technology, University of Eastern Finland, Kuopio, Finland; [3] Department of Gastroenterology and Metabolism, Poznan University of Medical Sciences, Poznan, Poland;

Objective: Obesity is a global burden and leading cause of chronic diseases and disability. Recently, Glucagonlike peptide1 (GLP1) agonists have become essential in obesity management, but side effects and expense limit their use. GLP1 is an incretin secreted from Lcells located in distal part of intestine after food ingestion. However, the nutrients fail to induce sustained GLP1 secretions. We hypothesize that porous silicon (PSi) particles enable sustained nutrient delivery with minimal caloric load to the distal intestine and promote a sustained endogenous GLP1 release.
Method: To test this hypothesis, thermally hydrocarbinzed (THCPSi) particles were used for delivery of αLinolenic acid (αLA). Obese male C57BL/6NCrl mice were fed with highfat diet for 9 weeks and divided into four groups: i) control, ii) empty THCPSi, iii) free αLA, and iv) αLAloaded THCPSi. All doses were prepared in water containing 2% DMSO+0.5% CMC, then orally gavage once daily for 5 weeks at 1hr before lights off. Body weight was recorded each week, and indirect calorimetry was performed using the Phenomaster system.
Results: αLAloaded THCPSi particles significantly ($p<0.05$) reduced body weight gain compared to control and empty THCPSi, whereas free αLA did not. AUC of cumulative food intake was significantly reduced with αLAloaded THCPSi particles compared to control ($p<0.01$), and free αLA ($p<0.05$). Interestingly, the AUC of plasma GLP1 levels over 5 hours were significantly ($p<0.05$) stimulated with αLAloaded THCPSi particles compared to all controls (iiii), demonstrating sustained GLP1 release over time.
Conclusion: In conclusion, targeted delivery of nutrients to the distal intestine using THCPSi particles represents a novel approach for appetite control via endogenous GLP1 secretions and obesity management.

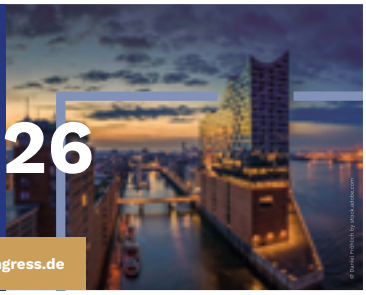

1

OC 12 FLOW of Signals: Signalling & Pathophysiology

OC1206

Statins modulate thermosensitive TRP channels and voltage gated sodium channels

George Oprita; Dan Domocos; Adelina Paduraru; Ines Pombeiro Stein 1; Ramona Babes 2; Andreas Leffler 1; Alexandru Babes 3
Anatomy, Physiology and Biophysics, Faculty of Biology, University of Bucharest, Bucharest, Romania; 1 Anästhesiologie, Medizinische Hochschule Hannover, Hannover, Germany; 2 Biophysics, „Carol Davila“ University of Medicine and Pharmacy, Bucharest, Romania; 3 Department of Anatomy, Animal Physiology and Biophysics, Faculty of Biology, University of Bucharest, Bucharest, Romania;

Objective: Statins are among the most prescribed drugs worldwide and their main effect is the reduction of blood cholesterol. Even though statin treatment is generally well tolerated, reports indicate that patients can develop myalgia, which usually disappears once the medication is stopped. Animal studies, however, reveal a potent analgesic effect of shortterm statin treatment, in both acute and chronic pain models. Transient Receptor Potential (TRP) and voltage gated sodium (Nav) channels are essential for peripheral nociception and have been shown to be modulated by various endogenous and exogenous molecules.
Method: All recordings were conducted on heterologous expression systems, such as HEK293T and ND7/23 cells, transfected with various ion channels, as well as mouse dorsal root ganglion (mDRG) neurons and cardiomyocytes derived from human induced pluripotent stem cells. The experimental procedures consisted in calcium microfluorimetry and patch clamp recordings, in both voltage clamp and current clamp configurations.
Results: We discovered that rosuvastatin acts as a TRPM8 agonist and modulates its cold sensitivity and simvastatin can activate both TRPA1 and TRPV1 via specific molecular determinants. Additionally, we have uncovered that simvastatin is a potent blocker, with a low micromolar IC_{50}, of both tetrodotoxin (TTX)sensitive as well as TTXresistant Nav channels, namely the cardiac Nav1.5 and the nociceptor specific Nav1.8 channels. Selective TRP channel antagonists were able to significantly block the statin dependent activation of mDRG neurons in primary cultures. Lastly, acute simvastatin treatment led to clear modulations of both neuronal and cardiac action potentials and firing rates.
Conclusion: This study reveals intricate and previously unknown statin interactions, which may explain why myalgia can occur during patient treatment and how they can lead to significant analgesia in various rodent pain models.

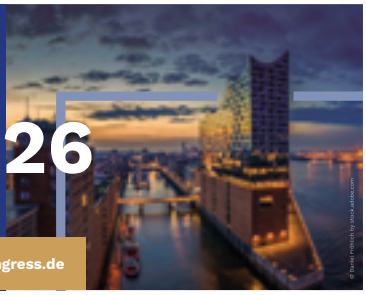

OC 13 FLOW of Urine: Kidney disease

OC1301

Hemoglobin Oxygen Affinity Shapes Renal Oxygen Handling and Is Linked to Acute Kidney Injury Risk: Evidence for a Renal Oxygenation Paradox

Robert Labes; Dario von Wedel [1]; Vera Anna Kulow; Laetitia Malotka; Julian Felber [1]; JanHendrik B. Hardenberg [2]; Nils Daum [3]; Moritz Thiele [1]; Cem Erdogan; Sophie Claire Reimers [3]; KaiUwe Eckardt [4]; Philipp Enghard [4]; Felix Balzer [1]; Sascha Treskatsch [3]; Michael Fähling Institut für Translatioinal Physiologie, Campus Charité Mitte, Charité - Universitätsmedizin Berlin, Berlin, Germany; [1] Institut für Medizinische Informatik, Campus Charité Mitte, Charité - Universitätsmedizin Berlin, Berlin, Germany; [2] Medizinische Klinik mit Schwerpunkt Nephrologie und Internistische Intensivmedizin, Campus VirchowKlinikum, Charité - Universitätsmedizin Berlin, Berlin, Germany; [3] Klinik für Anästhesiologie mit Schwerpunkt operative Intensivmedizin, Campus Charité Mitte, Charité - Universitätsmedizin Berlin, Berlin, Germany; [4] Medizinische Klinik mit Schwerpunkt Nephrologie und Internistische Intensivmedizin, Campus Charité Mitte, Charité - Universitätsmedizin Berlin, Berlin, Germany;

Objective: Hemoglobin oxygen affinity, commonly expressed as p50, determines the balance between oxygen loading and unloading, yet its physiological and clinical relevance for organ oxygenation remains poorly understood. We investigated whether variability in p50 is associated with acute kidney injury (AKI) and explored potential mechanisms in a translational approach.
Method: Two independent clinical cohorts of a tertiary hospital were analyzed, including perioperative patients (n=16,778) and critically ill patients (n=22,122). Associations between p50 and AKI were assessed using multivariable models and sensitivity analyses. To investigate mechanistic links, hemoglobin oxygen affinity was pharmacologically shifted in mice using the rightshifter RSR13. Transcriptomic responses were analyzed under baseline and rhabdomyolysisinduced AKI (RIAKI) conditions.
Results: P50 exhibited marked interindividual variability, with many patients showing rightshifted oxygen dissociation curves (p50 > 29 mmHg; perioperative: 47.7%; critically ill: 61.8%). Elevated p50 was independently associated with increased AKI risk (perioperative: $p = 0.005$; critically ill: $p < 0.001$), following a nonlinear relationship with a threshold above approximately 32 mmHg. This association remained robust across sensitivity analyses and was modified by anemia. In mice, pharmacological rightshifting activated hypoxia- and stressassociated pathways in the kidney, including HIF and p53 signaling, whereas opposing responses were observed in the heart. Under RAKI conditions, these renal responses were further amplified.
Conclusion: Increased oxygen unloading as expressed as elevated p50 does not uniformly improve tissue oxygenation but may impair renal oxygen handling. We propose a “renal oxygenation paradox”, in which reduced hemoglobin oxygen affinity promotes hypoxialike renal responses despite preserved systemic oxygen content. P50 may therefore represent a simple and accessible marker to identify patients at increased risk of AKI.

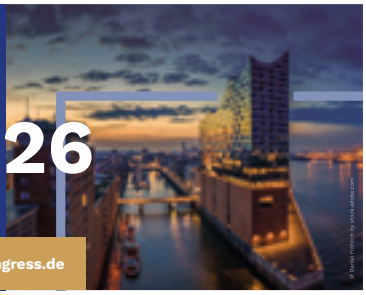

OC 13 FLOW of Urine: Kidney disease

OC1302

Therapeutic Targeting of the ANGPT2/TIE2 Signaling Axis Improves Diabetic Nephropathy in the BTBR OB/OB Mouse

Amanda Marks
Hultström; Marie Jeansson
Immunology, Genetics, & Pathology, Uppsala University, Uppsala, Sweden;

Objective: Diabetes is a chronic disease affecting more than 530 million people worldwide and is associated with serious complications including diabetic cardiomyopathy, coronary artery disease, atherosclerosis, and diabetic nephropathy. Diabetic nephropathy, is a leading cause of chronic kidney disease and endstage renal failure and substantially increases cardiovascular risk. Current therapies primarily target metabolic risk factors, dyslipidemia, and inflammation; however, additional vascular mechanisms beyond atherosclerosis contribute to disease progression and remain underexplored.
The connection between T2DM , CKD, is driven by common biological processes involving the Angiopoietin2 (ANGPT2) and TIE2 signaling pathway. In diabetes, hyperglycemia and advanced glycation endproducts disrupt ANGPT/TIE2 signaling, leading to increased ANGPT2 expression, oxidative stress, and endothelial dysfunction. Elevated circulating ANGPT2 levels correlate with kidney disease severity identify the ANGPT2–TIE2 axis as both a biomarker and a potential therapeutic target in diabetic nephropathy.
Method: This study evaluated the therapeutic value of a novel humanized antibody (ABX) that binds ANGPT2 and restores TIE2 signaling. 4weekold, BTBR ob/ob diabetic mice received weekly injections of ABX (25mg/kg) or vehicle control, until 11weeks of age. BTBR WT mice served as a nondiabetic, lean controls. Diabetic nephropathy was evaluated using urinary albumin and creatinine ratio (uACR), diabetes induced structural changes and microvascular injury were assessed using electron microscopy and PAS stained kidney sections.
Results: ABX treatment prevented diabetesinduced renal dysfunction measure by uACR levels. It also maintained endothelial fenestrations in peritubular and glomerular capillaries (electron microscopy), reduced glomerular hypertrophy and prevented glomerular basement membrane thickening and foot process effacement when compared with vehicletreated diabetic mice.
Conclusion: Taken together, these findings suggest that targeting ANGPT2 with ABX mitigates diabetic nephropathy and preserves renal microvascular structure in experimental type 2 diabetes.

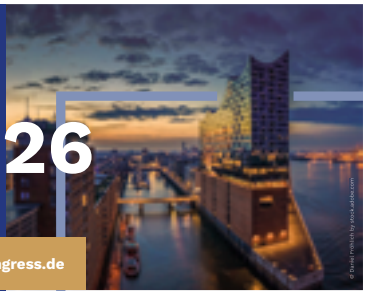

OC 13 FLOW of Urine: Kidney disease

OC1303

Proteinuria - a critical parameter for urinary tract infections in patients with chronic kidney disease

Laura Vang Sparsø; Aimi Hamilton; Mathias Skov; Henrik Birn [1]; Rikke Nielsen [2]; Helle A. Praetorius
Department of Biomedicine, Aarhus University, Aarhus, Denmark; [1] Dept. of Nephrology, Aarhus University Hospital Skejby, Aarhus, Denmark; [2] Department of Cell Biology, Institute of Anatomy, University of Aarhus, Aarhus, Denmark;

Objective: Urinary tract infections (UTIs) are common, and patients with chronic kidney disease (CKD) are particularly susceptible. We investigated whether proteinuria promotes UTI susceptibility using complementary *in vitro* and *in vivo* approaches.
Method: Proteinuria was induced in mice using an inducible podocin knockout model ($NPHS2^{fl/fl}$ crossed with tamoxifeninducible UBCCre/ERT2; Crenegative littermates as controls). Four weeks after induction, mice underwent instillation of 5×10^5 uropathogenic *Escherichia coli* (UPEC, O6:K13:H1) by direct injection into the bladder. After 24 hours, urine, bladder, kidney, and blood were collected, and bacterial burden was quantified by colonyforming unit counts. Urinary protein excretion was assessed by total protein measurement and SDS–PAGE. UPEC growth was analysed in urine from CKD patients with and without proteinuria, healthy volunteers (standardised to 300 mOsm/kg, pH 7.0), and mice by flow cytometry. Protein degradation was assessed by SDS–PAGE. Statistical analyses were performed using oneway ANOVA or Student's ttest, as appropriate.
Results: Proteinuric mice exhibited significantly higher bacterial loads in urine (p=0.0037), bladder (p=0.002), and kidney (p=0.0128), and a higher incidence of bacteraemia (p=0.0003) compared with controls (n=10–11). Urine from proteinuric CKD patients (ACR >300 mg/g) supported increased UPEC growth and delayed growth stagnation compared with nonproteinuric CKD patients with comparable eGFR. Albumin supplementation (2 mg/ml) to healthy urine did not affect bacterial growth; however, proteolytic degradation of albumin, induced by transient pH shift, significantly increased UPEC growth (n=8, p=0.006), an effect abolished by heat inactivation of urinary proteases. Consistently, UPEC growth was markedly enhanced in urine from proteinuric mice compared with controls (n=11–13, p<0.0001).
Conclusion: Proteinuria is associated with increased UTI severity in mice and enhanced UPEC growth in urine from both proteinuric mice and humans. This effect depends on proteolytic processing of urinary proteins, suggesting that filtered plasma proteins may serve as substrates that promote bacterial proliferation and contribute to increased UTI susceptibility in CKD.

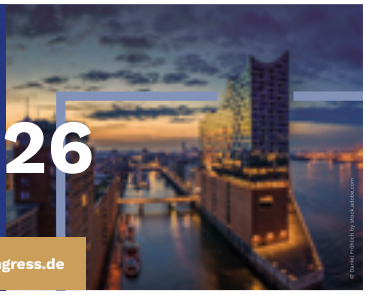

OC 13 FLOW of Urine: Kidney disease

OC1304

The role of zinc during improvement of serum calcification propensity by dialysis

Ioana Alesutan; Azmat Sohail; Barbara Ketterer; Anson Antony; Beatrice Toegel; Adela Tiffner; Margot Egger; Benjamin Dieplinger [1]; Andreas Pasch; Edward R. Smith [2]; Jakob Voelkl
Institut für Physiologie und Pathophysiologie, Johannes Kepler Universität Linz, Linz, Austria; [1] Abteilung für Labormedizin, Konventhospital Barmherzige Brueder Linz und Ordensklinikum Linz Barmherzige Schwestern, Linz, Austria; [2] Abu Dhabi Healthcare Company, Abu Dhabi, United Arab. Emirate;

Objective: Serum calcification propensity (T50 test) is a stress test on the strength of the endogenous mineral buffering system. This system prevents ectopic formation of calciumphosphate complexes and a weaker mineral buffering as in chronic kidney disease could carry an increased risk for secondary calciprotein particle (CPP) formation. However, the components of the mineral buffering system are only partially understood. Therefore, we investigated the role of zinc on mineral buffering in dialysis.
Method: Blood was collected from controls and dialysis patients before and after a dialysis session. Artificial serum preparations were used for an exact predefined environment. Serum calcification propensity (T50) was determined by a nephelometric method and the biological response to serum was investigated in primary human aortic vascular smooth muscle cells (VSMCs).
Results: T50 showed rather constant cyclic alterations with three dialysis sessions, but remained stable in controls. The increased expression of procalcific markers in VSMCs exposed to predialysis serum was lower in postdialysis serumexposed VSMCs or when serum was subjected to prior centrifugation for CPP removal. In postdialysis serum, T50 increased together with reduction of phosphate levels, but phosphate adjustment was not sufficient to equalize T50 to predialysis values. Zinc levels in serum and in isolated synthetic CPPs was increased after dialysis. Moreover, addition of the zinc chelator TPEN lowered T50 in postdialysis serum. In artificial serum, zinc increased T50 values, and this effect was modified by TPEN and albumin.
Conclusion: The cyclical alterations of mineral buffering in dialysis patients may involve a functional contribution of zinc.

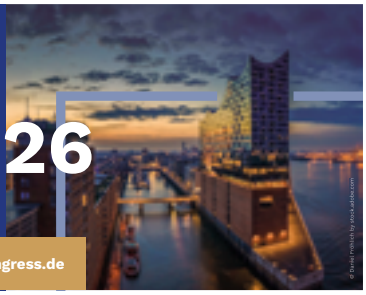

OC 13 FLOW of Urine: Kidney disease

OC1305

EP4 receptor agonism attenuates profibrotic signaling in translational human models of renal fibrosis

Camilla Merrild; Michael Schou [1]; Aisha Nadukkandy; Mia Gebauer Madsen [2]; Anna Krarup Keller [2]; Lene Niemann Nejsum; Henricus Antonius Maria Mutsaers; Lin Lin [1]; Rikke Nørregaard Department of Clinical Medicine, Aarhus University, Aarhus, Denmark; [1] Department of Biomedicine, Aarhus University, Aarhus, Denmark; [2] Department of Urology, Aarhus University Hospital, Aarhus, Denmark;

Objective: Chronic kidney disease (CKD) affects about 10% of the adult population and is characterized by progressive renal fibrosis, which is largely driven by Transforming Growth Factor- β (TGFβ). While activation of the prostaglandin E2 EP4 receptor has shown antifibrotic potential in animal studies, its effects in translational human renal fibrosis models remain to be elucidated. Here, we evaluated the antifibrotic effects of the EP4 receptor agonist Rivenprost in two renal fibrosis models: human precisioncut kidney slices (PCKS) and a 3D human glomerular model (GlomSpheres).
Method: Human PCKS were prepared from macroscopically healthy cortical tissue obtained from tumor nephrectomies and were cultured ex vivo. Fibrosis was induced with TGFβ (10 ng/ml) with or without the EP4 receptor agonist Rivenprost (75 µM). Fibrotic responses were assessed by Sirius red staining, RTqPCR, western blotting, and bulk RNA sequencing. Key antifibrotic effects were evaluated independently in the GlomSpheres using the same techniques as for the PCKS.
Results: TGFβ stimulation induced a significant profibrotic response, reflected by upregulation of profibrotic markers, including *COL1A1*, *FN*, and *ACTA* in human PCKS, while cotreatment with Rivenprost significantly inhibited this (RTqPCR, n=52). Representative Sirius red staining and western blot analyses confirmed increased interstitial fibrosis and fibronectin protein expression following TGFβ stimulation – both of which were significantly reduced by Rivenprost treatment. Bulk RNA sequencing of the human PCKS (n=8) identified 303 differentially expressed genes between TGFβ and TGFβ+Rivenprost conditions. Rivenprost treatment resulted in the downregulation of fibrosis associated genes and pathways related to collagen metabolism. Similar antifibrotic effects of Rivenprost were observed in the GlomSpheres, including reduced Sirius red staining and downregulation of pathways associated with wound healing and extracellular matrix organization in the bulk RNA sequencing dataset (n=6).
Conclusion: Rivenprost attenuated TGFβdriven profibrotic signaling across two translational renal fibrosis models, supporting further evaluation of EP4 agonism as an antifibrotic strategy in CKD.

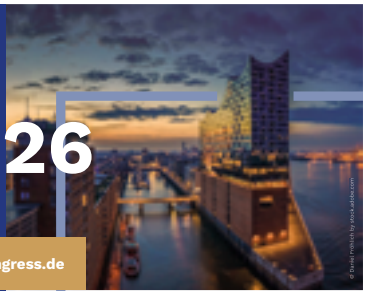

OC 13 FLOW of Urine: Kidney disease

OC1306

NFAT5 Deficiency in the Kidney Triggers Systemic MultiOrgan Inflammation

Vera Anna Kulow; Kristina Engel [1]; Laetitia Malotka; Cem Erdogan; Ina Maria Schießl [2]; Michael Fähling; Bayram Edemir [3]
Institut für Translatioinal Physiologie, Campus Charité Mitte, Charité - Universitätsmedizin Berlin, Berlin, Germany; [1] Lehrstuhl für Physiologie, Pathophysiologie und Toxikologie, Universität Witten/Herdecke, Witten, Germany; [2] Department of Biomedicine, Aarhus University, Aarhus, Denmark; [3] Zentrum für Biomedizinische Ausbildung und Forschung (ZBAF), Lehrstuhl für Physiologie, Pathophysiologie und Toxikologie, Universität Witten/Herdecke, Witten, Germany;

Objective: While NFAT5 is a key regulator of renal osmoadaptation to hyperosmotic stress, its loss in collecting duct cells may have consequences beyond the kidney. Kidney injury is increasingly understood as a driver of clinically relevant interorgan crosstalk, promoting inflammation in distant organs such as the lung and liver. In a previous study, we demonstrated that NFAT5 deficiency leads to a strong inflammatory response and plays an important role in cytokine signaling. Building on these findings, we investigated whether NFAT5 deficiency initiates a kidneyderived inflammatory program that connects renal fibrosis and inflammation with systemic multiorgan pathology.
Method: We generated collecting ductspecific Aqp2Cre$^{+/}$mediated *Nfat5* knockout (*Nfat5*KO) mice and collected kidneys, lungs, heart, spleen, and liver between 1869 weeks of age. Aqp2Cre$^{+/-}$ mice were served as control. Spatial transcriptomics was performed on kidneys, while bulk NGS, histological analyses and immunostainings were conducted across all organs.
Results: *Nfat5*KO kidneys developed an insipiduslike phenotype characterized by tubular damage and extensive fibrosis. Spatial transcriptomics revealed infiltration and activation of immune cells in the kidney. With prolonged knockout of *Nfat5*, these activated immune cells disseminated systemically, initially forming large T- and Bcell granulomas in the lungs. Advanced aging (>60 weeks) revealed infiltration of the liver by the same immune cell population.
Conclusion: Chronic NFAT5 deficiency initiates renal fibrosis and inflammation that evolves into systemic multiorgan pathology via immune cell dissemination. This reveals a novel kidneylungliver inflammation axis with potential implications for chronic kidney disease management.

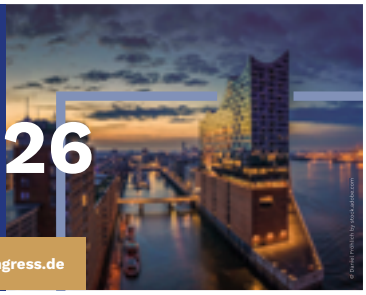

OC 14 FLOW of Blood: Systemic cardiovascular physiology

OC1401
Mechanistic insights into microvascular dysfunction in INOCA using human resistance arteries

Jessica Meades; Thomas Jepps [1]; Ylva Hellsten
Nutrition, Exercise and Sports, Biomedicinsk Institut (BMI), University of Copenhagen, Copenhagen, Denmark; [1] Integrative Circulation, Institute of Biomedical Sciences, University of Copenhagen, Copenhagen, Denmark;

Objective: Ischaemia with no obstructive coronary arteries (INOCA) is characterised by symptoms of myocardial ischaemia in the absence of significant coronary artery disease on angiography and predominantly affects women. INOCA encompasses two major endotypes, microvascular dysfunction and vasospasm, although the underlying mechanisms remain poorly understood.
Method: In an ongoing clinical study, paired gluteal biopsies from patients with INOCA and agematched controls are used to isolate small resistance arteries (200–450 µm diameter) for ex vivo wire myography and proteomic analysis. Vascular segments are assessed for endothelialdependent relaxation, smooth muscle responsiveness, and pharmacological vasoactivity to evaluate peripheral microvascular function and identify diseaserelated differences. Data are presented as mean ± SEM. Concentration–response curves were analysed using 2way ANOVA with Tukey's multiple comparison test, while EC50 comparisons were analysed using unpaired ttests.
Results: Preliminary analyses reveal sexdependent differences in noradrenalineinduced vasoconstriction in patients with INOCA, with female vessels (N=4) showing significantly reduced sensitivity compared to males (N=3) (pEC50 = 6.59 ± 0.11 vs 7.28 ± 0.26, respectively; $P < 0.05$), suggesting altered adrenergic responsiveness as a contributor to INOCA heterogeneity.
Additionally, in the presence of the nitric oxide synthase inhibitor LNAME (100 µM), acetylcholineinduced relaxation showed significantly reduced potency in patients compared to controls (N=5/group) (pEC50 = 7.59 ± 0.05 vs 7.85 ± 0.08, respectively; $P < 0.05$), suggesting greater dependence on nitric oxidemediated vasodilation in the patient group.
Conclusion: The broader project will examine vascular adaptations in patients with INOCA in response to exercise training and/or colchicine treatment. Together, these studies aim to provide mechanistic insight into INOCA pathophysiology and support development of improved therapeutic strategies.

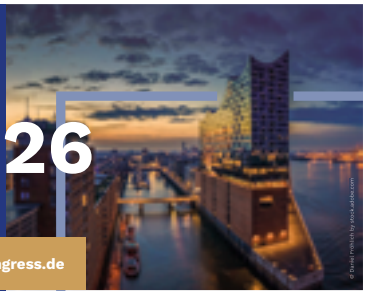

OC 14 FLOW of Blood: Systemic cardiovascular physiology

OC1402

Use of heartforming organoids derived from human iPS cells carrying a mutation in the *MYBPC3* gene to study the role of cMyBPC in human heart development

Fiona Soehngen; Karina Ivaskevica; Birgit Piep; Felix Osten; Annika Franke [1]; Lika Drakhlis [1]; Robert Zweigerdt [1]; Theresia Kraft; Sarah Konze Institute of Molecular and Cell Physiology, Hannover Medical School, Hannover, Germany; [1] Leibniz Research Laboratories for Biotechnology and Artificial Organs (LEBAO), Clinic for Cardiac, Thoracic, Transplantation and Vascular Surgery, Hannover Medical School, Hannover, Germany;

Objective: Hypertrophic cardiomyopathy (HCM), the most common inherited cardiac disease, is in many cases linked to mutations in sarcomeric proteins. Particularly, mutations in *MYBPC3*, encoding the cardiac myosinbinding protein C (cMyBPC), represent one of the most frequent genetic causes. To date, the underlying diseaserelevant mechanisms remain incompletely understood, particularly with respect to early developmental processes. The aim of this study was therefore to establish a human, threedimensional, *in vitro* model to investigate genotypedependent effects of a *MYBPC3* mutation during early cardiac tissue development.
Method: In this study, heartforming organoids (HFOs) were generated from human induced pluripotent stem cells (hiPSCs) carrying either a heterozygous or homozygous *MYBPC3* c.9272A>G mutation plus the corresponding isogenic control. This intronic mutation leads to incorrect splicing and thus introduces a premature stop codon, resulting in cMyBPC haploinsufficiency or loss, respectively. In the derived HFOs, formation efficiency, morphology, cellular composition, protein expression, and contractile function were assessed at d12 and d25 of HFO formation.
Results: All clones formed selforganized HFOs and showed spontaneous contraction. As expected, homozygous organoids exhibited an almost complete loss of cMyBPC, whereas heterozygous organoids showed reduced levels of cMyBPC. In the heterozygous, but more strongly in the homozygous mutant we observed impaired formation of the myocardial layer, reduced organoid size and increased morphological irregularity. Functional analyses of twitch kinetics showed a clear phenotype for the homozygous mutant HFOs with regard to reduced contraction amplitude, as well as slower contraction and relaxation velocities compared to the isogenic control.
Conclusion: In summary, this study establishes $MYBPC3_{mut}$ HFOs as a human, multicellular, threedimensional model system for mechanistic investigations on the role of cMyBPC in early embryonic development. Our findings indicate that *MYBPC3* deficiency may already affect early processes of cardiac tissue organization. This model provides a foundation for future studies on disease modelling and therapeutic development.

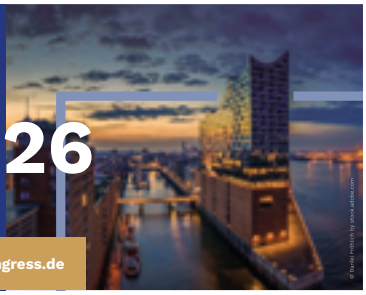

OC 14 FLOW of Blood: Systemic cardiovascular physiology

OC1403

Heterozygous Titin Deletion Alters Right Ventricular Stiffness and Remodelling in a Mouse Model of Pulmonary Hypertension

Kimberley Stein; Annika J. Klotz [1]; Marion Müller [2]; Anna Klinke [3]; Wolfgang Linke [1]; Daniela Wenzel
Systemphysiologie, Institut für Physiologie, RuhrUniversität Bochum, Bochum, Germany; [1] Institut für Physiologie II, Universitätsklinikum, Westfälische WilhelmsUniversität Münster, Münster, Germany; [2] IAF - Institut für Angewandte Forschung, Entwicklung und Weiterbildung, Katholische Hochschule Freiburg, Freiburg, Germany; [3] Klinik und Poliklinik für Kardiologie, Pneumologie, Angiologie und internistische Intensivmedizin, Klinik III für Innere Medizin, Universität zu Köln, Köln, Germany;

Objective: In pulmonary arterial hypertension, patients exhibit altered titin phosphorylation and increased right ventricular (RV) stiffness. To determine how titin influences pulmonary hypertension (PH), we induced the disease in heterozygous ($Ttn^{tm1a/+}$, TtnA) mice (titin translation stops after exon 3) and analysed RV structure and function.
Method: In WT and TtnA animals, treatment with Sugen 5416/hypoxia (HX) for 3 weeks induced PH. Cardiac function was assessed by pressurevolume catheter measurements or echocardiography (11.5 % (V) isoflurane). Isolated RV trabeculae were used for passive force measurements (PFM), morphometry was performed in wheat germ agglutinin (WGA)- stained heart sections. For statistics, oneway ANOVA and Tukey`s posthoc test were applied. For echocardiography, KruskalWallis and Dunn`s test and for PFM, twoway ANOVA and Tukey`s posthoc test were used.
Results: Hemodynamic analysis demonstrated the expected increase in RV endsystolic pressure in HXWT ($p<0.0001$ vs NXWT) and HXTtnA ($p<0.0001$ vs NXTtnA) mice, consistent with the successful induction of PH in both mouse lines. HXinduced PH resulted in RV hypertrophy in HXWT but not in HXTtnA animals. This was determined by morphometry of WGAstained heart sections (HXWT 300.0±12.1 μm^2 vs NXWT 216.4±5.1 μm^2, $p<0.0001$, all n=12; HXTtnA 249.9.1±8.7 μm^2, n=12 vs NXTtnA 216.4±5.1 μm^2, n=11, $p=0.05$) and echocardiography (HXWT vs NXWT, $p<0.0001$; HXWT vs NXTtnA, $p=0.08$). Systolic RV function (ESPVR) was elevated in HX for both genotypes (HXWT vs NXWT, $p<0.0001$; HXWT vs NXTtnA, $p=0.007$), whereas diastolic function differed: EDPVR was elevated in HXWT mice ($p<0.0001$ vs NXWT) demonstrating enhanced RV stiffness, but not in HXTtnA animals ($p=0.99$ vs NXTtnA). Impaired RV relaxation was observed by echocardiography in HXWT but not in HXTtnA, as isovolumetric relaxation time was enhanced in HXWT ($p=0.04$ vs NXWT) but not in HXTtnA ($p=0.09$ vs NXTtnA). These results were confirmed by PFM of isolated RV trabeculae in vitro at 20 % strain showing enhanced stiffness in HXWT ($p<0.0001$ vs NXWT) but not in HXTtnA ($p=0.6$ vs NXTtnA).
Conclusion: These data suggest that heterozygous titin deletion reduces RV stiffness and remodelling without compromising systolic function in a mouse model of PH. This highlights titin's critical role in diastolic function and adaptation to mechanical load.

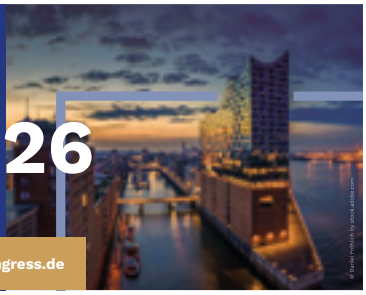

OC 14 FLOW of Blood: Systemic cardiovascular physiology

OC1404

DEL1deficiency exacerbates inflammatory cardiac remodeling in Angiotensin II– induced hypertension

Alina Maslakova; Maria Knyrim; Michael Marterstock; Anupam Das; Stephan Speier; Peter Mirtschink [1]; Triantafyllos Chavakis [2]; Andreas Deußen; Arka Baksi; Irakli Kopaliani Institut für Physiologie, Universitätsklinikum Carl Gustav Carus, Technische Universität Dresden, Dresden, Germany; [1] Institute of Clinical Chemistry, Faculty of Medicine, Carl Gustav Carus, TU Dresden, Dresden, Germany; [2] Abteilung für Klinische Pathobiochemie, Universitätsklinikum Carl Gustav Carus, Technische Universität Dresden, Dresden, Germany;

Objective: Hypertension results in increased inflammation in the heart that contributes to cardiac remodeling and functional impairment, yet the mechanisms that regulate these cardiac inflammatory responses are not completely understood. We investigated the constitutive role of developmental endothelial locus1 (DEL1), a secreted immunomodulatory glycoprotein that regulates leukocyte recruitment and inflammation resolution, in cardiac inflammation and remodeling during hypertension.
Method: Using DEL1 deficient ($Del1_{KO}$) and WT littermate mice, we revealed a dynamic time dependent pattern of cardiac remodeling following 14days of ANGII infusion.
Results: $Del1_{KO}$ mice developed early systolic dysfunction accompanied by diastolic alterations three days after ANGII infusion, whereas WTlittermates exhibited preserved systolic performance. Importantly, these functional differences occurred independent of arterial pressure. Flow cytometric analyses showed significant increased recruitment of neutrophils and inflammatory $Ly6C^{hi}$ monocytes into $Del1_{KO}$ hearts during at this early phase of hypertension. This was accompanied by activation of the bone marrow hematopoietic compartment, characterized by an early expansion of longterm hematopoietic stem cells, followed by a transient increase in hematopoietic progenitor stem populations during the intermediate phase (after 7days) of hypertension. During later stages of hypertension (after 14days), systolic function partially recovered in WTlittermate mice whereas only partial recovery was observed in $Del1_{KO}$ mice. However, this partial recovery was accompanied by exaggerated hypertrophic remodeling and increased cardiac fibrosis.
Conclusion: Together, these findings identify DEL1 as an endogenous regulator of cardiac inflammation that restrains early cardiac inflammatory recruitment at the onset of hypertension and supports balanced cardiac adaptation during prolonged hypertensive stress.

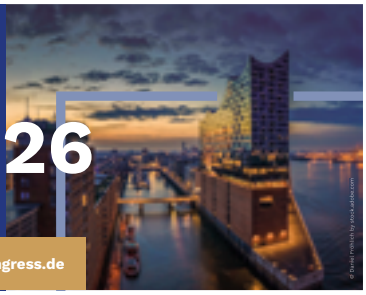

OC 14 FLOW of Blood: Systemic cardiovascular physiology

OC1405

Selective titin cleavage disrupts cardiac mechanical homeostasis to drive diastolic dysfunction and fibroblast activation

Johanna Freundt; Paulina Hartmann; Andreas Unger; Christine Löscher; Franziska Koser; Annika J. Klotz; Lydia Wachsmuth [1]; Michaela Door [2]; Susanne Hille [3]; Richard Holtmeier [1]; Jonathan Kirk [2]; Cornelius Faber [1]; Verena Hoerr [1]; Oliver J. Müller [3]; Wolfgang Linke Institut für Physiologie II, Universitätsklinikum, Westfälische WilhelmsUniversität Münster, Münster, Germany; [1] Clinic of Radiology, University of Münster, Münster, Germany; [2] Section of Cardiology, Dept. of Medicine, University of Chicago, Chicago, United States; [3] Translationale kardiovaskuläre Forschung, Klinik für Innere Medizin III, Universitätsklinikum SchleswigHolstein, Kiel, Germany;

Objective: Titin, the largest human protein, forms the elastic sarcomeric backbone, providing passive stiffness and lengthdependent activation in cardiomyocytes. Whereas titin mutations cause inherited cardiomyopathies, ischemic and chemotherapyinduced injury also provoke proteolytic cleavage of titin's elastic segment, resulting in the appearance of longenigmatic "T2" titin species. However, the effects of acute titin stiffness loss remain unknown.
Method: We developed a knockin mouse enabling selective invivo cleavage of cardiac titin springs. The mouse model contains a recognition site for tobacco etch virus protease (TEV) within the Iband titin spring near the T2 proteolytic hotspot, which we activated specifically in the beating heart by TEV overexpression using AAV9TEV plasmid (under the cTnT promoter) via tailvein injection, with AAV9GFP serving as control. We used multimodal analysis, including cMRI, echocardiography, confocal and electron microscopy, transcriptomics and proteomics, to elucidate the consequences of acute, cleavageinduced, titin stiffness loss for cardiac structure and mechanical function.
Results: Following AAV9TEV injection, cardiac titin cleavage, assessed on loose protein gels, started at day (D)34, reaching ~40% at D6, and plateauing at ~5560% at D1013 postinjection. No titin cleavage was observed in AAV9GFP injected hearts or in the skeletal muscles of AAV9TEVinjected mice. On immunofluorescently stained tissue sections, an antibody that recognizes the TEVcleaved sequence revealed a mosaic pattern of titincleaved and uncleaved cardiomyocytes at a proportion consistent with gel electrophoresis results. Echocardiography and cMRI, performed at regular intervals between D0 and D13 postinjection, demonstrated that titin cleavage does not dilate the heart but reduces chamber size and impairs ventricular filling, resulting in a restrictive phenotype and diastolic dysfunction in the presence of largely preserved systolic dysfunction. Mechanical assays of isolated cardiomyocytes revealed diminished restoring forces causing loss of elastic recoil, explaining the restrictive filling pattern. Invivo cleavage disrupted junctions, including integrin linkages and connexin43 gap junctions, widened intermyocyte space without hypertrophy or hyperplasia, and drove rapid fibroblast activation and extracellular matrix remodeling, followed by fibrosis. Omics analyses confirmed the absence of cardiomyocyte hypertrophy but activation of cellmatrix crosstalk and ECM remodeling, next to cytoskeletal reorganization and enhanced protein quality control mechanisms. However, attempted compensatory mechanisms failed, leading to decompensated heart failure by D13.
Conclusion: These findings establish that proteolytic cleavage of elastic titin perturbs cardiac mechanical homeostasis mainly by impairing elastic recoil and disrupting intra- and intercellular crosslinks, quickly driving diastolic dysfunction, matrix remodeling, and heart failure.

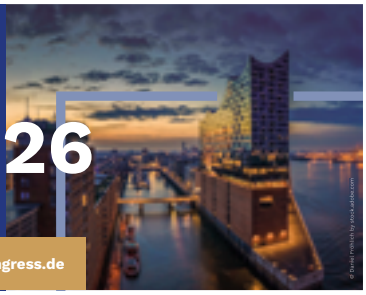

OC 14 FLOW of Blood: Systemic cardiovascular physiology

OC1406

Combined PKC- and AKT/ERKlinked receptor activation induces endocytic Ttubule loss in adult rat cardiomyocytes

Alexandra Kuhn; Tilmann Volk; Thomas Seidel [1]
Institut für Zelluläre und Molekulare Physiologie, Friedrich
Alexander
Universität Erlangen
Nürnberg,
Erlangen, Germany; [1] Innere Medizin, Infektiologie, Arztpraxis Weimar, Weimar, Germany;

Objective: The Ttubule (TT) system plays a key role in cardiac excitationcontraction coupling. Maladaptive remodeling in chronic heart failure (HF) leads to TT loss, contributing to contractile dysfunction. However, the mechanisms at the cellular level remain unknown. We recently identified NFkB signaling as a potential cause of TT loss. Since the NFkB upstream regulators protein kinase C (PKC) and AKT/ERK are implicated in cardiac remodeling, we investigated the receptormediated activation of these pathways on the tsystem.
Method: Left ventricular cardiomyocytes were isolated from adult female rats (anesthetized peritoneally with ketamine 100mg/kg and xylazine 10mg/kg before killing) and cultured with different PKC/NFkB or AKT/ERK/NFkB activators (angiotensin II [A], phenylephrine [P], endothelin1 [E], IGF1 [I], EGF, TNFα, IL1α, IL18). After 24 hours of culture, they were stained with Di8ANEPPS or used after 2 hours of culture for a dextranbased endocytosis assay, and stained with AM466. Confocal microscopy was used to quantify TT distance (TTD) and intracellular dextran. PKC and IkBα protein levels were analyzed by Western blotting (WB). Mixedeffects models with fixed effects for groups and random effects for biological replicates were applied.
Results: Cells treated with A+P+E+I showed a reduced abundance of TTs, indicated by increased TTD (0.89±0.05 µm, n=40/6, p<0.01; control: 0.73±0.03 µm, n=40/6). A+P+E (n=35/6) or IGF1 alone (n=42/6) showed no significant TT loss. Cells treated with A+P+E+I showed an increased internalization of extracellular dextran (0.7%±0.03% of myocyte volume, n=60/7, p=0.01). Dextranpositive intracellular structures displayed a TTlike shape and were no longer labeled by the membrane dye, consistent with internalized TT membrane. Exposure to A+P+E+EGF (n=41/6), EGF (n=40/6), TNFα (n=66/10), IL1α (n=78/11), IL18 (n=76/12), TNFα+IL1α (n=36/5) or IL18+IL1α (n=45/6) showed no significant TT loss. WB analysis (n=7) revealed an increased phosphorylation of PKCspecific sites and an increased expression of the NFkB response protein IKBα in A+P+E±I treated groups, but not in groups treated with the other substances.
Conclusion: Combined activation of PKClinked receptors and the IGF1dependent AKT/ERK pathway synergistically induces TT loss in rat cardiomyocytes. These findings suggest that the crosstalk between neurohormonal and growth factor signaling may induce TT remodeling, consistent with NFkBmediated TT internalization.

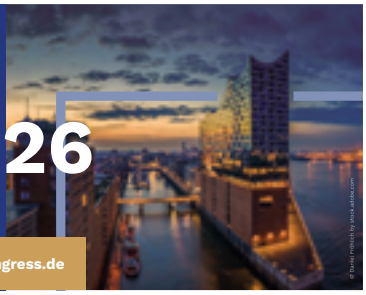

OC 15 FLOW of Knowledge: Methods and teaching in Physiology

OC1501

”A Riddle a Day Helps Learning to Stay” - The Physiology Advent Calendar: A Gamified Teaching Concept to Promote Conceptual Thinking in Preclinical Medical Education

Martin Pauli
Neurophysiology, Institute of Physiology, University of Würzburg, Würzburg, Germany;

Objective: Gamification has been shown to raise motivation and activate students in medical education. However, establishing gamification concepts remains challenging, as the time and effort required for design, construction, and implementation often pose substantial barriers.
Method: Here we present the **Physiology Advent Calendar**, a gamification concept based on Moodle, H5P, and Level Up! that has been developed and tested at the Physiological Institute of the University of Würzburg. Framed around the familiar advent calendar tradition, the concept delivers one activating physiology riddle per day throughout the Christmas season, designed to strengthen conceptual thinking and promote fascination with physiology among undergraduate medical students.
Results: Considering the upcoming Christmas season, we demonstrate the variability, feasibility, and pitfalls of the concept and invite to join a collaborative model.

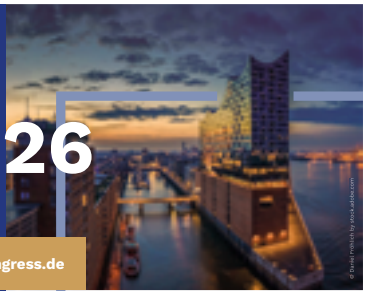

OC 15 FLOW of Knowledge: Methods and teaching in Physiology

OC1502

M[1]ündlich – S(t)imulation of CompetencyOriented Learning in Physiology

Lisa Eiring; Sven Benson [1]; Joachim Fandrey; Katrin ProstFingerle; Sandra Winning Abteilung Physiologie, Universitätsklinikum Essen, Essen, Germany; [1] Institut für Medizinische Psychologie und Verhaltensimmunbiologie, Universitätsklinikum, Universität DuisburgEssen, Essen, Germany;

Objective: Medical students often enter oral exams with insufficient preparation, especially in articulating knowledge under stress. To improve communication and structured answering, we developed a peerteachingbased exam training simulating oral exams.
Method: A total of approximately 190 thirdsemester medical students participated in the study. In groups of five, they alternated between the roles of teacher or learner. They simulated two oral exams under tutor (trained medical students of higher semesters) supervision with a time interval of three months. Each session included extensive structured feedback. This study was designed as a largescale, curriculumintegrated, quasiexperimental study of a peerled oral exam training intervention. The Ethics Committee of the Medical Faculty of the University of DuisburgEssen had approved the study. Participation was voluntary and based on informed consent.
Results: PTBET was associated with increased students‘ confidence in their own competences during exams and reduced perceived exam stress. After participation students reported higher selfassessment scores, with more students rating themselves higher and fewer reporting poor performance. Stress levels decreased in the second round, with more students experiencing no or only mild stress. Most students appreciated the peergroup format being effective and high numbers planned to include it in their prospective preparation for oral exams. The tutors also noted an improvement after the second round, particularly in terms of the quality of the students' presentations: the depth of information and the structure of the answers had improved considerably. Students’ later exam outcomes showed a favorable trend in internal followup exams and the oralpractical part of the first section of the German National Medical Licensing Examination (M1).
Conclusion: Peerbased simulation of oral exams may support communication skills and exam awareness while being associated with reduced stress. It offers a valuable complement to the traditional medical curriculum and is easily adaptable to other disciplines.

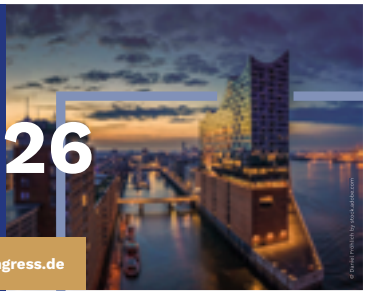

OC 15 FLOW of Knowledge: Methods and teaching in Physiology

OC1503

Medical students' misconceptions regarding heart rate and blood pressure measurements in the age of smartwatchbased biohacking

Robert Patejdl; Alexey Diyakov [1]; Gesine Reichart [2]; Elias Vogel [1]
Physiology, Institute for Biomedical Research, HMU Health and Medical University Erfurt, Erfurt, Germany; [1] Institute for Biomedical Research, HMU Health and Medical University Erfurt, Erfurt, Germany; [2] Physiology, Rostock University Medical Center, Rostock, Germany;

Objective: Cardiovascular parameters as heart rate, blood pressure, heart rate variability (HRV) and parameters associated with autonomic nervous system function are highly relevant in medicine, but also in exercise and sports physiology as well as in biopsychological concepts aiming at optimizing sleep, stress and general wellbeing.
Whereas practical classes in physiology at medical schhols aim at teaching the basic concepts of cardiovascular physiology and the techniques used for measuring these parameters are based upon classical methodology, both the general population and patients increasingly use wearable devices as smartwatches and fitnesstrackers.
While these techniques are not yet covered in physiology curricula or textbooks, they offer an opportunity to discuss methodological, biophysical and physiological issues with students, taking advantage of the broad availybility of devices and the students' familiarity with their handling.
Method: We conducted a survey at five medical faculties in Germany. The overall rate at which students used wearable devices to measure parameters of cardiovascular function was assessed. Students were then asked to report both their attitudes toward learning cardiovascular physiology in general and the perceived difficulty of concepts. Furthermore, they were asked questions reflecting their knowledge on the basic principles behind measuring blood pressure, heart rate and other parameters.
Results: In total, 469 students responded. The majority of respondents (mean age 23.1 ± 3.5 years, 64.0% female), 64.8% reported using smartwatches. Most smartwatch users tracked heart rate (99.7%), peripheral arterial oxygen saturation (63.8%), and electrocardiogram (49.0%). Only 9.9% reported measuring blood pressure.
Out of the questions regarding the underlying principles of smartwatch based measurements, lack of knowledge and misconceptions were identified in a consistently high proportion of students. For instance, correct answers were not more frequent than expected by chance regarding the detection principle for heartbeat: 53% of respondents agrees to the suggestion that heart rate is measured by mechanical detection of pressure signals at the wrist. In this case, correct response rates were not higher in smart watch users when compared to no-nusers. Surprisingly, correct answers regarding the principle of blood pressure estimation were given more frequent by students not using smartwatches when compared to those using smart watches for cardiovascular parameter assessment (44.4% vs. 31.5%, p=0.006).
Conclusion: Assessing students' concepts and knowledge regarding smartwatchbased measurements of cardiovascular parameters can be a first step to guide curricular coverage of this field. Considering the the rapidly growing rate of use by patients, clincians and healthy persons in the context of "biohacking" and "self optimization" there is an urgent need for implementing smartwatchbased measurements into medical curricula.

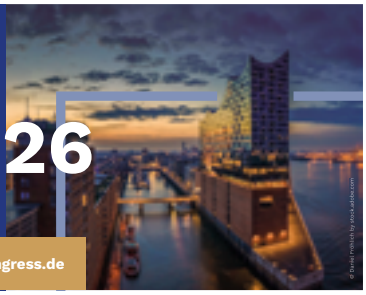

OC 15 FLOW of Knowledge: Methods and teaching in Physiology

OC1504

Medical Students' Critical Online Information Selection and Use - An EyeTracking Study

Maruschka Weber; Josephine Kluge; Dave Brunsch; Maximilian Dörre; Verena Klose Medical Department, Institute of Neurophysiology, Goethe University of Frankfurt, Frankfurt a. M., Germany;

Objective: Medical students increasingly use online information for their studies. We investigate students' successful task solving strategies during internet search within the framework of 'Critical Online Reasoning' (COR) and its development in the first 2 years of the medical curriculum.
Method: Eyetracking data was collected of 20 firstyear medical students solving a clinical case during free internet search (30 min). One year later, data was collected of these students solving again a clinical case, this time with the help of a set of preselected webpages, as analysis of the first survey showed that the acquisition of sources is not restricting.
Results: Task performance (maximum score 12) of the firstyear medical students widely ranged from 2 to 9 score points (mean 5.13 ±0.47, normal distribution p=0.38). The upper performing third (6 high performers (HP), score 7.71 ±0.45) differed significantly (p<0.01) from the lower third (6 low performers (LP), score 3.08 ±0.29). Surprisingly, they all could have achieved in average 11.80 ±0.12 points (out of maximal 12) with the information content of their visited webpages, which they named useful and trustworthy. Eyetracking investigations revealed, that even though all students spent very similar total fixation time on taskrelevant text passages on webpages they named useful and trustworthy (HP 124.17s ±32.42, LP 121.94s ±24.81; p=1.00), HP visually fixated more taskrelevant information within these text passages (p<0.01). In addition, the ratio of seen to used information (used for the written answer of the task) was significantly higher in HP (0.74 ±0.05) than LP (0.54 ±0.07; p=0.05), despite their similar writing time (HP 6.80 min ±0.91, LP 6.02 min ±1.20, p=0.87). Ongoing analysis of the secondyear students will shed light on a possible developmental effect of those strategies and COR skills along the medical curriculum, as domain specific knowledge needed for the task is taught in a preclinical physiology seminar, but COR skills are not promoted.
Conclusion: Medical students' COR performance was less determined by retrieval of taskrelevant webpages and text passages, than by collecting taskrelevant information within the selected text passages. Thereby, HP gathered more information and used a higher ratio of this information for generating the answer. Possibly, LP experienced high cognitive load or different epistemic beliefs. Analysis of the second survey will reveal the development of those COR skills and strategies.

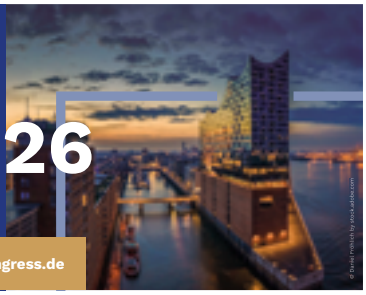

OC 15 FLOW of Knowledge: Methods and teaching in Physiology

OC1505
Evaluating Two Approaches for Identifying NonFunctional Distractors in MultipleChoice Examinations

Alfredo J. López Dávila; Hossein Shahla; Dominik Weigand; Jan Carl Becker; Alexander Oksche German Institute for State Examinations in Medicine, Pharmacy, Dentistry and Psychotherapy (IMPP), IMPP, Mainz, Germany;

Objective: Effective distractors are essential for highquality multiplechoice questions (MCQs). Functional distractors should attract lowerperforming examinees more frequently than higherperforming examinees. In classical test theory (CTT), distractor quality is commonly assessed using distractor discrimination indices based on pointbiserial correlations. Distractor discrimination indices should be negative and can be calculated as the correlation between respondents' test score and their performance on the distractor (i.e., a dichotomous variable coded 1 for respondents who select the distractor and 0 for respondents who select any other option (r_{PB_D}method)). An alternative method proposed by Attali and Fraenkel (rPB_{DC}method) includes only examinees selecting either the distractor or the correct answer. This study compared both methods regarding their utility for detecting potentially non-functional distractors.
Method: Data were obtained from a national medical licensing examination administered to 4,700 candidates. The examination consisted of 320 MCQs with five response options each, yielding 1,280 distractors. Distractor discrimination indices were calculated using both rPB_D and rPB_{DC}. Analyses focused on “inversions,” defined as distractors showing positive rPB_D index but negative rPB_{DC} index. The magnitude of the difference between both indices was also examined descriptively.
Results: Only 36 of 1,280 distractors (2.8%) demonstrated inversions between methods. Among these, the difference in distractor discrimination index exceeded 0.10 in 9 distractors, ranged from 0.05 to 0.10 in 8 distractors, from 0.01 to 0.05 in 16 distractors, and were below 0.01 in 3 distractors. Furthermore, only 8 distractors (0.6% of all distractors) showed rPB_{DC} values below −0.05 despite positive rPB_D values. Across all distractors, the mean difference between methods was 0.037, indicating minimal overall divergence.
Conclusion: In this examination context, the modified rPB_{DC} approach provided little additional benefit over the conventional rPB_D method for identifying nonfunctional distractors. Both methods yielded highly comparable results, while the modified approach excludes information from alternative distractors. Further research should evaluate whether these findings generalize across different examinations and populations.

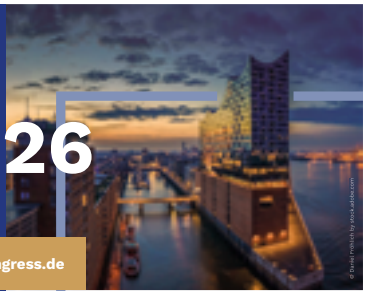

OC 15 FLOW of Knowledge: Methods and teaching in Physiology

OC1506

Diffdigester.unijena.de: a tool for optimized selection of restriction enzymes for plasmid identification in cloning procedures

Martin Gühmann; Stefanie Reuter; Ralf Mrowka
Experimentelle Nephrologie, Klinik für Innere Medizin III, FriedrichSchillerUniversität Jena, Jena, Germany;

Objective: Differential digests, also known as test or diagnostic digests, are a standard method in molecular cloning used to confirm whether a cloned plasmid is the target plasmid. However, selecting the right restriction enzyme for a differential digest by hand may be challenging and timeconsuming. To simplify this task, we created a free online tool called diffdigester.unijena.de (https://diffdigester.unijena.de).
Results: This tool finds restriction sites with regular expressions and displays the resulting DNA fragments as they would appear on a gel. The user can sort these gels by enzyme name or by dissimilarity of the restriction patterns between the different DNA sequences. This shows the most distinct pattern first and helps choosing the best enzyme to distinguish between desired and undesired ligation products. Additionally, the tool works with unrelated sequences, broadening its applications.
Conclusion: Thus, diffdigester.unijena.de is a quick, reliable, and freetouse tool for planning differential digests to verify ligation products from cloning.

P01 Postergroup: Renal Vascular & Glomerular Function

P0101
Development of SuperResolution Ultrasound Imaging Methods for In Vivo Characterisation of Renal Microvascular Disease

Amy Mcdermott; Iman Taghavi 1; Natalia Perez Jimenez 1; Mostafa Amin Naji 1; Jørgen Arendt Jensen 1; Charlotte Mehlin Sørensen
University of Copenhagen, København, Denmark; 1 Department of Health Technology, Center for Fast Ultrasound Imaging, Technical University of Denmark, Lyngby, Denmark;

Objective: Microvascular remodelling is a key feature of diabetic kidney disease (DKD) and hypertension, yet current imaging approaches lack the resolution required for comprehensive in vivo assessment of renal microvascular structure and haemodynamics. This project aimed to develop and optimise advanced renal imaging methodologies for the characterisation of microvascular disease in preclinical models of cardiometabolic kidney injury.
Method: Spontaneously Hypertensive Rats (SHR), Zucker Diabetic Fat (ZDF) rats, and corresponding control strains were studied to investigate renal microvascular remodelling. In vivo ultrasound superresolution imaging (SRI) and superresolution ultrasound using erythrocytes (SURE) methods were optimised for renal vascular imaging and haemodynamic assessment. Imaging workflows were developed to improve microvascular visualisation, vessel tracking, and flow quantification within the kidney. Complementary ex vivo imaging was performed using vascular perfusion with Microfil followed by highresolution microcomputed tomography (ZEISS XRadia 410 Versa µCT) to enable threedimensional vascular reconstruction. Imageprocessing pipelines were developed for quantitative assessment of vascular remodelling.
Results: Preliminary work has established robust imaging acquisition protocols and computational workflows for multimodal renal vascular imaging. Optimisation of SRI and SURE techniques has demonstrated the feasibility of highresolution in vivo visualisation of renal microvascular structure and flow dynamics. Ongoing analyses in hypertensive and diabetic rat models aim to characterise diseaseassociated alterations in renal vascular architecture and haemodynamics. Development of semiautomated processing pipelines is expected to improve the reproducibility and efficiency of quantitative vascular phenotyping across imaging platforms.
Conclusion: This work establishes an integrated imaging framework for highresolution assessment of renal microvascular disease in preclinical models. The optimisation of in vivo ultrasound superresolution imaging alongside advanced computational analysis provides a platform for detailed mechanistic investigation of renal haemodynamics and microvascular remodelling, supporting future translational development of noninvasive imaging biomarkers

P01 Postergroup: Renal Vascular & Glomerular Function

P0102

Autoimmunoglobulintriggered extracellular vesicles link exopherlike waste removal to immune complex clearance in membranous nephropathy

Nick Arkan; Marie Adler [1]; Pablo Saez [1]
Institut für Zelluläre und Integrative Physiologie, Zentrum für Experimentelle Medizin, Universitätsklinikum HamburgEppendorf, Hamburg, Germany; [1] Cell Communication and Migration Laboratory, University Hospital HamburgEppendorf, University of Hamburg, Hamburg, Germany;

Objective: Kidney podocytes maintain the filtration barrier through their interdigitating foot processes (FPs), interconnected by slit diaphragms (SDs). In membranous nephropathy (MN), circulating autoantibodies bind to FP antigens such as THSD7A. The resulting glomerular immune complex (IC) are used for MN diagnostics. Recently, our group identified autoimmunoglobulintriggered extracellular vesicles (AITEVs) link glomerular IC clearance to FP effacement. Strikingly, AITEV biogenesis shares fundamental features with exopher formation in proteotoxicstressed C. *elegans* neurons and murine cardiomyocytes, suggesting a conserved waste removal mechanism. Here, we investigate the evolutionary parallels of AITEV formation and exopher biology in an *in vitro* THSD7AMN model.
Method: Human podocytes overexpressing THSD7A were exposed to labeled antiTHSD7A antibodies. Highresolution confocal live allowed in vivo tracking of labeled THSD7A- and 1433 antibodies. The functional involvement of 1433 was assessed by pretreatment with a 1433 inhibtor (R18). Cells were subsequently fixed and stained for oxidative stress, vesicular markers (1433, annexin A1), and potential contributors to vesicle biogenesis (NCAM1, annexin A2).
Results: Autoantibody binding particularly at thin actin processes that contain THSD7A, initiates small aggregate formation at peripheral podocyte membranes. Live imaging revealed that these IC translocate to the juxtanuclear region, fusing into larger aggregates. Subsequently, plasma membrane budding generates AITEVs containing the antibodyantigenaggregates, 1433, annexin A1 and NCAM1. Pretreatment with R18 strongly reduced membranebound rbTHSD7A aggregate formation and translocation, while confocal live imaging confirmed absence of juxtanuclear aggregates. This parallels the role of 1433 as dyneinlinked adaptor protein in aggregate transport during C. *elegans* exopher formation.
Conclusion: While the initial trigger differs — extracellular autoantibody binding in MN vs. intracellular proteotoxic stress in C. *elegans* — AITEV and exopherformation converge on 1433dependent aggregate translocation, plasma membrane budding, and ejection of proteotoxic cargo. Both mechanisms operate in terminally differentiated cells, when degradation pathways are overwhelmed. The dual role of AITEVs in extra- and intracellular waste removal, and their molecular and morphological resemblance to exopherformation, positions podocyte membrane budding within a broader framework.

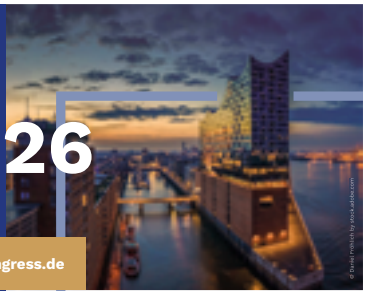

P01 Postergroup: Renal Vascular & Glomerular Function

P0103

A link between caldesmon and renin expression: an exploratory study

Sina Schumacher; Stephanie Probst; Bettina Scharner; Vladimir T. Todorov [1]
Physiology and Pathophysiology, University Witten/Herdecke, Witten, Germany; [1] Zentrum für Biomedizinische Ausbildung und Forschung (ZBAF), Lehrstuhl für Physiologie, Pathophysiologie und Toxikologie, Universität Witten/Herdecke, Witten, Germany;

Objective: Renin produced by the juxtaglomerular (JG) cells in the afferent arterioles of the kidney is a central regulator of systemic blood pressure and renal perfusion through activation of the renin–angiotensin system. Angiotensin II acts as a potent vasoconstrictor of vascular smooth muscle cells and is therefore essential for the maintenance of vascular tone and blood pressure homeostasis. Caldesmon, a key regulator of actin–myosin interactions, has emerged as an important modulator of vascular tone, cytoskeletal remodeling, and renal microvascular function, where it contributes to smooth muscle relaxation and regulation of vascular resistance. Using RNA sequencing of JG cells isolated from renincell specific Gsα knockout mice, in which cAMP signaling required for renin synthesis is impaired, we observed reduced expression of both renin and caldesmon. This finding raises the question of whether caldesmon and renin may directly influence each other's expression and whether caldesmon contributes to the regulation of JG cell function and vascular resistance within the afferent arteriole.
Method: To investigate a potential link between caldesmon and renin regulation, we used the human reninexpressing cell line Calu6 to analyze the effects of caldesmon knockout on renin expression, its stimulation, cellular proliferation, and cell–cell interactions. Cells were stimulated to induce high levels of renin expression and subsequently analyzed in a caldesmon knockout background.
Results: Preliminary data indicates that caldesmon knockout in Calu6 cells reduces renin expression, suggesting a potential functional interaction between caldesmon and renin production.

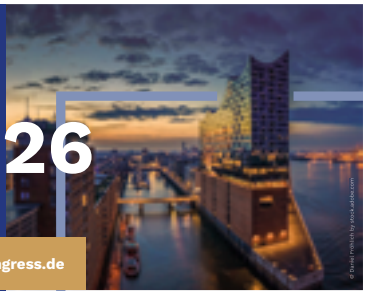

P01 Postergroup: Renal Vascular & Glomerular Function

P0104

Mechanistic response of the podocytes endolysosomal system upon antibody mediated stress

Rebecca Reidick; Katrin Neumann [1]; Stephanie Zielinski [1]; Elena Tasika [1]; Catherine Meyer Schwesinger [1]; Wiebke Sachs [1]
Universitätsklinikum HamburgEppendorf, Hamburg, Germany; [1] Institut für Zelluläre und Integrative Physiologie, Zentrum für Experimentelle Medizin, Universitätsklinikum HamburgEppendorf, Hamburg, Germany;

Objective: Podocytes are highly specialized cells of the glomerular filtration barrier that are frequently exposed to autoantibodymediated injury. Recent studies identified a new cellular response mechanism in which injured podocytes release extracellular vesicles (EVs) into the urine upon podocyte antigen targeting by autoantibodies, termed autoimmunoglobulintriggered (AIT)EVs. These vesicles contain endolysosomal proteins, suggesting a potential involvement of the endolysosomal pathway in AITEV biogenesis and release. The endolysosomal system is not only involved in protein degradation but regulates, among others, intracellular trafficking, membrane turnover, and cellular stress responses. However, its specific involvement in podocyte injury is unknown. This project investigates whether the identity and subcellular localization of podocyte proteins that are targeted by autoantibodies, differentially influences endolysosomal pathway activation, thereby shaping the podocyte stress response, including AITEV formation and release.
Method: Antibodymediated podocyte injury was induced in BALB/c mice using rabbit polyclonal antibodies (abs) targeting podocyte proteins expressed at distinct subcellular compartments of the glomerular filtration barrier (GFB), including THSD7A, MRC2, and GLEPP1. Functional and structural podocyte responses were assessed by longitudinal urinary albumintocreatinine ratio measurements and EV analyses from urine samples collected every second day. Serum parameters including albumin, creatinine, cholesterol, and triglycerides were analyzed from blood samples obtained at day 14. Day 14 kidney tissue was used for highresolution confocal microscopy, while isolated glomeruli will be analyzed by immunoblotting.
Results: Antigenspecific podocyte injury resulted in distinct structural, functional and EVassociated responses. Functionally, antiTHSD7Aabs induced marked proteinuria accompanied by elevated serum cholesterol levels, while antiMRC2abs and antiGLEPP1abs showed no nephrotic phenotype. Immunofluorescence microscopy exhibited antigenspecific injury patterns. AntiTHSD7A induced classical GFBassociated IgG deposits with strong complement C3 positivity, while mice exposed to antiMRC2abs showed punctate GFBassociated IgG deposits. Mice receiving antiGLEPP1abs exhibited limited aggregatelike GFBassociated IgG deposition. Preliminary findings suggest temporal dynamics in urinary AITEV release, which differs depending on the targeted antigen.
Conclusion: The extent of functional podocyte impairment and pattern of antibody accumulation at the GFB depends on the subcellular localization of the targeted protein.

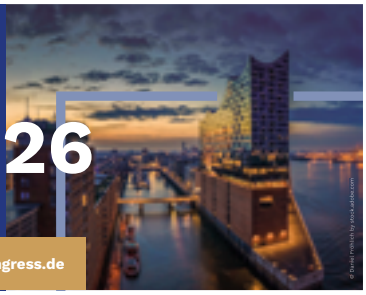

P01 Postergroup: Renal Vascular & Glomerular Function

P0105

Lysosomal impairment protects against antibody mediated podocyte injury

Wiebke Sachs; Desiree Loreth; Karen Lahme; Vincent BöttcherDierks; Ashnoor Kaur Soni; Stephanie Zielinski; Johannes Brand; Elena Tasika; Catherine MeyerSchwesinger
Institut für Zelluläre und Integrative Physiologie, Zentrum für Experimentelle Medizin, Universitätsklinikum Hamburg
Eppendorf, Hamburg, Germany;

Objective: The endolysosomal system is not only central for protein degradation but is also involved in a plethora of cellular processes, including the mediation of immune response, metabolism, signaling and membrane repair. As podocytes rely on the ubiquitin proteasome system (UPS) to maintain their proteostasis under physiologic conditions, the role of the endolysosomal system for podocyte health remains elusive. Podocyte injury is accompanied by proteotoxic stress and abnormal protein accumulations even though, both the endolysosomal and proteasome system are induced. We here assess the impact of the lysosomal system on the podocytes' resilience to antibodymediated injury.
Method: A mouse model of the lysosomal storage disorder mucolipidosis type II (MLII), which is caused by mutations in the nacetylglucosamine phosphotransferase leading to lysosomal enzyme missorting, was treated with antiTHSD7A antibody to induce podocyte injury. Disease progression was monitored clinically, and podocyte injury was assessed histologically. Changes in the degradative machinery were assessed using biochemical and histologic approaches. Further, the formation and abundance of podocytederived extracellular vesicles released into the urine were analysed via ImageStream.
Results: THSD7A antibodychallenged MLII mice were clinically inconspicuous whereas wildtype littermate controls presented with proteinuria and hyperlipidemia. Podocyte exact morphology measurement procedure (PEMP) revealed a tighter filtration slit density in MLII mice in comparison to their littermate controls. Interestingly, histologic assessment of Limp2+ lysosomes revealed increased amounts of Limp2 at the filtration slit, intercalating with the nephrin signal in MLII mice but not in littermate controls. Monitoring of podocytederived extracellular vesicle release to the urine revealed increased amounts in the urine of MLII mice in comparison to wildtype littermates.
Conclusion: Mucolipidosis type II mice are protected in antibodymediated injury, possibly due to an increased release of extracellular vesicles which might be an additional process to relief podocytes from increased proteotoxic stress. Also increase Limp2 levels at the podocyte membrane could indicate an involvement of Limp2+ lysosomes in maintaining podocyte plasma membrane homeostasis.

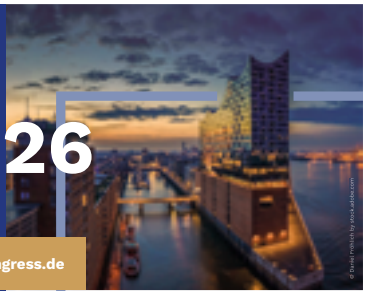

P01 Postergroup: Renal Vascular & Glomerular Function

P0106

Nephrin as a Novel Substrate of A Disintegrin And Metalloproteinase 10 (ADAM10)

Alina Lampert; Xueyu Li; Lisa SeipoldZimmermann [1]; Julia Reichelt; Desiree Loreth; Lukas Blume; Helga Vitzthum; LenaMarie Reimers; David Rosenbaum [1]; Simonas Gaudatis [1]; Karen Lahme; Sarah Frömbling; Christopher Kosub [2]; Stephanie Zielinski; Felix Mejia [3]; Marcia L. Moss [3]; Thorsten Wiech [4]; Tobias N. Meyer [5]; Paul Saftig [1]; Catherine MeyerSchwesinger Institut für Zelluläre und Integrative Physiologie, Zentrum für Experimentelle Medizin, Universitätsklinikum HamburgEppendorf, Hamburg, Germany; [1] Biochemisches Institut, ChristianAlbrechtsUniversität zu Kiel, Kiel, Germany; [2] Nephrologie/ Rheumatologie und Endokrinologie/Diabetologie, III. Medizinische Klinik, Universitätsklinikum HamburgEppendorf, Hamburg, Germany; [3] Verra Therapeutics, Lansing, United States; [4] Institut für Pathologie, Sektion Nephropathologie, Zentrum für Diagnostik, Universitätsklinikum HamburgEppendorf, Hamburg, Germany; [5] Klinik für Nephrologie, Diabetologie, Dialyse, Asklepios Klinik Barmbek, Hamburg, Germany;

Objective: The autoimmune kidney diseases minimal change disease (MCD) and membranous nephropathy (MN) are the leading cause of nephrotic syndrome in children and adults, respectively. A hallmark of both diseases is podocyte injury leading to a disruption of the glomerular filtration barrier (GFB) and clinically manifesting as nephrotic syndrome, characterised by massive proteinuria, hypoalbuminemia, edema, and hyperlipidemia. Podocytes form the slit diaphragm, a key component of the GFB, through the transmembrane proteins nephrin and neph1 on their foot processes. In the podocytopathies MCD and MN, these highly specialised epithelial cells are targeted by autoantibodies. Having recently demonstrated that the sheddase A Disintegrin And Metalloproteinase 10 (ADAM10) cleaves the major podocyte antigens in MN, we now aim to characterise its interaction with the MCD autoantigen nephrin.
Methods and Results: The distinct colocalization pattern of ADAM10 and nephrin was visualised in porcine and human kidney tissue using proximal ligation assays and superresolution confocal imaging. The colocalization signal got markedly pronounced along the podocyte foot processes and aggregated in the cytosol in MCD patient biopsies. Physical interaction of both proteins was confirmed by coimmunoprecipitation. Following treatment with ADAM10 inhibitors, fulllength nephrin levels stabilized, while extracellular Nterminal shedding products and intracellular Cterminal nephrin fragments decreased in porcine glomeruli; notably, this effect was absent for neph1. These findings remained consistent in HEK cells upon pharmacologic inhibition and genetic deletion of ADAM10. Regulated intramembranous proteolysis (RIP) was analysed using γsecretase inhibitors in pig glomeruli and HEK cells as well as γsecretase deficient HEK cells. All approaches showed a stabilization of Cterminal nephrin fragments.
Conclusion: Our findings identify nephrin as novel substrate of ADAM10 in health and disease undergoing subsequent RIPmediated processing of its Cterminal fragments. Whether these small proteolytic products exert signalling functions, analogous to Notch1, remains to be elucidated. The altered ADAM10–nephrin colocalization pattern in MCD suggests that this interaction might represent a critical regulatory node in podocyte injury and disease pathogenesis that warrants further studies.

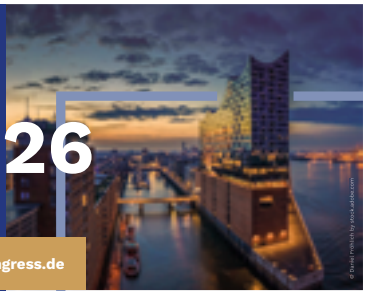

P01 Postergroup: Renal Vascular & Glomerular Function

P0107

Glomerular filtration rate and its association to inflammation and obesity in older subjects

Shalini Choudhary; Luca Verroest [1]; Jari Jokelainen [2]; Juha Auvinen [2]; Kari Mäkelä [3]; Mari Hämälainen [4]; Olli Kampman [5]; MarjoRiitta Jarvelin [6]; Sirkka Keinänen Kiukaanniemi [7]; KarlHeinz Herzig [8]; Ghulam Shere Raza [8] Department of Physiology, University of Oulu, Oulu, Finland; [1] Unit of Internal Medicine and Biomedicine, University of Oulu, Oulu, Finland; [2] Faculty of Medicine, Center for Life Course Health Research, University of Oulu, Oulu, Finland; [3] Research Unit of Biomedicine, Biocenter of Oulu, Oulu University, Oulu, Finland; [4] The Immunopharmacology Research Group, Faculty of Medicine and Life Sciences, University of Tampere, Tempere, Finland; [5] Faculty of Medicine and Life Sciences, Seinäjoki Central Hospital, University of Tampere, Tempere, Finland; [6] Department of Epidemiology and Biostatistics, School of Public Health, Imperial College London, London, United Kingdom; [7] Center for Life Course Health Research, Research Unit of Population Health, University of Oulu, Oulu, Finland; [8] Department of Physiology, Institute of Biomedicine and Internal Medicine, University of Oulu, Oulu, Finland;

Objective: Ageing is associated with progressive structural and functional changes in multiple organs, including kidneys. Renal ageing is characterized by nephron loss, reduced renal blood flow, and declining estimated glomerular filtration rate (eGFR), which collectively contribute to decreased kidney function. Ageing and obesity are potential contributors to chronic kidney disease (CKD), yet the mechanisms linking metabolic dysfunction and renal impairment in elderly populations remain poorly understood. We hypothesized that reduced eGFR in older adults is associated with obesityrelated metabolic dysfunction and systemic lowgrade inflammation.
Method: To investigate our hypothesis, we examined the association between eGFR and anthropometric, metabolic, and inflammatory markers in the elderly. 699 participants (293 men and 406 women; 68.9 ± 0.5 years) were included in a crosssectional analysis. Clinical measurements, anthropometric and circulating inflammatory markers were assessed. Spearman correlations were calculated to explore the relationship between eGFR and metabolic variables. Multivariate linear regression models were adjusted for cardiometabolic and lifestylerelated confounding factors.
Results: Men exhibited a higher prevalence of type 2 diabetes and hypertension, greater waist circumference, and elevated levels of inflammatory markers IL6 and YKL40 compared to women. In contrast, women displayed higher circulating levels of leptin and adiponectin and significantly reduced eGFR compared to men. eGFR showed significant inverse associations with HOMA2B, leptin, IL1ra, progranulin, and resistin. No significant correlations were observed between eGFR and BMI, waist circumference, blood pressure, CRP, IL6, and adiponectin. The association between eGFR and leptin, IL1ra, progranulin, resistin, and HOMA2B remained significant after adjustment.
Conclusion: In conclusion, reduced GFR in elderly participants was associated with markers of metabolic dysfunction and lowgrade inflammation, suggesting that these pathways may be involved in renal impairment in ageing. These findings suggest that inflammatory markers may affect renal microvascular regions, including the vasa recta of the kidney medulla, and should be further explored in future studies.

P01 Postergroup: Renal Vascular & Glomerular Function

P0108

Characterisation of AutoImmunoglobulinTriggered Extracellular Vesicles (AITEV) in Membranous Nephropathy

Nick Arkan; Vincent BoettcherDierks; Katrin Neumann; Karen Lahme; Desiree Loreth; Catherine MeyerSchwesinger
Institut für Zelluläre und Integrative Physiologie, Zentrum für Experimentelle Medizin, Universitätsklinikum HamburgEppendorf, Hamburg, Germany;

Objective: Membranous Nephropathy (MN) is the most common cause for nephrotic syndrome in adults. It is triggered by autoantibody binding to podocyte foot processes in the subepithelial space of the blood urine barrier. These antigenantibody complexes are finally released to the urine by podocytes as **AutoImmunoglobulinTriggered Extracellular Vesicles** (**AITEVs)**. AITEVs are a subtype of EVs that carry the antigenautoantibody complexes. The aim of this study is to further characterize AITEVs by establishing a specific marker profile of damaged podocyte surface membranes.
Method: MN patient's and healthy control urine was collected (n = 16). Total urinary EVs were isolated by differential ultracentrifugation, including a preclearing step for patient urines. AITEVs were discerned via 1433 and huIgG4 positivity by flow cytometry. Main focus was to identify the presence proteins associated with surface membrane stress. Further, confocal microscopy of control and MN patient biopsies was used to assess, if podocyte damage leads to a differential expression pattern of our markerproteins.
Results: Our analysis identified membranestress related proteins, like dystrophyassociated fer1like protein (dysferlin) and *4hydroxy2nonenal (*4HNE). The dysferlin is involved in membrane repair, while 4HNE *detects due to oxidated stress peroxidized lipids.* Flow cytometry of patient urine revealed a significant increase in the amount of AITEVs positive for both proteins when compared to controls. However, the amount of dysferlinpositive EVs varied between patients. Confocal microscopy showed that while in sections, dysferlin is expressed by endothelial cells and huIgG4 localizes to the capillary lumen, in MN patient biopsies huIgG4 was found in the subepithelial space and dysferlin at the glomerular filatration barrier and within the podocyte cytoplasm. Both proteins were present within urinaryspace aggregates (AITEVs) in MN.
Conclusion: Our data provides evidence for increased podocyte surface stress in MN using dysferlin and 4HNE as marker proteins and suggests that AITEV detection in patient urines may be suitable as a noninvasive diagnostic tool for podocyte injury.

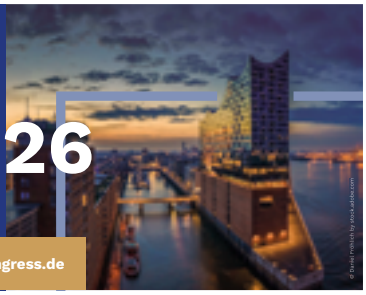

P01 Postergroup: Renal Vascular & Glomerular Function

P0109
Understanding the impact of kidney epithelial cells internalizing plasma proteins in doxorubicin proteinuric mice

Iben Skov Jensen; Vladyslava Ditiashova; Teri Hreha; Caroline KH Skands; Magdalena O Dubik; Jesper B Møller; Gitte R. Hinrichs; Per Svenningsen
Department of Molecular Medicine, University of Southern Denmark, Odense, Denmark;

Objective: Proteinuria is a negative prognostic marker of chronic kidney disease progression. When plasma proteins enter the renal tubules, the microenvironment changes dramatically, driving kidney damage and fibrosis. Yet, the underlying mechanisms are poorly understood. Further, while both male and female patients exhibit kidney damage related to proteinuria, males tend to have worse outcomes than females, indicating a profound sex difference in the kidney's response to proteinuria. This project aimed to investigate how internalization of plasma proteins into kidney epithelial cells influences cellular stress and damage during proteinuria in both adult males and females.
Method: We induced nephrotic syndrome with an intravenous injection of doxorubicin (Dox) 10 µg/g bodyweight in male and female BalB/CbyJ mice. On day 7 after injection, mice received an intravenous injection of fluorescently labeled plasma proteins, and the kidneys were harvested 2 hours later. Singlecell suspension of kidneys was sorted into proximal ($EpCAM1^{neg}$) and distal ($EpCAM1^{pos}$) epithelial cells with or without fluorescent plasma protein uptake. The 4 cell populations were analyzed by RNA sequencing.
Results: Seven days after Doxinjection, male and female mice displayed a similar degree of proteinuria, hypoalbuminemia, and increased plasma lipids. Immunolabeling of the kidneys showed internalized plasma proteins in megalin- as well as uromodulin, NCC- and AQP2p-ositive epithelial cells. Female mice, however, internalized plasma proteins to a much lesser extent. The difference between male and female mice was even more striking in the transcriptome of the sorted proximal and distal epithelial cells, where proteinuria caused a significant differential expression of ~4500 genes, both in the proximal and distal tubule in male mice, while only ~350 genes were affected in female mice.
Conclusion: This study showed that epithelial cells internalize plasma proteins throughout the nephron in nephrotic mice, but this occurs in a sexspecific manner. We speculate that this sex difference could be key to understanding the negative impact of plasma proteins in proteinuric kidney diseases.

P01 Postergroup: Renal Vascular & Glomerular Function

P0110

AITEV characterization in membranous nephropathy patients and generation of a nanobodybased detection tool

Laura Johanna Becerra Moreno; Karen Lahme; Catherine MeyerSchwesinger; Tobias N. Meyer [1]; Björn Rissiek [2]
Institut für Zelluläre und Integrative Physiologie, Zentrum für Experimentelle Medizin, Universitätsklinikum HamburgEppendorf, Hamburg, Germany; [1] Nephrology, Asklepios Klinikum
Barmbek, Hamburg, Germany; [2] Institut für Immunologie, Universitätsklinikum HamburgEppendorf, Hamburg, Germany;

Objective: In membranous nephropathy (MN), podocytes are targeted by autoantibodies, leading to deposition of immune complexes and ultimately damaging the kidney filtration barrier. Recently, AutoImmunoglobulinTriggered Extracellular Vesicles (AITEVs) carrying diseaserelevant antigens and autoantibodies were identified in the urine of MN patients and described as a novel autoantibodyinduced podocytederived vesicle population. This study investigated whether AITEVs represent an alternative noninvasive biomarker source for diagnostic and disease monitoring.
Method: To validate AITEVs as a novel biomarker, we detected bound autoantibodies by immunoblot, quantified the abundance and characterized specific markers by flow cytometry in longitudinal MN patient urine samples. The transgenic mouse line “LamaMice” was selected for immunization with MN patient AITEVs given their capability to solely produce camelid heavy chain antibodies, and thereby, nanobodies specific to MN marker molecules to facilitate more suitable detection assays and a more detailed characterization of AITEVs.
Results: Immunoblot analyses of AITEVs isolated from longitudinal urine samples of MN patients enabled the detection of bound autoantibodies, including cases with negative serum autoantibody titers, demonstrating their potential as a sensitive noninvasive biomarker for disease monitoring. Furthermore, flow cytometry analyses identified a distinct molecular fingerprint of AITEVs in MN, supporting their disease specificity. Building on these findings, we immunized “LamaMice” with MNderived AITEVs to generate and validate AITEVspecific nanobodies for more robust detection assays and a deeper molecular characterization of AITEVs.
Conclusion: Urinary AITEVs represent a promising noninvasive biomarker source for membranous nephropathy. Combined assessment of urinary AITEV abundance and bound autoantibodies may enable improved prognostic stratification and longitudinal monitoring of immunologic disease activity in MN patients.

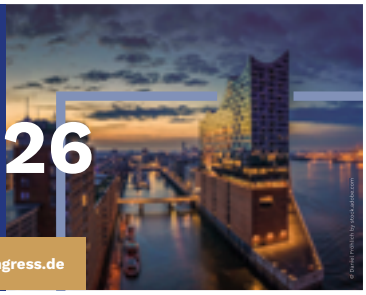

P01 Postergroup: Renal Vascular & Glomerular Function

P0111
Vascular constriction and dilation are tightly regulated, which directly affect blood pressure and perfusion

Yipeng Chen; Minze Xu; Kirschner Karin
Institut für Translatioinal Physiologie, Campus Charité Mitte, Charité - Universitätsmedizin Berlin, Berlin, Germany;

Objective: Under challenging events such as renal injury caused by ischemiareperfusion, vascular function is severely disturbed. Restoring vascular function after a harmful event can improve renal function. Studies have shown that treatment with polyamines can improve renal function in renal ischemiareperfusion injury and adenine nephropathy. The mechanism by how polyamines affect renal function. To investigate the mechanisms of three polyamines on the regulation of renal vascular function.
Method:
Microvascular Perfusion
Results:
Vascular dilatory effect on AA and EA mediated by spermidine.
Conclusion: Our previous experiments have verified the feasibility of this experiment. Polyamine compounds may suggest a dilatory effect on renal blood vessels. In the next experiments, we will explore the physiological mechanism of this effect and verify and explore the relationship with Kir channels. The insights gained from this study may help improve our understanding of renal vascular regulation and help develop new treatments for kidney injury.

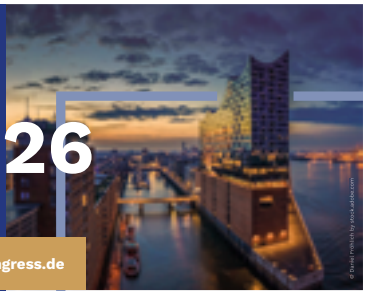

P01 Postergroup: Renal Vascular & Glomerular Function

P0112

The functional role of nephrocytes in the immune response of *Drosophila melanogaster*

Paris HazeltonCavill; Moritz Lassé; Tobias B. Huber; Sybille Köhler Nephrologie/Rheumatologie und Endokrinologie/Diabetologie, III. Medizinische Klinik,
Universitätsklinikum HamburgEppendorf, Hamburg, Germany;

Objective: Nephrocytes are specialised endocytic cells analogous to mammalian podocytes, however emerging transcriptomic and proteomic datasets suggest additional immuneassociated functions. We investigated whether nephrocytederived TEP2 contributes to systemic immune regulation and nephrocyte functional adaptation in *Drosophila.*
Method: TEP2 was specifically depleted using the nephrocytetargeted *Sns*Gal4 driver with validation of expression using FISH. Haemolymph proteomics enabled analysis of systemic immune changes. Changes in nephrocyte function were assessed by FITCAlbumin uptake assay, as well as immunofluorescence of the endocytic machinery. Wounding by pricking was used as an immune challenge model.
Results: We demonstrate strong expression of the immune factor TEP2 within nephrocytes. Cellspecific TEP2 knockdown altered the haemolymph immune proteome supporting a role for nephrocytes in circulating immune factor regulation. Baseline structure and function of these cells were largely preserved. Despite preserved baseline function, nephrocytes exhibited subtle remodelling characterised by altered nuclear DAPI intensity, changes in endocytic receptor abundance and increased lysosomal staining. Following immune challenge, control nephrocytes demonstrated enhanced endocytic uptake, as measured by increased FITCAlbumin fluorescence. This adaptive response was absent in TEP2 knockdown flies, revealing a TEP2dependent mechanism linking immune challenge to nephrocyte function.
Conclusion: Nephrocytes are not simply passive filtration cells. Our findings identify them as dynamic contributors to systemic immune regulation and reveal a previously underappreciated link between nephrocyte function and immune homeostasis.

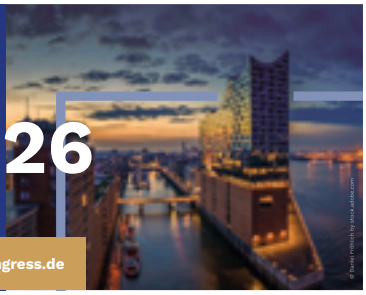

P01 Postergroup: Renal Vascular & Glomerular Function

P0113

First crossspecies proteomic glomerular cell atlas

Arvid Hutzfeldt; Uta Wedekind [1]; Yifan Tan [2]; Wiebke Sachs [1]; Lukas Blume [1]; Stephanie Zielinski [1]; Elena Tasika [1]; Favian Hatje [1]; Fatih Demir [2]; Vera Christine Wulfmeyer [2]; Moritz Lassé; PierreLouis Tharaux [3]; Thorsten Wiech [4]; Catherine MeyerSchwesinger [1]; Markus M. Rinschen [2] Nephrologie/Rheumatologie und Endokrinologie/Diabetologie, III. Medizinische Klinik, Universitätsklinikum HamburgEppendorf, Hamburg, Germany; [1] Institut für Zelluläre und Integrative Physiologie, Zentrum für Experimentelle Medizin, Universitätsklinikum HamburgEppendorf, Hamburg, Germany; [2] Department of Biomedicine, Aarhus University, Aarhus, Denmark; [3] Unité Mixte de Recherche (UMR)S1155, National Institute for Health and Medical Research (INSERM), Sorbonne Universités, Tenon Hospital, Paris, France; [4] Institut für Pathologie, Sektion Nephropathologie, Zentrum für Diagnostik, Universitätsklinikum HamburgEppendorf, Hamburg, Germany;

Objective: The glomerulus consists of three functionally distinct cell types, namely podocytes, mesangial cells, and endothelial cells. While singlecell RNA sequencing (scRNAseq) has provided transcriptomic cell type assignments, proteomewide characterization from human tissue is lacking. We built the first cell typeresolved proteomic atlas of human glomerular cells to validate transcriptomic marker assignments at the protein level, assess mousetohuman translatability, and provide a resource for disease gene interpretation.
Method: Human glomeruli were isolated from healthy parts of tumor nephrectomy tissue and podocytes, mesangial cells, and endothelial cells separated by FACS. Cell type specific proteomes were quantified by mass spectrometry and compared against equivalent mouse glomerular cellular fractions. Celltype separation, distinct protein expression validations were performed by qPCR and highresolution confocal microscopy.
Results: We identified 8,150 proteins across the three cell types, of which 1,818 were significantly enriched in one population over both others in two independent comparisons. This set of highly specific proteins represents the first unbiased, proteomewide cell type enrichment resource for human glomerular cells. Comparison with scRNAseq data revealed only moderate correlation (R = 0.4), confirming that transcript abundance does not reliably predict proteinlevel cell type enrichment. Crossreferencing our proteomic data with genes known to be causally implicated in FSGS and nephrotic syndrome confirmed the cell type assignments to podocytes (including KANK1 and PLCE1), mesangial cells (including CUBN), and endothelial cells (KANK 4). Additionally, 93, 44, and 61 surfaceexposed proteins were identified among endothelial, mesangial, and podocyte markers respectively, representing candidates for cell typespecific diagnostic or therapeutic targeting. Crossspecies comparison revealed several proteins with switched cell type enrichment between human and mouse glomeruli, the most striking being FGF1, which is podocyteenriched in humans specifically.
Conclusion: We present the first proteomic atlas of human glomerular cell types, confirming disease gene localization assignments from transcriptomics and identifying surface protein candidates for targeted therapy. Species differences in cell type enrichment, exemplified by FGF1, highlight the need for humanspecific proteomic validation in experimental nephrology.

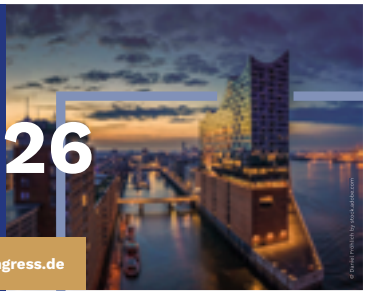

P01 Postergroup: Renal Vascular & Glomerular Function

P0114

The ubiquitinproteasome system and its effects on membrane dynamics in Drosophila nephrocytes

Michelle Bouchard; Paris HazeltonCavill; Karl K. Alornyo; Catherine MeyerSchwesinger [1]; Sybille Köhler; Tobias B. Huber
Nephrologie/Rheumatologie und Endokrinologie/Diabetologie, III. Medizinische Klinik, Universitätsklinikum HamburgEppendorf, Hamburg, Germany; [1] Institut für Zelluläre und Integrative Physiologie, Zentrum für Experimentelle Medizin, Universitätsklinikum HamburgEppendorf, Hamburg, Germany;

Objective: The ubiquitinproteasome system (UPS) is a highly conserved mechanism for protein degradation and essential for cellular proteostasis. The fruit fly *Drosophila melanogaster* harbors the proteolytic subunits prosβ1 (PSMB6), prosβ2 (PSMB7), and prosβ5 (PSMB5), as well as the immunoproteasomal subunits prosβ2(related)R1 and prosβ5(related)R1. The UPS also includes the transcription factor ewg (NRF1) and the enzymes uch (UCHL1) and ube3a (UBE3A).
Garland nephrocytes in larvae and pericardial nephrocytes in adults are used for these studies. While some proteasome and immunoproteasomal functions are understood in humans, their role in *Drosophila* nephrocytes remains unknown.
This project aims to define the functional role of the proteasome in nephrocytes and investigate how disruptions affect the recycling and degradation processes of conserved podocyte proteins.
Method: Nephrocytespecific depletion of proteasomal subunits and UPSassociated factors was used to assess filtration capacity, cellular morphology, and vesicular processing across developmental stages.
Results: Preliminary data indicate that loss of proteasomal subunits leads to pronounced morphological alterations and impaired filtration, with various subunits showing defects already in larvae. UPSassociated enzymes show weaker or agedependent phenotypes. Sexspecific differences in filtration capacity are detectable in young adults but become less pronounced with age.
Lysotracker staining additionally reveals changes in vesicular acidification upon depletion of proteasomal subunits, indicating altered lysosomal activity.
Conclusion: Together, these findings highlight a central role of the proteasome in maintaining nephrocyte structure and function. Future work will address how proteasomal impairment affects endocytic and recycling pathways as well as exocytosis, and how these alterations relate to conserved podocyte mechanisms in mammals.

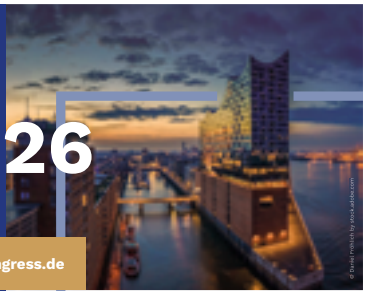

P02 Postergroup: Vascular Smooth Muscle Physiology

P0201

Nicotinamide adenine dinucleotide induces vasorelaxation in rat basilar arteries under normoglycemic and hypoglycemic conditions

Alexander Horack; Rüdiger Köhling; Rudolf Schubert [1]
OscarLangendorffInstitute for Physiology, University of Rostock, Rostock, Germany; [1] Physiologie, Medizinische Fakultät, Universitätsklinikum Augsburg, Augsburg, Germany;

Objective: Nicotinamide adenine dinucleotide (NAD) is increasingly recognized as a regulator of metabolic and vascular function. Beyond its established role in cellular energy metabolism and immunerelated signaling, NAD has been proposed to act as an extracellular signaling molecule with neurotransmitterlike and vasoactive properties. Previous studies have shown that NAD can modulate vascular tone in coronary, aortic, and mesenteric vessels. However, its functional effects in the cerebral vasculature, particularly under metabolically compromised conditions, remain insufficiently characterized.
Method: We examined the direct vascular effects of NAD on isolated basilar arteries from 3–4monthold Wistar rats using wire myography. All procedures followed institutional and legal guidelines for animal experimentation. Rats were anaesthetized with ether by inhalation prior to tissue harvesting. After verification of vessel viability, arterial segments were precontracted with U46619, a thromboxane A2 receptor agonist, and exposed to cumulative concentrations of NAD. To assess whether reduced glucose availability alters NADmediated vascular responses, a separate series was performed under hypoglycemic conditions by lowering buffer glucose to 10% of standard levels.
Results: NAD induced concentrationdependent relaxation of precontracted basilar arteries compared with control conditions. In the biologically clustered linear mixed model, significant effects were observed for condition ($p = 0.0247$), concentration ($p < 0.0001$), and the condition × concentration interaction ($p < 0.0001$; n = 12 NADtreated and 11 control animals). Post hoc analysis showed greater relaxation in the NAD group at higher concentrations. At the highest concentration, the response differed from control by −17.78 ± 4.42 percentage points (mean ± SEM; $p = 0.0002$). Under hypoglycemic conditions, baseline NAD reactivity did not differ between groups before glucose reduction. In the postintervention curves, the technical repeatedmeasures ANOVA showed no significant condition effect or condition × concentration interaction, whereas the biologically clustered model showed a significant interaction without a significant condition effect. Corrected post hoc comparisons revealed no significant difference at any concentration (n = 15 hypoglycemic and 14 control animals).
Conclusion: These findings indicate that NAD exerts direct vasorelaxant effects in rat basilar arteries. Reduced extracellular glucose was not associated with a uniform attenuation of NADinduced relaxation, although the clustered analysis suggests that the concentrationresponse profile may differ under hypoglycemic conditions. NAD may therefore contribute to cerebrovascular tone regulation under metabolic stress and represents a relevant signaling pathway for future studies on cerebrovascular dysfunction.

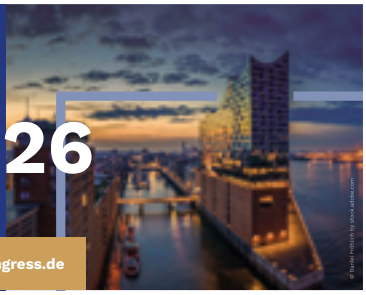

P02 Postergroup: Vascular Smooth Muscle Physiology

P0202

Longchain ceramides promote pulmonary vascular remodeling in PHLHD by dysregulating mitochondrial function

Huimin Jia; Qiuhua Li; Christoph Knosalla; Wolfgang M. Kübler; Mariya M. Kucherenko [1] Institut of Physiology, CharitéUniversitätsmedizin Berlin, corporate member of the Freie Universität Berlin and Humboldt Universität zu Berlin, Berlin, Germany; [1] Deutsches Herzzentrum der Charité, Berlin, Germany;

Objective: Elevated circulating levels of long chain ceramides (LCC) are linked to adverse cardiovascular outcomes, yet their role in pulmonary hypertension secondary to left heart disease (PHLHD) remains unclear.
Results: By metabolomic analyses, we identified increased levels of LCC 16:0 and 18:0 in pulmonary arteries (PA) of PHLHD patients compared to controls. This finding was replicated in a PHLHD rat model induced by surgical aortic banding (AoB). Consistent with ceramides´ documented ability to dysregulate mitochondrial function, we identified 114 proteins involved in mitochondrial membrane organization, transport, and respiration as dysregulated in PAs from PHLHD patients, while the expression level of neutral sphingomyelinase (nSMase) which generates ceramide from sphingomyelin was increased. In isolated rat PA smooth muscle cells, inhibition of nSMase by GW4869 rescued mitochondrial morphology and ATP production while reducing proliferation.
To probe for the therapeutic potential of ceramide inhibition *in vivo*, AoB rats received intraperitoneal (i.p.) injections of GW4869 (3 mg/kg, thrice weekly) from week 4 to 9 postAoB. GW4869 treatment did not significantly affect left ventricular systolic pressure or weight but significantly reduced right ventricular systolic pressure and hypertrophy. Echocardiographic analysis revealed that GW4869 partially restored PA acceleration time (PAAT), tricuspid annular plane systolic excursion (TAPSE), and PA radial strain, indicating improved pulmonary vascular and right ventricular function. Immunostaining of histological lung samples for αSMA and CD31 confirmed that ceramide inhibition significantly reduced PA medial thickening.
Conclusion: Here we report a new pathomechanistic role for LCC as drivers of pulmonary vascular remodeling in PHLHD via dysregulation of mitochondrial function. Targeting ceramide biosynthesis may present a promising strategy to improve pulmonary and right ventricular hemodynamics independent of left heart function.

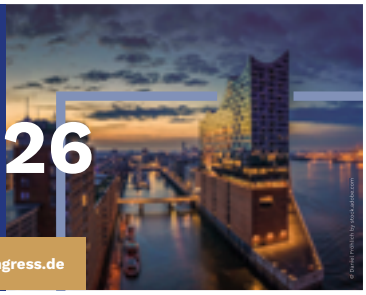

P02 Postergroup: Vascular Smooth Muscle Physiology

P0203

LPP as a mechanotransducer controlling vascular smooth muscle cell homeostasis in a sexdependent manner

Hangjun Ou; Alexandra Sporkova; Markus Hecker
Department of Cardiovascular Physiology, Institute of Physiology and Pathophysiologygie, Heidelberg university, Heidelberg, Germany;

Objective: Lipomapreferred partner (LPP) is a zyxin family protein that localizes to focal adhesions. Although LPP regulates actin dynamics and vascular repair, its role in sexdependent vascular protection remains unclear. This study aims to investigate the sexdependent role of LPP in vascular smooth muscle cells (VSMCs) and its underlying molecular mechanisms.
Method: Primary VSMCs from homozygous male or female *Lpp*$^{fl/fl}$ mice were isolated and transduced with a Cre recombinaseexpressing adenoassociated viral vector. Knockdown efficiency was analysed by immunofluorescence and Western blot. 2Dcell proliferation was monitored using the PHI0 Cellwatcher device. To better mimic the 3D vascular environment, VSMC spheroids were prepared for functional assays, including migration and contraction/relaxation assay on collagen matrices.
Results: AAV9based transduction achieved a minimum 95% reduction in LPP expression, as confirmed by both Western blot and immunofluorescence analysis. In male but not female VSMCs, LPP deficiency significantly ($p < 0.05$) accelerated 2D proliferation and enhanced 3D migration. Moreover, LPPdeficient VSMC spheroids showed impaired contractile responses to KCl and an attenuated caffeineinduced mobilization of intracellular calcium. Preliminary analyses indicate a divergent functional response between sexes, with ongoing experiments characterizing sexspecific migration kinetics and signaling cascades.
Conclusion: Our findings demonstrate that LPP is essential for maintaining the contractile VSMC phenotype and vascular integrity. Upon injury or overt biomechanical stress, the decline/loss of LPP causes switching to the synthetic phenotype, thereby facilitating maladaptive vascular remodeling. The observed sexdependency of the protective effects of LPP may provide new insights into the sexual dimorphism of cardiovascular diseases and the role of mechanotransducers in vascular physiology.

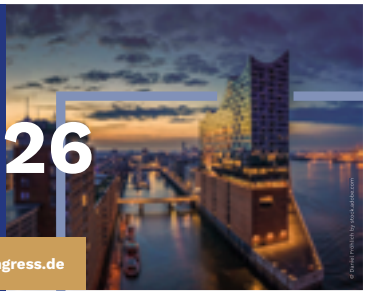

P02 Postergroup: Vascular Smooth Muscle Physiology

P0204

Pericyte contact alters endothelial cell metabolism by promoting exchange of lactate through SLC16A3

Mahdieh Safarzad; Sebastian Kempf [1]; Roman Vuerich [1]; Rüdiger Popp [1]; Timo Frömel [1]; Jiong Hu [1]; Ingrid Fleming [2]
Centre for Molecular Medicine, Institute for Vascular Signalling, Goethe University Frankfurt, Frankfurt am Main, Germany; [1] Centre for Molecular Medicine, Institute for Vascular Signalling, Goethe University, Frankfurt am Main, Germany; [2] Institute for Vascular Signalling, Goethe University Frankfurt am Main, Frankfurt a. M., Germany;

Objective: Intimate crosstalk between endothelial cells and pericytes is fundamental for vascular development and stability, yet the metabolic dimension of this interaction remains poorly defined.
Method: Using a filterbased coculture system that mimics the shared basement membrane of the microcirculation, we performed integrated multiomics analysis to investigate how direct contact reprograms both cell types.
Results: Initial contact did not induce quiescence, but instead triggered a transient, lowlevel endothelialtomesenchymal transition (EndMT)like state in endothelial cells, characterized by upregulation of genes involved in extracellular matrix production, including collagen isoforms, and PDGFR signaling, without loss of endothelial identity. Concomitantly, pericytes reshaped endothelial metabolism, increasing glycolysis and elevating intracellular pyruvate and lactate. Proteomic analysis of the contact interface revealed enrichment of solute carriers, most notably the lactate transporter SLC16A3. Functional studies demonstrated that pericytes act as a glycolytic partner, shuttling lactate to endothelial cells via SLC16A3. This lactate did not fuel the TCA cycle but instead served as a signaling metabolite, driving widespread alterations in the endothelial acetylome and lactylome, particularly affecting proteins involved in glycolytic metabolism. In vitro, exogenous lactate potentiated cytokineinduced EndMT and upregulated lactylationassociated genes. The physiological relevance of this lactate shuttle was confirmed in vivo, where endothelialspecific deletion of Slc16a3 in mice impaired retinal angiogenesis, reducing vessel density and endothelialpericyte overlap without affecting endothelial proliferation.
Conclusion: These findings establish that vessel maturation is orchestrated by a metabolically gated phase of plasticity initiated upon first contact, wherein a targeted EndMTlike program and pericytedriven lactate signaling coordinate vascular network assembly.

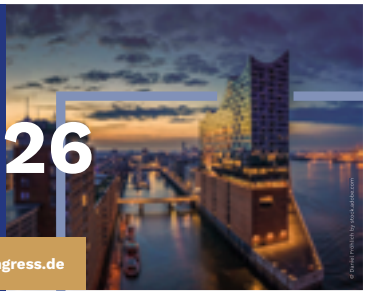

P02 Postergroup: Vascular Smooth Muscle Physiology

P0205

Comparing ChR2 and hOPN5 for Gastric Pacemaking

Lennart Evers; Johannes Riebeling; David Zipf; Markus Vogt; Lena-Christin Conradi 1; Michael Ghadimi 1; Robert Patejdl 2; Tobias Brügmann 3
Vegetative Optogenetics , Institute of Cardiovascular Physiology , University Medical Center Göttingen, Göttingen, Germany; 1 Clinic for General, Visceral and Pediatric surgery, University Medical Center Göttingen, Göttingen, Germany; 2 Physiology, Institute for Biomedical Research, HMU Health and Medical University Erfurt, Erfurt, Germany; 3 Institute of Cardiovascular Physiology, University medical center, Goettingen, Göttingen, Germany;

Objective: Gastroparesis is characterized by delayed gastric emptying in the absence of mechanical obstruction caused by dysfunction of the enteric nervous system and interstitial cells of Cajal. Typical symptoms include nausea, vomiting, bloating, early satiety, and epigastric pain. We compared the mechanism and potential of the optogenetic tools Channelrhodopsin2 (ChR2) and human Neuropsin (hOPN5) for to directly stimulate smooth muscle cells (SMC) for gastric pacemaking.

Method: Antral smooth muscle strips and intact stomachs from transgenic ChR2eYFP and hOPN5eYFP mice were stimulated using blue light (470 nm) or UV light (385 nm), respectively. Isometric force generation and intragastric pressure were analyzed and antral SMC strips of transgenic mice treated with 1 µM µM nifedipine, 30 µM carbenoxolone (CBX) and increasing concentrations of alltrans retinal. Longterm stimulation experiments were performed by repeated UVlight stimulation once per minute for 5 min followed by a 5 min pause, repeated over 2 h.
Results: Expression was restricted to SMC and found in ~one third of SMC in ChR2 and hOPN5 mice. Optogenetic stimulation induced force generation and increased intragastric pressure in both mouse models. In ChR2positive strips, bluelightinduced contractions were completely abolished by nifedipine, indicating dependence on extracellular calcium influx through Ltype Ca^{2+} channels. In contrast, nifedipine had no significant effect on UVlightinduced force generation in hOPN5 strips ($p = 0.65$), suggesting Ca^{2+}release from intracellular stores. ATR incubation was required for light responses in hOPN5 tissue. The halfmaximal ATR concentration required for hOPN5 activation was 370 ± 150 nM (N=3, n=10). CBX significantly reduced the maximum force of ChR2mediated contractions, indicating that lightinduced activation spreads from ChR2positive to neighboring negative SMC via gap junctions. In contrast, CBX increased the lightinduced force in hOPN5expressing tissues. Confocal Ca^{2+} imaging of hOPN5positive SMC showed that Ca^{2+} transients in single cells did not excite neighboring non expressing SMC.
Furthermore, hOPN5mediated force generation remained stable during a 2h stimulation period, with no significant decrease in response amplitude ($p > 0.20$).
Conclusion: Both ChR2 and hOPN5 enable reliable optogenetic stimulation of gastric smooth muscle. However, they have distinct but complementary mechanisms of action with important impact on the gene transfer for future treatment of gastroparesis.

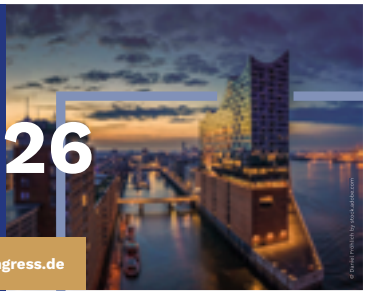

P02 Postergroup: Vascular Smooth Muscle Physiology

P0206

Aurora kinase A drives lung vascular remodeling by shortening primary cilia in pulmonary hypertension

Runhe Qin
Institute of Physiology, CharitéUniversitätsmedizin Berlin, Berlin, Germany;

Objective: Primary cilia (PC) are sensory organelles that coordinate mechanical and biochemical signalling in vascular cells and help maintain pulmonary vascular homeostasis. We previously showed that PC are shortened and less frequent in pulmonary vascular cells in pulmonary hypertension (PH) , and that PC loss contributes to pulmonary vascular remodelling and the development of PH. As Aurora kinase A (AURKA) regulates ciliary disassembly for cell cycle progression, we hypothesized that AURKA may contribute to PC loss and cellular phenotype changes characteristic for PH in lung vascular cells in response to characteristic PH stimuli.
Method: Human pulmonary artery smooth muscle cells (hPASMC) and human pulmonary artery endothelial cells (hPAEC) were stimulated with TGFβ (10 ng/mL) or PDGF (10 ng/mL), or exposed to hypoxia (1% oxygen). PC abundance and length were assessed by immunofluorescence staining for acetylated αtubulin and ARL13B. Cell migration was quantified using woundhealing assays. Cell proliferation was quantified by BrdUincorporation assays. AURKA activity, hPASMC hypertrophy and hPAEC endothelialtomesenchymal transition (EndoMT) was assessed by immunoblotting for phosphorylated AURKA and its downstream target HDAC6 as well as the hPAEC and hPASMC markers CD31 and αsmooth muscle actin (αSMA), respectively.
Results: In hPASMC and hPAEC, TGFβ increased AURKA activity while reducing PC number and length. Analogous effects were detected after stimulation with PDGF or hypoxia, suggesting AURKAdependent deciliation as a shared response to characteristic PH stimuli. In line with this view, AURKA inhibition with MK5108 (1 μM) increased PC length and the proportion of ciliated cells following treatment with PHlike stimuli. In parallel, MK5108 reduced stimulusinduced αSMA upregulation in hPAEC and hPASMC by 39.2% or 19.0%, respectively, indicating suppression of mesenchymal transition and hypertrophic responses. Finally, MK5108 attenuated TGFβinduced proliferation and migration of hPASMC and hPAEC.
Conclusion: These findings identify AURKA activation as novel pathomechanism in PH, in that AURKA promotes lung vascular cell deciliation and subsequent transition to a PH phenotype . Pharmacological inhibition of AURKA may hence present a novel therapeutic strategy for the treatment of PH.

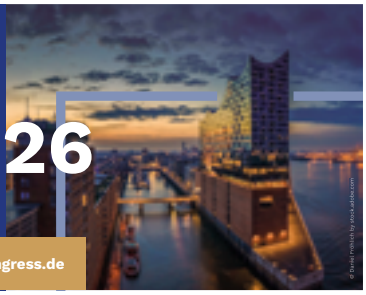

P02 Postergroup: Vascular Smooth Muscle Physiology

P0207
Exploring the molecular mechanism of the bidirectional contractile effect of Angiotensin II in murine vasculature

Lubomir Lubomirov; Chukwuanyinonso Ikeotuonye; Michael Andriske [1]; Vladimir T. Todorov Biomedical Center for Education and Research (ZBAF), Institute of Physiology and Pathophysiology, Witten/ Herdecke University, Witten, Germany; [1] Research Group Physiology of Senses, Faculty of Biology und Biotechnology, RuhrUniversity Bochum, Bochum, Germany;

Objective: Pathophysiologic activation of ReninAngiotensin System (RAS) parallels various cardiovascular diseases such as heart failure, hypertension, chronic kidney disease and arteriosclerotic disease. Present work has explored the molecular mechanism of the contractile effect of the effector hormone Angiotensin II (ANGII) in murine vasculature.
Method: Contractility of murine superior mesenteric- (MA), tail- (TA), interlobar- (IA) and saphenous- (SA) arteries was studied by wiremyography. Phosphorylation of 20 kDa myosinregulatorylightchain (MLC_{20}) and targeting subunit of myosinlightphosphatase, MYPT1 at position Serine668 (MYPT1S668, ProteinkinaseGsite) were determined with western blotting.
Results: Application of 60mM K^+ increased force to 8.8 mN in MA, 11.4 mN in TA, 5.8 mN in IA and 12.3 mN in SA, respectively. Treatment of all vessels with maximal concentrations of $a_1$agonist, phenylephrine, increased force similarly. The mechanical removal of endothelium did not affected the contractile effect of 60mM K^+, but abolished the acetylcholineinduced relaxation. In all vessels with intact endothelium, application of maximal concentrations of ANGII (1µM) induced transient rise in force (peak), followed by a decline and stabilization (plateau). While in TA and SA the ANGIIpeak was similar to the force obtained with 60mM K^+, in MA and IA these values were only ~30% of those detected in high K^+. In TA and SA, removal of endothelium was without effect on ANGIIpeak but increased the plateau to 33% and ~22% of high K^+ ($p<0.05$). By contrast, in MA and IA neither peak nor plateau were affected by endothelial removal. Interestingly, while the contractile response of repetitive application of ANGII was abolished in visceral arteries (IA and MA), in SA and TA this response was preserved. In addition, in isolated segments of SA the timecourse of $MLC_{20}$and MYPT1S668phosphorylations showed similarity with the forcekinetic observed in contractile the experiments.
Conclusion: The present work provides evidence that the contractile effect of ANGII involves a rapid transient rise in force followed by force decline and plateau. Our work also suggests that in visceral arteries the ANGIIcontractile effect is not dependent from vascular endothelium, whereas in peripheral resistive vessels the relaxing component of ANGIIplateaucontraction is to a great extent endothelium dependent.

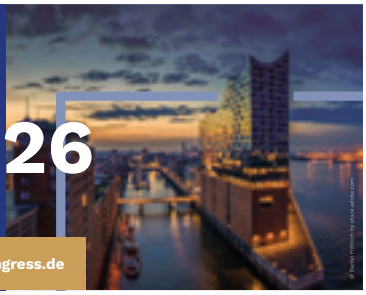

P02 Postergroup: Vascular Smooth Muscle Physiology

P0208

Septic associated lactic acidosis impairs human vascular smooth muscle cell contractility

Stefanie Ruhs; Philipp Terpe [1]; Michael Bucher [1]
Universitätsklinik und Poliklinik für Innere Medizin, Herz- und Thoraxchirurgie, Universitätsklinikum, MartinLutherUniversität HalleWittenberg, Halle (Saale), Germany; [1] Clinic for Anaesthesiology and Surgical Intensive Care, Julius Bernstein Institute of Physiology, MartinLuther University HalleWittenberg, Halle (Saale), Germany;

Objective: Sepsis, a lifethreatening organ dysfunction caused by a dysregulated host response to infection, is associated with a high mortality (20 to 50%). During sepsis, lactic acidosis (LA) with elevated serum lactate levels (>2 mmol/L) is frequently observed and associated with poor clinical outcomes. The septic vasculature exhibits reduced responsiveness to vasopressors, leading to systemic vasodilation and therapyresistant arterial hypotension. The resulting vasoplegia and the mechanisms linking lactic acidosis to vascular smooth muscle cell (VSMC) dysfunction and phenotypic alterations remain insufficient understood. The aim of this study was to investigate the effect of lactic acidosis on VSMCs contractility, compared to control conditions, as a surrogate of vascular functionality. Furthermore, these results were compared with the effects observed under acidosis alone and after addition of Na^+lactate.
Method: Human aortic smooth muscle cells (HAoSMCs) were treated for 48 h with lactic acidosis (LA, pH 6.8), hydrochloric acid (HCl, pH 6.8), Na?lactate (pH 7.4), and corresponding controls (pH 7.4; mannitol, pH 7.4, as a hyperosmolarity control). To assess cell contractility, cells were stained with CalceinAM (cytoplasmic staining) and Hoechst (nuclear staining) and imaged before and after ionomycin stimulation using a Cytation3 digital microscope. Image analysis was performed using Gen5 Image Prime 3.08 software.
Results: Ionomycininduced cell contractions were quantified in a concentrationdependent manner using the relative lengthtowidth (L/W) ratio. Assuming an ellipsoidal cell geometry and constant cell volume (spherical approximation), relative L/W changes were converted into percentage contraction, which was independent of the initial cell shape. The maximal contractile response (V_{max}) and the ionomycin concentration at 50% of the maximal contraction (EC_{50}) were calculated for each experimental condition. HCl- and LAinduced acidosis reduced maximal contractile capacity (V_{max}) and enhanced EC_{50}, indicating impaired contractile function and/or altered calcium handling. These findings indicate a predominantly acidotic effect, as both mannitol and Na^+lactate increased V_{max} and reduced EC_{50} values compared to control conditions.
Conclusion: In summary, acidosis, rather than lactate itself, is the primary determinant of impaired VSMC contractility, potentially involving altered calcium sensitivity/handling.

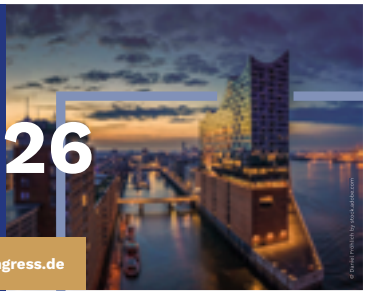

P02 Postergroup: Vascular Smooth Muscle Physiology

P0209

Multiple potassium channels contribute to ETCORM induced vasorelaxation

Asli Altayeva; Rudolf Schubert
Physiology, Institute of Theoretical Medicine, Medical Faculty, University of Augsburg, Augsburg, Germany;

Objective: The 21st century is associated with industrial expansion and rapid urbanization, thus, leading to a continuous dependence on fossil fuels, which eventually results in combustion of persistent, odorless gas. In particular, carbon monoxide (CO), which can accumulate outdoors and indoors by causing permanent exposure to air pollution, affecting people's wellbeing. A previous study has concluded that in rat mesenteric arteries, COinduced vasodilation is mediated exclusively by Kv7 channels . In mesenteric arteries Kv7 channels dominate at the mRNA level, whereas BK channels also constitute a considerable fraction in saphenous arteries. As the exact role of BK channels in COevoked vasodilation remains unclear, the hypothesis that COinduced vasodilation in saphenous arteries is mediated by both Kv7 and BK channels was tested.
Method: Contractile responses of endotheliumdenuded saphenous arteries of 12weeks old male rats were studied using myography. Realtime PCR was performed to determine potassium channel expression at the mRNA level. Enzyme triggered carbon monoxide releasing molecules (ETCORM) were used as CO donors.
Results: Simultaneous mRNA expression analysis in mesenteric and saphenous arteries showed that isoforms of Kv7 (KCNQ) channels are expressed at slightly higher levels in mesenteric compared to saphenous arteries. Pretreatment of vessels with potassium channel inhibitors demonstrated that ETCORM induced vasodilation is considerable when only Kv7 channels are available, but only moderate when solely BK channels remain accessible.
Conclusion: Our data show that both Kv7 and BK channels account for substantial proportions of the mRNA for potassium channels in saphenous arteries. Both channels contribute to ETCORMinduced vasodilation, with BK channels playing a smaller role.

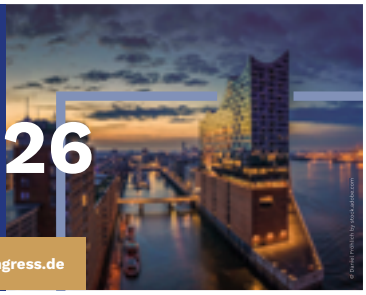

P02 Postergroup: Vascular Smooth Muscle Physiology

P0210

Integrin β2mediated activation of procalcific signaling in vascular smooth muscle cells by extracellular matrix protein 1

Anson Antony; Sabine Knipp; Arndt Rohweder; Azmat Sohail; Alexander Kasbary; Adela Tiffner; Beatrice Toegel; Mehdi Razazian; Sheyda Bahiraii; Manousos Makridakis [1]; Antonia Vlahou [1]; Jakob Voelkl; Ioana Alesutan
Institut für Physiologie und Pathophysiologie, Johannes Kepler Universität Linz, Linz, Austria; [1] Center of Systems Biology, Biomedical Research Foundation of the Academy of Athens, University of Athens, Athens, Greece;

Objective: Medial vascular calcification is highly prevalent and associated with increased risk for cardiovascular events and mortality in chronic kidney disease (CKD). This process is regulated by vascular smooth muscle cells (VSMCs) and involves extracellular matrix remodeling in the vasculature. The present study investigated the potential involvement of extracellular matrix protein 1 (ECM1) in VSMC calcification and the underlying mechanisms.
Method: Experiments were performed *in vitro* in calcifying primary human aortic VSMCs and *ex vivo* in mouse aortic explants.
Results: ECM1 expression was upregulated in VSMCs during procalcific conditions, and ECM1 knockdown suppressed calcification mediuminduced procalcific marker expression as well as calcification of VSMCs. Conversely, exposure to recombinant human ECM1 protein promoted procalcific marker expression and augmented procalcific signaling and calcification of VSMCs during procalcific conditions. Inhibition of integrin β2 with a neutralizing antibody or silencing of the *ITGB2* gene blunted ECM1induced procalcific signaling in VSMCs. In addition, silencing of *ITGB2* had protective effects on VSMC calcification during procalcific conditions. Increased *ECM1* mRNA expression in calcification medium was mediated by the procalcific transcription factor CBFA1, as its pharmacological inhibition was able to abrogate this effect. In mouse aortic explants, Cbfa1 inhibition reduced phosphateinduced procalcific signaling and calcification, effects paralleled by suppression of *Ecm1* mRNA expression and altered distribution in the medial layer.
Conclusion: ECM1 is upregulated and promotes VSMC calcification during procalcific conditions, effects mediated at least in part by integrin β2. Thus, ECM1integrin β2 signaling may play an important role in vascular calcification during pathological conditions such as CKD.

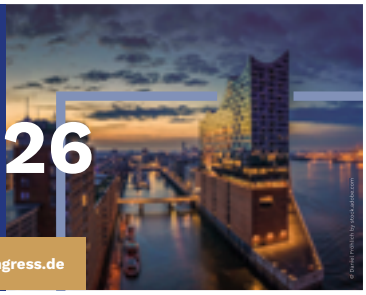

P02 Postergroup: Vascular Smooth Muscle Physiology

P0211

Role of 5HT2B serotonin receptors in coronary vasoconstriction in isolated rodent hearts

Wassim Fakhreddine; Katrin Porath; Falko Lange; Rüdiger Köhling; Timo Kirschstein
Oscar Langendorff Institut für Physiologie, Universitätsmedizin Rostock, Rostock, Germany;

Objective: Serotoninmediated coronary spasms are potential causes of myocardial ischemia. Effects of serotonin are receptorspecific and therefore potentially pharmacologically modifiable. However, while most studies concentrated on 5HT4 receptors, the literature on 5HT2B receptors also expressed in coronary vessels is scarce.
Method: The objective of the present study was to explore the role of 5HT2B receptors on serotonininduced vasoconstriction in the coronary vascular bed of the isolated rodent heart. To this aim, rat hearts were mounted on a Langendorff apparatus and perfused with oxygenated and bicarbonatebuffered electrolyte perfusion solution containing 10 mmol/l glucose (~330 mOsm/kg H2O). To assess the effect of serotonin antagonists LY272015 (5HT2B) and SB221284 (5HT2B/C) on serotonininduced vasoconstriction, we first applied perfusion solution containing serotonin and then added either antagonist to the bath. Our measures were the electrocardiogram, the aortic pressure and the left ventricular systolic pressure.
Results: Serotonin (5 µM) alone caused an increase of the aortic pressure, indicating an increase of coronary resistance, but had virtually no effect on the other two measures. This increase was reversed by both antagonists (5 µM) suggesting that at least 5HT2B was responsible for the serotonin effect. Preliminary data with the NO synthase inhibitor LNAME indicated that the relaxing effect of LY272015 was not mediated by NO.
Conclusion: These results suggest that the serotonin effect on coronary perfusion in isolated rodent hearts is mediated, among other mechanisms, via 5HT2B receptors, but independent of NO production.

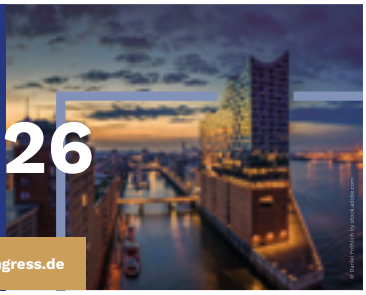

P02 Postergroup: Vascular Smooth Muscle Physiology

P0212

Elastogenesis in the pregnant uterus as a paradigm to reinstate elasticity in organs Alicia Schneider
Vascular Research Centre, Institut für Kardiovaskuläre Physiologie, Goethe University, Frankfurt a. M., Germany;

Objective: Elastolysis contributes to severe diseases such as aortic aneurysms. The uterus is a unique adult mammalian tissue capable of reactivating elastogenesis during pregnancyinduced expansion. Understanding the mechanisms governing this process may enable therapeutic strategies for elastolytic diseases.
Method: Timeresolved singlecell RNA sequencing was performed to define elastogenesisassociated gene programs in the pregnant uterus and compared them with cardiac tissue. Multiomic profiling integrating transcription and chromatin accessibility was used to infer regulatory states. In vivo SILAC proteomics quantified tissuespecific protein turnover across pregnancy. Hormonestimulated primary fibroblasts were analyzed in vitro.
Results: The uterus exhibits dynamic transcriptional remodeling in the nonpregnant state across the estrous cycle, reflecting hormone responsiveness. During pregnancy, singlecell analysis identifies uterine fibroblasts and smooth muscle cells as key drivers of extracellular matrix remodeling, with induction of *Eln* and *Fbn1*.
SILAC proteomics revealed striking, pregnancyspecific elastin renewal in the uterus, with approximately 44.6% newly synthesized elastin at gestational day 14, indicating extensive structural protein turnover. Skeletal muscle shows no detectable elastin incorporation, indicating a tissuespecific program, while liver shows lowlevel incorporation (~6%) as ECM remodeling baseline. Postpartum samples show activation of PTENassociated signaling, suggesting a temporally restricted remodeling and apoptotic program restoring the prepregnancy state. Regulatory mechanisms are further resolved using snATACseq.
In vitro, estrogen induces *Eln* and *Fbn1*, whereas progesterone exerts antagonistic effects.
Conclusion: Pregnancy activates a distinct hormonally driven gene regulatory network that reactivates elastogenesis in the adult uterus. Defining this program may provide therapeutic strategies to induce elastic fiber regeneration in elastolytic cardiovascular disease.

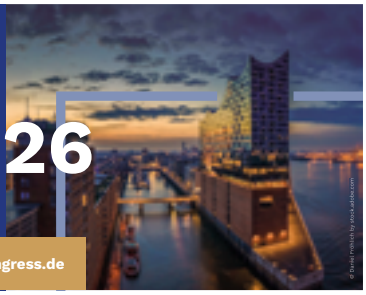

P02 Postergroup: Vascular Smooth Muscle Physiology

P0213

Combined inhibition of K_v7 and BK_{Ca} channels reveals a role for Ltype Ca^{2+} channels in enhancing contractility of male mouse urethral smooth muscle

Neha Gupta; Gerard Sergeant; Mark Hollywood; Keith Thornbury; Caoimhin Griffin
Life & Health Science, Dundalk Institute of Technology, Dundalk, Ireland;

Objective: Myogenic tone of vascular smooth muscle cells (VSMC) relies on Ca^{2+} influx via voltagedependent Ltype Ca^{2+} channels (LTCC). In VSMC, opening of LTCC is regulated by activation of largeconductance Ca^{2+}activated K^+ channels (BK_{Ca}) and voltagedependent K^+ channels encoded by KCNQ (K_v7) (Ma *et al.*, 2020), which when opened or closed hyperpolarize or depolarize VSMC respectively, thus, working in concert to modulate myogenic tone via LTCC activation or deactivation (Dopico *et al.*, 2018). This raises the question of whether modulation of smooth muscle tone via regulation of LTCC by combined actions of BK_{Ca} and K_v7 channels is limited to the vascular system, or also occurs in visceral tissues.
In the urinary tract, LTCC contribute to excitationcoupling in urethral smooth muscle cells (USMC) in numerous species, contributing to myogenic tone and maintenance of continence . In contrast to VSMC, LTCC do not contribute to USMC tone, or responses to adrenergic agonists or nerve stimulation, despite expression of the channels (Gupta *et al.*, 2023). Reasons for noncontribution of Ltype channels to murine USMC contractility remain unclear. Drawing from the known actions of K_v7 and BK_{Ca} channels in VSMC, we hypothesized that basal activation of K_v7 or BK_{Ca} channels in USMC would inhibit LTCC, dampening their contribution to USMC contractions.
Method: We examined effects of BK and Kv7 blockade on urethral smooth muscle contractions in wildtype mice, using isometric tension recordings of urethral contractions, and instu Ca^{2+} imaging of urethral smooth muscle Ca^{2+} signals in tissues from animals expressing a genetically encoded Ca^{2+} reporter exclusively in smooth muscle. (ActaGCaMP8.1 mice).
Results: In isometric tension experiments, when urethral rings were precontracted by phenylephrine (PE, 1 μM, $\alpha_1$adrenoreceptor agonist), or contracted by electrical field stimulation (EFS), neither XE991 (10 μM, K_v7 inhibitor) nor iberiotoxin (300nM, BK_{Ca} inhibitor) had any effect. However, a combination of iberiotoxin and XE991 induced phasic contractions superimposed on PE responses, and enhanced EFSevoked contractions, which were all reversed by nifedipine (LTCC inhibitor). During *in situ* Ca^{2+} imaging of USMC, combination of XE991 and iberiotoxin converted asynchronous, localized intracellular Ca^{2+} signals to coordinated, propagating intercellular waves, which were abolished by nifedipine. Ca^{2+} influx via Orai channels is critical for USMC Ca^{2+} signalling, and precontracted urethral rings were relaxed by GSK7975A or Synta 66 (Orai inhibitors). Under these conditions, nifedipinesensitive phasic activity was evoked by XE991, while iberiotoxin addition had no effect. This suggested Ca^{2+} influx via Orai was linked to BK_{Ca} activation
Conclusion: Our data suggest that LTCC do not contribute to mouse USMC contractions under normal conditions due to basal activation of K_v7 and BK_{Ca} channels whose latter activation is linked to Ca^{2+} influx via Orai channels.

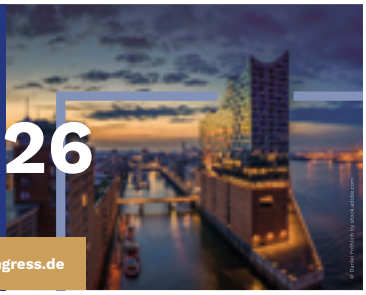

P03 Postergroup: Vascular Disease

P0301

Skin Microvascular Responses to Exercise in Children with Type 1 Diabetes

Ivana Potocnik; Tadej Battelino [1]; Klemen Dovc [1]; Nejka Potocnik
Medical faculty, Institute of Physiology, University of Ljubljana, Ljubljana, Slovenia; [1] University Medical Centre Ljubljana, University Children's Hospital, Department of Endocrinology, Diabetes and Metabolic Diseases,, Ljubljana, Slovenia;

Objective: Type 1 diabetes mellitus (T1D) is a chronic metabolic disorder marked by insulin deficiency and persistent hyperglycaemia. Although clinical complications such as retinopathy and neuropathy develop later in life, vascular dysfunction begins much earlier. Microvascular impairments are believed to precede and promote longterm complications. This study examined skin blood flow responses to exercise in children with T1D compared with healthy, physically active peers.
Method: Sixteen physically active children (8 with T1D, HbA1c = 7.82 ± 0.82%; 8 age, sex, and VO2maxmatched controls) performed graded cycling to exhaustion under controlled environmental conditions. Skin blood flow at the fingertip (glabrous; LDFp) and forearm (nonglabrous; LDFf) was assessed using laser Doppler flowmetry (PeriFlux 6000, Perimed) before and after 15 min of passive recovery. Mean arterial pressure (MAP) and cutaneous vascular conductance (CVCp, CVCf) were calculated. Logtransformed data were analysed by twoway repeatedmeasures ANOVA (time × group).
Results: For LDFp, significant main effects of time ($F(1,14)=17.22$, $p<0.001$) and group ($F(1,14)=7.72$, $p=0.01$) were observed, with no interaction. Similar results were found for CVCp. Fingertip perfusion and conductance were lower in T1D both before and after exercise (postexercise CVCp: 3.05 ± 1.25 vs. 1.67 ± 0.63, $p=0.015$). After adjusting for preexercise glucose, differences were no longer significant. LDFf, CVCf, and MAP changes were unaffected by group.
Conclusion: Reduced glabrous skin perfusion in children with T1D appears primarily related to acute hyperglycaemia rather than chronic vascular dysfunction, highlighting the importance of glycaemic stability for preserving thermoregulatory control.

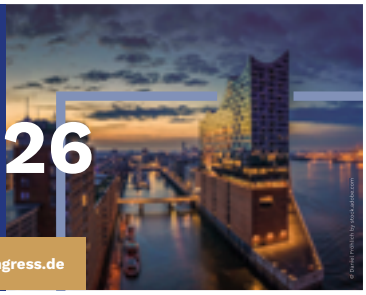

P03 Postergroup: Vascular Disease

P0302
Growth differentiation factor 6 drives endothelial maladaptation in pulmonary hypertension due to left heart disease

Qiuhua Li; Mariya M. Kucherenko [1]; Netra Nambiar Veetil [2]; Huimin Jia; Shaofei Liu [2]; Szandor Simmons; Wolfgang Kübler
Institut für Physiologie, Campus Charité Mitte, Charité - Universitätsmedizin Berlin, Berlin, Germany; [1] Deutsches Herzzentrum der Charité, Berlin, Germany; [2] Charité – Universitätsmedizin Berlin, Berlin, Germany;

Objective: Pulmonary hypertension due to left heart disease (PHLHD) is characterized by endothelial dysfunction and pulmonary vascular remodeling; yet, the molecular drivers of these changes remain unclear. Given the central role of bone morphogenetic protein (BMP) signaling in pulmonary arterial hypertension, we investigated its contribution to endothelial alterations in PHLHD.
Results: Pulmonary artery endothelial cells (PAECs) from PHLHD patients and rats with aortic banding (AoB)induced PHLHD showed impaired BMP signaling, characterized by reduced BMPR2 expression, decreased SMAD1/5/8 phosphorylation in response to BMP2, and increased proliferation and migration. Transcriptomic and protein profiles of pulmonary arteries revealed upregulation of growth differentiation factor 6 (GDF6) and the BMP antagonist gremlin 1 (GREM1) in both human and experimental PHLHD. In healthy PAEC, exogenous GDF6 activated BMP, TGFβ, and ERK1 pathways. In contrast, in PHLHD PAEC, BMP signaling was suppressed, whereas TGFβ and ERK1 pathways were hyperactivated. Downstream analyses identified GDF6 to activate ERK1 via VEGFR2, leading to increased TGFβ expression and SMAD3 activation through TGFBR1. In turn, this cascade induces GREM1 which further inhibits BMP signaling. Functionally, GDF6 enhanced proliferation and migration in healthy PAEC, whereas GDF6 knockdown normalized the phenotype of PHLHD PAEC. *In vivo*, lungspecific silencing of GDF6 reduced pulmonary vascular remodeling and normalized pulmonary and right ventricular hemodynamics and function.
Conclusion: Collectively, these findings identify GDF6 as a key pathogenic mediator of endothelial dysregulation in PHLHD and highlights its potential as a therapeutic target.

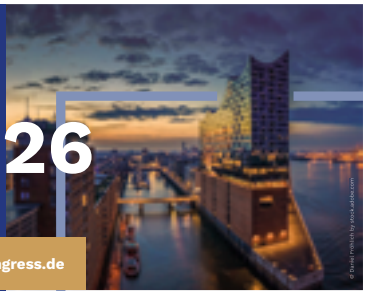

P03 Postergroup: Vascular Disease

P0303

Single cell sequencing reveals a distinct cellular response to vascular pressure in a model of unilateral carotid artery atherosclerosis of mice

Victoria Jurisch; Alicia Schneider; Melina Lopez; Longyuan Jia; Xin Wen; Wesley Abplanalp; Timothy Warwick; Fatih Alcicek; David M. Leistner [1]; Ralf P. Brandes Institut für Kardiovaskuläre Physiologie, Universitätsklinikum, Johann Wolfgang GoetheUniversität, Frankfurt a. M., Germany; [1] Medizinische Klinik III, Kardiologie, Universitätsklinikum, Johann Wolfgang GoetheUniversität, Frankfurt a. M., Germany;

Objective: Hypercholesterolemia and hypertension are key risk factors for atherosclerosis. As prohypertensive agents raise complex secondary response mechanisms, the direct impact of pressure is difficult to study. To address this, we developed a mouse model in which only the hemodynamic environment differs between the two carotid arteries while systemic conditions remain identical.
Method: Mice were rendered hypercholesterolemic by AAV8PCSK9 delivery and Western diet. Unilateral carotid hypertension was induced by transverse aortic constriction (TAC). Vascular ultrasound, histological analysis, and singlecell and µMACE RNA sequencing were performed on both carotid arteries at early and late time points after TAC. Ultrasound confirmed 123% increase in flow rate in the right carotid artery in the right carotid artery by day 3 after TAC.
Results: In the context of hypercholesterolemia, this hemodynamic imbalance led to localized plaque formation in the right carotid artery, with histological evidence of lipid deposition and vascular fibrosis 10 weeks after surgery. Singlecell and µMACE RNA sequencing revealed coordinated temporal remodeling of the vascular wall after TAC. At day 1, endothelial cells acquired a turbulent flowassociated program, with increased expression of *Edn1, Vcam1*, and *Icam1*. *Trp53* expression was also elevated, consistent with an early stress- and apoptosisassociated response. Among the mechanosensitive changes, Bmp4 emerged as a putative endothelialspecific candidate gene. By day 3, remodeling had expanded beyond the endothelium, with a marked proliferative phase driven mainly by primed fibroblasts. This was accompanied by the emergence of an activated smooth muscle cell population. Over time, the right carotid artery showed progressive remodeling with enhanced infiltration of neutrophils and macrophages. Endothelial cells progressively lost arterial identity, with the arterial endothelial cell fraction declining from ~80% at day 1 to ~56% at day 70. This shift was accompanied by an expansion of EndMTlike, lipidresponsive, inflammatory, proliferative, and lymphatic states.
Conclusion: This model isolates flow- and pressuredriven effects on atherogenesis and reveals early endothelial mechanosensing, stress responses, and fibroblast activation as key events linking altered hemodynamics to vascular remodeling and plaque development.

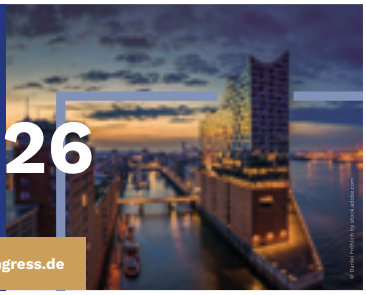

P03 Postergroup: Vascular Disease

P0304
Sex Differences in Middle Cerebral Artery Dysfunction in Alzheimer's Disease: From Mouse Model to Aβ and Tau Oligomers

Maria Hovmann Andresen; Vladimir V. Matchkov; Eugenio Jimenez Gutierrez
Department of Biomedicine, Aarhus University, Aarhus, Denmark;

Objective: Alzheimer's Disease is the leading cause of dementia. Hallmarks of the disease include pathophysiological accumulation of amyloidbeta oligomers and tau fibrils. These proteins have been shown to accumulate inside the walls of pial vessels. The vascular effect of these AD hallmarks is, however, unknown.
Method: We measure functional changes in middle cerebral arteries (MCA) from wildtype mice (C57Bl/6NRJ) and from 3xTg AD mice using a wire myograph. We exposed MCAs to different concentrations of amyloid oligomers (Cab40 ,Cab42: 1 nM and 1 uM) and tau fibrils (Ctau: 5 nM and 50 nM) for one hour and investigated their contractility using cumulative concentrations of U46619 (10 nM - 3 uM) and relaxation with the carbonic anhydrase inhibitor acetazolamide (ATZ) on vessels preconstricted with U46619 and compared it with control vessels and vessels from 3xTg AD mice.
Results: Preliminary findings indicate an interesting response of female murine vessels when exposed to the proteins one by one, a pattern also observed when male vessels were exposed to all the proteins. Furthermore, a similar response was identified in vessels from female 3xTg AD mice. However, during incubation, vessels from male mice demonstrated a constrictive response compared to those from female mice.
Conclusion: This study demonstrates that the isolated proteins induce vascular disturbances, as observed in 3xTg AD females. The combination of the three peptides, resembling a more comprehensive model of patient pathology, suggests a prominent effect on vascular function. These results highlight the influence of AD proteins on vascular function, which may affect blood flow dynamics during AD progression.

P03 Postergroup: Vascular Disease

P0305

Microvascular and Macrovascular Dysfunction in Patients with Chronic Kidney Disease and Hypertension

Justina Mihaljevic; Dubravka Mihaljevic [1]; Ana Marincic Žagar [2]; Zdenko Boras [3]; Dina Šišljagic [4]; Ines Drenjancevic [2]
Department of Radiology, Clinical Hospital Centre Osijek, Osijek, Croatia; [1] Department of Internal Medicine, Institute of Nephrology, Clinical Hospital Centre Osijek, Osijek, Croatia; [2] Department of Physiology and Immunology, Clinical Hospital Centre Osijek, Osijek, Croatia; [3] Department of Surgery, Urology, Orthopedics, Physical Medicine and Rehabilitation, Clinical Hospital Centre Osijek, Osijek, Croatia; [4] Department of Gynecology, Clinical Hospital Centre Osijek, Osijek, Croatia;

Objective: This study aimed to investigate differences in hemodynamic, microvascular and body composition parameters among patients with chronic kidney disease (CKD), hypertension (HTN) and healthy controls.
Method: This crosssectional study included 76 participants: CKD (N=22), HTN (N=27), and controls (N=27). Smokers and patients with diabetes were excluded. Participants underwent impedance cardiography (ICG), laser Doppler flowmetry (LDF), and body composition analysis (Maltron BioScan 920 II). Group differences were analysed using oneway ANOVA with post hoc tests. Ethical approval was obtained (#2158614624121); all participants provided informed consent (ClinicalTrials.gov: NCT06316284).
Results: ICG showed higher systolic blood pressure (SBP; 143±14 vs. 125±8 mmHg, p=0.0001), diastolic blood pressure (DBP; 85±13 vs. 77±8 mmHg, p=0.0145), mean arterial pressure (MAP; 100±13 vs. 88±8 mmHg, p=0.0005), and systemic vascular resistance index (SVRI; 2452±501 vs. 1955±548 dyn·s·cm?5·m², p=0.0055), with lower stroke volume (SV; 95±19 vs. 110±18 mL, p=0.0209) and total arterial compliance index (TACI; 0.9±0.2 vs. 1.15±0.2 mL/m²/mmHg, p=0.0053) in CKD patients compared to controls. HTN patients also had higher SBP (143±18 vs. 125±8 mmHg, p<0.0001), DBP (85±9 vs. 77±8 mmHg, p=0.0132), and MAP (98±10 vs. 88±8 mmHg, p=0.0012), with lower TACI (0.92±0.34 vs. 1.15±0.2 mL/m²/mmHg, p=0.0058) compared to controls. No significant differences were found among CKD and HTN groups, although CKD patients showed a trend toward higher SVRI and lower SV and TACI values.
LDF demonstrated reduced acetylcholineinduced dilation (AChID; 9.4±5.6 vs. 14.15±5.8, p=0.0112) in CKD patients versus controls, indicating impaired endothelialdependent microvascular function. HTN patients also showed lower AChID values (10.7±5.3), without statistical significance.
Body composition analysis showed higher BMI in HTN patients compared to controls (28.4±4.3 vs. 25.8±2.9 kg/m², p=0.0435).
Conclusion: CKD patients exhibited significant macrovascular and microvascular dysfunction, emphasizing the systemic vascular impact of CKD on vasculature and the importance of cardiovascular risk assessment in this population.
Supported by Faculty of Medicine research grants IP23MEFOS2026, IP18MEFOS2024, and IP20MEFOS2025 (PI: Ines Drenjancevic).

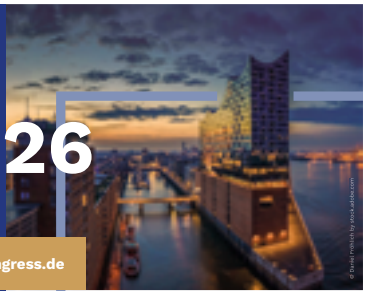

P03 Postergroup: Vascular Disease

P0306

Arteriosclerosis in 3D spheroids – Impact of NSAIDs on smooth muscle cell foam cell formation

Risto Hoffmockel; Thomas Korff
Cardiovascular Physiology, Institute for physiology and pathophysiology, RuprechtKarlsUniversität Heidelberg/Universitätsklinikum Heidelberg, Heidelberg, Germany;

Objective: Smooth muscle cells (SMC) play an important role in the pathogenesis of arteriosclerosis as they may acquire a foam cell phenotype after being chronically exposed to cholesterol. The specific role of SMCderived foam cells in the progression of atherosclerotic plaques remains unclear. In this context, we investigated whether SMC foam cell formation is affected the by nonsteroidal antiinflammatory drugs (NSAIDs) the use of which may alter plaque stability and bears a risk of cardiovascular events.
Method: To investigate the effect of NSAIDs on human aortic smooth muscle cells (hAoSMC), a 3D spheroid model was exploited, that supports cellular quiescence and a high level of differentiation. hAoSMC spheroids were exposed to watersoluble cholesterol (Chol:MCD) to mimic a proarteriosclerotic environment and were treated with ibuprofen (10µM) or diclofenac (2µM). Migration of Chol:MCDstimulated hAoSMC, as measured by the number of outgrowing cells originating from a spheroid was inhibited by NSAID treatment (DMSO: 72.3±7.0; ibuprofen: 50.8±3.0, $p<0.01$, n=5; diclofenac: 30.8±11.3, $p<0.01$, n=4; Student's ttest). However, accumulation of cholesterol in hAoSMC spheroids was not altered by NSAID treatment as evidenced by fluorescence (confocal) microscopybased detection of lipid droplets. Analyses of gene expression by qPCR ($\Delta\Delta C_T$ method) showed that diclofenactreated hAoSMC decreased *ACTA2* expression (2^ddCT=0.41±0.22, $p<0,01$, n=7) as compared to control conditions. Furthermore, both diclofenac and ibuprofen decreased *HMGCR* (diclofenac: 2^ddCT=0.45±0.31, $p<0.01$; ibuprofen: 2^ddCT=0.66±0.29, $p=0.02$, n=7) expression in Chol:MCDtreated hAoSMC (compared to Chol:MCD control), while *ABCA1* expression was suppressed (2^ddCT=0.49±0.40, $p=0.02$, n=7) by diclofenac only. Likewise, RNAseqbased gene set enrichment analyses (n=3) indicated that diclofenac but not ibuprofen significantly altered the hAoSMC transcriptome (e.g. Gene Ontology - Biological Process: chemotaxis (↓, adj. $p<0.01$), regulation of inflammatory response (↓, adj. $p<0.01$), nuclear division (↑, adj. $p<0.01$)). Among the most strongly regulated genes, expression of the immunomodulatory interleukin 24 *(IL24)* was significantly downregulated in diclofenac/Chol:MCDtreated spheroids (5.26fold change, adj. $p<0.01$ vs. Chol:MCD treatment).
Conclusion: In summary, the NSAID diclofenac may lower the contractile capacity of hAoSMCs and affect the phenotype of hAoSMCderived foam cells by decreasing gene expression associated with cholesterol generation (*HMGCR*) and efflux (*ABCA1*). Moreover, diclofenac promotes expression of proliferationassociated genes while decreasing antiproliferative gene expression (e.g. *IL24*). Regular use of diclofenac could thus lead to a phenotypic change of SMC located in atherosclerotic lesions, which may accelerate the development of vulnerable plaques in the long run.

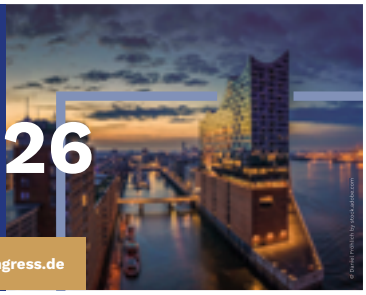

P03 Postergroup: Vascular Disease

P0307

Temporal Proteomic Remodeling of Cerebral Arteries in Hypertensive Rats

Joakim A. Bastrup; Catarina Rippe [1]; Karl Swärd [1]; Thomas Jepps [2] Department of Biomedical Sciences, University of Copenhagen, Copenhagen, Denmark; [1] Department of Experimental Medical Science, Lund University, Lund, Sweden; [2] Integrative Circulation, Institute of Biomedical Sciences, University of Copenhagen, Copenhagen, Denmark;

Objective: Hypertension is a major risk factor for neurological disorders, such as stroke and dementia, yet the molecular mechanisms linking chronic hypertension to cerebrovascular dysfunction remain poorly understood. Here, we investigated temporal proteomic remodeling of the cerebrovasculature in male spontaneously hypertensive rats (SHRs) and normotensive WistarKyoto (WKY) controls at 30 and 40 weeks of age, representing the progression of untreated hypertension from early adulthood to midlife.
Method: Discoverybased proteomics, histological analyses, and RNAsequencing data integration were performed on cerebrovascular samples from 30- and 40weekold male SHRs and WKY rats.
Results: Proteomic profiling revealed a significant agedependent remodeling of the cerebrovascular proteome in SHRs, partially associated with reduced expression of serum response factor (SRF) and its downstream regulon. Pathway analysis demonstrated a transient upregulation of mitotic (Mphase) proteins at 30 weeks, consistent with maladaptive smooth muscle cell proliferation. By 40 weeks, expression of proliferative markers had normalized, whereas extracellular matrix (ECM)associated proteins showed pronounced divergence. These molecular changes were supported by histological evidence of increased mediatocircumference ratio and collagen deposition, indicating progressive vascular remodeling.
Conclusion: Chronic hypertension induces a temporal shift in cerebrovascular remodeling, progressing from early maladaptive smooth muscle proliferation to later ECMdriven structural remodeling. These findings suggest that the mechanisms underlying hypertensive vascular injury evolve over time and may require stagespecific therapeutic interventions to reduce the risk of neurovascular disease.

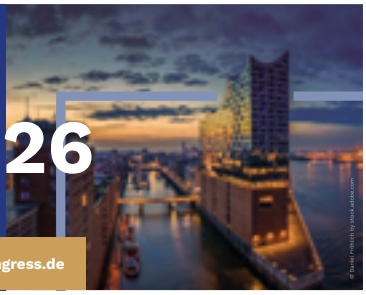

P03 Postergroup: Vascular Disease

P0308

Gestational Diabetes Mellitus alters insulin signaling and FABP4 expression in the human fetoplacental vasculature

Maria de Leyre Villar Ballesteros; Clara M. Hengst; Talita Aygün; Heike Brendel; Jennifer Mittag; Alexander Frühauf [1]; Cahit Birdir [1]; Paul D. Taylor [2]; Henning Morawietz Division of Vascular Endothelium and Microcirculation, Department of Medicine III, Dresden University of Technology, Dresden, Germany; [1] Department of Obstetrics and Gynecology, Center for Feto/neonatal Health, Dresden University of Technology, Dresden, Germany; [2] Department of Women & Children's Health, School of Life Course Sciences, King's College London, London, United Kingdom;

Objective: Gestational diabetes mellitus (GDM) is the most common complication in pregnancy and associated with adverse maternal and fetal outcomes. It impairs placental endothelial function and blood flow, thereby increasing the longterm risk of metabolic and cardiovascular diseases in the offspring. However, the molecular mechanisms driving endothelial dysfunction in the fetoplacental circulation remain incompletely understood. This study aimed to characterize alterations in vascular reactivity and insulin signaling in the fetoplacental vasculature of GDM pregnancies and to identify potential therapeutic targets to improve endothelial function in the offspring.
Method: Human fetoplacental vessels and human umbilical vein endothelial cells (HUVECs) were obtained from normoglycemic (NG) and GDM pregnancies. Vascular reactivity was assessed using a Mulvany myograph to evaluate insulinmediated vasodilation. Protein expression of key insulin signaling components was analyzed by Western blotting in both fetoplacental vessels and HUVECs. In addition, differential gene expression analysis was performed in NG and GDM HUVECs using bulk RNA sequencing, followed by validation on the protein level by immunofluorescence staining.
Results: Insulinmediated vasodilation was significantly impaired in fetoplacental vessels from GDM pregnancies compared with NG controls and associated with a reduction in total insulin receptor protein expression. Consistently, insulin signaling through the PI3K/AKT/eNOS pathway was inhibited, as evidenced by diminished insulininduced AKT phosphorylation in GDMderived HUVECs. Bulk RNA sequencing revealed a significant upregulation of fatty acid–binding protein 4 (FABP4) in GDM HUVECs. FABP4 has been implicated in insulin resistance and endothelial dysfunction. The upregulation of FABP4 was subsequently confirmed on the protein level by immunofluorescence.
Conclusion: In conclusion, these findings demonstrate that maternal GDM induces insulin resistance and endothelial dysfunction in the fetoplacental vasculature, likely mediated by impairment of the AKT/eNOS signaling pathway. Further studies will determine whether the increased expression of FABP4 plays a causal role in fetoplacental vascular impairment or represents a marker of endothelial dysfunction in GDM.

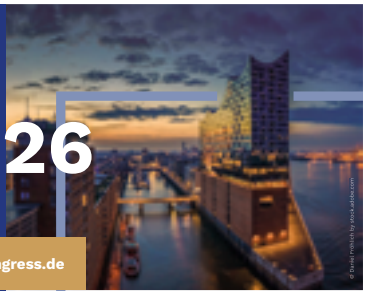

P03 Postergroup: Vascular Disease

P0309

Effects of the flavonoid Fisetin on small artery dysfunction in ageing and dietinduced metabolic stress in mice

Beijia Zhang; Line Fleischer Hach [1]; Maria Vestergaard Christensen; Raquel Feliciano [1]; Juliette Tavenier [1]; Yu Wang [2]; Ove Andersen [1]; Line Jee Hartmann Rasmussen [1]; Lars Jørn Jensen Dept. of Veterinary and Animal Sciences, Faculty of Health and Medical Sciences, University of Copenhagen, Frederiksberg, Denmark; [1] Department of Clinical Research, Copenhagen University Hospital Amager and Hvidovre, Hvidovre, Denmark; [2] Dept. of Pharmacology and Pharmacy, LKS Faculty of Medicine, University of Hong Kong, Pok Fu Lam, Hong Kong;

Objective: Ageing and metabolic stress from sedentary behavior and hypercaloric diet increase the risk of cardiovascular and neurodegenerative diseases, partly through small artery dysfunction and blood flow dysregulation. However, whether the flavonoid fisetin can mitigate age- and dietrelated vascular dysfunction remains unclear. We aimed to characterize small artery dysfunction in young versus old mice with or without metabolic stress, assess the therapeutic potential of fisetin, and determine the role of Rhokinase in disease mechanisms.
Method: All animal procedures were approved by the authorities. Male C57BL/6NTac mice were assigned to fisetin or vehicle (20 mg/kg, 2 days/week for 4 weeks). Young (3.5 months; N=32) and old (18 months; N=30) mice received control or highfat/highfructose diet for 10 weeks (N=7–8 per condition). Isolated 3rdorder mesenteric arteries (150–200 µm) were studied by pressure myography (60 mmHg, 37°C, pH 7.40). We assessed vasoconstriction (KCl, noradrenaline), endotheliumdependent dilation (acetylcholine), myogenic tone (60120 mmHg), structural remodeling, and stiffness. Rhokinase inhibition (Ripasudil, 400 nM), senescence marker p16 (qPCR), and advanced glycation endproducts (AGE) expression (immunofluorescence) were evaluated. Data were analyzed by 2- or 3way ANOVA (age, diet ± fisetin; $P<0.05$).
Results: Ageing increased body weight ($P<0.0001$) and noradrenaline contractility ($P<0.05$), while impairing endothelial function and promoting hypertrophic remodeling ($P<0.05$). Obesogenic diet increased body weight ($P<0.0001$), reduced endothelial function ($P<0.05$) and myogenic tone ($P<0.001$), and induced structural remodeling ($P<0.05$–0.01). Age×diet interactions occurred for myogenic tone and stiffness ($P<0.001$). Fisetin attenuated noradrenergic hypercontractility, remodeling, endothelial dysfunction, and reduced myogenic tone (young lean mice, only). Rhokinase inhibition reduced myogenic tone in young vehicle- and all fisetintreated groups, indicating reduced Rhokinase activity with age, and an apparent partial recovery by fisetin. p16 increased with age, and endothelial AGE accumulation was elevated in old mice and young obese mice, however, with no fisetin effects.
Conclusion: Overall, fisetin may improve small artery function governing blood pressure and flow, potentially via its known antioxidant and antiinflammatory actions.

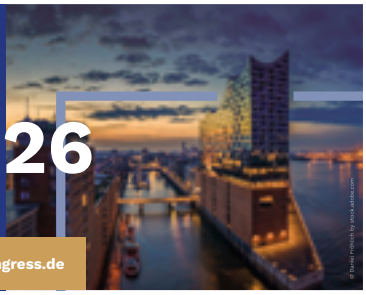

P03 Postergroup: Vascular Disease

P0310

Early changes in microvessel function and structure in a mouse model of metabolic syndrome (db/db mouse): effects of treatment with empagliflozin and enalapril

Julia Sophie Schröter Bonk; Cem Erdogan; FalkBach Lichtenberger; Elizaveta Pavlova [1]; Andreas Patzak; Karin Michaela Kirschner; Pratik Hemant Khedkar Institut für Translatioinal Physiologie, Campus Charité Mitte, Charité - Universitätsmedizin Berlin, Berlin, Germany; [1] AG HerzKreislaufRegulation, Institut für Translationale Physiologie, Charitè - Universitätsmedizin Berlin, Berlin, Germany;

Objective: Type 2 diabetes mellitus is associated with vascular complications that contribute substantially to cardiovascular and renal morbidity. However, early microvascular alterations preceding overt structural damage remain incompletely understood. We investigated early functional and molecular changes in resistance arteries of db/db mice and assessed whether treatment with the SGLT2 inhibitor empagliflozin, alone or combined with the ACE inhibitor enalapril, modulates these alterations.
Method: Male and female db/db mice and db/+ controls were studied at 18 weeks of age after receiving vehicle, empagliflozin, or combined empagliflozin + enalapril over 8 weeks via drinking water.
Vascular function of mesenteric arteries was assessed by wire myography. Statistics comprised nonparametric multiple contrast tests (MCTP) for group comparisons and cubic mixedeffects models (MM) for concentrationresponse curves.
Results: Db/db mice were obese and hyperglycaemic (54.59 ± 5.00 vs. 27.55 ± 2.96 g; 690.68 ± 75.31 vs. 166.22 ± 20.43 mg/dL), while wall/lumen ratio of mesenteric arteries was unchanged.
Phenylephrineinduced constriction was increased in mesenteric arteries from db/db mice ($p = 0.025$, MCTP). Acetylcholineinduced endothelial relaxation was impaired in db/db mice (genotype effect $\beta = 34.72 \pm 4.60$, $p < 0.001$, MM), with reduced NOindependent endothelial relaxation (genotype effect $\beta = 10.698 \pm 3.891$, $p = 0.008$, MM).
Empagliflozin lowered serum glucose (318.94 ± 82.40 mg/dL; $p < 0.001$, MCTP) and restored NOindependent relaxation ($\beta = 8.585 \pm 3.743$, $p = 0.026$, MCTP). Mesenteric arteries showed increased
expression of MMP2, MMP14, Col1a1, and Col1a2 in diabetes ($p \leq 0.025$, MCTP), whereas empagliflozin + enalapril reduced Col1a2 expression ($p = 0.031$, MCTP).
Conclusion: These findings indicate that early diabetic vasculopathy in db/db mice is characterized by functional endothelial impairment and molecular remodelling before manifest structural vascular damage. Treatment with empagliflozin improved vascular function while combined empagliflozin + enalapril treatment modulated early extracellular matrixassociated alterations, supporting vascular protection as a potential mechanism contributing to the combined benefit of SGLT2 and reninangiotensinaldosteronesystem inhibition.

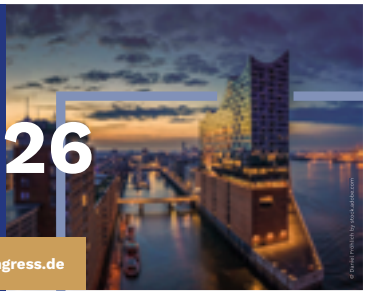

P03 Postergroup: Vascular Disease

P0311

Dexamethasone Inhibits Abdominal Aortic Aneurysm Progression in Rats, though with Major Catabolic Effects

Peter Nørrelund Alrø; Nikolaj Horskær Madsen; Jes Sanddal Lindholt; Jane Stubbe [1] Cardiothoracic and Vascular Surgery, Odense University Hospital, Odense, Denmark; [1] Cardiovascular and Renal Research, Institute of Molecular Medicine, University of Southern Denmark, Odense, Denmark;

Objective: Abdominal aortic aneurysm (AAA) is a chronic, localized dilatation of the abdominal aorta, and represents a significant cause of mortality among elderly men, particularly following aneurysm rupture. Currently no effective pharmacological therapy exists to prevent AAA progression. The underlying pathogenesis includes chronic vascular inflammation driving extracellular matrix degradation. Based on this, we hypothesize that the glucocorticoid receptor agonist dexamethasone- a wellrecognized antiinflammatory agent widely used for long term treatment in other conditionshave the potential to inhibit AAA expansion.
Method: In sedated male SpragueDawley rats AAA was induced by intraluminal porcine pancreas elastase infusion in the infra renal region. The following day dexamethasone treatment (0.1mg/kg) was initiated by gavage either daily (DD, n=13) or saline (n=15) for 9 consecutive days or every other day (DEOD, n=11) or saline (n=6) for 14 days and in accordance with approved animal protocol and ARRIVE guidelines.
Results: AAA expansion was significantly reduced by dexamethasone treatment both when given every other day (DEOD, 41.4±14.9%) or daily (DD, 50.2±41.9%) compared to controls (116.8 ±64.9, $p<0.0002$) determined by ultrasound measurements. As dexamethasone reduced body weighs up to 20% DD rats and controls were euthanized at day 10 (mean body weight:285.4±14.3g vs) while DEOD continued until day 14 (332.9±16.3g) with a subset of the controls (day 10: 366.1±20.4g/day 14: 404±11.7g). Body composition by DXA scans on postsurgery day 14, showed no change in bone mineral content ($p=0.64$), nor bone density ($p<0.07$), while both body fat (39,5±9.2g vs.27.0 ±4.4g, n=13,6, $p<0.03$) and lean body mass (274.6±11.7g vs.327.7±12.2g, n=13,6. $p<0.0001$) significantly decreased in the DEOD group compared to controls. Histological assessment of aneurysm cross sections showed no difference in elastin content by Millers staining ($p=0.28$) nor in infiltration neutrophils (myeloperoxidase positive cells, $p=0.10$), nor in area of vascular smooth muscle cells (ACTA2 positive cells, $p=0.14$).
Conclusion: Dexamethasone can prevent AAA expansion but is associated with loss of body fat and lean body mass. Thus, it is not recommended as treatment option in the tested doses.

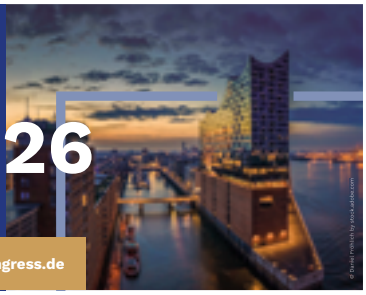

P03 Postergroup: Vascular Disease

P0312

Extracellular vesicles as potential mediators of vascular protection in atherosclerotic disease progression

André Atef Borchardt; Laura Ginsbach; Emanuel Rodrigez; Nadashree Krishnasamy; Lisa Peters; Alexander Melnikow; Toralf Kaiser [1]; Peter Ahnert [2]; Holger Kirsten [2]; Martin Witzenrath [3]; Wolfgang Kübler; Szandor Simmons
Institut für Physiologie, Campus Charité Mitte, Charité - Universitätsmedizin Berlin, Berlin, Germany; [1] German Rheumatology Research Center Berlin, Berlin, Germany; [2] Institut für Medizinische Informatik, Statistik und Epidemiologie, Universität Leipzig, Leipzig, Germany; [3] Medizinische Klinik mit Schwerpunkt Infektiologie und Pneumologie, Campus Charité Mitte, Charité - Universitätsmedizin Berlin, Berlin, Germany;

Objective: Cardiovascular disease remains a leading cause of death worldwide, with atherosclerosis as a major underlying pathology (WHO 2021). While mechanisms driving atheroprogression are well studied, endogenous factors counteracting vascular inflammation remain poorly understood. Extracellular vesicles (EVs), once considered cellular debris, are now recognized as mediators of intercellular communication in health and disease. We hypothesized that circulating EVs in patients with stable atherosclerosis contributes to vascular protection by attenuating endothelial dysfunction and formation of foam cells from macrophages.
Method: Plasmaderived EVs were analyzed in three cohorts: patients with diagnosed atherosclerosis and no history of cardiovascular events (CVE) (LIFEHeart stable; n=86), patients with diagnosed atherosclerosis and a history of CVE (LIFEHeart unstable; n=56); and a populationbased cohort of control donors without atherosclerosis or a history of CVE (LIFEAdult; n=77). EVs were isolated from plasma using size exclusion chromatography and characterized by nanoparticle tracking analysis (NTA).
Results: Mean EV size was 72 ±1.2 nm in the control cohort, and similar (75 ±1.3 nm) in the LIFEHeart stable cohort but increased to 87 ±2.2 nm in the LIFEHeart unstable cohort. Lineage tracing nanoflow cytometry revealed a higher number of monocytederived EVs in both atherosclerosis cohorts than in the control group, reaching $8.3x10^5$ ±$1.4x10^5$ EVs/ml in LIFEHeart stable and $7.6x10^5$ ±$1.4x10^5$ EVs/ml in LIFEHeart unstable, compared to $3.2x10^5$ ±$5.9x10^4$ EVs/ml in LIFEAdult patients. Macrophagederived EVs were 1.8fold higher in the LIFEHeart unstable cohort ($2,4x10^5$ ±$3.8x10^4$ EVs/ml) compared to LIFEHeart stable and LIFE Adult cohorts (both $1.3x10^5$ ±$3.2x10^4$ EVs/ml). Functionally, EVs from LIFEHeart stable patients enhanced endothelial migration in human umbilical vein endothelial cell by 1.2fold, and reduced foam cell formation in THP1 cells by 30% compared to coculture with EVs isolated from LIFEAdult patients.
Conclusion: Circulating EVs from patients with clinically stable atherosclerosis exhibit functional properties consistent with vascular protection, including enhancement of endothelial migratory capacity and reduction of foam cell formation. A deeper understanding of intercellular communication via EVs may fuel the identification of novel biomarkers and therapeutics for vascular stabilization in atherosclerotic disease.

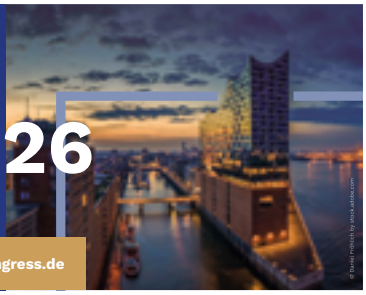

P03 Postergroup: Vascular Disease

P0313

Hemodynamic Transition from Normotension to Hypertension Assessed by Impedance Cardiography

Ana Stupin; Ivana Tolj [1]; Ivo Vincetic [2]; Ivana Jukic; Ines Drenjancevic; Marin Vuckovic [3]; Sandra Saric [3]; Nikolina Kolobaric; Zrinka Mihaljevic; Marko Stupin [3]
Department of Physiology and Immunology, University Hospital Center Osijek, Osijek, Croatia; [1] Department of Nephrology; Department of Internal Medicine, University Hospital Center Osijek, Osijek, Croatia; [2] Department of Radiology, University Hospital Center Osijek, Osijek, Croatia; [3] Department of Cardiovascular Disease, University Hospital Center Osijek, Osijek, Croatia;

Objective: Early alterations in vascular and cardiac function may precede overt hypertension; however, the integrated progression of arterial compliance, vascular resistance, and cardiac workload across the early blood pressure spectrum remains incompletely characterized. This study aimed to assess progressive changes in arterial compliance, systemic vascular resistance, and cardiac workload across normotensive, prehypertensive, and early hypertensive adults, and to evaluate their interrelationships using impedance cardiography.
Method: Sixtyone adults were classified as normotensive (NT; SBP ≤129 mmHg, DBP ≤84 mmHg; N=16), prehypertensive (PREHT; SBP 130–139 mmHg, DBP 85–89 mmHg; N=21), and untreated stage 1 hypertensive (HT; SBP 140–159 mmHg, DBP 90–99 mmHg; N=24), based on 24hour ambulatory blood pressure monitoring. Groups were matched for age and sex. The study was conducted in accordance with the Declaration of Helsinki. Continuous beattobeat hemodynamic and blood pressure measurements were obtained under standardized resting conditions using impedance cardiography (Cardioscreen® 2000, Medis, Ilmenau, Germany). Total arterial compliance index (TACI), systemic vascular resistance index (SVRI), and left cardiac work index (LCWI) were analyzed.
Results: TACI progressively decreased from NT (1.042 ± 0.226) to PREHT (0.936 ± 0.199) and HT (0.808 ± 0.254), with a significant betweengroup difference (P = 0.012); post hoc analysis showed significantly lower TACI in HT vs NT (P = 0.011). SVRI showed a gradual increase across NT (2016 ± 382), PREHT (2202 ± 512), and HT (2407 ± 579), without statistical significance (P = 0.079). LCWI also increased across groups (NT: 3.7 [3.2–4.4]; PREHT: 4.0 [3.3–4.6]; HT: 4.3 [3.7–4.9]) without significant differences (P = 0.171).
Conclusion: These findings indicate early and progressive hemodynamic alterations across the blood pressure spectrum, characterized by reduced arterial compliance and increasing vascular resistance and cardiac workload. Despite limited statistical significance for all parameters, the observed trends and physiologically coherent relationships support the presence of early vascular and cardiac functional changes already evident in prehypertensive individuals.

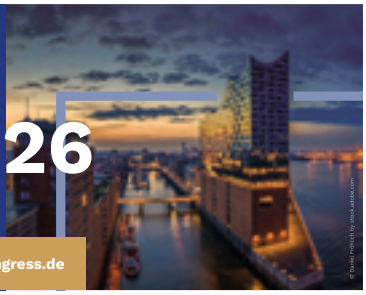

P03 Postergroup: Vascular Disease

P0314

Effects of CarnosineEnriched Chicken Meat on Microvascular Reactivity in Patients with Chronic Coronary Syndrome

Dora Uršic; Nikolina Kolobaric; Ines Drenjancevic; Zrinka Mihaljevic; Ana Stupin; Aleksandar Kibel; Ivana Jukic
Department of Physiology and Immunology, University Hospital Center Osijek, Osijek, Croatia;

Objective: Endothelial dysfunction and impaired microvascular reactivity contribute significantly to the progression of chronic coronary syndrome (CCS), highlighting the need for novel dietary strategies with potential vasoprotective effects. This study investigated the effects of carnosineenriched chicken meat consumption on endotheliumdependent and independent microvascular reactivity in patients with CCS using laser Doppler flowmetry (LDF).
Method: In this randomized doubleblind study, 38 patients with CCS were assigned to consume either regular chicken meat (Control group, n = 19) or carnosineenriched chicken meat (Carnosine group, n = 19) for three weeks. Microvascular reactivity was assessed by laser Doppler flowmetry (MoorVMSLDF, Axminster, UK). Measurements included postocclusive reactive hyperemia (PORH), acetylcholineinduced dilation (ACh ID), sodium nitroprussideinduced dilation (SNP ID), and local thermal hyperemia (LTH). Endotheliumdependent and independent vasodilatory responses were evaluated before and after the intervention under standardized laboratory conditions. Hemodynamic parameters were simultaneously monitored to assess the overall cardiovascular effects of dietary carnosine supplementation. The study was conducted in accordance with the Declaration of Helsinki.
Results: Following the intervention, the Carnosine group demonstrated significantly improved PORH and LTH responses, indicating enhanced endotheliumdependent microvascular vasodilation. SNPinduced dilation also significantly increased, suggesting improved endotheliumindependent vasodilation. No significant changes were observed in ACh ID. Additionally, systolic, diastolic, and mean arterial pressure were reduced after consumption of carnosineenriched chicken meat.
Conclusion: Carnosineenriched chicken meat exerts beneficial effects on microvascular function in patients with CCS by improving both endotheliumdependent and independent vasodilation. In addition, carnosine intake lowers arterial blood pressure, suggesting a favorable impact on hemodynamic function and overall microvascular health.

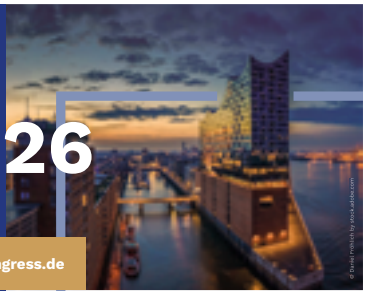

P04 Postergroup: Transcriptional & epigenetic reviving of disease

P0401

RADIAnT: Novel statistical method for RNADNA interaction calling helps identify generegulatory RNAs in EndMT

Simonida Zehr; Emma C. Walsh [1]; Alessandro Bonetti [1]; Matthias Leisegang; Ralf P. Brandes; Marcel H. Schulz; Timothy Warwick
Institut für Kardiovaskuläre Physiologie, Universitätsklinikum, Johann Wolfgang GoetheUniversität, Frankfurt a. M., Germany; [1] Department of Biochemistry, University of Cambridge, Cambridge, United Kingdom;

Objective: Chromatinlocalised RNAs play diverse roles in gene regulation and nuclear architecture. Mapping genomewide RNADNA interactions is possible using a variety of molecular methods, including using bridging oligonucleotides to ligate RNA and DNA in proximity. While molecular methods have progressed, a robust computational method for calling biologically meaningful RNADNA interactions from these data is lacking.
Method: Herein, we present *RADIAnT* (**R**NA **A**nd **D**NA **I**nteractions **A**nalysed 'n' **T**ested), a readstointeractions pipeline for the statistical analysis of RNADNA ligation data. *RADIAnT* calls interactions against a datasetspecific background that models expected interaction frequency of a given bin with a given RNA. Therefore, a *distancespecific background* is calculated for each RNA r as the number of reads that were sequenced at a given *distance*, normalized by the total number of reads for RNA r. This background helps control for nascent RNA. To account for genomewide regional biases (resulting from techniqual artifacts or sequence biases), a *binspecific background* is constructed in the same manner (mean RNA frequency at each given *bin*). The two background models are unified in a manner that favors the more conservative value for testing. Observed interaction counts of each RNA in the sequenced interactome are tested using a Poisson test ($\alpha = 0.05$). To account for multiple testing, we apply the method described by Benjamini & Hochberg.
Results: Applying both classification- and correlationbased benchmarking, we found that *RADIAnT* outperforms previously proposed methods in the accurate recall of genomewide RNADNA interactions.
In a use case, we studied the RNAchromatininteractome in the physiologically- and pathologically relevant process of endothelialtomesenchymal transition (EndMT). As an *in vitro* model, human umbilical vein endothelial cells (HUVECs) were treated with interleukin1 beta (IL1β) and transforming growth factor beta 2 (TGFβ2) to induce a phenotypic switch. We appliead *RADIAnT*to RADICLsequencing of both control (endothelial) and treated (EndMT) cells and integrated the results with nuclear RNAsequencing (nucRNAseq), and ATACseq to identify dynamically chromatinassociated RNAs. By depleting candidate chromatinassociated lncRNAs (siRNAmediated knockdown), their gene regulatory behaviour at bound target genes important to endothelial phenotype maintenance could be validated.
Conclusion: These data demonstrate how effective RNADNA interaction calling with *RADIAnT* can help to place RNAs at key points in gene regulatory networks governing cellular behaviour.

P04 Postergroup: Transcriptional & epigenetic reviving of disease

P0402
Adaption of tumor cell proliferation to chronic acidosis involves E2F transcription factor family

Anne Riemann; Virginie Dubourg; Mandy Rauschner; Sarah Reime; Oliver Thews JuliusBernsteinInstitut für Physiologie, Medizinische Fakultät, MartinLutherUniversität HalleWittenberg, Halle (Saale), Germany;

Objective: The microenvironment of solid tumors is often characterized by a lack of nutrients and of oxygen (hypoxia), as well as an increase in the proton concentration (acidosis). Acute acidosis can block tumor cell proliferation, resulting in a G_1/G_0 cell cycle arrest. However, when tumor cells remain in an acidic environment chronically, they seem to adapt and regain their proliferative capacity after a certain period of time.
Method: In this study, we compare breast (MCF7) and prostate (AT1) cancer cells under acute acidosis (24 h pH 6.6) and chronically acidic conditions (5 weeks pH 6.6) in HEPES/ MESbuffered RPMI media. As a control, cells grew under physiologic conditions (pH 7.4) for 24 h or 5 weeks. Subsequently, cells were subjected to RNA sequencing and analysis of proliferation.
Results: Transcriptome analysis followed by functional analysis revealed a global modulation of the expression of genes involved in proliferation. During acute acidosis the expression of genes repressing proliferation like CDKN1A ($p21^{Cip1}$) and CDKN1B ($p27^{Kip1}$) was increased, while expression of genes promoting proliferation like CDK1/2 (cyclindependent kinase 1 and 2), MCM5 (minichromosome maintenance protein complex 5) and CLSPN (claspin) was reduced. However, this trend in the regulation of the expression either disappeared or is even reversed in acidosisadapted cells, and thus proliferation is reestablished. Involved in this modulation are changes in the activity of the E2F transcription factor family. Except for E2F4, all family members studied displayed distinctive changes in their expression when comparing acute with chronic acidic conditions. After 24 h incubation at pH 6.6, expression of E2F family members was highly reduced. After 5 weeks however, acidic tumor cells had either higher expression (for instance of E2F1, E2F3 and E2F7) or displayed no changes when compared to control cells grown in media pH 7.4.
Conclusion: In conclusion, over longer time periods in an acidic microenvironment the tumor cells can adapt and maintain high levels of proliferation even when extracellular pH stays low. This will in turn affect overall tumor growth and consequently clinical outcome of patients.

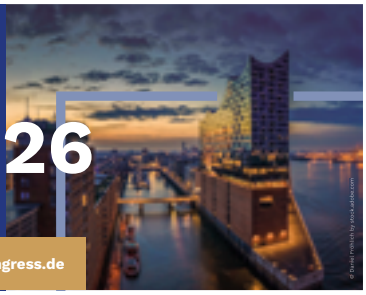

P04 Postergroup: Transcriptional & epigenetic reviving of disease

P0403
Mapping noncoding sequence variation to cardiovascular disease via gene regulatory RNADNA interactions

Astha Khanduri; Ralf P. Brandes; Timothy Warwick
Institut für Kardiovaskuläre Physiologie, Universitätsklinikum, Johann Wolfgang GoetheUniversität, Frankfurt a. M., Germany;

Objective: This work investigates how nonprotein coding sequence variants mechanistically contribute to the pathogenesis of cardiovascular disease
Method: The effects of sequence variants on the formation of RNADNA interactions was analysed by conducting predictions of interaction propensity using our previously published tool TriplexAligner. Variantharbouring transcripts were constructed from publicly available datasets from the GWAS Catalog and dbSNP, before their genomewide interaction profiles were compared to respective reference transcripts.
Results: Regions of ncRNAs predicted to be involved in RNADNA interactions by our previously published method TriplexAligner were found to have a higher rate of diseaserelevant genetic variation than proteincoding exon, indicating the potential importance of noncoding RNAs to the development of disease. By computationally modelling the formation of RNADNA interactions by almost 500 wildtype and variant RNA sequences, a repertoire more than 13,000 predicted gene regulatory variationsensitive ncRNADNA interactions was assembled, where sequence variation in the ncRNA is predicted to abrogate the interaction of the affected RNA at gene regulatory loci. Using these data, we assembled ncRNAcentric gene regulatory networks, which can be used to derive predicted transcriptional consequences of RNA sequence variants. Example analyses showed ncRNA sequence variation to be putatively linked with the regulation of blood pressure via regulation of key genes involved in solute transport.
Conclusion: This work shows that noncoding genetic variation has the potential to modulate cardiovascular diseaserelevant gene regulatory programs via abrogation of gene regulatory RNADNA interactions. Using computational and molecular methodologies, we will prioritize candidate variant ncRNAs which could be used to further enhance our understanding of individual disease risk in the future.

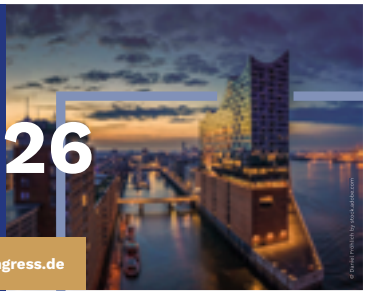

P04 Postergroup: Transcriptional & epigenetic reviving of disease

P0404

miR21 reduces inflammatory responses in marcophages and is increased in patients with chronic coronary syndrome

Gerhild Euler; Lukas Harbaum [1]; Abdullah Alnajjar; Kevin Kaloshi; Julian Kreutz [2]; Michael Malysa [1]; Rainer Schulz [3]; Bernhard Schieffer [1]; Mariana Parahuleva [1] Physiologisches Institut, Justus Liebig Universität, Gießen, Germany; [1] Angiologie und internistische Intensivmedizin, Klinik für Kardiologie, Universitätsklinikum Marburg, Marburg, Germany; [2] Klinik für Kardiologie, Philipps Universität Marburg, Marburg, Germany; [3] Fachbereich Medizin, Physiologisches Institut, JustusLiebigUniversität Gießen, Gießen, Germany;

Objective: In atherosclerosis, macrophages contribute to plaque formation that provokes coronary artery disease. Just recently, we identified microRNA 21 (miR21) in human coronary atherosclerotic plaques. Since the differentiation of monocytes to macrophages is a prerequisite for lodging of macrophages in the atherosclerotic plaque, we investigated the influence of miR21 on macrophage differentiation and determined miR21 expression in different monocyte subsets in patients with acute and chronic coronary artery syndrome (ACS vs. CCS).
Method: The monocytic human cell line, THP1, was used in the study. For induction of macrophage differentiation to proinflammatory M1, THP1 monocytes were stimulated with PMA (phorbol12myristate13acetate, 5 ng/ml) for 3 days, followed by stimulation with IFNγ (20 ng/ml) and LPS (10 pg/ml) up to 3 days.
Results: The marker genes for M1 polarization, IL1β and TNFα, increased under this stimulation. In addition, increased expression of miR21 was observed. Treatment of THP1 cells with antagomiR21 prior to M1stimulation enhanced TNFα expression, thereby indicating that miR21 suppresses proinflammatory release of cytokines in M1 cells. Furthermore, miR21 expression was analyzed in peripheral blood probes from patients with ACS during catheterization of the culprit artery and 48h and 3 months thereafter. Blood samples were taken from CCS patients at the same times. Monocytes were sorted by FACS into classical (CD14++CD16–), intermediate (CD14++CD16+), and nonclassical (CD14+CD16++) subsets. Interestingly, miR21 expression increased only in CCS patients. In classical monocytes, a transient increase within 48 h was detected, in nonclassical monocytes miR21 increased after 3 months and in intermediate monocytes miR21 was elevated at all time points.
Conclusion: In conclusion, miR21 represses proinflammatory cytokine release in macrophages and may thereby attenuate atherosclerotic processes. Elevated levels of miR21 in monocytes from CCS patients may attenuate proinflammatory responses and thus contribute to more stable plaques, whereas low miR21 levels in monocyte from ACS patients may lead to unstable plaques that are prone to rupture.

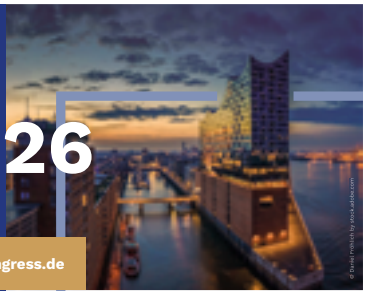

P04 Postergroup: Transcriptional & epigenetic reviving of disease

P0405

RoquinDependent Regulation of microRNA Stability in Cardiac Remodeling after Ischemic Injury

Nadja Itani; Rolf Schreckenberg; Rainer Schulz; Péter Bencsik [1]; Péter Ferdinandy [1]; KlausDieter Schlüter
Physiologisches Institut, JustusLiebigUniversität Gießen, Gießen, Germany; [1] Department of Pharmacology and Pharmacotherapy, Semmelweis University, Budapest, Hungary;

Objective: Cardiac ischemia and subsequent reperfusion are major contributors to myocardial injury and adverse postinfarct remodeling. While microRNAs are recognized as key regulators of these processes, the mechanisms controlling microRNA stability in the cardiac context remain incompletely understood. The RNAbinding protein Roquin has emerged as an important posttranscriptional regulator, yet its role in the cardiovascular system has not been investigated to date. This study aimed to characterize the expression of Roquin in the cardiovascular system and to identify Roquindependent regulatory pathways involved in postischemic remodeling.
Method: Primary rat cardiomyocytes and human AC16 cardiomyocytelike cells were used to investigate the role of Roquin under ischemic stress conditions. In vivo ischemia–reperfusion experiments as well as in vitro hypoxia–reoxygenation models were performed to mimic postischemic cardiac injury. Roquin expression and downstream signaling pathways were analyzed by quantitative PCR and Western blotting to assess the regulation of microRNAs and target gene expression.
Results: For the first time, Roquin expression was characterized in the cardiovascular system and found to be dynamically regulated under hypoxic conditions, suggesting a role in cellular stress adaptation. Mechanistically, a novel Roquin2–miR23b5p–ZBTB20 signaling axis was identified. Roquin regulated the expression of miR23b5p, which in turn modulated ZBTB20 mRNA expression. Functional analyses indicated that maintenance of Roquin expression following hypoxic stress may exert cardioprotective effects by stabilizing ZBTB20 expression and thereby influencing cellular pathways associated with survival and remodeling.
Conclusion: These findings identify Roquin as a previously unrecognized regulator in the cardiovascular system and establish the Roquin2–miR23b5p–ZBTB20 axis as a novel posttranscriptional signaling pathway involved in cardiac stress responses. Collectively, this work provides new insights into the regulation of cardioprotective pathways and highlights Roquin as a potential therapeutic target for limiting adverse cardiac remodeling following ischemic injury.

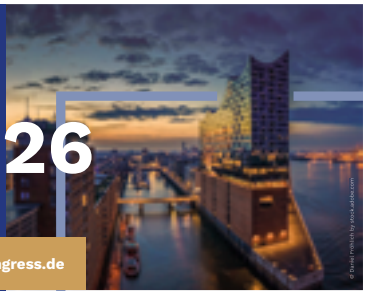

P04 Postergroup: Transcriptional & epigenetic reviving of disease

P0406

HMGB2 is an RNADNA triplexassociated protein essential for endothelial cell function

Marie Elisabeth Bayer; Julia Stötzel; Timothy Warwick; Agnes Yasmine Krüger; Maximilian Braun [1]; Kirsten Schaubruch [2]; Ralf Heermann [2]; Ilka Wittig [3]; Matthias Leisegang; Harald Schwalbe [4]; Ralf P. Brandes
Institut für Kardiovaskuläre Physiologie, Universitätsklinikum, Johann Wolfgang GoetheUniversität, Frankfurt a. M., Germany; [1] Institute for Organic Chemistry and Chemical Biology, Johann Wolfgang GoetheUniversität, Frankfurt a. M., Germany; [2] Institute of Molecular Physiology, Microbiology and Biotechnology, Mainz, Germany, Johannes GutenbergUniversity, Mainz, Germany; [3] Molekulare Bioenergetik, Universitätsklinikum, Johann Wolfgang GoetheUniversität, Frankfurt a. M., Germany; [4] Institute for Organic Chemistry and Chemical Biology, Johann Wolfgang GoetheUniversität, Frankfurt, Germany;

Objective: RNADNA triplexes formed by long noncoding RNAs are emerging regulators of gene expression in the cardiovascular system. Usually for RNA/DNA interactions, proteins like readers and writes are established, but whether these proteins also exist for RNADNA triplexes is unknown.
Method: RNADNA interacting proteins were identified by a global allinall approach. For this, ImmunoprecipitationMass Spectrometry using antibodies against dsDNA or RNADNA hybrids was performed. Proteins specifically interacting with the *MEG3:TGFBR1* triplex present in HUVECs were determined using Isolation of DNAassociated proteins. Interaction between HMGB2 and *MEG3:TGFBR1* triplex was investigated using Electromobility shift assay (EMSA) and Surface Plasmon Resonance (SPR). *TGFBR1* response was analysed by HMGB2 or *MEG3* knockdown and overexpression.
Results: Over 100 nuclear proteins associated with RNADNA triplexes were identified. Proteins with HMGbox domains were overrepresented, HMGB2 being the top hit. EMSAs confirmed interaction between HMGB2 and *MEG3:TGFBR1* triplex *in vitro*. Binding capacity was validated using SPR. The function of *MEG3* in the *MEG3:TGFBR1* triplex is suppressing gene expression. Knockdown of *MEG3* therefore increased *TGFBR1* expression. Importantly, also knockdown of the *MEG3:TGFBR1* binding HMGB2 had the same effect (siRNA, 48h, HUVEC, Oneway ANOVA, p= 0,0141). Overexpression of either HMGB2 or *MEG3* decreased *TGFBR1* expression. Mutants lacking *MEG3's* triplexforming region or HMGB2's box 2 abolished its effects on gene expression.
Conclusion: HMGB2 is an RNADNA triplex binding protein which contributes to the function of *MEG3* in its action at the *TGFBR1* locus. HMGB2 was required for the specific RNADNA triplex gene regulatory function of *MEG3*.

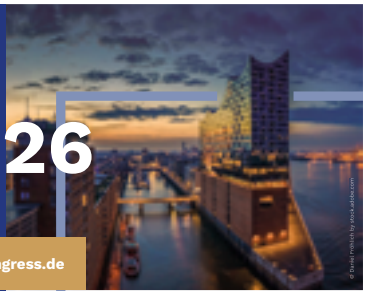

P04 Postergroup: Transcriptional & epigenetic reviving of disease

P0407

Sorafenib triggers cachexia by impeding transcriptional function of the SET1/MLL epigenetic regulator complex

Baoyu Zhou; Bushra Khan; Chiara Lanzuolo [1]; Valentina Rosti [1]; Philina Santarelli [1]; Andreas Pich [2]; Theresia Kraft; Mamta AmruteNayak; Arnab Nayak
Institut für Molekular- und Zellphysiologie, Medizinische Hochschule Hannover, Hannover, Germany; [1] Istituto Nazionale Genetica Molecolare 'Romeo ed Enrica Invernizzi', Milan, Italy; [2] Institute of Toxicology, Hannover Medical School, Hannover, Germany;

Objective: Certain chemotherapies are frequently associated with cachexia, a severe musclewasting syndrome that significantly impairs prognosis in cancer patients. Understanding mechanistic insights of chemotherapyinduced cachexia is essential to improve treatment strategies. This study aimed to investigate whether the tyrosine kinase inhibitor (TKI) sorafenib induces cachexia and to clarify its molecular mechanisms.
Method: Differentiated skeletal muscle cells were treated with either Sorafenib, Imatinib, or Nilotinib, and analyzed using transcriptomics, quantitative proteomics methods. Sarcomere structure, calcium transients, mitochondrial respiration, ATP production, and contractility were assessed. Chromatin immunoprecipitation (ChIP) analysis was used to detect chromatin signaling associated with TKI treatment.
Results: Sorafenib reduced the level of the active epigenetic mark i.e, histone 3 lysine 4 trimethylation on key musclespecific genes. This was due to impaired chromatin binding of SET1A, the catalytic subunit of the SET1/MLL histone methyl transferase complex, to chromatin upon Sorafenib treatment. Affected genes were involved in sarcomere structure (e.g., *MyHC* isoforms), sarcoplasmic reticulum Ca^{2+} handling (e.g., *Atp2a1, Ryr1*), and mitochondrial oxidative phosphorylation. Consequently, Sorafenibtreated muscle cells exhibited sarcomere disorganization, loss of calcium transients, impaired mitochondrial respiration and severe loss of contraction. Knockdown of SET1A phenocopied Sorafenibinduced cachexia, further confirming the essential role of SET1A in this process. Notably, other tyrosine kinase inhibitors, Imatinib and Nilotinib, did not cause similar effects.
Conclusion: Sorafenib induces cachexia by disrupting SET1Amediated epigenetic and transcriptional regulation in skeletal muscle cells, suggesting that the SET1Adependent chromatin signaling pathway may be a potential therapeutic target for chemotherapyassociated muscle atrophy.

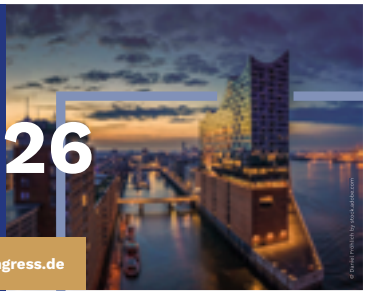

P04 Postergroup: Transcriptional & epigenetic reviving of disease

P0408

The role of myonuclei vs epigenetic traces in skeletal muscle memory

Einar Eftestøl; Martin F. Strand [1]; Mads Bengtsen [2]; Jo C. Bruusgaard [1]; Kristian Gundersen University of Oslo, Oslo, Norway; [1] Kristiania University College, Oslo, Norway; [2] Norwegian Directorate of Health, Oslo, Norway;

Objective: Muscle subjected to anabolic steroids or strength training display increased myonuclear number and hypertrophy. Upon removal of the stimulus, the hypertrophy is reversed, yet the myonuclei are preserved. When reintroduced to a hypertrophic stimulus, muscles respond better than naiive muscles. The memory storage mechanism has so far mainly been attributed to a permanent accretion of myonuclei, yet other longlasting changes like epigenetic traces might also play a role.
Method: We performed ATACseq analysis on purified myonuclei from two muscles after a 2week testosterone treatment and after a 7week (quadriceps) and 13week (EDL) washout period without testosterone in female mice in order to study chromatin accessibility. Myonuclei were specifically tagged using an antibody against PCM1 and purified by magnetic isolation using secondary antibodycoated microbeads. The cellular response to testosterone treatment was analyzed by visualizing nuclei (DAPI), myonuclei (PCM1) and fiber perimeter (dystrophin) on cryocross sections.
Results: Testosterone treatment for 2 weeks led to increased muscle weight, myonuclear number and fiber crosssectional area, confirming effects from previous studies.
A csaw/edgeR analysis comparing testosterone treatment to sham identified 4395 differentially accessible loci (FDR≤0.05), and following gene ontology and KEGG analyses showed many genes and pathways linked to hypertrophy, cytoskeletal remodeling, protein synthesis and degradation, and myonuclear remodeling.
After the washout period, we found only very few out of the 4395 loci were still altered, and these were connected to only 4 genes, namely Mapk14, Actr3B, Umad and Hddc2. They can thus be considered as putative memory loci/genes, although their role in skeletal muscle is still to be completely understood.
Conclusion: Previous attempts to identify memory genes also found only a handful of putative candidates, and there was no consensus between the previous studies or with our study. More functional experiments should be performed to follow up on the putative memory genes, yet for now myonuclear permanency perhaps still recides as the most important basis for a muscle memory.

P04 Postergroup: Transcriptional & epigenetic reviving of disease

P0409

Not so NEATly noncoding: a novel nuclear microprotein encoded by the lncRNA NEAT1 modulates DNA replication and cell proliferation

Anne Birke; Stefan Günther [1]; Carsten Künne [1]; Witold Szymanski [2]; Johannes Graumann [2]; Matthias Leisegang [3]; Ingrid Fleming [4]; Mauro Siragusa Institute for Vascular Signalling, Goethe University Frankfurt am Main, Frankfurt a. M., Germany; [1] Max Planck Institute for Heart and Lung Research, Bioinformatics and Deep Sequencing Platform, Bad Nauheim, Germany; [2] Institute & Core Facility of Translational Proteomics, BiochemicalPharmacological Centre, PhilippsUniversität Marburg, Marburg, Germany; [3] Vascular Research Center, Goethe University, Frankfurt a. M., Germany; [4] Department of Molecular Medicine, Institute for Vascular Signalling, Goethe University Frankfurt, Frankfurt a. M., Germany;

Objective: Microproteins (miPs) encoded by long noncoding RNAs (lncRNAs) are an emerging class of molecules with potential roles in vascular biology. However, their function remains largely unknown. This study focused on the characterization of a 71 amino acid miP encoded by the lncRNA NEAT1 in human endothelial cells, i.e. miPNEAT1.
Results: In endothelial cells expressing a FLAGtagged miPNEAT1 fusion protein, miPNEAT1 localized to the nucleus (FLAG immunofluorescence) and elicited the disruption of promyelocytic leukaemia nuclear bodies, suggesting a possible involvement in the regulation of gene expression. FLAGmiPNEAT1 immunoprecipitates from nuclear endothelial cell extracts were analysed by mass spectrometry to identify proteins interacting with the miP. This analysis identified interactions with proteins involved in DNA replication, including the DNA helicase complex, and nucleotide metabolism. As a consequence, in miPNEAT1expressing cells, genes related to cell proliferation, migration and angiogenesis were significantly downregulated, while genes associated with inhibition of cell growth were upregulated. Consistent with these alterations, miPNEAT1expressing endothelial cells exhibited reduced cell proliferation and migration.
Conclusion: Altogether, these results suggest that endothelial miPNEAT1 is a novel nuclear microprotein involved in the regulation of fundamental processes, including nuclear body organization, DNA replication and cell proliferation.

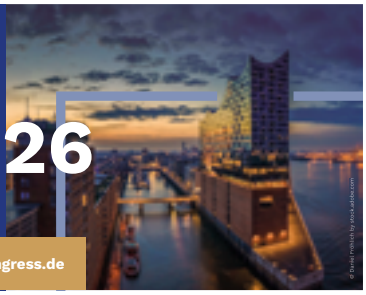

P04 Postergroup: Transcriptional & epigenetic reviving of disease

P0410

Dynamic assembly of accessory proteins drives SWI/SNF function through differentiation

Yinuo Zhou; Zhanhua Xing; Katalin Pálfi; Ilka Wittig [1]; Ralf P. Brandes; Matthias Leisegang; James Oo Institut für Kardiovaskuläre Physiologie, Universitätsklinikum, Johann Wolfgang GoetheUniversität, Frankfurt a. M., Germany; [1] Molekulare Bioenergetik, Universitätsklinikum, Johann Wolfgang GoetheUniversität, Frankfurt a. M., Germany;

Objective: SWItch/Sucrose NonFermentable (SWI/SNF) is a chromatin remodeling complex that actively maintains genomewide chromatin accessibility. BRG1 is the central, enzymatically active subunit of SWI/SNF, but accessory subunits are required for complex function. SWI/SNF aberrations occur in tumorigenesis and cardiovascular diseases. The molecular basis of locusspecific functions of SWI/SNF is incompletely understood. We hypothesize that cellspecific complex assembly and targeting facilitate cellspecific differentiation.
Method: Differentiation of human iPSCs into endothelial cells (ECs) and cardiomyocytes (CMs) was induced to study SWI/SNF alterations during lineage specification. CUT&RUN, ATACseq, and RNAseq were performed to characterize SWI/SNF remodeling activities through differentiation. Complexome profiling and IPMS were performed to identify both the constitutive and stagespecific subunit composition. Protein candidates were selected for perturbation in loss- and gainoffunction conditions. A degronbased (dTAG) system was used to allow rapid degradation of candidate proteins using FKBP mutant knockin iPSC lines.
Results: CUT&RUN revealed hundreds to thousands of differential BRG1 peaks during iPSCEC differentiation, indicating cell typespecific localization of SWI/SNF in a dynamic manner. Nuclear complexomics demonstrated dynamic complex composition during differentiation with constitutive and stagespecific SWI/SNF interactors. To determine the relevance of these dynamics, GLTSCR1, a GBAFspecific subunit, was studied in detail as it showed cell stage specific expression. Depletion of GLTSCR1 impaired progression of iPSCs from phasebright colonies to loosening and then elongated morphology of mesoderm cells, and downregulated mRNA levels of mesoderm markers.
Conclusion: These findings suggest that SWI/SNF differentially targets specific genomic loci and that this might in due to cellspecific complex assembly. GLTSCR1, as one of the candidate interactors, helps facilitate SWI/SNF targeting specificity during differentiation.

P05 Postergroup: Renal Tubular Disease

P0501

Creatine: From an athletes' supplement to therapy in GATMassociated kidney disease

Tanja Link; Allein Plain; Vanessa Mikicz [1]; Anja Süß; Katrin Pollok [2]; Eva Wacker [1]; Ben Davies [3]; Detlef Böckenhauer [4]; Markus Reichold; Jonathan Schäffler [5]; Ralph Witzgall [1]; Katja Dettmer [6]; Robert Kleta [7]; Felix Knauf [8]; Richard Warth
Medizinische Zellbiologie, Institut für Physiologie, Universität Regensburg, Regensburg, Germany; [1] Institut für Molekulare und Zelluläre Anatomie, Universität Regensburg, Regensburg, Germany; [2] Medical Cell Biology, University of Regensburg, Regensburg, Germany; [3] Genetic Modification Service, The Francis Crick Institute, London, United Kingdom; [4] Department of Pediatric Nephrology, UZ Leuven, Leuven, Belgium; [5] Department of Medical Cell Biology , Institute for Physiology, University Regensburg, Regensburg, Germany; [6] Institute of Functional Genomics, University of Regensburg, Regensburg, Germany; [7] Centre for Nephrology, Royal Free Hospital, University College London, London, United Kingdom; [8] Knauf laboratory, Division for Nephrology and Hypertension, Mayo Clinic, Rochester, United States;

Objective: Several missense mutations in the glycine amidinotransferase gene (GATM or AGAT) cause an autosomal dominant renal Fanconi syndrome, leading to the formation of filamentous aggregates of the mutated GATM, e.g. p.T336A, in the proximal tubules. This is accompanied by cell damage, fibrosis, and progressive loss of kidney function. GATM catalyzes the transfer of a guanidino group from arginine to glycine. The resulting guanidinoacetate is a precursor of creatine. It is known that GATM expression is negatively regulated by creatine. Accordingly, this study investigated whether creatine supplementation could suppress mutated GATM expression and thereby inhibit the presumed pathomechanism.
Method: Wildtype and GatmT336A knockin mice, which develop aggregates of the mutated GATM in the proximal tubules like the patients, received creatine supplementation (2% creatine plus 8% sucrose) in their drinking water. After three weeks, urine, blood, and kidney samples were collected for analysis. Gene expression was quantified by RTqPCR, protein levels by Western blotting and immunofluorescence, and creatine metabolism by mass spectrometry.
Results: Urinary creatine concentrations were significantly increased following creatine supplementation, whereas no changes were observed in creatinine or guanidinoacetate concentrations. Creatine supplementation tripled serum creatine concentrations and slightly elevated creatinine concentrations in both genotypes, while reducing serum guanidinoacetate concentrations by approximately 30%. GATM mRNA expression was similar between wildtype and T336A knockin mice under control conditions but led to a decline to approximately half the baseline level in both genotypes after creatine supplementation. Untreated T336A knockin mice showed doubled GATM protein levels as in wildtype animals, which is likely due to a prolonged halflife of the filamentous mutant GATM. Creatine supplementation decreased the amount of GATM protein to half the baseline level in both genotypes after three weeks, confirmed by immunofluorescence.
Conclusion: In summary, results from the GATMT336A knockin mouse model indicate that dietary creatine supplementation effectively reduces mutant GATM protein expression in the kidney and attenuates aggregate formation. A clinical study will evaluate the benefits of creatine supplementation in affected induviduals.

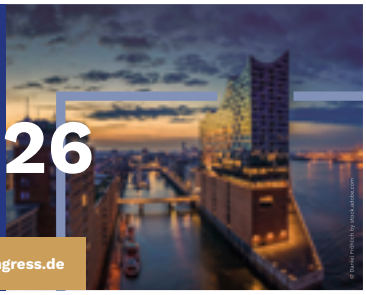

P05 Postergroup: Renal Tubular Disease

P0502

Polycystin2 pore mutations associated with autosomal dominant polycystic kidney disease (ADPKD) impair ion channel function of polycystin2/polycystin1 complexes

Frauke Wagner; Tobias Staudner; Bardha Azemi; Linda Geiges; Christoph Korbmacher; Alexandr V. Ilyaskin
Institut für Zelluläre und Molekulare Physiologie, FriedrichAlexanderUniversität ErlangenNürnberg, Erlangen, Germany;

Objective: ADPKD is one of the most common inherited kidney disorders, characterized by renal cyst formation ultimately leading to endstage renal disease. Mutations occur in the *PKD1* or *PKD2* genes, encoding polycystin1 (PC1) or polycystin2 (PC2), respectively. PC2 can form a homomeric ion channel, but when coexpressed with PC1 preferentially assembles as PC2/PC1 heteromeric ion channel with a 3:1 stoichiometry. The (patho)physiological role of PC2/PC1 channels remains poorly understood. As previously reported, diseaseassociated missense mutations in the pore loop of PC2 alter ion channel function of PC2 homomeric channels (Staudner et al., *J Biol Chem*, 2024). Here, we characterized the impact of these mutations (F629S, C632R, R638C) on the formation and function of heteromeric PC2/PC1 channels using a recently established PC2/PC1 gainoffunction (GOF) construct (Staudner et al., *FEBS Letters*, 2025).
Method: PC2/PC1GOF channels with or without pore mutations were heterologously expressed in *Xenopus laevis* oocytes and analyzed using the twoelectrode voltage clamp technique. Currents were measured in the absence or presence of extracellular divalent cations (Ca^{2+}/Mg^{2+}), which partially inhibit PC2/PC1 channel activity. Cell surface expression and complex formation were assessed by western blotting combined with surface biotinylation and coimmunoprecipitation, respectively.
Results: In the F629S and C632R mutants, maximal inward currents were almost completely abolished both in the presence and absence of extracellular Ca^{2+}/Mg^{2+} (F629S: 0.5±0.3 µA, n=42; C632R: 0.1±0.1 µA, n=42; control: 3.9±2.2 µA, n=30 in the absence of Ca^{2+}/Mg^{2+}; mean ± SD; $p<0.0001$; ANOVA). In contrast, currents produced by the R638C mutant were largely preserved under divalentfree conditions (2.1±0.9 µA, n=41; mean ± SD), but were strongly reduced in the presence of Ca^{2+}/Mg^{2+}, indicating increased susceptibility to divalent cationmediated inhibition. None of the mutations significantly affected cell surface expression (n=3) or heteromerization of PC2/PC1 (n=3). Thus, PC2/PC1 complexes with pore mutations in PC2 assemble and traffic normally to the cell surface but exhibit impaired ion channel function.
Conclusion: In conclusion, our finding that pathogenic PC2 pore mutations affect PC2/PC1 ion channel function supports the pathophysiological role of this heteromeric channel in ADPKD. The development of methods to restore PC2/PC1 ion channel function may provide a novel therapeutic strategy in ADPKD.

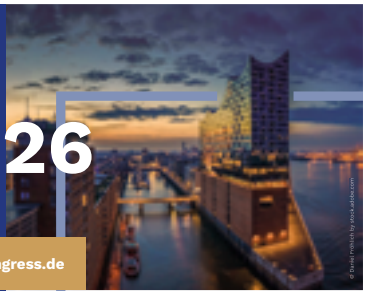

P05 Postergroup: Renal Tubular Disease

P0503

Urinary metabolomics of potassium chlorideinduced acidosis in rats and humans with chronic kidney disease

Pedro Henrique Imenez Silva; Michiel L.A.J. Wieers; Crissy F. Rudolphi; Martin Gritter; KuangYu Wei; Liffert Vogt [1]; Martin H. de Borst [2]; Joris I. Rotmans [3]; Ewout J. Hoorn Internal Medicine, Erasmus Medical Center, Rotterdam, The Netherlands; [1] University of Amsterdam, Amsterdam, The Netherlands; [2] Department of Internal Medicine, University Medical Center Groningen, Groningen, The Netherlands; [3] Department of Internal Medicine, Leiden University Medical Center, Leiden, The Netherlands;

Objective: Potassium repletion has been proposed as a strategy to mitigate kidney function decline in individuals with chronic kidney disease (CKD) consuming a lowpotassium diet. However, the accompanying anion may influence this effect. Potassium chloride (KCl) supplementation has been associated with metabolic acidosis, a condition linked to adverse outcomes in CKD, potentially offsetting the benefits of potassium supplementation. The mechanisms underlying KClinduced metabolic acidosis remain unclear. This study aimed to investigate the acidbase and metabolic effects of KCl supplementation.
Method: We integrated detailed urinary acidbase characterization with metabolomics analyses of urine samples collected in two previous studies in which KCl administration reduced plasma bicarbonate. One study was conducted in rats with shamoperated or 5/6 nephrectomy rats receiving 0.1% or 2.5% KCl in the diet for 4 weeks and the other in humans with CKD stages G3bG4 receiving KCl supplementation for 2 weeks. Untargeted metabolomics analysis was performed with 24h urine samples from rats (n = 89/group) and humans (n = 18) via ultrahighperformance liquid chromatographytandem mass spectrometry. Rat data were analyzed using twoway ANOVA with FDR correction, while human data were evaluated using paired Wilcoxon tests before and after KCl supplementation. Supervised multivariate classification with featureimportance scoring were used to identify metabolites contributing to group separation in the rat metabolome.
Results: Ammoniagenesisassociated pathways, typically activated during acidosis and responsible for its correction, were unresponsive to KCl loading in rats and humans. In agreement, net acid excretion was not stimulated by KCl intake despite the reduction in plasma bicarbonate. Significant alterations were observed in metabolites associated with hepatic metabolism: In rats, KCl loading activated the urea cycle, potentially reflecting impaired ammonium excretion and enhanced reabsorption. In humans, the excretion of bile acid metabolites was strongly affected, although whether this reflects altered ammonium metabolism remains unclear. Nitrogen metabolism was broadly affected in both species, alongside a marked decrease in the excretion of several imidazolecontaining metabolites, which can serve as intracellular pH buffers.
Conclusion: KCl loading suppresses both net acid excretion and the excretion of imidazolecontaining metabolites in rats and humans, while also altering systemic metabolism through mechanisms that extend beyond the kidney. Our study suggests that KCl both attenuates ammoniagenesis and reduces ammonium excretion efficiency in rats, while in humans ammoniagenesis is likely similarly attenuated, but effects on ammonium excretion efficiency remain unclear. Collectively, we characterized extensive metabolomic effects of KCl supplementation across species, involving both renal and extrarenal pathways.

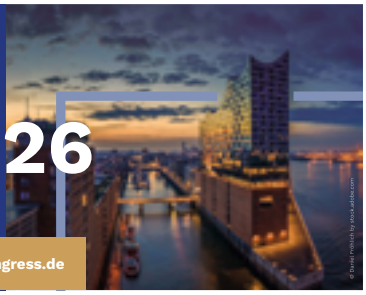

P05 Postergroup: Renal Tubular Disease

P0504

Challenged Urine Bicarbonate Excretion Dynamically Reflects ShortTerm Changes in CFTR Function in People with Cystic Fibrosis

Amalie Quist Rousing; Peder Matzen Berg; Mads V. Sørensen; Søren JensenFangel [1]; Hanne Vebert Olesen [2]; Majbritt Jeppesen [1]; Jens Leipziger Department of Biomedicine, University of Aarhus, Aarhus, Denmark; [1] Department of Infectious Diseases, University of Aarhus, Aarhus, Denmark; [2] Department of Paediatrics and Adolescent Medicine, University of Aarhus, Aarhus, Denmark;

Objective: Renal cystic fibrosis transmembrane conductance regulator (CFTR) function is essential for urinary HCO_3^- excretion and is markedly impaired in people with CF (pwCF). Challenged urinary HCO_3^- excretion following an oral $NaHCO_3$ load may serve as a simple in vivo biomarker of CFTR function, reflecting both the extent of CFTR dysfunction and therapyinduced rescue. This study evaluates the sensitivity and rapid reversibility of this biomarker. We investigated challenged urine HCO_3 excretion in pwCF treated with triple CFTR modulator therapy (elexacaftor/tezacaftor/ivacaftor, ETI), before, during, and after a short therapy interruption, and examined the association with systemic acidbase and volume parameters, and ETI plasma concentrations.
Method: 27 pwCF underwent a 90minute oral $NaHCO_3$ challenge test before, during, and after a randomized ETI interruption (12, 36, or 60 hours). Urine was collected at baseline and 90 minutes after $NaHCO_3$ ingestion for electrolyte and acidbase measurements. Baseline venous blood samples were obtained for electrolyte, acidbase, and ETI plasma concentration measurements. 16 healthy control participants and 22 CF carriers also completed the challenged test.
Results: ETI treatment interruption was associated with a reduced challenged urine HCO_3 excretion in pwCF (Δ: 1.29 mmol/90 min., 95% CI: 0.4 to 2.2), whereas systemic electrolyte and acidbase parameters were unchanged. Challenged urine HCO_3^- excretion was markedly modulated by spot urine NH_4^+ concentration (65% lower per 2fold higher urine NH_4^+), forming the basis for a way to normalize test responses to varying baseline acidbase and hydration status. CF carriers demonstrated intermediate HCO_3^- excretion capacity – higher than pwCF off ETI and lower than healthy controls (Δ: 3.42 and 5.09 mmol/90 min, respectively). ETI plasma concentration analyses are pending.
Conclusion: Challenged urine $HCO3^-$ excretion is sensitive to shortterm changes in ETItherapy, supporting its dynamic reflection of CFTR function and its use as an *in vivo* biomarker in pwCF. Adjustment for systemic acidbase status using baseline spot urine NH_4^+ reduces variation and improves interpretation of test responses. The ability to detect reversible changes in CFTR function during shortterm changes may support clinical assessment of treatment adherence and individualized optimization of CFTR modulator therapy.

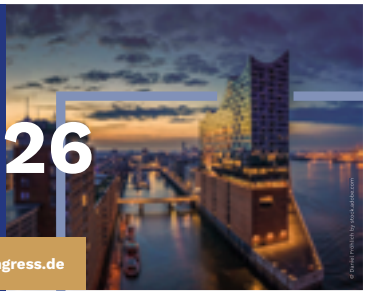

P05 Postergroup: Renal Tubular Disease

P0505
Effect of hydrostatic pressure on transport of macromolecules and water in renal cell lines

Samuel Sandegaard; Dorothee Günzel [1]; Rita Rosenthal [1]; Jeppe Praetorius
Department of Biomedicine, Aarhus University, Aarhus, Denmark; [1] Institut für Klinische Physiologie, Campus Benjamin Franklin, Charité - Universitätsmedizin Berlin, Berlin, Germany;

Objective: In the mammalian proximal tubule a hydrostatic pressure gradient exists of ≈ 10 mmHg from tubule lumen to interstitium. Three pathways for transport are available in epithelia: transcellular, and paracellular through either the bi- or tricellular junctions. We hypothesized that this hydrostatic gradient might play a role in the poorly understood nearisotonic water transport of the proximal tubule by driving water through the tricellular junction, in turn increasing macromolecule transport through a solvent drag mechanism.
Method:
The effect of hydrostatic pressure was studied on two leaky epithelial cell lines (LLCPK1 and MDCK II), and the tight MDCK C7 cells (+/- knockdown of tricellular protein tricellulin to increase macromolecule and water permeability). When confluent, cells were mounted in Ussing chambers connected to classic glass bubble lifts, allowing an increase in water column height on one side of the epithelium of up to 10 cm H_2O (≈ 7.3 mmHg). The fluorescent molecule fluorescein (332 Da) was added to the apical chamber, and samples were taken from the basolateral chamber for analysis of dye accumulation by a plate reader.
Results: Pilot experiments showed decreased permeability to fluorescein in the presence of 10 cm H_2O apical hydrostatic pressure in leaky cell lines (LLCPK1 (31.2%, n=5) and MDCK II (26.7%, n=4)). In the tight MDCK C7 controls (n=8), no change in permeability was observed. In MDCK C7 tricellulin knockdown cells, the effect of pressure was largest (44.8%, n=7).
Conclusion: Contrary to our hypothesis, apical pressure tends to decrease macromolecule transport, likely due to closing of the lateral intercellular space. Further results will be presented at Physiology in Focus 2026.

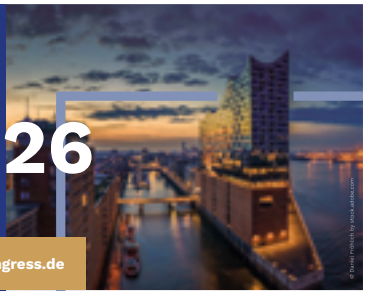

P05 Postergroup: Renal Tubular Disease

P0506

Lithium Treatment Alters Principal and Intercalated Cell Marker Expression in $mCCD_{cl1}$ cells

Xabier Sørtvedt; Birgitte Moenster Christensen
Department of Biomedicine, Aarhus University, Aarhus, Denmark;

Objective: Lithium (Li) is widely used to treat bipolar disorder, but up to 40% of patients develop Liinduced Nephrogenic Diabetes Insipidus (LiNDI). In rodents, the development of LiNDI includes a remodeling of the collecting duct (CD). The fraction of AQP2expressing principal cells decreases, while the fraction of H^+ATPaseexpressing intercalated cells increases. Moreover, Ecadherin and betacatenin are absent in the basal plasma membrane of a subset of CD cells. The $mCCD_{cl1}$ cell line expresses ENaC allowing entry for Li and the cells respond to vasopressin and Li. The aim is to examine the potential of $mCCD_{cl1}$ cells as a model for the Liinduced cellular remodeling.
Method: mCCDcl1 cells were treated for 2, 3 and 4 weeks with either 1 mM LiCl or NaCl (controls). Cells were embedded in paraffin for immunohistochemistry or lysed for immunoblotting. Multiple unpaired ttests with welch correction were applied on the fraction of control mean values from densitometric analyses of immunoblots. Results are given as mean ± SD.
Results: Two weeks of 1 mM LiCl treatment decreased AQP2 levels to 41.1 ± 10.9% of control levels (100 ± 15.4%, $p<0.01$, $n = 6$). After four weeks of Li treatment, AQP2 levels were reduced to 39.6 ± 4.8% of controls (100 ± 8.9%, $p<0.01$, $n = 8$ [Li], n = 9 [con]). The decrease in AQP2 levels preceded any increase in H^+ATPase levels, which was not observed until 3 weeks of Li (129.7 ± 26.6% vs Con: 100 ± 14.1%, $p<0.05$; $n = 6$). After four weeks, H^+ATPase levels increased to 171.9 ± 25.5% when compared to controls (100 ± 12.6%, $p<0.01$, $n = 8$ [Li], $n = 9$ [con]). No changes in betacatenin levels were observed. Ecadherin levels were reduced to 91.9 ± 7.2 % of control levels (100 ± 5.1%, $p<0.05$, $n= 8$ [Li], $n = 9$ [con] after 4 weeks of treatment. Preliminary immunohistochemistry data showed Ecadherin and betacatenin localized at the basal and lateral plasma membrane domains of mCCDcl1 cells in control conditions as observed *in vivo*.
Conclusion: In conclusion, $mCCD_{cl1}$ cells exhibit potential to serve as an *in vitro* model for studying cellular remodeling in LiNDI and could aid the prevention or alleviation of LiNDI.

P05 Postergroup: Renal Tubular Disease

P0507

Kidney Tubular Function and Adverse Outcomes in Chronic Kidney Disease

Peder Matzen Berg; Jesper Frank Andersen; Sebastian Nielsen [1]; Jakob Nyvad [1]; Niels Henrik Buus; Henrik Birn [1]; Mads Vaarby Sørensen; Jens Georg Leipziger
Department of Biomedicine, University of Aarhus, Aarhus, Denmark; [1] Department of Renal Medicine, Aarhus University, Aarhus, Denmark;

Objective: Kidney function is typically assessed using eGFR and uACR, which primarily reflects glomerular function. However, most kidney tissue is comprised of the tubulointerstitial compartment. We recently developed the urine ammoniumpH index (uAPI) as a measure of kidney tubular function. Here, we assessed the prognostic relevance of a low uAPI, as a measure of impaired tubular function, and if its integration could improve clinical management.
Method: Seven independent cohorts of patients with CKD (n=818) were followed for up to 5 years (median: 4.9 years, IQR: 3.55). The primary outcome was CKD progression (sustained ≥50% eGFR reduction, sustained eGFR<15, or initation of kidney replacement therapy). Secondary outcomes were annual eGFR decline, acute kidney injury, metabolic acidosis, hyperkalemia, acute hospitalizations, cardiovascular outcomes, and allcause mortality.
Associations between a low uAPI and outcomes were assessed using an individual patient data metaanalysis approach by cox proportional hazards models (time to first event analyses, e.g. CKD progression), negative binomal regression analyses (count analyses, e.g. hospital admissions), and mixedeffects models for repeated measures (for annual eGFR decline). Analyses were adjusted for demographics and risk factors (including eGFR, uACR, diabetes status, and systolic blood pressure).
Using our initial two cohorts as development cohort (n=150) and the remaining cohorts as validation cohort (n=668), we assessed the potential clinical relevance of integrating the uAPI in clinical management.
Results: A low uAPI was associated with an adjusted 7.3fold higher risk of CKD progression (95% CI: 3.316), a larger annual eGFR decline and a significantly increased risk for all other secondary outcomes. Adding the uAPI to the KDIGO heatmap or the kidney failure risk equation improved classification (6070%) and discrimination (34%) and decreased the proportion of patients classified as needing nephrology referral in both the development (~54% to ~46%) and validation cohort (~64% to ~54%) without missing any kidney events.
Conclusion: Poor tubular function, as indicated by low a uAPI, is independently associated with adverse outcomes and faster eGFR decline in CKD. Inclusion of the uAPI into standard risk stratification approaches may potentially optimize referral patterns, decrease patient burden, and optimize health care resource utilization.

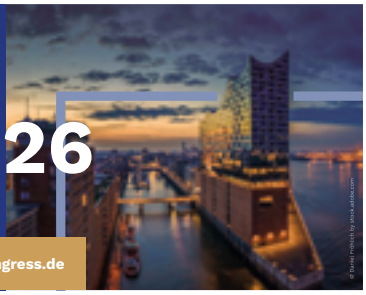

P05 Postergroup: Renal Tubular Disease

P0508

Regulation of Klotho expression in murine models of chronic kidney disease and human kidney slices

Natasja P. Simonsen; Jasmine C. L. Atay; Stanislava Pankratova [1]; Mirolyuba Ilieva [2]; Rikke Nørregaard
Department of Clinical Medicine, Aarhus University, Aarhus, Denmark; [1] Department of Veterinary and Animal Sciences, University of Copenhagen, Frederiksberg, Denmark; [2] Department of Pathology, Rigshospitalet, Copenhagen, Denmark;

Objective: Chronic kidney disease (CKD) affects about 10% of the population and is characterized by progressive fibrosis and loss of renal function. Klotho is a renoprotective protein enriched in the kidney with proposed antifibrotic properties. This study investigated alterations in Klotho expression in murine CKD models and human kidney slices (HKS).
Method: CKD was induced in C57BL/6 mice by 0.2% adenine diet (2–4 weeks), unilateral ureteral obstruction (UUO; 3–7 days), or intraperitoneal injection of folic acid (250 mg/kg; 2–4 weeks). Anesthesia was induced by inhalation of 35 % sevoflurane for the UUO surgery or sacrifice. Macroscopically healthy cortical tissue from tumor nephrectomies was prepared as 250300 µm precisioncut slices and incubated for 24–48h with or without transforming growth factor (TGF). Klotho expression was assessed by qPCR, western blotting, and immunohistochemistry.
Results: In adeninefed mice, Klotho mRNA was reduced by 64 ± 22% at 2 weeks and 86 ± 9% at 4 weeks, while protein levels decreased by 74 ± 6% and 69 ± 10%, respectively. In UUO kidneys, Klotho mRNA decreased by 78 ± 4% at 3 days and 85 ± 7% at 7 days, with protein reductions of 80 ± 6% and 72 ± 6%, respectively. Folic acid reduced Klotho mRNA by 28 ± 10% at 4 weeks but no changes occurred at 2 weeks. In HKS, Klotho expression decreased by over 85% after 24–48 h incubation.
Conclusion: Together, these data indicate that significant Klotho downregulation occurs by CKD induction in various animal models and HKS. This suggests that Klotho deficiency is prevalent in CKDinduced fibrosis and may serve as an important diagnostic marker and therapeutic target.

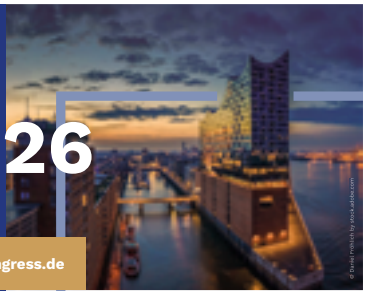

P05 Postergroup: Renal Tubular Disease

P0509

Effects of acute phosphate intake on mineral buffering and autonomic nervous system in healthy adults

Adela Tiffner; Helmut K. Lackner [1]; Azmat Sohail; Beatrice Toegel; Elisabeth Riegel; Gregor Mitter; Barbara Ketterer; Mehdi Razazian; Sheyda Bahiraii; Margot Egger; Benjamin Dieplinger [2]; Andreas Pasch; Edward R. Smith [3]; Daniel Cejka; Ioana Alesutan; Jakob Voelkl Institut für Physiologie und Pathophysiologie, Johannes Kepler Universität Linz, Linz, Austria; [1] Institut für Physiologie, Medizinische Universität Graz, Graz, Austria; [2] Abteilung für Labormedizin, Konventhospital Barmherzige Brueder Linz und Ordensklinikum Linz Barmherzige Schwestern, Linz,
Austria; [3] Abu Dhabi Healthcare Company, Abu Dhabi, United Arab. Emirate;

Objective: Phosphate is considered a cardiovascular toxin and has been suggested to stimulate the sympathetic nervous system. Its detrimental effects are at least partially mediated by calciprotein particles (CPP), with secondary CPP2 particularly recognized to induce vascular dysfunction, inflammation and calcification. CPP2 formation in blood is part of a physiological mineral buffering system, which is impaired and associated with mortality in chronic kidney disease. This study investigated the acute effects of excessive phosphate uptake in healthy volunteers.
Method: In an exploratory study with a crossover design, 28 healthy human medical students received either 1200 mg of phosphorus or NaCl control per os. After 4.5 hrs, a stress test with measurement of heart rate variability was conducted, and blood and urine were collected. Individual mineral buffering strength in serum samples was determined by the serum calcification propensity (T50) test and by measuring the resulting hydrodynamic radius of CPP2. In a second study cohort, the treatment arms were expanded to include a third group receiving magnesium and zinc supplementation alongside phosphate to strengthen the mineral buffering system.
Results: Compared with NaCl, the phosphate treatment increased serum phosphate, PTH and urinary phosphate excretion. These alterations were paralleled by increased serum calcification propensity (lower T50) and higher hydrodynamic radius of CPP2. Phosphate intake also altered the highfrequency component of heart rate variability in some phases of the stress paradigm. In the second study cohort, similar results were observed, but magnesium and zinc supplementation failed to alter the effects of phosphate intake.
Conclusion: Acute intake of larger phosphate amounts reduces T50 and increases CPP2 radius in healthy volunteers, indicating a weakening of the mineral buffering system. This effect is apparently accompanied by changes in vegetative nervous system activity. Supplementation with magnesium and zinc at the dosage investigated was insufficient to improve T50 or to alter other effects of phosphate loading.

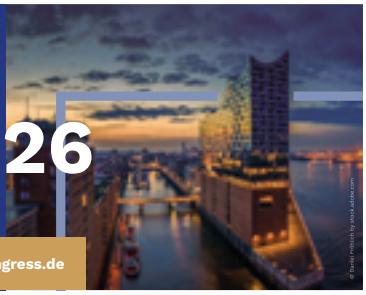

P05 Postergroup: Renal Tubular Disease

P0510

Regulation of Renal and Intestinal Magnesium Handling in a Mouse Model of Autosomal Dominant Hypocalcemia

Angele Frisdal; Wouter van Megen [1]; Henrik Dimke
Department of Molecular Medicine, University of Southern Denmark , Odense, Denmark; [1] Institute of Anatomy, University of Zurich, Zurich, Switzerland;

Objective: Autosomal dominant hypocalcemia type 1 (ADH1) is a form of hypoparathyroidism caused by gainoffunction mutations in the calciumsensing receptor (CASR), leading to hypocalcemia that is not always associated with hypercalciuria (van Megen, EBioMedicine, 2022). Some ADH1 patients also develop hypomagnesemia and require Mg^{2+} supplementation (Roszko, JBMR, 2022). In the kidney, Mg^{2+} is reabsorbed through the paracellular pathway in the proximal tubule and the TAL. Additional Mg^{2+} transport occurs through TRPM6 and TRPM7 channels in the distal convoluted tubule, which are also expressed in the colon. However, the effects of chronic CASR activation on these pathways remain poorly understood. This study aims to investigate the mechanism whereby ADH1 can alter renal and intestinal Mg^{2+} handling.
Method: *Casr* gainoffunction *Nuf* mice were studied under baseline conditions or when given a high or low dietary Mg^{2+} for 14 days, with an additional group receiving low dietary Mg^{2+} for 7 days. Mice were placed in metabolic cages for urine and feces collection. Mice were anesthetized with isoflurane (1.5%, inhalation) before sacrifice.
Results: In *Nuf* mice, baseline plasma Mg^{2+} was significantly lower compared to wild type (WT) mice (0.814 ± 0.036 mM vs. 0.592 ± 0.028 mM, $p<0.0001$). In contrast, urinary Mg^{2+} excretion remained unchanged. These parameters were also unchanged under high or low Mg^{2+} diets. After 14 days on the high Mg^{2+} diet, plasma Mg^{2+} remained unchanged (0.806 ± 0.059mM vs. 0.761 ± 0.042mM, $p=0.619$). Surprisingly, after 14 days on a lowMg^{2+} diet, mice showed a severe phenotype and reached the human endpoints; therefore, the lowMg^{2+} diet was reduced to 7 days. After 7 days on the low Mg^{2+} diet, plasma Mg^{2+} remained unchanged between the groups (0.225 ± 0.021mM vs. 0.240 ± 0.027mM, $p=0.631$). Furthermore, at baseline condition, *TRPM6* expression was significantly reduced in *Nuf* mice compared with WT mice in the kidney (1.000 ± 0.051 vs. 0.814 ± 0.041, $p = 0.044$) and colon (0.928 ± 0.147 vs. 0.562 ± 0.061, $p=0.019$), whereas TRPM7 expression was unaffected in both tissues.
Conclusion: Chronic CASR activation in ADH1 reduces plasma Mg^{2+} levels and decreases *TRPM6* expression in the kidney under baseline conditions, supporting a role for altered magnesium homeostasis in ADH1.

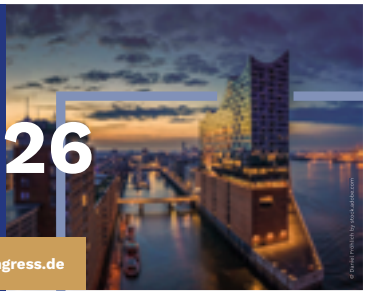

P06 Postergroup: Hypoxia & pulmonary functions

P0601

Intracellular calcium and mucin secretion in airway epithelial cells

Giorgio Fois; Annika Armbruster; Manfred Frick
Institute of General Physiology, University of Ulm, Ulm, Germany;

Objective: Mucin secretion is essential for lung health. Mucins are released via exocytosis of mucin granules from secretory cells of the airway epithelium. Exocytosis is a conserved mechanism in eukaryotic cells and is triggered by intracellular calcium $[Ca^{2+}]_i$. We hypothesize that different $[Ca^{2+}]_i$ levels may regulate distinct secretory pathways, thereby contributing to baseline or stimulated mucin secretion in human airway epithelial cells. This study aims to assess the relationship between calcium dynamics and mucin secretion using complementary imaging and secretionbased readouts.
Method: We analyzed immortalized human airway epithelial cells that were differentiated at airliquid interface were analysed using livecell calcium imaging and secretion assays. Using this approach, we examined the relationship between spontaneous $[Ca^{2+}]_i$ fluctuations and mucin release under unstimulated conditions. In parallel, candidate calciumsensing proteins were evaluated as potential mediators of secretion.
Results: Preliminary analyses suggest that small fluctuations in intracellular calcium $[Ca^{2+}]_i$ are associated with mucin granule exocytosis. Consistent with this finding, highaffinity calciumsensing proteins, including synaptotagmins, are being evaluated as candidate mediators of granule fusion under lowcalcium conditions
Conclusion: These findings support a role for $[Ca^{2+}]_i$ in the regulation of mucin secretion in human airway epithelial cells. Ongoing work aims to define the calciumdependent mechanisms that shape secretion sensitivity and to clarify how these processes contribute to airway epithelial function.

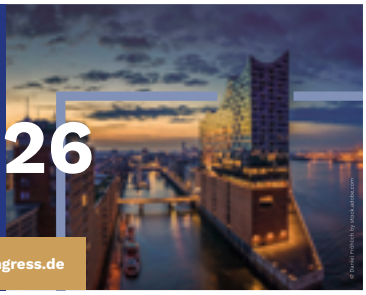

P06 Postergroup: Hypoxia & pulmonary functions

P0602

The role of thermo- and mechanosensitive TRPV1 and TRPV4 channels in the development and progression of ventilatorinduced lung injury

Wolfgang Kübler; Laura Michalick [1]
Institut für Physiologie, Campus Charité Mitte, Charité - Universitätsmedizin Berlin, Berlin, Germany; [1] Institute of Physiology, German Heart Center, Charité University Medicine Berlin, Berlin, Germany;

Objective: Mechanical ventilation induces endothelial barrier failure and pulmonary edema, contributing to ventilatorinduced lung injury (VILI), yet underlying mechanisms remain incompletely understood. In previous work, we identified a critical role for the mechanosensitive Ca^{2+} channel TRPV4 in VILI, with new pilot data pointing towards a synergism of TRPV4 with thermosensitive TRPV1 channels. As temperature is an increasingly recognized yet underexplored modulator of lung injury, we probed for a contribution of thermosensitive TRPV1 to TRPV4mediated VILI.
Method: To assess the relevance of mechanical and temperaturedependent TRPV1/4 activation *in vivo* and *ex vivo,* wildtype, *Trpv1*$^{-/-}$, and *Trpv4*$^{-/-}$ mice or their respective isolated perfused lungs (IPL) were subjected to low (7 ml/kg) or high (20 ml/kg) tidal volume ventilation at 2040°C. Lung injury was assessed by realtime monitoring of lung weight gain (in IPL) or postmortem wettodry lung weight ratio, BALF protein content and the extravasation of intravenously injected human serum albumin (HSA) as measures of lung vascular permeability *in vivo*. In parallel, human pulmonary microvascular endothelial cells were exposed to static or cyclic stretch (0 or 18% elongation) at 20, 30, or 40°C, in the presence or absence of TRPV1 (SB366791) or TRPV4 (HC067047) antagonists, and TRPV1–TRPV4 interactions were quantified by proximity ligation assay (PLA). TRPV1/4 expression levels were determined by Western blot and qPCR in both lung tissue and endothelial cells.
Results: *In vivo* and *ex vivo*, the severity of VILI increased with ventilation temperature, reflected by increased pulmonary edema, vascular permeability, and lung weight gain, respectively. VILI was reduced in both *Trpv1*$^{-/-}$ and *Trpv4*$^{-/-}$ mice compared to wild type. *In vitro*, cyclic stretch increased TRPV1–TRPV4 interactions as determined by PLA, and this effect was further enhanced at 40°C as compared to 20°C. TRPV1 or TRPV4 antagonists reduced PLA signals, indicating that functional blockade of either channel attenuates temperature- and stretchinduced TRPV1–TRPV4 interactions.
Conclusion: Here, we demonstrate a crucial synergism of both thermo- and mechanosensitive TRPV1 and TRPV4 in VILI, in that temperature- and stretchdependent TRPV1–TRPV4 interactions promote endothelial dysfunction and edema formation in response to mechanical overventilation, whereas lower inspired gas temperatures protect from VILI. These findings suggest that targeting thermo- and mechanosensitive TRP channels and/or ventilation at low inspired gas temperatures may represent a new strategy to mitigate VILI.

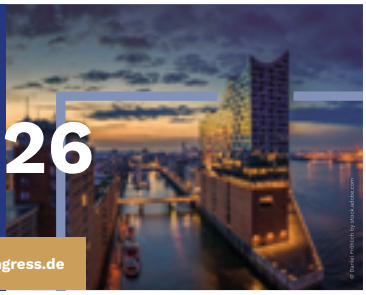

P06 Postergroup: Hypoxia & pulmonary functions

P0603

Pharmacologic inhibitors of cellular oxygen sensors – novel treatment options for neuroblastoma?

Anna Daniela Dorsch; Pauline Fessen; Sascha TroschkeMeurer [1]; Holger N Lode [2]; Carsten C. Scholz
Institute of Physiology, University Medicine Greifswald, Greifswald, Germany; [1] Department of Pediatric Oncology and Hematology, University Medicine Greifswald, Greifswald, Germany; [2] Abteilung Allgemeine Pädiatrie - Nephrologie, Klinik und Poliklinik für Kinder und Jugendmedizin, Universitätsklinikum Greifswald, Greifswald, Germany;

Objective: Neuroblastoma is the most common solid malignant extracranial tumor of childhood, with a 5year eventfree survival rate in the highrisk stage below 50 % under standard therapy. Prolyl4hydroxylase domain (PHD) 13 proteins are cellular oxygen sensors, that hydroxylate the transcription factor HypoxiaInducible Factor (HIF) subunits 1α and 2α, marking them for proteasomal degradation. In hypoxia, PHD13 are no longer active, allowing for HIFα accumulation and HIF target gene transcription. Pharmacologic PHD13 inhibitors (PHIs) are clinically approved for the treatment of renal anemia. Preclinical studies suggest that PHIs can also be potential treatments for some cancers. We previously observed that the PHI FG4592 increases apoptosis in the neuroblastoma cell line Kelly. In this study, various neuroblastoma cell lines were used to assess different PHIs as possible novel treatment option.
Method: Five different neuroblastoma cell lines (SHEP2, CHLA20, CHLA90, LAN1, COGN519) were treated with various PHIs (FG4592, AKB6548, GSK1278863, BAY853934, DMOG), assessing cell survival, confluency and apoptosis every eight hours for up to seven days, using livecell imaging (LCI). Successful PHI treatment was analyzed by efficient HIF1α stabilization and expression of the HIFα targets PHD2 and PHD3.
Results: First results show that GSK1278863 reduces neuroblastoma LAN1 and CHLA20 cell confluency after approximately 5 days of treatment and simultaneously increases caspase activity, indicating that apoptosis caused reduced cell confluency. DMOG slowed down cell growth of several cell lines. Interestingly, other PHIs did not majorly alter cell growth or apoptosis, indicating PHI selective effects. PHImediated HIF1α stabilization and induction of PHD2 and PHD3 were both PHI and cell typespecific.
Conclusion: Although all investigated compounds inhibit the PHDs and stabilize HIFα, only GSK1278863 and DMOG affect neuroblastoma cell growth, albeit apparently through different effects. Overall, this demonstrates a compoundspecific effect that is therefore likely independent of HIF.

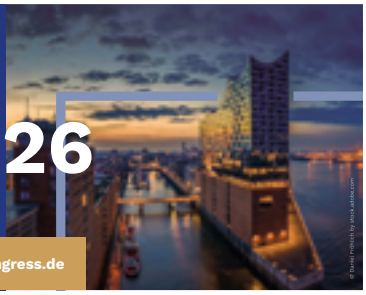

P06 Postergroup: Hypoxia & pulmonary functions

P0604

Multilevel regulation of RUNX2 drives pulmonary vascular remodeling in pulmonary hypertension due to left heart disease (PHLHD)

Poyi Hu; Mariya M. Kucherenko [1]; Qiuhua Li; Wolfgang Kübler
Institute für Physiologie , Charité - Universitätsmedizin Berlin, Berlin, Germany; [1] Deutsches Herzzentrum der Charité, Berlin, Germany;

Objective: Pulmonary hypertension (PH) is a serious complication of left heart disease (LHD), characterized by increased pulmonary vascular pressures and resistance and extensive vascular remodeling. Our previous work identified that upregulation of Runtrelated transcription factor 2 (RUNX2) in pulmonary artery smooth muscle cells (PASMC) contributes to disease progression by promoting cell proliferation, osteogenic transformation, calcification, and pulmonary artery (PA) stiffening. Accordingly, pharmacological inhibition of RUNX2 effectively reversed PH in preclinical models (*Liu et al., 2024*). Yet, the regulatory pathways underlying RUNX2 activation in PHLHD remain incompletely understood. Here, we investigated RUNX2 regulation in PHLHD at the posttranscriptional and posttranslational levels.
Method: Small RNA sequencing identified *miR320* as a potential posttranscriptional regulator of RUNX2 via four predicted binding sites within the RUNX2 3′UTR. RUNX2 acetylation in human pulmonary arteries was analyzed by coimmunoprecipitation and associated with haemodynamic severity. RUNX2 phosphorylation and nuclear translocation were determined by Western blotting and immunofluorescence staining. PASMC proliferation and osteogenic calcification were evaluated using Ki67 immunostaining and Alizarin Red staining *in vitro* and in a rat PHLHD model induced by aortic banding.
Results: *miR320* expression was reduced in PAs of PHLHD patients compared with LHD patients without PH. Inhibition of *miR320* increased RUNX2 expression and the propensity for calcification in healthy PASMC, whereas treatment with a *miR320* mimic reduced RUNX2 protein levels in PHLHD PASMC.
At the posttranslational level, nuclear RUNX2 acetylation was increased in PA samples of PHLHD patients and correlated with elevated pulmonary arterial systolic pressure and transpulmonary pressure gradient. Further, RUNX2 phosphorylation at Ser319 and nuclear localization were promoted by growth differentiation factor 6 (GDF6), which we recently identified as important driver of PHLHD. Accordingly, treatment of healthy PASMC with exogenous GDF6 increased cell proliferation in a RUNX2dependent manner, whereas *in vivo* knockdown of GDF6 in a rat model of PHLHD induced by aortic banding reduced PA wall thickness and calcification.
Conclusion: These findings establish RUNX2 as a central component of a multilevel regulatory network in PHLHD, providing novel mechanistic insights into pulmonary vascular remodeling and identifying potential targets for therapeutic intervention.

P06 Postergroup: Hypoxia & pulmonary functions

P0605

Human coronary and pulmonary arterial endothelial cells respond similarly to chronic hypoxia

Maren Hedden; Lena SchmidtHutten; Valentin Osterhage; Fiona Kleinsang; Alina Haack; Rainer H. Böger; Juliane Hannemann
Institute of Clinical Pharmacology and Toxicology, University Medical Center HamburgEppendorf, Hamburg, Germany;

Objective: The human coronary and pulmonary vasculature respond in opposite ways to hypoxia – nitric oxide (NO)mediated vasodilation occurs in the coronary arteries, whilst vasoconstriction occurs in the pulmonary arteries. We have previously shown that accumulation of asymmetric dimethylarginine (ADMA) is involved in hypoxic pulmonary hypertension. We therefore studied the regulation of the endothelial NOADMA pathway in primary human coronary (HCAEC) and pulmonary arterial endothelial cells (HPAEC) in normoxia (NX; 21 % O_2) and hypoxia (HX; 1 % O_2).
Method: HCAEC and HPAEC were cultured to subconfluence in NX and HX for 24 to 72 hours, respectively. Cells were harvested and lysed, and RNA expression (RTqPCR) of vascular endothelial growth factor A (VEGFA) as well as RNA expression, protein expression (Western Blotting), and enzyme activities (LCMS/MS) of dimethylarginine dimethylaminohydrolase (DDAH)1 and 2, endothelial nitric oxide synthase (NOS3, eNOS), and protein arginine Nmethyltransferases (PRMTs) were measured.
Results: HX significantly upregulated VEGFA mRNA expression to about 2.5fold above NX in both cell lines. DDAH1 mRNA expression showed no major regulation by HX, whilst we noted a slight, but significant upregulation of DDAH2 mRNA at 48 and 72 h of HX in HCAEC and at 72 h of HX in HPAEC (both $p < 0.05$). These changes were mirrored at the protein level. However, DDAH enzyme activity, measured by LCMS/MS as the amount of $d_7$citrulline converted from d_7ADMA, was not significantly changed by up to 72 hours of HX as compared to NX in either of the two endothelial cell types. NOS3 mRNA expression was downregulated by 30 – 40 % in both cell types, while protein expression transiently increased in HCAEC during HX. NOS enzyme activity as measured by the conversion rate of $d_4$arginine to $d_4$citrulline displayed a similar trend but showed no significance. In HPAEC eNOS protein expression and activity remained unchanged.
Conclusion: Despite diametrically opposite responses of endotheliummediated vasodilation to hypoxia in vivo, we observe no major differences in expression nor activity of the genes and enzymes involved in the endothelial NOADMA pathway in endothelial cells of pulmonary and coronary origin, respectively. Despite an increase in gene and protein expression of DDAH2 in both cell lines, no effect on DDAH activity was measured. In contrast, the slight temporary increase of eNOS protein expression in HCAECs was reflected as a trend in NOS activity. However, this slight difference does not explain the contrasting responses of the coronary and pulmonary epithelium. Therefore, we speculate that in vivoresponses are orchestrated by interactions of the endothelium with adjacent cell types.

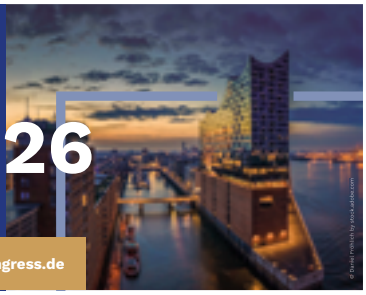

P06 Postergroup: Hypoxia & pulmonary functions

P0606
Identification of the core exocytic machinery for surfactant secretion in type II alveolar epithelial cells

Hongyu Miao; Philipp Kolb; Manfred Frick
Institute of General Physiology, Ulm University, Ulm, Germany;

Objective: Secretion of surfactant in the lung alveoli is essential for maintaining lung function. Surfactant reduces surface tension by forming a dynamic interfacial film at the airliquid interface (ALI) within the alveoli in a surface areadependent manner. This contributes to the stabilization of the alveoli during exhalation and facilitates alveolar distension during lung inflation. Dysregulation of surfactant secretion can cause severe respiratory failure, the most notable example being infant respiratory distress syndrome (IRDS) in premature babies, who have insufficient surfactant secretion in their alveoli. Alveolar type II epithelial (ATII) cells secrete surfactant via exocytosis of lamellar bodies (LBs), which are intracellular structures that store surfactant. Soluble Nethylmaleimidesensitive factor attachment protein receptors (SNAREs) are ultimately responsible for catalyzing LBplasma membrane fusion; however, their functional characterization in ATII cells remains unclear. The aim of this project is to identify the complete inventory of SNARE proteins in ATII cells.
Method: In this project, we examined the expression of SNARE proteins in rat primary ATII cells and human iPSCderived ATII cells at three levels: transcript (RTPCR), protein (Western blot and immunofluorescence), and functional (fusion assay). All cells were maintained in alveolar organoid culture.
Results: Our results indicate high expression of Stx3, Stx4, Syt7, Vamp3, Vamp8, and Snap23 in ATII cells. Immunofluorescence images revealed the colocalization of Syt2, Syt7, and Vamp8 with LBs in ATII cells. There is no significant difference in expression or fusion assay results between primary and organoidderived cells. We are in the process of knocking out these proteins using CRISPRCas9 gene editing to validate their functional relevance and the role of LB exocytosis in fusion assays.
Conclusion: The overall aim is to fully understand the core exocytic machinery that regulates surfactant secretion. Molecules that selectively target these machineries may have further potential in treating respiratory failure.

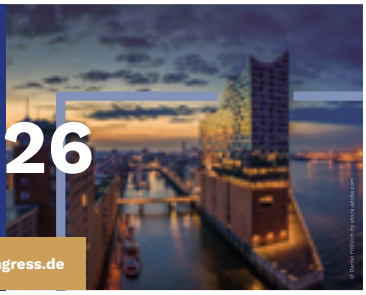

P06 Postergroup: Hypoxia & pulmonary functions

P0607

HIFmTOR crosstalk in retinal pigment epithelium metabolism: Implications for agerelated macular degeneration

Lennart Stiene; Joachim Fandrey; Yoshiyuki Henning
Institut für Physiologie, Universitätsklinikum Essen AöR, Essen, Germany;

Objective: Agerelated macular degeneration (AMD) is the leading cause of blindness among the elderly population in industrialized countries. Previous studies have suggested that metabolic dysregulation in the retinal pigment epithelium (RPE), a monolayer of cells adjacent to the photoreceptors, represents an early hallmark of AMD. Hypoxia at the RPE/photoreceptor interface is another hallmark of AMD, which is also linked to stabilization of hypoxiainducible factors (HIF). HIF orchestrates a cascade of adaptations to ensure the survival of hypoxic cells, including the induction of a glycolytic switch that may contribute to metabolic dysregulation. In addition, hypoxia is linked to the inhibition of the mechanistic target of rapamycin (mTOR). Our preliminary work, together with findings from other groups, suggests the existence of a tight crosstalk between HIF and mTOR signaling that might be central to metabolic homeostasis. Thus, we aimed to comprehensively characterize the crosstalk of the two HIF isoforms HIF1 and HIF2 and the mTOR complexes mTORC1 and mTORC2 under normoxia and hypoxia.
Method: Using the human RPE cell line ARPE19, we are currently investigating the interdependence of HIF1, HIF2, mTORC1, and mTORC2 by targeted siRNAmediated knockdown experiments. Pathway alterations are being analyzed by Western blot and qRTPCR.
Results: Our preliminary results demonstrate that mTORC1 activity predominated under normoxia, while HIF1α, HIF2α and mTORC2 were downregulated. Under hypoxia, mTORC1 was downregulated and mTORC2 as well as HIFs were upregulated.
Conclusion: Based on the expected findings, targeted modulation of this crosstalk offers a highly promising approach to prevent early RPE bioenergetic failure and AMD progression.

P06 Postergroup: Hypoxia & pulmonary functions

P0608

Beyond Hypersecretion: Characterizing the Basal Mucin Exocytic Pathway in Human Epithelial Cells

Annika Armbruster; Veronika Neubauer; Selina Kindig; Giorgio Fois; Manfred Frick
Institute of General Physiology, University of Ulm, Ulm, Germany;

Objective: Airway mucus is essential for pulmonary host defense, trapping inhaled threats for removal by mucociliary clearance. Mucin glycoproteins are released from secretory epithelial cells through SNAREmediated exocytosis at a low baseline rate and a high stimulated rate. The baseline rate supports steadystate mucociliary clearance while stimulated mucin secretion occurs in response to airway inflammation, with mucin hyperproduction causing pathologic airflow obstruction and infection. While the pathways for pathological hypersecretion in conditions such as asthma, COPD, and cystic fibrosis are well characterized, the machinery driving baseline mucin secretion remains poorly defined. This study aims to characterize the specific SNARE proteins that mediate basal mucus release to provide insight into the fundamental mechanisms of airway homeostasis.
Method: We differentiated immortalized primary human airway epithelial cells in airliquid interface (ALI) cultures. We determined the most abundantly expressed SNAREassociated genes in secretory and goblet cells in a qPCR analysis, focusing on syntaxins (STX), synaptotagmins (SYT), vesicleassociated membrane proteins (VAMP) and synaptosomeassociated proteins (SNAP). Based on these findings, we performed CRISPR/Cas9 gene knockouts for STX3 and SYT7 to evaluate their roles in baseline mucus secretion.
Results: We found that STX3 and SYT7 are the most abundantly expressed SNARE proteins. We established a CRISPR/Cas9based gene knockout for these targets in immortalized small airway bronchial cells.
Conclusion: Using these knockout models, we will be able to determine the effect of lacking the respective SNARE protein on mucus secretion. Defining the distinct core exocytic machineries of baseline and stimulated secretion opens new avenues for therapy.

P06 Postergroup: Hypoxia & pulmonary functions

P0609

Spheroids reveal hypoxiadriven spatial restriction of adenoviral infection

Tamara Büttner; Xiaoyan Wang; Brenda Krishnacoumar; Athanasios Papadamakis; Suna Cicek; Yves Schild; Sandra Winning; Elisabeth LittwitzSalomon; Anja Ehrhardt [1]; Ulf Dittmer [2]; Wibke Bayer; Joachim Fandrey; Anna Malyshkina
Abteilung Physiologie, Universitätsklinikum Essen, Essen, Germany; [1] Fakultät für Gesundheit (Department für Humanmedizin), Universität Witten/Herdecke, Witten, Germany; [2] Institut für Virologie, Universitätsklinikum Essen, Universität DuisburgEssen, Essen, Germany;

Objective: Hypoxia is a hallmark of solid tumors and represents a major barrier for effective cancer therapies, including oncolytic virotherapy. While adenoviruses are widely studied as oncolytic agents, the impact of hypoxic tumor microenvironments on viral infection and spatial spread remains incompletely understood. In this study, we investigated how oxygen availability influences adenovirus infection in twodimensional (2D) cultures and threedimensional (3D) tumor spheroids.
Results: We first confirmed hypoxia responsiveness in commonly used adenovirus research cell lines (HEK293A and A549) as well as in KP4 pancreatic cancer cells, demonstrating hypoxiainduced HIF1α stabilization. Hypoxia markedly reduced adenoviral protein production in 2D cultures across all cell lines. To model oxygen gradients found in solid tumors, we established stable KP4 spheroids using a hangingdrop approach supplemented with methylcellulose. Spatial analysis of HAdV5_GFPinfected spheroids revealed that productive infection was largely restricted to the welloxygenated outer rim when infection occurred during spheroid formation and hypoxia development. In contrast, infection performed under normoxic conditions prior to spheroid formation resulted in a more uniform distribution of infected cells throughout the spheroid.
Conclusion: Together, these findings demonstrate that hypoxia not only suppresses adenoviral replication but also shapes the spatial pattern of infection in 3D tumor models, highlighting the importance of incorporating hypoxiarelevant 3D systems in preclinical evaluation of oncolytic adenoviruses.

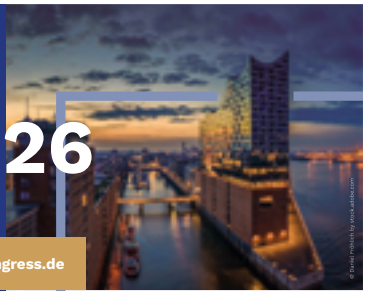

P06 Postergroup: Hypoxia & pulmonary functions

P0610

From Injury to Fibrosis: Investigating EndothelialMacrophage Crosstalk in IPF

Susanne Wespel; Annika Armbruster; Irina Shalashova [1]; Philipp Kolb; Johanna Diehm; Sarah Groetzner [1]; Muriel Lizé [1]; Manfred Frick
Institute of General Physiology, University of Ulm, Ulm, Germany; [1] Immunology and Respiratory Disease Research, Boehringer Ingelheim Pharma GmbH and Co. KG, Biberach an der Riß, Germany;

Objective: Idiopathic pulmonary fibrosis (IPF) is a progressive and fatal lung disease with limited therapeutic options. Monocytederived macrophages are increasingly recognized as key regulators of inflammation, tissue repair, and fibrosis. Signals originating from the diseased alveolar niche are thought to impair homeostatic macrophage differentiation and promote profibrotic phenotypes. This study investigates how endothelial injury influences macrophage polarization in IPFrelevant conditions.
Method: Human pulmonary microvascular endothelial cells (HPMECs) were exposed to thrombin, an IPFassociated cytokine cocktail, or a recently established trauma cocktail to induce endothelial damage *in vitro*. Barrier integrity, monocyte adhesion, and inflammatory gene and protein expression were assessed to validate endothelial dysfunction. Conditioned media from damaged HPMECs were transferred to primary human macrophages. Macrophage polarization was analyzed using a customdesigned CyTOF panel and gene expression profiling. In addition, phagocytic and efferocytotic capacities were investigated.
Results: All stress conditions induced substantial endothelial dysfunction, characterized by impaired barrier integrity, enhanced monocyte adhesion, and increased expression of proinflammatory markers. The custom CyTOF panel enabled discrimination of conditioned mediatreated macrophages into M0, M1, M2a, and M2clike phenotypes.
Conclusion: These findings demonstrate that endothelial injuryassociated secretomes modulate macrophage fate and provide a suitable model to investigate endothelialimmune crosstalk in IPF. Supernatants inducing pronounced proinflammatory and/or profibrotic macrophage phenotypes will be further characterized by mass spectrometry to identify signaling mediators involved in macrophage polarization. This work contributes to understanding dysregulated cellcell communication in IPF and may help identify novel therapeutic targets.

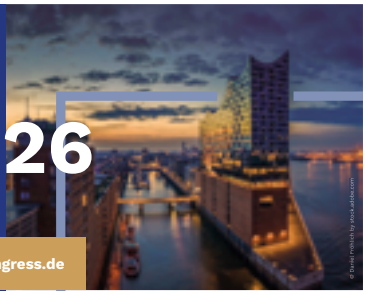

P07 Postergroup: Neuoscience & Behavior

P0701

Networkwide functional changes as underlying mechanism of deepbrain stimulation in dystonia

Denise Franz; Marco Heerdegen; Fabiana Santana Kragelund; Konstantinos Spiliotis [1]; Angelika Richter [2]; Franziska Richter [3]; Rüdiger Köhling
OscarLangendorffInstitute of Physiology, Rostock University Medical Center, Rostock, Germany; [1] Civil Engineering, Applied Mathematics and Complex Systems, Democritos University of Thrace, Komotini, Greece; [2] Veterinary Medicine, Institute of Pharmacology and Toxicology, University of Leipzig, Leipzig, Germany; [3] Institute of Pharmacology, Toxicology and Pharmacy, Tierärztliche Hochschule Hannover, Hannover, Germany;

Objective: Deep brain stimulation (DBS) of the internal globus pallidus/entopeduncular nucleus improves dystonia, but its mechanisms and stimulation parameters remain insufficiently understood. This study examined whether continuous pallidal DBS induces timedependent and networkwide changes in synaptic and intrinsic excitability across the motor system in the *dtsz* hamster model of spontaneous generalized dystonia.
Method: Dystonic hamsters received continuous pallidal DBS (130 Hz, 60 µs, 50 µA) for either shortterm (3 h) or longterm (11 d). Behavioural efficacy was assessed *in vivo*. Ex vivo electrophysiology was then performed in acute slices within minutes after stimulation, including patchclamp recordings in striatum, motor thalamus and motor cortex, and highdensity microelectrode array recordings in cerebellar cortex. In parallel, a largescale computational network model of basal gangliathalamocortical circuits was used to analyse frequencydependent DBS effects and optimise stimulation parameters.
Results: DBS was most effective at 130 Hz and produced distinct, durationdependent network adaptations. In striatal medium spiny neurons, shortterm DBS reduced miniature EPSC frequency while increasing intrinsic firing, whereas longterm DBS attenuated synaptic depression and decreased intrinsic excitability. In motor thalamus, longterm DBS increased baseline postsynaptic current frequency, shortened interevent intervals and enhanced inhibitory current amplitude, without direct 130 Hz entrainment. In motor cortex, excitatory input became more temporally clustered and disinhibition could evoke prolonged burst activity. In cerebellar cortex, dystoniarelated reductions in firing rate, spike amplitude and network centrality were shifted towards healthy control patterns after DBS. Computational modelling supported the experimental data by showing that higher stimulation frequencies restore thalamic output towards a more physiological tonic mode.
Conclusion: Pallidal DBS induces distributed plastic reorganisation across basal gangliathalamocortical and cerebellothalamocortical loops rather than a purely local effect. Therapeutic benefit depends on both stimulation duration and temporal repatterning of network activity. These findings provide a mechanistic basis for optimising DBS protocols in dystonia.

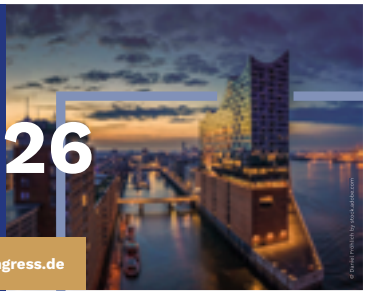

P07 Postergroup: Neuoscience & Behavior

P0702

SCN2A variantdriven, brain statedependent in vivo mesoscale activity patterns in the developing mouse cortex

Sonja Nevelchuk; Yury Kovalchuk; Olga Garaschuk
Department of Neurophysiology, Institute of Physiology, University of Tübingen, Tübingen, Germany;

Objective: Ongoing neuronal activity during early postnatal development is essential for proper circuit formation. The SCN2A^{A263V} gainoffunction variant, associated with earlyonset epileptic encephalopathy, enhances neuronal excitability during a critical developmental window when Nav1.2 is the dominant sodium channel at the axon initial segment. How this hyperexcitability reshapes largescale patterns of intrinsic cortical activity remains unclear.
Method: Combining widefield Ca^{2+} imaging, simultaneous EMG recording in headfixed neonatal (postnatal day 6) mice, we characterized intrinsic cortical activity patterns across active (REM) and quiet (NREM) sleep, awake, and motion states in SCN2A^{A263V} mutants and wildtype mice (here and below n= 11/13 WT and mutant mice).
Results: We found that mutant mice preserve overall vigilance state architecture, but their cortical Ca^{2+} signals are more frequent, have smaller amplitudes and distributions of event origins across cortical regions that are similar to wild type (WT). Unlike WT cortical activity, which shows clear statedependent modulation of event features (e.g., size,), mutant activity appears less differentiated across vigilance states, suggesting a partial erosion of the brain statespecific activity patterns.
Furthermore, we examined the spatial and directional organization of cortical activity at the network level. Dimensionality analysis of event spatial footprints suggested that WT Ca^{2+} signaling is more spatially stereotyped, while mutant events appear to have a more diffuse repertoire of spatial configurations. To test this directly, we quantified withinanimal eventtoevent similarity and found that it was significantly reduced in mutants by two metrics – dwellweighted cosine similarity ($p=0.02$) and binary footprint overlap ($p=0.01$), confirming that the mutant cortex generates less reproducible spatial patterns from event to event.
Analysis of wave propagation revealed that Ca^{2+} waves in mutant mice traveled shorter net distances ($p=2x10^3$) with conserved total path length ($p=0.02$), indicating less directionally committed propagation.
Conclusion: Together, these findings reveal a coherent phenotype: the hyperexcitable mutant cortex fires more readily, but the activity it generates is weaker, shorterlived, and less directionally structured, producing waves that fail to propagate across the cortex as effectively as in WT. Crucially, these events appear to be less reproducible, potentially degrading the consistent, patterned activity signals that the developing brain relies on to guide circuit formation.

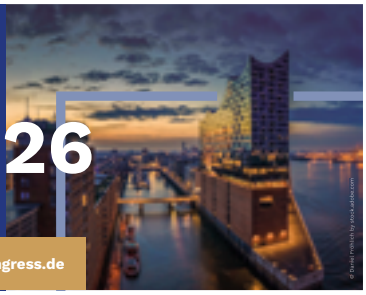

P07 Postergroup: Neuoscience & Behavior

P0703

Thermoneutral Housing Reshapes Sex Differences in Mouse Thermal Preference

Jiaming Kang; Jan Roedel; Katharina Zimmermann
Klinik für Anästhesiologie, Friedrich Alexander Universität Erlangen Nürmberg, Erlangen, Germany;

Objective: Sex differences in temperature preference are well documented in inbred mice, with females preferring warmer environments. Since standard 22°C housing increases metabolic rate relative to 30°C, we tested whether these differences are intrinsic or result from adaptation to 22°C housing.
Method: Fortyfour C57BL/6J mice, 21 males and 23 females, were tested before and after 4 weeks of thermoneutral housing (TNH) at 30 ± 1°C. Thermal preference was assessed in a circular gradient ring across three floortemperature ranges: 5–30°C, 15–40°C, and 20–45°C. Behavior was quantified as cumulative percent time and cumulative distance across 12 temperature zones.
Results: Under standard housing, mice showed temperaturedependent sex differences, with females displaying greater warmseeking than males in the 15–40°C and 20–45°C gradients, but not the 5–30°C gradient. TNH increased sex separation in the 5–30°C gradient while reducing it in warmer gradients. Cumulative time curve shifted between sexes from 0.099 to 0.617, 1.033 to 0.637, and 1.274 to 0.620 across gradients; corresponding to percent changes of −23.43% (p=0.1107), +8.84% (p=0.3756), and +10.05% (p=0.0004), respectively, with comparable effects for cumulative distance. These changes were driven mainly by increased cold avoidance and reduced warmseeking in females.
Conclusion: In conclusion, longterm thermoneutral housing altered the magnitude and spatial pattern of sex differences in thermal preference primarily through adaptation of females. Housing temperature is an important contextual factor shaping sex differences in thermoregulatory behavior, with implications for behavioral and metabolic studies. Experiments were approved by the Government of Lower Franconia under permit 55.2.2253221014.

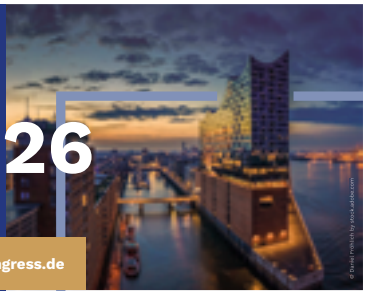

P07 Postergroup: Neuoscience & Behavior

P0704

Strength of ECGbased cardiorespiratory coupling as autonomous system surrogate of tonic experimental pain

Jose Eduardo Perez Najar; Felix Maximilian Kuon; ChiaraSophie Krüger [1]; Thomas Schiemann; Jürgen Lorenz
Faculty of Life Sciences, Hamburg Applied Science University, Hamburg, Germany; [1] Osteopathic Research Institute, Hamburg, Germany;

Objective: Currently, there is only a limited amount of methods for objective assessment of the autonomous component of pain perception. Heart rate variability (HRV) is a central tool for noninvasive assessment of the autonomic system behavior and its combination with respiratory signals offers a more precise evaluation of specific autonomic regulatory pathways. Cardiorespiratory coupling (CRC) reflects coordinated autonomic control through phenomena such as vagallymediated respiratory sinus arrhythmia (RSA). The aim of the present study was to test the sensitivity of a novel CRC surrogate derived from 12lead ECG recordings in 22 healthy subjects exposed to cold pressor pain and no pain control conditions.
Method: We used a wavelet transformbased framework for CRC assessment using 12lead ECG recordings, from which RR intervals and ECGderived respiration (EDR) signals are extracted. Wavelet coherence and crossspectral power are combined into a timevarying CRC metric, enabling analysis of autonomic dynamics with specificity in both time and frequency. This framework is applied to recordings from 22 healthy subjects exposed to four repeated alternations between a painful Cold Pressor Test and nonpainful warm water control condition while on a fixed acoustically paced breathing rhythm at 12 breath/min. A linear mixed model analysis is used to assess the effects of condition and repeated exposure on CRC metrics.
Results: Cold water exposure reduced CRC coupling energy 31% relative to warm water in early exposure periods, with a progressive reversal in later periods up to 82% recovery, resulting in a significant condition by period interaction. The same type of results were found for phaseconsistent coupling measured by a wavelet coherence value across periods.
Conclusion: This pattern suggests an initial disruption of vagallymediated CRC under repeated painrelated sympathetic activation. It also demonstrates significant habituation over repeated exposures. We conclude that this waveletbased CRC metrics can be used to detect timevarying autonomic dynamics in response to pain.

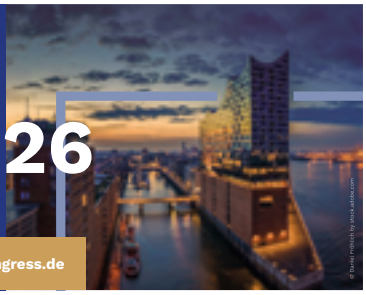

P07 Postergroup: Neuoscience & Behavior

P0705

Singlecell spatial transcriptomic profiling of nonneuronal changes to acute ischemic stroke in aged female mice

Line Mathilde Brostrup Hansen; Christian Stæhr; Dmitry D. Postnov [1]; David Boas [2]; Lasse Sommer Kristensen; Jørgen Kjems [3]; Vladimir V. Matchkov
Department of Biomedicine, Aarhus University, Aarhus, Denmark; [1] Center of Functionally Integrative Neuroscience, Aarhus University, Aarhus, Denmark; [2] Department of Biomedical Engineering, Neurophotonics Center, Boston University, Boston, United States; [3] Interdisciplinary Nanoscience Center, Aarhus University, Aarhus, Denmark;

Objective: Acute ischemic stroke (AIS) represents a global health burden, with approximately 7.63 million new incidences annually. Despite advances in recanalization therapies, complications such as noreflow and futile reperfusion frequently limit functional recovery. The mechanisms underlying these phenomena remain poorly understood. Notably, biological sex significantly influences AIS outcomes, with females experiencing a higher proportion of strokerelated mortality and poorer functional recovery. Despite this, preclinical stroke research predominantly relies on male subjects, leaving a critical knowledge gap regarding femalespecific responses to ischemic injury.
Method: We investigated acute changes in gene expression following AIS in aged female mice. A transient middle cerebral artery occlusion was induced in six 24–26 weekold female C57BL/6J mice utilizing one hour of awake photothrombotic occlusion, followed by 24 hours of reperfusion. Coronal brain sections were analyzed using CosMx spatial molecular imaging (NanoString Technologies), with singlecell identity prediction performed by reference to Allen Brain Atlas.
Results: Spatial transcriptomics profiling revealed a rich cellular landscape across the coronal brain slices, identifying a total of 283,258 nonneuronal cells, including 52,604 vascularassociated cells spanning endothelial and smooth muscle cells, arteriolar and capillary pericytes, and vascular leptomeningeal cells, as well as 193,591 glial cells, of which 67,112 were astrocytes.
Using this highresolution dataset, spatial mapping of celltypespecific transcriptional changes within the ischemic core and periinfarct penumbra was performed. Cells were compared with paired contralateral regions, serving as internal controls to detect gene expression signatures and pathway activations important for dynamic vascular and glial responses to ischemic injury, which may be particularly important for functional recovery following AIS reperfusion in female stroke biology.
Conclusion: Ischemiareperfusion in aged female mice triggers expression profile changes in nonneuronal cell types that may be associated with stroke outcome severity.

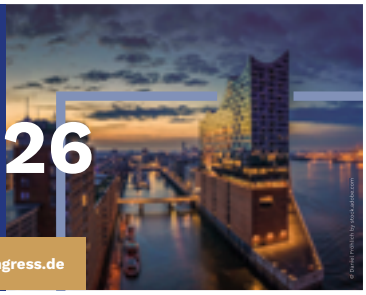

P07 Postergroup: Neuoscience & Behavior

P0706

What lizards teach us about the hippocampus? An evolutionary comparative approach

Niels
Röhrdanz; Kira Kaiser; Peer Wulff
Systems Neuroscience, Physiologisches Institut, Christian Albrechts Universität zu Kiel, Kiel, Germany;

Objective: For centuries, the hippocampus has been a primary focus of neuroscience research. Despite the vast number of studies and the dramatic scientific advances, many questions remain unanswered. Whereas the hippocampus has been primarily studied in mammals, there is a broad consensus that homologues exist in all amniotes. Adopting an evolutionary comparative approach may shift our perspective and, by analysing similarities and differences, may help to identify core features of hippocampal processing.
Method: In pursuit of a comparative approach, we conducted a series of experiments on the lizard Anolis carolinensis to examine its hippocampal homologue at the structural, functional, and behavioural levels.
Results: In Experiment 1, we analysed the expression of marker genes of the hippocampus and its subregions. We found spatially restricted marker gene expression, delineating a hippocampal homologue with DGlike and CAlike subregions in medial, dorsomedial, and dorsal cortices.
In Experiment 2, we implemented IEG imaging as a readout of hippocampal activity. We find increased activity in the medial, dorsomedial, and dorsal cortices five minutes after exposure to a novel context, as would be expected in a hippocampal homologue.
In experiment 3, we investigated whether *Anolis carolinensis* can form hippocampusdependent memory using a contextual fear conditioning paradigm. Conditioned animals showed significantly increased head movement during reexposure after one day.
Conclusion: These results support the hypothesis of general homology between the reptilian cortex and the mammalian hippocampus in structure and function, down to the level of subregions. We will now inquire how this general homology is realized in the lizard at the level of subregional connectivity, principal cell properties and synaptic function.

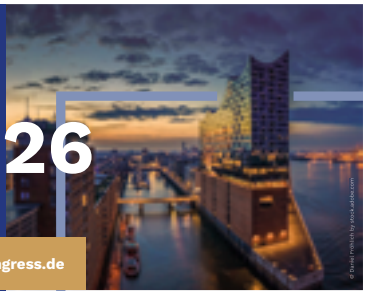

P07 Postergroup: Neuoscience & Behavior

P0707

β-Oxidation couples metabolic state to neuronal autophagy

Veronika Fritz; Natalia Kononenko
Physiologie, University Hospital, Köln, Germany;

Objective: Neurons operate under exceptionally high energetic demand to sustain synaptic transmission and ion homeostasis. While glucose metabolism has long been considered their dominant energy source, accumulating evidence suggests that neurons retain a previously underappreciated capacity to engage fattyacid βoxidation (FAO). In parallel, autophagy preserves neuronal homeostasis by clearing damaged organelles and protein aggregates. Notably, autophagy deficiency leads to striking regionspecific outcomes: ATG5 loss causes degeneration of cerebellar Purkinje cells, whereas cortical neurons display relative resilience. The metabolic basis of this differential vulnerability remains unclear.
Results: Here, we tested whether CPT1Adependent FAO supports cortical neuronal function under autophagy deficiency. In wildtype (WT) neurons maintained under glucoserich conditions, pharmacological inhibition of CPT1 with etomoxir had minimal effects on Ca^{2+} dynamics and intracellular ATP levels, indicating that FAO is largely dispensable when glycolytic substrates are available. In contrast, ATG5deficient cortical neurons exhibited pronounced sensitivity to FAO inhibition. Blocking CPT1 significantly altered Ca^{2+} signaling and caused a marked reduction in ATP levels, revealing a previously unrecognized metabolic dependency.Consistent with this adaptive rewiring, CPT1A expression is dynamically regulated across development and brain regions, and in vivo disruption of βoxidation leads to agedependent cortical neuronal loss.
Conclusion: Together, our findings identify autophagy and βoxidation as tightly interconnected pathways that coregulate neuronal energy homeostasis, excitability, and survival. We propose that autophagy deficiency induces a substrate shift toward fatty acid utilization, and that this metabolic flexibility represents a key determinant of cortical neuronal resilience. Dysregulation of CPT1Adependent FAO may therefore contribute to selective vulnerability in neurodegenerative disorders.

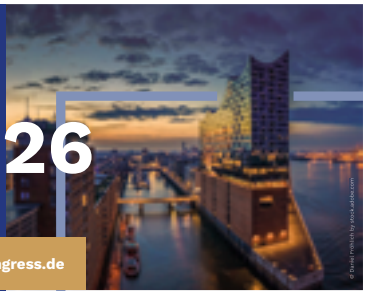

P07 Postergroup: Neuoscience & Behavior

P0709

CAPGDF15, a ProGDF15Derived Peptide, Suppresses Appetite and Promotes Metabolically Favorable Weight Loss

Casper M. Sigvardsen; Cecilie B. Lindqvist; Christian T. Voldstedlund; Joan M. M. Pasano; Josephine Maria Kanta [1]; Nicoline R. Andersen [2]; Camilla C. Hansen; Amanda Wiggenhorn [3]; Sebastian B. Jørgensen [4]; Jonathan Z. Long [3]; Erik A. Richter Department of Nutrition, Exercise and Sports, University of Copenhagen, Copenhagen, Denmark; [1] Biomedical Sciences, University of Copenhagen, Copenhagen, Denmark; [2] Health and Medical Sciences, University of Copenhagen, Copenhagen, Denmark; [3] Pathology, School of Medicine, Stanford University, Stanford, United States; [4] External Exploration and Innovation Unit, Novo Nordisk, Måløv, Denmark;

Objective: A novel endogenous secreted peptide derived from the GDF15 preprotein, CAPGDF15, was discovered in 2023, yet its physiological role remains largely uncharacterized. Here, we aimed to determine the effects of CAPGDF15 on appetite regulation and metabolic homeostasis.
Method: Dietinduced obese (DIO) C57BL/6Ntac mice were treated daily with CAPGDF15 for 21 days to assess food intake and body composition. Metabolic adaptations were assessed using indirect calorimetry with realtime pairfeeding controls, while mitochondrial respiration was investigated using high resolution respirometry of liver, skeletal muscle and adipose tissue. Neural engagement was evaluated in acutely treated lean C57BL/6NTac mice using cFos immunostaining combined with 3D brain modeling (GA. i.p. 75 mg/kg Pentobarbital and 4.75 mg/kg Lidocaine).
Results: CAPGDF15 acted as a potent anorexigenic agent, reducing food intake and body weight by 38.3% and 21.7%, respectively (twoway repeated measure ANOVA, Tukey's posthoc test; $p<0.0001$ and $p<0.05$, VEH n=4, CAP n=7). Acute treatment activated canonical appetiteregulating brain regions within the dorsal vagal complex, pons, and hypothalamus (n=8 in both groups). Prolonged treatment induced metabolically favorable weight loss, with a greater reduction in fat mass (69.2%) and liver fat content (61.3%) compared with caloric restriction alone (Oneway ANOVA; Tukey's posthoc test; n=5 in both groups, both $p<0.05$). Despite reduced nocturnal activity, CAPGDF15treated mice exhibited increased energy expenditure and maintained core body temperature, whereas pairfed controls showed a ~1°C temperature reduction following caloric restriction. CAPGDF15 treatment also increased wholebody lipid oxidation with approximately 10% greater reliance on lipidderived energy during the light phase (Twoway repeated measure ANOVA, $p<0.0001$, n=10). Whereas Western blot analyses (n=5) showed no alteration in expression or phosphorylation status of lipolytic enzymes, preliminary respirometry data (n=3) suggest elevated mitochondrial proton leak in liver and eWAT, alongside elevated fatty acidsupported respiration in eWAT.
Conclusion: CAPGDF15 is an endogenous peptide that, when administered exogenously, suppresses appetite and promotes a metabolically active state conducive to fat loss, through both central appetiteregulating pathways and peripheral mechanisms potentially including mitochondrial uncoupling in liver and adipose tissue.

P07 Postergroup: Neuoscience & Behavior

P0710
Topdown control of olfactory processing during flexible behavior in mice

Athanasios Manolis; Samuele Negri; Kathrin Sauter; Sebastian H. Bitzenhofer Neural Circuit Physiology Group, Center for Molecular Neurobiology Hamburg, University Medical Center HamburgEppendorf, Hamburg, Germany;

Objective: Behavioral flexibility requires the brain to adapt sensory processing according to context and experience. While feedback projections from higher association areas are known to influence early sensory activity, how they shape information flow across distributed brain networks remains poorly understood. We investigate how feedback from the lateral entorhinal cortex (LEC) and hippocampus (HP) modulates processing in primary olfactory areas, namely the olfactory bulb (OB) and piriform cortex (PIR), to support flexible behavior.
Method: The mouse olfactory system provides a unique model to study topdown modulation because the OB receives extensive feedback from cortical and limbic structures without an intervening thalamic relay. We combine anatomical tracing, highdensity electrophysiological recordings, and optogenetic manipulations to characterize feedback pathways and their functional impact. Electrophysiological recordings of singleunit activity and local field potentials are performed simultaneously in OB, PIR, LEC, and HP in awake, headfixed mice during odordependent behavioral tasks. Viral tracing approaches are used to map connectivity and identify projection neuron populations.
Adult mice underwent stereotactic viral injections and headbar implantation under isoflurane anesthesia (1–3% in oxygen, inhalation). For histological analyses, mice were deeply anesthetized and transcardially perfused with 4% paraformaldehyde.
Results: Preliminary anatomical analyses confirm extensive feedback connectivity between higher association areas and primary olfactory regions. Retrograde tracing reveals distinct populations of neurons in PIR and LEC projecting to the OB, providing a structural framework for subsequent functional investigations. Electrophysiological experiments assess how neuronal population dynamics and interarea coordination are modulated by odors and how optogenetic perturbation of feedback pathways alters these responses.
Conclusion: Our findings establish the anatomical substrate underlying topdown modulation in the olfactory system and provide a foundation for investigating how feedback circuits dynamically regulate sensory processing. This work aims to uncover general principles by which higher association areas shape information flow and support flexible behavior.

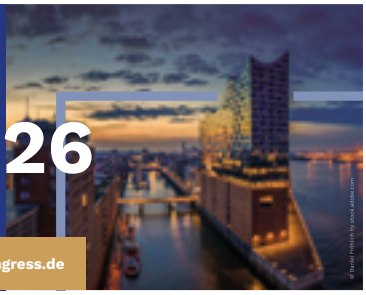

P07 Postergroup: Neuoscience & Behavior

P0711

Beneficial effects of voluntary running on cognition and hippocampal plasticity in APP/PS1 mice

Thomas Endres; Jennifer Zucker; Monique Klausch 1; Georgia Ioanna Kartalou; Elke Edelmann 2; Kurt Gottmann 3; Volkmar Leßmann 2
Institute of Physiology, Otto-von-Guericke University Magdeburg, Magdeburg, Germany; 1 AG Neuroanatomie, Institut für Anatomie und Zellbiologie, Universitätsmedizin Greifswald, Greifswald, Germany; 2 Institut für Physiologie, Medizinische Fakultät, Otto-von-Guericke-Universität, Magdeburg, Germany; 3 Institute of Neuro- and Sensory Physiology, Heinrich Heine University Düsseldorf, Düsseldorf, Germany;

Objective: The development of effective therapeutic strategies for Alzheimer's disease (AD) remains a major challenge in neuroscience. This study aimed to evaluate whether two non-invasive interventions, voluntary running and environmental enrichment, can attenuate cognitive decline and ADlike pathology in the APP/PS1 mouse model of AD.

Method: APP/PS1 mice were assigned to voluntary running, environmental enrichment, or standard housing conditions. Interventions began at four months of age, shortly before the onset of pronounced cognitive deficits, and continued for two months. Spatial memory was assessed using the Morris water maze, and fear learning was evaluated by contextual fear conditioning. In addition, BDNF and amyloidbeta (Aβ) protein levels were quantified in the hippocampus and frontal cortex by ELISA. Hippocampal longterm potentiation and spine density were also examined to assess synaptic plasticity.

Results: Voluntary running was particularly effective in reducing cognitive deficits and enhancing synaptic plasticity in APP/PS1 mice. It also restored spine density in the CA1 region of the hippocampus and reduced Aβ protein accumulation. These effects were more pronounced than those observed under environmental enrichment or standard housing conditions.

Conclusion: Our findings suggest that voluntary running can ameliorate cognitive impairments, improve synaptic plasticity, restore hippocampal spine density, and reduce Aβ accumulation in APP/PS1 mice. Voluntary running may therefore represent a promising non-invasive approach for attenuating AD pathologylike symptoms.

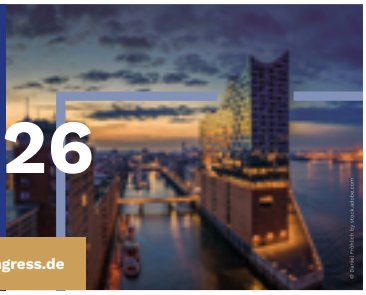

P07 Postergroup: Neuoscience & Behavior

P0712

Dopamine Projections to Dorsal Striatum Subregions during Fear and Reward Learning

Daphne Zafiri; Sevil Duvarci
Life Sciences, Institute of Neurophysiology, Uniklinik Frankfurt, Goethe University Frankfurt, Frankfurt a. M., Germany;

Objective: Dopamine (DA) projections to the dorsal striatum have long been associated with motor control, action selection and reinforcement learning. However, whether they contribute to fear and safety learning, as well as reward processing, remains less well understood. The dorsal striatum is composed of anatomically and functionally distinct subregions, each receiving dopaminergic input from different subpopulations of DA neurons.
Method: In this study, we used fiber photometry to record activity from DA terminals throughout the dorsal striatum in mice during associative fear and extinction learning, as well as operant reward conditioning.
Results: We found that DA projections to distinct dorsal striatal subregions exhibit heterogeneous activity patterns during aversive and appetitive learning paradigms.
Conclusion: Together, these findings provide insights into the subregionspecific organization of dopaminergic projections to the dorsal striatum and their potential roles in encoding emotionally and motivationally relevant learning processes.

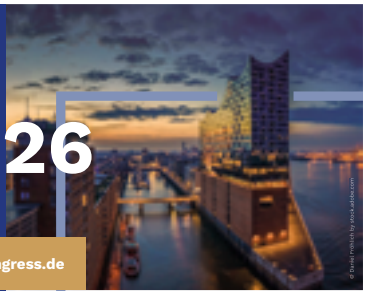

P07 Postergroup: Neuoscience & Behavior

P0713

Temporal Organization of Olfactory Bulb Activity Shapes Information Propagation Across the Mouse Olfactory Network

Samuele Negri; Athanasios Manolis; Kathrin Sauter; Sebastian H. Bitzenhofer Neural Circuit Physiology Group, Center for Molecular Neurobiology Hamburg, University Medical Center HamburgEppendorf, Hamburg, Germany;

Objective: The mechanisms governing the propagation of sensory information across distributed brain networks remain incompletely understood. A fundamental question is how activity generated in primary sensory regions is transmitted to downstream targets and which neuronal features determine effective communication between interconnected brain areas. Olfactory system provides a powerful model to address this question because it contains a relatively short and welldefined pathway linking sensory and associative regions, while odor information is sampled within discrete temporal windows determined by respiration. We hypothesized that the temporal structure of neuronal activity, and particularly the degree of synchrony among neurons, is a key determinant of information propagation across the olfactory network.

Method: Experiments were performed in mice in accordance with current European and national regulations governing animal research.

To characterize direct connectivity originating from the olfactory bulb, we employed the recently developed anterograde transsynaptic tracer ATLAS.

Neural activity was simultaneously recorded from the olfactory bulb, piriform cortex, lateral entorhinal cortex, and hippocampus of headfixed mice through acute extracellular recordings using silicon probes. To investigate the role of temporal activity patterns in information propagation, olfactory bulb output neurons were optogenetically stimulated with different light intensities and durations.

Results: ATLAS tracing confirmed direct olfactory bulb connectivity with multiple downstream olfactory regions, including the piriform cortex and lateral entorhinal cortex, consistent with established anatomical pathways. Optogenetic activation of olfactory bulb output neurons elicited robust responses in downstream regions, demonstrating effective propagation of activity across the olfactory network. Importantly, propagation efficacy depended strongly on the temporal structure of stimulation. Although increased light intensity enhanced local activation within the olfactory bulb, brief and temporally precise stimulation protocols produced more reliable downstream responses than prolonged stimulation paradigms. These findings suggest that propagation of sensory information in the olfactory system is not simply driven by how strongly neurons are activated, but rather by the synchrony of neural activity. In particular, brief and welltimed activation appears to be more effective than prolonged stimulation.

Conclusion: Together, these results suggest that synchrony and temporal precision are fundamental determinants of information propagation across sensory networks. By combining anatomical tracing, largescale electrophysiological recordings, and optogenetic perturbations, this work provides new insight into the circuit mechanisms underlying communication between sensory and associative brain regions and establishes a framework for investigating how learning may reshape information flow across the olfactory system.

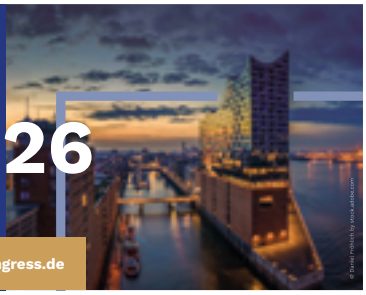

P08 Postergroup: In vivo nevrophysiology & connectivity

P0801
Object Coding in the Dentate Gyrus during Novel Object Recognition

Vladimir Zavialov; Josef Bischofberger
Department of Biomedicine, University of Basel, Basel, Switzerland;

Objective: The hippocampus is crucial for learning, memory, and spatial navigation. Activity of hippocampal principal neurons is also modulated by nonspatial features of the environment, including object location and identity. In the dentate gyrus (DG), mossy and granule cells exhibit objectassociated changes in their spatial firing maps. However, these responses are heterogeneous and remain poorly characterized. We examined how object introduction and exchange in a novel object recognition test (NORT) affected the activity of excitatory neurons in the DG. Recent studies also hint at the involvement of dendritetargeting somatostatinexpressing interneurons (SOMINs) in noveltyassociated responses. That is why we tested how the suppression of SOMINactivity modulated objectassociated responses and object preference.
Method: Using in vivo calcium imaging, we monitored neuronal activity in mice exploring a Ymaze, where objects were spatially separated in two maze arms. Opto- and chemogenetics were used for the suppression of SOMINactivity. All experiments were conducted according to federal and cantonal regulations. Carprofen (0.06 mg/ml in drinking water) was administered to the mice 1 day before and 3 days after the surgeries. Additionally, buprenorphine (GRIN lens implantation, 0.1 mg/kg) or carprofen (virus injection, 5 mg/kg) were injected subcutaneously. During the surgeries, isoflurane (12% in oxygen) was supplied via a gas mask.
Results: Object introduction let to a decrease in the firing map similarity in corresponding arms compared to the entry arm that remained empty (0.11±0.01 and 0.11±0.01 vs 0.22±0.02, $p<0.0001$, Friedman test with Dunn's multiple comparisons test, n=446 cells). This effect was preserved during the optogetic silencing of SOMINs (0.15±0.01 and 0.13±0.01 vs 0.24±0.01, $p=0.001$, Friedman test with Dunn's multiple comparisons test, n=467 cells). In the NORT, the cells showed higher firing map similarity in the arm where the same object was present compared to the arm where the object was exchanged (0.29±0.02 vs 0.20±0.02, $p<0.0001$, Friedman test with Dunn's multiple comparisons test, n=446 cells). Optogenetic suppression of SOMINs disrupted the object specificity of firing maps, reversing this difference (0.11±0.01 vs 0.19±0.02, $p=0.001$, Friedman test with Dunn's multiple comparisons test, n=467 cells). On the behavioral level, chemogenetic suppression of SOMINs disrupted novel object preference (descrimination index 0.09±0.07 for identical objects vs 0.14±0.07 for different objects, $p=0.68$, Wilcoxon test, n=7) compared to vehicle control (descrimination index 0.05±0.06 for identical objects vs 0.33±0.10 for different objects, $p=0.02$, Wilcoxon test, n=7).
Conclusion: Together, these findings suggest that SOMINmediated inhibition is critically important for objectspecific coding in the DG and object discrimination.

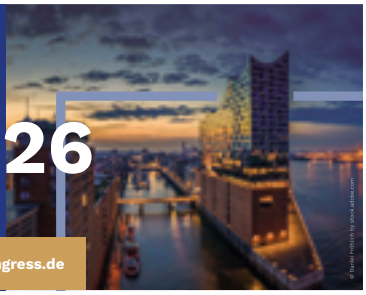

P08 Postergroup: In vivo nevrophysiology & connectivity

P0802

Reciprocal firing rate changes of dopamine substantia nigra neurons associated with increased head acceleration, speed of locomotion and rotational behavior of mice during open field locomotion

Daniela Freitag; Pascal Vogel; Jochen Roeper
Interdisziplinären Zentrums für Neurowissenschaften, Goethe
Universität, Frankfurt a. M., Germany;

Objective: Dopamine substantia nigra (DA SN) neurons are important for voluntary movement control.

Method: We performed chronic multielectrode recordings in awake freely moving male C57Bl/6N mice, aged 8–16 weeks, while simultaneously tracking their movements in an open field. We identified putative DA SN (pDA SN) neurons by their response (>50% reduction of mean firing rate) to the systemically injected D2receptor agonist quinpirole.

Results: In accordance to Da Silva et al. (2018), our data set of n=83 (N=31) pDA SN neurons confirmed the diversity of electrical activity changes associated with selfpaced movement initiation: only 7% of pDA SN neurons (n=6/83) significantly increased their firing rates (baseline to max: +2.8±2.2Hz, mean±SD) in a 500ms time window around accelerometerdefined initiation of selfpaced movements. A larger fraction (~24%, n=20/83) of pDA SN neurons transiently decreased their firing rates (baseline to min: 1.6±0.4Hz, mean±SD) in the same time window. Similar patterns were observed in association with deeplabcutbased, speeddefined movement initiations, with 10% of pDA SN (n=8/83) transiently increased (baseline to max: +2.3 ± 1.9Hz, mean ± SD) and a smaller fraction of 2% (n=2/83) transiently decreased their firing rate (baseline to min: 0.5 ± 0.1Hz, mean ± SD). Furthermore, reciprocal firing rate changes of pDA SN neurons also occurred in association with contralateral rotations (left; firing rate increase of +3.9 ± 4.1Hz in n=5/83, firing rate decrease of 1.1 ± 0.5Hz in n=17/83) or ipsilateral rotations (right; firing rate increase of +0.7 ± 0.9Hz in n=7/83, firing rate decrease of 0.8 ± 1.3Hz in n=11/83).

Conclusion: We currently focus on the role of pDA SN neuron ensemble patterns in initiating movement transitions.

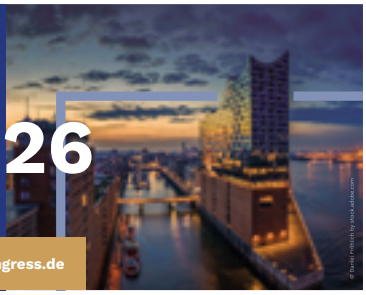

P08 Postergroup: In vivo nevrophysiology & connectivity

P0803

Enhanced spinal network excitability in ALS patients produces abnormal Hreflex recovery when employing the double stimulation paradigm

Robert Patejdl; Sebastian Wölk [1]
Physiology, Institute for Biomedical Research, HMU Health and Medical University Erfurt, Erfurt, Germany; [1] Physiology, Rostock University Medical Center, Rostock, Germany;

Objective: The Hreflex constitutes a monosynaptic spinal reflex pathway and is considered the neurophysiological counterpart of the Achilles tendon reflex. Using a modified doublestimulation protocol, it is possible to distinguish the temporal properties of spinal excitatory and inhibitory processes. In the context of ALS, this technique may yield clinically important information about impairments of motor system function.
Method: Hreflex recovery was evaluated in 15 patients with ALS and 82 individuals without ALS, among them 12 agematched healthy controls (HC). The experimental setup comprised 14 different interstimulus intervals (ISIs) covering a total duration of up to one second.
Results: Compared with healthy controls, patients with ALS showed Hreflex recovery already at interstimulus intervals (ISIs) of 30 and 50 ms. Within the ISI range of 50–200 ms, recovery amplitudes were significantly greater in the ALS group than in agematched controls. These findings indicate increased excitability of spinal neuronal networks in ALS, reflected by an earlier onset and enhanced magnitude of Hreflex recovery.
Conclusion: These alterations likely reflect changes in neuronal network activity and can be attributed to modifications in both segmental spinal circuits and supraspinal regulatory pathways. Further studies on the underlying synaptic pathophysiology and altered network dynamics are needed.

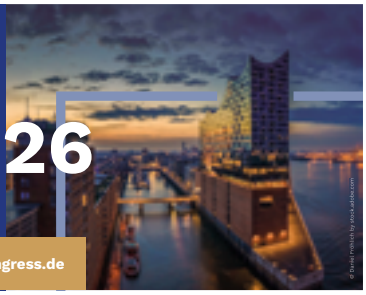

P08 Postergroup: In vivo nevrophysiology & connectivity

P0804

KATP channels are open in vivo and prevent depolarization block in medial substantia nigra dopamine neurons, enabling intrinsic oscillations

Richard EggerMackrodt; Niklas HammerBahador [1]; Jochen Roeper [2]
Institute of Neurophysiology, Goethe University Frankfurt, Frankfurt a. M., Germany; [1] Department of Psychiatry, University Hospital Frankfurt, Frankfurt a. M., Germany; [2] Interdisziplinären Zentrums für Neurowissenschaften, GoetheUniversität, Frankfurt a. M., Germany;

Objective: In vivo dopamine (DA) substantia nigra (SN) neurons are spontaneously active and show different action potential discharge patterns. While the expression of dominantnegative KATP channel mutants eliminated in vivo burst firing selectively in medial SN DA neurons (Schiemann et al., 2012), a direct electrogenic effect of open KATP remains elusive.
Method: To close this gap, we combined *in vivo* wholecell recordings in the midbrain of adult DATCre mice with cellspecific pharmacological manipulations of KATP channels, by applying the KATP channel inhibitor tolbutamide or the activator NN414 via the recoding pipette. Additionally, we used *in vitro* patchclamp recordings to further analyze the underlying biophysical identity of oscillatory bursting DA neurons.
Results: We discovered a prominent contribution of open KATP channels to the membrane potential in 1/3 of tolbutamidedialyzed DA neurons (n= 20/60). Furthermore, KATP channel inhibition reduced the spontaneous occurrence of transient hyperpolarizing pauses (“valleys”), while KATP channel enhancement increased their rate. Using unbiased hierarchical clustering, we identified four distinct clusters of valleys in vivo, of which one was affected by pharmacologically altering KATP channel function. These KATPdependent valleys were characterized by being long (~1s), deep (45 mV) and with a slow onset (0.03 mV/ms). Surprisingly, injection of negative current in vivo was sufficient to rescue the burstpause pattern. To differentiate between open KATP channels preventing the depolarization block for synaptically induced bursting in vivo (i.e. “state setter” (Kedia et al., 2024)) or enabling the entire burstpause pattern intrinsically we isolated DA neurons synaptically in vitro and performed stepwise hyperpolarizations. Surprisingly, we discovered that a subset of calbindinpositive DA neurons in the medial SN intrinsically generate membrane potential oscillations resulting in repetitive burst discharges.
Conclusion: In summary, our data demonstrate that KATP channels are open in vivo and prevent depolarization block in calbindinpositive medial SN DA neurons. Thereby, they enable oscillatory bursting. These results are consistent with our previous extracellular *in vivo* study (Schiemann et al., 2012). Here we identified the underlying biophysical mechanism, where a strong KATP channel current enables an intrinsic oscillator (i.e. KATP as a state setter).

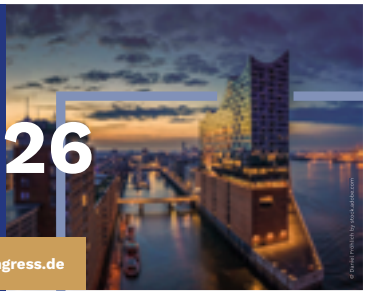

P08 Postergroup: In vivo nevrophysiology & connectivity

P0805

Multimodal analysis of GABAergic transmission within the motor cortex of the dystonic hamster

Sarah Rahause; Ella Nissen; Max Hörnschemeyer; Johannes Nolte; Fabiana Santana Kragelund; Rüdiger Köhling; Denise Franz
OscarLangendorffInstitute of Physiology, Rostock University Medical Center, Rostock, Germany;

Objective: This study investigates GABAergic transmission in the motor cortex of the dystonic dt^{sz} hamster to characterise cortical contributions to dystonia. We focus on glutamate decarboxylase GAD67 as a marker of GABA synthesis.
Method: We combine Western blot analyses of the motor cortex of adult and juvenile animals with an organotypic slice culture model, live/dead assays, extracellular recordings of local field potentials, and immunohistochemical analyses of GAD67 and Factin. This approach allows us to assess molecular, structural, and functional properties of inhibitory networks.
Results: We find agedependent alterations in the GABAergic system. Juvenile dt^{sz} hamsters show no difference in total GAD67 protein expression compared to wildtype animals, whereas adult dt^{sz} hamsters show increased GAD67 levels that persist after pallidal deep brain stimulation. Cell viability in WT and dt^{sz} slice cultures increases over time, reaching approximately 80–90% after 48–72 hours. Electrophysiologically, juvenile WT slice cultures exhibit spontaneous local field potentials that increase upon blockade of GABAergic inhibition with gabazine. In contrast, juvenile dt^{sz} slice cultures show no spontaneous activity under baseline conditions or after gabazine application. Confocal analysis reveals reduced GAD67 immunofluorescence in dt^{sz} motor cortex slices and a tendency toward reduced Factin structure.
Conclusion: The results indicate an agedependent and likely compensatory dysregulation of GABAergic transmission in the dystonic motor cortex, consistent with impaired inhibitory network function and altered cortical excitability.

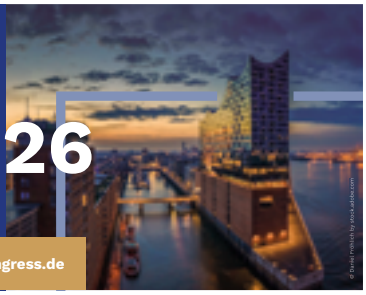

P08 Postergroup: In vivo nevrophysiology & connectivity

P0806
Microglia regulate hippocampal network dynamics via THIK1 dependent IL1β release

Michael Surala; Ecem Tütüncü; Luna Šošo Zdravkovic; Zoltan Gerevich; Jörg Rolf Paul Geiger; JonasFrederic Sauer [1]; Christian Madry

Institut für Neurophysiologie, Charité - Universitätsmedizin Berlin, Berlin, Germany; [1] Systemic Neurophysiology, CIPMM, Universität des Saarlandes, Homburg, Germany;

Objective: Microglia maintain brain homeostasis through continuous neuropil surveillance, a process dependent on the twopore domain potassium channel THIK1. While THIK1 is essential for both surveillance and IL1β release, affecting microglianeuron communication, its specific role in neuronal function remains unexplored. This study aims to investigate the impact of THIK1 in modulating neuronal network activity.
Method: Using acute mouse brain slices in combination with electrophysiology and pharmacological and genetic interventions, we investigated the consequences of THIK1 blockade on hippocampal synaptic transmission and CA1 gamma oscillations. Furthermore, we characterized THIK1 mediated cytokines and purinergic signaling in dependence of neuronal activity.
Results: We demonstrate that THIK1 is a critical regulator of hippocampal network state. Genetic deletion or acute pharmacological blockade of THIK1 resulted in a profound increase in gamma oscillation power and altered synaptic transmission in CA1 pyramidal cells. Mechanistically we uncovered that the increase in gamma power is driven by attenuation in IL1β signaling.
Conclusion: Our study identifies THIK1 as a homeostatic regulator of hippocampal network activity. We establish a specific microglianeuron interaction generating THIK1–IL1β dependent neuronal feedback, thereby constraining network hyperexcitability.

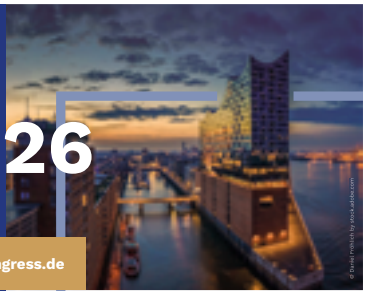

P08 Postergroup: In vivo nevrophysiology & connectivity

P0807

Loss of endosomal SodiumHydrogen Exchanger NHE6 rewires metabolism in primary astrocytes

Lara Sach; Heidi Nielsen [1]; Blanca Aldana [2]; Stine Falsig Pedersen
Department of Biology, Insitute of Cell biology and physiology, University of Copenhagen, Copenhagen, Denmark; [1] Department of Drug design and pharmacology, University of Copenhagen, Copenhagen, Denmark; [2] Department of Veterinary and animal sciences, University of Copenhagen, Frederiksberg, Denmark;

Objective: SodiumHydrogen Exchanger NHE6 (SLC9A6) regulates endosomal pH and ion homeostasis. SLC9A6 mutations lead to the devastating neurodevelopmental disease Christianson Syndrome, with symptoms including epileptic seizures, nonverbal status and the attenuation of weight and growth gain. *Ex vivo* research found that loss of NHE6 in primary neurons leads to reduced arborization of neuronal circuits, trafficking deficits and diminished longterm potentiation. However, effects of NHE6 loss on glial cells have been extensively understudied. Here, we use primary cultures of wild type (WT) and NHE6 knockout (KO) cortical astrocytes to study the effect of NHE6 loss on the astrocyte metabolic landscape.
Method: Using multiple techniques including proteomic profiling, Seahorse XF analysis, GCMS metabolic isotope tracing and confocal imaging we investigated the impact of NHE6 KO on glucose- and lipid metabolism pathways.
Results: While our proteomic data showed significant changes in protein expression related to glucose metabolism and oxidative phosphorylation, we did not find any changes in glycolytic rate or mitochondrial respiration, and extracellular lactate concentration was unchanged between cell types. Notably, NHE6 KO astrocytes exhibited diminished phosphorylation of the pyruvate dehydrogenase complex (PDHA) indicating higher pyruvate uptake into the mitochondria. Treatment with palmitate plus bovine serum albumin (BSA) increased PDHA phosphorylation and elevated mitochondrial activity only in KO astrocytes and this effect was diminished by inhibiting endocytosis. Strikingly, similar changes were observed with BSA alone, suggesting that albumindriven metabolic changes may contribute to the NHE6 KO phenotype. In conclusion, NHE6 loss drives major metabolic proteomic changes but only mild functional metabolic effects in KO astrocytes.
Conclusion: Ongoing studies suggest that NHE6 loss in astrocytes compromises neuronal health in coculture. We hypothesize that KO astrocytes remodel their metabolism to compensate for loss of NHE6 which essentially impacts their ability to support neurons metabolically.

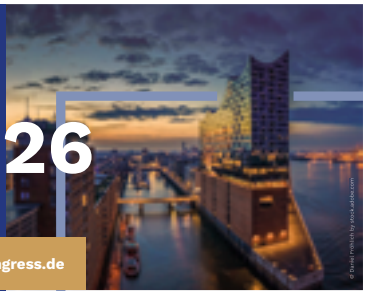

P08 Postergroup: In vivo nevrophysiology & connectivity

P0808

Comparative Characterization of Functional Network Emergence in Dorsal and Ventral Forebrain Organoids Derived from Human Induced Pluripotent Stem Cells

Tomas Fanutza; Maximilian Borgmeyer; Zino Aufenacker; Nina Wittenmayer; Christian Wozny
IMM Institute for Molecular Medicine, MSH Medical School Hamburg, Hamburg, Germany;

Objective: Recent advances in human induced pluripotent stem cell (hiPSC)derived threedimensional (3D) neural organoids have provided transformative platforms for modeling human brain development, regional specification, and diseaserelevant neuronal circuit formation in vitro. Cerebral organoids recapitulate critical features of early human brain neurodevelopment, including cellular heterogeneity, structural organization, and progressive neuronal maturation. We employ regionspecific brain organoid models with a focus on the cortex, dorsal forebrain organoids (DfOs) and ventral forebrain organoids (VfOs), to investigate how distinct developmental trajectories shape neuronal identity, morphology, and functional network properties.
Method: Using immunohistochemistry combined with confocal microscopy, we assess regional and neuronal populations by quantifying differential expression patterns of synaptic proteins across both models. To determine functional maturation, we perform wholecell patchclamp electrophysiology in acute organoid slices to characterize intrinsic membrane properties, neuronal excitability, and spontaneous synaptic transmission, with particular emphasis on glutamatergic and GABAergic synaptic events. In parallel, Sholl analysis of reconstructed neurons from patched cells is used to evaluate dendritic complexity and morphological maturation, enabling comparative assessment of neuronal architecture between dorsal and ventral forebrainderived neurons.
Results: By directly comparing these parameters between DfOs and VfOs, we aim to delineate regionspecific differences in neuronal development, synaptic integration, and network stabilization over time. Our overarching goal is to define how dorsal and ventral forebrain programs differentially contribute to the emergence and longterm maturation of functional human neuronal circuits.
Conclusion: This work will advance mechanistic understanding of human forebrain development and provide robust in vitro models for investigating circuit dysfunction in neurodevelopmental and neuropsychiatric disorders such as autism spectrum disorders, major depressive disorder, and Alzheimer's disease.

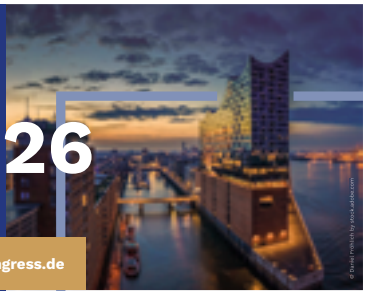

P08 Postergroup: In vivo nevrophysiology & connectivity

P0809

In vivo awake Neuropixels recordings of putative dopamine neurons in the substantia nigra reveal statetransition coding during selfpaced locomotion

Yingning Lu; Pascal Vogel [1]; Jochen Roeper [1]
Institute of Neurophysiology, Goethe University Frankfurt, Frankfurt a. M., Germany; [1] Interdisziplinäres Zentrum für Neurowissenschaften, GoetheUniversität, Frankfurt a. M., Germany;

Objective: Substantia nigra (SN) dopamine (DA) neurons exhibit diverse firing patterns around movement transitions, but their exact relationships to state transitions are not yet fully resolved.
Method: To investigate their role in motor control, we conducted highdensity, singleshank Neuropixels 1.0 recordings in awake, headfixed mice performing spontaneous locomotion on a treadmill.
Results: We recorded ~3000 units across the full depth of the probe over 30 sessions (N = 11). Across this population, 48% (n = 1500) responded to rest–movement transitions, with n = 882 showing excitation (+6.0 ± 6.3 Hz; mean ± SD) and n = 618 inhibition (−3.8 ± 4.4 Hz; mean ± SD), indicating widespread, transitionassociated rate modulation. Focusing on n = 251 putative DA (pDA) units (8% of all recorded units) based on firing rate and waveform criteria, and localized within the SN by DiI/TH histology, n = 110 pDA SN units showed onsetrelated modulation, with 26% (n = 65; +3.0 ± 3.5 Hz; mean ± SD) being excited and 18% (n = 45; −1.4 ± 1.2 Hz; mean ± SD) inhibited. At movement offset, 34% (n = 85) were significantly modulated, split between inhibitory (n = 41; −2.9 ± 5.8 Hz; mean ± SD) and excitatory (n = 44; +1.5 ± 1.0 Hz; mean ± SD) responses, and 56% (n = 141) responded at both transitions. **Conclusion:** These patterns are comparable to those recorded in freely moving mice (da Silva et al., 2018). We are now extending our study to the use of 4shank Neuropixels 2.0 probes to sample across the mediolateral extent of the SN in male and female mice. In addition to singleunit rate changes, we will focus our analysis on LFP–spike coupling and firing correlations among pDA SN neurons during selfinitiated rest–movement transitions.

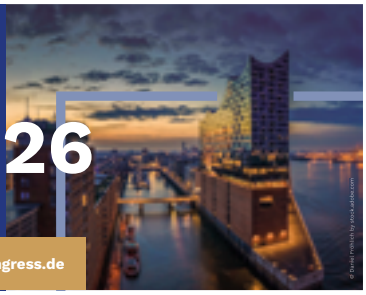

P08 Postergroup: In vivo nevrophysiology & connectivity

P0810
Mapping of projectionspecific inputs to the nucleus reuniens

Sören Brandt; Andreas Weiß; Kira Kaiser; Niels Röhrdanz; Peer Wulff Systems Neuroscience, Physiologisches Institut, ChristianAlbrechtsUniversität zu Kiel, Kiel, Germany;

Objective: The nucleus reuniens (nRE) of the thalamus is reciprocally connected to the medial prefrontal cortex (mPFC) and to the hippocampus and is thought to be a key node in hippocampalprefrontal communication. Whereas efferents of the nRE mainly project to hippocampus and mPFC, the nRE receives input from many additional cortical and subcortical structures, which modulate its activity and thus hippocampalprefrontal communication. To understand how the diverse inputs to the nRE may shape hippocampalprefrontal communication we set out to map the projectionspecific afferents of this nucleus.
Method: To dissect projectionspecific inputs to the nRE and compare them to previously reported nonprojectionspecific inputs, we first injected a retrograde AAV expressing Crerecombinase into the hippocampus and simultaneously delivered Credependent AAVhelper viruses expressing the avian leukosis and sarcoma virus receptor (TVA) and the rabies glycoprotein into the nRE. After 21 days, we injected the glycoproteindeleted rabies virus that expressed envelope protein from the avian sarcoma leucosis virus (EnvA) into the nRE. 10 days later, brains were fixed, sectioned, and immunohistochemically stained. Secondary neurons were imaged and analyzed using the SHARCQPipeline and customized scripts.
Results: Here, we present a monosynaptic rabies virusbased tracing approach, combined with a semiautomated analysis pipeline based on SHARCQ, to investigate the inputs to nRE neurons that project to the hippocampal CA1 region. We have developed customized scripts as addons to inform not only about detected cells per brain region but also about regions devoid of labeled cells, to reveal the anatomical hierarchy of identified brain regions and to normalize cell counts by area to account for sampling asymmetry. Brain regions providing afferents to hippocampusprojecting nRE neurons were largely consistent with previous nonprojectionspecific retrograde tracing studies.
Conclusion: The approach we present here provides a methodological framework for dissecting projectionspecific neuronal circuits and in its specific application offers new insights into the functional organization of the mPFCnREhippocampus network.

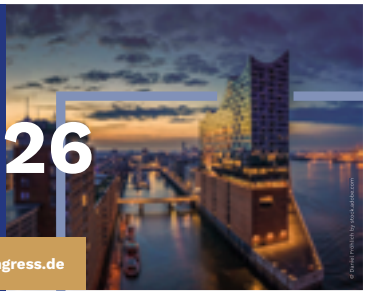

P08 Postergroup: In vivo nevrophysiology & connectivity

P0811
Brainwide Monosynaptic Input Mapping of Nucleus Accumbens Neurons

Natasha Nadeem Khan; Ximena Icaria SalinasHernandez; Sevil Duvarci Life Sciences, Institute of Neurophysiology, Uniklinik Frankfurt, Goethe University Frankfurt, Frankfurt a. M., Germany;

Objective: The nucleus accumbens (NAc) is a key component of the mesolimbic dopamine (DA) system that plays a central role in motivation, reward processing and adaptive learning. Our recent work demonstrated that DA neurons projecting to NAc are also critical for encoding an extinction prediction error (EPE) signal crucial for driving fear extinction learning. Specifically, EPEencoding DA neurons selectively target the anteromedial (amNAc), but not the posteromedial NAc (pmNAc), suggesting functional specialization along the anteroposterior axis of the medial NAc. However, the circuit architecture underlying these subregionspecific differences remains poorly understood, particularly with respect to dopamine D1 receptor- and D2 receptorexpressing medium spiny neurons (D1- and D2MSNs), the principal output neurons of the NAc.
Method: Here, we performed cell typespecific wholebrain rabies tracing to map the monosynaptic inputs to D1- and D2MSNs across the anteroposterior axis of the medial NAc using transgenic mouse lines selectively expressing Cre recombinase in D1MSNs or D2MSNs.
Results: Comparative analysis of brainwide inputs revealed unique patterns of afferent organization across both MSN subtypes and NAc subregions.
Conclusion: Together, these findings provide comprehensive anatomical insights into understanding how NAc circuits mediate fear extinction learning.

P08 Postergroup: In vivo nevrophysiology & connectivity

P0812

Electrophysiological characterization of seizure generation mechanisms in a genetic rat model of absence epilepsy

Annika Lüttjohann; Eleni Nikalexi; Jonas Terlau [1]; Thomas Budde; HansChristian Pape Institute of Physiology I, Münster University, Münster, Germany; [1] Derpartment of Neurosurgery, Translational Neurotechnology Laboratory, Technical University of Munich, Munich, Germany;

Objective: Spikewavedischarges (SWD) are the electrophysiological hallmark of absence epilepsy. SWD are known to be generated in the thalamocortical network and a seizure onset zone was identified in the somatosensory cortex (S1). Rhythmic cortical 59 Hz oscillations are often seen to precede SWD activity in a wellvalidated genetic rat model of absence epilepsy (GAERS), but are also seen in seizurefree periods. We aimed to elucidate critical spatiotemporal dynamics in the communication between S1 and thalamus required for SWD generation.
Method: Mulisite local field potential recordings, local electrical doublepulse stimulation and local pharmacological inhibition were performed in S1 and different thalamic nuclei of freely behaving GAERS. Local field potentials were analyzed by nonlinear association analysis, wavelet analysis and current source density analysis.
Results: Inhibition of the centromedian thalamic nucleus (CM) resulted in a selective suppression of the spike component while rhythmic cortical 59 Hz oscillations remained present. The amplitude of the spike component in the cortical LFP was correlated to the degree of S1CM communication as assessed by current source density analysis. Surprisingly, wavelet analysis and nonlinear association analysis revealed higher spectral power and stronger coupling between S1 and CM for interictal compared to preictal 59 Hz oscillations. However, coupling strength during preictal oscillations was higher than during passive wakefulness. Double pulse stimulation during 59 Hz oscillations was more likely to induce epileptic afterdischarges compared to stimulation during passive wakefulness. While no overall differences in cortical excitability were revealed, phasespecific differences in excitability were noticed during the oscillation.
Conclusion: Our findings highlight the importance of S1CM communication for SWD generation and indicate that an intermediate coupling between S1 and CM is most favorable for SWD generation. Moreover, 59 Hz oscillations represent highrisk periods for seizure generation. Preictal 59 Hz oscillations display a unique electrophysiological profile in absence epileptic rats that might pave the way for qualification as biomarker for SWD generation and seizure prediction.

P08 Postergroup: In vivo nevrophysiology & connectivity

P0813

Selective Cav1.3inhibition reduces dopamine substantia nigra neuron in vivo firing and striatal dopamine transients during exploration in male mice

Johannes Boehm; Pascal Vogel [1]; Niklas HammerBahador [2]; Nadine Ortner [3]; Jochen Roeper [1]
Neurophysiology, Goethe University Frankfurt a.M., Frankfurt a.M., Germany; [1] Interdisziplinären Zentrums für Neurowissenschaften, GoetheUniversität, Frankfurt a. M., Germany; [2] Department of Psychiatry, University Hospital Frankfurt, Frankfurt a. M., Germany; [3] Division of Medical Physics and Biophysics, Medical University Graz, Graz, Austria;

The Dihydropyridine (DHP)sensitive LType calcium channels $Ca_v1.3$ and $Ca_v1.2$ serve diverse physiological functions and are also present in dopamine (DA) neurons of the substantia nigra (SN). Previous studies from our group have demonstrated that $Ca_v1.3$ channels act as linear fullrange amplifiers of firing rates (FR) specifically in lateral DA SN neurons projecting to the dorsolateral striatum (DLS). This amplifier function of $Ca_v1.3$ channels is dampened by clinically relevant doses of isradipine (ISR) (Shin et al. 2022, Science Advances).
In this study we investigated the in vivo effect of ISR in awake and freely moving mice during open field exploration using chronic extracellular recordings. Consistently to the in vitro study we were able to observe a significant decrease of 24% in mean firing rates of lateral pharmacologically identified DA SN neurons (n=28, N=3). In open field behaviour we found no obvious differences between ISR and vehicle (VEH) injection.
Based on previous research by Koralek and Costa (Koralek & Costa, 2021, Science Advances) suggesting the crucial role of electrical activity in DA SN neurons in selectively invigorating exploitative behavior in mice, we hypothesized that an ISRinduced decrease in firing rates of lSN neurons might influence exploitative or explorative behavior. To investigate this hypothesis, we trained a group of mice (6 male WT and 10 male and female $Ca_v1.2$DHP/ mice) to perform a twopoke sequence learning task, rewarded with sugarwater, where rewarded exploitative action sequences could be distinguished from other explorative actions. After reaching plateau performance characterized by stable exploitative poking of the target sequence, we administered ISR or VEH i.p. 15 minutes prior to placing the animals in the operant chamber and opened an additional exploration port. ISR injection resulted in the selective decrease of explorative dopamine transients in male mice, while female mice remained unchanged.

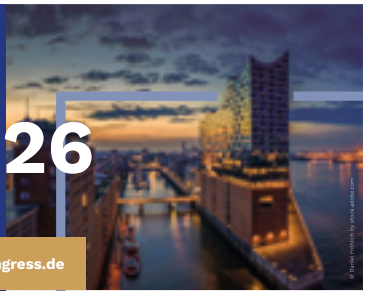

P08 Postergroup: In vivo nevrophysiology & connectivity

P0814
Interactions of catecholaminergic signaling in the brain

Alexander Dieter; Lena Eschholz; J. Simon Wiegert
Neurophysiology, Medical Faculty Mannheim, Heidelberg University, Mannheim, Germany;

Objective: Neuromodulators play a central role in regulating brain states such as arousal, learning and cognition. Yet how distinct neuromodulatory systems interact remains poorly understood. Recent advances in the genetic targeting of these systems and the emergence of fluorescent indicators sensitive to individual neuromodulators now allow the simultaneous monitoring of distinct neuromodulatory populations with high molecular specificity and temporal precision.
Method: Here, we investigate interactions between the locus coeruleus noradrenergic system (LCNE) and the ventral tegmental area dopaminergic (VTADA) system in mice by using spectrally distinct calcium indicators to selectively target LCNE and VTADA neurons in the same animal. All experiments were performed in compliance with German law according to the directive 2010/63/EU of the *European Parliament* on the protection of animals used for scientific purposes and in accordance with the 3R principles. During preparative surgeries, animals were anesthetized via inhalation of isoflurane in air (5 % for induction, 12 % for maintenance).
Results: We found that spontaneous activity in the two systems is negatively coupled during both rest and locomotion. A temporal analysis indicates that LCNE activity precedes and suppresses VTADA dynamics. Consistent with this finding, we identified anatomical and functional evidence for LCNE release within the VTA. Furthermore, exposure to a natural stressor as well as optogenetic activation of LCNE neurons causally reduced VTADA activity.
Conclusion: Thus, our findings suggest a negative interaction between these two catecholaminergic systems, which is governed by the LCNE system.

P09 Postergroup: Cation & non selective channels

P0901

Functional subclasses of cultured sensory neurons from pig and mouse

Marc Behrendt; Sabrina Soares; Zeinab Abbasi; Lisa Tiebl; Hans Jürgen Solinski; Roman Rukwied; Richard Carr; Martin Schmelz
Experimental Pain Research, Mannheim Center for Translational Neuroscience (MCTN), Heidelberg University, Mannheim, Germany;

Objective: The translational value of rodent pain models is limited by pronounced species differences in primary sensory neuron organization and function. Pig nociceptors resemble human ones more closely than those in mice, yet functional data on porcine sensory neurons - especially concerning the expression and activity of painrelated signaling proteins - remain scarce.
Method: Cultured pig and mouse dorsal root ganglion (DRG) neurons were investigated using calcium imaging combined with chemo- and electrostimulation to enable a comparative functional classification of sensory neurons as well as the characterization of nociceptive signaling mechanisms.
Results: Of the pig neurons examined, a substantial proportion responded to the TRPV1 agonist capsaicin (CAP+; 39.8%), the TRPM3 agonist pregnenolone sulfate (PS+; 31.1%), or to both agonists (19.1%). The mean cell diameters of the pig neurons differed significantly between the groups, with CAP+/PS+ neurons being the smallest (33.67 µm), CAP/PS- neurons the largest (50.42 µm), and the other groups having mean diameters in between (CAP+/PS: 39.85 µm; CAP/PS+: 40.49 µm). Larger pig neurons responded more frequently to both electrical rectangular (RE) and slow (250 ms) sine wave (SW) stimuli, and the mean diameter of the responding cells was significantly larger than that of the nonresponding cells.
The activation thresholds determined using increasing stimulus intensities (550 mA) did not differ significantly between large and small pig neurons, neither for slow nor for fast (20 ms) SW stimuli. Small cells responded significantly more frequently to ten consecutive fast SW stimuli of increasing intensity, but not to ten slow SW stimuli. While the thresholds for RE stimuli did not vary greatly within and between the chemically defined subclasses of pig neurons, the thresholds for slow SW stimuli were higher in PS+ (30.4 mA) than in PS- (22.8 mA) cells. Blockade of the action potential by a substantial reduction in extracellular sodium prevented calcium responses following RE stimulation, yet in some neurons slow SW stimuli still evoked calcium transients.
Treatment of pig or mouse neurons with tetrodotoxin (TTX; 1 µM) resulted in a significant reduction in calcium responses to RE and slow SW stimuli in all cells. In mouse CAP- neurons, TTX led to a significantly greater reduction in calcium responses to RE stimuli than in cells treated with a Nav1.7Nav1.8 blocker combination (P050+A80). In mouse CAP+ cells, the effect of TTX on RE calcium responses was not significantly stronger than that of P050+A80, nor was it in mouse neurons stimulated with SW stimuli.
Conclusion: The combined use of chemo- and electrostimulation together with selective ion channel inhibition enables a refined functional classification of sensory neuron subtypes in pig and mouse DRG cell cultures and highlights the pig as a potentially more translationally relevant model for human nociceptor biology and pain signaling.

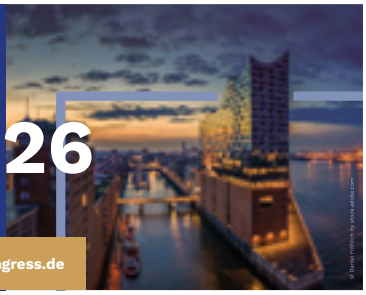

P09 Postergroup: Cation & non selective channels

P0902
Otenabant is a Selective Antagonist of Human PIEZO1

Vincent Jaquet; Reetta Penttinen [1]; Gorane RodríguezUrquirizar [2]; Cyril Castebou; Yves Cambet; Nicolas Rosa; Mathilde Bourdin; Bita Asghariastanehei [3]; Franciele de Lima [3]; Marie Martin [3]; Elie Nader [3]; Selma A. Serra [2]; José M. FernándezFernández [2]; Nicoletta Murciano [1]; Philippe Connes [3]; Stéphane Egée [4]; Hélène Guizouarn [5]; Lars Kaestner [6]; Niels Fertig [1]; Maria Giustina Rotordam [1]; Nicolas Demaurex

Department of Cell Physiology and Metabolism, University of Geneva, Genève, Switzerland; [1] Nanion Technologies GmbH, München, Germany; [2] Laboratori de Fisiologia Molecular, Universitat Pompeu Fabra, Barcelona, Spain; [3] Laboratoire interuniversitaire de Biologie de la Motricité, Université Claude Bernard Lyon I, Villeurbanne, France; [4] Station Biologique de Roscoff, Roscoff, France; [5] Université Côte d'Azur, Nice, France; [6] Theoretical Medicine and Biosciences, Saarland University, Homburg, Germany;

Objective: PIEZO1 mechanosensitive cation channels translate mechanical cues into intracellular Ca^{2+} and Na^{+} elevations, enabling cells to respond to physical alterations in their environment. PIEZO1 contributes to red blood cells (RBC) volume homeostasis and gainoffunction PIEZO1 mutations cause hereditary xerocytosis (HX), a rare mostly compensated hemolytic anemia, and aberrant channel activation exacerbates sickling and vascular dysfunction in sickle cell disease. Despite strong genetic and physiological evidence supporting PIEZO1 as a therapeutic target, potent and selective inhibitors are limited, and existing compounds show modest specificity or poorly explored mechanisms. Improved pharmacological tools are needed.
Method: We conducted a highthroughput screen of FDAapproved drugs to identify PIEZO1 inhibitors. Compounds were tested at concentrations of 10 µM in a monocytic cell line, using intracellular Ca^{2+} elevations evoked by the PIEZO1 agonist Yoda1 as readout. The inhibitory activity of the best hit was validated and compared to existing PIEZO1 inhibitors using electrophysiological analysis, orthogonal PIEZO1dependent assays across cell lines and human RBCs. As functional proof, we investigated the impact of three PIEZO1 inhibitors on RBC deformability by ektacytometry, after Yoda1 prestimulation.
Results: This screen identified Otenabant, a selective Cannabinoid Receptor Type 1 (CB1) antagonist, as a potent PIEZO1 inhibitor. Otenabant dosedependently inhibited Ca^{2+} elevations mediated by endogenous or exogenously expressed human PIEZO1, but was ineffective against mouse Piezo1, revealing speciesspecific channel differences. Otenabant inhibited mechanosensitive currents elicited by shear stress in fibroblasts and by repeated poking in PIEZO1expressing HEK293 cells, altering the currents activation and inactivation kinetics, and prevented Yoda1induced hyperpolarization in RBCs. Otenabant was able to reverse the negative impact of Yoda1 on RBC deformability.
Conclusion: These findings demonstrate the utility of Yodabased screening for discovering PIEZO1 antagonists and identify Otenabant as a promising chemical scaffold for developing selective PIEZO1 inhibitors with therapeutic potential.

P09 Postergroup: Cation & non selective channels

P0903

Sphingosine1 phosphate activates volumeregulated anion channels through Gβγ signaling

Yulia Kostritskaia; Sumaira Pervaiz; Anna Klemmer; Malte Klüssendorf; Tobias Stauber Institute for Molecular Medicine, MSH Medical School Hamburg, Hamburg, Germany; Institute for Molecular Medicine, MSH Medical School Hamburg, Hamburg, Germany;

Objective: The volumeregulated anion channel (VRAC) plays a critical role in regulatory volume decrease by mediating the release of chloride ions and organic osmolytes. Beyond cell volume regulation, VRAC contributes to several essential cellular processes, including membrane potential regulation, glutamate release, and apoptosis. Moreover, VRAC permeability to antibiotics and anticancer drugs highlights its therapeutic relevance. Although osmotic swelling is a wellknown activator of VRAC, increasing evidence suggests that VRAC can also be activated under isovolumetric conditions through protein kinase D (PKD) dependent mechanisms. Sphingosine1phosphate (S1P), an important signaling lipid acting through G proteincoupled receptors (GPCRs), has been reported to activate VRAC in several cell types. This study aimed to investigate the mechanism of S1Pinduced VRAC activation and to determine the involvement of GPCRmediated G protein signaling pathways.
Method: S1Pinduced VRAC activation was examined in multiple cell types using wholecell patchclamp electrophysiology. The role of S1P receptors was assessed using genomic knockout of S1PR1 in HeLa cells, as well as pharmacological inhibition with S1PR1 antagonists (W123 and W146) and the S1PR2 antagonist JTE013. The S1PR1selective agonist SEW2871 was used to evaluate receptor specificity. To investigate downstream signaling mechanisms, toxinbased suppression of receptorcoupled G proteins was performed. Pertussis toxin was used to inhibit Gαi/o signaling, while gallein was applied to block Gβγ subunit effector interactions.
Results: Genomic knockout of S1PR1 in HeLa cells, as well as pharmacological inhibition with the S1PR1 antagonists W123 and W146, significantly reduced S1Pinduced VRAC activation. In contrast, inhibition of S1PR2 with JTE013 had no effect. Furthermore, the S1PR1selective agonist SEW2871 mimicked S1Pinduced VRAC activation, indicating that S1P activates VRAC primarily through S1PR1 in HeLa cells.
Investigation of downstream signaling pathways showed that inhibition of Gαi/o signaling with pertussis toxin did not suppress S1Pinduced VRAC currents, excluding a major role for Gαi/o proteins. However, blockade of Gβγ signaling with gallein significantly reduced VRAC activity, suggesting that Gβγ dimers are involved in channel activation. Notably, S1P failed to activate VRAC in HEK293T cells, which lack endogenous Gβγresponsive phospholipase Cβ (PLCβ) isoforms.
Conclusion: Our findings demonstrate that S1P activates VRAC through an S1PR1mediated signaling pathway involving Gβγ subunits and PLCβ, likely leading to PKD activation and subsequent channel opening. These results identify S1PR1mediated Gβγ–PLCβ signaling as a key molecular mechanism underlying isosmotic VRAC activation.

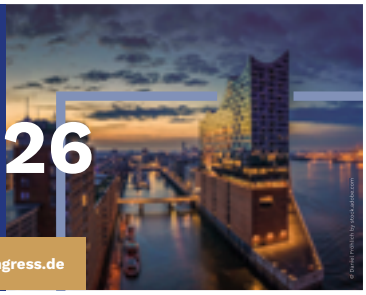

P09 Postergroup: Cation & non selective channels

P0904

Functional characterization of putative gainoffunction mutations in the Nterminal cytoplasmic domain of TRPM3

Emelie Dehmer; Júlia CastroMarsal; Doris Newel; Olaf Pinkenburg; Johannes Oberwinkler
Institut für Physiologie und Pathophysiologie, PhilippsUniversität Marburg, Marburg, Germany;

Objective: Transient Receptor Potential Melastatin 3 (TRPM3) is a nonselective cation channel activated by thermal stimuli and chemical agonists including pregnenolone sulfate (PregS). In peripheral nociceptors, it plays a key role in the detection of noxious heat and the development of inflammatory thermal hyperalgesia. In these cells, TRPM3 channel activity is inhibited by GPCR activation through direct interaction of Gβγ subunits with a short sequence in the cytosolic Nterminal region of TRPM3 channels. In addition to nociceptors, TRPM3 is also strongly expressed in the CNS. Patients with certain gainoffunction (GOF) mutations present with a variety of neurodevelopmental symptoms, including severe developmental delay, epileptic seizures and sometimes altered somatosensory perception. However, these symptoms do not occur uniformly in all patients, and may depend, at least partially, on the precise mutation present in the carrier. A606T and D614V are two putative GOF mutations identified in patients with comparatively mild neurological symptoms. Both mutations are located in the Nterminal cytoplasmic domain of TRPM3, in or very close to the interaction site for Gβγ proteins. However, it is not yet known how these mutations interfere with channel function.
Method: Using HEK293T cells for heterologous expression, we studied the functional characteristics of these pathological TRPM3 mutations with wholecell patchclamping.
Wildtype channels and a better characterized severe TRPM3 GOF mutation (V1002M) served as controls.
Results: We initially confirmed that A606T and D614V are gainoffunction mutations. However, more detailed experiments revealed that the underlying mechanism of the increased channel activity are different. TRPM3A606T channels do not show an altered response to PregS, but the inhibition by GPCR activation is weaker than in wildtype channels. On the other hand, D614V mutant channels do not show a weaker inhibition after GPCR activation, but an altered currentvoltage relationship with increased inward currents resulting in a doubly rectifying I/V relationship. Our data also indicate in this mutant a leftshifted doseresponse curve when stimulating with PregS, reminiscent of the wellcharacterized V1002M mutant. However, compared to V1002M, the functional alterations of the D614V mutation are weaker, in keeping with the reportedly milder neurological symptoms of the patient.
Conclusion: In conclusion, these findings demonstrate that mutations occuring in close spatial proximity can cause very different functional properties. These results will help to better understand the functional consequences of pathological TRPM3 mutations and possibly guide treatment options.

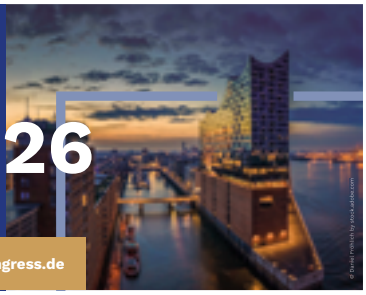

P09 Postergroup: Cation & non selective channels

P0905

Activity of different HCN channels during pacemaker depolarization studied by an actionpotential clamp at singlechannel resolution

Klaus Benndorf; Uta Enke; Andrea Schweinitz; Debanjan Tewari; Christian Sattler; Ralf Schmauder; Christoph SchmidtHieber [1]
Institute of Physiology II, University Hospital Jena, Jena, Germany; [1] Institute of Physiology I, University Hospital Jena, Jena, Germany;

Objective: Rhythmic activity in specialized pacemaker neurons and cardiomyocytes is necessary to control such fundamental functions as alertness and the heart rate, respectively. Four HCN channel isoforms have been identified to generate the pacemaker current, I_h, I_q or I_f. These isoforms differ in activation speed, voltage dependence, singlechannel conductance, and cAMP sensitivity.
Method: We expressed murine HCN1, HCN2 and HCN4 channels in *Xenopus* oocytes and studied the timedependent singlechannel conductance during the pacemaker depolarization at room temperature by using a dynamic action potential (AP) clamp at femtosiemens resolution.
Results: In one approach, we applied trains of neuronal APs as command. At an AP frequency of 10 Hz, the open probability (P_o) was unchanged during pacemaker depolarization for all three isoforms whereas at an AP frequency of 2.77 Hz, the activation and deactivation gating was robust for HCN1, minor for HCN2 and absent for HCN4. This indicates that HCN1 is the primary neuronal HCN pacemaker channel. Simulations suggest that its role in rhythmic neurons is to trigger the initial pacemaker depolarization. Furthermore, we applied trains of human sinoatrial node APs as command. At the slow AP frequency of 0.298 Hz (room temperature!), HCN2 and HCN4 channels show a slow increase of P_o from ~0.1 to ~0.25, matching the pacemaker depolarization, whereas HCN1 channels are too fast to play this role.
Conclusion: mHCN1 is the primary HCN pacemaker channel in neurons whereas in sinoatrial node cells of the human heart only HCN2 and HCN4 are kinetically suitable to generate pacemaking.

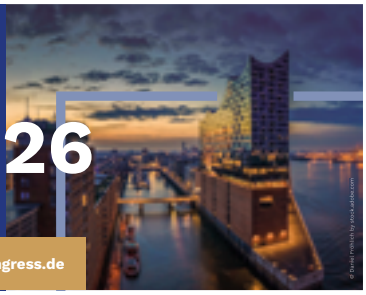

P09 Postergroup: Cation & non selective channels

P0906

Cx43 and its short isoform GJA120k are both contributing to the migration enhancing effect of Cx43

Christina Buchberger; Petra Kameritsch [1]; Hanna Mannell; Kristin Pogoda
Physiologie, Insitut für Theoretische Medizin, Universität Augsburg, Augsburg, Germany; [1] WalterBrendelCentre of Experimental Medicine, Institute of Surgical Research, LMU Klinikum Großhadern, München, Germany;

Objective: Connexin43 (Cx43) mediates intercellular communication via gap junctions but also exerts channelindependent functions. The Cterminal domain alone enhances migration channelindependently. Recent evidence shows that short Cx43 isoforms, consisting of the Cterminal domain, are generated by alternative translation and naturally occurring additionally to the fulllength Cx43 protein. Here, we investigated the role of the predominant expressed truncated Cx43 isoform GJA120k in cell migration of HeLa cells *in vitro*.
Method: To enable selective functional studies, HeLacells were transfected with GJA120kGFP or the translationdeficient mutant Cx43M213LGFP. Expression and localization were analyzed in HeLacells using Western blotting and IF staining. Functional effects on cell migration were investigated using timelapse video microscopy in woundhealing assays.
Results: Western blots confirmed expression of fulllength protein and GJA120k in HeLaCx43 as well as selective expression of GJA120k or Cx43M213L in the corresponding transfected HeLa cells. IF microscopy showed a membraneassociated, localization of Cx43 and Cx43M213L, and GJA120k in the cytosol, whereas Cx43M213L lacked cytosolic signal. Woundhealing assays revealed that both fulllength Cx43 (n=4) and GJA120k (n=5) significantly increased migration compared to controls (HeLaCTL: 61±4 µm, HeLaGFP: 62±3 µm, HeLaCx43: 172±4 µm, HeLaGJA120k: 142±8 µm; $p<0.01$). Cx43M213L (n=3) showed only slightly increased migration (HeLaCx43M213LGFP: 94±6 µm; $p<0.05$).
Conclusion: Our results showed that both GJA120k and the fulllength Cx43 mutant Cx43M213L increased migration, but to a different extent. However, the strongest effect on migration was observed when both fulllength Cx43 and GJA120k are expressed. suggesting that Cx43 and its short isoform GJA120k cooperatively contribute to the migrationenhancing effect of Cx43.

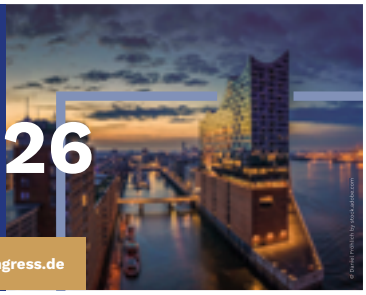

P09 Postergroup: Cation & non selective channels

P0907

How are TRPM1 channels inhibited by G proteins?

Júlia CastroMarsal; Franziska Schneider; Marc Behrendt; Raissa Enzeroth; Olaf Pinkenburg; Johannes Oberwinkler
Institut für Physiologie und Pathophysiologie, PhilippsUniversität Marburg, Marburg, Germany;

Objective: In the dendritic tips of ONbipolar cells, TRPM1 is found in a multiprotein complex together with mGluR6, which is thought to negatively regulate TRPM1 activity through G protein signaling. In the presence of light, less glutamate is released from photoreceptors, reducing the activation of mGluR6, which leads to the disinhibition of TRPM1 channels and to ONbipolar cell depolarization. Given the difficulty of studying TRPM1 channels in heterologous systems, the details of the negative regulation between mGluR6 and TRPM1 channels are still unclear.
TRPM3 channels, which are closely related to TRPM1, are inhibited by binding to Gβγ proteins, and the interaction site has been mapped in TRPM3. Interestingly, this short (10 aa) Nterminal Gβγinteracting sequence is also found in TRPM1.

Method: Using HEK293T cells for heterologous expression, we investigated TRPM1 inhibition produced by GPCR activation with wholecell patchclamping. We specifically tested the hypothesis that Gβγmediated inhibition of TRPM1 occurs by Gβγbinding to the same binding site sequence as in TRPM3.

Results: Testing different $G_{i/o}$coupled receptors, we found a larger inhibition when coexpressing TRPM1 with the morphineactivated μOR than with the glutamateactivated mGluR6. We therefore used μOR for further experiments. The nonhydrolyzable GDP analog GDPβS deactivates Gproteins. Applying this substance intracellularly reduced TRPM1 inhibition, indicating a dependence on the Gprotein activity. Furthermore, TRPM1 inhibition was abolished by the additional overexpression of a Gβγbinding peptide (βARKct), demonstrating that Gβγ subunits are responsible for TRPM1 inhibition. TRPM1 inhibition was not reduced during the intracellular application of AMPPCP, a nonhydrolyzable ATP analogue which inhibits several enzymes potentially implicated in a $G_i$regulated pathway, such as PKA or adenylate cyclase. This indicates that these downstream enzymes are not involved in TRPM1 inhibition. Importantly, a mutant TRPM1 without the Gβγinteracting sequence did not show any inhibition after μOR or mGluR6 activation. Preliminary results show that TRPM1 currents can be reduced significantly by coexpressing Gβγ subunits, but not when coexpressing $Gα_i$ or $Gα_o$ proteins.

Conclusion: In conclusion, our results suggest that TRPM1 channels are inhibited by direct interaction with Gβγ proteins on the same Gβγinteracting site that was previously identified in TRPM3.

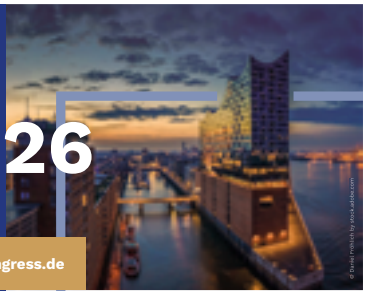

P09 Postergroup: Cation & non selective channels

P0908
Ion Selectivity of TMEM175 Channels

Jayashree Erappanakoppalu Veerabhadra; Sönke Cordeiro; Thomas Baukrowitz
Physiologisches Institut, ChristianAlbrechtsUniversität zu Kiel, Kiel, Germany;

Objective: TMEM175 is initially described as a K^+ ion channel expressed on lysosomal membranes. Structural and functional studies show the channel being also conductive for proton (H^+). The K^+ selectivity filter of TMEM175 channels is described to be distinct from the other classical potassium ion channels with their common motif (GYG) suggesting novel ionselectivity. Independent of whether the channels conduct K^+ and/or protons they are thought to play a pivotal role in lysosomal pH homeostasis. The aim of this project was to shed light on the ion selectivity of TMEM175 channels, especially on the molecular basis underlying this ion selectivity.
Method: Taking advantage of the plasma membrane localization of TMEM175 after heterologous expression, we examined its ion selectivity and proton conductance in HEK293 cells using wholecell patchclamp recordings under varying extracellular ionic and pH conditions.
Results: Extracellular acidification elicited a robust inward proton current with an activation time course of 3.81 s. Biionic measurements confirmed the cation selectivity profile of TMEM175, with $P_{Cs^+} = P_{Rb^+} > P_{K^+} > P_{Na^+}$. Most K^+ channels conduct NH_4^+ to some extent, although NH_4^+ conductance is typically similar to or lower than K+ conductance. In contrast, we found that TMEM175 conducts NH_4^+ with an approximately eightfold higher conductance than K+ and activates with a time constant 81.4 s. Because lysosomes, due to their low luminal pH, act as intracellular NH_4^+ sinks, we next examined whether TMEM175 affects cellular NH_4^+ handling. Using NH_4^+ pulse experiments, we found that heterologous expression of TMEM175 in HEK293 cells significantly alters intracellular pH responses and cellular NH_4^+ content. Finally, to define the permeation pathway for NH_4^+, we mutated residues implicated in K+ and/or proton conductance
Conclusion: We found beside their K^+ and proton conductance TMEM175 also possess a large NH_4^+ conductance. By this TMEM175 might play a significant role in lysosomal NH_4^+ homeostasis.

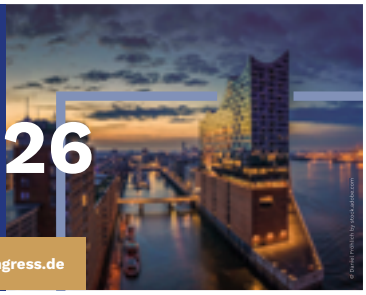

P09 Postergroup: Cation & non selective channels

P0909

The role of TRPM8 in the shaking behaviors of mammals and birds

VioletaMaria Caragea; RamonaAndreea Bivoleanu; Mirela Iodi Carstens [1]; Earl Carstens [1]; Katharina Zimmermann [2]; Tudor Selescu
Department of Anatomy, Animal Physiology and Biophysics, Faculty of Biology, University of Bucharest, Bucharest, Romania; [1] Department of Neurobiology, Physiology and Behavior, College of Biological Sciences, University of California, Davis, Davis, United States; [2] Klinik für Anästhesiologie, FriedrichAlexanderUniversität ErlangenNürmberg, Erlangen, Germany;

Objective: A common thermoregulatory behavior in mammals is shaking the body around the spinal axis, to quickly remove water from fur. This behavior is known as “wet dog shakes” (WDS). The role of the Transient Receptor Potential Melastatin 8 (TRPM8) ion channel - the main cool and cold receptor expressed in sensory nerve endings, as a trigger for WDS in wet animals, is not yet well understood. Also, there is a lack of knowledge on the shaking behavior of birds, both regarding its temperature dependence and pharmacological elicitation.
Method: Young adult Wistar rats, C57BL/6 mice (wildtype and *Trpm8/*) and Plymouth Rock chickens underwent temperaturecontrolled waterspraying tests, as well as systemic administration of the selective TRPM8 agonist Cryosim1 (33 mg/kg; intraperitoneal in rodents; subcutaneous in chickens). The following behaviors were scored: in rats and mice - WDS bouts, head or body grooming; in chickens - body and head shakes, feather ruffling, preening, and corner crowding. The consistency of spraying was verified using feedback from a thermal imaging camera, with dorsal surface temperature of the animals being recorded along the waterspraying experiments. The average dorsal temperature after waterspraying was about 13/14.5/17 °C (cold) and 35/32/30 °C (warm) in rats, mice and chickens, respectively.
Results: In rodents, a WDS bout started with the rotation of the head and neck as it propagated towards the tail. In rats, Cryosim1 and icilin elicited a comparable number of WDS bouts within 30 min (approx. 120 WDS bouts). Also in rats, waterspraying had a striking temperaturedependent effect: during the first minute after spraying, cold water evoked an average of 4.2 WDS bouts, while warm water elicited no WDS.
In mice, Cryosim1 elicited no observable behavioral changes in *Trpm8/-* animals, whereas in wildtype mice it elicited both WDS and grooming. In wildtype mice, waterspraying evoked WDS behaviors with a shorter latency at cold water, while this temperaturedependent effect was not present in *Trpm8/-* mice.
In chickens, the shake bouts were always preceded by feather ruffling. Vigorous body shaking was followed by head shaking with an amplitude of up to 180°, while the neck was extended forward and eyelids were closed. Cryosim1 elicited specific shaking behaviors in chickens, followed by crowding in the corners of the arena, in a sleeplike behavior, within 2 min after injection. The waterspraying evoked shaking was quantified by summing the shake bouts, each weighted by its timing during the first minute from spraying. This score revealed that cold waterspraying evoked more short latency shake bouts compared to warm waterspraying.
Conclusion: In conclusion, we showed that spraying animals under laboratory conditions, with temperaturecontrolled water, evokes shaking in a temperaturedependent manner in rats, mice and chickens, and chemical stimulation of TRPM8 elicits shaking behaviors in both mammals and birds.

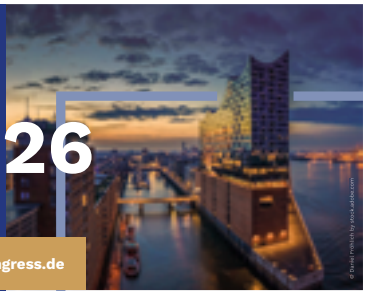

P09 Postergroup: Cation & non selective channels

P0910

Ruminal TRP channels: a comparison of mRNA expression by native tissues, primary cultures and organoids

Franziska Liebe; Saeed Khomeijani Farahani [1]; Ilka Slosarek; David Manneck [2]; Dorothee Günzel [3]; Friederike Stumpff [2]
Institute of Veterinary Anatomy, Freie Universität Berlin, Berlin, Germany; [1] Department of Human Medicine, Physiology, Medical School Berlin, Berlin, Germany; [2] Physiology, Institute for Molecular Medicine, Health and Medical University Potsdam, Potsdam, Germany; [3] Klinische Physiologie, Campus Benjamin Franklin, Charité - Universitätsmedizin Berlin, Berlin, Germany;

Objective: Previous research indicates that large quantities of Na^+, NH_4^+, Ca^{2+}, and Mg^{2+} are absorbed by the rumen of cattle and sheep, with TRPV3, TRPV4, TRPM6 and TRPM7 having emerged as likely pathways. An overview of the expression of other TRP channels and their conservation in cell cultures is lacking.
Method: Ruminal epithelium from four sheep (permit G 0087/21 and G 0098/21) was used for bulk mRNA sequencing of the native tissues („T“), or of cells cultured on inserts either after three passages in primary culture („PC“) or from organoids („OG“, 10 passages). Transcriptome analysis (RNAseq) was performed by Novogene (Cambridge, UK) using the *Ovis aries* reference genome, ARSUI_Ramb_v3.0. Values are given as median $\log_2$(FPKM+1) (25% quantile/75% quantile). Expression was assumed at $\log_2$(FPKM+1) > 0.3. For easier comparison of PC and OG to T, $\log_2$(FPKM+1) values are given in % of the value in T, with significant differences ($p<0.05$, Anova on Ranks) indicated by (*).
Results: In samples from native ruminal tissues (N=4), median $\log_2$(FPKM+1) of TRPM4, TRPM6, TRPV3, TRPV4, TRPM7, TRPV2, and TRPV6 was at 4.66 (4.56/4.71); 3.62 (3.5/3.68); 3.49 (3.41/3.6); 3.33 (3.3/3.39); 2.87 (2.84/2.91); 2.09 (2.06/2.15) and 1.25 (1.22/1.36). TRPM2 showed marginal expression at 0.56 (0.53/0.59). The values for TRPA1, TRPV1, and TRPC1 were at 0.17 (0.15/0.2), 0.16 (0.14/0.19) and 0.07 (0.06/0.08), probably reflecting noise. Expression in PC did not differ significantly from that in OG. Relative to median $\log_2$(FPKM+1) in T, TRPM6 was at 25% (PC) and 18%(OG*), TRPV4 at 134% (PC*) and 126% (OG), TRPV3 at 59% (PC*) and 73% (OG), TRPV6 at 15% (PC*) and 23% (OG), TRPM2 at 29% (PC) and 2% (OG*). TRPM4, TRPM7, and TRPV2 were nearly identical in PC, OG, and T. All other channels, including TRPV5 and TRPM8, were near zero in all three groups, except for TRPC1, which was significantly higher in OG (1.61 (1.57/1.65) and PC (1.07 (0.99/1.25)) than in T (0.07 (0.06/0.08)).
Conclusion: The expression pattern of members of the TRP channel family in the native tissue is remarkably well conserved using two different cell culture approaches. Confirming conclusions drawn from other studies, the data demonstrate robust expression of the nonselective cation channels TRPV3 and TRPV4 and the magnesium channels TRPM6 and TRPM7. Expression of the epithelial calcium channel TRPV6 was marginal. Future studies on the rumen should explore the roles of TRPM4 and TRPV2.

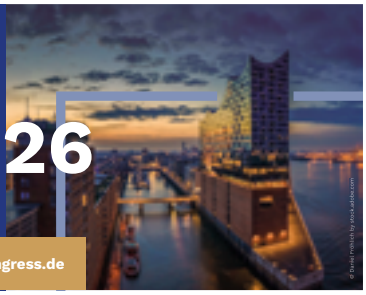

P09 Postergroup: Cation & non selective channels

P0911

An aquaglyceroporin governs cellular water and CO_2 conductance relevant for vesicular mineral formation in a marine animal model

Marian Hu
Physiologisches Institut, ChristianAlbrechtsUniversität Kiel, Kiel, Germany;

Objective: Many organisms ranging from protists to vertebrates and humans generate $CaCO_3$ biominerals involving endocytotic uptake of extracellular fluids. These fluids are modified within endocytotic vesicles to produce an amorphous mineral precursor that is exocytosed to form mineralized structures. In this process, water must be removed from endocytotic vesicles and the cell to promote concentration of calcification substrates and production of a waterfree mineral.
Method: In this work we used a suite of methods ranging from whole animal experiments over molecular and biochemical analyses to heterologous characterizations of channel proteins. Whole animal experiments were used to study the effect of spAQP9 inhibition and morpholino knockdown on skeletogenesis. Gene expression analyses, in situ hybridization and single cell transcriptomics were used to study spatiotemporal expression patterns of spAQP9 along the early embryonic development. Immunocytochemistry using a custom made antibody was performed to identify the subcellular localization of the channel. Finally, heterologous expression of spAQP9 in xenopus oocytes was used to study the water and CO_2 permeability of this channel.
Results: Using the sea urchin larva as a marine model system we demonstrate that the aquaglyceroporin (spAQP9) is involved in the cellular calcification process. spAQP9 is found exclusively in the calcifying primary mesenchyme cells (PMCs) and mineralization is associated with increased spAQP9 expression underlining its role in skeleton formation. Heterologous expression of sp*AQP9* in *Xenopus laevis* oocytes demonstrated that this channel conducts water and carbon dioxide. The water conductance by spAQP9 is sensitive to phloretin with an IC_{50} of ~38 µM and treatment of larvae with phloretin or knockdown of spAQP9 impaired skeleton formation. Immunohistological analyses revealed localization of spAQP9 in vesicles with different subcellular distribution depending on the calcification activity of PMCs. Finally, we developed an *invivo* assay to measure cellular and vesicular water permeability in PMCs and found a significant water permeability of the plasma membrane and membranes of calciumrich vesicles.
Conclusion: The results of this work highlight the importance of water transport mechanisms in the mineralization process. Translocation of water channels like spAQP9 into vesicular structures may represent an important feature to remove water from endocytotic vesicles. Here aquaporins like spAQP9 can represent key players that serve a dual function as a water and CO_2 conductance pathway and thereby can support ion concentration and carbon transport, two processes that are of fundamental importance to promote intracellular mineral precursor formation.

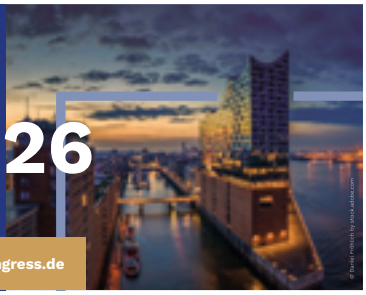

P09 Postergroup: Cation & non selective channels

P0912

Mutations causing autosomal dominant polycystic kidney disease (ADPKD) differentially affect the formation and function of heteromeric polycystin2/polycystin1 ion channels

Tobias Staudner; Bardha Azemi; Frauke Wagner; Linda Geiges; Christoph Korbmacher; Alexandr V. Ilyaskin
Institut für Zelluläre und Molekulare Physiologie, FriedrichAlexanderUniversität ErlangenNürnberg, Erlangen, Germany;

Objective: ADPKD is caused by mutations in *PKD1* and *PKD2*, encoding polycystin1 (PC1) and polycystin2 (PC2). PC2 alone can form homotetrameric ion channels, but when coexpressed with PC1, it preferentially forms heterotetrameric PC2/PC1 channels with a 3:1 stoichiometry. The physiological role of polycystins as ion channels is still unclear, but altered ion channel function of mutant polycystins may contribute to the pathophysiology of ADPKD. The aim of this study was to systematically investigate the impact of distinct pathogenic mutations on the assembly and function of heteromeric PC2/PC1 channels.
Method: Established gainoffunction (GOF) constructs for homomeric PC2 channels (Wang et al., *EMBO Reports*, 2019) and heteromeric PC2/PC1 channels (Staudner et al., *FEBS Letters*, 2025) were heterologously expressed in *Xenopus laevis* oocytes and analyzed using twoelectrode voltage clamp technique. Complex formation was assessed by coimmunoprecipitation.
Results: Our electrophysiological approach, based on measurements of reversal potentials and divalent cationmediated current inhibition, allowed assessment of the impact of Cterminal truncations in PC2 and PC1 on PC2/PC1 heteromerization efficiency. Interestingly, truncating mutations impaired the assembly of functional PC2/PC1 channels to different degrees depending on the length of the deleted fragment in PC2 (R742X>Y836X>R872X; n=2545; p<0.0001; ANOVA) or PC1 (E4128X>C4208X; n=3047; p<0.0001; ANOVA). These functional results were consistent with biochemical analysis of PC2/PC1 complex formation (n=23). In contrast, Cterminal truncations of PC2 had no effect on homomeric PC2 channel formation and function. Indeed, maximal currents mediated by truncated PC2GOF constructs were similar to those of control PC2GOF channels without truncation (e.g., R742X: 6.0±3.2 µA, n=62; control: 6.1±3.0 µA, n=37; mean ± SD; p=0.7542; MannWhitney). Furthermore, pathogenic mutations in the PC2 pore region (F629S, C632R, R638C) or disrupting a critical disulfide bond in the extracellular TOP domain of PC2 (C331S) reduced cation conductance of heteromeric PC2/PC1 channels without preventing complex assembly.
Conclusion: Taken together, our data demonstrate that ADPKD mutations differentially affect the formation and function of heteromeric PC2/PC1 ion channels, underscoring their pathophysiological relevance. Therefore, the development of mutationspecific strategies to restore impaired PC1/PC2 ion channel function may open new therapeutic perspectives.

P09 Postergroup: Cation & non selective channels

P0913

Increased Ca^{2+} influx and altered cell signaling in HEK 293 cells expressing the TRPV4 mutant E278K

Jian Hasan; Julia Liekfeldt [1]; Philipp Lutze [1]; Mirjam Krautwald; Martin Landsberger [2]; Heinrich Brinkmeier [1]
Institute of Pathophysiology, University Medicine Greifswald, Greifswald, Germany; [1] Institute of Physiology, University Medicine Greifswald, Greifswald, Germany; [2] Hochschule Fresenius Heidelberg, Heidelberg, Germany;

Objective: Missense mutations in the gene coding for the mechanosensitive cation channel TRPV4 can cause skeletal dysplasias and peripheral neuropathies in humans. Though it is likely that altered Ca^{2+} influx through the mutant channels play a role for disease pathology in some cases, the precise pathomechanisms of most of the TRPV4 mutations are still unknown. To study the cell physiological function of the TRPV4 mutant E278K, YFPtagged mutant and the wildtype (WT) TRPV4 proteins were expressed in HEK 293 cells using an inducible promotor system (FlpIn™ TREx™ , Invitrogen).
Method: Cell growth and viability were studied and intracellular Ca^{2+} concentrations monitored with the fluorescent Ca^{2+} indicator Fura2. TRPV4 gene expression, detectable by YFP fluorescence was reproducibly induced by the addition of 0.01 µM doxycycline to the culture medium.
Results: After 24 h of induction, cytoplasmic Ca^{2+} concentrations (given as Fura2 fluorescence ratios, excitation: 340/380 nm) were increased in cells expressing the TRPV4 mutant E278K (1.15 ± 1.12; WT: 0.45 ± 0.05; means ± STD). The rise of $[Ca^{2+}]_i$ could be widely reverted by application of 1 µM of the specific TRPV4 channel blocker HC067047 (ratio: 0.62 ± 0.1). In both cell lines cytoplasmic Ca^{2+} concentrations rose within 5 min to a plateau in response to the TRPV4 activator GSK1016790A (GSK101, 40 nm). Only in cells expressing the TRPV4 WT channel, the PCK activator PMA (0.1 µM) caused a marked increase of $[Ca^{2+}]_i$, while the PCK inhibitor Gö6976 (5 µM) reduced $[Ca^{2+}]_i$ to basal levels in both cell lines. Pharmacological stimulation of TRPV4 channels and rise of $[Ca^{2+}]_i$ by GSK101 was still possible. Calmidazolium (CDZ, 2 µM), a synthetic calmodulin inhibitor caused a similar effect as shown for Gö6976. $[Ca^{2+}]_i$ was reduced to basal levels in both cell lines, but in the presence of CDZ stimulation of TRPV4 channels by GSK101 was not possible. Further studies on signal transduction pathways using a Rho kinase inhibitor and a RhoA inhibitor did not show consistent effects. In addition to the increased $[Ca^{2+}]_i$, cells expressing the E278K mutant showed a tendency to detach from the surface of the culture dish after 24 h of induction of gene expression. After 72 h, 90% of the cells were found in the supernatant, while only 12% of the cells expressing the WT channel showed this behaviour. Cell rounding and detachment could be completely inhibited by addition of 2 µM HC067047.
Conclusion: We conclude that the TRPV4 missense mutation E278K causes gain of function of the channel leading to increased cytoplasmic calcium levels in HEK 293 cells and further to cell rounding and detachment. This is most likely caused by Ca^{2+} induced effects on the cytoskeleton or by altered gene expression of cytoskeletal proteins. Furthermore, the described phenotype of TRPV4E278K expressing cells requires basal levels of PCK activity and the Ca^{2+}/calmodulin signal transduction pathway.

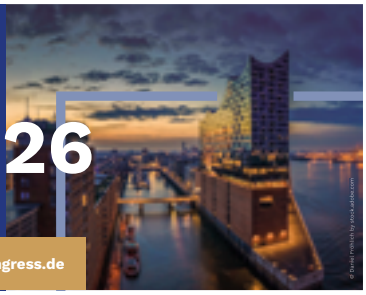

P09 Postergroup: Cation & non selective channels

P0914

Salivary gland organoids as a model to study claudin10bdependent ion transport and fluid secretion

Evgeniya Kochina; Maryl Brandy Sielatchom Foyang; Arnold Tsamo Tetou [1]; Friederike Stumpff [2]; Dorothee Günzel
Klinische Physiologie, Campus Benjamin Franklin, Charité - Universitätsmedizin Berlin, Berlin, Germany; [1] Klinik für Nieren- und Hochdruckerkrankungen, Zentrum für Innere Medizin, Medizinische Hochschule Hannover, Hannover, Germany; [2] Physiology, Institute for Molecular Medicine, Health and Medical University Potsdam, Potsdam, Germany;

Objective: Claudin10b (Cldn10b) is a tight junction protein involved in paracellular ion transport in epithelial tissues. Mutations in *CLDN10B* cause HELIX syndrome, a rare disorder associated with hypohidrosis, electrolyte imbalance and salivary gland dysfunction. Since salivary secretion depends on tightly regulated ion and fluid transport processes, we investigated the role of Cldn10b in salivary gland epithelial physiology using organoidbased models.
Method: Salivary gland organoids were generated from inducible Cldn10b knockout (C10b iKO) mice and cultured both as 3D Matrigel structures and as 2D monolayers on permeable supports. Functional characterization was performed using Ussing chamber recordings together with a novel intraluminal potential measurement technique allowing realtime electrophysiological assessment in intact 3D organoids. Live imaging was performed to demonstrate secretory lumen swelling responses.
Results: Immunofluorescence staining confirmed the presence of acinar, ductal, myoepithelial and progenitor cell populations within the organoids. Tamoxifeninduced deletion of Cldn10b resulted in reduced transcript and protein expression, confirming efficient knockout induction. Electrophysiological analyses revealed altered responses in C10b iKO organoids compared to controls in both Ussing chamber and intraluminal potential measurements, supporting a role for Cldn10b in epithelial ion transport. In addition, bulk RNA sequencing was performed to identify molecular pathways affected by Cldn10b deficiency.
Conclusion: Overall, this study establishes salivary gland organoids as a physiologically relevant platform for investigating epithelial transport mechanisms and demonstrates the importance of Cldn10b for normal salivary gland function. The integration of intraluminal potential recordings with conventional electrophysiological approaches provides a complementary strategy to study bioelectrical properties of epithelial organoids and may contribute to a better understanding of HELIX syndrome pathophysiology.

P09 Postergroup: Cation & non selective channels

P0915
A unique claudin2 transmembrane interface enables increased strand dynamics

LauraSophie Beier; Xian Shi [1]; Felix Odhiambo Otenga [2]; Gilles Carpentier [3]; Patrick M. Marsch [2]; Michael J. Grey [4]; Shikha Nangia [2]; Jerrold R. Turner [1]
Physiologisches Institut, ChristianAlbrechtsUniversität Kiel, Kiel, Germany; [1] Department of Pathology, Laboratory of Mucosal Barrier Pathobiology, Brigham and Women's Hospital and Harvard Medical School, Boston, United States; [2] Department of Biomedical and Chemical Engineering, Syracuse Biomaterials Institute, Sysracuse University, Syracuse, United States; [3] Laboratoire GlyCRRET, Faculté des Sciences et Technologie, Université Paris Est Créteil Val de Marne, Créteil, France; [4] Department of Medicine, Division of Gastroenterology, BethIsreal Deaconess Medical Center and Harvard Medical School, Boston, United States;

Objective: Claudins are critical for epithelial homeostasis and the formation of selectively permeable barriers. Claudins 2 and 15 form paracellular cation channels that are essential for nutrient absorption within the intestine. While knockout of both claudins results in death due to malabsorption, deletions of either one claudin are viable, indicating compensation and functional redundancy. Yet, their expression is differentially regulated during development and in disease, suggesting unique properties of either claudin 2 or 15 to meet tissuespecific needs.

We hypothesize that differences in the molecular interactions underlying claudin2 and 15 assembly contribute to strand dynamics and may explain the distinct expression patterns in development and disease.
Method: We used sequence alignments and structural predictions to compare claudins 2 and 15. To mimic tissue development, cellular migration assays were conducted. Claudin assembly was imaged using superresolution (STED) microscopy and manipulated by sitedirected mutagenesis. Channel conductivity was assessed by measuring transepithelial electrical resistance. Strand dynamics were observed in fluorescence recovery after photobleaching and pulsechasepulse assays.
Results: We identified an intermolecular interface between the second and third transmembrane helices of claudin2, anchored by an evolutionarily conserved glutamine residue at position 81, that is absent in claudin15 and all other claudins examined. This interface contributes to claudin assembly, paracellular channel conductivity and strand dynamics through separable mechanisms, providing the first demonstration that claudin channel function does not require polymerization. Substitution of three interface residues converts claudin2 strand dynamics to those of claudin15, providing evidence that molecular mobility within the tight junction is an intrinsic property of the claudin sequence.
Conclusion: Here, we defined a previously unrecognized interface that confers unique properties to claudin2. The findings challenge the prevailing assumption that claudins, while having remarkable sequence homology, also share interchangeable structural mechanisms. This provides a structural framework to understand the apparent functional redundancy of claudins 2 and 15 within the context of cellular requirements during development and in disease

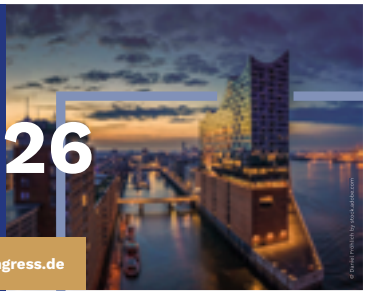

P10 Postergroup: Skeletal Muscle

P1001

Characterizing the in vivo structurefunction relationship of Iband titin compliance to skeletal muscle contraction performance using realtime, smallangle Xray diffraction resolved to 5 ms

Anthony Hessel; Cameron Hill [1]; Weikang Ma [2]; Charles Chung [3]
Institute of Physiology II, University Hospital Muenster, Münster, Germany; [1] Randall Centre for Cell & Molecular Biophysics, King's College London, London, United Kingdom; [2] Department of Biology, Illinois Institute of Technology, Chicago, United States; [3] Department of Physiology, Wayne State University, Detroit, United States;

Objective: Skeletal muscle contraction is not merely an allornothing response but is instead regulated by various sarcomeric proteins. The titin protein is a long filament that extends across the halfsarcomere as a freelyextensible viscoelastic element between the thin and thick filaments in the Iband, and runs along the thick filament backbone in the Aband. Current evidence points towards a role for Iband titin as a regulator of contractile performance, partially determined by the viscoelastic properties. To explore this feature, we studied intact rat extensor digitorum longus (EDL) muscle with a spontaneous global knockout of RBM20, leading to a longer and more compliant Iband titin.
Method: Intact EDL was harvested from homozygote and wildtype RBM20 KO rats and immediately used. Twitch and maximal tetanus contractions were produced in parallel with timeresolved (5 ms frames) muscle smallangle Xray diffraction (MyoXRD) to track thick filament structures. MyoXRD is a powerful technique where muscle tissue is exposed to powerful Xrays beams generated at particle accelerators (synchrotrons), which scatter off the organized sarcomeric proteins and produce a diffraction pattern. Diffraction patterns provide details about the configurations of the muscle motor proteins in real time during the experiments in vivo, allowing for clear timeresolved, structurefunction characterization of titin during contraction.
Results: Results indicate that homozygous muscle presents mechanical and structural signatures of impaired thick filament activation, and this is more pronounced in twitch than in tetanus. We further report on the activationdependence of the Aband titinbased ~3.9 nm reflection (e.g., M11) that arises in the Czone from periodic titin kinks, though to stabilization of some myosin heads in the docked / OFF configuration. We report that the titin M11 reflections undergo a noticeable change with activation, where one periodicity disappears (~3.90 nm) while another emerges (~3.97 nm), in relation to the relative activation state, suggesting an activationdependent change in the Aband titin configuration.
Conclusion: TOur results demonstrate that modifying Iband viscoelastic properties can alter contraction performance by regulating, but not impairing, thick filament contraction machinery. Iband titin compliance can be altered in healthy and diseased muscles via acute and chronic pathways. Evidence from this current study uncovers the mechansims by which titin can regulate contraction performance in healthy systems, and as well as why even a small mutation to Iband titin can cause dibelitating myopathies.

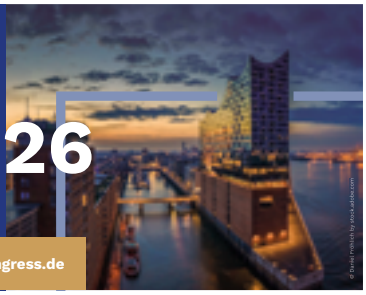

P10 Postergroup: Skeletal Muscle

P1002

Concentric- and eccentricbiased exercise training induce distinct proteomic phenotypes in rat soleus muscle

Stefan Braun
Molecular Muscle and Exercise Physiology, University of Bayreuth, Kulmbach, Germany;

Objective: Concentric (CON) and eccentric (ECC) muscle loading are two distinct forms of muscle activity, where in concentric movement the muscle is shortening against external load, while eccentric movement involves lengthening of the muscle against load that is typically too high to handle with muscle contraction itself. These loading modalities play a key role in muscle adaptation and have been widely implemented in training as well as therapeutic conditioning. We established a rat training model to compare proteomic adaptations to level versus downhill running.
Method: Rats were assigned to sedentary control (CTRL), level running (LEV; 1° incline/nearlevel condition; concentricbiased) or downhill running (DH; −20° decline; eccentricbiased). Training was performed for 60 min/day over 6 weeks. After training, rats were euthanized according to institutional animalwelfare approval, and hindlimb muscles as well as heart were collected. Soleus muscle samples were processed for proteomic analysis. Differentially abundant proteins (DAPs) were identified between groups (n = 3/group; Student's ttest), followed by Gene Ontology Biological Process enrichment analysis (GO:BP).
Results: Compared with CTRL, there were 479 significant ($p<0.05$) DAPs in the DH and 109 in the Lev group with 71 of these DAPs shared among the two exercise modalities. GO:BP analysis indicated a DHspecific enrichment of proteins associated with extracellular matrix organization, cell adhesion and force transmission. In contrast, proteins linked to mitochondrial biogenesis, oxidative metabolism and muscle development were less represented among DHassociated changes compared with LEVassociated changes.
Conclusion: Together, these data suggest that distinct muscle contraction modalities induce a distinct adaptive response in skeletal muscle. While CON muscle activity had a general lower effect on DAPs compared to CTRL than ECC muscle activity. DH running rats were especially enriched in proteins involved in connective tissue remodelling and inflammatory processes. This suggests, that ECC loading induces the development of ECM to make the loaded muscle more resilient against muscle damage induced by the lengthening effect of running downhill by passively increasing the rigidity and therefore decreasing the load passed onto the muscle tissue itself.

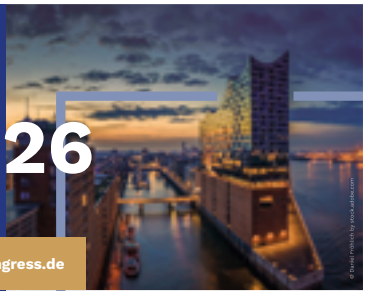

P10 Postergroup: Skeletal Muscle

P1003

Glycogenolytically derived ATP is essential for Ca^{2+} transients in skeletal muscle fibres

Niels Ørtenblad; Daniel Andersson [1]; Joachim Nielsen
Department of Sports Science and Clinical Biomechanics, University of Southern Denmark, Odense, Denmark; [1] Department of Physiology and Pharmacology, Department of Physiology and Pharmacology, Karolinska Institutet, Stockholm, Sweden;

Objective: Low muscle glycogen content impairs muscle function and is associated with deficits in excitation–contraction (E–C) coupling, including reduced membrane excitability and sarcoplasmic reticulum Ca^{2+} release. However, these findings are primarily associative, and the direct role of glycogenolytically derived ATP in E–C coupling remains unclear. Here we aimed to determine the direct effect of glycogen availability on cytosolic free Ca^{2+} concentration ($[Ca^{2+}]i$) in single muscle fibres using specific inhibitors of glycogen phosphorylase (GP).
Method: Single collagenasedissected fibres from mouse flexor digitorum brevis muscles were stimulated with 350 ms tetani at 15–150 Hz, and $[Ca^{2+}]i$ measured using Indo1. Glycogen availability was manipulated using two distinct GP inhibitors, 1,4dideoxy1,4iminoDarabinitol (DAB, 1 mM) and CP316,819 (40 µM). Measurements were performed in both independent fibres and paired experiments comparing control conditions with subsequent GP inhibition.
Results: GP inhibition caused a significant decrease in $[Ca^{2+}]i$ at all stimulation frequencies, with no effect on resting $[Ca^{2+}]i$. $[Ca^{2+}]i$ (mean±SD) was reduced to 40±38% (CP, n=40) and 41±39% (DAB, n=17) at 20 Hz, and to 79±45% (CP) and 73±22% (DAB, n=17) at 150 Hz. Notably, 58% of DABtreated fibres were nonresponsive to stimulation. Similar findings were obtained in paired experiments (DAB, n=12; CP, n=15).
Conclusion: These findings provide direct evidence that glycogenolytically derived ATP is essential for normal cytosolic Ca^{2+} transients, likely via effects on membrane excitability and/or SR Ca^{2+} release. The greater impairment at lower stimulation frequencies suggests a direct effect on SR Ca^{2+} release mechanisms.

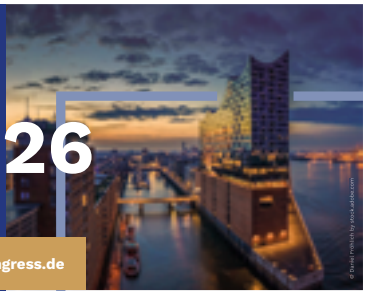

P10 Postergroup: Skeletal Muscle

P1004

Temporal transcriptomic remodeling of skeletal muscle following femoral artery ligation in normal and high fat diet mice

Emmanouella Michaela Xanthopoulou; Emily Shorter [1]; Liu Zhengye; Estela Santos Alves; Minying Cui; Baptiste Jude [2]; Ferdinand von Walden [2]; Johanna Lanner [1]
Department of Physiology and Pharmacology, Karolinska Institutet, Stockholm, Sweden; [1] Department of Physiology, Nutrition and Biomechanics, Swedish School of Sport and Health Sciences, Stockholm, Sweden; [2] Department of Women's and Children's Health, Karolinska Institutet, Stockholm, Sweden;

Objective: Peripheral artery disease (PAD) is a frequent complication of type 2 diabetes. The condition arises from reduced limb perfusion causing ischemia and progressive skeletal muscle impairment which is further aggravated by diabetesassociated metabolic stress. Current treatments aim to restore perfusion but do not fully recover muscle function, highlighting the need to better understand mechanisms driving PADrelated myopathy. While femoral artery ligation (FAL) is a wellestablished mouse model to study PAD, it is still unclear how ischemic skeletal muscle changes over time after injury and how metabolic stress affects these changes at the transcriptomic level.
Method: In the present study, adult female C57BL/6J mice, maintained on a normal diet (ND) or highfat diet (HFD) underwent unilateral femoral artery ligation. Anesthesia was induced with isoflurane (3–4%) and maintained at 1–3% delivered via a precision vaporizer. Gastrocnemius muscle was collected at 3 days, 1 week, 2 weeks, and 4 weeks postFAL, alongside muscles from dietmatched control mice. Bulk RNA sequencing was performed, followed by differential gene expression analysis using DESeq2, Gene Ontology pathway enrichment using EnrichR, and celltype deconvolution using CIBERSORTx with a published singlecell reference dataset (McKellar et.al. 2021).
Results: Our results demonstrate that femoral artery ligation induces a robust and highly timedependent remodeling of skeletal muscle at the transcriptomic level. Early responses (3 days to 1 week postFAL) are characterized by increased inflammation and impaired metabolic and mitochondrial programs. Over time, the muscle gradually reorganizes and recovers, returning toward a controllike state by 4 weeks after FAL. While this recovery pattern is observed in both normal diet and highfat diet mice, recovery in HFD mice appears delayed, with more sustained alterations in gene expression.
Conclusion: While diet seems to modulate the magnitude of early transcriptomic responses as well as recovery, the overall trajectory of transcriptomic regulation, pathway enrichment, and cell type composition is largely conserved between normal- and highfat diet mice, indicating that time after injury is the primary driver of postischemic muscle adaptation in the FAL mouse model of PAD.

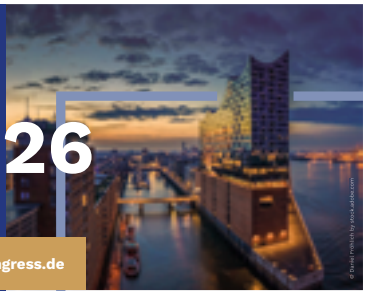

P10 Postergroup: Skeletal Muscle

P1005

Fibertypespecific phenotypes in skeletal muscle during earlystage inflammatory myopathy

Cecilia Leijding; Kristofer M Andreasson [1]; Yi Zhong; Victoria L Wyckelsma; Marta Murgia [2]; Tomas A Schiffer; Maryam Dastmalchi [1]; Stefan M Reitzner; Carl Johann Sundberg; Helene Alexanderson [1]; Takashi Yamada [3]; Mattias Carlström; Volker M Lauschke; Stefano Gastaldello; Daniel Andersson
Physiology and Pharmacology, Karolinska Institutet, Stockholm, Sweden; [1] Dept of medicine, Solna devision of Rheumatology, Karolinska Institutet, Stockholm, Sweden; [2] Dept of Biomedical Science, University of Padova, Padova, Italy; [3] Graduate school of Biomedical and Health Science, Hiroshima University, Hiroshima City, Japan;

Objective: Idiopathic inflammatory myopathies (IIM) are characterized by skeletal muscle weakness and accelerated fatigue, yet the mechanisms underlying muscle dysfunction remain poorly understood. This study investigates how type I and type II muscle fibers are differently affected in earlystage IIM.
Method: Muscle biopsies from patients with recentonset IIM and healthy controls were manually dissected into type I and type II muscle fibers and analyzed using mass spectrometrybased proteomics to identify fibertype specific molecular alterations. To further explore disease fibertype dependent molecular and physiological mechanisms, type I phenotypic muscles (m. soleus; SOL), and type II phenotypic muscles (m. extensor digitorum longus; EDL*),* from an experimental autoimmune myositis (EAM) mouse model or control mice were analyzed. EAM mice and controls were 6–8weekold female BALB/cAnNRj mice. Mice were immunized tailbase–wise with rat skeletal muscle myosin under sedation with 2% isoflurane mixed with oxygen. For muscle isolation, mice were sacrificed by cervical dislocation, and muscles were immediately isolated.
Results: Proteomic analyses showed molecular differences between IIM and control, with different responses in type I and II fibers across key signaling pathways. Mitochondriarelated pathways were extensively downregulated in type II fibers, while type I fibers showed comparatively preserved mitochondria. Type II fibers displayed aberrant expression of sarcomere proteins, typically not expressed in type II fibers. Interferon signaling pathway was upregulated in type II but not in type I fibers. Moreover, the EAM model displayed muscle weakness, increased fatigue, and altered expression of mitochondrial proteins in the type II dominant EDL muscles.
Conclusion: This study identifies muscle fibertype specific phenotypes in earlystage IIM, demonstrating that type II are more affected than type I fibers. The main disease mechanisms that affects type II muscle fiber include mitochondrial dysfunction, impaired contractile function and exacerbation of inflammatory signaling. These findings give new insight into mechanisms in earlystage IIM pathogenesis.

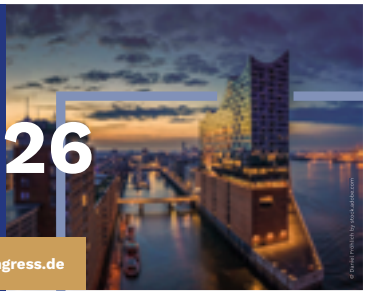

P10 Postergroup: Skeletal Muscle

P1006

When is enough enough? Biopsy number and reliability of MHC composition in human skeletal muscle

Rasmus Jensen; Joachim Nielsen; Peter Plomgaard [1]; Niels Ørtenblad
Department of Sports Science and Clinical Biomechanics, University of Southern Denmark, Odense, Denmark; [1] Centre for Physical Activity Research, Copenhagen University Hospital, København, Denmark;

Objective: Myosin heavy chain (MHC) distribution, quantified by gel electrophoresis of needle biopsy samples, is the gold standard for characterising skeletal muscle fibre type composition. Little is known about how the estimate improves when additional biopsies are obtained. Here we quantified the reliability of MHC composition estimates as a function of biopsy number using a leaveout design.
Method: Withinsubject variability was assessed in 6 biopsies from each of 11 male subjects (n = 66 biopsies total), obtained before, during, and after cycling to exhaustion from both legs. MHC distribution was determined by SDSPAGE with Coomassie staining. Reliability of singles, duplicates, and triplicates was quantified using a leaveout design, with agreement against an independent criterion from the remaining biopsies expressed as CV and mean absolute deviation. ICC(1,k), SEM, and MDC95 were derived from a oneway randomeffects model and extrapolated using the SpearmanBrown formula.
Results: Mean (95% CI) MHC composition was 48.7% (44.2–53.1), 43.3% (38.4–48.2), and 8.1% (5.8–10.3) for MHCI, MHCIIa, and MHCIIx. CV for single biopsies was 13.8%, 13.4%, and 64.3%, improving to 5.8%, 5.6%, and 26.9% for triplicates. ICC(1,k) for singles was 0.44, 0.63, and 0.34, improving to 0.70, 0.83, and 0.61 for triplicates. SEM for a single biopsy was 7.4, 5.8, and 4.5%point, with MDC95 of 20.6, 16.2, and 12.5%point; triplicates reduced MDC95 to 11.9, 9.3, and 7.2%point for MHCI, MHCIIa, and MHCIIx, respectively (mixed model). The largest single absolute deviation was 24.4%point for MHCI and 15.6%point for MHCIIa from a single biopsy. The right leg contained 3.4%point more MHCIIa than the left (P = 0.01). MHC distribution was unaffected by exercise (P = 0.71, 0.24, 0.31).
Conclusion: The precision of MHC composition estimates improves markedly when averaging more than one biopsy, with the greatest gain achieved by moving from a single biopsy to two. The SEM and MDC95 reported here provide an empirical basis for biopsynumber decisions in study design.

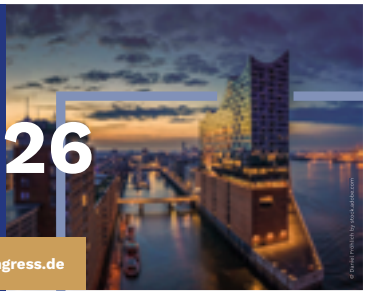

P10 Postergroup: Skeletal Muscle

P1009

Effect of exercise intensity on nextday subcellular glycogen distribution in human skeletal muscle

Joachim Nielsen; Camilla T. Schytz; Mathias D.H. Jensen; Niels Ørtenblad; Kasper D. Gejl
Department of Sports Science and Clinical Biomechanics, University of Southern Denmark, Odense, Denmark;

Objective: The subcellular localization of glycogen particles influences skeletal muscle function in humans. In particular, intramyofibrillar glycogen has been associated with ion handling in ex vivo preparations and endurance performance in vivo. However, it remains unknown whether glycogen distribution can be altered on a daily timescale. This study tested the hypothesis that high exercise intensity mediates a nextday redistribution of glycogen toward the intramyofibrillar compartment.
Method: Nine healthy men aged 22–26 years completed a randomized crossover design with three days of standardized training and diet, followed by a baseline muscle biopsy on day 4 before either a lowintensity (15 min at 40% Wmax) or highintensity (8 × 30 s at 150% Wmax) exercise bout. A second biopsy was obtained the following day (nextday). Subcellular glycogen localization was assessed using transmission electron microscopy.
Results: Exercise intensity did not affect nextday glycogen localization. In the lowintensity trial, intramyofibrillar glycogen content (% of total glycogen; mean [95% CI]) was 7.4 [6.5–8.3] and 10.9 [9.1–12.7] at baseline and nextday, respectively, while corresponding values in the highintensity trial were 7.7 [6.4–9.0] and 9.9 [8.2–11.6]. By bootstrapping, the change from baseline to nextday was 3.4 [1.9–5.3] and 2.3 [0.7–5.0] in the low- and highintensity trials, respectively. The betweentrial difference in change was −1.1 [−4.4 to 2.0]. Across trials, the change was 2.8 [1.1–4.7].
Conclusion: In conclusion, exercise intensity did not affect nextday glycogen localization. However, intramyofibrillar glycogen content increased from baseline to nextday, suggesting that factors independent of exercise intensity may regulate glycogen redistribution on a daily timescale.

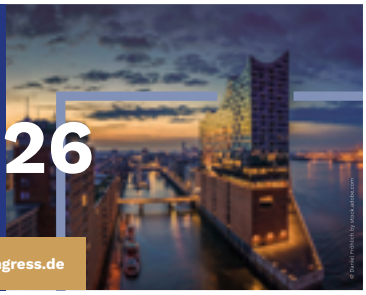

P10 Postergroup: Skeletal Muscle

P1010

Temperature dependence of actin and thin filament sliding along cardiac alpha- and betamyosin molecules

Marina Zefi; Petra Uta; Theresia Kraft; Tim Scholz
Institute of Molecular and Cell Physiology, Hannover Medical School, Hannover, Germany;

Objective: Different isoforms of striated muscle myosinII motor proteins such as cardiac alpha- and betamyosin are generally considered to have distinct functional properties such as actin filament sliding velocity. Alphamyosin is regarded the fast and betamyosin the slow postnatal cardiac myosin isoform. However, in many species both myosin isoforms can work friendly together in mixed myocardial tissue apparently without interfering with each other's function.
Due to experimental limitations such as increasing protein, myofibril or myocyte damage, only few data exist regarding alpha- and betamyosin velocities at higher temperatures. This raised the question whether alpha- and betamyosin might move actin with approximately equal velocity at body temperature.
Method: We used myosin extracted from porcine atrial and ventricular myocardium to gain mainly alpha- and betamyosin preparations and compared their actin sliding velocities in an in vitro motility assay, in which fluorescently labelled actin or thin filaments are moved in the presence of ATP by surfaceimmobilized myosin molecules.
Results: Varying the temperature between 15 and porcine body temperature of 39°C, we found that with increasing temperature the difference between actin sliding velocities on alpha- and betamyosin decreased progressively. While at 15°C, a temperature often used in muscle fiber, cell, or myofibril experiments, atrial myosin moved actin filaments with 0.638 µm/s almost fivetimes faster than ventricular betamyosin with 0.129 ± 0.024 µm/s, approaching body temperature of 39°C this difference decreased to 1.3fold faster movement on alphamyosin (13.972 ± 1.872 vs. 9.214 ± 0.753 µm/s). As not unregulated actin filaments but native thin filaments are the physiological interaction partner of myosin we also tested the temperature dependence of cardiac thin filament sliding velocities and found a comparable progressive decrease of speed differences with increasing temperature.
Conclusion: We conclude that at physiological temperature cardiac alpha- and betamyosin move actin with almost equal velocity which suggests that in mixed myocardial tissue both myosin isoforms could work together without interfering with each other's function.

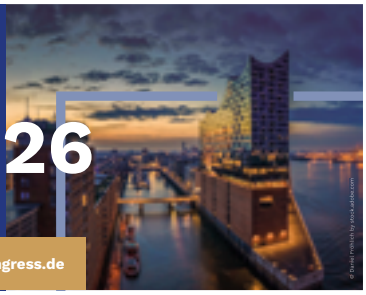

P10 Postergroup: Skeletal Muscle

P1011

Blockage of autophagy causes severe skeletal muscle disruption in a mouse model for myofibrillar myopathy 6

Kerstin Filippi; Kathrin GrafRiesen; Maithreyan Kuppusamy [1]; Andreas Unger [2]; Kenichi Kimura [3]; Martin Matijass [1]; Henrique Baeta [1]; Magdalena Podlacha [4]; Daniel Haertter [5]; Martin Wiemann; Grzegorz Wegrzyn [4]; Cornelia Kornblum [6]; Jens Reimann [6]; Wolfgang A. Linke [2]; Pitter F. Huesgen [1]; Wolfram S. Kunz [7]; Bernd K. Fleischmann; Michael Hesse Institute of Physiology I, University Hospital Bonn, Bonn, Germany; [1] Central Institute for Engineering, Electronics and Analytics (ZEA), Forschungszentrum Jülich, Jülich, Germany; [2] Institut für Physiologie II, Universitätsklinikum, Westfälische WilhelmsUniversität Münster, Münster, Germany; [3] University of Tsukuba, Ibaraki, Japan; [4] Department of Molecular Biology, University of Gdansk, Gdansk, Poland; [5] Institute of Pharmacology and Toxicology, University Medical Center Göttingen, Göttingen, Germany; [6] Department of Neurology, University Bonn Medical Center, Bonn, Germany; [7] Institute of Experimental Epileptology and Neurocognition, University Bonn Medical Center, Bonn, Germany;

Objective: Patients carrying the BAG3 mutation p.P209L (c.626C>T) develop severe myofibrillar myopathy (MFM6) and neuropathy. MFM6 is characterized by rapidly progressive muscle dystrophy in childhood and restrictive cardiomyopathy, limiting life expectancy to approximately 20 years. BAG3, as part of the chaperoneassisted selective autophagy (CASA) complex, plays a critical role in muscle protein turnover.
Method: To elucidate the pathomechanism of the skeletal muscle phenotype, we utilized a humanized mouse model overexpressing a BAG3_P209LGFP fusion protein under the ubiquitous CAG promoter.Skeletal muscle function was assessed by in vivo and ex vivo force measurements, while histological, proteomic, and transcriptomic analyses were performed to characterize structural and molecular alterations. In addition, autophagic flux and mitochondrial integrity were investigated using complementary in vitro and in vivo approaches.
Results: The CAGBAG3_P209L mice displayed reduced body weight and pronounced skeletal muscle weakness, with significant deficits in maximal force development. Histological analysis revealed sarcomere disintegration, extensive inflammation, protein aggregation, and increased number of centralized nuclei. Proteomic and transcriptomic profiling indicated impaired protein homeostasis, elevated protein synthesis, loss of sarcomeric proteins, and dysregulation of autophagyrelated pathways. Followup in vivo and in vitro analyses further demonstrated a severe blockage of autophagic flux as central disease mechanism. The imbalance between protein degradation and synthesis suggests an inadequate compensatory response. Mitochondria were also morphologically and functionally altered, likely as a secondary consequence and contributing to muscle dysfunction.To assess therapeutic potential, we delivered shRNA targeting hBAG3 via AAV/rh10 into skeletal muscle at postnatal day 15. Treated mice displayed significant functional improvement, improved sarcomere integrity, and reduced inflammation, protein aggregates, as well as centralized nuclei.
Conclusion: In conclusion, this novel BAG3_P209L transgenic mouse model recapitulates key molecular and functional hallmarks of MFM6, providing valuable insights into disease mechanisms and demonstrating impaired autophagic flux as a central pathogenic mechanism in BAG3associated MFM6.

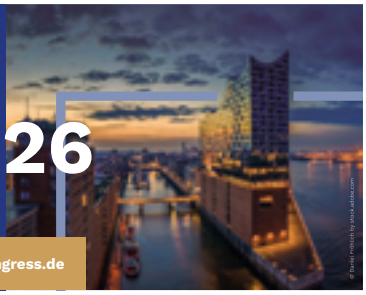

P10 Postergroup: Skeletal Muscle

P1012

Muscle, microbiome and metabolism: a feedback loop in Duchenne muscular dystrophy

Anthony Marullo; Friederike Uhlig; Ken O´Halloran
Department of Physiology, University College Cork, Cork, Ireland;

Objective: We have previously shown that male mice raised without a gut microbiome show sexspecific impairment of skeletal muscle forcegenerating capacity, indicating that the metabolic output of resident bacteria reaches and affects muscle. This led us to characterise gutmuscle interactions in Duchenne muscular dystrophy (DMD), where the muscle itself becomes the primary source of metabolic disturbance.
Method: In the *mdx* mouse, loss of dystrophin drives ongoing muscle breakdown, releasing catabolic byproducts and immune mediators that alter the nutrients and signals reaching the gut. The microbial community adapts to this altered supply by shifting its composition and functional capacity to match the now available substrates. To follow how the reshaped microbial metabolism modulates the host, we combined metagenomics, metabolomics (plasma, faecal, diaphragm), and transcriptomics (ileum, colon, diaphragm). Microbial functional capacity (KEGG Orthologs) was related to faecal and plasma metabolites, with host transcription confirming the metabolic consequences locally (gut) and systemically (diaphragm).
Results: The adapted community featured lower shortchain fatty acid and bilesalt hydrolase capacity and elevated lipopolysaccharide levels, leaving a systemic SCFA deficit, accumulated luminal bile acids, and depleted indoles, impairing AhR signalling. Elevated 3methylhistidine tracked muscle breakdown across all compartments. Circulating lipopolysaccharide accompanied TLR4associated inflammation in the diaphragm, alongside a suppressed ileal immune profile with a structurally intact barrier.
Conclusion: Together these data place the microbiome within the dystrophic disease process as a metabolic intermediary, its output reshaped by the metabolic stress of muscle breakdown and regenerative demand, ultimately contributing to further exacerbate the disease. Our work reveals targets for adjunct therapies for DMD.

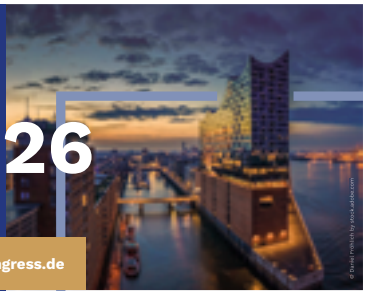

P11 Postergroup: New & old hormones

P1101

PARP1 associates with the mineralocorticoid receptor to enhance transcriptional activity

Karolin Philipp; Claudia Grossmann
JuliusBernsteinInstitut für Physiologie, Medizinische Fakultät, MartinLutherUniversität HalleWittenberg, Halle (Saale), Germany;

Objective: The mineralocorticoid receptor (MR) is a ligandactivated nuclear receptor that regulates transcriptional programs involved in electrolyte homeostasis, inflammation, and cardiovascular remodeling. Efficient steroid hormone receptordependent transcription requires the coordinated recruitment of chromatinassociated coregulators and transcriptional complexes. Poly(ADPribose) polymerase 1 (PARP1) is an important regulator of chromatin organization and transcriptional activity and has been implicated in steroid receptormediated gene regulation. However, whether PARP1 functionally associates with the MR remains poorly understood.
Method: To investigate the MRPARP1 interaction, HEK293derived cell systems were analyzed using coimmunoprecipitation and subcellular fractionation followed by Western blot analysis. PARP1 enrichment was quantified relative to lysate controls and normalized to total protein staining or MR expression. In addition, MRdependent reporter gene assays were performed to assess the functional impact of PARP1 on MRmediated transcriptional activity.
Results: MR expression increased PARP1 enrichment in eluate fractions without markedly altering total cellular PARP1 expression levels, indicating enhanced recruitment rather than increased protein abundance. Aldosterone treatment further enhanced PARP1 enrichment under several experimental conditions. As expected, subcellular fractionation demonstrated aldosteronedependent redistribution of MR from cytosolic toward nuclear and chromatinassociated fractions, whereas PARP1 localization remained predominantly nuclear/chromatinassociated. Domain mapping experiments revealed that MR constructs containing the Cterminal CDEF domains showed the strongest PARP1 enrichment, while the isolated Nterminal AB domain displayed only weak association. Functional reporter gene assays demonstrated dose- and timedependent activation of MR signaling by aldosterone. PARP1 deficiency reduced MRdependent reporter gene activity, suggesting that PARP1 enhances transcriptional efficiency of MR.
Conclusion: In conclusion, our findings identify PARP1 as a potential MRassociated coregulator and suggest that ligand activation and the Cterminal MR domains promote efficient PARP1 recruitment. Future studies will investigate the role of PARP1 in MRassociated chromatin remodeling and transcriptional regulation at endogenous target genes.

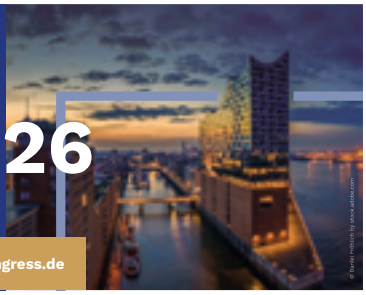

P11 Postergroup: New & old hormones

P1102

Serum- and GlucocorticoidRegulated Kinase 1 (SGK1) Mediates HypoxiaInduced Oxidative Stress and Mitochondrial Dysfunction Through NADPH oxidase Signaling

Asmaa Khalifa; Nis Halland [1]; Marc Nazare [1]; Agnes Görlach; Andreas Petry
Experimental and Molecular Pediatric Cardiology Department, German Heart Center Munich, TUM University Hospital, Germany., München, Germany; [1] Integrated Drug Discovery, Sanofi, Frankfurt a. M., Germany;

Objective: Hypoxia induces oxidative stress and mitochondrial dysfunction, contributing to maladaptive cellular responses in cardiovascular disease. Serum- and glucocorticoidregulated kinase 1 (SGK1) is a stressresponsive kinase implicated in cellular adaptation; however, its role in hypoxiainduced signaling remains incompletely understood. This study investigated the contribution of SGK1 to oxidative stress pathways in response to hypoxia.

Method: H9C2 cardiomyoblasts and HMEC1 endothelial cells were exposed to hypoxia (1% O_2). SGK1 signaling was modulated using the pharmacological inhibitor Comp16y and genetic approaches including wildtype (SGK1WT), constitutively active (SGK1CA), and kinasedead (SGK1DK) constructs. NADPH oxidase signaling was modulated through siRNAmediated knockdown or the NOX1/NOX4 inhibitor GKT137831. Reactive oxygen species (ROS), mitochondrial morphology, metabolic activity, cellular senescence, and angiogenic responses were assessed.

Results: Hypoxia induced a timedependent increase in SGK1 expression accompanied by phosphorylation of its downstream target GSK3β and induction of the NADPH oxidase components p22phox and NOX4. SGK1 inhibition by Comp16y or expression of SGK1DK prevented p22phox and NOX4 induction and significantly attenuated hypoxiainduced ROS production, whereas expression of SGK1CA increased ROS levels. Inhibition of NADPH oxidase signaling attenuated SGK1mediated ROS generation, supporting a functional interaction between SGK1 and NADPH oxidases. Furthermore, inhibition of SGK1 or NADPH oxidases improved mitochondrial network integrity and reduced hypoxiainduced metabolic adaptation, cellular senescence, and endothelial tube formation.

Conclusion: SGK1 is a key regulator of hypoxiainduced oxidative stress and mitochondrial dysfunction and may represent a therapeutic target in hypoxiaassociated disease.

P11 Postergroup: New & old hormones

P1103

Physiological Amelioration of Nanosilver and Arsenic Toxicity by *Moringa oleifera* Leaf Extract in Experimental Rats

Faiza Bashir; Saima Sharif [1]; Shagufta Naz [1]
Zoology, Department of Zoology, University of Narowal, Narowal, Pakista, Narowal, Pakistan; [1] Zoology, Lahore College for Women University, Lahore, Pakistan;

Objective: The coexistence of heavy metals and AgNPs in biological systems represent a multifaceted toxicological scenario that is not completely understood until now. A noticeable gap is still present in the research, particularly, related to their chronic combined impacts of oral exposure on biochemical and hematological parameters, and on the presence of tissue residual content of these elements in vital organs such as the liver. Therefore, the current study aims to bridge that gap by investigating the therapeutic potency of Moringa leaves extract against hepatic injury owing to the accretion of elements and systemic toxicity brought by exposure to nanosilver and arsenic in albino rats.
Method: Sprague Dawley rats (270) of 5 weeks old were randomly allocated into fifteen groups, receiving daily, oral doses of high and low concentrations of Moringa extract (3 g/kg and 2 g/kg body weight), AgNPs (150 mg/kg and 100 mg/kg bw), and As (16.4 mg/kg and 10.25 mg/kg bw), individually and in combinations over 12 weeks. Blood and liver were collected at 4, 8, and 12 weeks for haematology and biochemical analysis.
Results: Exposure to (AgNPs), (As), or both (AgNPs+As) led to significant decline in good fat (HDLC) contents and erythrocytes indices, including Hb, RBC, PCV, and MCHC levels, coupled with elevated MCV, creatinine, total cholesterol, and triglyceride activities besides bioaccumulation of arsenic and silver in liver tissue in dose and time dependent way in comparison to control and Moringa treated animals across three months. Rats treated with Moringa extract alone at both dosages exhibited improved blood parameters and a decline in creatinine and lipid markers levels throughout the study period. However, partial restoration of blood and biochemical indices was observed, along with a notable a dose dependent and time dependent reduction in residual silver and arsenic bioaccumulation, when Moringa extract was coadministered with toxicants either individually or in combination in each month of experiment.
Conclusion: The findings support the protective potential of *Moringa oleifera* in reducing liver and kidney damage, likely due to its antioxidant and antiinflammatory properties, highlighting its significance as a natural protective agent against environmental pollutants.

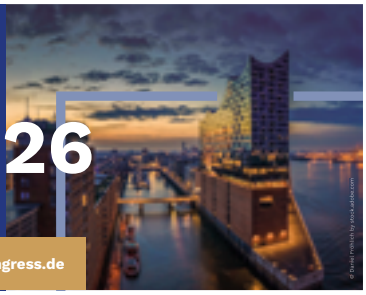

P11 Postergroup: New & old hormones

P1104

REVERB Signaling Modulates the Circadian Regulatory Axis for GlucagonLike Peptide1 Secretion in Enteroendocrine LCells

Ravikant Sharma; Ghulam Shere Raza; KarlHeinz Herzig
Department of Physiology, Institute of Biomedicine and Internal Medicine, University of Oulu, Oulu, Finland;

Objective: Circadian regulation of enteroendocrine function is an important determinant of metabolic homeostasis. Enteroendocrine Lcells possess intrinsic clock machinery that drives rhythmic GLP1 secretory responses, and disruption of BMAL1 impairs timedependent GLP1 secretion. REVERB is another key component of clock machinery involved in metabolic regulation, but its role in GLP1 secretion is poorly defined.
Method: We hypothesized that REVERB activation modulates basal GLP1 secretion in a circadian phasedependent manner. STC1 cells were synchronized with forskolin (20 μM) and treated with vehicle or the REVERB agonist SR12418 (1 μM). Clockgene expressions were measured at 0, 6, 12, 18, and 24 h postsynchronization (n = 6), while basal GLP1 secretion was quantified for 2 h at 8, 14, 20, and 26 h postsynchronization (n = 3).
Results: SR12418 repressed and reshaped *Bmal1* rhythmic expression, supporting engagement of the REVERB clockoutput pathway. *Reverb* expression was timedependent, but SR12418 did not increase overall transcript abundance. In vehicletreated cells, basal active GLP1 secretion did not show a significant overall time effect. In Dunnett's posthoc comparison against 0 h, only the 26 h endpoint reached significance ($p < 0.01$).
Conclusion: Together, these data support REVERB clockoutput signaling as a regulator of the temporal organization of basal GLP1 secretion in synchronized enteroendocrine cells.

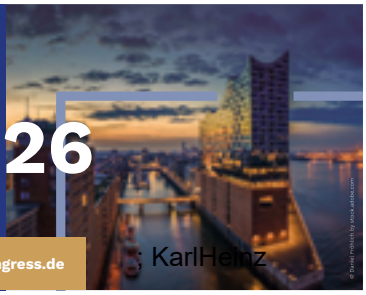

P11 Postergroup: New & old hormones

P1105

Associations of Habitual Coffee Intake with Testosterone and Cardiometabolic Markers: the Northern Finland Birth Cohort 1966 Study

Luca Verroest; Jari Jokelainen [1]; Shalini Choudhary [2]; Juha Auvinen [1] ; MarjoRiitta Jarvelin [3]
Herzig [4]; Ghulam Shere Raza [4]
Unit of Internal Medicine and Biomedicine, Medicine, University of Oulu, Oulu, Finland; [1] Faculty of Medicine, Center for Life Course Health Research, University of Oulu, Oulu, Finland; [2] Department of Physiology, University of Oulu, Oulu, Finland; [3] School of Public Health, Department of Epidemiology and Biostatistics, Imperial College London, London, United Kingdom; [4] Department of Physiology, Institute of Biomedicine and Internal Medicine, University of Oulu, Oulu, Finland;

Objective: Coffee is a widely consumed source of bioactive compounds globally, yet its associations with circulating metabolites, sex hormones, and cardiometabolic markers remain incompletely characterised. We investigated these associations in a large populationbased cohort, with particular attention to sexspecific hormonal profiles and metabolomic signatures.
Method: Crosssectional data from 2,264 participants (47% men) of the Northern Finland Birth Cohort 1966 (NFBC1966) at age 46 were analysed using sexstratified Spearman correlations and multivariable linear regression models adjusted for BMI, educational attainment, smoking, physical activity, and alcohol intake.
Results: Higher coffee intake groups showed lower total and visceral fat and higher skeletal muscle mass, while BMI was comparable across groups. Inverse correlations were observed between coffee intake and circulating branchedchain amino acids (BCAAs) in both sexes. In men, higher coffee intake was correlated to a more favourable glucose–insulin profile and a distinct hormonal pattern: multivariableadjusted models showed positive associations with total testosterone (β = +0.29 nmol/L per cup/day), bioavailable testosterone, and sex hormone–binding globulin (SHBG), alongside inverse associations with free testosterone and the free androgen index (FAI). In women, hormonal associations were more limited, with positive associations for SHBG and inverse associations for free testosterone and FAI.
Conclusion: Habitual coffee consumption was associated with a leaner body composition, lower circulating BCAAs, and a sexspecific hormonal profile that may be metabolically relevant, particularly in men. Future longitudinal and intervention studies are needed to establish causality and identify the coffeederived bioactive compounds involved.

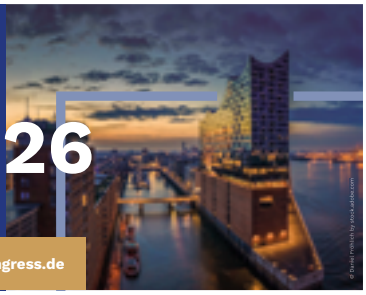

P11 Postergroup: New & old hormones

P1106

Global metabolic depression in human villous trophoblast cells after exposure to hypoxia

Mia Joeli Persikowski; Laia Pagerols Raluy [1]; Jonathan R. Sierla; Dominique Singer; Julia Heiter
Neonatologie, Universitätsklinikum HamburgEppendorf, Hamburg, Germany; [1] Kinderchirurgie, Universitätsklinikum HamburgEppendorf, Hamburg, Germany;

Objective: Fetal Growth Restriction (FGR) affects approximately 10% of pregnancies and is a leading cause of postnatal and longterm complications. FGR can result from a mismatch between the fetus' nutritional needs and the placenta's ability to supply them. Recent research suggests that hypoxic stress impairs mitochondrial metabolism in placental cells, with the inhibition of oxidative phosphorylation outlasting the transient decline in mitochondrial content. This study tested the hypothesis that placental O_2 consumption is temporarily replaced by anaerobic glycolysis, and examined whether a longer recovery phase allows for a more complete restoration of mitochondrial activity.
Method: Human villous trophoblastic (BeWo) cells were cultured under normoxic and hypoxic conditions for 48h and recovered under normoxic conditions for either 24 or 48h. Mitochondrial content was assessed via flow cytometry before and after hypoxic incubation and after 24 and 48h of recovery. Oxidative and glycolytic metabolism were analyzed using a respirometric analyzer (Seahorse, Agilent) by recording the O_2consumption rate (OCR) and the extracellular acidification rate of normoxic, hypoxic and recovered cells. All data were analyzed by oneway ANOVA with Tukey's posthoc test and are presented as means ± standard deviations, with significance considered at $p < 0.05$.
Results: Mitochondrial content was significantly reduced in hypoxic cells (16.0%) compared to normoxic controls (77.7%), with partial recovery observed after 24 (20.0%) or 48h (47.9%). Consistently, the OCR declined under hypoxic conditions and showed an even more significant reduction after recovery. While glycolytic function increased modestly after hypoxia, it decreased significantly after recovery.
Conclusion: The findings indicate that placental cells reduce their mitochondrial content in response to reduced O_2 availability. Even after a prolonged period of reoxygenation, mitochondrial content recovers only gradually. Furthermore, a sustained impairment of oxidative phosphorylation is observed, which is not compensated for by increased anaerobic glycolysis and thus indicates global metabolic depression.

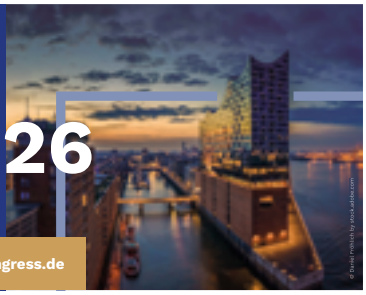

P11 Postergroup: New & old hormones

P1107

Just a little prick: Careful cell contacts enabled by ceramic nanostraws

Noah Brechmann; Tamara Büttner [1]; Bernd Walkenfort [2]; Buena Delos Reyes [2]; Daniel Schäfer [3]; Sebastian Schlücker [3]; Dirk Mayer [4]; Mike Hasenberg [2]; Joachim Fandrey [1]; Karsten Seidl; Sandra Winning [1]
Fraunhofer IMS Duisburg, Duisburg, Germany; [1] Abteilung Physiologie, Universitätsklinikum Essen, Essen, Germany; [2] Imaging Center Essen, Electron Microscopy Unit, University of Duisburg Essen, Germany; [3] Physical Chemistry I, University of DuisburgEssen, Essen, Germany; [4] Institute of Biological Information Processing, Bioelectronics (IBI3), Forschungszentrum Jülich GmbH, Jülich, Germany;

Objective: Nanostraw arrays represent a novel and promising approach for the controlled delivery of substances into cells characterized by very little cellular activation or damage. Herein, we describe a sensitive strategy to establish intracellular contact with human macrophagelike differentiated THP1 cells.
Method: Macrophages must function under stressful *invivo* conditions in oxygendeprived tissues with inflammation. THP1 cells stayed healthy and did not show signs of activation when cultured on nanostraw arrays.
Results: Importantly, we found convincing evidence for the successful delivery of gold nanoparticles and fluorescencelabeled antibodies into THP1 cells. Future applications of nanostraw arrays are the functionalization with silane coating to immobilize proteins and/or the analysis of membrane located ion channels in THP1 cells by electrophysiology.
Conclusion: Our findings demonstrate that nanostraw arrays can enable intracellular contact for substance delivery and they might also allow measurements of the cellular membrane potential under stressful culture conditions like hypoxia in the future, in particular for immune cells.

P11 Postergroup: New & old hormones

P1108

Characterization of the immune response against AAV- mediated optogene transfer in pigs

Sai Sudha Yalamarthi; Marie Freier; Sören Hauck [1]; Philipp Ströbel [1]; Dirk Beutner [2]; Tobias Brügmann
Institute of Cardiovascular Physiology, University medical center, Goettingen, Göttingen, Germany; [1] Institute of Pathology, University medical center, Goettingen, Göttingen, Germany; [2] Department of Otolaryngology, University medical center, Goettingen, Göttingen, Germany;

Objective: Bilateral laryngeal paralysis is characterized by fixed vocal folds, which can result in life threatening dyspnea. The posterior cricoarytenoid muscle (PCM) is solely responsible for the abduction of vocal folds. Unfortunately, current treatment options have several disadvantages and cannot reliably restore phonation and respiration. A promising therapeutic approach is direct optogenetic stimulation of PCM for laryngeal pacemaking. In this project, we aimed to explore the gene transfer, optical stimulation and to characterize the immune response in pigs.

Method: We injected various amounts of AAV serotypes 2/6 and 2/9 expressing Channelrhodopsin2 (ChR2) in fusion with mCherry directly into PCMs of 26, 2 months old landrace pigs. PCM were stimulated optically (465 nm, ~1.5 mW/mm^2, 20 Hz, 40 ms) and electrically (100 Hz, 2 ms biphasic). Neutralizing antibodies (NAb) were detected by analysing the transduction efficiency after incubation with sera by flow cytometry and total antibodies against AAV capsids with ELISA. Immunofluorescence staining with the sera on HEK293 cells expressing respective proteins was performed to detect antibodies against ChR2 or mCherry. The cellular immune response was characterized by analyzing the PBMCs with flow cytometry. All data shown as mean ± sem.

Results: 914 days after gene transfer, expression of ChR2/mCherry and lightinduced contractions were observed in PCM in dependence of AAV particle numbers. However, several pigs developed marked immune cell infiltration, leading even to functional alteration in 16 out of 26 pigs. AAV injection led to production of NAbs in all pigs, which was more pronounced in case of AAV2/6 (14 pigs) compared to AAV2/9 (12 pigs). Notably, pigs injected with AAV2/9 also developed antibodies against AAV2/6. Antibodies developed against AAV2/6 (1837 ± 293.4 ng/mL, n=14 pigs) were significantly higher than against AAV2/9 (620 ± 49.5 ng/mL, n=12 pigs, twotailed unpaired T test, p=0.0006). 10 pigs developed antibodies against mCherry but none against ChR2. Pigs with high immune cell infiltration in PCM had higher frequencies of $CD8^+$ and $CD8^+CD4^+$ T cells (24.9 ± 3.2% of $CD3^+$ T cells) than pigs without immune cell infiltration (18.68 ± 4.9% of $Cd3^+$ T cells, n=3 pigs).

Conclusion: Optogenetic laryngeal pacemaking successfully stimulated the contraction of PCM and thus opening of vocal folds in pigs, but immune cell infiltration primarily driven by AAV and mCherry has led to muscle degradation.

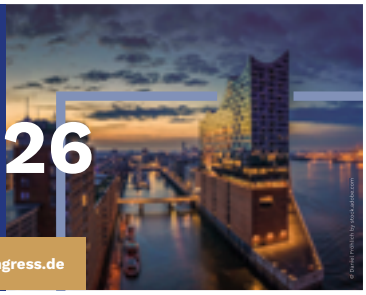

P11 Postergroup: New & old hormones

P1109
Bonespecific IFITM5 is present in extracellular vesicles

Kenneth Schöneck; Funda Celik; Lukas Daniel Sandoval Flores; Anke Baranowsky [1]; Sandra Paradies
Institute of Osteology and Biomechanics, University Medical Center HamburgEppendorf, Hamburg, Germany; [1] Clinic for Trauma Surgery and Orthopaedics, University Medical Center HamburgEppendorf, Hamburg, Germany;

Objective: Interferoninduced transmembrane protein 5 (IFITM5) is predominantly expressed by boneproducing osteoblasts. Pathogenic variants in the encoding gene *IFITM5* lead to the autosomaldominant inherited disease osteogenesis imperfecta (OI), commonly known as brittle bone disease. Clinically, IFITM5related OI patients are characterized by low bone mass, recurrent fractures and severe skeletal deformities. The majority of patients carry the monoallelic variant c.14C>T in the 5'UTR of *IFITM5*, generating a new start codon, leading to the addition of five amino acids to the Nterminus of the protein. Mouse model studies revealed that the absence of Ifitm5 does not result in a skeletal phenotype, whereas the transgenic expression of the diseasecausing variant strongly impairs skeletal development and results in perinatal lethality, thus indicating a gainoffunction variant. However, the molecular function of IFITM5 and the consequence of the diseasecausing variant remain unknown.

Method: Functional analyses were conducted using IFITM5overexpressing HEK293 and osteoblastlike cell lines. We analysed the cell culture supernatant via Western blot analysis, isolated and characterized extracellular vesicles (EVs) via ultracentrifugation and nanoparticle tracking analysis as well as mass spectrometry (MS). Immunofluorescence microscopy experiments were performed to study the topology of the wildtype IFITM5 and the diseasecausing variant of IFITM5. Furthermore, coimmunoprecipitation experiments in combination with MS were conducted to identify potential protein interaction partners.
Results: We could show that IFITM5 forms dimers at the plasma membrane but is also released to the extracellular matrix. The characterization of EVs from cell culture supernatant revealed that IFITM5 is present not only in EVs derived from overexpressing cells but also in EVs derived from primary mouse osteoblasts. Our topology studies showed that the Nterminus of the wildtype IFITM5 and the diseasecausing variant of IFITM5 protrudes into the extracellular matrix. Interestingly, the OIrelated bone matrix protein SPARC, also known as osteonectin, seems to be a promising candidate for protein interaction to IFITM5.
Conclusion: The presence of wild type IFITM5 and the diseasecausing variant of IFITM5 in EVs and the potential interaction with SPARC are promising findings to decipher the role of IFITM5 for bone matrix mineralisation.

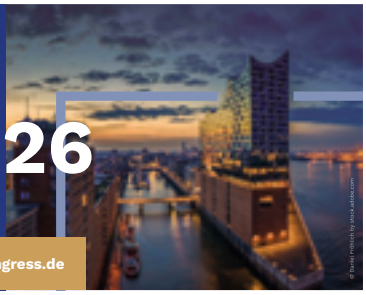

P11 Postergroup: New & old hormones

P1110

Regulation of fibroblast growth factor 23 (FGF23) by mechanosensor Piezo1

Sina Hülße; Martina Feger; Michael Föller
Institut für Physiologie, Universität Hohenheim, Stuttgart, Germany;

Objective: Under physiological conditions, fibroblast growth factor 23 (FGF23) is produced in bone and mainly regulates renal phosphate and vitamin D handling. Further production sites and effects in disease are described. Piezo1 is a mechanosensitive nonspecific cation channel playing an important role in bone remodeling, fracture healing, or osteogenesis. The intracellular signaling orchestrating the production of FGF23 is not fully understood. Here, we sought to decipher the role of Piezo1 in the regulation of FGF23.
Method: UMR106 osteoblastlike cells were used. Gene expression was determined by qRTPCR, and intracellular Ca^{2+} concentration was assessed by Fluo4 fluorescence. Transcriptome analysis was accomplished by a gene chip and stable *Piezo1* knockdown in UMR106 cells by the CRISPR/Cas9 method.
Results: As a result, UMR106 cells expressed Piezo1. Transcriptome analysis revealed that chemical Piezo1 activator Yoda1 strongly upregulated FGF23 suppressor dentin matrix acidic phosphoprotein 1 (DMP1). Yoda1 and Jedi2, another PIEZO1 agonist, downregulated and Piezo1 antagonist $GdCl_3$ upregulated *Fgf23* mRNA transcript levels. CRISPR/Cas9based Piezo1 knockdown did not affect cell viability, but abrogated the Yoda1dependent increase in intracellular Ca^{2+} and *Dmp1* gene expression as well as suppression of *Fgf23*.
Conclusion: Taken together, Piezo1 is a powerful regulator of FGF23 production in UMR106 osteoblastlike cells.

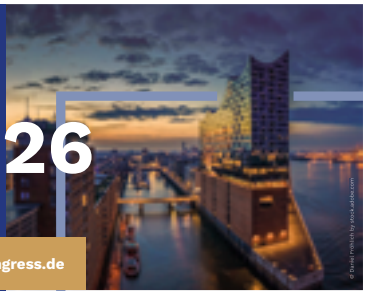

P11 Postergroup: New & old hormones

P1111

Functional characterization of a new angulin isoform: ILDR1v7

Amelie Johanna Moll; Felicitas E.M. Gnielka; Jörg Piontek; Carlos AyalaTorres; Susanne Krug
Klinische Physiologie, Campus Benjamin Franklin, Charité - Universitätsmedizin Berlin, Berlin, Germany;

Objective: Tight junctions (TJ) are essential for epithelial barriers, regulating paracellular permeability and tissue homeostasis. Angulins are tight junction (TJ) proteins that localize to tricellular contacts and regulate tricellular TJ organization. A novel seventh immunoglobulinlike domaincontaining receptor 1 isoform (ILDR1v7) was identified and cloned from intestinal tissues and cell lines, suggesting functional relevance in the intestinal epithelium. This study aims to characterize ILDR1v7 regarding its sequence, localization, and function within the epithelial barrier.
Method: Comparative sequence analyses was used to analyse the isoform for conserved and isoformspecific features. Tagged ILDR1v7 constructs were stably expressed in MDCK II and HT29/B6 intestinal cells with different angulin knockouts (LSRKO, ILDR1KO, and LSR/ILDR1doubleKO). Clones were characterized in respect to ILDR1v7 localization, its influence on TJ protein expression and barrier function performing electrophysiological measurement in Ussing chambers, like transepithelial resistance, dilution potentials and FITCdextran fluxes.
Results: Sequence alignment revealed that ILDR1v7 corresponded to the predicted isoform ILDR1X3 and was highly conserved with other angulins in the Nterminal Iglike domain and transmembrane region. The cytoplasmic domain displayed distinct features, including a proline substitution and a deletion removing a dileucine motif. Proper localization required free access to the Nterminus, as only Cterminally tagged ILDR1v7 localized in TJs, with enrichment at tricellular TJs. ILDR1v7 had no obvious effect on barrier properties in MDCK II.
Conclusion: ILDR1v7 is a structurally distinct, tricellularenriched ILDR1 isoform whose function is likely masked by angulin redundancy. Ongoing experiments with stepwise angulin knockouts in intestinal HT29/B6 cells are determining whether ILDR1v7 recruits tricellulin and restores barrier integrity, which would define its specific role in the intestinal TJ.

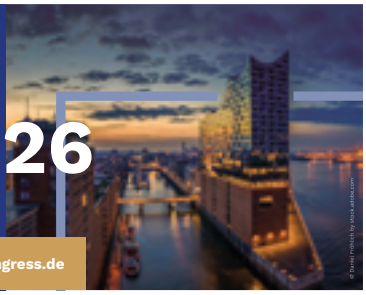

P11 Postergroup: New & old hormones

P1112
Inflammatory Bladder Cancer: Unpacking the HIFLysM or Treg Axis

Anne Tersteegen; Clara Roggendorf; Vivienne Schneider; Sandra Winning; Joachim Fandrey
Abteilung Physiologie, Universitätsklinikum Essen, Essen, Germany;

Objective: Chronic inflammation and hypoxic conditions are key drivers of tumor initiation and progression in solid malignancies, including bladder cancer. Hypoxiainducible factors (HIFs) act as central regulators of cellular adaptation to low oxygen tension and critically influence both tumor cells and immune responses. This study aims to elucidate mechanistic links between chronic inflammation, immune regulation, and the functional role of HIF1α and HIF2α in myeloid immune cells (LysM) and regulatory T cells (Tregs) during the early phases of inflammationdriven bladder carcinogenesis.
Method: An established murine combination model is employed that integrates recurrent bacterial cystitis induced by transurethal instillation of $5x10^8$ (in 50 µl PBS) uropathogenic *E. coli 536* (UPEC) with chemical carcinogenesis triggered by *N*butyl*N*(4hydroxybutyl)nitrosamine (BBN, 0,05 % v/v in drinking water). Conditional knockout mouse lines with celltypespecific deletion of *Hif1a* and/or *Hif2a* in myeloid cells and Foxp3? Tregs are used to dissect the contribution of HIFdependent signaling pathways to inflammation, immune cell recruitment, tumor microenvironment remodeling, and early tumor development.
Results: Preliminary data shows an increased *Hif1a* expression, mostly in the cytosol as well as increased lymphocyte infiltration ($CD45^+$, $CD4^+$cells and Tregs) into the tumor in the combined (UPEC + BBN) model. This effect is even more pronounced in mice deficient for *Hif1a* in myeloid cells.
Conclusion: The findings are expected to advance the understanding of tumorassociated immune responses and may identify novel targets for preventive and immunotherapeutic strategies in patients with chronic inflammatory bladder diseases.

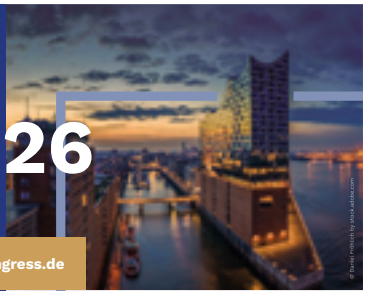

P11 Postergroup: New & old hormones

P1113
ER stress response by site2 protease is essential for bone formation

Maike Buck; Judith Zeidler; Thomas Höger; AssilRamin Alimy [1]; Anke Baranowsky [1]; Kenneth Schöneck; JanOle Schulze [2]; Timur Alexander Yorgan; Thorsten Schinke; Sandra Paradies Institute of Osteology and Biomechanics, University Medical Center HamburgEppendorf, Hamburg, Germany; [1] Clinic for Trauma Surgery and Orthopaedics, University Medical Center HamburgEppendorf, Hamburg, Germany; [2] Institute for Computational Systems Biomedicine, University of Hamburg, Hamburg, Germany;

Objective: The site2 protease (S2P), encoded by *MBTPS2* on the X chromosome, is a Golgiresident intramembranecleaving zinc metalloprotease. Following initial cleavage by site1 protease (S1P), S2P releases membranebound transcription factors, which are essential for physiological processes such as the regulation of lipid biosynthesis and the endoplasmic reticulum (ER) stress response. Surprisingly, although S2P is ubiquitously expressed, pathogenic *MBTPS2* missense variants affect primarily the skeleton. Such variants cause an Xlinked recessive form of osteogenesis imperfecta (XOI), characterized by bone fragility, severe skeletal deformities and short stature. OI is the largest group of hereditary skeletal disorders primarily affecting boneforming osteoblasts, whose main function is the synthesis and secretion of collagen type I (Col1) to form the bone matrix. To date, the molecular pathomechanism underlying the S2Prelated skeletal alterations remains poorly understood.
Method: We established S2Pdeficient HAP1 cells, a human haploid cell line, as an appropriate cell culture model. Gene expression was analysed by quantitative PCR and transcriptome array and protein expression by Western blot and mass spectrometry. The cell viability of S2Pdeficient HAP1 cells was assessed by flow cytometry. In addition, we generated a conditional knockout mouse model with loss of *Mbtps2* predominantly in osteoblasts. The skeleton of *Mbtps2*deficient mice was visualised by Xray and primary osteoblasts and the collagen network by electron microscopy and gene expression was analysed by transcriptome array.
Results: Hemizygous mice exhibited premature lethality. Xray and histological analysis of 2weeksold mutant mice revealed failure of proper bone formation, short stature, skeletal deformities and multiple fractures. Primary osteoblasts showed downregulation of osteoblastspecific proteins and upregulation of ER stressassociated apoptosis markers, consistent with signs of apoptosis on electron microscopy of *Mbtps2*deficient mice. Similarly, ER stressrelated proteins were upregulated in S2Pdeficient HAP1 cells, although flow cytometry revealed no significant change in cell viability. Contrary to previous reports suggesting ER retention, Col1 was found to be secreted in both the mutant mice and Col1overexpressing S2Pdeficient HAP1 cells. Further analysis identified TANGO1 (transport and Golgi organization protein 1 homolog) as a missing component of the vesicular Col1 secretion machinery in S2P deficiency.
Conclusion: These findings suggest that impaired ER stress resolution is crucial for bone formation and loss of S2P disrupts TANGO1dependent vesicle formation, impairing large cargo secretion and potentially explaining the observed Col1 network disorganization. The compensatory mechanism by which Col1 is secreted in S2P deficiency remains to be elucidated.

P11 Postergroup: New & old hormones

P1114

Kupffer Cells as Key Targets of Hepatic Cadmium Handling: Putative Uptake Mechanisms of Ionic and ProteinBound Cadmium

Nicole Mangazeev; Allein Plain Reyes; Annika Kiel [1]; Angela KralemannKöhler [1]; Teresa Kern; Marie Bergmeier; Jan Schulte am Esch [2]; WingKee Lee Physiology & Pathophysiology of Cells and Membranes, Medical School OWL, Bielefeld University, Bielefeld, Germany; [1] Department of General and Visceral Surgery, Medical School OWL, Bielefeld University, Bielefeld, Germany; [2] Department of General and Visceral Surgery, Protestant Hospital of Bethel Foundation, University Hospital OWL of the Bielefeld University, Bielefeld, Germany;

Objective: Cadmium (Cd) is a toxic heavy metal that accumulates in the liver and can form complexes with serum proteins such as albumin (Alb), transferrin (Tf), and metallothionein (MT). While hepatocytes are considered primary targets of Cd toxicity, the role of resident Kupffer cells (KCs) in hepatic cadmium handling remains incompletely understood. This study aimed to investigate the uptake and cellular responses of KCs and hepatocytes to ionic and proteinbound Cd species.
Method: Primary rat KCs were isolated by liver perfusion and Percoll gradient centrifugation and characterized by **Western blot** and **qPCR**. Immortalized Kupffer KUP5 and the hepatocyte AML12 cell lines were treated with $CdCl_2$, CdTf, CdAlb, and CdMT for 24 hours prior to metabolic activity (**MTT)** and cell viability (**trypan blue)** assays. Uptake of fluorescentlylabeled Tf and Alb was monitored by **live cell imaging**. Expression (mRNA, protein) of putative receptors (TFR1, SLC22A17, megalin) and transporters (DMT1, ZIP8, ZIP14) after Cd exposure were determined.
Results: Compared to AML12, KUP5 were more sensitive to $CdCl_2$ with lower EC_{50} values (5.25 µM vs. 27.98 µM, n = 4) in MTT assay. CdMT had no effect (105% ± 9.6 SE), whereas CdAlb (64.12% ± 9.4 SE) and CdTf (66.15% ± 7.8 SE) significantly reduced metabolic activity paralleled with morphologic alterations yet no significant change in live/dead cell numbers (n = 3). In contrast, ionic Cd caused ~70% reduction of total cell number. In KUP5 cells, fluorescentlylabeled Tf was peripherally distributed, suggesting recycling, whereas perinuclear Alb indicated lysosomal trafficking. TFR1, SLC22A17, DMT1, ZIP8, and ZIP14 mRNA were elevated in both primary and immortalized KCs compared to hepatocytes, while megalin protein was not detectable. $CdCl_2$ did not alter TFR1 and SLC22A17 protein expression (n = 3), but increased ZIP8 after 24 h (1.269 ± 0.066 fold; n = 3). CdTf significantly augmented TFR1 protein (1.183 ± 0.051 fold, n = 3), whereas CdMT decreased SLC22A17 expression after 24 h (0.446 ± 0.180 fold; n = 3).
Conclusion: Our data demonstrate ionic and complexed Cd species are internalized by KUP5 cells causing Cd species dependent stress responses through metabolic and morphologic adaptations, highlighting the importance of KCs and Cd speciation in hepatic Cd handling.

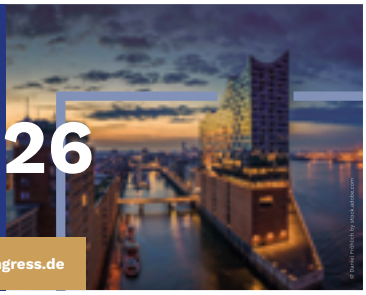

P11 Postergroup: New & old hormones

P1115

Triiodothyronine (T3) is a direct agonist of human acidsensing ion channel 3

Lu Qin; Viktoria Rakowski; Michal Stawarski; Dominik Wiemuth; Stefan Gründer
Institut of physiology, RWTH Aachen University, Aachen, Germany;

Objective: Human acidsensing ion channel 3 (hASIC3) is a protongated Na^+ channel expressed in the peripheral and central nervous systems. However, unlike rodent ASIC3, only a small fraction of hASIC3 can be activated at physiological pH, whereas full activation requires alkaline preconditioning (pH 8.0). Recently, we have shown that the thyroid hormone triiodothyronine (T3) is a positive allosteric modulator of rat ASIC3 (rASIC3). The purpose of this study was to characterize the action of T3 on hASIC3.
Method: hASIC3 and rASIC3 were expressed in *Xenopus* oocytes and currents recorded by TwoElectrodeVoltageClamp (TEVC).
Results: Surprisingly, we found that T3 directly activates hASIC3. In oocytes expressing hASIC3, but not rASIC3, T3 induced a sustained inward current independent of extracellular pH changes. The current evoked by 10 µM T3 was > 2fold larger than that induced by pH 5.0 following pH 8.0 preconditioning. T3evoked currents were Na^+ selective (E_{rev} = +31.2 mV) and inhibited by the classical ASIC inhibitor amiloride (IC_{50} = 264.6 µM). Using rathuman ASIC3 chimeras, we identified the distal region of the extracellular domain of hASIC3 as being critical for T3induced activation. Moreover, the potentially diseasecausing polymorphism hASIC3P385A strongly reduced T3evoked currents without affecting protoninduced activation. Because proline 385 has previously been implicated in glutamate binding to ASIC1a, our results suggest that T3 may activate hASIC3 through a related ligandbinding pocket.

Conclusion: Our findings identify T3 as a new endogenous agonist of hASIC3 with potential relevance for human disease.

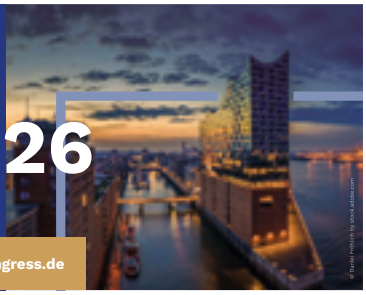

P12 Postergroup: Cardiac electrophysiology ECG

P1201
Algorithmbased evaluation of systolic time intervals in an *in vivo* murine model

Rajkumar Rajanathan; Halvor Osterby Guldbrandsen; Vladimir V. Matchkov; Tina Myhre Pedersen
Department of Biomedicine, Aarhus University, Aarhus, Denmark;

Objective: Despite great advances in the diagnosis and treatment of cardiovascular diseases, a high prevalence and mortality worldwide remain for these disorders. Continued refinement of existing methodologies, and development of new approaches, is therefore vital to improve cardiovascular assessment. Standardization of interpretation of physiological data is important both experimentally and clinically, as manual analyses may lead to bias and reduce accuracy. Here, we aimed to develop a standardized, algorithmbased approach for evaluation of simultaneous blood pressure and electrocardiogram (ECG) recordings, to assess electromechanical cardiac function.
Method: We used ~9 monthold C57BL6/J mice. Simultaneous blood pressure and ECG were recorded in anesthetized (mechanically ventilated ~2% isoflurane in 1 L/min 100% O_2) mice, and in freely moving mice with implanted telemetry probes (HDX11, DSI; insertion under isoflurane anaesthesia, and buprenorphine for analgesia). Phenylephrine (0.3 mg/kg i.p.) was administered in both anaesthetized and awake mice to induce cardiovascular changes and validate the sensitivity of the computational approach. Additionally, in anaesthetized mice, electrical pacing (600 - 678 BPM) was used for further validation. Obtained data were analysed using a tailored MATLAB script, identifying the QRS complex and simultaneous minima and maxima of the second derivative of the pressure trace, indicating aortic valve opening and closing.
Results: In both anesthetized and alert telemetry animals, the MATLAB script correctly identified fiducial points of the ECG and blood pressure recordings The systolic time intervals, including the electromechanical systole, the preejection period, and left ventricular ejection time were thereby determined. As expected, systolic time intervals were prolonged after administration of phenylephrine and shortened with increasing pacing rate.
Conclusion: Our computational algorithm reliably identified the alterations in electromechanical cardiac properties. These findings highlight the potential of algorithmic cardiovascular signal analysis to improve throughput, to reduce bias and increase sensitivity in both basic research and clinical applications.

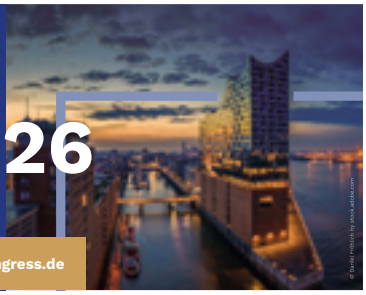

P12 Postergroup: Cardiac electrophysiology ECG

P1202

Respiratory heart rate variability as a biomarker of cardiac interception?

Max Lennart Schneider; Lucas Bohlen; Jürgen Lorenz [1]
Research Department, Osteopathie Schule Deutschland, Hamburg, Germany; [1] Faculty of Life Sciences, Hamburg Applied Science University, Hamburg, Germany;

Objective: The interoceptive system senses, processes, and regulates internal bodily states (e.g., cardiac and respiratory signals), partly through afferent and efferent pathways of the autonomic nervous system. Interestingly, both interoceptive and autonomic functions are impaired in diverse health conditions. Heart rate variability (HRV) refers to the variation in time between consecutive heartbeats, which reflects autonomic function and is strongly influenced by breathing cycles (i.e., respHRV). Since both respHRV and cardiac interoception are vagally mediated through efferent and afferent pathways, respectively, this exploratory crosssectional study investigated whether respHRV predicts cardiac interoception.
Method: We collected electrocardiographic recordings from healthy adults (n=25) during paced breathing (618 breaths/min) and analyzed respHRV in the frequency domain of RR intervals (within a bandwidth centered around the pacedbreathing frequencies). Interoceptive outcomes included: (1) cardiac interoceptive accuracy (HCT), (2) interoceptive sensibility (MAIA2, BPQ, IAS, NRS), (3) interoceptive attention (IATS), and (4) metacognitive awareness (CAC). Data were analyzed using generalized linear mixed models.
Results: Participants with higher respHRV, across all breathing rates, showed significantly higher interoceptive accuracy (HCT) ($p < 0.05$) and interoceptive sensibility (MAIA2 and NRS, not BPQ and IAS) (both $p < 0.001$), but not interoceptive attention (IATS) and interoceptive awareness (CAC) (both $p > 0.05$). Additionally, higher respHRV was significantly associated with lower breathing rates ($p < 0.001$) and female gender ($p < 0.001$).
Conclusion: Our preliminary findings suggest that respHRV could serve as a potential biomarker of cardiac interoception. However, due to the small sample size and absence of respiration rate measurements, our findings must be interpreted cautiously and future studies are needed.

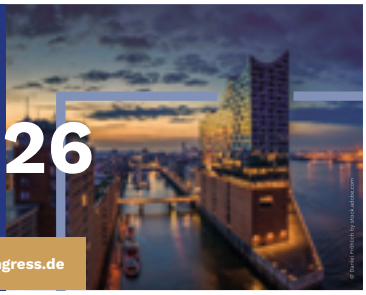

P12 Postergroup: Cardiac electrophysiology ECG

P1203

Using an adapted Langendorff perfusion setup for optogenetic investigation of autonomic control of the heart

Elena Meier; Jan Rebers; Jonas Heer; Pia Iaconianni; Josef Madl; Peter Kohl; Callum ZgierskiJohnston; Franziska SchneiderWarme
Institute for Experimental Cardiovascular Medicine, Medical Faculty and Medical Center, University of Freiburg, Freiburg, Germany;

Objective: The intracardiac nervous system (icNS) plays a central role in heart rhythm and pump function. Increasing evidence suggests that agerelated remodelling of the icNS contributes to cardiac electrophysiological dysfunction. However, structural and functional alterations of the icNS remain poorly understood, due to methodological limitations in studying neurocardiac communication in intact cardiac tissue. We aim to establish an adapted Langendorff perfused system enabling selective neuronal stimulation to investigate autonomic regulation of the heart.
Method: We use transgenic mouse models expressing Channelrhodopsin2 (ChR2eYFP) selectively in cholinergic neurons (ChATChR2 mice) or adrenergic neurons (THChR2 mice), enabling fluorescent labelling and targeted activation of parasympathetic or sympathetic neurons. For functional analysis, we established an adapted Langendorff perfusion system, where we cannulate the descending aorta rather than the ascending aorta. In contrast to conventional preparations, we excise the heart within the thoracic cavity, allowing us to preserve intracardiac and extracardiac sympathetic ganglia and their axonal projections to the heart. Functional readouts are pseudoECG recordings and dyebased optical mapping.
Results: The adapted Langendorff perfusion setup enables viable ex vivo heart maintenance. Initial functional experiments indicate that optogenetic activation of ChATChR2 neurons reduces heart rate, delays AV nodal conduction, and induces ventricular arrhythmias, consistent with findings from our previous study using different concentrations of carbachol. As an additional method, we used electrical stimulation of the stellate ganglion guided by the sympathetic chain as an anatomical landmark, which results in an increased heart rate. Nevertheless, electrode placement remains technically demanding.
Conclusion: Experiments with optogenetic and electrical stimulation are ongoing. Excision of the musculus longus colli to expose the stellate ganglion is expected to improve electrode positioning and reproducibility. The platform is also compatible with pharmacological and neurohumoral stimulation. In future studies, we will coactivate both autonomic branches using optogenetics and electrical or pharmacological stimulation to investigate their functional integration in murine hearts and their role in regulating cardiac function and arrhythmia susceptibility in the ageing heart.

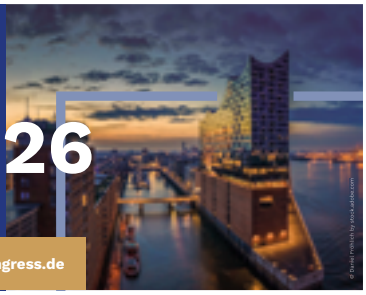

P12 Postergroup: Cardiac electrophysiology ECG

P1204

Comparative Physiology Meets Human Preterm Neonates: Revealing an Unexpected Mismatch in Heart Rate and Metabolic Scaling

Dominique Singer; Jochim Koch [1]; Lisa P. Huth [2]; Anna Perez [3]; Julia Heiter [3]
Neonatologie, Universitätsklinikum HamburgEppendorf, Hamburg, Germany; [1] Ratzeburg, Germany; [2] Mainz, Germany; [3] Children's Hospital, Neonatology and Pediatric Critical Care Medicine, University Medical Center Eppendorf, Hamburg, Germany;

Objective: According to allometric scaling laws, heart rate and specific basal metabolic rate increase with decreasing body mass. The human fetus deviates from this relationship by maintaining a heart rate of approximately 140 bpm throughout gestation—significantly lower than that predicted for its body mass. This reflects a state of hypometabolism, favored by the absence of thermogenesis, and acts as an adaptation to the intrauterine lowoxygen environment. Hence, it remains to be determined whether, and to what extent, heart rate and metabolic rate in preterm neonates adjust toward their allometrically predicted levels after birth.
Method: To address this question, an observational study was conducted involving 28 preterm infants with birth weights ranging from 590 to 1,495 g. Heart rate data from the first 28 days of life were retrieved from patient monitoring records and analyzed using statistical timeseries analysis. Additionally, a systematic literature search identified 12 eligible studies (published between 1962 and 2009), in which resting energy expenditure was measured in a total of 593 preterm infants via indirect calorimetry. From these studies, 410 data points—covering the first 58 days of life—were extracted and fitted using logarithmic regression.
Results: Despite substantial scatter in the heart rate data, a trend line was established, rising from approximately 150 to 170 bpm and described by the regression function: HR [bpm] = 5.558 ln(day) + 148.696 ($p < 0.001$, R^2 = 0.791, SEE = 2.804). For the specific metabolic rate, a surprisingly uniform postnatal increase from roughly 2.0 to 3.5 W/kg was observed, following the equation: sMR [W/kg] = 0.387 ln(day) + 1.852 ($p < 0.001$, R^2 = 0.605, SEE = 7.532). When compared to the overall body mass (BM) relationship of heart rate (HR [bpm] = 241 BM [kg]^0.25) and specific basal metabolic rate (sBMR [W/kg] = 3.4 BM [kg]^0.25), respectively, the heart rate of a 1,000 g reference neonate remained disproportionately low, whereas the postnatal metabolic increase attained or even exceeded the allometrically predicted level. The emergent divergence between heart rate, and thus cardiac output, on the one hand, and metabolic rate on the other, might contribute to the elevated susceptibility of preterm neonates to minor hemodynamic disturbances.
Conclusion: The comparative analysis suggests that a mismatch in heart rate and metabolic scaling may be a previously unrecognized marker of immaturity in human preterm neonates.

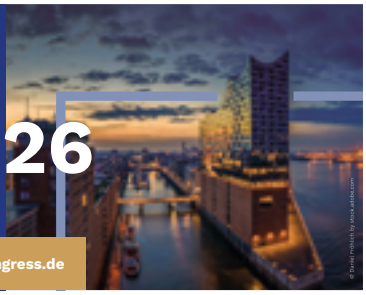

P12 Postergroup: Cardiac electrophysiology ECG

P1205

Cellular Phenotype of a Novel Mutation in the Cardiac Pacemaker Channel HCN4 Leading to Sinus Node Dysfunction and Left Ventricular Noncompaction

MohammadTaha Abdollahnia; Merten Prüser [1]; Miriam Reiss [1]; Pascal Syren [1]; Martin Both [2]; Antje D Ebert [3]; Timon Seeger [1]; Norbert Frey [1]; Andreas Draguhn [2]; Patrick A Schweizer [1] Internal Medicine III, Heidelberg University Hospital, Heidelberg, Germany; [1] Department of Cardiology, Angiology and Pneumology, Heidelberg University Hospital, Heidelberg, Germany; [2] Department of Neuro- and Sensory Physiology, Institute of Physiology and Pathophysiology, Heidelberg University, Heidelberg, Germany; [3] Department of Cardiology and Pneumology, University Medical Center Göttingen, Göttingen, Germany;

Objective: The HCN4 channel mediates the “funny current” (I_f) in cardiac pacemaker cells, which underlies the spontaneous depolarization that contributes importantly to cardiac automaticity. Dysfunction in HCN4 activity has been associated with sinus node dysfunction (SND), atrial fibrillation (AF) and structural cardiac abnormalities such as left ventricular noncompaction (LVNC), although the underlying pathophysiological mechanisms remain unresolved. We sought to investigate this combined phenotype and the molecular mechanisms of ion channel dysfunction in a novel familial HCN4 mutation.

Method: We performed patchclamp recordings of heterologously expressed HCN4 channels with/without the mutation using HEK293 cells. Furthermore, patientspecific induced pluripotent stem cells (hiPSCs) of a patient and isogenic controls were generated to further characterize the mutation.

Results: We detected the novel mutation in the poreforming region of the HCN4 channel in members of a German family comprising SND, AF and LVNC and clinically characterized the phenotype. Using patchclamp experiments, our preliminary data showed that homomeric expression of the HCN4 mutation leads to lossoffunction. Coexpression of HCN4 channels with/without the mutation causes a leftward shift of the activation curve and an overall reduction in current density. Interestingly, cotransfected HEK293 cells showed a broad distribution of current amplitudes, rather than a single peak between homomeric WT or mutant channel expression. We successfully generated hiPSCs of the index patient and respective isogenic control cells lacking the mutation to analyse the physiological effects of the mutation after further differentiation to cardiomyogenic cells.

Conclusion: We present a novel familial HCN4 mutation associated with a combined arrhythmogenic and structural cardiac phenotype. Patch clamp experiments in HEK293 cells suggest a mutation induced reduction in HCN4 activity, which might contribute to the clinical phenotype. Additional studies using the newly generated hiPSC lines may provide further insight into the pathomechanisms causing the combined structural and arrhythmogenic phenotype.

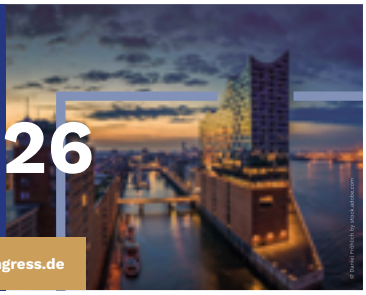

P12 Postergroup: Cardiac electrophysiology ECG

P1206
Cardiac Conduction System of Elephants and Tenrecs

Kirstine Calloe; Carsten Grøndahl [1]; Sara Andreia Rodrigues Abreu [2]; Eva Dervas [3]; Udo Hetzel [4]; Ditte Mai Myrup Albinus [5]; Hannah Louise Tornøe [6]; Mads Frost Bertelsen [7]; Stamatios Alan Tahas [7]; Morten B Thomsen [8]
Department of Veterinary and Animal Sciences, University of Copenhagen, Frederiksberg, Denmark; [1] Copenhagen Zoo, Frederiksberg, Denmark; [2] Aalborg Zoo, Aalborg, Denmark; [3] VetsuisseFaculty, Institute of Veterinary Pathology, University of Zurich, Zürich, Switzerland; [4] Institut für Veterinärpathologie, VetsuisseFakultät, Universität Zürich, Zürich, Switzerland; [5] Dept. of Parasitology and Pathobiology, University of Copenhagen, Frederiksberg, Denmark; [6] Department of Veterinary and Animal Sciences, University of Copenhagen, Frederiksberg, Denmark; [7] Copenhagen Zoo, Frederiksberg, Denmark; [8] Department of Biomedical Sciences, University of Copenhagen, Copenhagen, Denmark;

Objective: Afrotheria (“African beasts”) constitute a diverse superorder of mammalian species that diversified from the other major mammalian clades in the early Cretaceous, 145100 million years ago. Contemporary Afrotheria exhibits minimal morphological resemblance and shows a large variation in size; while elephants (*Elephantidae*) currently are the largest landliving animal, the tenrecs (*Tenrecidae*) weigh from a few grams to a little more than a kilogram. **Method:** We hypothesized that ventricular activation in the elephant heart depends on a transmural Purkinje fibre network. To investigate the effect of body size, we extended the histological and electrophysiological characterization to include the tenrec.

Results: We found that the elephant heart does have a transmural Purkinje network whereas the tenrec predominantly expresses a subendocardial network. The morphology of the Purkinje fibres is different in the two taxa. While the Purkinje fibres of the elephant are large and ovoid, those of the tenrec are smaller and harder to distinguish from working cardiomyocytes. Electrocardiography further revealed that the electrical activation pattern of the hearts was different, likely reflecting the differences in distribution of the conduction system, with the elephant heart activating in an apextobase direction, whereas the tenrec heart showed considerably more variation in the activation pattern, but an overall basetoapex direction activation pattern.

Conclusion: The results support that a transmural Purkinje fibre network is a prerequisite for a coordinated activation of the ventricular free walls in larger animals.

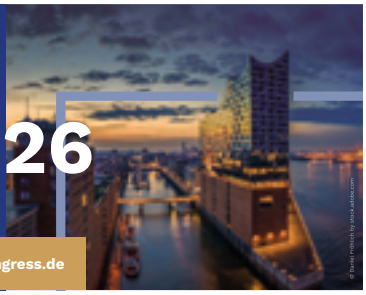

P12 Postergroup: Cardiac electrophysiology ECG

P1207

3D Cardiac Rotation from SmartphoneRecorded EASIVectorcardiography as a Surrogate for BreathingFrequency Estimation

Felix Maximilian Kuon; Markus Riemenschneider; Jürgen Lorenz
Faculty of Life Sciences, Hamburg Applied Science University, Hamburg, Germany;

Objective: Accurate assessment of respiratory rate is essential for interpreting heart rate variability (HRV), as respiratory sinus arrhythmia (RSA) contributes a significant component of vagallymediated HRV. Conventional ECGderived respiration (EDR) methods rely either on RRinterval modulation or on singlelead QRS amplitude changes, capturing only a onedimensional projection of the threedimensional (3D) thoracic heart movement during breathing. Both approaches have their limits due to lack of percission or interindividual differences in autonomic function.
Method: We developed a 3D EDR approach (HeartmovementEDR) exploiting beattobeat rotational displacement of the cardiac dipole. FrankXYZ vectorcardiograms were reconstructed from a compact fourelectrode EASI system recorded via a smartphone application. The angular displacement of the Rpeak cardiac vector was expressed as the Euclidean norm of its azimuthal and polar components. Continuous wavelet transform ridge analysis were applied within a unified Python pipeline. In a pilot study with 19 healthy adults (12 male, mean age 33.4 ± 7.5 years) performing acoustically paced breathing (6–18 breaths/min), HeartmovementEDR was compared against RRIntervalEDR and RAmplitudeEDR. Additionally HeartmovementEDR was compared with EDR results from a standard HRV software package (KubiosHRV Premium).
Results: HeartmovementEDR achieved the highest mean signaltonoise ratio (6.01 ± 3.83 dB vs. 4.62 ± 5.64 dB and 3.20 ± 4.24 dB; KruskalWallis $p < 0.001$) and the lowest mean absolute error (0.016 Hz vs. 0.050 Hz and 0.032 Hz) from the paced breathing reference. Compared with KubiosEDR, HeartmovementEDR showed superior accuracy below 10 breaths/min.

Conclusion: These results demonstrate that a standard smartphone app with only four electrodes suffices to derive robust 3D breathingfrequency estimates over the range of slow to moderately fast breathing rates, offering a practical tool for mobile HRV monitoring and vagallyactivating intervention protocols.

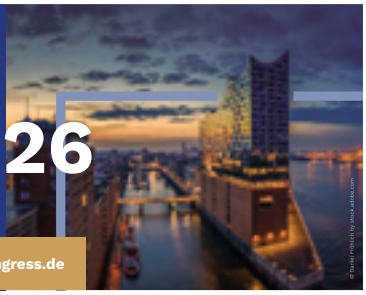

P12 Postergroup: Cardiac electrophysiology ECG

P1208

Redlight optogenetic G_i activation promotes atrial fibrillation by shortening atrial refractoriness

Caspar Robert Timpe; Daniela Malan; Wanchana Jangsangthong; Philipp Sasse
Institute of Physiology I, University Bonn, Bonn, Germany;

Objective: Atrial fibrillation (AF) is a prevalent cardiac arrhythmia caused by reentrant electrical activity promoted by heterogeneous refractoriness. Vagal G_i signaling activates G proteincoupled inwardly rectifying potassium channels and has been implicated in AF generation. To investigate the spatial and temporal requirements of G_i signaling for AF induction, we developed an optogenetic approach for precise control of cardiac G_i activation with light.
Method: We generated a novel flox mouse line for αMHCCredependent, heartspecific expression of the $G_i$coupled longwavelengthsensitive Cone opsin (hLWO).
Langendorffperfused hearts were illuminated with red light (625 nm), and atrial action potentials were recorded using sharp microelectrodes. Atrial effective refractory period (aERP) was measured using S1S2 pacing. AF susceptibility was evaluated using burst pacing (100 Hz, 3 s, 1–2.5 mA).
Results: Optogenetic activation of hLWO (44 µW/mm²) induced a sustained reduction in atrial action potential duration (APD_{90}) by 50.9±6.7% (n=4), comparable to Carbachol (CCh, 1 µM; 40.3±3.9%, n=3). By varying pulse duration and light intensity, we determined a halfmaximal light dose of 3.8 µW/mm² and an optimal stimulation protocol of 100 ms pulses at 1 Hz for sustained APD_{90} shortening. Optogenetic G_i activation shortened aERP by 13.6±2.3 ms (n=5), whereas CCh reduced aERP by 26.3±7.8 ms (n=4), indicating stronger refractoriness shortening during pharmacological stimulation.
Under control conditions, AF was only rarely inducible (22.3±7.7%, n=8), whereas optogenetic G_i activation (116 µW/mm²) significantly increased AF inducibility to 54.9±12.9% (n=8; paired ttest, p=0.0127). Likewise, CCh increased AF inducibility to 40.1±5.8% compared to control conditions (3.3±3.3%, n=5; paired ttest, p=0.0022). Successful AF induction was associated with stronger optogenetic induced APD_{90} shortening (34.1±5.7%, n=8) compared to hearts in which AF was not inducible (17.5±3.2%, n=7; unpaired ttest, p=0.0302), suggesting that a critical degree of APD shortening is required for sustained AF induction.
Conclusion: We established optogenetic control of atrial G_i signaling using hLWO, providing a powerful tool to investigate the timing, localization, and sensitivity of $G_i$dependent mechanisms underlying AF.

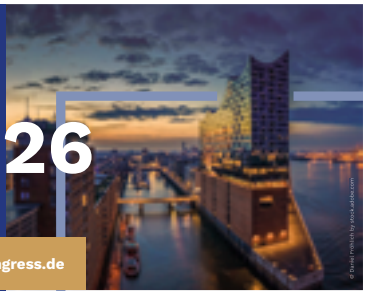

P12 Postergroup: Cardiac electrophysiology ECG

P1209

Calcium Modulates SERCA2a Activity in Human Atrial Myocytes

Andrea Brunetti; Yong Li [1]; Nefeli Pavlidou [2]; David Revuelta; Evaldas Girdauskas [3]; Carmen Dessauer [1]; Christina E. Molina
Experimentelle HerzKreislaufforschung, Zentrum für Experimentelle Medizin, Universitätsklinikum HamburgEppendorf (UKE), Hamburg, Germany; [1] Department of Integrative Biology and Pharmacology, McGovern Medical School, University of Texas Health Science Center Houston, Houston, United States; [2] DZHK Nord Germany, Hamburg, Germany; [3] Klinik und Poliklinik für Herz- und Gefäßchirurgie, Universitäres Herz- und Gefäßzentrum Hamburg, Universitätsklinikum HamburgEppendorf (UKE), Hamburg, Germany;

Objective: This project aims to identify novel mechanisms regulating SERCA2a nanodomain signaling in human atrial cardiomyocytes and to determine how these mechanisms are altered in atrial fibrillation (AF). By uncovering the role of Ca^{2+}dependent adenylyl cyclase regulation of local cAMP dynamics, this work may contribute to the development of targeted therapeutic strategies to restore excitation–contraction coupling and calcium homeostasis in AF. Ultimately, these findings could support future precision medicine approaches aimed at improving cardiac rhythm stability and reducing arrhythmogenic remodeling in patients with atrial fibrillation.
Method: Myocytes were isolated from atrial samples of patients in sinus rhythm (CtlSR) and atrial fibrillation (AF). Cardiomyocytes were transduced with the SERCA2atargeted FRET cAMP biosensor Epac1PLN. After 48 h in culture, realtime cAMP dynamics were measured following IBMX (100 µM), PDE8 inhibition (PF06427878, 30 nM), modulation of Ltype Ca^{2+} channels (BayK, nifedipine), inhibition of SOCE/TRPC channels (SKF96365), stretchactivated channels (gadolinium), ryanodine receptor activation (caffeine), and AC5/6 inhibition (vidarabine). Patchclamp recordings quantified sarcoplasmic reticulum Ca^{2+} load before and after stimulation. AC presence and activity within the SERCA2a nanodomain were assessed by RTqPCR and immunoprecipitationbased proteomics.
Results: When CtlSR human atrial myocytes were treated with PF, cAMP levels were unexpectedly halved. This reduction was also observed upon Ca^{2+} (1 mM), BayK and caffeine, but only in CtlSR not in AF cells. Interestingly, blocking Ca^{2+} release from ryanodine receptors or other calcium entry through channels present on the plasma membrane other than the Ltype, led to increased cAMP levels. RTqPCR and activity assays performed on the immunoprecipitants of SERCA2a confirmed the presence of AC5/6 and the involvement of Ca^{2+} in the regulation of SERCA2a activity and the dysregulation in AF. Vidarabine application on top of IBMX promoted a decrease of cAMP levels, further confirming a functional participation of AC5/6 in the regulation of cAMP. This reduction was not observed in the AF myocytes. Complementary, patchclamp revealed significant differences in sarcoplasmic reticulum Ca²? load when measured befor or after a stimulation train in CtlSR myocytes.
Conclusion: These findings identify a previously unrecognized Ca^{2+}dependent feedback mechanism regulating local cAMP signaling within the SERCA2a nanodomain in human atrial myocytes, which is lost in case of AF. Our data support for the first time a functional role of AC5/6 in shaping compartmentalized cAMP dynamics. Together, these results provide new insights into mechanisms controlling excitation–contraction coupling.

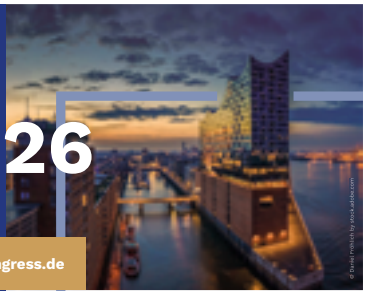

P12 Postergroup: Cardiac electrophysiology ECG

P1210

Simplistic, modelindependent protocol for assessing dynamic action potential duration adaptation

Paavo Virtanen; Huy Tran; Jussi Koivumäki
BioMediTech, Faculty of Medicine and Health Technology, Tampere University, Tampere, Finland;

Objective: Adaptation of action potential duration (APD) to heart pacing rate is a fundamental electrophysiological property of cardiomyocytes. Although computational models aim to reproduce this phenomenon, there is currently no standardised approach for simulating APD adaptation, particularly under dynamic pacing conditions. This study proposes a simple and broadly applicable dynamic restitution protocol that incorporates physiologically relevant pacing variability and aims to ease crossmodel comparisons.
Method: We developed a purposefully minimalistic dynamic APD restitution protocol designed to be modelindependent, require minimal user input, and incorporate periodic variations in pacing cycle length (CL) to reflect physiological heart rate variability. The protocol is evaluated by comparing its performance against two conventional approaches: a “mathematical” approach involving approximately 1000 action potential cycles to ensure steadystate convergence, and a “practical” approach using only tens of cycles to reach a quasisteadystate. The protocol was applied across multiple human atrial and ventricular cell models, including conditions reflecting atrial fibrillationrelated remodelling.
Results: The proposed protocol captures the twophase APD adaptation response to changes in pacing CL, characterized by an initial rapid decrease followed by a slower adaptation phase toward steadystate. Compared with traditional approaches, the protocol provides comparable insights while reducing computational requirements. Importantly, the inclusion of periodic pacing variability enabled differentiation of shortterm memory properties across different cardiac cell models and under pathological conditions such as atrial fibrillation.
Conclusion: The dynamic APD restitution protocol offers a simple, efficient, and informative alternative to existing simulation approaches. Its minimal requirements and physiological relevance make it suitable for broad adoption across modelling frameworks, potentially improving standardisation and enabling more consistent crossstudy comparisons of cardiac electrophysiological dynamics.

P13 Postergroup: Diastolic Function - a matter of relaxation

P1301

Distinct cardiac proteomic and phosphoproteomic profiles distinguish obesityindependent heart failure with preserved versus reduced ejection fraction

Franziska Koser; Mahmoud Abdellatif [1]; Theresa Bock [2]; Marcus Krüger [3]; Simon Sedej [4]; Wolfgang Linke Institut für Physiologie II, Universitätsklinikum, Westfälische WilhelmsUniversität Münster, Münster, Germany; [1] Division of Cardiology, Medical University of Graz, Graz, Austria; [2] Institute for Genetics, University of Cologne, Cologne, Germany; [3] Cologne Excellence Cluster on Cellular Stress Responses in AgingAssociated Diseases (CECAD), Universität zu Köln, Köln, Germany; [4] Kardiologie, Universitätsklinik für Innere Medizin, Medizinische Universität Graz, Graz, Austria;

Objective: The underlying pathomechanisms of human heart failure with preserved ejection fraction (HFpEF) remain poorly understood, although lowgrade systemic inflammation and endothelial dysfunction have been implicated. Here, we aimed to identify cardiac proteomic and phosphoproteomic signatures that distinguish nonobese HFpEF from heart failure with reduced ejection fraction (HFrEF), using nonfailing donor hearts as controls.
Method: Left ventricular myocardial tissue from explanted or nonfailing donor hearts (Medical University Graz) was classified as Control (Ctrl), HFpEF, or HFrEF (mean EF [%]: 63 [Ctrl], 62 [HFpEF], 24 [HFrEF]; mean age 58.1±9.5; mean BMI 26.6±2.7 kg/m²) and analysed by quantitative mass spectrometry (N=67/group).
Results: Cardiac proteome analysis identified 49 significantly regulated proteins (fold change >1.5, p<0.05) in HFpEF and 160 in HFrEF vs Ctrl hearts, out of 1813 detected cardiac proteins. Gene Ontology enrichment analysis of significantly regulated proteins in HFpEF vs Ctrl hearts revealed enrichment of the terms ”complement activation” and ”innate immune response”. Both terms were also enriched in HFrEF vs Ctrl hearts, indicating lowgrade systemic inflammation as a shared disease feature. However, the extent and phenotype of inflammatory remodelling differed between HF subtypes. Complement activation and myeloidassociated inflammation were moderate in HFpEF but more pronounced in HFrEF, reflected by more upregulated inflammatory proteins. Humoral immune activation and thromboinflammatory remodelling were observed only in HFrEF. Among the 19 proteins uniquely regulated in HFpEF, but not HFrEF, vs Ctrl hearts, two were notable: upregulated THBS4, indicating activation of the THBS4ATF6 unfolded protein response axis, and downregulated CDH13, suggesting impaired adiponectinmediated antiinflammatory signalling. Phosphoproteomic alterations in nonobese HFpEF and HFrEF vs Ctrl hearts primarily involved sarcomeric proteins (e.g., titin, desmin), which were predominantly hyperphosphorylated.
Conclusion: Both HF subtypes showed lowgrade systemic inflammation independent of obesity, with HFpEF displaying a milder complementpositive, myeloidactive phenotype than HFrEF, which exhibited stronger inflammatory activation with additional humoral and thromboinflammatory features. THBS4- and CDH13related pathways may represent HFpEFspecific targets. Systemic inflammation may contribute to altered sarcomeric protein phosphorylation.

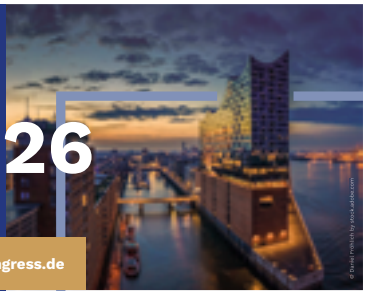

P13 Postergroup: Diastolic Function

P1302

Loss of the deubiquitinase OTUB1 induces an HFpEFlike phenotype in mice altering sarcomere, cytoskeleton- and MAPK signaling- associated proteins

Nina Oechsler; Sarah Costantino [1]; Amalia RuizSerrano [2]; Yulia L. Volkova [2]; Alexander Akhmedov [3]; Nicole Olgunelma [4]; Manuela Gesell Salazar [5]; Leif Steil [5]; Stefan Simm [6]; Uwe Völker [7]; Francesco Paneni [1]; Carsten C. Scholz Institute of Physiology, University Medicine Greifswald, Greifswald, Germany; [1] Department of Cardiology, Center for Translational and Experimental Cardiology, University Hospital Zurich, Zurich, Switzerland; [2] Institute of Physiology, University of Zurich, Zurich, Switzerland; [3] Center for Molecular Cardiology, University of Zurich, Zurich, Switzerland; [4] Institute for Bioanalytics, University of Applied Sciences Coburg, Coburg, Germany; [5] Interfaculty Institute for Genetics and Functional Genomics, University Medicine Greifswald, Greifswald, Germany; [6] Hochschule für angewandte Wissenschaften, Coburg, Germany; [7] Interfakultäres Institut für Genetik und Funktionelle Genomforschung, Universität Greifswald, Greifswald, Germany;

Objective: Heart failure with preserved ejection fraction (HFpEF) accounts for approximately 50% of all heart failure cases. Due to an incomplete understanding of the molecular mechanisms driving HFpEF progression, no causal pharmacological therapy is currently available. We previously observed that murine embryos with constitutive global *Otub1* knockout (KO) develop an increased ventricular wall diameter and heart weight. Therefore, we investigated the role of OTUB1 in cardiac homeostasis in detail.
Method: Cardiac function was assessed in adult mice with either induced wholebody or cardiacspecific *Otub1* KO using echocardiography. In addition, proteomic analysis of heart tissues from cardiacspecific *Otub1* KO mice was performed. Proteins of interest were further investigated by immunoblotting.
Results: Global and cardiacspecific *Otub1* KO led to a phenotype comparable to HFpEF, characterized by reduced cardiac output, increased left ventricular mass, extended isovolumetric relaxation and contraction time, and a preserved ejection fraction. Analysis of hearts from WT mice and mice with global *Otub1* KO revealed upregulation of sarcomere and cytoskeletal components, including actin nucleation factor Leiomodin2 (a predominantly cardiac protein) and βActin, suggesting a restructuring of the heart. Additionally, *Otub1* loss led to upregulation of MAP3K1 (an upstream activator of the ERK and JNK signaling pathways) as well as of the apoptosis- and autophagyrelated proteins PDCD10 and Beclin1, which are also relevant for cardiac homeostasis.
Conclusion: Overall, our results show that OTUB1 is an important protein for cardiac homeostasis, affecting sarcomere, cytoskeleton- and MAPK signaling- associated proteins and *Otub1* deletion induces an HFpEFlike phenotype. Studying the underlying mechanisms will likely contribute to our understanding of the molecular mechanisms leading to HFpEF and may aid in the development of a novel treatment option.

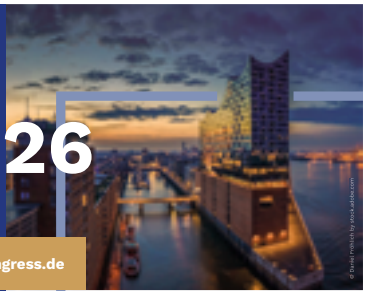

P13 Postergroup: Diastolic Function - a matter of relaxation

P1303

HFpEF, HFrEF, or maybe HFimpEF? On the Role of Ventricular Deformation and Echocardiographic Analysis Methods in the Classification of Heart Failure in Diabetic Mice

Andre Heinen; Axel Gödecke
Institut für Herz- und Kreislaufphysiologie, HeinrichHeineUniversität und Universitätstklinikum Düsseldorf, Düsseldorf, Germany;

Objective: Preclinical mouse models of heart failure are typically classified based on ejection fraction (EF) into heart failure with preserved EF (HFpEF), heart failure with reduced EF (HFrEF), or heart failure with improved EF (HFimpEF). Recently, we described a T2DMrelated mouse model (dietinduced obesity combined with lowdose streptozotocin; DIOSTZ), in which animals develop a strong HFpEF phenotype with reduced cardiac output, decreased enddiastolic volume, increased LVfilling pressure, and reduced global longitudinal strain (GLS), which is a HFpEF diagnostic criterion. From a geometric point of view, a reduction in GLS could only be reconciled with a preserved EF if the global ventricular shape is altered. However, various echocardiographic methods for the determination of LVvolumes and EF may be affected to varying degrees by changes in ventricular shape.
Method: Here we investigate ventricular deformation in the DIOSTZ HFpEF mouse model, and the impact of ventricular deformation on commonly used echocardiographic approaches for EF determination. Ventricular length (apexbase), height (anteriorposterior), and width (septallateral) were determined during diastole and systole using echocardiographic long and short axis images. Eccentricity indices (EI) were calculated (PSLAEI, length/height; and SAXEI, height/width) to describe ventricular deformation. Furthermore, EF were determined using onedimensional shortaxis diameter (EFSAX 1D), twodimensional PSLA area (EFPSLA 2D), or Simpsonmethod (EFSimpson 3D) derived volume estimates. (n=19 for DIOSTZ HFpEF group, and n=8 for chow treated control group; unpaired ttest comparison)
Results: During diastole, only minor differences in ventricular shape were detected between DIOSTZ HFpEF animals and healthy chow group. In contrast, during systole PSLAEI was highly increased (3.96±0.61 vs. 3.02±0.29, $p<0.05$), and SAXEI was reduced (1.09±0.08 vs. 1.17±0.07, $p<0.05$) in the DIOSTZ group demonstrating the occurrence of HFpEFrelated ventricular deformation. Determination of EF using EFSAX 1D indicated a robust increase in EF in DIOSTZ hearts (80.2±6.6% vs. 70.1±5.7%, $p<0.05$), whereas EFPSLA 2D resulted in a trend towards reduced EF (58.3±5.8% vs. 62.3±4.2%, $p=0.067$), and finally EFSimpson 3D showed a preserved EF (62.0±3.4% vs. 61.1±1.5%, $p=0.396$).
Conclusion: These data, obtained using an established HFpEF mouse model, show that the choice of echocardiographic analysis method has a significant impact on EFbased classification into a heart failure subtype.

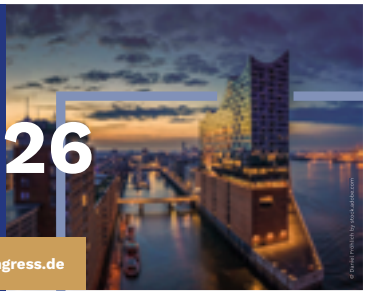

P13 Postergroup: Diastolic Function - a matter of relaxation

P1304

The SGLT2 inhibitor, Dapagliflozin, Decreases Mitochondrial Oxygen Consumption in a Murine Model of Heart Failure with Preserved Ejection Fraction

Anna Vingborg; Elina Kovalenko; Markus M. Rinschen; Tina Myhre Pedersen; Vladimir V. Matchkov
Department of Biomedicine, Aarhus University, Aarhus, Denmark;

Objective: Globally, the prevalence of hypertension and metabolic disease, including diabetes mellitus, is rapidly rising. These factors are important contributors to the development of heart failure with preserved ejection fraction (HFpEF). It is wellknown that sodiumglucose cotransporter2 inhibitors (SGLT2i) possess cardioprotective properties in heart failure. SGLT2i have previously been proposed to mediate cardiac protection by shifting substrate utilization towards fatty acid oxidation with subsequent generation of ketone bodies. Nevertheless, SGLT2irelated changes in glucose metabolism within HFpEF remain to be further elucidated.
Hypothesis: SGLT2 inhibition alters cardiac mitochondrial respiration during glucose utilization, thereby attenuating the progression of HFpEF.
Method: Male C57BL/6JRj mice were assigned to; I) vehicletreatment receiving a normal diet, II) vehicletreatment receiving a western diet (WD) combined with Nnitro1arginine methyl ester (LNAME, 600 mg/kg/day) in the drinking water; and III) treatment with a SGLT2i (dapagliflozin; 10 mg/kg diet (DAPA)) in chow combined with WD and LNAME for 6 weeks.
Echocardiography (anesthesia: inhaled isoflurane; induction 34%, maintenance 12%) was conducted prior to the initiation of the intervention period and repeated at the end of the study. At sacrifice, mitochondrial respiration in cardiac tissue was assessed using the OROBOROS O2kFluoRespirometer. $P<0.05$ is considered statistically significant.
Results: The E/e' ratio, a parameter for diastolic function, was increased in the HFpEFgroup compared to controls and this was improved with DAPA towards control values ($P=0.042$ and $P=0.51$, respectively, n=79). Furthermore, mitochondrial oxygen consumption in cardiac tissue from the HFpEFgroup was significantly increased compared with controls, though this was normalized with DAPA treatment ($P=0.008$ and $P=0.003$, respectively, n=69).
Conclusion: Decreased mitochondrial oxygen consumption may contribute to the cardioprotective effects of SGLT2i in HFpEF.

P13 Postergroup: Diastolic Function - a matter of relaxation

P1306

Coronary flow reserve and capillary density is preserved in mice with HFpEF

Katrine Hegelund Rasmussen; Eliott Hamann [1]; Oliver Holm [1]; Thomas Jepps; Ylva Hellsten [1]; Morten B Thomsen
Integrative Circulation, Institute of Biomedical Sciences, University of Copenhagen, Copenhagen, Denmark; [1] Department of nutrition, exercise and sports, University of Copenhagen, Copenhagen, Denmark;

Objective: Coronary microvascular dysfunction (CMD) is associated with developing cardiomyopathies, especially heart failure with preserved ejection fraction (HFpEF). The pathogenesis of HFpEF is poorly understood and patients with diastolic dysfunction together with a reduced coronary flow reserve (CFR) have a 5fold increase of HFpEF hospitalizations later in life. This highlights the need of developing translational animal models with a focus on CFR to understand the connection between CMD and HFpEF progression.
Aim: The present study investigates coronary function by quantifying CFR and capillary density in a HFpEF mouse model.
Method: C57BL6/NRj male mice were randomized to two groups: One group (HFpEF, n=24) received highfat diet (HFD) and water with 1 g/L of LNAME for 16 weeks. The control group (n=23) received control chow and water. Exercise capacity was tested by running distance on a treadmill. CFR was assessed in vivo by pulsewave Doppler and ex vivo in isolated hearts. Capillary density was quantified by CD31 lectin histology.
Results: Ejection fraction was similar in HFpEF mice and controls (60±9 versus 57±12%; P>0.05). HFpEF mice exhibited exercise intolerance by a shorter maximal running distance compared to control mice (201±89 versus 290±90 m; P=0.001). CFR in vivo (HFpEF: 2.76±0.4 and controls: 2.56±0.6; P=0.19) and ex vivo (HFpEF: 4.7±2.1 and controls: 4.4±1.5; P=0.64) were similar in the two groups. Capillary density staining showed no difference between the groups (HFpEF: 2974±150 versus controls: 2990±263 capillaries/mm2; P=0.9).
Conclusion: Our findings indicate that coronary flow reserve and capillary density remain unaltered in this mouse model of HFpEF.

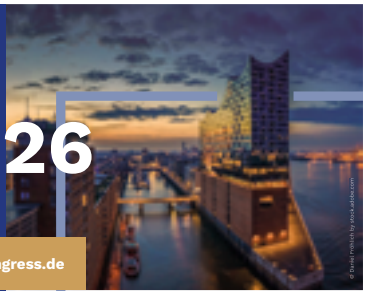

P13 Postergroup: Diastolic Function

P1307

Myotoxin II, a snake venom Lys49 phospholipase A_2 homolog, induces calcium release from intracellular stores in rat cardiomyocytes

Isabel QuirósGutiérrez; JiaHao Zhao [1]; Kathrin Kowalski; Bruno Lomonte [2]; Julián Fernández [2]; José María Gutiérrez [2]; Natalie Weber [1]; Theresia Kraft; Alfredo J. López Dávila Institute of Molecular and Cell Physiology, Hannover Medical School, Hannover, Germany; [1] Institute of Molecular and Translational Therapeutic Strategies, Hannover Medical School, Hannover, Germany; [2] Facultad de Microbiología, Instituto Clodomiro Picado, Universidad de Costa Rica, San José, Costa Rica;

Objective: Secreted phospholipase A_2 ($sPLA_2$) myotoxins are cytotoxic proteins found in snake venoms. Catalytically active $sPLA_2$ enzymes and Lys49 $sPLA_2$ homologues that lack enzymatic activity induce skeletal muscle necrosis, a hallmark of snakebite envenoming. Previous studies have shown that $sPLA_2$ myotoxins disrupt the sarcolemma, inducing calcium influx and increasing intracellular calcium concentrations. However, the effects of $sPLA_2$ myotoxins on intracellular organelles remain poorly understood.
Method: To characterize the intracellular effects of MtII, a Lys49 $sPLA_2$ homologue from the venom of *Bothrops asper*, single ventricular cardiomyocytes were isolated from male Lewis rats and used as a model for studying striated muscle. Cardiomyocyte hypercontraction was used as a surrogate marker for cell death. The animals were anaesthetized using a vaporizer with 5% isoflurane and euthanized by cervical dislocation. The cardiomyocytes were obtained by enzymatic digestion and mechanical dissociation of slices from the left ventricle. All animal procedures were conducted in accordance with German animal protection law and EU Directive 2010/63/EU, and were approved by the local authorities in Lower Saxony (LAVES, Oldenburg, Germany).
Results: Exposure to 25 µg/mL of MtII at 37 °C under physiological extracellular calcium concentrations resulted in hypercontraction of cardiomyocytes at 9.8 ± 1.8 s (mean ± SEM; n = 35). By contrast, under calciumfree extracellular conditions, hypercontraction occurred significantly later at 24.4 ± 3.3 s (mean ± SEM; n = 35; p = 0.005). Pharmacological inhibition of a key calciumhandling protein (i.e., DHPR channels) did not influence the time taken for hypercontraction to occur.
Conclusion: Our findings suggest that MtII induces calcium release from intracellular stores, probably by disrupting the membranes of mitochondria and sarcoplasmic reticulum. Intracellular calcium release may contribute to the increase in cytosolic calcium, in addition to the calcium influx from the extracellular fluid through the disrupted sarcolemma. This is likely to explain the shorter time to hypercontraction when MtII was administered in the presence of extracellular calcium. Further mechanistic studies will be performed to evaluate these hypotheses. This *ex vivo* model provides a valuable framework for understanding the cytotoxic mechanisms of Lys49 myotoxins.

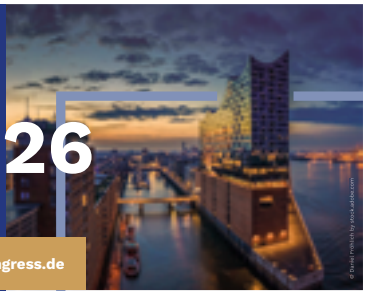

P13 Postergroup: Diastolic Function - a matter of relaxation

P1308

In vivo evaluation of cardiomyocytespecific AKAP7 gamma/delta deficiency in the mouse

Karoline Morhenn; Hariharan Subramanian [1]; Helga Vitzthum; Viacheslav O. Nikolaev [1]; Heimo
Ehmke Institut für Zelluläre und Integrative Physiologie, Zentrum für Experimentelle Medizin, Universitätsklinikum HamburgEppendorf, Hamburg, Germany; [1] Institute of Experimental Cardiovascular Research, University Medical Center HamburgEppendorf, Hamburg, Germany;

Objective: In heart failure, myocardial Ca^{2+} homeostasis is impaired, resulting in altered contraction and relaxation. Cellular mechanisms include changes in the SERCA/phospholamban (PLN) complex reducing SR Ca^{2+} filling. A kinase anchoring protein 7 γ/δ isoforms (AKAP7g/d) have been shown *in vitro* to enhance SERCA activity by anchoring PKA to the SERCA/PLN complex. We therefore investigated *in vivo* effects of cardiomyocytespecific (CM) AKAP7g/d deletion on cardiac function in two mouse models of heart failure. We expected superinhibition of SERCA, resulting in cardiac insufficiency and accelerated development of experimentally induced heart failure.
Method: All data were collected from CMspecific AKAP7g/ddeficient mice (KO) and their wildtype littermates (WT) in accordance with current EU legislation. Echocardiographic analysis was conducted in isofluraneanaesthetized mice at baseline and after i.p. injection of 0.9% NaCl or isoproterenol (2 mg/kg). Heart failure was induced by transverse aortic constriction (TAC) or ligation of the left anterior descending artery (MI); shamoperated animals served as controls (i.p. anesthesia by medetomidine 0.5 mg/kg, midazolam 5 mg/kg, fentanyl 0.05 mg/kg). Cardiac function was assessed by echocardiography 2, 6, and 10 weeks post operation; organs were taken 1112 weeks post operation. PLN and RyR phosphorylation and SERCA expression were analyzed by immunoblot. Collagen was assessed in Sirius Red/Fast Greenstained cardiac crosssections.
Results: Basal heart function and morphology did not differ between KO and WT (n=10). Acute isoproterenol injection did not induce genotypespecific effects in cardiac function (n=5). TAC and MI led to similar increases in heart weight compared to sham in both genotypes (TAC: n=711, LAD: n=914), and similar decreases in ejection fraction and fractional shortening (TAC: n=814, LAD: n=818). Longterm survival after TAC and MI was unchanged. Cardiac collagen was slightly enhanced in WT after TAC, while KO appeared protected (n=5). Following MI, no genotypespecific effect was observed (n=5). PLN Ser16 and Thr17 and RyR Ser2808 phosphorylation, and SERCA expression, were unaffected by AKAP7g/d deletion in both heart failure models (TAC: n=69, LAD: n=6).
Conclusion: Despite the wellknown *in vitro* effects of AKAP7γ/δdependent PKA anchoring to the SERCA/PLN complex, CMspecific AKAP7γ/δ deletion in mice had no detectable physiological or pathophysiological consequences *in vivo*.

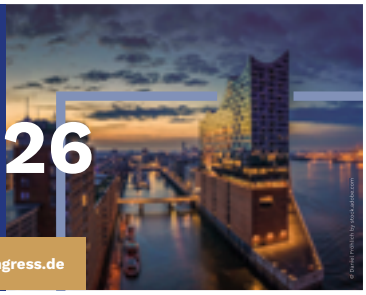

P13 Postergroup: Diastolic Function - a matter of relaxation

P1309
Functional investigation of dilated cardiomyopathy mutation in βcardiac myosin light chain 2

Rima Sarkar
Institute of Molecular and Cell Physiology, Hannover Medical School, Hannover, Germany;

Objective: To determine the functional consequences of the D94A mutation in βcardiac myosin regulatory light chain 2 (MLC2v), which is associated with dilated cardiomyopathy (DCM), and to understand how this mutation contributes to impaired cardiac contractility and pathological cardiac remodeling.
Method: Native βcardiac myosin was isolated from human left ventricular tissue. Recombinant human wildtype (WT) and D94A mutant MLC2v proteins were expressed in *E. coli*. A reconstitution system was developed to exchange native MLC2v with WT or mutant MLC2v in human cardiac myosin with high exchange efficiency. In vitro actin filament gliding (motility) assays were performed to measure myosindriven actin sliding velocity. Motility of native thin filaments (nTFs) interacting with WT and mutant myosin was also analyzed. $Ca^{2?}$ sensitivity of thin filament activation was assessed.
Results: The D94A mutation caused a significant reduction (~30%) in actin filament gliding velocity compared to WT myosin. Native thin filament motility was also reduced in the presence of mutant myosin. No change in $Ca^{2?}$ sensitivity of thin filament activation was observed between WT and mutant conditions.These findings indicate that the mutation impairs myosin motor performance without affecting $Ca^{2?}$dependent regulatory mechanisms.
Conclusion: The D94A mutation in MLC2v disrupts cardiac myosin motor function, leading to reduced actin filament sliding and impaired contractile performance. These functional deficits occur without altering $Ca^{2?}$ sensitivity, suggesting that the mutation primarily affects mechanical aspects of the myosin motor. Ongoing studies aim to further define the kinetic and mechanical basis of this impairment to better understand DCM pathology and support the development of targeted therapeutic strategies.

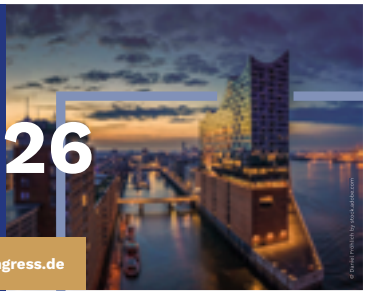

P14 Postergroup: Capturing Calcium Connections

P1401

KCa channels regulate ROS balance and cell survival in lung cancer cells

Johannes Jung; Albrecht Schwab; Héctor Noguera Hurtado Physiologisches Institut II, Universitätsklinikum, Westfälische Wilhelms Universität Münster, Münster, Germany;

Objective: KCa1.1 and KCa3.1 channels are overexpressed in nonsmall cell lung cancer and contribute to tumor cell migration and survival. They localise to the plasma and inner mitochondrial membranes, affecting membrane potential, cell volume and mitochondrial function. We aim to identify the role of KCa channels in lung cancer cells harboring two common driver mutations under various metabolic stresses.
Method: We used the human lung adenocarcinoma cell lines A549 (KRASmutated) and PC9 (EGFRmutated). Pharmacological inhibition of KCa channels was performed by membranerestricted inhibitors (iberiotoxin) and lipophilic compounds (paxilline and senicapoc). Functional assays included: cytosolic and mitochondrial ROS measurements with DCFDA and mitoSOX, respectively, mitochondrial respiration via Seahorse, and cell viability by ATP assay, after acute or 24hour treatments. Metabolic stress was induced by glucose deprivation and/or hypoxia.
Results: KCa1.1 and KCa3.1 channels are expressed in A549 and PC9 cells. KCa1.1 mRNA increases with paxilline blockade, indicating a compensatory response. Inhibition of KCa1.1 with paxilline causes the greatest rise in cytosolic ROS in both cell types under different glucose concentrations (25, 5.5 and 0.5 mmol/L glucose; N = 4). Iberiotoxin (plasmamembrane KCa1.1 inhibitor) shows no effect. Unexpectedly, the combination of KCa3.1 and KCa1.1 blockage by senicapoc and paxilline shows a lower increase in cytosolic ROS than paxilline treatment. In PC9 cells, senicapoc and paxilline increase mitochondrial ROS (senicapoc: 10.5±7.9%; paxilline: 13.3±1.6%), while dual blockage is synergistic (27 ± 4%). Blockage of KCa3.1 and KCa1.1 decreases mitochondrial respiration. Senicapoc alone and combined with paxilline reduces cell viability after 24hours. Finally, we find that KCa channels are upregulated under severe stress (1% O2 and 0.5 mmol/L glucose) which may serve as an adaptive mechanism for cancer cell survival.
Conclusion: KCa3.1 and KCa1.1 channels regulate mitochondrial redox balance, respiration, and cell survival in KRAS- and EGFRmutated lung cancer cells. Their function remains crucial for survival under severe metabolic stress.

P14 Postergroup: Capturing Calcium Connections

P1402

Calcium signals in the human zona glomerulosa

Gabriel Stölting; Cara Gebauer [1]; Ute Scholl [2]; Frederike Butz [3] Medizinische Klinik mit Schwerpunkt Nephrologie und Internistische Intensivmedizin, Campus VirchowKlinikum, Charité - Universitätsmedizin Berlin, Berlin, Germany; [1] Center of Genomic Medicine, Berlin Institute of Health at Charité, Berlin, Germany; [2] Medizinische Klinik mit Schwerpunkt Nephrologie und Internistische Intensivmedizin, Campus Mitte, Charité - Universitätsmedizin Berlin, Berlin, Germany; [3] Department of Surgery CCM|CVK, Charité – Universitätsmedizin Berlin, Berlin, Germany;

Objective: Production of the mineralocorticoid aldosterone in the zona glomerulosa (ZG) of the adrenal gland is primarily governed by the extracellular concentrations of angiotensin II (Ang II) and K^+. Such stimulation of the ZG has been shown to trigger electrical and chemical pathways converging on oscillatory fluctuations of intracellular calcium in ZG cells. Gainoffunction mutations in the ion channels and transporters involved cause increased calcium signaling, resulting in uncontrolled aldosterone release in a disease called primary aldosteronism.
Much of our current knowledge stems from clinical observations and animal model systems, primarily in mice. However, there are notable differences in the expression of ion channels and transporters between humans and mice including the absence of the mostfrequently mutated channel in aldosteroneproducing adenomas, KCNJ5.
Method: To understand the importance of these differences in controlled experiments, we established acute slice preparations from human adrenal gland samples of patients undergoing (partial) adrenalectomies. We stained these slices with organic calciumsensitive dyes and used fluorescence microscopy to quantify calcium signaling.
Results: As in model systems, human ZG cells exhibited intracellular calcium fluctuations in response to angiotensin II, but with frequencies and patterns distinct from those of murine ZG cells. Ang IIdependent calcium signaling was not observed along the whole outer cortex but in distinct clusters. Subsequent stainings for aldosterone synthase revealed a discontinuous expression pattern in agreement with the reported formation of (micro)nodules, even in patients without primary aldosteronism.
Conclusion: The results demonstrate significant functional differences between human and murine ZG cells. This highlights the need for further investigations of humanspecific calcium signaling mechanisms in both healthy and diseased adrenal glands. Our system allows for such investigations as well as pharmacological interventions aimed at mitigating primary aldosteronism.

P14 Postergroup: Capturing Calcium Connections

P1403

Inhibition of the mitochondrial $K_{Ca}3.1$ channel has anticancer effects in lung and breast cancer

Héctor Noguera Hurtado; Christina Kick [1]; Luca Matteo Todesca [2]; Joana Massa [1]; Weronika Wilczak; Emma Etmar Bulk; Jana Osthues [1]; Dominika Ciechanska; Oliver Koch [1]; Martina Düfer [1]; Bernhard Wünsch [1]; Ildikó Szabó [2]; Albrecht Schwab
Physiologisches Institut II, Universitätsklinikum, Westfälische Wilhelms Universität Münster, Münster, Germany; [1] Insitute of Pharmaceutical and Medicinal Chemistry, University of Münster, Münster, Germany; [2] Department of Biology, University of Padova, Padova, Italy;

Objective: Mitochondria regulate metabolism, redox balance, and apoptosis. Ion channels of the inner mitochondrial membrane impact bioenergetics and cell survival. This project investigates how targeting mitochondrial $K_{Ca}3.1$ channels (mito$K_{Ca}3.1$) with novel TPP^+conjugated inhibitors affects cancer cell behavior.
Method: To evaluate the function of mito$K_{Ca}3.1$, we used lung and breast cancer cell lines. Two novel senicapoc derivatives conjugated with TPP^+ were employed to inhibit the mitochondrial channel. Cells were treated either acutely or for 24h, and various assays were conducted: measurements of mitochondrial membrane potential (DY_m), cell migration, cell viability, and mitochondrial metabolism. In addition, we used transmission electron microscopy and RTqPCR.
Results: We validated the new senicapoc derivatives (mitosen and mitorevsen) by measuring DY_m in lung and breast cancer cell lines. Blocking K^+ influx through mito$K_{Ca}3.1$ hyperpolarizes the DY_m. Since mitochondrial function influences energy conversion and signaling pathways that support cancer progression, we investigated whether inhibiting mito$K_{Ca}3.1$ affects cell migration. After treating lung cancer cells with mitosen for 24h, cell translocation (control: 111±16 µm, mitosen: 42±5 µm) and cell velocity (control: 0.50±0.04 µm/min; mitosen: 0.28±0.03 µm/min) decreased. Additionally, we showed that acute application of channel inhibitors increased mitochondrial reactive oxygen species, and a 24h treatment led to endoplasmic reticulum stress. Basal respiration, ATPlinked respiration, and maximal respiration were reduced after 24h of treatment with mitosen. We confirmed that cell viability decreased in both singlecell and spheroid tumor models following mitosen treatment. Furthermore, blocking mito$K_{Ca}3.1$ resulted in mitochondrial swelling, as well as loss of mitochondrial cristae (control: 3.35±0.13 a.u.; mitosen: 2.43±0.11 a.u.). In addition, circular cristae are present in 18% of mitochondria treated with mitosenicapoc.
Conclusion: We find that the mitoKCa3.1 channel regulates mitochondrial activity and cancer cell behaviors like migration and survival. Inhibiting mito$K_{Ca}3.1$ disrupts mitochondrial ion regulation and affects metabolic and stress responses. Remarkably, mitosenicapoc works at concentrations up to 60 times lower than senicapoc.

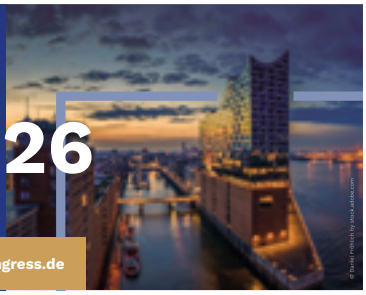

P14 Postergroup: Capturing Calcium Connections

P1404

Mechanotransduction Across Scales: Integrating Optogenetics, Calcium Imaging, and Sequencing

Rittik Bhati; Heidi Peussa; Märi Isomäki; Arri Priimägi [1]; Teemu O. Ihalainen; Soile Nymark; Huy Tran
Faculty of Medicine and Health Technology, Tampere Institute for Advanced Study, Tampere University, Tampere, Finland; [1] Faculty of Engineering and Natural Sciences, Tampere University, Tampere, Finland;

Objective: Ca^{2+} ion is a key messenger in many critical intracellular processes, allowing cells to adapt to mechanical cues and new environmental conditions. However, it remains unclear how cells interpret Ca^{2+} transient kinetics into longterm memories in gene expression pathways. Answering this question remains challenging as most transcriptomic methods do not yield spatial information, an important aspect in studying Ca^{2+} responses in tissues.
Method: Here, we present a lightbased experiment setup that combines 1) the smart photonic Disperse Red 1 (DR1) system (Fedele et al., 2020; Peussa et al., 2023) which enables the application of reproducible mechanical stimuli to cells and 2) the photoconvertible fluorescent protein pDendra (Hasle et al., 2020) for multilevel cell labeling and sorting for subsequent RNA sequencing. Both lightbased systems can be controlled independently with noncompeting wave lengths using commonly available confocal microscopes.
Results: The flexibility of the DR1 system and multilevel cell labeling by optogenetics allows us to acquire transcriptomic responses following mechanical stimulations with limited degree of temporal and spatial information.
Conclusion: When combined with Ca^{2+} imaging, this strategy can provide a dynamic framework for linking mechanical stimulation, calcium signaling dynamics and downstream gene expression responses at various subpopulation levels.

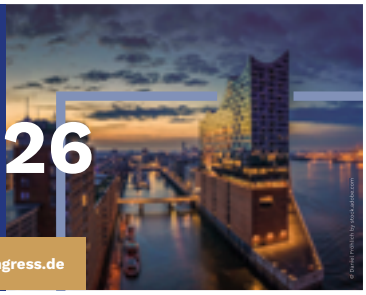

P14 Postergroup: Capturing Calcium Connections

P1405

Neuronal Ca2+ signaling is regulated by the deubiquitinating enzyme UCHL1

Finn Hennig; Sarah Frömbling; Alexandre Bouron [1]; Desiree Loreth; Catherine MeyerSchwesinger
Institut für Zelluläre und Integrative Physiologie, Zentrum für Experimentelle Medizin, Universitätsklinikum HamburgEppendorf, Hamburg, Germany; [1] Laboratoire Chimie et Biologie des Métaux (LCBM), Université Grenoble Alpes, Grenoble, France;

Objective: UCHL1 is the most abundant brain protein and besides being involved in proteasomal degradation as a deubiquitinating enzyme (DUB), the exact role is not yet understood. C57BL/6 mice deficient for UCHL1 display an agedependent accumulation of ubiquitinated proteins and a dying back axonal degeneration showing progressing motor impairment. Interestingly, mutations in the gene encoding UCHL1 are associated with Parkinson‘s disease. In this study, we investigated whether alteration in neuronal Ca2+ signaling could be causative for the motoric phenotype.
Method: Proteomic, biochemical and histological approaches were used to determine changes in neuronal Ca2+ homeostasis in constitutive UCHL1 deficient mice (KO) compared to wildtype (WT) littermates using primary neuronal cultures or total brains from embryonic to adult stages. Cervical dislocation under anesthesia (3.5% isoflurane or ketamine 120 mg/kg, xylazine 16 mg/kg, i.p) was used for brain extraction.
Results: Proteomic analysis of P5 brains (n=3) revealed upregulation of important Ca2+ signaling regulating proteins, like CamKII, SERCA, AMPAR and the VGCC Cav1.2, under UCHL1 deficiency, which was further confirmed by preliminary biochemical and histological analysis (n=6). Further, alteration in the size and morphology of Ca2+ storingorganelles (ER, mitochondria and lyso/autophagosomes) could be detected by electron microscopy and histology of E15 primary neuronal cultures (pNCs). Further and interestingly, UCHL1 DUB activity in pNCs is decreased upon intracellular Ca2+ rise induced by the application of ionomycin (1µM).
Conclusion: UCHL1 deficiency leads to alteration in neuronal Ca2+ homeostasis thereby influencing the expression of important intracellular Ca2+ regulating proteins in the brain. This might contribute to the progressive motoric phenotype of UCHL1 deficient mice.

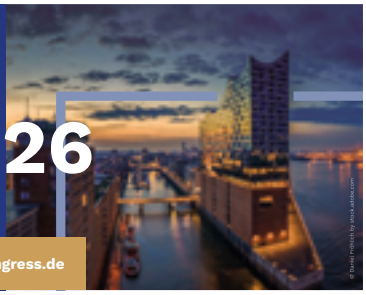

P14 Postergroup: Capturing Calcium Connections

P1406

Insights into the plasma membrane association of Extended Synaptotagmin 3

Veronika Thallmair; Saara Lautala [1]; Theresa Jolie; Alina Wlodarczyk; Sebastian Thallmair [2]; Dominik Oliver [3]
Institut für Physiologie und Pathophysiologie, PhilippsUniversität Marburg, Marburg, Germany; [1] Frankfurt Institute for Advanced Studies, Frankfurt a. M., Germany; [2] GoetheUniversität Frankfurt, Frankfurt a. M., Germany; [3] Department of Neurophysiology, Institute of Physiology and Pathophysiology, Philipps University Marburg, Marburg, Germany;

Objective: Membrane contact sites between the ER and the PM are sites of coordinated Ca2+ influx and nonvesicular lipid transport between the ER and the PM. They are indispensable for lipid homeostasis at the PM as they harbor lipid transfer proteins like for example Nirs, ORPs/OSHs and GramD proteins. Thereby they regulate among others phosphoinositide, diacylglycerol and cholesterol levels at the PM. ERPM contact sites are established by protein tethers which connect both membranes and Extended Synaptotagmins (ESyts) are the most abundant ERPM tethering family in mammals. ESyts are ERresident and regulate ERPM connectivity via reversible association with lipids at the PM. Understanding PM association of ESyts is fundamental to fully understand ERPM tethering and lipid transfer across ERPM contact sites.
Method: Here, we study PM binding ESyt 3, an understudied member of the ESyt protein family. ESyt3 contains three C2 domains and the most Cterminal C2 domain (C2C) has been shown to bind to PI(4,5)P2. However exact lipid binding properties of ESyt3 are unknown. We independently address PM association of the individual C2 domains as well as of a large unstructured linker between C2B and C2C. We use coarsegrained molecular dynamics simulations as well as cellular approaches. In living CHO cells we manipulate PM lipid content by either recruitment of phosphoinositide phosphatases or via activation of phospholipase Cβ while simultaneously imaging PM association of GFPtagged C2 domains via Total Internal Reflection Fluorescence (TIRF) microscopy.
Results: With our combinatorial approach of experiments and computation we identified that the C2C of ESyt3 not only binds to PI(4,5)P2 but also binds to PI4P. Moreover, we identified two different configurations of PM association of the C2C domains with different lipid binding profiles. Further, we identified R813, K814 and R854 as key residues for phosphoinositide binding. In addition to the C2C domain, we first identified that the unstructured linker between C2B and C2C is also a key region for PM association of the fulllength protein. Its PM association is strongly dependent on its aromatic residues. Finally, we also investigated PM association of the C2AB domains and identified for the first time that they bind to PI.
Conclusion: We identified so far unknown proteinlipid interactions with physiological impact on ERPM tethering and lipid transfer across ERPM contact sites.

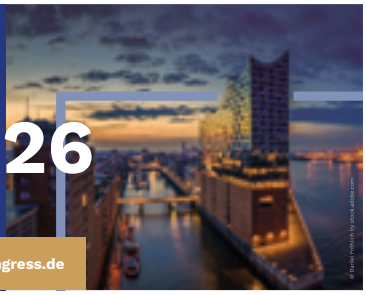

P14 Postergroup: Capturing Calcium Connections

P1407

Impact of a novel mutation in a mitochondria - ER contact site protein on cell physiology

Christine S. Gibhardt
Universitätsmedizin Göttingen, Göttingen, Germany;

Objective: Mitochondria are essential for cellular energy metabolism and their function is influenced by their internal organization and organelle contact sites. Especially, mitochondriaendoplasmic reticulum (ER) contact sites (MERCs) are of particular importance, as they regulate calcium (Ca^{2+}) signaling, lipid transfer and redox signals. Altered MERCs have been frequently discussed in the context of cancer in recent years. Additionally, their role in immunity has been explored.
This project aims to evaluate the impact of a novel mutation in a MERCresiding protein on cellular signaling, mitochondrial function and cell physiology in patientderived cells. Patients with a homozygous mutation in the ERlocalized oxidoreductase exhibit a specific clinical presentation characterized by autoimmunity.
Method: Using a variety of methods, we intend to gain new insights into cellular alterations by analyzing Ca^{2+} signaling (Fura2AM, FRETbased mitochondrial Ca^{2+} sensors), mitochondrial function (TMRE, OCR), proliferation and MERC organization (electron microscopy).
Results: We observed elevated mitochondrial Ca^{2+} levels, disturbed mitochondrial function and MERCs, as well as a highly proliferative phenotype in patientderived fibroblasts. Furthermore, we aim to uncover cellular alterations by using proteome analysis to better understand the determinants causing the autoimmune disorder and to elucidate the underlying cellular changes that lead to the patients clinical presentation.
Conclusion: Here, we demonstrate how a mutated MERC protein affects cell physiology in patientderived cells to gain more insights into disease development.

P14 Postergroup: Capturing Calcium Connections

P1408

The role of ttype calcium channels in sensory processing and arousal regulation in *Drosophila melanogaster*

Anatoli Ender; Davide Raccuglia; David Owald
Institut für Neurophysiologie, Charité Universitätsmedizin Berlin, Berlin, Germany;

Objective: Throughout the day, our brains are constantly bombarded by external stimuli, most of which get filtered out in order to extract behaviourally relevant information. This sensory filtering process continues even during sleep, with only salient stimuli capable of waking us up. While some of the brain regions and circuits involved in sleep and sensory filtering are known, the underlying neuronal mechanism remains largely unclear.
Sleep is highly conserved across vertebrates and invertebrates, making *Drosophila* an ideal model to investigate these mechanisms. Slow wave oscillations have previously been identified in the R5 network of the central complex, which encodes sleep drive in *Drosophila*. Furthermore, recent work has shown that network synchrony in this brain region establishes a neural filter that promotes quiescence. We hypothesise that intrinsic membrane currents in R5 neurons are critical for establishing a sensory filter that, while promoting sleep, retains the capacity to allow the animal to detect and respond to salient stimuli.
Method: To characterise the intrinsic properties and mechanisms underlying sensory processing of R5 neurons, we performed *in vivo* wholecell patch clamp and GCaMP recordings of R5 cells in the central complex. Behavioural arousal assays were performed in sleepdeprived animals to assess the functional relevance of the identified channels.
Results: We identified a networkindependent activity component in R5 neurons that correlates with the animal's sleep need, being present in sleepdeprived animals but absent in wellrested flies. *In vivo* patch clamp recordings revealed calcium currents in R5 neurons that become apparent only after blocking sodium currents, indicating a cellintrinsic calcium conductance. Targeted knockdown of the *Drosophila* Ttype Ca_V3 channel abolished these calcium currents and reduced the sensitivity of R5 neurons to visuallyevoked stimuli.
Conclusion: We propose a dual function of ttype currents: amplifying incoming signals and generating arousal windows at the output level. Our data suggest that ttype currents define in- and output gates of a sensory filter and contribute to a lesser extent to the pacemaking of sodium bursts in R5 neurons. Together, these findings suggest that intrinsic Ttype calcium channel activity in R5 neurons links sleep need to sensory sensitivity, providing a cellular mechanism by which the sleeping brain maintains selective arousability to salient stimuli.

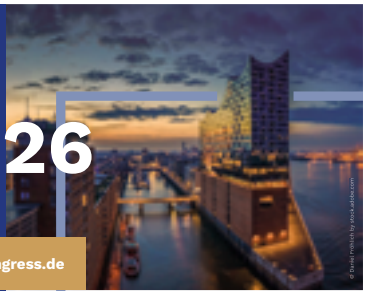

P14 Postergroup: Capturing Calcium Connections

P1409

How central is the cytosolic calcium level? From *in vitro* measurements to mathematical modeling

Bhati Rittik; Heidi Peussa; Aapo Tervonen; Jari Hyttinen; Soile Nymark; Teemu O. Ihalainen; Huy Tran
Faculty of Medicine and Health Technology, Tampere Institute for Advanced Study, Tampere University, Tampere, Finland;

Objective: Calcium ion (Ca^{2+}) is an essential second messenger for intracellular and intercellular signaling, enabling cells to navigate complex environments and ensure accurate differentiation during development as well as the maintenance of physiological functions. Most mathematical models of Ca^{2+} dynamics assume a multitude of ion channels that measure highdimensional properties of the cellular environment and integrate their readouts into a single cytosolic Ca^{2+} signal. However, relying on this onedimensional Ca^{2+} signal seems insufficient to explain the complexity of downstream cellular responses.
Method: Through live imaging of Ca^{2+} dynamics in epithelial MadinDarby canine kidney (MDCKII) cells, we observed that cytosolic Ca^{2+} levels at rest are far from stable, instead exhibiting a nonperiodic blinking behavior triggered primarily by sporadic Ca^{2+} influx through Piezo1 channels. When Ca^{2+} influx was maintained by opening Piezo1 channels with the drug Yoda1, we observed Ca^{2+} oscillations in all cells, driven by the same feedback mechanism responsible for the classic ATPdriven Ca^{2+} oscillation. These oscillations persisted only until a high cytosolic Ca^{2+} concentration (~400 nM) was reached.
Results: Through stability analysis of a simple Ca^{2+} model, we demonstrated that Ca^{2+} feedback mechanisms must be partially insulated from the cytosolic Ca^{2+} level within a cellular subcompartment. In this compartment, intracellular Ca^{2+} response kinetics should operate near criticality to maximize sensitivity to small perturbations, albeit at the expense of specificity (i.e., the ability to distinguish the source and amplitude of perturbations).
Conclusion: Our findings show the limit of the cytosolic Ca^{2+} level, which has been the most accessible with the use of dyes and fluorescent reporters. They highlight the importance of studying Ca^{2+} dynamics in subcompartments, as well as other modes of signal transduction.

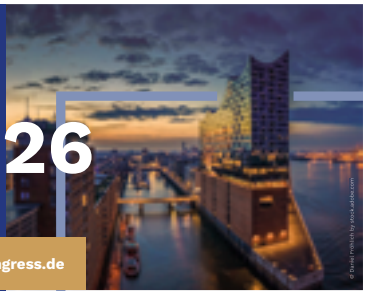

P14 Postergroup: Capturing Calcium Connections

P1411

Extracellular linker of ASIC1a accounts for isoformspecific modulation by the chaperone PCYOX1L

Samuel Kühs; Michal Stawarski; Sven Kuspiel; Eva Kläser; Stefan Gründer
Institut of physiology, RWTH Aachen University, Aachen, Germany;

Objective: Acidsensing ion channels (ASICs) are modulators of neuronal excitability. Recent proteomic analyses identified prenylcysteine oxidase 1 like (PCYOX1L) as a novel ASIC1ainteracting partner. PCYOX1L is ubiquitously expressed in neurons, facilitates ASIC1a oligomerization and trafficking to the plasma membrane, and its genetic ablation markedly impairs hippocampal longterm potentiation. Although PCYOX1L is presumed to function as a chaperone, the precise ASIC1aPCYOX1L interaction interface remains unknown. Since PCYOX1L is secreted, it is suspected to interact with the extracellular domain (ECD) of ASIC1a. Intriguingly, we found that PCYOX1L robustly potentiated rat ASIC1a (rASIC1a) but not chicken ASIC1a (cASIC1a) currents, suggesting a previously unrecognized speciesspecific modulatory mechanism.
Method: To delineate the putative PCYOX1L binding site, we generated a panel of chimeric rat/chicken ASIC1a constructs. These constructs were transiently expressed in HEK293 cells with a double KO of ASIC1a and PCYOX1L. Whole cell patchclamp recordings quantified total ASIC1amediated currents with and without PCYOX1L. To validate the dependence of oligomerization on PCYOX1L, clear nativePAGE experiments were performed.
Results: Functional screening of the rat/chicken ASIC1 chimeras identified a short linker in the ECD responsible for the dependence on PCYOX1L. Assessing oligomerization using clear nativePAGE confirmed these findings. Furthermore, single point mutations in the linker connecting β9 and α4 of the rASIC1a ECD were sufficient to eliminate PCYOX1L dependence of rASIC1a.
Conclusion: Collectively, these results pinpoint a discrete linker region within the ASIC1a ECD as the determinant of the speciesspecific modulation by PCYOX1L. This motif represents a potential pharmacological target for the selective regulation of ASIC1a activity.

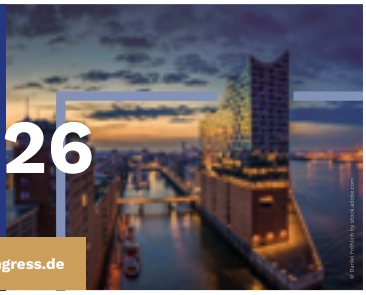

P14 Postergroup: Capturing Calcium Connections

P1412

K^+ channelmediated regulation of neutrophil migration and tumor immune infiltration in NSCLC

Alexa Heuer; Dominika Ciechanska; Sandra Schimmelpfennig; Maicol Mancini [1]; Antonio Maraver [1]; Salome Barbakadze [2]; Steffanie Bode [2]; Albrecht Schwab; Friedemann Kiefer [2] Physiologisches Institut II, Universitätsklinikum, Westfälische Wilhelms Universität Münster, Münster, Germany; [1] Institute of Cancer Research of Montpellier, Montpellier, France; [2] European Institute for Molecular Imaging, University Münster, Münster, Germany;

Objective: Neutrophils are early responders in innate immunity, rapidly migrating to sites of infection or inflammation. For efficient chemotaxis, K^+ channels such as $K_{Ca}3.1$ are essential, as they regulate membrane potential and cell volume. Therefore, K^+ channels also influence immune cell infiltration in tumors, highlighting their potential as therapeutic targets for modulation of the tumor microenvironment.
Method: In this study, we investigated neutrophil behavior in response to C5a and CXCL1 and examined the role of K^+ channels using targeted pharmacological inhibition. Livecell imaging of isolated murine neutrophils was applied to analyze chemotaxis *in vitro*. Moreover, $K_{Ca}3.1$ was inhibited in mice bearing non–small cell lung cancer (NSCLC) tumors using senicapoc. Tumors were analyzed by confocal microscopy. The neutrophiltolymphocyte ratio was used as marker of immune cell composition. Comparison of neutrophiltolymphocyte ratio between treated and untreated tumors was performed to assess the impact of $K_{Ca}3.1$ on the tumor microenvironment.
Results: Chemotaxis experiments showed increased directionality and translocation of neutrophils in response to CXCL1 compared to C5a. Inhibition of $K_{Ca}3.1$ using senicapoc impaired chemotaxis toward both chemoattractants, confirming the established role of $K_{Ca}3.1$ in neutrophil migration. For the analysis within the tumor microenvironment, a workflow was established enabling comparison of the neutrophiltolymphocyte ratio between the tumor core and the peripheral 250 µm region in confocal images. Our data demonstrate differential distributions of neutrophils and $CD8^+$ T cells within these regions. Neutrophils were further visualized by lightsheet microscopy, providing a threedimensional representation of their distribution.
Conclusion: Taken together, our findings highlight $K_{Ca}3.1$ as a potential therapeutic target for modulation of neutrophil migration and immune cell infiltration in NSCLC. These results support further investigation of ion channel targeting as a strategy to shape the tumor immune microenvironment.

P15 Postergroup: Hypoxia & pulmonary functions (applications, preclinical models)

P1501

Advancing preclinical models for investigating retinal degeneration and identifying novel therapeutic approaches

Annika Schubert; Anna Malyshkina; Bettina Budeus [1]; Claudia Padberg; Joachim Fandrey; Yoshiyuki Henning
Institut für Physiologie, Universitätsklinikum Essen AöR, Essen, Germany; [1] Institute of Cell Biology (Cancer Research), University Hospital Essen, University of DuisburgEssen, Essen, Germany;

Objective: The degeneration and atrophy of retinal pigment epithelium (RPE) cells, a monolayer of supportive cells that are crucial for photoreceptor health, play a central role in retinal degenerative diseases such as agerelated macular degeneration (AMD). Therefore, studying RPE degeneration in appropriate preclinical models is highly important for understanding underlying mechanisms and screening for potential new therapeutics.
Method: To overcome limitations of the widely used human ARPE19 cell line, which progressively loses its characteristic RPEspecific phenotype, we investigated two alternative RPE models. First, an improved fourweek longterm maturation protocol was applied to ARPE19 cells to promote redifferentiation. Second, a primary porcine RPE (ppRPE) culture was established using pig eyes obtained from a slaughterhouse. Due to the anatomical and physiological similarities between porcine and human eyes, including retinal structure and gene expression patterns, porcine models are highly relevant as preclinical models for studying human diseases.
Results: The ARPE19 maturation protocol resulted in an improved morphology, and an RPElike metabolic phenotype and gene expression pattern. Using this longterm ARPE19 model, we also evaluated two clinically approved drugs (Vorinostat and Ruxolitinib) currently used for other diseases for their potential to reduce oxidative stress and hypoxiainduced cell death, both hallmarks of advanced AMD. Both drugs showed promising results, demonstrating protective effects against RPE degeneration in this model. Therefore, we are currently evaluating the efficacy of these drugs in the ppRPE model.
Conclusion: Together, these models provide valuable preclinical platforms for investigating AMDrelated pathophysiology and evaluating novel therapeutic strategies.

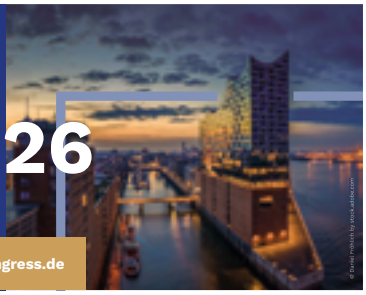

P15 Postergroup: Hypoxia & pulmonary functions (applications, preclinical models)

P1502

Effects of nocturnal periodic breathing on cerebral blood flow response at high altitude: a randomised, crossover study

Rachel Turner; Johanna Roche [1]; Giovanni Vinetti; Hannes Gatterer; Christoph Siebenmann Institute of Mountain Emergency Medicine, Eurac Research, Bolzano, Italy; [1] Pulmonary Division and Sleep Disorders Center, University Hospital of Zürich, Zürich, Switzerland;

Objective: Hypoxic exposure increases the ventilatory response to changes in arterial partial pressure of carbon dioxide ($PaCO_2$), which predisposes to ventilatory instability, commonly giving rise to central sleep apnoea and the characteristic nocturnal periodic breathing (nPB) observed at highaltitude. During nPB, cyclical alternations between apnoea and postapnoeic hyperpnoea generate pronounced oscillations in both $PaCO_2$ and arterial oxygen saturation (SaO_2). However, to what extent this cyclical stimulus exerts a sustained influence on the cerebrovasculature remains unclear. Therefore, we investigated whether inhibiting nPB at altitude contributes to a differential waking cerebral blood flow (CBF) response and acute mountain sickness (AMS) prevalence at 4000 m.
Method: In a randomized, placebocontrolled, singleblind, crossover trial, nine healthy men completed two 3day sojourns in a hypobaric chamber at a simulated altitude of 4,000 m. During one sojourn nPB was inhibited (nPB) by continuous monitoring and individual adjustment of inspiratory CO_2 fraction throughout each night, whereas during the other sojourn nPB was left unprevented (nPB+). CBF was assessed before chamber entry at sea level, the morning after the first night (TP1), the afternoon after the first night (TP2) and the following afternoon (TP3) via highresolution, duplex sonography of both extracranial arteries. Resting cardiorespiratory measurements and AMS severity were assessed directly prior to each CBF measure and each subsequent morning.
Results: Cerebral blood flow was not different between sojourns at any timepoint (sojourn: p = 0.920, time × sojourn: p = 0.624). AMS scores (sojourn: p = 0.137, time × sojourn: p = 0.328) and cardiorespiratory variables (sojourn: all $p \geq 0.079$, time × sojourn: all $p \geq 0.118$) throughout the sojourns were also similar.
Conclusion: nPB inhibition did not affect ventilation, AMS prevalence or the CBF response associated with a threeday hypobaric hypoxia sojourn. However, it remains unclear whether nPB and indeed diurnal PB exert a specifically beneficial or detrimental effect during early acclimatisation, plus longer exposures remain to be investigated.

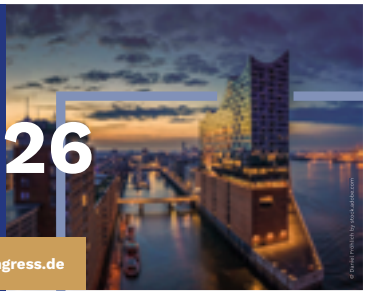

P15 Postergroup: Hypoxia & pulmonary functions (applications, preclinical models)

P1503

Blood gas and acidbase parameter variations in regard to experimental and clinical applications

Mario Lira; Ali Kashefi; Khosrow Mottaghy
Extracorporeal Circulation Laboratory, Institute of Physiology, Medical Faculty RWTH Aachen University, Aachen, Germany;

Objective: Blood gas parameters are measured under noflow conditions establishing the relationship between O_2 Saturation and PO_2. However our investigations demonstrate that the deformability of red blood cells under shear flow is an important factor because it affects the velocity of O_2 uptake and release. The purpose of this study is to evaluate the degree of gas exchange during sheared blood flow and its influence upon O_2 uptake and CO_2 removal.
Method: Specially designed purediffusive membrane lungs (oxygenators) were inserted into a recirculating circuit driven by small blood pumps. One oxygenator was used for arterializing venous blood coming from a reservoir, which collects venous blood from a desoxygenator configured to provide the desired inlet venous blood gas data. This experimental circuit enabled us to reveal the dynamic flow process of blood gas exchange, closely according to the in vivo situation.
Results: Blood gas and acidbase parameters were measured under given flow conditions. PCO_2 was artificially increased up to 80 mmHg simulating lung insufficiency under a constant blood flow rate, and the course of its drop to arterial values as a function of time was monitored during the application of the artificial membrane lung. Furthermore, we report the obtained bicarbonate kinetics and acidbase parameters. These results can be applied to evaluate the necessary total surface area and blood/gas flow conditions for a membrane lung, and its gassing strategy to achieve physiologically arterialized blood gas parameters.
Conclusion: The obtained results can be used for designing new, highperformance oxygenators optimized to improve the oxygen uptake rate and the extracorporeal CO_2 removal in severe lung diseases. This research was funded by the European Union´s Horizon Europe research and innovation programme under grant agreement No. 101130006.

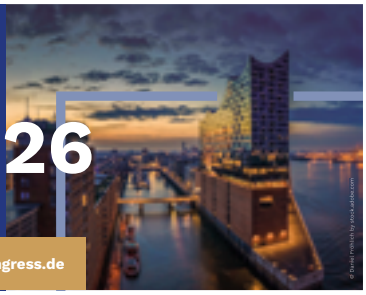

P15 Postergroup: Hypoxia & pulmonary functions (applications, preclinical models)

P1504

Regulatory functions of cold on oxygen transport and human performance: a review

Dominique Gagnon; Stephen Cheung [1]
Helsinki Clinic for Sport and Exercise Medicine, Helsinki, Finland; [1] Kinesiology, Brock, St. Catharines, Canada;

Objective: Cold exposure impairs exercise performance through multiple physiological mechanisms. Hyperoxia can restore exercise capacity in the cold, thus highlighting oxygen availability as a key limiting factor.
Results: At the lungs, cold air induces bronchoconstriction, although increased ventilation can partly compensate for reduced respiratory efficiency. Temperature also regulates oxygen diffusion properties, reducing oxygen unloading capacity and impairing delivery to active muscle tissue. O_2 diffusion coefficient is reduced by 3% per °C but its solubility is increased by approximately 1.4% per °C, ultimately compromising the unloading portion of the oxygen transport pathway by 1.6% per °C. Moreover, cold exposure affects vascular regulation by decreasing blood flow and convective oxygen transport through sympathetically mediated vasoconstriction. This vasoconstriction may suppress ATP and nitric oxidemediated vasodilation generally observed with from exercise, further reducing oxygen availability to exercising muscles. Interestingly, and despite a lower oxygen diffusion coefficient, a compensatory increase in oxygen extraction via a steeper blood flow / oxygen consumption curve, from increased blood pressure or otherwise, partly offsets these limitations. Finally, mitochondrial ATP production may be compromised by ion leakage and altered fatty acid metabolism during muscle cooling, potentially limiting force generation and muscular performance.
Conclusion: Although numerous studies have reported local muscle lower tissue oxygen saturation during exercise under cold conditions (520%), methodological inconsistencies have contributed to variable findings. Despite some physiological compensation, cold may severely and negatively influence muscle function and exercise capacity through integrated disruption pathways in oxygen transport, vascular regulation, and oxidative metabolism.

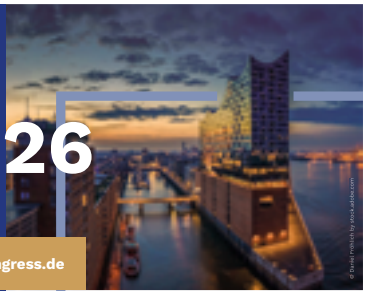

P15 Postergroup: Hypoxia & pulmonary functions (applications, preclinical models)

P1505

Phospholipid optimized Artificial Oxygen Carrier For Clinical Application

Fjorarba Mamaj; Fabian Nocke; Katja Siebecke [1]
Institute of Physiological Chemistry, University Hospital Essen, Essen, Germany; [1] Institute of Physiology, University Hospital Essen, Essen, Germany;

Objective: Artificial oxygen carriers (AOC) such as our lecithinmodified nanoscale oxygen carriers (LENOX) have proven to be an effective treatment against hypoxia. They consist of a perfluorodecalin core with an albumin/lecithin shell, and this nanoemulsion is miscible with aqueos media (e.g. cell culture medium, volume substitution solutions, blood). For clinical translation, of LENOX, a defined product is an important prerequisite and since LENOX shall also be applied intravenously, the requirements on the final product and its components are very high. Especially the natural component lecithin (a nondefined mixture of many different phospholipids and impurities) could be a bottleneck.
In this work we analyze the impact of different commercially available and clinically approved clearly defined phospholipid mixtures on the LENOX synthesis process and nanoemulsion characteristics.
Method: LENOX were synthesized as described previously, except for exchanging the lecithin with different predefined phospholipid compositions. The final products were analyzed by dynamic light scattering for particle size distribution and by a rheometer for viscosity. A light microscope was used to detect possible larger particles > 1 µm. Finally, the oxygen release was determined by a respirometer as a test of functionality.
Results: As compared to the original LENOX formulation, we aimed for minimal impact on the shearthinning rheological properties of the nanoemulsion, a similar or narrowed particle size distribution and preserved functionality for the novel LENOX versions. We identified preserved rheological and functional properties in combination with a measurable difference of particle size distributions for the different phospholipid compositions used for LENOX synthesis.
Conclusion: In conclusion, we could define a set of phospholipid compositions resulting in a stable and highly functional LENOX formulation. This results in a clearly defined product and allows a step forward towards clinical approval.
Acknowledgement
We thank Lipoid GmbH for providing the phospholipid compositions.

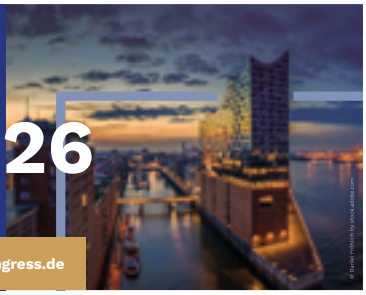

P15 Postergroup: Hypoxia & pulmonary functions (applications, preclinical models)

P1506

The DDAH1 and DDAH2 genes affect the adaptation response of the lung circulation to high altitude hypoxia – Results of ALTIGENE: a Mendelianrandomized study at 3,450 m

Rainer H. Böger; Kilian Thompson; Marcus Lifke; Juliane Hannemann Institute of Clinical Pharmacology and Toxicology, University Medical Center HamburgEppendorf, Hamburg, Germany;

Objective: Reduced release of the endotheliumderived vasodilator nitric oxide (NO) has is involved in hypoxic pulmonary vasoconstriction. In previous studies, we observed that increased levels of the NO synthesis inhibitor, ADMA, are prospectively associated with high altitude pulmonary hypertension (HAPH). ADMA is enzymatically cleared by dimethylarginine dimethylaminohydrolase (DDAH)1 and 2. We previously reported that the single nucleotide polymorphisms (SNPs) DDAH1 rs233112 and DDAH2 rs805304 are associated with the incidence of high altitude pulmonary hypertension after longterm altitude exposure. We now performed a prospective, Mendelianrandomized study to analyse whether these SNPs affect the pulmonary vasoconstrictor and respiratory adaptation to high altitude.
Method: Out of a large group of 249 volunteers aged between 18 and 40 years who were genotyped, we included 39 healthy young volunteers who were homozygous major or homozygous minor carriers of the DDAH1 rs233112 or the DDAH2 rs805304 SNPs, with the respective other SNP in heterozygous state. Each subject was studied at baseline in Hamburg (6 m above sea level) and on days 1, 2, 4, and 7 during a 7day sojourn at 3,450 m above sea level at the High Altitude Research Station Jungfraujoch, Switzerland. Blood samples, respiratory function, and cardiac function (echocardiography) were repeatedly tested.
Results: Haematocrit increased with lower arterial oxygen saturation at altitude with no significant differences between the genetically defined groups. However, pulmonary vascular resistance and systolic pulmonary artery pressure showed different trends between participants who were homozygous major or homozygous minor for DDAH1 rs233112, with higher pulmonary artery pressure in homozygous carriers of minor allele (p=0.044). This was paralleled by slight increases in ADMA and a significant increase in Lornithine. In the systemic circulation, LVEF was higher in carriers of the minor allele than in those homozygous for the major allele. In addition, homozygous carriers of the major allele of DDAH1 rs233112 showed more severe symptoms of acute mountain sickness. Individuals who were homozygous major for DDAH2 rs805304 showed a smaller increase in pulmonary pressure and less fatigue than homozygous carriers of the minor allele, but they experienced a transiently increased bronchial obstruction at high altitude.
Conclusion: The DDAH1 SNP rs233112 and the DDAH2 SNP rs805304 have a multi-dimensional effect on the adaptation of both the pulmonary and systemic circulation at high altitude. They also affect respiratory adaptation and the incidence of acute mountain sickness. Thus, our data provide strong genetic and functional evidence for an involvement of the Larginine/ADMA/DDAH/NO signal transduction pathway in the adaptation of the pulmonary and systemic vasculature to chronic high altitude hypoxia.

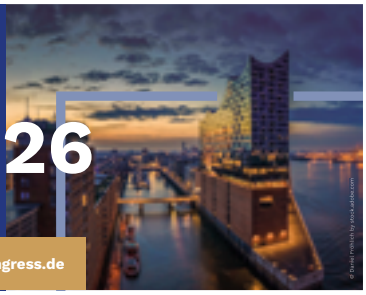

P15 Postergroup: Hypoxia & pulmonary functions (applications, preclinical models)

P1507

Generation and characterization of urinary bladder organoids

Vivienne Schneider; Joachim Fandrey; Nora Koll; Sandra Winning
Abteilung Physiologie, Universitätsklinikum Essen, Essen, Germany;

Objective: Urinary bladder carcinoma (UBC) is associated with chronic inflammation and a drop of oxygen in the tumor microenvironment. Thus, the hypoxiainducible factor 1 (HIF1) is a potential prognostic marker for poor outcome in UBC holding an important role in the urothelium. Ninety percent of UBC arise from urothelial cells, which can be categorized into basal, intermediate, and umbrella cells. In this project, urinary bladder organoids (UBO) will be used to analyze the underlying signaling pathways of UBC formation and the additional role of urinary tract infections.
Method: UBO were generated under normoxic conditions and characterized under roxadustat stimulation using microscopy and quantitative mRNA analysis for their cellular composition and HIF target gene expression as well as protein analysis for HIF expression.
Results: This revealed the expression of typical urothelial cell markers like cytokeratin 5, 14 and 20 as well as uroplakin 1b. Further, roxadustat induced accumulation of HIF1a protein and HIF target gene expression.
Conclusion: We successfully proved UBO to show important features of the urothelium. Next, we will try to generate murine UBO with *Hif*1a knockout. Ultimately, we plan to infect the organoids with uropathogenic *E. coli* and treat them with carcinogens to analyze critical aspects of UBC formation.
The resulting data will help to deepen our understanding of the relationship between HIF, urinary tract infections and UBC.

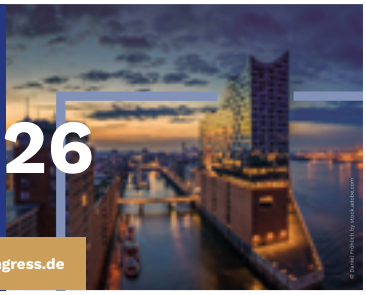

P15 Postergroup: Hypoxia & pulmonary functions (applications, preclinical models)

P1508

Establishment of a human alveolar coculture model to investigate epithelial - immune communication

Philipp Kolb; Susanne Wespel; Achim Riecker; Johanna Diehm; Hongyu Miao; Manfred Frick
Institute of General Physiology, University of Ulm, Ulm, Germany;

Objective: The alveolar niche is the central functional unit of the lung and consists of highly specialized epithelial and immune cell populations that play essential roles in maintaining alveolar homeostasis. Human in vitro models that recapitulate the cellular complexity of the alveolar niche remain limited. Here, we describe the establishment of a human alveolar coculture model consisting of induced pluripotent stem cell (iPSC)derived alveolar epithelial cells and human monocytederived alveolar macrophages.
Method: Human iPSCs were differentiated via definitive endoderm and anterior foregut endoderm stages into NKX21positive lung progenitors, which were subsequently specified into alveolar type 2like cells (iAT2s) and maintained as alveolospheres. Differentiation towards alveolar type 1like cells (iAT1s) was induced through modulation of YAP/TAZ signaling by LATS inhibition. Cellular identity was assessed by immunofluorescence staining, morphological characterization, and gene expression analysis. iAT2s expressed canonical alveolar markers and demonstrated functionality through inducible surfactant release associated with fusion of lamellar bodies with the plasma membrane. iAT1like cells displayed characteristic flattened morphology and expression of AT1associated markers. To establish the immune compartment of the model, human peripheral blood monocytes isolated from buffy coats were differentiated into alveolar macrophagelike cells using established cytokinebased differentiation protocols. Differentiated macrophages exhibited alveolar macrophagelike morphology and expression of associated markers.
Results: All three cell populations were successfully maintained under coculture conditions. Interactions between epithelial and immune cells were observed, including strong cellular attachment and indications of intercellular dye transfer between the epithelial and immune compartments.
Conclusion: This model provides a human in vitro platform for investigating epithelial–immune interactions within the alveolar niche and may enable future studies on stretchinduced signaling and inflammatory responses in lung disease.

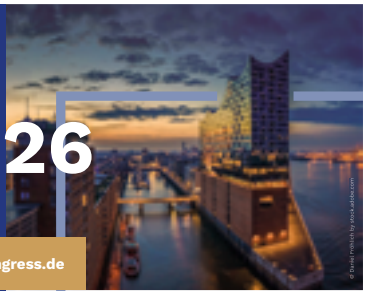

P15 Postergroup: Hypoxia & pulmonary functions (applications, preclinical models)

P1509

Attenuation of Thermal and Cardiovascular Strain via Skin Capsaicin Application During Prolonged HighIntensity Interval Exercise

Athanasios Zavvos; Iro Kaltsoni; Evangelia Soukara; Panagiotis Miliotis; Maria Koskolou; Nickos Geladas
Department of Physical Education and Sport Science, National and Kapodistrian University of Athens, Dafni, Greece;

Objective: Prolonged highintensity interval exercise induces significant thermal strain by elevating core body temperature (Tre). This study investigated whether the skin application of capsaicin can attenuate thermal strain and enhance the sensation of thirst during such exercise.
Method: Seventeen physically active men participated on two separate occasions: without (Con) and with capsaicin application (Caps). In the Caps condition, four patches—each containing 4.8 mg of capsaicin—were applied to four anatomical sites: the pectoralis major, the trapezius, and on the rectus femoris of each leg. Wearing standard athletic attire (Tshirt and shorts), participants rested for 30 minutes before the exercise protocol. The protocol consisted of six 4min bouts at 7075% of VO2max. Rectal temperature (Tre), skin temperature (Tskin) at four sites (chest, arm, thigh, and leg), local sweating rate (SwR), and heart rate (HR) were recorded continuously throughout the experimental protocol. Additionally, thirst sensation (TS) and thermal sensation were assessed. Environmental conditions were maintained at 21.3±1.13°C and 39±6.7% relative humidity (RH).
Results: Capsaicin application resulted in a lower Tre (Caps: 37.45±0.05°C vs Con: 37.60±0.05°C, $p \leq 0.001$, d=0.47) and Tskin (Caps: 32.13±0.21°C vs Con: 32.34±0.21°C, $p \leq 0.001$, d=0.28) compared to Con. Conversely, SwR (Caps: 0.97±0.02 mg/cm²/min vs Con: 0.44±0.22 mg/cm²/min, $p \leq 0.001$, d=4.25) was higher in Caps. Additionally, HR (Caps: 146±3.39 vs Con: 148±3.39 bpm, $p \leq 0.01$, d=0.59) was lower in Caps. Regarding TS (Caps: 4.80±0.41 vs Con: 4.80±0.41, p=0.94, d=0.01), no significant difference was observed. In contrast, thermal sensation (Caps: 7.00±0.32 vs Con: 6.00±0.32, $p \leq 0.001$, d=0.86) was higher in Caps compared to Con.
Conclusion: Skin application of capsaicin during prolonged highintensity interval exercise appears to enhance the thermoregulatory heat loss, reducing both Tre and Tskin via an increased SwR, thereby contributing to the mitigation of thermal strain. The minor reduction of HR, despite a higher thermal sensation, implies less cardiovascular strain with capsaicin application. Lastly, capsaicin does not appear to alter thirst sensation during exercise.

P15 Postergroup: Hypoxia & pulmonary functions (applications, preclinical models)

P1510

Cardiorespiratory Coupling is a robust Marker of respirationrelated vagal Modulation across Sleep, Stress and ApneaRelated Conditions Using HighFrequency Heart Rate Variability and Respiration Signals

Woolyn Cho; Katrin Schröder
Zphys1, University clinic, Goethe Univeristy, Frankfurt a. M., Germany;

Objective: Cardiorespiratory coupling reflects the interaction between autonomic cardiac regulation and respiration. Because respiration strongly modulates highfrequency heart rate variability (HFHRV), this coupling may indicate physiological state changes during sleep, stress and respiratory disturbances. This project aimed to develop a reproducible computational pipeline to assess respirationrelated vagal modulation across different physiological conditions.
Method: Publicly available datasets were analysed, including one CAP Sleep control recording, the drive01 stress recording and the a01 ApneaECG recording. ECG signals were bandpass filtered, R peaks were detected and RR intervals were interpolated to 4 Hz. Respiratory signals, when available, were filtered and resampled to the same time base. HFHRV was calculated as spectral power in the 0.15–0.40 Hz band using Welch analysis. Magnitudesquared coherence between HRV and respiration was assessed in 60 s sliding windows with 30 s overlap.
Results: In the CAP Sleep analysis, N3like windows showed higher HFHRV than N2like windows (2.83×10^{-4} vs. 8.77×10^{-5}; n = 70 vs. 104), while HF coherence differed only moderately (0.645 vs. 0.678). In drive01, rest windows showed higher HFHRV than stress windows (0.1090 ± 0.0239 vs. 0.0274 ± 0.0061; n = 27 each), whereas HF coherence was similar between conditions. In the ApneaECG analysis, apneasuspect windows showed lower HFHRV than normal windows (0.000387 vs. 0.002342; n = 197 each). Validation against minutewise apnea annotations showed high precision (0.934) but low sensitivity (0.196).
Conclusion: HFHRV showed physiologically plausible changes across sleep, stress and apnearelated conditions and appears to be a robust marker of respirationrelated vagal modulation. Coherence provided complementary information but was more sensitive to parameterization and signal quality.

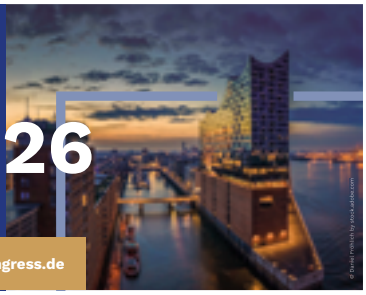

P16 Postergroup: Endothelial biology & Systemic Vascular Physiology

P1603

Differential effects of calcineurin (PPP3CB) on angiotensin II signaling in male and female vasculature

Alexander Nolze; Sindy Rabe; Stefanie Ruhs [1]; Nicole Strätz; Katja Quarch; Conny Köhler [2]; Claudia Grossmann
JuliusBernsteinInstitut für Physiologie, MartinLutherUniversität HalleWittenberg, Halle (Saale), Germany; [1] Universitätsklinik und Poliklinik für Innere Medizin, Herz- und Thoraxchirurgie, Klinik für Anästhesiologie und operative Intensivmedizin, MartinLutherUniversität HalleWittenberg, Halle (Saale), Germany; [2] Klinik für Herzchirurgie, Medizinische Fakultät, MartinLutherUniversität HalleWittenberg, Halle (Saale), Germany;

Objective: Cardiovascular diseases exhibit notable sex differences, with angiotensin II (AngII) contributing to these disparities. The ubiquitously expressed beta subunit of calcineurin (PPP3CB), a serine/threonine phosphatase, has been implicated in mediating AngIIinduced cardiac pathology. Therefore, this study aimed to investigate the sexdependent role of calcineurin in AngIIdriven vascular alterations.
Method: Male and female mice globally lacking PPP3CB were subjected to AngII infusion by osmotic minipumps for 28 days (500 ng/kg/min). Pumps were implanted under isoflurane anesthesia (2 % in 100 % O_2, 1 L/min). Systolic blood pressure in mice was assessed noninvasively using the tailcuff method and with pressure and wire myography vessel function was analyzed. Aortic samples were subjected to histological and RNASeq analysis. Primary aortic vascular smooth muscle cells (aVSMCs) served as model to investigate proliferation/wound closure and explore signaling mechanisms by qPCR.
Results: AngII elicited a less pronounced increase in blood pressure in female mice, independent of calcineurin, without affecting vessel wall thickness or lumen size. Functional assays revealed AngIIinduced and calcineurindependent endothelial dysfunction exclusively in males. In aVSMCs of male mice, AngII promoted proliferation and wound closure via Tgfb1 signaling but not in those of female mice. Transcriptomic analysis of aortic samples with GSEA and IPA revealed differential expression of extracellular matrixassociated genes in both sexes including collagen 1 and fibronectin 1. While male mice showed a calcineurindependent regulation, which included Egfr, Tgfb1 and Ctgf, signaling in females was independent of calcineurin and Tgfb1. Downstream of Egfr, aVSMCs of male mice exhibited PKC pathway activation, while aVSMCs of female mice predominantly engaged ERK/MAPK signaling to regulate Ctgf expression.
Conclusion: These findings demonstrate that calcineurin has different roles in AngII signaling in males and females and thereby contributes to sexdependent differences in vascular pathophysiology. Recognizing these sexspecific mechanisms highlights the need for tailored strategies in the prevention and management of cardiovascular diseases.

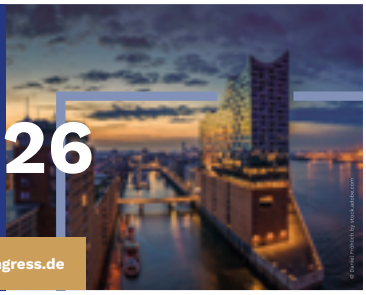

P16 Postergroup: Endothelial biology & Systemic Vascular Physiology

P1604

Hypothalamic BloodBrain Barrier Integrity and Autonomic Function Following EarlyLife Hypoxia and GramPositive Bacterial Challenge in the Neonatal Rat

Anna O´Connell; Maria Luis Dias Casacão; Karen O´Connor; Ken O´Halloran; Fiona McDonald
Department of Physiology, University College Cork, Cork, Ireland;

Objective: Preterm infants frequently require cardiorespiratory support resulting in prolonged hospitalisation, increasing the risk of hypoxia and nosocomial infection respectively. Hypothalamus is a key regulatory of autonomic balance. There is evidence that hypoxia and inflammation alone disrupt bloodbrain barrier (BBB) integrity and stimulate glia in this important region.
We aimed to investigate whether chronic intermittent hypoxia (CIHH) and lipoteichoic acid combined with peptidoglycan (LTA+PGN), independently or synergistically, compromise BBB integrity in the paraventricular nucleus (PVN) and supraoptic nucleus (SON), and influence blood pressure in a neonatal rat model.
Method: Dams and litters were either left at normoxia or placed in an environmental chamber where FiO2 was manipulated to generate intermittent hypoxia (8%)/hyperoxia (30%)/normoxia (21%) (CIHH) between postnatal day (PND) 3 and 12. On PND13, pups received intraperitoneal saline or LTA+PGN. BBB permeability was assessed via fluorescent tracer extravasation visualised by confocal microscopy. Extra/intravascular fluorescence ratios were quantified in capillaries (n=5–6). Brains were also used for neuroglial characterisation. A separate cohort underwent *in vivo* systemic blood pressure assessment under urethane anaesthesia (n=34). To further investigate the direct effect of hypoxia and grampositive bacterial challenge on astrocyte inflammatory signalling, primary astrocyte cell cultures were exposed to hypoxia and/or LTA+PGN treatment. NFκB transcriptional activity as well as cytokine analysis including IL6, IL1β and IL10 was assessed.
Results: LTA+PGN increased the extra/intravascular fluorescence ratio in the magnocellular and intermediocellular regions of the PVN (Gas × LTA+PGN, p=0.02 and p=0.01 respectively). Blood pressure was unaffected by either intervention.
Conclusion: LTA+PGN and CIHH increased PVN BBB permeability, but this effect was not additive. The implication of this finding is that it could facilitate central cytokine signalling but was not demonstrated to modulate blood pressure. Further studies will examine the local hypothalamic stress.

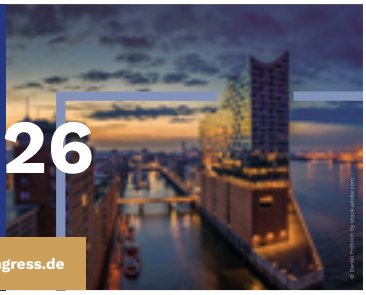

P16 Postergroup: Endothelial biology & Systemic Vascular Physiology

P1605

The mechanical pulse meter allows an exact comparison of pulse transit time between the left and right wrist

Thomas Braun
Dr. Braun Praxisklinik, Rötz, Germany;

Objective: Preliminary studies have shown that the mechanical pulse meter (mPm) allows a precise measurements of the pulse wave transit time between the heart and the left wrist. These studies have also revealed a correlation between this transit time and blood pressure. The present study aimed to compare the arrival time of the pulse wave at both wrists (radial artery).
Method: The mPm is a noninvasive, and easily performed examination method, which converts the movement of the arterial wall into electrical voltage using a microdynamo. The timepoint at which the artery expands most rapidly is also when the electrical voltage is highest (M). In a preliminary anatomical study, it was measured in situ that the path of blood from the heart to the right wrist is 5 to 6 cm shorter than to the left. Fiftyseven people, 22 female and 35 male, between 19 and 89 years of age (mean 48.7 years, standard deviation +/- 19.98), participated in the study. The examination was performed with the participants lying supine, arms relaxed in supination at their sides. Measurements were taken simultaneously on both wrists.
Results: In individuals under 25 years of age, the transit time difference (M earlier on the right than the left) was 0.01 seconds (SD +/- 0.018), which corresponds to a pulse wave velocity of approximately 5 to 6 m/s. As systolic blood pressure increases, the point at which the pulse wave is measured first shifts from right to left. This effect becomes statistically significant above 145 mmHg and is highly significant ($p<0.01$) above 155 mmHg (0.023 seconds, SD +/- 0,024). This kind of shift was also found with the rise of the diastolic blood pressure above 85 mmHg ($p<0.05$). No genderrelated significance was found in the overall group.
Conclusion: This study compared the time points of fastest arterial wall expansion at both wrists using mPm. While in young individuals this time point occurred on average 0.01 seconds earlier on the right wrist than on the left, the values shifted to the left with increasing systolic and diastolic blood pressure. The measurements did not provide a causal explanation for this phenomenon, but is the first to show it. Other methods like piezoelectric measurement did not show this shift. Further studies with further optimization of the equipment and larger comparison groups are necessary.

P16 Postergroup: Endothelial biology & Systemic Vascular Physiology

P1606

AKR1A1 is a denitrosase in endothelial cells and impact on endothelial cell metabolism

Riham Rafea; Mauro Siragusa; Stefan Günther [1]; Rahul Chakraborty; LoredanaMirela Lupu; Witold Szymanski [2]; Johannes Garumann [2]; Beate Fisslthaler; Ingrid Fleming
Institute for Vascular Signalling, Goethe University Frankfurt am Main, Frankfurt a. M., Germany; [1] Max Planck Institute for Heart and Lung Research, Bioinformatics and Deep Sequencing Platform, Bad Nauheim, Germany; [2] Institute of Translational Proteomics, Department of Medicine, PhilippsUniversität Marburg, Marburg, Germany;

Objective: Aldoketo reductase family 1 member A1 (AKR1A1) is traditionally recognized for its role in biogenic aldehyde reduction. However, recent evidence suggests it also functions as a denitrosase, regulating protein Snitrosation. Therefore, the goal of this study was to assess whether it affects nitric oxide (NO) signalling and function in endothelial cells.
Method: AKR1A1 levels were modulated via siRNAmediated knockdown and overexpression approaches. We employed a multilayered analysis integrating transcriptomic profiling (RNAseq), proteomics and untargeted metabolomics. Protein Snitrosation was assessed using the biotin switch technique. Functional validation included fibronectin adhesion, monocyteendothelial interaction, Proliferation and spheroidbased sprouting assays.
Results: AKR1A1 was expressed by cultured endothelial cells under basal conditions and its siRNAmediated knockdown resulted in altered endothelial cell metabolism. LCMS/MS based metabolomics analyses revealed that the lack of AKR1A1 increases metabolites that linked to NO signaling i.e., Lcitrulline, AMP, GMP, the pentose phosphate pathway intermediate; ribose 5phosphate and glutathione (GSH and GSSG). The latter changes could be accounted for by the Snitrosation of pyruvate kinase M2 (PKM2). Indeed, it was possible to demonstrate that the overexpression of AKR1A1 abolished the Snitrosation of PKM2. Transcriptomic and proteomic analysis revealed that AKR1A1 may potentially affect pathways linked to NO. This was confirmed in as much as eNOS expression in AKR1A1 depleted cells, and correlated with a decrease in ICAM1 and VCAM1 expression as well as monocyte adhesion. There were also significant changes in genes linked with G protein coupled receptor signalling and extracellular matrix regulation. Fitting with these observations AKR1A1deficient cells adhered better to fibronectin and demonstrated a proangiogenic phenotype i.e., both migration and sprouting from endothelial cell spheroid were increased.
Conclusion: Our data highlight the importance of AKR1A1 as a denitrosase in the endothelium that regulates PKM2 Snitrosation and endothelial cell metabolism as well as function. These results suggest AKR1A1 may be a target in strategies to improve endothelial cell function and reestablish the Snitrosoproteome in conditions of low NO bioavailability.

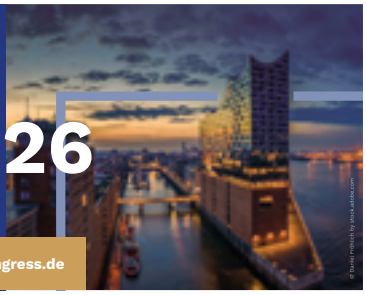

P16 Postergroup: Endothelial biology & Systemic Vascular Physiology

P1607

Cterminal FGF23 Promotes Endothelial Glycocalyx Collapse and Impairs Endothelial Function in Hemodialysis Patients

Benedikt Fels; Josephine Koch; Tamara Kunze; Carl Vahldieck; Caspar F. Franssen [1]; Jacob van den Born [1]; Kristina Kusche
Institut für Physiologie, Universität zu Lübeck, Lübeck, Germany; [1] Department of Nephrology, University Medical Center Groningen, University of Groningen, Groningen, The Netherlands;

Objective: Cardiovascular disease and endothelial dysfunction are highly prevalent in chronic kidney disease (CKD). Elevated plasma fibroblast growth factor 23 (FGF23) levels in CKD are associated with increased cardiovascular risk. The functional properties of the surface of endothelial cells (ECs), forming the inner vascular layer, are crucial for the maintenance of vascular health. Hallmarks of endothelial dysfunction include damage to the endothelial glycocalyx (eGC), stiffening of the underlying cortex, and consequently disturbed vascular function. However, the influence of FGF23 on endothelial nanomechanics remains poorly understood. We therefore investigated whether elevated FGF23 directly alters endothelial nanomechanics, functions, and thereby contributes directly to endothelial dysfunction.
Method: Human umbilical vein endothelial cells were incubated with uremic sera from hemodialysis patients with low (≤2,000 RU/mL; n=6) or high (≥30,000 RU/mL; n=6) FGF23 levels, as well as with recombinant intact FGF23 and Cterminal FGF23 (30 ng/mL each). eGC height and cortex stiffness were assessed by atomic force microscopy. eGC components and cortical Factin were validated by immunofluorescence staining, and immunecell adhesion as well as NO production were evaluated.
Results: Sera from patients with high FGF23 reduced eGC height by 17%, increased eGC stiffness by +63%, and enhanced cortical stiffness by +18% compared with serum from patients with low FGF23. Recombinant Cterminal FGF23, but not intact FGF23, induced similar effects compared to unstimulated controls (eGC height: 41%; eGC stiffness: +79%; cortical stiffness: +36%). Cterminal FGF23, similarly, increased actin polymerization by +20%, whereas intact FGF23 had no effect. FGF23 specificity was confirmed by using a blocking antibody. Cterminal FGF23, but not intact FGF23, also leads to higher numbers of adherent monocytes to the endothelial surface, as well as impaired NO bioavailability.
Conclusion: Cterminal FGF23, but not intact FGF23, induces damage of endothelial surface structures – thereby leading to impaired vascular functions. These findings support a vasculopathological role for Cterminal FGF23 in hemodialysis patients.

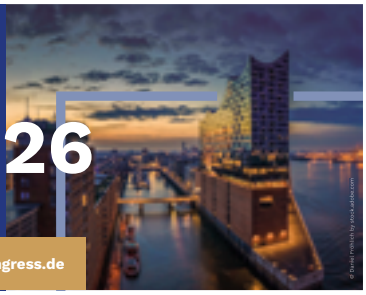

P16 Postergroup: Endothelial biology & Systemic Vascular Physiology

P1608

Timeofday variation in complementdriven endothelial glycocalyx nanomechanics in cardiovascular pathology

Isaiah Joseph Ting; Benedikt Fels; Kristina Kusche; Carl Vahldieck
Institut für Physiologie, Universität zu Lübeck, Lübeck, Germany;

Objective: Cardiovascular events peak in the early morning, yet the endothelial mechanisms underpinning this temporal vulnerability remain poorly defined. The luminal endothelial glycocalyx (eGC) and the subjacent actinrich cortical layer jointly regulate barrier function, mechanotransduction, and nitric oxide (NO) bioavailability. We previously showed that complement anaphylatoxins C3a and C5a, rapidly generated during acute cardiovascular inflammation, directly injure this functional unit: C3a engages C3aR1Rac1 signalling to drive cortical stiffening, glycocalyx shedding, and reduced NO bioavailability, while C5a acts via C5aR1RhoA to further stiffen the cortical layer. Whether this complementglycocalyx injury axis is itself temporally organised across the 24hour day has not been investigated.
Method: We extended this work with a retrospective timeofday reanalysis of nanomechanical and biomarker data from 63 individuals with an acute ischaemic cardiovascular event treated by emergency percutaneous coronary intervention, using this cohort as a human model of innate immunevascular activation. Serumdriven endothelial responses, comprising eGC height and stiffness, cortical stiffness, syndecan1, C3a, and C5a, were stratified by blood sampling time into 6hour bins (Morning, Afternoon, Evening, and Night), then modelled using 24hour cosinor analysis to resolve temporal acrophases, principal component analysis to identify covarying endothelialinflammatory axes, and Spearman correlations to relate complement load to nanomechanical injury severity.
Results: Morningcollected sera (06:00<12:00) induced a marked endothelialinjury phenotype associated with elevated cortical stiffness, syndecan1, C3a, and C5a alongside reduced eGC height and stiffness compared with afternoon and evening sampling (all FDRadjusted $p<0.001$). Cosinor modelling placed acrophases for cortical stiffness, syndecan1, C3a, and C5a in the early morning (~07:0007:40), directly opposing evening acrophases for eGC height and stiffness (~19:0519:18).
Conclusion: Complementdriven injury to the endothelial surface layer is not temporally uniform. It is phaselocked to the established circadian window of greatest cardiovascular risk, implicating clock time as a physiologically relevant and insufficiently characterised determinant of endothelial vulnerability at the innate immunevascular interface.

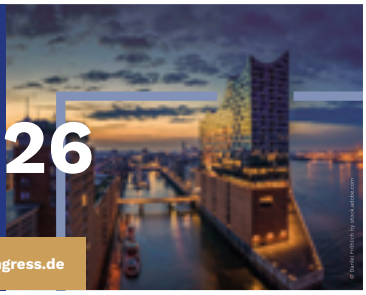

P16 Postergroup: Endothelial biology & Systemic Vascular Physiology

P1609

DIASILAC Proteomics Reveals CoatingDependent Endothelial ECM Remodeling Under Flow

Fatih Celal Alcicek; Parviz Ghezellou; Jana Wurzel; Katalin Pálfi; Victoria Jurisch; Xin Wen; Longyuan Jia; Ilka Wittig [1]; Ralf P. Brandes
Institut für Kardiovaskuläre Physiologie, Universitätsklinikum, Johann Wolfgang GoetheUniversität, Frankfurt a. M., Germany; [1] Molekulare Bioenergetik, Universitätsklinikum, Johann Wolfgang GoetheUniversität, Frankfurt a. M., Germany;

Objective: Endothelial cells respond to shear stress differently depending on the composition of the extracellular matrix (ECM). We observed that under flow, human umbilical vein endothelial cells (HUVECs) align faster on fibronectincoated surfaces than on gelatincoated surfaces. However, the ECM remodeling mechanisms underlying this difference remain unclear. This study investigated how coating type influences endothelial ECM remodeling and turnover under static and flow conditions using a stable isotope labeling with amino acids in cell culture (SILAC) proteomics approach.
Method: HUVECs were cultured on gelatin- or fibronectincoated surfaces to reach confluence. Medium was then changed to SILAC medium and cell were further cultured under static or laminar flow conditions for additional 24 h and 72 h (15 dynes/cm2). Samples were then decellularized and the remaining ECM fraction was subjected to mass spectrometrical analysis using a Bruker TIMS/TOF machine in data independent acquisition (DIA) mode. Total ECM abundance was evaluated using iBAQ values, while MS1/MS2 lightheavy raw intensities and heavy fraction analyses were used to assess newly synthesized ECM and to determine remodeling dynamics.
Results: A total of 261 ECMassociated proteins were identified in all experimental groups. Most ECM proteins were common to both conditions suggestive for a constitutive endothelial ECM core composition. There were, however, substantial quantitative differences in ECM abundance between groups. The median log2 iBAQ values increased from 0.93 and 0.96 in static gelatin 24h and static fibronectin 24h to 1.20 and 1.24 in static gelatin 72h and static fibronectin 72h, respectively; while flow groups showed lower median values in the range 0.49–0.74. Overall ECMassociated abundance signatures were strongest for the static fibronectin 72h samples. In addition, fibronectinassociated conditions showed a greater number of proteins linked to remodeling and adhesion such as FN1, THBS1, HSPG2, CCN1, CCN2, TGM2, LOXL2, IGFBP7, PXDN, MMRN1, and SERPINE1.
Newly synthesized ECM was most prominent in the static fibronectin 72h samples. The proteins with the highest heavy fractions included CCN2 (0.81), CCN1 (0.79), HSPG2 (0.78), FN1 (0.73), SERPINE1 (0.67), LOXL2 (0.64), VWF (0.63), HHIP (0.62), THBS1 (0.62), and COL18A1 (0.61), reflecting active ECM remodelling and deposition of newly synthesised matrix. In contrast, several structural ECM proteins showed relatively stable heavy fractions across conditions, indicating lower turnover dynamics.
Conclusion: Fibronectin coating supports earlier and more active endothelial ECM remodeling under flow conditions, which may contribute to faster endothelial adaptation and alignment under shear stress compared to gelatin coated surfaces.

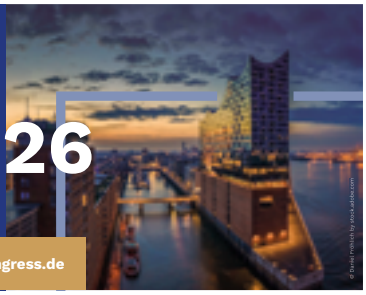

P16 Postergroup: Endothelial biology & Systemic Vascular Physiology

P1610

Characterisation of the role of *EMILIN1* c.1606C>T mutation in aortic aneurysms (AA) using human induced pluripotent stem cells (hiPSCs)

Yanhui Zhang
Institute of Physiology I, University Hospital Bonn, Bonn, Germany;

Objective: Patients with *EMILIN1* mutations experience a broad range of symptoms, including AA formation. They suffer from early disease onset and severe disease progression, but the underlying mechanisms remain unclear. Our project aims to better understand the role of *EMILIN1* in AA development.
Method: We generated a homozygous genomeedited hiPSC line carrying the patientspecific *EMILIN1* c.1606C>T (p.Gln536*) mutation (*EMILIN1 C1606T)* and characterized their pluripotency and differentiation potential. The mutated hiPSC line was differentiated into endothelial cells (hECs) and vascular smooth muscle cells (hVSMCs), and their functional characteristics were analysed through tube formation and migration assays. Additionally, the structure of the cytoskeleton and the extracellular matrix was investigated via immunofluorescence staining.
Results: We confirmed the pluripotency of the EMILIN1 C1606T hiPSC line based on the ability to differentiate into the three germ layers (95.79 ± 2.136% TBXT+, 99.02 ±0.9812% SOX17+, 92.22±4.597% TUBB3+). While EMILIN1 C1606T hECs showed similar proliferation, tube formation and migration ability, in hVSMCs, a decreased migration was observed. Additionally, the mutant hVSMCs exhibited cytoskeletal changes and alterations in extracellular matrix (ECM) components.
Conclusion: We have successfully generated a mutant EMILIN1 c.1606C>T hiPSC line, which provides a platform to investigate the contribution of EMILIN1 to AA formation in vitro. Our results indicate that hVSMCs are more affected by this mutation than hECs. In future experiments, TGF and integrin signalling will be addressed.

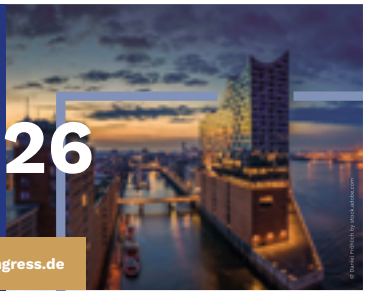

P16 Postergroup: Endothelial biology & Systemic Vascular Physiology

P1611

Role of endothelial AT1 receptors in hypertension mediated bone marrow activation and organ damage

Vakhtang Kilauridze; Alina Maslakova; Anne Klotzsche vonAnnelm; Carmen Hentsche; Antje Messer; Bianca Müller; Birgit Zatschler; Stephan Speier; Arka Baksi; Irakli Kopaliani
Institut für Physiologie, Universitätsklinikum Carl Gustav Carus, Technische Universität Dresden, Dresden, Germany;

Objective: Hypertension induces profound alterations in the bone marrow microenvironment, particularly within the myeloid niche, priming hematopoietic cells for an exaggerated inflammatory response that contributes to hypertensive organ damage. Although endothelial angiotensin II type 1 (AT1) receptors play a key role in translating angiotensin II (AngII) stimuli, the contribution of the endothelium in transferring this hypertensive stimulus to the bone marrow is not fully understood
Method: To address this question, we used a mouse model with an inducible endothelial deletion of the AT1a receptor combined with a constitutive AT1b knockout. After induction, mice underwent either sham surgery or implantation of an AngII osmotic pump. Bone marrow angiogenesis was assessed, through immunostaining and niche activation, through flow cytometry. Subsequent organ damage was evaluated by echocardiography, cardiac histology and qPCR. We monitored blood pressure using the tailcuff method and determined endothelial dysfunction via Mulvany myography.
Results: Preliminary bonemarrow analysis revealed a lower percentage of longterm hematopoietic stem and progenitor cells in KO mice, alongside a lower vessel percentage area. KO mice also displayed lower markers for fibrosis like COL1A1 and COL3A1 in the qPCR of heart. Echocardiography reinforced these results, showing reduced relative wall thickness and left ventricular mass. Mice lacking AT1 receptors also had lower blood pressure after AngII stimulation compared to WT treated mice.
Conclusion: Together, these data indicate a bone marrow niche less primed for a severe immune response. Which in turn may be a key factor in reducing end organ damage in hypertension.

P16 Postergroup: Endothelial biology & Systemic Vascular Physiology

P1612

GAbinding protein transcription factor subunit alpha GABPA sustains endothelial angiogenic function, histone gene expression and RNAchromatin structures

Praveenya Tirunagari; Agnes Yasmine Krüger; Timothy Warwick; Stefan Günther [1]; Alfredo CabreraOrefic [2]; Ilka Wittig [3]; Ralf P. Brandes; Matthias Leisegang Institut für Kardiovaskuläre Physiologie, Universitätsklinikum, Johann Wolfgang GoetheUniversität, Frankfurt a. M., Germany; [1] Max Planck Institute for Heart and Lung Research, Bad Nauheim, Germany, Bad Nauheim, Germany; [2] Institute of Biochemistry, JustusLiebigUniversität, Gießen, Germany; [3] Molekulare Bioenergetik, Universitätsklinikum, Johann Wolfgang GoetheUniversität, Frankfurt a. M., Germany;

Objective: GAbinding protein transcription factor subunit alpha (GABPA) is a broadly expressed transcription factor implicated in proliferation and metabolic control. While previously linked to endothelial promoter regulation and retinal angiogenesis, its role in endothelial cell biology remains unclear. Here, we identify GABPA as a critical regulator of endothelial angiogenic function and uncover a noncanonical mechanism linking GABPA to histone gene expression and RNAchromatin structures.
Method: GABPA knockdown was performed in human umbilical vein endothelial cells (HUVECs) to assess its role in endothelial function. Endothelial proliferation, migration, VEGFAmediated spheroid outgrowth, and tube formation were analyzed. To define the underlying mechanism, RNAseq was performed following GABPA depletion. CUT&RUN was used to assess GABPA chromatin occupancy. To identify potential noncanonical mechanisms, complexome profiling and GABPA immunoprecipitation followed by mass spectrometry were conducted. RNADNA hybridassociated signals were examined using S9.6 staining. In addition, GABPA RNA immunoprecipitation followed by RNAseq (RIPseq), dsDNA RIPseq, and integrative analysis of Triplexseq, CUT&RUN, RNAseq, RIPseq, and RADICLseq datasets were performed to identify potential GABPAdependent RNAchromatin interactions.
Results: GABPA knockdown impaired endothelial function by decreasing proliferation, migration, VEGFAmediated spheroid outgrowth, and tube formation. Transcriptomic analysis revealed broad suppression of E2F/Sphase genes and coordinated downregulation of 48 replicationdependent histone genes. Notably, these differentially expressed genes showed only minimal overlap with GABPA chromatin occupancy by CUT&RUN, suggesting that their regulation is not primarily mediated by direct promoter binding. Complexome profiling identified a nuclear complex containing GABPB1 and the RNA helicase DDX41. GABPA depletion significantly reduced the nuclear S9.6 signal, indicating a role in maintaining RNADNA hybridcontaining structures. RIPseq demonstrated association of GABPA with histone transcripts, which displayed substantial RNase H resistance and enrichment in dsDNA RIPseq, consistent with their incorporation into noncanonical RNAchromatin assemblies. Integrative analysis further identified plausible GABPAdependent functional and structural triplexforming RNAs and their corresponding DNA regions.
Conclusion: Together, these data support a model in which GABPA, in concert with GABPB1 and DDX41, sustains endothelial angiogenic function by maintaining histone gene expression and RNAchromatin structures, potentially including RNADNA triplex interactions.

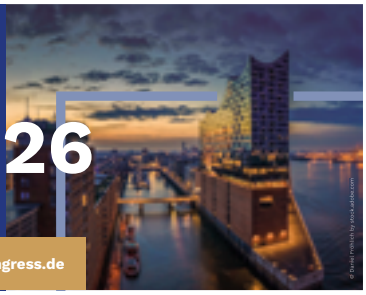

P16 Postergroup: Endothelial biology & Systemic Vascular Physiology

P1613

Reduced Antioxidant Capacity Already Present in Prehypertension Across the Early Blood Pressure Spectrum

Zrinka Mihaljevic; Ivo Vincetic [1]; Nikolina Kolobaric; Ivana Tolj [2]; Marko Stupin [3]; Ana Marincic Zagar; Ivana Jukic; Ines Drenjancevic; Sandra Saric [3]; Ana Stupin Department of Physiology and Immunology, University Hospital Center Osijek, Osijek, Croatia; [1] Department of Radiology, University Hospital Center Osijek, Osijek, Croatia; [2] Department of Nephrology; Department of Internal Medicine, University Hospital Center Osijek, Osijek, Croatia; [3] Department of Cardiovascular Disease, University Hospital Center Osijek, Osijek, Croatia;

Objective: Oxidative stress and reduced antioxidant capacity are proposed contributors to vascular dysfunction and early cardiovascular alterations preceding hypertension. However, their systemic changes across the early blood pressure spectrum remain incompletely defined. This study aimed to assess oxidative stress markers and antioxidant capacity across normotensive, prehypertensive, and early hypertensive adults.

Method: Fortynine adults were classified as normotensive (NT; SBP ≤129 mmHg, DBP ≤84 mmHg; N=13), prehypertensive (PREHT; SBP 130–139 mmHg, DBP 85–89 mmHg; N=19), and untreated stage 1 hypertensive (HT; SBP 140–159 mmHg, DBP 90–99 mmHg; N=24), based on 24hour ambulatory blood pressure monitoring. Groups were matched for age and sex. The study was conducted in accordance with the Declaration of Helsinki. Plasma thiobarbituric acid reactive substances (TBARS) were used as a marker of lipid peroxidation, and ferric reducing antioxidant power (FRAP) was used to assess total antioxidant capacity. Group comparisons were performed using oneway analysis of variance (oneway ANOVA), followed by HolmSidak post hoc multiple comparison test.

Results: TBARS showed no significant differences across groups (NT: 0.818 ± 0.041; PREHT: 0.840 ± 0.050; HT: 0.835 ± 0.054; P = 0.496). In contrast, FRAP differed significantly between groups (P = 0.004), with lower values in PREHT and HT compared with NT. Post hoc analysis confirmed significantly lower FRAP in NT vs PREHT (P = 0.004) and NT vs HT (P = 0.020), with no difference between PREHT and HT (P = 0.378).

Conclusion: These findings indicate alterations in systemic redox balance across early blood pressure categories, driven primarily by changes in antioxidant capacity. The observed pattern suggests that reduced antioxidant defenses may be an early feature of blood pressure elevation, while lipid peroxidation appears less affected at this stage. Further studies in larger cohorts are warranted to clarify the temporal dynamics of redox alterations in early cardiovascular remodeling.

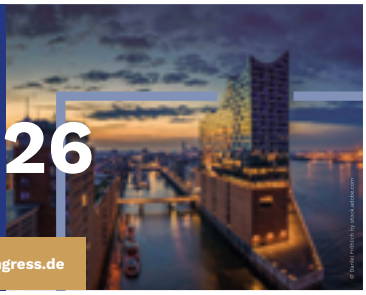

P17 Postergroup: Metabolism in Physioloy

P1701

OLFML2B marks hepatocyte identity loss and stromal remodeling in hepatocellular carcinoma: a multidataset transcriptomic analysis

Mehmet Ridvan Ozdede; Ahmed Sait Bozyil [1]
Physiology, Necmettin Erbakan University, Konya, Türkiye; [1] PhysiologyMedicine, Firat University, Elazig, Türkiye;

Objective: The olfactomedin/olfactomedinlike (OLFM/OLFML) family has not been systematically characterized in hepatocellular carcinoma (HCC). We investigated whether OLFMfamily expression patterns are associated with tumor status, hepatocyte identity, stromal remodeling and survival in HCC.
Method: Public transcriptomic datasets were analyzed, including TCGALIHC RNAseq data (371 primary tumors, 50 solid tissue normal samples), GSE25097 (268 tumors, 243 adjacent nontumor, 40 cirrhotic and 6 normal liver samples) and GSE14520/GPL3921 (225 tumors, 220 adjacent nontumor samples). OLFM1, OLFM4, OLFML1, OLFML2A, OLFML2B, OLFML3 and MYOC were available across the validation datasets. Expression differences were assessed using nonparametric tests with BenjaminiHochberg correction. Module scores were calculated from genewise zscore averages for hepatocyte identity, fibrosis/ ECM, CAF/stellatecell activation, TGFβ signaling, EMT/invasion, proliferation, immuneinflammatory, endothelial/angiogenesis and MCT/lactate transport signatures. Spearman correlations were used for genemodule associations.
Results: OLFML2A and OLFML2B were consistently increased in HCC tumors across datasets. In TCGALIHC, OLFML2A and OLFML2B were tumorenriched (FDR=1.52×10^{21} and 5.32×10^{25}, respectively). In GSE14520, both genes were also higher in tumors than adjacent nontumor tissue (OLFML2A FDR=2.29×10^{19}; OLFML2B FDR=1.09×10^{15}). By contrast, OLFML3, OLFM1 and OLFML1 were relatively enriched in nontumor/adjacent liver. OLFML2B showed the most reproducible association with hepatocyte identity loss (TCGA r=0.408; GSE25097 r=0.718; GSE14520 r=0.451), proliferation, CAF/stellate activation, TGFβ signaling, EMT/invasion and fibrosis/ECM signatures. OLFML2Bhigh samples showed increased MKI67, TOP2A, FAP, ACTA2, POSTN, MMP9, COL1A1 and COL1A2, with reduced ALB, TTR, ASGR1 and HNF4A. In TCGALIHC, OLFML2B showed a nominal association with poorer overall survival, but this did not remain significant after multipletesting correction.
Conclusion: These findings suggest that OLFML2B captures a reproducible HCC transcriptional state characterized by hepatocyte identity loss and stromalremodeling activity. Further validation using singlecell, spatial and proteinlevel datasets is required to define its cellular source and functional relevance.

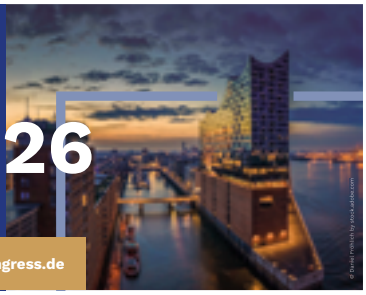

P17 Postergroup: Metabolism in Physioloy

P1702
ContextDependent Functions of WT1 in Visceral Adipose Tissue

Helena Landstorfer; Xheni Meçi; Philipp Koch; Karin Michaela Kirschner; Holger Scholz Institut für Translatioinal Physiologie, Campus Charité Mitte, Charité - Universitätsmedizin Berlin, Berlin, Germany;

Objective: Obesity constitutes a major global health burden giving rise to cardiovascular disease and metabolic disorders. In particular, expansion of visceral (intraabdominal) white adipose tissue (WAT) correlates with increased morbidity and mortality. On the other hand, “browning”, i.e. the appearance of heatproducing adipocytes in WAT, is considered metabolically beneficial. The transcription factor WT1 is expressed in progenitor cells (preadipocytes) in visceral WAT and has been implicated in maintaining the white adipocyte fate of these fat depots. Remarkably, heterozygous *Wt1* knockout mice display browning of their visceral WAT with improved glucose tolerance and reduced hepatic steatosis on highfat diet (HFD).
Since induced WAT browning is a promising tool to combat obesity and metabolic disease, we aimed at further exploring the role of WT1 in this process and in adipose tissue homeostasis in general.
Method: Mice with conditional *Wt1* inactivation in visceral WAT progenitor cells were generated and phenotyped. *Wt1* gene targeting was achieved by mating a *Pdgfrα*Cre deleter line with mice harboring loxP sites in their *Wt1* gene.
Results: Surprisingly, conditional *Wt1* knockout mice ($Wt1^{fl/fl}$; PdgfrαCre) were obese with enlarged visceral and subcutaneous fat depots, hepatic steatosis, and hypertrophy of white adipocytes. Bulk RNA sequencing following *Wt1* silencing in primary visceral preadipocytes combined with Cut&Run analyses identified *Wnt4*and *Pcx* (*pyruvate carboxylase*) as candidate WT1 target genes. Consistently, retroviral overexpression of *Wnt4* markedly impaired adipogenic differentiation of 3T3L1 cells. Bioinformatic analysis of publicly available singlenucleus RNA sequencing data (GSE176171) revealed heterogeneity among preadipocyte populations in visceral WAT of mice. Mice kept on highfat diet (HFD) displayed a reduced fraction of preadipocytes and an increased portion of macrophages compared with mice receiving normal chow. Expression levels of *Wt1* and total cell numbers of *Wt1*expressing preadipocytes were significantly reduced in mice on HFD.
Conclusion: Collectively, these findings suggest that WT1 marks and regulates a specialized preadipocyte subtype that limits adipogenic differentiation in visceral adipose tissue. Integrating *in vivo* genetic models with singlecell transcriptomic and *in vitro* approaches provides a powerful tool to dissect transcriptional networks regulating adipose tissue homeostasis.

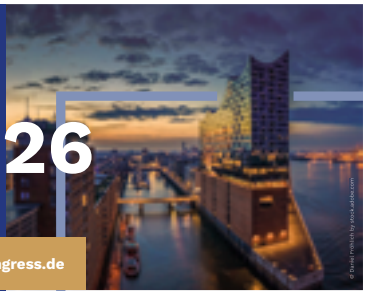

P17 Postergroup: Metabolism in Physioloy

P1703

GLP1 Receptor Blockade Alters BetaCell Activity and Functional Network Organization in Pancreatic Islets

Maja Duh; Eva Paradiž Leitgeb; Lana Kralj; Lidija Križancic Bombek; Jasmina Kercmar; Maša Skelin Klemen; Andraž Stožer; Marko Gosak

Institute of Physiology, University of Maribor, Faculty of Medicine, Maribor, Slovenia;

Objective: Pancreatic beta cells regulate glucosedependent insulin secretion through coordinated Ca^{2+} dynamics. While GLP1 signaling potentiates betacell activity, its role in shaping multicellular betacell dynamics remains unclear. We investigated how GLP1 receptor inhibition with exendin9 (ex9) alters collective betacell dynamics and functional network organization in pancreatic islets.

Method: Acute pancreatic tissue slices from C57BL/6J mice were loaded with a fluorescent Ca^{2+} indicator and imaged by confocal microscopy during sequential glucose stimulation. Control islets were stimulated twice with 10 mM glucose, separated by 6 mM substimulatory intervals, whereas experimental islets were treated with the GLP1 receptor antagonist ex9 (100 nM) during the second substimulatory and stimulatory interval. We quantified activation dynamics, Ca^{2+} signaling parameters, and spatial distributions of functionally defined cell subpopulations, and used wavelet and network analyses to assess oscillatory frequency composition and collective betacell organization.

Results: Control islets showed reproducible activation across repeated glucose stimulations; GLP1R blockade markedly delayed collective activation, increasing the average activation delay by approximately 50 %. While control islets exhibited a slight increase in betacell activity during repeated stimulation, activity in ex9treated islets remained largely unchanged. Wavelet analysis indicated preserved but frequencyshifted oscillatory activity under ex9. At the network level, functional connectivity analysis revealed reduced connectivity during repeated stimulation in control islets, whereas ex9 partially preserved overall network stability. Spatial analysis showed that first responder cells in control islets remained preferentially localized near the islet periphery during both stimulation intervals. In contrast, ex9 redistributed first responder cells toward the islet interior. Hub cells remained centrally localized in both groups.

Conclusion: Our findings indicate that endogenous GLP1 signaling is not only important for potentiating betacell activity, but also for preserving the spatial and functional organization of collective islet dynamics. GLP1R blockade delays coordinated activation, reshapes oscillatory activity, and disrupts the peripheral organization of first responder cells. These results suggest that GLP1 signaling supports robust multicellular coordination in pancreatic islets, with potential implications for understanding how incretinbased mechanisms modulate islet function beyond their direct insulinotropic effects.

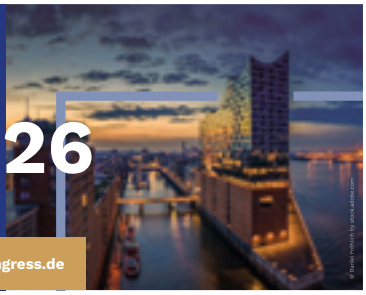

P17 Postergroup: Metabolism in Physioloy

P1704

Effects of Arginine Vasopressin on Pancreatic a and ß Cells: GlucoseDependent Modulation and ReceptorSpecific Responses

Nastja Murko
Institute of Physiology, Faculty of Medicine, University of Maribor, Maribor, Slovenia;

Objective: Arginine vasopressin (AVP) has been implicated in the regulation of pancreatic islet function; however, its effects on α and β cells remain incompletely understood. We investigated the glucose dependence, receptor specificity, and intracellular signaling mechanisms underlying AVPinduced responses in pancreatic islet cells.

Method: Acute pancreatic tissue slices from C57BL/6J mice were used for functional imaging and hormone secretion experiments. Cytosolic Ca2+ dynamics in α and β cells were monitored using confocal microscopy during stimulation with AVP or receptorspecific agonists and antagonists under different glucose conditions and in the presence of cAMPmodulating agents. Dynamic insulin secretion measurements were performed using perifusion experiments on pancreatic tissue slices. Ca2+ events were analyzed as previously described, and receptor expression was additionally assessed using RNAscope.

Results: AVP exerted glucosedependent effects on both α and β cells. At low glucose concentrations, AVP selectively increased αcell activity without affecting β cells. At stimulatory glucose concentrations, AVP enhanced Ca2+ signaling in both cell types. Reduction of intracellular cAMP levels by epinephrine suppressed AVPinduced responses in β cells, indicating a permissive role of cAMP signaling. AVP responses displayed a bellshaped concentration dependence, with maximal activation at lower concentrations and reduced responses at higher concentrations, consistent with IP3 receptor properties. Insulin secretion also displayed a bellshaped dependence on AVP concentration. Increased αcell activity observed at higher AVP concentrations coincided with reduced δcell activity, suggesting that enhanced αcell responses may partially result from diminished δcell–mediated paracrine inhibition. Pharmacological profiling together with RNAscope analysis indicated that AVP acts predominantly through V1b receptors.

Conclusion: Our findings demonstrate that AVP modulates pancreatic α- and βcell activity in a glucose- and cAMPdependent manner. In addition to direct receptormediated effects, AVP may regulate αcell activity indirectly through altered δcell paracrine signaling. These results identify AVP as an important modulator of intraislet communication and glucosedependent hormone secretion.

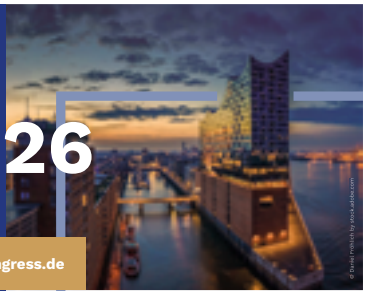

P17 Postergroup: Metabolism in Physioloy

P1705

HIF1α Stabilization Restores Immune Metabolism in Hereditary Hemorrhagic Telangiectasia

Nelson Niski; Joachim Fandrey; Anna Wrobeln
Abteilung Physiologie, Universitätsklinikum Essen, Essen, Germany;

Objective: Hereditary Hemorrhagic Telangiectasia (HHT) is an autosomal dominant vascular disorder caused by mutations affecting transforming growth factorbeta (TGFβ) signaling. It is characterized by multisystemic vascular dysplasia, called arteriovenous malformations, as well as immune dysregulation. Hypoxiainducible factors (HIFs) are central regulators of cellular adaptation to hypoxia and play key roles in immune regulation and cellular metabolism. Crosstalk between TGF- β and HIF signaling is essential for maintaining immune homeostasis.
Method: In this study, we demonstrate that $CD4^+$ T cells from HHT patients exhibit significantly reduced *HIF1A* gene expression, accompanied by decreased transcription of HIF target genes compared to unaffected controls. In addition,low cytometry analyses revealed that pharmacological inhibition of prolyl hydroxylases using Roxadustat effectively stabilizes HIF1α protein expression in $CD4^+$ T cells, $CD14^+$ monocytes, $CD8^+$ Tells, $CD56^+$ NK cells, and $CD19^+$ B cells. This was accompanied by upregulated gene expression of *HIF1A* and its target genes in $CD4^+$ T Cells.
Results: Functional metabolic profiling using Seahorsebased T cell activation assays identified marked differences between HHT and nonHHT cells. Additionally, the Glycolytic Stress Assay revealed reduced glycolytic capacity in HHT $CD4^+$ T cells and $CD14^+$ monocytes compared to unaffected cells, confirming impaired metabolic responsiveness in HHT. Following Roxadustat treatment, a restoration of glycolysis was observed.
Conclusion: In summary, these findings underscore the central role of HIF1α signaling in regulating immune cell metabolism and function. Suppressed HIF1α signaling result in metabolic dysfunction and impaired immune responses and suggests pharmacological HIF stabilization as a promising therapeutic strategy for restoring immune dysfunction in HHT.

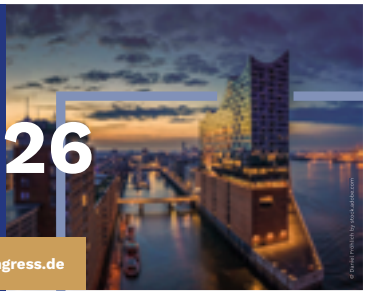

P17 Postergroup: Metabolism in Physioloy

P1706
ACSS2 as a Regulator of Muscular Lactate Homeostasis

Niclas Rausch; Christopher Allen Bishop; Maximilian Kleinert
Department of Molecular Physiology of Exercise and Nutrition, German Institute of Human Nutrition (DIfE) PotsdamRehbruecke, Nuthetal, Germany;

Objective: Regular exercise remains a cornerstone of publichealth recommendations for preventing obesity and type 2 diabetes. Highintensity exercise improves postprandial glucose handling and corresponds with drastic increases in blood lactate levels. Chronic hyperlactatemia, however, is linked to adiposity and disease. Recent work highlights the relevance of a lactatemediated posttranslational modification (i.e., lactylation) as a regulatory link between cellular metabolism and epigenetic mechanisms. The lactylation of histone proteins modifies the chromatin structure, which affects accessibility and the expression of genes. Nonhistone proteins show altered structure and activities when lactylated. The addition of lactate to lysine residues requires lactylCoA as a metabolic precursor, a conversion catalyzed by lysineacyltransferases. ACSS2 was identified as a lactylCoA synthetase in tumor cells. Its contribution to skeletal muscle (SkM) lactylation remains unexplored but might uncover novel lactateregulated pathways.
Method: We utilize C2C12 myocytes and *ex vivo*incubated isolated mouse muscles to study the molecular effects of ACSS2 inhibition on cellular lactate dynamics. Muscle biopsies from highfat diet (HFD)- and controlfed male C57BL/6J mice were analyzed for ACSS2 expression and intracellular lactate levels.
Results: In C2C12 cells, *Acss2* mRNA expression increases 3fold with differentiation (n=48 per group, $p<0.0001$, Unpaired ttest). The acute inhibition of ACSS2 reduces panlactylation levels by 25 % *in vitro* (n=3 per group, $p<0.05$, Twoway ANOVA and Fisher's LSD test). *Ex vivo*incubated soleus muscles show reduced intramuscular lactate under ACSS2 inhibition (0.22 mM vs. 0.14 mM lactate/ µg protein, n=6 per group, $p<0.01$, Twoway ANOVA and Fisher's LSD test). HFDfed mice have higher SkM lactate (0.20 vs. 0.26 mM lactate/ µg protein, n=8 per group, $p<0.001$, Unpaired ttest) and 85% higher ACSS2 levels than controls (n=67 per group, $p<0.01$, Unpaired ttest).
Conclusion: ACSS2 is highly abundant in mature SkM and increases with chronic HFDfeeding in mice. Inhibition of ACSS2 impairs lactylation *in vitro* and alters intracellular lactate handling *ex vivo*. Future work will utilize stable isotopes to trace lactate under ACSS2 inhibition, and epigenetic tools to study functional consequences of ACSS2mediated lactylation. The molecular insights will be further complemented with SkM biopsies of humans with obesity.

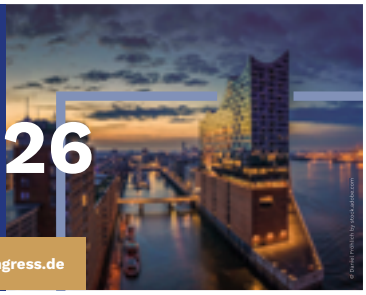

P17 Postergroup: Metabolism in Physioloy

P1707
Gestational Diabetes Mellitus modifies serum calcification propensity

Azmat Sohail; Julia Lastinger; Beatrice Toegel; Andreas Pasch; Ioana Alesutan; Peter Oppelt; Jakob Voelkl
Institut für Physiologie und Pathophysiologie, Johannes Kepler Universität Linz, Linz, Austria;

Objective: Spontaneous ectopic formation of calciumphosphate crystals in blood is prevented by an endogenous mineral buffering system. The strength of the mineral buffering system can be assessed by the serum calcification propensity test (also known as T50 test), where weaker mineral buffering has been associated with increased mortality in diabetes mellitus and the general population. Gestational Diabetes Mellitus (GDM) is typically temporary, but it increases a woman's lifetime risk of cardiovascular events. Thus, the impact of GDM on serum calcification propensity was investigated.
Method: Serum calcification propensity (T50) was investigated in pregnant women with and without known GDM as well as in artificial serum preparations.
Results: T50 was shortened in patients with GDM, accompanied by increased serum phosphate and calcium levels but without alterations in fetuinA concentrations. In patients with GDM, T50 was correlated to glucose concentrations during oral glucose tolerance test. Artificial glycation of fetuinA by methylglyoxal also led to a shortened T50 in artificial serum preparations. Similarly, incubation of human serum with methylglyoxal before serum calcification propensity testing shortened T50.
Conclusion: GDM may be linked to lower T50 (increased serum calcification propensity). Increased glycation of fetuinA in diabetic conditions may contribute to deranged mineral buffering.

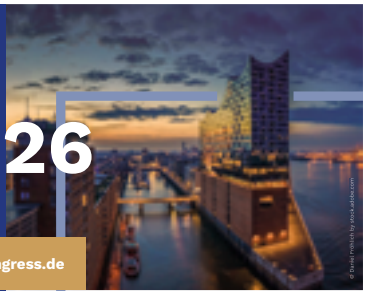

P17 Postergroup: Metabolism in Physioloy

P1708

Role of metabolism and mitochondrial function during iPSCderived cardiomyocyte differentiation for mediating sensitivity towards genotoxic noxae

Michelle Westerhoff; Roohallah Ghodrat [1]; Andreas S. Reichert [1]
Insitute of Cardiovascular Physiology, Medical Faculty and University Hospital Düsseldorf, Düsseldorf, Germany; [1] Institute of Biochemistry and Molecular Biology I, Medical Faculty and University Hospital Düsseldorf, Düsseldorf, Germany;

Objective: Since the 1960s, doxorubicin (Dox) has been administered as a chemotherapy agent for the treatment of solid tumors and hematological malignancies in adults and children. However, the precise mechanisms underlying Doxinduced cardiotoxicity which manifest within weeks to years after the initial application are still unresolved. Beyond its effect on nuclear and cytosolic processes, mitochondrial alterations are thought to play a major role in cardiotoxicity. However, previous studies relied on comparatively high Dox doses and prolonged exposure times that poorly mimic the clinical situation, where plasma concentrations decline rapidly within the first hour after infusion.
Method: Therefore, we established a shortpulse Dox treatment model in human inducedpluripotent stem cells (iPSCs) and iPSCderived cardiomyocytes (iCMs) to mimic clinically relevant plasma concentrations and to decipher the role of mitochondria as mediators of cardiotoxicity.
Results: Here, iPSCs exhibit higher sensitivity to mild and transient Dox exposure than iCMs, independently of pronounced DNA damage responses or reduced differentiation potential. Both, iPSCs and iCMs displayed persistent mitochondrial impairments, including increased mitochondrial fragmentation, reduced ATP levels, and altered metabolism. Notably, Dox treatment in iPSC stage prior to cardiac differentiation persistently altered the transcriptional landscape of derived iCMs, including downregulation of genes associated with cardiac contractility and metabolism. Concomitant, we observed impaired contractility in iCMs possibly associated with altered calcium handling.
Conclusion: Together, these findings suggest that Doxinduced mitochondrial dysfunction, especially prior to cardiac differentiation, contributes to longterm alterations in bioenergetic and contractile properties of cardiomyocytes and may represent a mechanism underlying cardiotoxicity in childhood cancer survivors.

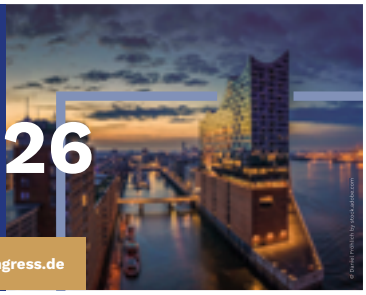

P17 Postergroup: Metabolism in Physioloy

P1709

Treatment of obese mice with Atglistatin following cardiac I/R results in alterations to adipose tissue biology

Pia Hebar; Heba Zabri; Dominik Semmler; Simone Gorressen; Stefan Lehr [1]; Jens W. Fischer; Katharina Bottermann
Institute of Pharmacology, University Hospital, Heinrich Heine University Düsseldorf, Düsseldorf, Germany; [1] German Diabetes Center (DDZ), Düsseldorf, Germany;

Objective: Obesity is classified as a primary risk factor for cardiovascular disease, including myocardial infarction (MI). White adipose tissue (WAT) function is considerably compromised in obese subjects. MI exerts both, an acute stimulatory effect on WAT lipolysis, as well as a chronic effect on WAT metabolic and secretory function.
Method: The murine ATGLinhibitor Atglistatin was utilised to characterise the role of WAT function over extended periods following cardiac ischaemia/reperfusion (I/R) injury in obese C57BL/6J male and female mice. Morphology, structural and functional characteristics of cardiac tissue, subcutaneous (iWAT), visceral (gWAT) WAT and blood were analysed. A closedchest model was used to induce cardiac I/R (anaesthesia: ketamine/xylazine (100/10 mg/kg BW), isoflurane (1.52%), analgesia: buprenorphine (0.05 - 0.1 mg/kg body weight)) following a 9week highfat/highsucrose diet. Atglistatintreatment started the day after ischemia. Mice were euthanised by cervical dislocation or CO2 24 hours and 28 days after I/R.
Results: Acute activation of lipolysis was absent in both male and female mice following I/R. The analysis of the lipolytic gene profile post I/R yielded contradictory results between males and females, with the former demonstrating a reduction and the latter an increase in gene expression of hormonesensitive lipase (*Lipe)* in gWat. In addition to cardiac I/R, treatment with Atglistatin resulted in a comparable relative loss of body weight and a reduction in gWAT mass in both sexes. Ischemic Atglistatintreated male mice demonstrated additionally smaller adipocytes in iWat, while this was unchanged in females. Atglistatintreatment reduced circulating leptin and increased circulating ghrelin indicating enhanced appetite in males. No alterations in cardiac function were achieved in either sex after Atglistatintreatment compared to vehicle.
Conclusion: In obese mice, the initial lipolytic response to I/R appears to be diminished. Although the treatment led to a reduction in body weight and an alteration in adipose tissue biology, no beneficial impact on cardiac function was observed after I/R.

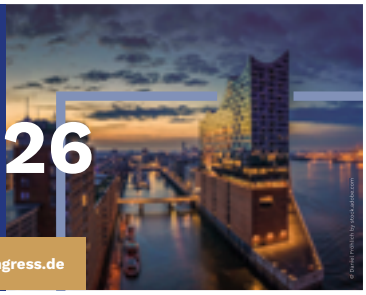

P17 Postergroup: Metabolism in Physioloy

P1710

Dissecting chain lengthspecific effects of mediumchain fatty acids on glucometabolic regulation in obese mice

Ye Cao; Wenke Jonas [1]; Niclas Rausch; Maximilian Kleinert
Department of Molecular Physiology of Exercise and Nutrition, German Institute of Human Nutrition (DIfE) PotsdamRehbruecke, Nuthetal, Germany; [1] Department of Experimental Diabetology, German Institute of Human Nutrition (DIfE) PotsdamRehbruecke, Nuthetal, Germany; Department of Molecular Physiology of Exercise and Nutrition, German Institute of Human Nutrition (DIfE) PotsdamRehbruecke, Nuthetal, Germany;

Objective: Mediumchain fatty acids (MCFAs) are widely used in clinical and nutritional settings, including ketogenic diets, typically in mixed formulations. While associated with increased energy expenditure and improved metabolic regulation in healthy and obese individuals, the contribution of distinct MCFAs remains unclear. To address this, we compared the acute glucometabolic effects of individual evenchain MCFAs on glucose metabolism and energy expenditure in obese mice.
Method: Male dietinduced obese (DIO) mice received a single oral gavage of triacylglycerols containing C6 (caproic acid), C8 (caprylic acid), or C10 (capric acid), with lard as a longchain fatty acid (LCFA) control. Circulating glucose and βhydroxybutyrate were monitored for 4 h. Energy expenditure and food intake were measured by indirect calorimetry, and body weight was determined before and at 24 h post gavage. Based on initial screening, C8 was further evaluated against lard using an oral insulin stimulation test.
Results: MCFA administration elicited pronounced chainlengthdependent glucometabolic responses. Both C6 and C8 induced robust ketogenic responses, with βhydroxybutyrate reaching ~2.3 mmol/L at 60 min ($p<0.01$ vs C10 and lard). C8 significantly increased oxygen consumption within 5 h compared with lard ($p<0.05$), indicating an acute elevation in energy expenditure. This was accompanied by reduced food intake (~55% vs lard at 24 h, $p<0.01$) and a decrease in body weight (~3%). Based on its distinct metabolic profile, C8 was selected for further metabolic characterization using an insulinstimulation test. C8 increased insulin secretion at 1 h postgavage. Following glucose administration, C8 further enhanced earlyphase insulin secretion (~4fold at 5 min, $p < 0.0001$ vs lard), whereas lardtreated mice showed a delayed insulin response. In parallel, mice gavaged with C8 displayed an attenuated early glucose excursion.
Conclusion: MCFA chain length critically determines metabolic responses in the context of obesity. C8 induces a coordinated glucometabolic response, characterized by enhanced ketogenesis, increased energy expenditure, reduced energy intake, and improved glucose handling. These findings highlight that enriching C8 may enhance the metabolic efficacy of MCFAbased nutritional strategies, including ketogenic diets, for the treatment of glucometabolic diseases.

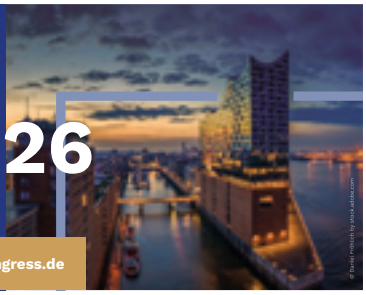

P17 Postergroup: Metabolism in Physioloy

P1711
Isolated Effects of Lactate on Lipolysis and Adipose Tissue Signaling in Humans

Julia Röja; Sebastian Edman; Emily Shorter [1]; William Apró; Johanna T. Lanner; Marcus Moberg [2]
Physiology, Nutrition and Biomechanics , Swedish School of Sport and Health Sciences, Stockholm, Sweden; [1] Department of Physiology, Nutrition and Biomechanics, Swedish School of Sport and Health Sciences, Stockholm, Sweden; [2] Physiology, Nutrition and Biomechanics, Swedish School of Sport and Health Sciences, Stockholm, Sweden;

Objective: Lactate has been proposed as a regulator of lipid metabolism and lipolysis. Beyond its metabolic role, lactate has emerged as a signaling molecule that can induce protein lactylation. Lactate is often investigated in the context of exercise metabolism. Here, we instead set out to isolate the effects of lactate on lipid regulation and adipose tissue signaling under resting conditions.
Method: Eighteen healthy adults (9 female, 9 male) underwent a 60min venous infusion of sodium lactate (125 µmol/kg fatfree mass/min) or isotonic saline. Blood and adipose tissue biopsies were collected before, immediately after, and 60 min after infusion. Plasma lactate and serum free fatty acid concentrations were measured spectrophotometrically, while hormone concentrations were determined using enzymelinked immunosorbent assays. Adipose tissue protein lactylation and protein expression and phosphorylation related to GPR81PKAmediated lipolytic signaling were assessed by immunoblotting. Data were analyzed using twoway repeatedmeasures ANOVA and are presented as mean ± SD. Bulk RNA sequencing was performed on biopsy samples collected preinfusion and 60 min postinfusion using an Illumina platform, generating ≈50 million reads per sample.
Results: Plasma lactate levels peaked at 5.9 ± 0.37 mmol/L at the end of the lactate infusion (p<0.0001 vs. saline; n=12 vs. 12). Free fatty acid concentrations decreased by 27% from 0.58 ± 0.25 to 0.42 ± 0.12 mmol/L (p<0.001 vs. saline; n=12 vs. 12), whereas no change was observed in insulin, epinephrine, or norepinephrine levels during the lactate infusion (p>0.05 vs. saline; n=12 vs. 12). Adipose tissue phosphorylation of PKA substrates, $CREB^{Ser133}$ and HSL^{Ser660} were not altered by lactate infusion (p>0.05 vs. saline; n=12 vs. 6). Lactate infusion increased adipose tissue protein lactylation (Llactyllysine) by 22% compared with saline infusion (p=0.0337; n=12 vs. 6). Bulk RNA sequencing identified 29 differentially expressed genes (DEGs) in adipose tissue specifically responsive to lactate infusion ($padj$<0.05 vs. saline). Pathway enrichment analysis indicated activation of kinase- and stressresponse pathways, including serine/threonine kinase activity and neurotrophic signaling.
Conclusion: In conclusion, lactate infusion decreased circulating free fatty acid concentrations, independent of systemic hormonal responses, and was accompanied by increased adipose tissue protein lactylation, suggesting a direct role for lactate in human lipid regulation.

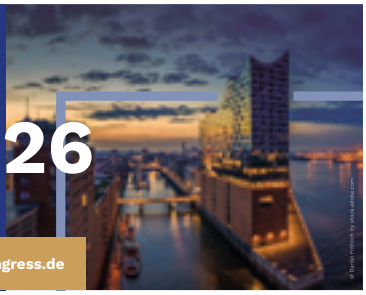

P17 Postergroup: Metabolism in Physioloy

P1712

Long noncoding RNA PCAT19 protects and bookmarks DNA replication origins during endothelial cell quiescence

James Oo; Katalin Pálfi; Ralf P. Brandes
Institut für Kardiovaskuläre Physiologie, Universitätsklinikum, Johann Wolfgang GoetheUniversität, Frankfurt a. M., Germany;

Objective: Endothelial cells remain quiescent for long periods, yet rapidly reenter the cell cycle when vascular repair is required. This proliferationquiescence switch is essential for endothelial growth, reendothelialisation and regeneration. We previously identified the endothelialenriched long noncoding RNA PCAT19 as a regulator of this switch. In quiescent endothelial cells, PCAT19 binds the replication protein RPA2 and limits its phosphorylation, thereby restraining replication stress signalling, DNA damage and inappropriate proliferative entry. However, how PCAT19 functions at DNA replication sites together with RPA2 and other interacting proteins remained unclear.
Results: RNADNA interaction mapping (RADICLseq) identified approximately 1,100 PCAT19associated chromatin loci in endothelial cells. Overlap with genome annotation and histonemark datasets showed that these sites are enriched at active regulatory regions, including promoters and enhancers, which are often linked to replication origins. Integration with replication timing maps (Repliseq), which show when genomic regions are copied during S phase, then revealed that PCAT19associated loci are indeed enriched at replicationinitiation zones and biased toward early replication sites. UHRF1 emerged as an important second PCAT19associated factor with domainmapping suggesting that PCAT19 binds regions of UHRF1 that influence its function in DNA methylation maintenance. Subsequent methylation profiling (5mC meCUT&RUN), which maps methylated chromatin regions, revealed marked differences between proliferating and quiescent endothelial cells, and PCAT19associated loci closest to replicationinitiation regions were enriched near these methylation changes. UHRF1 chromatin profiling further showed altered UHRF1 occupancy after PCAT19 perturbation.
Conclusion: These findings suggest that PCAT19 helps maintain replicationlinked chromatin states during endothelial quiescence and may support safe cellcycle reentry during vascular repair. Ongoing work aims to test whether controlled depletion of PCAT19 can improve endothelial growth and regeneration in plaquelike models of vascular disease without increasing replication stress, opening potential therapeutic avenues for endothelial cellstate transitions.

P17 Postergroup: Metabolism in Physioloy

P1713

Redox Regulation of ExerciseInduced Insulin Sensitization: Insights from Humans and Drosophila

Christian T. Voldstedlund; Jonathan J. Petrocelli [1]; Alina Malita [2]; Kim A. Sjøberg; Haopeng Xiao [1]; Carlos HenriquezOlguin; Casper M. Sigvardsen; Farina L. Schlabs; Jesper Havelund [3]; Nils J. Færgeman [3]; Jørgen F. P. Wojtaszewski; Bente Kiens; Thomas Elbenhardt Jensen; Kim Rewitz [2]; Edward T. Chouchani [1]; Erik A. Richter
Department of Nutrition, Exercise and Sports, University of Copenhagen, Copenhagen, Denmark; [1] Department of Cell Biology, DanaFarber Cancer Institute, Harvard Medical School, Boston, United States; [2] Department of Biology, University of Copenhagen, Copenhagen, Denmark; [3] University of Southern Denmark, Odense, Denmark;

Objective: Insulinstimulated glucose uptake is markedly enhanced in skeletal muscle following a single bout of exercise, yet the underlying molecular mechanisms remain incompletely understood. Therefore, we investigated the physiological and molecular mechanisms underlying exerciseinduced improvements in skeletal muscle insulin sensitivity.
Method: We investigated the role of reversible cysteine oxidation in exerciseinduced insulin sensitization in men using a oneleg exercise model combined with quantification of leg glucose uptake, skeletal muscle redox proteomics, metabolomics, and functional validation in Drosophila using a recently developed assay for assessing glucose uptake. Reversible cysteine oxidation was quantified using a CPTMSbased redox proteomics workflow that enables stoichiometric assessment of reversible cysteine oxidation in human skeletal muscle.
Results: Across 5,791 cysteines, insulin induced a global reductive shift in oxidation in muscle from both legs, while prior exercise did not induce a sustained elevation of global oxidation. Instead, exercise modified cysteine oxidation in a sitespecific and compartmentalized manner. Subsequent analysis coupled with metabolomics identified redoxsensitive proteins involved in glycogen metabolism (GDE), glucose handling (PDK2/G6PD), and insulin signaling (PP1B). Although both GDE and PDK2 exhibited significant correlations with leg glucose uptake, only PP1B and G6PD were identified as potential regulators of insulinstimulated glucose uptake using a newly developed leg musclespecific assay in Drosophila.
Conclusion: Collectively, these findings identify selective cysteine redox remodelling as a mechanism potentially linking exercise to enhanced insulin sensitivity.

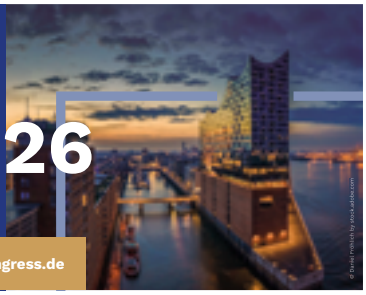

P18 Postergroup: K Channels

P1801

Dynamic coupling reloaded - functional characterization of diseaserelated *KCND2* variants affecting Kv4.2 channel inactivation gating

Anna Babenhauserheide; Yongqiang Zhang; Stefan Kindler [1]; Robert Bähring
Institut für Zelluläre und Integrative Physiologie, Universitätsklinikum HamburgEppendorf (UKE), Hamburg, Germany; [1] Institut für Humangenetik, Universitätsklinikum HamburgEppendorf (UKE), Hamburg, Germany;

Objective: In a cohort of patients with earlyonset global developmental delay, partly accompanied by epileptic seizures, heterozygous missense variants were identified in the *KCND2* gene. *KCND2* encodes the voltagegated K^+ channel αsubunit Kv4.2, the molecular substrate of a somatodendritic Atype current, which regulates low frequency firing and dendritic excitation and plays a central role in synaptic plasticity. The newly identified *KCND2* variants lead to amino acid exchanges in or near a conserved PVP motif in the S6 segment of Kv4.2, known to be involved in the dynamic coupling of voltage sensor and gate in the process of closedstate inactivation. The purpose of this study was to examine whether and how the amino acid substitutions alter channel function.
Method: *Xenopus laevis* oocytes (harvested from anesthetized frogs; 1.2 g tricaine/l tap water) were injected with cRNA encoding wildtype (WT) and mutant Kv4.2 channel proteins and the auxiliary subunits KChIP2b and DPP6s. Kv4.2 channels were analysed in different configurations under voltage clamp.
Results: In a heteroternary configuration (Kv4.2 WT + mutant + KChIP2b + DPP6s) all newly identified *KCND2* variants (V402L, P403S, P403T and I405M) caused slowed macroscopic inactivation and slowed tail current deactivation kinetics. The recovery from inactivation was also slowed, and the voltage dependence of steadystate inactivation was shifted in the positive or negative direction. The most prominent effects compared to homoternary WT were seen for heteroternary P403T channels (time constants from tripleexponential fits: 28, 241 and 1251 ms instead of 26, 86 and 617 ms; tail current deactivation time constant: 19 ms instead of 0.8 ms; recovery time constant: 166 ms instead of 16 ms; voltage of halfmaximal steadystate inactivation: 83 mV instead of 63 mV). Thus, we find complex alterations in Kv4.2 channel inactivation gating, compatible with both gainoffunction (at positive voltages above threshold) and lossoffunction (at negative voltages below threshold).
Conclusion: Our findings strongly suggest that pathogenic *KCND2* missense variants affecting a short domain including the PVP motif modify Kv4.2 channel inactivation gating, dysregulate neuronal excitability and thus cause earlyonset global developmental delay and epilepsy.

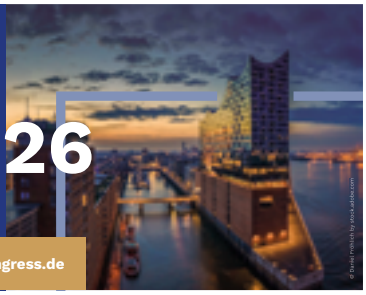

P18 Postergroup: K Channels

P1802
Potassium channel modulation enhances KRAStargeted therapy in PDAC

Weronika Wilczak; Albrecht Schwab; Zoltan Pethö
Physiologisches Institut II, Universitätsklinikum, Westfälische Wilhelms Universität Münster, Münster, Germany;

Objective: Pancreatic ductal adenocarcinoma (PDAC) is driven by oncogenic KRAS mutations in more than 90% of patients. Durable therapeutic responses remain limited, despite KRAS inhibitors recently entered clinical development. Therefore, rational combination strategies are urgently needed.
Method: We established a heterotypic 3D spheroid platform composed of PDAC cancer cells, pancreatic stellate cells, and endothelial cells embedded in extracellular matrix to recapitulate key features of the tumor microenvironment. Dose–response analyses of three selective $KRAS^{G12D}$ inhibitors, zoldonrasib, MRTX1133, and daraxonrasib, were performed in KRASmutant spheroids. Based on potency and reproducibility, the $KRAS^{G12D}$ inhibitor MRTX1133 was selected for further experiments. Membrane potential dynamics were monitored using cancer cells expressing the fluorescent voltagesensitive reporter rEstus. Finally, we performed a drug repurposing screen of clinically tested K^+ channel modulators in combination with MRTX1133 using the spheroid platform.
Results: KRAS inhibition selectively reduced viability in KRASmutant models (generated with Panc1 or AsPc1 cells), while KRAS wildtype cells (BxPC3) were largely unaffected. Highdose MRTX1133 (1 µM) reduced spheroid viability by 63%, while 1 nM had minimal effect. Screening of K^+ channel modulators identified compounds that enhanced sensitivity to KRAS inhibition. Notably, combining 1 nM MRTX1133 with the K_V7 inhibitor linopirdine reduced spheroid viability by 41%. Acute treatment induced heterogeneous alterations in membrane polarization, with a subset of cells exhibiting hyperpolarization, suggesting functional coupling between oncogenic KRAS signaling and ion transport mechanisms. Complementary assays showed that dual KRAS and K_V7 inhibition reduced PDAC cell migration, while TGFβ secretion decreased approximately 2- to 4.8fold.
Conclusion: Our data support a role for K^+ channel modulation in enhancing KRAStargeted therapy in PDAC.

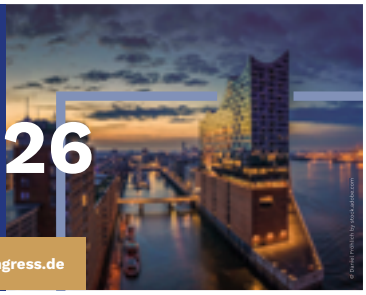

P18 Postergroup: K Channels

P1803

Biophysical properties of K_v7/KCNQ/Mchannels in hippocampal mossy fibre boutons

Luise Wehle; Ricardo Murphy [1]; Henrik Alle; Johan F. Storm [1]; Jörg Rolf Paul Geiger Institut für Neurophysiologie, Charité - Universitätsmedizin Berlin, Berlin, Germany; [1] Physiology Section, Institute for Basic Medical Sciences, University of Oslo, Oslo, Norway;

Objective: Hippocampal mossy fibres, the axons of dentate gyrus granule cells, exhibit electrical resonance in the thetatogamma frequency range, thought to arise from K_v7 channel activity. This impedance property may contribute to frequencydependent subthreshold signal integration along the mossy fibre pathway.

Method: To characterise the underlying Mcurrent (I_M), XE991sensitive currents were recorded using the wholemossy fibre bouton (MFB) patchclamp configuration in acute hippocampal slices of Wistar rats at 35 °C (postnatal day 19 – 35, decapitated during deep anaesthesia with isoflurane). All voltage values are corrected for liquid junction potentials, data represent mean ± standard deviation.

Results: Steadystate activation of I_M yielded a halfactivation voltage ($V_{1/2}$) of −46.3 mV and slope factor k = 8.9 mV (10 µM XE991, n = 7), comparable to results obtained at 3 µM XE991 ($V_{1/2}$ = −46.1 mV, k = 9.0 mV, n = 3). The K_v7 activator retigabine leftshifted activation to $V_{1/2}$ = −80 mV (n = 2), corroborating the K_v7 identity. Having blocked K_v1, K_v3 and BK channels pharmacologically, I_M stabilised the resting membrane potential (RMP) at −64.8 ± 2.2 mV, subsequent application of XE991 depolarised MFBs to −48.8 ± 2.7 mV (n = 7). XE991 increased input resistance from 1.62 ± 0.28 to 1.92 ± 0.36 GΩ (−90 to −80 mV step), reflecting minimal K_v7 channel recruitment at RMP. The maximum steadystate XE991sensitive conductance amounted to 3.17 ± 0.86 nS (n = 7). Activation time constant (τ_{act}) ranged from ~45 ms at −50 mV to ~23 ms at +20 mV, and deactivation time constant (τ_{deact}) from ~32 ms at −60 mV to ~10 ms at −90 mV.

Conclusion: Our biophysical characterisation of K_v7 channels provides key parameters for modelling K_v7dependent electrical resonance in hippocampal mossy fibres.

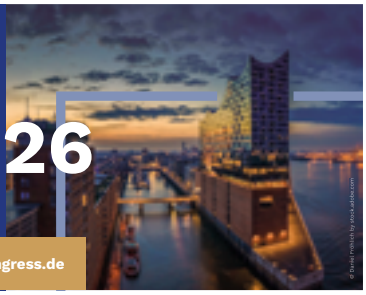

P18 Postergroup: K Channels

P1804

KCNH3 lossoffunction variant associated with epilepsy and neurodevelopmental delay enhances Kv12.2 channel inactivation

Christiane K. Bauer; Frederike L. Harms [1]; Robert Bähring
Institut für Zelluläre und Integrative Physiologie, Universitätsklinikum Hamburg Eppendorf (UKE), Hamburg, Germany; [1] Institut für Humangenetik, Universitätsklinikum HamburgEppendorf (UKE), Hamburg, Germany;

Objective: The *KCNH* (EAG) gene family encodes Kv10, Kv11 and Kv12 voltagegated K^+ channels, which are critically involved in the control of cardiac and neuronal excitability. Pathogenic gainoffunction variants in *KCNH1* and *KCNH5*, encoding Kv10 channels, can cause neurodevelopmental syndromes including seizures, whereas a plethora of lossoffunction variants in *KCNH2*, encoding the Kv11.1 ("hERG") channel, are known to underlie the cardiac longQTsyndrome 2 (LQT2). Here, we provide the first evidence of a link between a *KCNH3* missense variant and human neurological disease, established in a young girl presenting with neurological symptoms including nocturnal seizures. Trio exome sequencing revealed a heterozygous *de novo* missense variant, NM_012284.3:c.1112C>T; p.(Ala371Val), in the *KCNH3* gene, which encodes the neuronal Kv channel αsubunit Kv12.2. The amino acid substitution is located in the transmembrane segment S5 at a site highly conserved in all EAG channels. The analogous variant in *KCNH2* is known to cause LQT2.
Method: Kv12.2 wildtype and mutant channels were analyzed using the twoelectrode voltage clamp technique in *Xenopus laevis* oocytes and the wholecell patch clamp technique in CHO cells. Oocytes (harvested from anesthetized frogs; 1.2 g tricaine/l tap water) were injected with corresponding cRNAs, and CHO cells were transiently transfected with corresponding cDNAs using Lipofectamine.
Results: Electrophysiological characterization of the *KCNH3* p.(Ala371Val) variant demonstrated lossoffunction of the mutant Kv12.2 channels, and strongly reduced current amplitudes in a dominantnegative manner were observed upon coexpression of wildtype and mutant channel subunits. Recordings in elevated external K^+ reduced the rectification of Kv12.2 conductance as predicted by the GHK current equation, allowing the detection and biophysical analysis of currents mediated by A371V Kv12.2 channels. Strikingly different from wildtype channels, A371V Kv12.2 channels exhibit accelerated inactivation kinetics (5fold) and a dramatic negative shift in the voltage dependence of inactivation by more than 100 mV. Even in heteromeric wildtype + A371V Kv12.2 channels, inactivation was strongly enhanced, leading to significant current reduction at physiological potentials.
Conclusion: Our results propose *KCNH3* as a new disease gene associated with a neurodevelopmental phenotype including seizures, in line with murine knockout data (Zhang et al 2010, Nat Neurosci 13:1056).

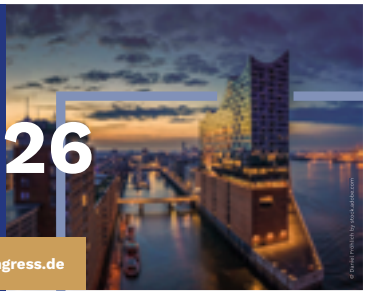

P1805

P18 Postergroup: K Channels

Investigating the mechanisms of KvSmediated trafficking in KCNQ Channels

Rajeshwari Bisen; Aparna Renigunta [1]; Dominik Oliver; Vijayaram Kumar Renigunta Department of Neurophysiology, Institute of Physiology and Pathophysiology, Philipps University Marburg, Marburg, Germany; [1] Klinik II für Pädiatrische Nephrologie, Transplantationsnephrologie und Allgemeine Kinderheilkunde, Standort Marburg, Universitätsklinikum Gießen und Marburg GmbH, Marburg, Germany;

Objective: Voltagegated potassium (Kv) channels assemble as tetramers to mediate K^+ efflux across the plasma membrane upon membrane depolarization. Silent Kv (KvS) subunits typically require coassembly with Kv2 subunits to form functional channels. However, recent evidence has revealed that KvS subunits also modulate Kv7 (KCNQ) channels, uncovering a previously unrecognized aspect of their function
Method: To investigate the KvSmediated regulation of KCNQ channels, we characterized nature of KvSKCNQ protein association using immunocytochemistry (ICC), surface biotinylation and Retention Using Selective Hooks (RUSH) systems. By expressing Kv8.1/Kv8.2 Cterminal exchange chimeras in *Xenopus* oocytes, we isolated the specific role of the KvS Cterminus in surface expression of KCNQ subunits. Finally, coimmunoprecipitation and surface quantification assays were used to determine whether calmodulin (CaM) is a necessary part of the KvSKCNQ complex
Results: Consistent with our previous observations, Kv8.1 increased KCNQ plasma membrane trafficking, while Kv8.2 decreased it. Together, our assays demonstrated that KvS subunits act as βlike auxiliary subunits rather than classical poreforming αsubunits. Oocyte surface quantification revealed that the KvS Cterminus directly modulates this KCNQ trafficking. However, unlike typical KCNQ channels, we did not detect CaM in the KvSKCNQ complex. Furthermore, when coexpressed with Kv8.1, both CaMbindingdeficient and BFNCassociated KCNQ mutants successfully exited the endoplasmic reticulum (ER)
Conclusion: We propose that Kv8.1 can replace CaM as a chaperone for ER export, driving KCNQ forward trafficking through a CaMindependent mechanism. This establishes KvS subunits as a novel class of KCNQ trafficking regulators, offering new physiological insights into channelopathies caused by disrupted CaMKCNQ interactions.

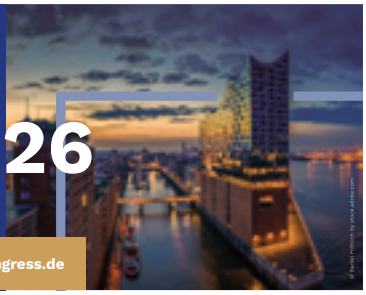

P18 Postergroup: K Channels

P1806

Selective control of intrinsic in vitro bursting by somatodendritic Kv7 channels in VTA dopamine neurons projecting to the medial shell of the nucleus accumbens

Tabea Ziouziou; Emanuel Lopes [1]; Christopher Knowlton [2]; Carmen Canavier [2]; Stephanie Cragg [1]; Jochen Roeper [3]
Institute of Neurophysiology, Goethe University Frankfurt, Frankfurt a. M., Germany; [1] University of Oxford, Oxford, United Kingdom; [2] Louisiana State University, New Orleans, United States; [3] Interdisziplinäres Zentrum für Neurowissenschaften, GoetheUniversität, Frankfurt a. M., Germany;

Results: Dopamine (DA) neurons projecting to the nucleus accumbens (NAcc) exhibit biophysical properties and firing patterns distinct from other DA midbrain neurons (Lammel et al. 2008; Knowlton, Ziouziou et al. 2021). While most *in vitro* electrophysiology studies on DA neurons focus on singlespike activity, our study identified a subset of ventral tegmental area (VTA) DA neurons projecting to the medial shell of the NAcc (mNAcc) that spontaneously generated short (24 spikes) highfrequency burst discharges (max frequency 53.3±16.1 Hz, n=3, N=4). Using retrograde tracing and *in vitro* patchclamp recordings in coronal midbrain slices from adult male and female C57BL6/N mice, we found that this intrinsic burst activity was sparse under control conditions (20%, n=3/15) but was potentiated by pharmacological inhibition of somatodendritic and proximal axonal Kv7 channels by 10 µM XE991 (80%, n=18/22). In contrast, less than 20% of core NAccprojecting VTA DA neurons (n=4/24) and none of the lateral shellprojecting VTA DA neurons (n=0/25) showed burst firing in the presence of XE991. The observed *in vitro* burst firing resembled *in vivo* plateau bursting (Otomo et al. 2020) with a depolarizing shift (6.1±2.4 mV, n=22, N=4) in subsequent action potential thresholds within the burst. To probe how mNAcc DA axons respond to burst pattern discharge, we used fastscan cyclic voltammetry to measure DA release in coronal slices. DA release evoked by bipolar electrical stimulation with *in vitro* burstlike patterns (4 pulses, 100 Hz) reported this activity in mNAcc better than other striatal regions, with DA levels ~5 times those for a single pulse. Inhibition of Kv7 channels in mNAcc reduced DA release evoked by burstlike patterns (AUCcontrol: 3048±1000, n=34, N=7 vs. XE991: 2130±566, n=22, N=5).
Conclusion: In summary, our findings suggest that both somatodendritic and distal axonal Kv7 channels shape intrinsic fast burst discharges and phasic dopamine release in the mNAcc.

P18 Postergroup: K Channels

P1807

Kv4 channel gating modulation by pathogenic *KCND* variants affecting the pore helix

Pia Ullmann; Fabian Schönewald; Stefan Kindler [1]; Robert Bähring
Institut für Zelluläre und Integrative Physiologie, Universitätsklinikum HamburgEppendorf, Hamburg, Germany; [1] Institut für Humangenetik, Universitätsklinikum HamburgEppendorf, Hamburg, Germany;

Objective: The genes *KCND1* and *KCND2* encode the αsubunits of the voltagegated K^+ channels Kv4.1 and Kv4.2, respectively. These channels contribute to a somatodendritic Atype current, which controls neuronal excitation, discharge behaviour and synaptic plasticity. They are formed by four αsubunits, each with six transmembrane segments (S1S6), flanked by cytoplasmatic N- and Ctermini. A pore loop between S5 and S6 harbours the highly conserved K^+ selectivity filter sequence and a pore helix, critical for ion selectivity and high throughput permeation. Published pathogenic *KCND2* variants affect essential gating domains, whereas the majority of reported *KCND1* variants modify channel domains, which are less critical for channel function, such as the cytoplasmic N- and Ctermini. Here we report two novel missense variants affecting the pore helices of Kv4.1 and Kv4.2 (Kv4.1 A361E and Kv4.2 F361L) in patients with developmental delay and intellectual disability. The purpose of this study was to assess whether and how channel function is modulated by these amino acid exchanges.
Method: Wildtype and mutant channel proteins (Kv4.1 or Kv4.2) were heterologously expressed in *Xenopus laevis* oocytes, obtained from anesthetized frogs (1.2 g tricaine per liter tap water) and injected with respective cRNAs. Channels were characterized using the twoelectrode voltageclamp technique.
Results: Both pore helix variants are functional and mediate Atype currents. Macroscopic inactivation is accelerated in Kv4.1 A361E (initial time constant: 16 instead of 27 ms) but slowed in Kv4.2 F361L (initial time constant: 46 instead of 19 ms). The recovery from inactivation is moderately slowed in Kv4.1 A361E (time constant: 131 instead of 100 ms) but strongly accelerated in Kv4.2 F361L (time constant: 51 instead of 204 ms). Finally, the voltage dependence of steadystate inactivation remains virtually unchanged in Kv4.1 A361E ($V_{1/2}$: 61 instead of 59 mV) but is strongly shifted in the positive direction in Kv4.2 F361L ($V_{1/2}$: 47 instead of 67 mV).
Conclusion: Amino acid substitution in the Kv4.1 pore helix has less severe effects on channel function than a nonhomologous substitution in the pore helix of Kv4.2. The data are consistent with previous findings indicating that the effects of *KCND1* variants on channel function are less severe than those of *KCND2* variants. Prenatal selection in combination with the Xchromosomal localization of *KCND1* offers a possible explanation.

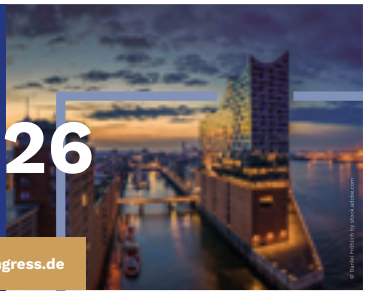

P18 Postergroup: K Channels

P1808

Selective inhibition of the Kv2.1/6.4 heteromeric potassium channel by Riluzole

Debanjan Tewari; Klaus Benndorf; Indra Schröder
Institute of Physiology II, University Hospital Jena, Jena, Germany;

Objective: Riluzole is an FDAapproved drug used clinically for the treatment of amyotrophic lateral sclerosis. However, its precise mechanism of action remains unclear. Previous studies have suggested that Riluzole exerts multiple effects on several types of ion channels. For instance, Kv1.5 and Kv4.2 potassium channels have been reported to be inhibited by Riluzole in their closed and inactivated states.
Method: Electrophysiology, Mutagenesis, and Molecular Docking
Results: Three concentrations of Riluzole (100, 250, and 500 µM) were initially tested to evaluate their effects on the electrophysiological properties of the Kv2.1/6.4 heteromeric channel. At a concentration of 500 µM, the activation conductancevoltage (G–V) curve was shifted approximately 15 mV toward more negative potentials, accompanied by a reduction in steadystate current amplitude. In addition, a decrease in the activation time constant was observed, suggesting altered channel gating kinetics. In contrast, the Kv2.1 homomeric channel was not significantly affected at the same concentration of Riluzole.
Conclusion: These preliminary findings suggest that the effects of Riluzole on Kv2.1/6.4 channels may be isoformspecific, indicating a possible selective interaction with heteromeric channel configurations.

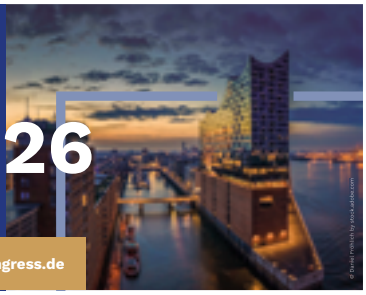

P18 Postergroup: K Channels

P1809

Conformational basis of TREK channel activation: revisiting the role of the downup transition and the lipidoccluded pore

Marianne Musinszki; Chun Kei Lam [1]; Edward Mendez Otalvaro [1]; Friederike Schulz; Elena B. Riel [2]; Anthony Ogwo; Kristin Rathje; Lea C. Neelsen; Bert de Groot [1]; Marcus Schewe [3]; Thomas Baukrowitz [3] Medical Faculty, Physiological Institute, Kiel University, Kiel, Germany; [1] Department of Theoretical and Computational Biophysics, Max Planck Institute for Biophysical Chemistry, Göttingen, Germany; [2] Department of Anesthesiology, Weill Cornell Medical College, New York, United States; [3] Physiologisches Institut, ChristianAlbrechtsUniversität zu Kiel, Kiel, Germany;

Objective: TREK/TRAAK twoporedomain potassium (K2P) channels are polymodally regulated membrane proteins that integrate physical and chemical stimuli, but the structural basis of their gating remains incompletely understood. Here, we combine systematic mutagenesis, electrophysiology, pharmacology, and molecular simulations to define how structural rearrangements in the M2/M3/M4 helical bundle control selectivity filter (SF) gating in TREK channels.
Method: We identify multiple gatingrelevant residues whose mutation strongly increases channel open probability. To predict structural consequences of these mutations, we apply a lowcost free energy framework based on nonequilibrium molecular dynamics simulations. This approach robustly classifies mutations according to their preferred conformational state and distinguishes mechanistically distinct gainoffunction phenotypes. Predictions are validated using electrophysiological recordings and a statesensitive norfluoxetine (NFx) assay, complemented by conventional molecular dynamics simulations and residue interaction analysis that resolve local structural rearrangements.
Results: Our results reveal at least two predictable, separable activation mechanisms. One class of mutations stabilizes an upstate conformation, characterized by a high activity SF state and disrupted interactions between M2, M3 and M4. A second, surprisingly common class activates the channels without a transition to the upstate, indicating that gainoffunction can arise from fardistributed perturbations within a largely downlike architecture.
We further show that diverse physiological stimuli—including intracellular pH changes, phospholipids, and PIP2—converge on stabilization of the upstate conformation, supporting a unified mechanism of physiological activation
Finally, functional and computational evidence is inconsistent with lipidocclusion models of gating. Instead, channel activity is best explained by conformational changes that regulate the SF through allosteric coupling to the transmembrane helical bundle.
Conclusion: Together, these findings provide a revised mechanistic framework for TREK/TRAAK channel activation and establish a general computational–experimental strategy for predicting mutationinduced conformational changes in ion channels.

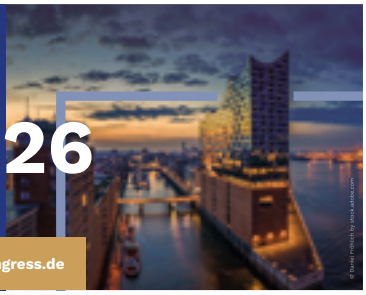

P18 Postergroup: K Channels

P1810

Analysing the voltage dependences of Atype potassium channel gating considering GHK rectification

Robert Bähring; Anna Babenhauserheide; Thomas Meurer; Christiane K. Bauer
Institut für Zelluläre und Integrative Physiologie, Universitätsklinikum HamburgEppendorf (UKE), Hamburg, Germany;

Objective: Rapid inactivation of ion channels may complicate the study of the voltage dependence of activation by analysing tail currents at a constant driving force. Therefore, the voltage dependence of Atype K^+ channel activation is usually determined by converting peak current amplitudes at different test voltages (iv curve) into conductance to obtain gv curves, assuming ohmic channel behaviour. However, most Kv channels show a form of rectification, which depends on the K^+ concentration gradient across the membrane, as described by the GoldmanHodgkinKatz (GHK) current equation. The purpose of this study was to test Kv4.2 Atype channels for the presence of GHK rectification, to convert iv data into activation curves that describe the voltage dependence of opening probability (Po) and to apply these curves to the analysis of pathogenic channel variants.
Method: Twoelectrode voltage clamp experiments were performed on Kv4.2expressing *Xenopus laevis* oocytes bathed in 2 or 98 mM K^+, and peak current amplitudes measured at different test voltages were converted into activation curves in an appropriate manner (Clay 2009, Front Cell Neurosci 3: 16). The oocytes were harvested from anesthetized frogs (1.2 g tricaine/l tap water) and injected with cRNAs coding for wildtype and mutant Kv4.2 channels and for the auxiliary subunits KChIP2b and DPP6s.
Results: Kv4.2 instantaneous iv relationships show outward rectification in 2 but not in 98 mM external K^+. Therefore, activation curves were generated accounting for GHK rectification. Boltzmann analysis of GHKcorrected activation curves yields a voltage of halfmaximal activation ($V_{1/2}$) of 23 mV (uncorrected gv curve: +4 mV) and a slope factor (k) of 13 mV (uncorrected gv curve: 21 mV). Unlike uncorrected gv curves, GHKcorrected activation curves saturate at voltages more positive than +20 mV and are thought to reflect the voltage dependence of Po. We applied this analysis to wildtype homomeric and wildtype + mutant heteromeric ternary Kv4.2 + KChIP2b + DPP6s channels. Corresponding Po windows, based on the overlap of activation and steadystate inactivation curves, reveal no gainoffunction for the Kv4.2 S6 mutants but a drastic gainoffunction for a Kv4.2 S4S5 linker mutant examined.
Conclusion: For Kv4.2 channels, iv data should be transformed considering GHK rectification, in order to obtain a measure of Po, especially if used to study the overlap of activation and inactivation curves.

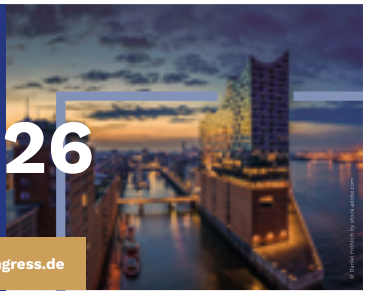

P18 Postergroup: K Channels

P1811

Targeting the modulator pocket in K2P channels: New activators for the family member TRAAK

Chaimae Benkerdagh; Jonathan Ralph [1]; Nathaniel Smith [1]; Han Sun [1]; Thomas Baukrowitz; Marcus Schewe
Physiologisches Institut, ChristianAlbrechtsUniversität zu Kiel, Kiel, Germany; [1] LeibnizForschungsinstitut für Molekulare Pharmakologie (FMP), Berlin, Germany;

Objective: Twopore domain potassium (K_{2P}) channels are widely expressed across tissues and respond to a broad range of physiological stimuli. Consequently, they participate in numerous physiological and pathophysiological processes, including pain, making them attractive therapeutic targets. The K_{2P} family comprises several members with distinct functional, structural, and pharmacological properties.
Here, we focus on the TREK subfamily, for which selective pharmacological targeting remains challenging, particularly for TRAAK. In this context, a recent study identified aprepitant as a novel and selective activator of TRAAK based on highthroughput screening and electrophysiological validation.
Method: Using a combination of molecular modeling and functional electrophysiological approaches, we investigated the pharmacological action of aprepitant and characterized its selectivity, putative binding site, and gating mechanism.
Results: Although aprepitant was previously reported to be selective for TRAAK, our data show that it also activates TREK2 to a comparable extent, while remaining inactive toward TREK1. Computational modelling suggest that aprepitant binds within the modulator pocket of TRAAK, at a site analogous to the ML335 binding site in TREK1. Consistently, electrophysiological analyses identified key residues within the modulator pocket that are critical for aprepitant binding.
Conclusion: Together, variations in bindingpocket architecture provide a framework for the rational design of more selective and, consequently, safer therapeutics for pain management.

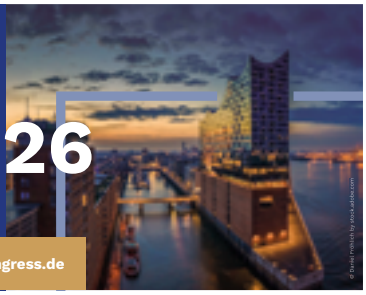

P18 Postergroup: K Channels

P1812

Functional Role of K2P Channels in the Regulation of Tone in Systemic Arteries

Lara Maria Astrid Heinrich; Rudolf Schubert
Physiologie, Medizinische Fakultät, Universitätsklinikum Augsburg, Augsburg, Germany;

Objective: Organ perfusion is regulated by arterial tone, which is determined by the membrane potential of vascular smooth muscle cells. Potassium (K^+) channels are key modulators of this membrane potential. Notably, twopore domain K^+ (K2P) channels contribute to the negative feedback regulation of vasoconstriction and pHdependent regulation of vascular tone. Although well studied in pulmonary circulation, their role in systemic circulation remains largely unexplored. We hypothesized that K2P channels, particularly TASK1 and TREK1 channels, contribute to tone regulation in the systemic circulation.
Method: Intact segments of adult rat systemic and pulmonary arteries (Arteria saphena, Arteria interlobaris) were studied ex vivo using wire myography. TREK1 channel function was investigated using the selective blockers spadin and PE2228, and the opener ML335. TASK1 channel function was examined using the selective blocker ML365 and AVE1231. Due to their small conductance, we aimed to unmask these K2P channels by blocking major potassium conductances using iberiotoxin (BK_{Ca} channels), DPO1 (Kv1.5 channels) and XE991 (Kv7 channels).
Results: We did not detect any relevant effect of spadin alone or in the presence of ML335, either in the absence or in the presence of IBTX+DPO1. Likewise, no relevant effect was detected for PE2228. ML335 reduced methoxamineinduced contractions, indicating a non-specific effect at the applied concentration. We did not detect any relevant effect of ML365 in the absence of IBTX+DPO1; however, ML365 increased vascular tone in the presence of IBTX+DPO1 and appeared more potent than the previously studied TASK1 blocker AVE1231, although nonspecific effects occurred at higher concentrations. Effects of AVE1231 were also detectable in pulmonary arteries in the presence of IBTX+DPO1 and IBTX+XE991.
Conclusion: Our data suggest that in A. saphena TREK1 channels do not contribute to basal or methoxamineinduced tone. In contrast, TASK1 channels contribute to negative feedback regulation of vasocontraction when dominant potassium conductances are suppressed, indicating a functional role for TASK1 channels in the regulation of systemic arterial tone.

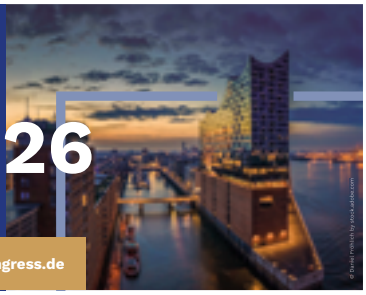

P18 Postergroup: K Channels

P1813

Functional analysis of a pathogenic *KCND2* variant affecting the linker between voltagesensor and pore module

Thomas Meurer; Stefan Kindler [1]; Robert Bähring
Institut für Zelluläre und Integrative Physiologie, Universitätsklinikum Hamburg Eppendorf (UKE), Hamburg, Germany; [1] Institut für Humangenetik, Universitätsklinikum HamburgEppendorf (UKE), Hamburg, Germany;

Objective: Voltagegated K^+ channels of the Kv4 subfamily play a central role in regulating neuronal excitability by mediating transient Atype currents. Kv4 channels are formed by four asubunits, each with six transmembrane segments (S1S6). A voltagesensor module (S1S4) is functionally linked to a pore module (S5S6), which is involved in forming the selectivity filter and the gate. Here, a new missense variant in *KCND2*, encoding the Kv4.2 asubunit, was identified in a patient with global developmental delay and epileptic seizures. The corresponding G309V amino acid substitution occurs in the S4S5 linker region, which couples the voltagesensor to the pore module. Alterations within this region are expected to critically influence channel function. The purpose of this study was to functionally characterize the Kv4.2 G309V variant, to assess whether the gating modifications may explain the patient phenotype, and to identify putative starting points of pharmacological intervention.
Method: Kv4.2 channels were analysed using the twoelectrode voltage clamp technique in *Xenopus laevis* oocytes. Oocytes (harvested from anesthetized frogs; 1.2 g tricaine/l tap water) were injected with cRNA encoding wildtype (WT) and G309V mutant Kv4.2 channels and the auxiliary subunits KChIP2b and DPP6s.
Results: G309V mutant Kv4.2 channels exhibit slowed and incomplete inactivation with a considerable residual fractional current at the end of a 3 s test pulse (initial time constant: 45 instead of 18 ms; residual fraction: 0.39 instead of 0.02). Although the voltage dependence of steadystate inactivation is shifted negative ($V_{1/2}$: 82 instead of 68 mV), the G309V inactivation curve shows Utype features. The modulatory effects were preserved in a heteroternary configuration (Kv4.2 WT + G309V + KChIP + DPP). In the light of the observed massive gainoffunction, therapeutic treatment of the patient with the neuroprotective substance riluzole, a known Kv4 channel inhibitor, is being considered and was therefore tested in our system. Riluzole (bathapplied at 500 mM) suppresses peak currents (50%), but has negligible effects on the special inactivation features of G309Vcontaining channels.
Conclusion: Our data reveal Utype features with massive gainoffunction at positive voltages as a novel modulatory effect in mutant Kv4.2 channels. The use of riluzole to counteract gainoffunction needs to be examined in greater detail before it can be considered as a therapeutic option.

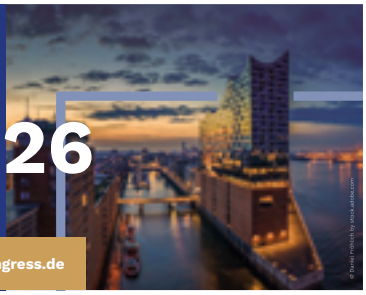

P18 Postergroup: K Channels

P1814

The Sea Urchin TMEM175 Channel: A Regulator of Vesicular pH and K+?

Caroline
Rott; Ornina Merza; Sönke Cordeiro; Marianne Musinszki; Marian Hu
Physiologisches Institut, Christian

The lysosomal transmembrane protein TMEM175 in humans and mammals, functions as a K^+ and proton channel critical for luminal and ion homeostasis. Recent studies identified lysosomes in osteoblasts as key organelles in bone formation. Given the evolutionary conserved function of lysosomes, we investigated the orthologous channel spTMEM175 in mineralizing primary mesenchyme cells (PMCs) of the in the sea urchin larva (Strongylocentrotus purpuratus), a marine model for biomineralization. In analogy to vertebrate osteoblasts, also in PMCs mineralization occurs within vesicles that internalize seawaterlike fluid. To date the role and function of spTMEM175 in mineralizing cells remains unknown. We used a suite of methods ranging from structural simulations over functional genomics to electrophysiological approaches and whole animal experiments to study the function and expression patters of the TMEM175 homologue in the mineralizing cells of the sea urchin embryo.

In the sea urchin larva single cell transcriptomic analysis and in situ hybridization as well as gene expression analyses demonstrate that spTMEM175 is mainly expressed in PMCs. To characterize its function, spTMEM175 was expressed in Xenopus laevis oocytes. Twoelectrode voltage clamp revealed that spTMEM175 encodes an ion channel that is activated by extracellular Mg^{2+} and alkaline pH, conditions mimicking seawater. Notably, currents increase further at Mg^{2+} concentrations beyond seawater levels and pH up to 9, resembling conditions in the mineralization vesicles. These findings suggest a role for spTMEM175 as a modulator for pH and ions in mineralizing vesicles.

Future work will determine ion selectivity and subcellular localization of spTMEM175 in PMCs to shed light on the role of this lysosomal ion channel in the mineralization process. This comparative approach will reveal conserved mechanisms of lysosomal ion transport in mineralizing systems.

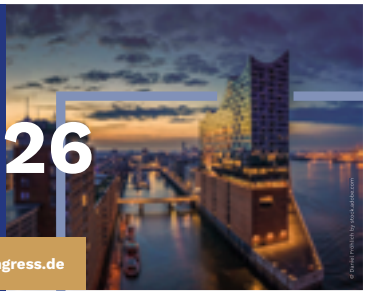

P19 Postergroup: Synaptic Signalling

P1901

Adolescent alcohol drinking affects the excitation/inhibition balance and synaptic plasticity in adult mouse dentate gyrus

Fang Zheng; Christian Alzheimer
Institute of Physiology and Pathophysiology, FriedrichAlexanderUniversität ErlangenNürnberg, Erlangen, Germany;

Objective: Excessive alcohol consumption during adolescence is regarded as a risk factor for the development of alcoholism later in life, yet the pathophysiological mechanisms remain largely unknown. Key players of glutamatergic and GABAergic neurotransmission are among the targets of alcohol in the brain. Here we used a mouse model of heavy adolescent drinking over two weeks to examine how binge drinking in early ages affects adult hippocampus with respect to: (1) excitation and inhibition (E/I) balance, (2) synaptic transmission and response to alcohol reexposure, and (3) gradient of synaptic plasticity along the longitudinal axis of the hippocampus.
Method: We performed wholecell voltageclamp recordings from granule cells (GCs) and field potential recordings in the middle molecular layer of dentate gyrus (DG).
Results: Heavy adolescent drinking disturbed the E/I balance of the total synaptic drive impinging on GCs¸ and also impaired LTP at the medial perforant path (mPP) - DG synapse, especially in dorsal DG. In both dorsal and ventral hippocampal slices from alcoholnäive adults, acute alcohol exposure tilted the E/I balance by enhancing synaptic inhibition and reducing synaptic excitation. Interestingly, when slices from adult mice with an earlier drinking experience were reexposed to alcohol, inhibitory synaptic drives were less augmented in both regions, whereas excitatory synaptic inputs onto granule cells were less suppressed only in ventral DG.
Conclusion: By revealing a dorsoventral gradient of susceptibility to early alcohol drinking, this finding adds to the everincreasing evidence for functional segregation of the two regions. Our study also demonstrates that heavy adolescent drinking has lasting consequences on how excitatory and inhibitory synaptic inputs are weighted in the DG. Finally, early binge drinking alters the impact of acute alcohol exposure on synaptic functions in adulthood, thereby possibly promoting relapse.

P19 Postergroup: Synaptic Signalling

P1902

Excitatory synaptic transmission onto parvalbumin interneurons preferentially governs gamma oscillation properties in acute human neocortical slices

Philip Steiskal; Ecem Tütüncü; Tobias Grünert; Zoltan Gerevich; Jörg Rolf Paul Geiger
Institut für Neurophysiologie, Charité - Universitätsmedizin Berlin, Berlin, Germany;

Objective: Distinct network oscillations coincide with different brain and behavioral states. Remarkably, changes in gammaband network oscillations (30100 Hz, γosc) are tightly linked to normal cognitive functions and to their impairment in pathological conditions. γosc emerge locally from feedback loops between excitatory pyramidal cells and inhibitory parvalbumin interneurons (PVI), that transform convergent excitatory input into precisely timed, strong perisomatic inhibition. While γosc are studied extensively in vivo, their underlying synaptic mechanisms in the human cortex as well as the role of excitatory drive onto PVI, remain to be elucidated.
Method: We established a highthroughput method (up to 32 slices/patient) to record local field potentials of lowfrequency γosc (20–30 Hz) induced by lowconcentration kainate under physiological ionic conditions in acute human neocortical slices. The high reliability (~90% responder rate) of these oscillations – exceeding that in mouse neocortex – enabled us to collect data from ≥500 slices from ≥50 epilepsy patients, to investigate the properties of in vitro γosc and to assess the pharmacological modulation of excitatory transmission.
Results: We found interregional and interlaminar differences in γosc properties. Antagonizing NMDA receptors increased γosc power, while broad AMPA receptor block strongly reduced power (ctrl (n=8): 1.03 norm., GYKI53655 (n=6): 0.42 norm. [median], $p < 0.001$ MannWhitney) and frequency (baseline: 23.96±2.34 Hz, GYKI: 8.63±0.85 Hz [mean±SEM], n=6, $p < 0.01$ paired t test). Notably, selective block of calciumpermeable AMPA receptors preferentially expressed on PVI produced a similar network effect (power – ctrl (n=22): 1.04 norm., NASPM (n=35): 0.58 norm. [median], $p < 0.01$ MannWhitney; frequency – baseline: 24.2±0.81, NASPM: 12.28±0.98 [mean±SEM], n=35, $p < 0.0001$ paired t test). Repeated γosc induction increased power, which was impaired by blocking mGluR1/5, critical for activitydependent PVI synaptic strengthening (ctrl (n=6): 1.88±0.13 norm., MPEP/JNJ16259685 (n=7): 1.37±0.18 norm. [mean±SEM], $p < 0.05$ Welch's t test).
Conclusion: Our results show the significance of excitatory transmission for maintaining γosc and identify excitatory input and synaptic plasticity of PVI as potential therapeutic targets in modulating γosc in neuropsychiatric diseases.

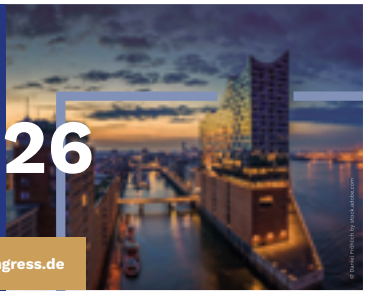

P19 Postergroup: Synaptic Signalling

P1903

Optogenetic mapping of Nucleus Reuniens Inputs to Hippocampal Microcircuits using Slice Electrophysiology

Ceylan
Scarlett Steinecke; Andreas Weiß; Elke Edelmann; Peer Wulff
Systems Neuroscience, Physiologisches Institut, Christian

Objective: The CA1 region of the hippocampus (Hip) receives excitatory inputs from the entorhinal cortex, CA3, and the thalamic nucleus reuniens (nRE), a key relay station between the medial prefrontal cortex (mPFC) and the Hip. Although behavioral data indicate that afferents from nRE, which make synaptic contacts in CA1 and subiculum, they are important for the topdown control of memory processes, the cellular mechanisms underlying its influence on hippocampal circuits remain largely unclear. This project investigates which neuronal subtypes in the Hip are recruited by nRE afferents and how these inputs modulate CA1 and subicular activity.

Method: In acute hippocampal brain slices of mice, optogeneticallyassisted slice electrophysiology was performed to enable selective optical stimulation of nRE afferents. Wholecell patchclamp recordings were performed on CA1 and subicular pyramidal neurons and interneurons. Neurons were characterized both based on their electrophysiological firing properties and responses to optical stimulation, as well as through passive filling with biocytin and subsequent posthoc identification based on their morphology and precise anatomical localization within the Hip.

Results: Different neuronal cell types have been examined in CA1 and subiculum for their responsiveness to nRE input. Ongoing recordings aim to disentangle which interneuron populations are recruited by nRE afferents.

Conclusion: Preliminary experiments suggest that nRE afferents recruit distinct neuronal populations within CA1 and subiculum. Delineation of recruited cell types will provide mechanistic insights into nREmediated modulation of mnemonic representations in the Hip.

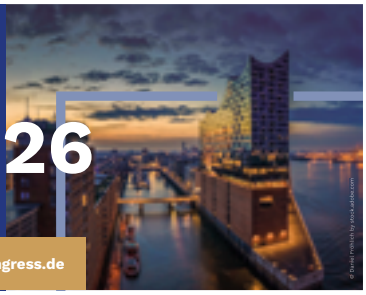

P19 Postergroup: Synaptic Signalling

P1904

Retroactive endogenous dopamine release gates timingdependent LTP at Schaffer collateral CA1 synapses of the mouse hippocampus

Babak Khodaie; Thomas Munsch; Elke Edelmann; Volkmar Leßmann
Institut für Physiologie, Medizinische Fakultät, Otto von Guericke Universität, Magdeburg, Germany;

Objective: Dopamine shapes reward and punishment induced learning in the mammalian brain and regulates LTP at Schaffer collateralCA1 synapses of the hippocampus that are involved in these learning processes. Spike timingdependent plasticity (STDP) paradigms at SCCA1 synapses are due to their short duration and action potential firing patterns considered as physiological stimulus for the induction of timingdependent LTP (tLTP) that might mimic memory relevant synaptic plasticity processes *in vivo*. Here, we investigated whether a 10 s long low repeat STDP paradigm can be gated by retroactive, endogenous dopamine release to develop tLTP at SCCA1 synapses.
Method: We prrepared acute mouse hippocampal slices from >2 months old animals and used whole cell patchclamp recordings in CA1 pyramidal cells to investigate STDP at Schaffer collateral inputs. We used 6 repeats (within 10 sec) of paired 1:1 or 1:4 pre- and postsynaptic action potential firing (Δt = +10 ms) to elicit timingdependent LTP (tLTP). Catecholaminergic modulation of tLTP (30 min after STDP stimulation) was characterized using bath applied D1 and D2 dopamine receptor antagonists and α- or βadrenergic inhibitors. To determine the critical time window of endogenously released dopamine at SCCA1 synapses required for successful induction of tLTP, we optogenetically inhibited dopamine release at different time points before (at 10 min), during (at 0 min), and after (at +10 min, or +20 min) stimulation with the STDP protocol.
Results: Using D1 and D2 receptor antagonists, our experiments revealed that canonical 6x 1:1 tLTP is strictly dependent on intact dopamine signaling at all SCCA1 synapses along the dorsoventral hippocampal axis, while postsynaptic burst firing during the 6x 1:4 protocol overcomes this requirement for DA signaling for tLTP in dorsal hippocampus. In contrast, endogenous noradrenaline release showed much weaker influence on tLTP. Our results obtained with optogenetic silencing of endogenous dopamine release revealed that the presence of DA is mandatory within a critical time window of 110 min after STDP induction to gate 6x 1:1 tLTP.
Conclusion: Our results show that low repeat tLTP is crucially regulated by endogenous dopamine release from catecholaminergic fibers in the CA1 region throughout the dorsoventral hippocampal axis. Overall, our data support the idea that reward- or punishmentrelated dopamine signaling can retroactively associate a specific experience with a temporally distant rewarding or punishing outcome.

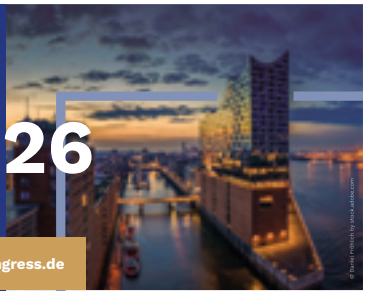

P19 Postergroup: Synaptic Signalling

P1905
Altered microgliaPVI interactions in DISC1 mutant mice

Luna Šošo Zdravkovic; Christian Madry; JonasFrederic Sauer [1]
Institut für Neurophysiologie, Charité - Universitätsmedizin Berlin, Berlin, Germany; [1] Systemic Neurophysiology, CIPMM, Universität des Saarlandes, Homburg, Germany;

Objective: Microglia, the resident immune cells of the brain, are involved in virtually all CNS disorders, with implications ranging from neuroprotection to neurodegeneration, depending on the activation state and the resulting impact on neuronal function. While their interactions with excitatory neurons are relatively wellexplored, there is only sparse knowledge on how microglia regulate GABAergic inhibition, for which parvalbumin positive interneurons (PVI) play a crucial role. PVIs are a key component in coordinating neuronal activity underlying memory formation, cognition and sensory information processing, but are also implicated in neuropsychiatric disorders. This study investigates microgliaPVI bidirectional interactions in the hippocampus of a *Disrupted inSchizophrenia 1* (DISC1) mouse model, characterized by impairment of PVIdependent network function reflected in aberrant gamma oscillatory network activity.
Method: Using electrophysiological and imaging techniques in vivo and in situ, microgliaPVI bidirectional interactions and network dynamics were investigated in the hippocampus of DISC1 mutant mice. Microglial morphology, lysosomal function, phagocytosis, and spatial proximity to PVI perisomatic regions were assessed. In addition, alterations in perineuronal nets (PNNs) and incorporation of PNN material in microglia were analyzed.
Results: Preliminary findings indicate alterations in microglial morphological and functional properties and their interactions with PVIs, associated with impaired network function in DISC1 mutant mice.
Conclusion: These findings unveil maladaptive microgliaPVI interactions associated with network dysfunction in DISC1 mice. Our study implicates microglial impairment in neuropsychiatric diseases, such as schizophrenia and major depression, which are genetically linked to DISC1.

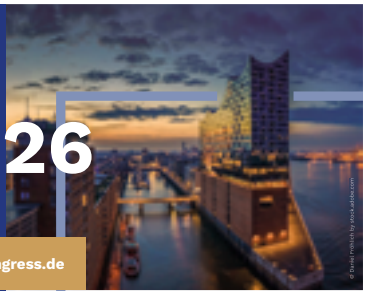

P19 Postergroup: Synaptic Signalling

P1906

Enhanced encoding of speech sounds at the first central auditory synapse

Christian Keine; Amarins N. Heeringa [1]; Tamara Radulovic; Ivan Milenkovic Department for Human Medicine, Carl von Ossietzky Universität Oldenburg, Oldenburg, Germany; [1] Department of Neuroscience, Carl von Ossietzky Universität Oldenburg, Oldenburg, Germany;

Objective: Understanding speech requires the brain to faithfully encode the rapid acoustic patterns of speech sounds, generated in the auditory nerve (AN), which carries all acoustic information from the ear to the brain. The AN represents vowels in two complementary ways: by how fastrateplace and temporal codes. Because the rateplace code saturates at higher sound levels, behavioral vowel discrimination depends increasingly on the temporal precision of AN spiking. Spherical bushy cells (SBCs) of the anteroventral cochlear nucleus receive large AN presynaptic terminals, i.e. endbulbs of Held and exhibit higher temporal precision compared to their AN input. However, whether this temporal enhancement improves the encoding of behaviorally relevant speech sounds and whether it does so through a temporal rather than a ratebased code remains unknown. We addressed this by using the SBC as a model in which the AN input (EPSPs) and the postsynaptic output (action potentials, APs) are recorded simultaneously, allowing a direct input–output comparison for vowels of different discrimination difficulty.
Method: We performed in vivo loosepatch recordings from SBCs in anaesthetized Mongolian gerbils during the presentation of three naturally spoken vowels chosen to span a range of perceptual discrimination difficulty established in prior behavioral studies. Recorded signals were decomposed into the AN input (all EPSPs) and the postsynaptic APs. For both input and output, we quantified temporal precision and assessed singlecell vowel discrimination using rate- and timing–based discrimination metrics.
Results: For every vowel tested, the temporal sparsity and precision of the SBC output were significantly greater than those of the AN input. Despite significant differences in firing rate between input and output, ratebased discrimination was generally poor and was not improved by the processing at the endbulb–SBC synapse. In contrast, timingbased discrimination was significantly enhanced at the SBC output relative to the AN input.
Conclusion: The improvement in timingbased vowel discrimination indicates a computational refinement of the temporal information that supports speechsound encoding, already evident at the first central synapse. Given that acoustically evoked inhibition increases temporal precision of the SBC output, the improved vowel discrimination we observe can likely be explained by the same inhibitory mechanism.

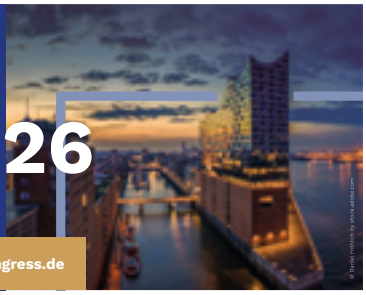

P19 Postergroup: Synaptic Signalling

P1907

Characterization of Inhibitory Interneurons in iPS Cellderived Ventral Forebrain Organoids

Zino Aufenacker; Tomas Fanutza; Christian Wozny
IMM Institute for Molecular Medicine, MSH Medical School Hamburg, Hamburg, Germany;

Objective: Cerebral organoids are threedimensional models derived from humaninduced pluripotent stem cells (hiPS cells). While human postmortem tissue and mouse models have traditionally been used to study neurodevelopmental and neuropathological processes, cerebral organoids now provide insights into regionspecific development and the formation of circuits relevant to neuropsychiatric diseases. They also give rise to personalised in vitro patient models. However, recent studies using cerebral organoids have mainly focused on excitatory neurons and modelling corticallike structures. In this study, we have characterised the morphology and function of emerging inhibitory interneurons in ventral forebrain organoids (VFO), which model the ventral forebrain including the ganglionic eminence.
Method: The growth of neuronal tissue is known to be tightly controlled by chromatin regulation. Here, we tested whether treatment with GSK343, an inhibitor of the histonelysine methyltransferase EZH2, would lead to a significant increase in inhibitory neurons in VFOs.
Results: We performed immunohistochemistry in combination with confocal microscopy and bioimaging analysis using FIJI to quantify neuronal marker protein expression, comparing GSK343- with DMSOtreated and untreated VFOs at several time points.
VFO slices were stained for cFos as an indicator of neuronal activity, and for parvalbumin (PV), calbindin (CB) and somatostatin (SST) to test for interneuronal diversity. Cleaved caspase3 was used to determine the degree of cell death. Furthermore, wholecell patchclamp electrophysiology was performed to evaluate the functional maturation of neurons in acute organoid slices.
Conclusion: Our model shows a great diversity of (inter)neurons replicating the wellknown distribution of different interneuron subtypes. It is therefore suitable for studying the role of dysfunctional interneurons in neurodevelopmental and neuropsychiatric disorders, such as autism spectrum disorder, epilepsy and Alzheimer's disease.

P19 Postergroup: Synaptic Signalling

P1908

Synaptic Connectivity of Layer 5 Pyramidal Neurons in the Mouse TeA Microcircuit

Emilia Thoma; Franz Xaver Mittermaier; Sabine Grosser [1]; Henrik Alle; Jörg Rolf Paul Geiger
Institut für Neurophysiologie, Charité - Universitätsmedizin Berlin, Berlin, Germany; [1] Institut für integrative Neuroanatomie, Charité - Universitätsmedizin Berlin, Berlin, Germany;

Objective: The mammalian neocortex is populated by distinct neuron types with different functions and contributions to signal integration. To try to understand circuit functions and computations in the neocortex, the underlying fundamental connectivity patterns with neuron subtype resolution must be investigated.
To this purpose, we investigate layer 5 pyramidal neurons in the mouse temporal association cortex (TeA). Layer 5 acts as the main output layer of the neocortex. Two distinct pyramidal neuron populations are the main constituents of layer 5, and are defined by their targets, with intratelencephalicprojecting neurons (L5IT) projecting to other areas of the telencephalon and extratelencephalicprojecting neurons (L5ET) projecting to subcerebral targets (Kalmbach et al., 2021).
Method: To study microcircuit connectivity of putative L5IT and putative L5ET neurons, we performed multineuron patchclamp recordings of up to eight simultaneously recorded neurons, selectively targeting pyramidal neurons expressing a fluorescence marker in acute brain slices from mouse TeA. To this end, we used a Sim1Cre driver mouse line to selectively label L5ET neurons. Sim1Cre mice were crossed with Ai9 mice, leading to endogenous expression of tdTomato in L5ET neurons. The selection of L5IT neurons was based on two criteria: the absence of tdTomato expression and the identification of their morphology. Post hoc, L5IT and L5ET neuron classification is further confirmed based on their morphological, electrophysiological and histochemical characteristics. To understand the underlying connectivity patterns and directionality questions, we are investigating microcircuit inter- and intratype connectivity of L5IT and L5ET neurons, specifically monosynaptic connections.
Results: The exploratory recordings were conducted on 89 neurons, of which 22 were identified as L5ET neurons. Overall we tested a total of 324 possible connections and found 25 monosynaptic connections. The overall connectivity of these neurons was found to be ~ 7.7% (25/324).
Conclusion: Our preliminary data suggest asymmetric connectivity between L5IT and L5ET cells in the TeA of mice, a pattern that has also been observed in other regions of the mouse neocortex. This feature has also been observed to be conserved in the human MTG (Mittermaier et al., *in preparation*).

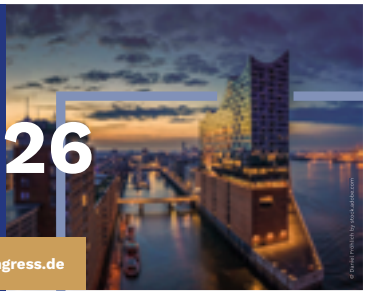

P19 Postergroup: Synaptic Signalling

P1909

Enhancing potassium channel function impairs synaptic activity of adultborn GABAergic interneurons in the mouse olfactory bulb

Yury Kovalchuk; Daria Dodon [1]; Myroslava Polozhentseva [1]; Natalie Kikot'ová; Volodymyr Shvadchak [1]; Olga Garaschuk
Department of Neurophysiology, Institute of Physiology, University of Tübingen, Tübingen, Germany; [1] Biochemistry and Biotechnology, Vasyl Stefanyk Precarpathian National University, IvanoFrankivsk, Ukraine;

Objective: Gainoffunction mutations of K^+ channels are implicated in neurodevelopmental disorders, neural network hyperexcitability, and severe drugresistant epilepsy, but the underlying mechanisms remain unclear. Here, using the mouse olfactory bulb (OB) as a model system, we analyzed how increased activity of voltagegated Kv1.2 channels impacts functional properties of inhibitory adultborn OB granule cells (GCs).
Method: Neural stem cells stemming from the subventricular zone of the lateral ventricles were virally modified in the rostral migratory stream en route to the OB to overexpress Kv1.2 channels together with the ratiometric Ca^{2+} indicator Twitch2B. Prior analyses of the transcriptome (bulk RNAseq) and morphology of the resulting Kv1.2overexpressing GS revealed a profound downregulation of genetic pathways encoding proteins involved in CNS development, neurogenesis, neuronal migration, and dendritic/axonal morphogenesis. Moreover, in the same cells, we have observed significant downregulation of pathways related to synapse assembly, including pre, trans, and postsynaptic elements (e.g., synaptic vesicle exo- and endocytosis; regulation of transsynaptic signaling; glutamate- and GABAergic synaptic transmission, etc.).
Results: By measuring spontaneous EPSCs and IPSCs from adultborn GCs in acute OB slices, we examined the RNAseq prediction of impaired synaptic integration of GCs with enhanced Kv1.2 channel function. The wholecell patchclamped GCs were filled with Alexa Fluor 594 dye, and their dendritic morphology was assessed using twophoton imaging. Subsequently, the EPSC/IPSC amplitudes and interevent interval distributions were compared between control and Kv1.2overexpressing groups. We found that Kv1.2overexpressing cells exhibited smaller amplitudes and lower event frequencies for both inhibitory and excitatory synaptic currents. However, the most profound effect, an almost 3fold increase in the respective EC50 value, was observed for the cumulative probability function, which describes the IPSC interevent interval distribution.
Conclusion: Taken together, the results of electrical recordings align well with the RNAseq data, revealing a key role of Kv1.2 channels in the development and synaptic integration of GABAergic neurons, and highlighting an unexpected mechanistic explanation for how Kv1.2 channel mutations might cause Developmental and Epileptic Encephalopathy.

P19 Postergroup: Synaptic Signalling

P1910
Positional fusion and synaptic shortterm facilitation at cerebellar parallel fibers

Robert Jacobi; Martin Pauli; Maximilian Zettner; AnnaLeena Sirén; Christian Stigloher [1]; Hartmut Schmidt [2]; Shigeki Watanabe [3]; Manfred Heckmann; Kristina Lippmann [2] Neurophysiology, Institute of Physiology, University of Würzburg, Würzburg, Germany; [1] Biocenter, University of Würzburg, Würzburg, Germany; [2] Carl Ludwig Institute for Physiology, University of Leipzig, Leipzig, Germany; [3] Solomon H. Snyder Department of Neuroscience, Johns Hopkins University, Baltimore, United States;

Objective: Learning and memory depend on brain circuits that translate transient activity patterns into rapid changes in synaptic strength. The cerebellar cortex enables motor learning with millisecond precision and relies on plasticity, particularly shortterm facilitation (STF) at Parallel FiberPurkinje cell (PF) synapses.
Method: We used electrical field stimulation followed by highpressure freezing and electron tomography of acute murine cerebellar slices to identify ultrastructural correlates of STF, capturing activitydependent presynaptic states with millisecond temporal and nanometer spatial resolution in nearnative circuits.
Results: During STF, presynaptic Active Zones (AZs) revealed rapid replenishment of membraneproximal synaptic vesicles (SVs). Widening of the electrondense material (EDM) underneath SVs containing the fusion machinery appears to be a dominant structural correlate of increased synaptic strength. A novel topographical mechanism of STF involves Munc133dependent priming and initial release at the AZ edge, followed by a positional shift of release toward the AZ center. Synaptotagmin 7 supports STF by enabling rapid replenishment and EDM extension at the AZ center.
Conclusion: We conclude that STF at PF AZs is encoded by coordinated increases in release probability, vesicle replenishment, and positional fusion, principles likely to be particularly relevant at larger human synapses.

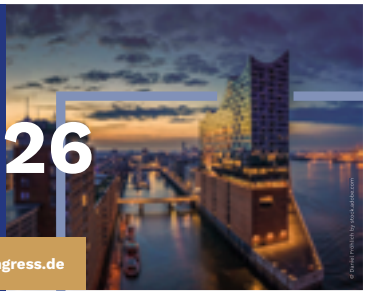

P19 Postergroup: Synaptic Signalling

P1911

Lactate as an alternative metabolic substrate modulates neuronal excitability, synaptic transmission, and sharp waveripple activity in mature cortical networks

Babak Khodaie; Martin Both [1]; Alexei V. Egorov; Oliver Kann
Institute of Physiology and Pathophysiology, Heidelberg University, Heidelberg, Germany; [1] Department of Neuro- and Sensory Physiology, Institute of Physiology and Pathophysiology, Heidelberg University, Heidelberg, Germany;

Objective: Lactate (Llactate) originating from the blood circulation and/or astrocytes, has been hypothesized to represent a major energy source for neurons during brain activation. However, the efficiency of lactate in fueling fast neuronal network oscillations such as gamma oscillations (~40 Hz) and sharp wave–ripples (SPWRs, with ripples at ~250 Hz), which underlie complex cortex functions such as perception and memory formation is less clear.
Method: Here, we studied the effects of glucose (10 mM) versus lactate (20 mM) as fuel on neuronal membrane excitability, synaptic transmission and SPWRs using electrophysiology in acute hippocampal slices from 4–6 week old mice. Animals were anesthetized with inhalation anesthetics (1.5% vol/vol isoflurane in a gas mixture of 70% nitrous oxide and 30 % O_2) prior to slice preparation. Spontaneous SPWRs were assessed by local field potential (LFP) recordings in hippocampal CA3 and CA1 regions. Synaptic transmission was assessed by Schaffer collateral (SC) stimulation to evoke field postsynaptic potentials (fPSPs) in stratum radiatum and stratum pyramidale in CA1. Intracellular recordings with sharp microelectrodes were performed to assess intrinsic membrane properties, including excitatory and inhibitory synaptic conductance in individual pyramidal cells. In addition, we tested lactate supplementation (6 mM) in lowglucose condition (2 mM).
Results: We find that (1) lactate attenuates both generation and propagation of SPWRs. (2) Lactate attenuates synaptic transmission at SCCA1 synapses. (3) Lactate alters intrinsic membrane properties and moderately increases action potential firing rate. (4) Lactate attenuates excitatory and inhibitory synaptic conductances, while the overall excitationinhibition balance is unaffected. (5) Lactate supplementation partially recovers SPWRs during glucose shortage.
Conclusion: Together, these findings indicate that lactate fuel affects synaptic transmission more severely than action potential firing in cortical network neurons. During glucose shortage, however, lactate can serve as a supplementary energy source.

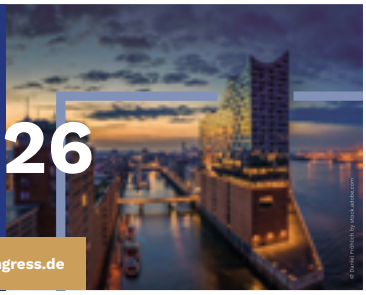

P19 Postergroup: Synaptic Signalling

P1912
Adolescent Stress: Persistent Synaptic & Mitochondrial Dysfunction - “Can Enriched Environment Prevent LongTerm Deficits?”

Nadja Treiber; Luisa Theißen; Franziska Ebert; Fang Zheng; Christian Alzheimer Institute of Physiology and Pathophysiology, FriedrichAlexander Universität ErlangenNürnberg, Erlangen, Germany;

Objective: Adolescent stress (AS) represents a critical risk factor for longlasting disruptions in hippocampal function that predispose to neuropsychiatric disorders even later in adulthood. By contrast, an Enriched Environment (EE) promotes resilience by enhancing cognition, supporting synaptic plasticity, and reducing depressivelike states. Activin A, a neuroactive cytokine of the TGFβ family, has emerged as a key mediator of these beneficial effects, highlighting its potential as a therapeutic target. Thus, this study investigates how AS induces persistent hippocampal dysfunction and whether poststress EE can reverse these alterations, with a particular focus on activin signaling.
Method: Using an oral corticosteronebased model of AS in mice (PND 3045), we applied a multidisciplinary approach combining *ex vivo* hippocampal electrophysiology and molecular profiling to assess synaptic plasticity and mitochondrial function in adulthood (PND 90120). Experiments were performed in both wildtype mice and transgenic mice with forebrainspecific disruption of activin receptor signaling to assess the contribution of activindependent mechanisms. Following AS or control treatment, animals were exposed to EE for three weeks (PND 4667), with weekly changing stimuli.
Results: AS induced persistent impairments in short- and longterm synaptic plasticity within the dentate gyrus. These deficits were aggravated in dnActRIB mice, which additionally displayed a pathological shift in excitatory–inhibitory balance, indicating that activin signaling constrains neuronal dysfunction after stress exposure. Mitochondrial alterations persisted into adulthood and were characterized by elevated spare respiratory capacity, suggesting altered metabolic compensation. Interestingly, EE restored ASassociated changes in shortterm plasticity selectively, suggesting that EE predominantly modulates presynaptic mechanisms rather than postsynaptic plasticity processes, and partially normalized mitochondrial function in an activindependent manner.
Conclusion: In conclusion, our findings identify adolescence as a critical window during which stress produces enduring hippocampal dysfunction. Importantly, EE promotes functional recovery from stressrelated neuronal and metabolic impairments, at least in part through activin. EE may therefore represent a promising strategy to enhance resilience and mitigate longterm stressrelated brain pathology.

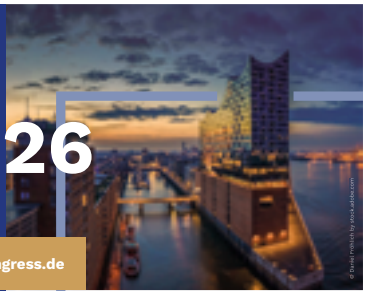

P19 Postergroup: Synaptic Signalling

P1913

Mechanisms of theta burst firing induced low repeat spike timingdependent plasticity (STDP) at hippocampal inputs to the mPFC of adult mice

Maxime Picard; Thomas Munsch; Susanne Meis; Christian Sattler; Thomas Endres; Volkmar Leßmann
Institut für Physiologie, Medizinische Fakultät, OttovonGuerickeUniversität, Magdeburg, Germany;

Objective: Fear extinction is a complex behavioural mechanism to reshape consolidated fear memories, involving neuronal circuits of hippocampus, mPFC, and amygdala. BDNF is a key regulator of fear extinction and neuronal plasticity alongside the hippocampusmPFC axis. However, whether BDNFdependent STDP in mPFC contributes to fear extinction is unknown.
Method: Here, we used patchclamprecordings in layer V neurons to record STDP at excitatory inputs in acute mPFC slices from adult mice. We established a new protocol that elicited timingdependent LTP (tLTP) with the least possible number of repeated pairings (Δt= +12 18 ms) of 1 presynaptic spike with a thetaburst of 4 postsynaptic spikes (1:4 pairing). We found that 12 repeats (at 0,1 Hz) of this protocol were sufficient to elicit tLTP in ILmPFC pyramidal cells under conditions of intact $GABA_A$ and $GABA_B$ receptor mediated inhibition. We used different pharmacological interventions to characterise the mechanisms of induction and expression of this 12x 1:4 tLTP protocol.
Results: Thirty min after stimulation with the 12x 1:4 STDP protocol, EPSP slope was increased to 154.4 +/- 15.2% and EPSP amplitude to 129.4 +/- 9.8% compared to negative control. Bath application of the NMDA receptor inhibitor APV (50 µM) did not block 12x 1.4 tLTP. In contrast, inhibition of Ltype voltage gated Ca^{2+}- channels with nifedipine (25 µM) blocked 12x 1:4 tLTP. Interestingly, bath application of the tyrosine kinase inhibitor k252a (100 nM) interfered with expression of 12x 1:4 tLTP.
Conclusion: Our preliminary results suggest induction of theta burst firingdependet tLTP via activation of Ltype voltage gated Ca2+ channels and an expression mechanism that involves BDNFdependent activation of TrkB receptors at hippocampal input synapses to layer V pyramidal cells in the IlmPFC. Further experiments involving TrkBreceptorbodies (TrkBFc) that can scavenge endogenously released BDNF are required to prove a role of BDNF/TrkB signalling at these HIPmPFC synapses. Moreover, we will investigate whether this possibly BDNFdependent 12x 1:4 tLTP is specific for hippocampal inputs or can be observed also at intracortical excitatory inputs within the ILmPFC. These experiments should reveal the role of endogenous BDNF secretion in physiological relevant low repeat tLTP in the ILmPFC.

Supported by DFG CRC1436 (TP A06), DFG LE 1020/71 and by the BMBF [German Center for Mental Health (DZPG; 01EE2305A)].

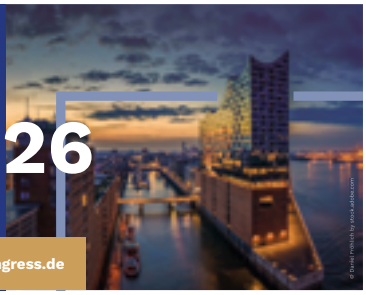

P19 Postergroup: Synaptic Signalling

P1914

Effects of selective inner or outer hair cell loss on auditory brainstem responses and cochlear amplification in conditional knockout mouse models

Matteo Spinelli; Dan Wang; Olga Gohr; Maike Claußen [1]; Christian Keine; Ivan Milenkovic
Department for Human Medicine, Carl von Ossietzky Universität Oldenburg, Oldenburg, Germany; [1] Department of Neuroscience, Carl von Ossietzky Universität Oldenburg, Oldenburg, Germany;

Objective: Progressive cochlear hair cell degeneration is a major cause of sensorineural hearing impairment, yet the quantitative relationship between hair cell loss and functional auditory deficits remains incompletely understood. Existing models rely on noise exposure, ototoxic drugs, or aging, which produce variable, often overlapping damage patterns across cell types. To overcome this limitations, we used tamoxifeninducible conditional mouse models expressing diphtheria toxin A to selectively ablate inner hair cells (IHC) or outer hair cells (OHC), and tracked auditory function longitudinally during progressive, celltypespecific hair cell loss.
Method: Conditional hair cell ablation was induced at postnatal days P14–15 via tamoxifen-dependent activation of diphtheria toxin A in vGluT3iCreER (IHCspecific) and Prestin-CreERT2 (OHCspecific) mouse lines. Auditory brainstem responses (ABR) and distortion product otoacoustic emissions (DPOAE) were recorded in mice of both sexes at P18–21, P25–30 and P60–72. Following functional assessments, hair cell loss was quantified in each animal by immunohistochemistry and confocal microscopy, enabling direct correlation of cellular degeneration with functional deficits.
Results: OHC ablation progressed from ~30% loss at P18–21 to ~70% at later stages. This was accompanied by reduced DPOAE amplitudes, with decreases of ~20 dB at early stages and up to ~40 dB at later time points, predominantly at midtohigh frequencies. ABR thresholds increased progressively, reaching shifts of ~40 dB in OHCablated mice at P60–72. In contrast, IHC loss progressed more gradually (~20% at P18–21, ~30% at P25–30, and ~40% at P60–72) and produced milder ABR threshold elevations, reaching ~20 dB at the latest stage. Consistent with the specificity cochlear amplification to OHC function, DPOAE amplitudes remained comparable to control levels following selective IHC ablation.
Conclusion: Using celltypespecific conditional ablation, we demonstrate that DPOAE measurements sensitively detect earlystage OHC degeneration, whereas selective IHC loss produces measurable ABR threshold elevations while preserving otoacoustic emissions. The differential functional signatures of OHC versus IHC loss obtained through controlled degeneration models may refine the interpretation of progressive cochlear pathology and inform the development of diagnostic strategies for distinguishing underlying mechanisms of hearing loss.

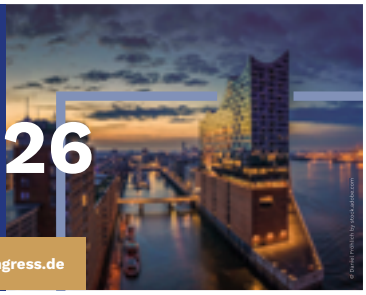

P19 Postergroup: Synaptic Signalling

P1915
Intersite synchrony of ripple oscillations as a central GABAergic function

Michael Hadler; Emily Aery Jones [1]; Henrik Alle; Jörg Rolf Paul Geiger Institut für Neurophysiologie, Charité - Universitätsmedizin Berlin, Berlin, Germany; [1] University of Maryland, Maryland, United States;

Objective: Neuronal oscillations are considered a noninvasive biomarker of intact brain network function and cognitive processes, founded in a delicate balance of neuronal excitation and inhibition. Particularly fast “ripple” oscillations (150 – 300 Hertz) are associated with memory consolidation and retrieval during states of rest, during which they synchronize large portions of the hippocampal network, yet little is known of the spatiotemporal components of this phenomenon.
Method: We reanalyze previously published in vivo multisite local field potential recordings in mouse hippocampus, including animal models of neurodegeneration, and compare this data to multielectrode array (MEA) recordings in an ex vivo model of ripple oscillations, allowing the highthroughput application of pharmacology and optogenetics.
Results: Ripple oscillations recorded in vivo in awake, resting mice display a profound heterogeneity in the extent of intrahippocampal synchrony. This “intersite synchrony” is paradoxically saturated in a mouse model of Alzheimer’s disease, which correlates with the reduced occurrence of ripple oscillations in these animals and not with changes in ripple power or duration. We recapitulate this heterogeneity in MEA recordings hippocampal brain slices and find that the extent of ripple intersite synchrony is primarily determined by GABAergic output and defacto independent of glutamatergic transmission. Surprisingly, ex vivo ripple synchrony is inversely correlated to the cellular excitability of fastspiking, parvalbuminpositive interneurons (PVIs), suggesting a link between GABAergic tone, the control of PVI activation, and the network’s capability to generate highly synchronized activity at rest.
Conclusion: In summary, our results show that hippocampal ripple oscillations exhibit pronounced variability in their spatiotemporal properties (intersite synchrony), which is altered in a mouse model of Alzheimer’s disease. We identify GABAergic signaling, rather than glutamatergic transmission, as the primary regulator of ripple synchrony, with parvalbuminpositive interneuron excitability playing a key modulatory role. These findings provide new insight into the mechanisms underlying hippocampal network coordination and suggest ripple synchrony as a potential biomarker of network dysfunction in neurodegeneration.

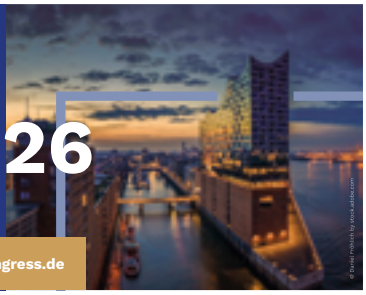

P19 Postergroup: Synaptic Signalling

P1916

Catecholaminergic Modulation of PrefrontalLateral Hypothalamic Circuit During Stress and Anxiety

Alisa Bakhareva; Zhasmina Ergasheva; Anne Petzold [1]; Tatiana Korotkova
Institute for Systems Physiology, University Of Cologne, Köln, Germany; [1] European Neuroscience Institute, A Joint Initiative of the University Medical Center Göttingen and the Max Plank Institute for Multidisciplinary Sciences, Göttingen, Germany;

Objective: Stress and anxiety help animals adapt to challenging environments, but when dysregulated, they contribute to numerous psychiatric disorders. The medial prefrontal cortex (mPFC) is involved in regulating stress and anxiety and exerts topdown control over subcortical regions, including the lateral hypothalamus (LH). Both norepinephrine and dopamine dynamics respond to stress and modulate neuronal activity in mPFC and LH. Yet it remains unclear how prefrontal–hypothalamic circuit mediates stress- and anxietyrelated adaptations, and how catecholamines shape this interaction.
Method: To dissect the role of vmPFCLH projections, we performed calcium imaging of vmPFCLH projections during innate stress- and anxietyrelated behaviours of mice. We then employed dualsite, dualcolor fibre photometry of GRAB sensors to simultaneously monitor norepinephrine and dopamine activity in vmPFC and LH. Furthermore, we combined TRAP labelling, retrograde tracing and *in situ* hybridisation to characterize the molecular identity of stressresponsive LHprojecting neurons in vmPFC.
Results: Our data revealed that vmPFCLH projections are functionally engaged during stress- and anxietyrelated responses, preferentially signalling behaviours relevant to the current challenge. Stressresponsive LHprojecting vmPFC neurons expressed receptors for both norepinephrine and dopamine, positioning them to integrate neuromodulatory signals during stress. Dualsite photometry revealed that norepinephrine dynamics were coordinated across vmPFC and LH, tracking anxiety, stressinduced anxiety, and anxietyrelieving behaviours. Dopamine signals also responded to stress and anxiety but displayed greater regional specialization.
Conclusion: Together, these findings identify the vmPFC–LH pathway as a catecholaminesensitive circuit that supports adaptive behavioural responses to stress and anxiety.

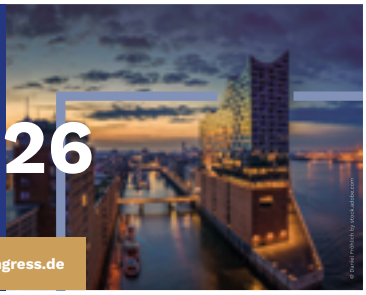

P20 Postergroup: Knowledge - Methods and teaching in Physiology

P2001
Physiology for the Next Generation

Stefan Galler
Biosciences and Medical Biology, University of Salzburg, Salzburg, Austria;

Objective: Physiology education and the further development of the discipline would benefit substantially if incoming university students already possessed relevant foundational knowledge. A solid preparation focused on functional relationships would provide an ideal basis for maintaining the necessary disciplinary orientation throughout the course of study, despite increasing specialization.
Method: This goal could be achieved through online courses for suitable uppersecondary students across Germanspeaking countries, taught by didactically experienced experts. Teaching should emphasize fundamental principles, avoid unnecessary complexity, and allow flexible participation without major entry barriers. Interactivity can be achieved by using a webbased response system that supports several hundred participants. It would be desirable for the German Physiological Society to assume patronage and establish a committee to develop a coordinated program, recruit suitable instructors, and raise awareness of the program in schools.
Results: Over several decades, the author has systematically prepared physiological teaching content and developed concepts specifically tailored to beginners. The entire course is designed as a continuously interactive format and uses a webbased realtime voting system. Initial experiences with uppersecondary students in the Austrian initiative “Schüler:innen an die Hochschulen” were highly encouraging. The author would like to encourage colleagues to participate in the program and help increase its visibility.
Conclusion: A broadly accessible interactive online program in physiology for suitable uppersecondary students is technically feasible. Suitable instructors who could collaborate within a coordinated program are available. The greatest challenge is to raise awareness of the program among potential participants. With longterm development, it appears realistic to foster a new generation of students who possess sound knowledge and disciplinary perspective and may thereby contribute to the sustainable further development of the field.

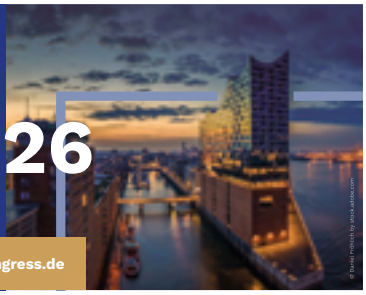

P20 Postergroup: Knowledge - Methods and teaching in Physiology

P2002

Impact of choice on life science student performance across varied laboratory practical assessments

Bernard Drumm; Caoimhin Griffin
Life & Health Science, Dundalk Institute of Technology, Dundalk, Ireland;

Objective: There is increasing awareness from universal design for learning (UDL) and teaching for understanding (TfU) frameworks that undergraduate assessments require a diverse array of methodologies to allow students to express learning and demonstrate performances of understanding. Despite the myriad of benefits that practical classes can impart, student performances is often evaluated from overreliance on traditional written reports, which evaluate a narrow range of student competencies. In Dundalk Institute of Technology (DkIT), we recently modified the assessment strategy of a 'Biotechnology' module within a third year BSc (Hons) programme in Biopharmaceutical Science to include 3 different modes (Moodle Quiz, Group Presentation and Written Report).
Method: Over 3 academic years, we found there was no statistical difference in student scores between the Moodle Quiz, Group Presentation and Written Report, and this was consistent each year (2020, n=24 students; 2021, n=13 students; 2022, n=29 students). However, when survey and focus group data was analyzed from these cohorts, it emerged that each assessment allowed students to practice different skill sets and express learning and understanding differently, with some assessments more suited to practicing (and presumably evaluating) specific skills over others.
Results: We designed an additional study in the same 3rd year Biotechnology module over 2 academic years (2023 - 2024), where students performed varied assessments as before (Moodle Quiz, Group Presentation and Written Report), and introduced a 4th assessment where students had a choice of which of modality they would engage with. We analysed student scores (n=72 students), and found that when asked to choose their final assessment 72.6% chose Moodle Quiz, 16.4% chose Written Report and only 11% chose Presentation. 58% of students chose the assessment in which they previously scored highest. However, almost the same proportion did not, and 29.3% of students even chose the assessment they had previously scored lowest. Interestingly, when scores in chosen assessment modality were tracked to scores with the same modality on first attempt, there was no statistical difference ($P>0.05$, n=72).
Conclusion: These data suggest providing students with a choice in assessment modality for practical classes does not result in increased scores. We conclude students select assessment modalities based on factors beyond prior grades.

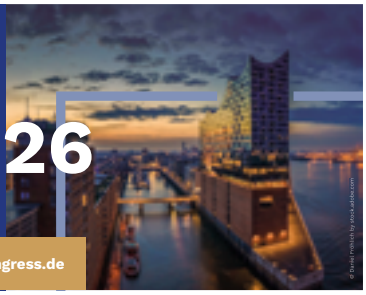

P20 Postergroup: Knowledge - Methods and teaching in Physiology

P2003

Study of Kidney Function in cohorts of Medical Students to teach Renal Physiology with large population data

Uta Binzen; Alexander Dieter [1]; Stefanie Nittka [2]; J. Simon Wiegert [3]; Wolfgang Greffrath [4]
Kardiovaskuläre Physiologie, Medizinische Fakultät Mannheim, Universität Heidelberg, Mannheim, Germany; [1] Universitätsmedizin Mannheim, Mannheim, Germany; [2] Institute for Clinical Chemistry, Medical Faculty Mannheim, Heidelberg University, Mannheim, Germany; [3] Neurophysiology, Medical Faculty Mannheim, Heidelberg University, Mannheim, Germany; [4] Mannheimer Zentrum für Translationale Neurowissenschaft, Neurophysiologie, Universitaetsmedizin Mannheim, Universität Heidelberg, Mannheim, Germany;

Objective: Assessing renal function is a core component of teaching renal physiology. Typically, student laboratory exercises involve measuring various renal parameters during antidiuresis and upon induced diuresis. However, precisely determining urine and plasma concentrations of various solutes in a student setting is laborious, timeconsuming, and errorprone. We address this challenge by analyzing a large set of parameters in a certified diagnostic laboratory and using population statistics to assess various functional parameters commonly used to infer kidney function.
Method: Students arrived in antidiuresis. Diuresis was then induced either by rapid water consumption (1.5 L) or by oral administration of furosemide (20–40 mg). Other students brought 24hour collected urine and provided an additional sample of spontaneous urine. The samples of each condition were chemically analyzed using automated laboratory analyzers. The urine output over time, glomerular filtration rates (GFR) and estimated eGFR were calculated. Clearance values were determined for creatinine, electrolytes, glucose, urea, and socalled ‘free water clearance’, as well as urine and plasma osmolarities during saluresis or water diuresis.
Results: Systematically collecting and analyzing urine and blood samples involving a professional clinical analysis institute helps to generate a large, highquality dataset providing detailed and individualized insights into kidney function and its immediate changes in the context of diuresis. This procedure offers the opportunity to involve students in the analysis and interpretation of large population data and to yield highquality results at the same time. By communicating laboratoryspecific preanalytical requirements, students also gain an understanding of the biochemical properties of urine. Obtained results were subsequently discussed in a seminar, which should improve overall understanding of the topic and satisfaction of the students. In addition, our study and the derived results can serve as an instructive template for theoretical instruction of preclinical medical students.
Conclusion: Analyzing urine and plasma samples from the renal function laboratory course in a clinical chemistry laboratory is feasible and didactic promising. In addition to providing detailed and individualized insights into kidney function and its immediate changes in diuresis, this procedure offers the opportunity to work with students to analyze larger datasets.

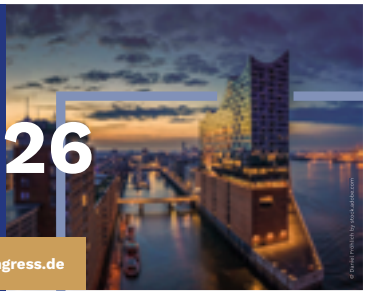

P20 Postergroup: Knowledge - Methods and teaching in Physiology

P2004

Standardised model samples in the physiology lab course: A didactic concept for determining glomerular filtration rate and potassium clearance

David Manneck; Friederike Stumpff
Physiology, Institute for Molecular Medicine, Health and Medical University Potsdam, Potsdam, Germany;

Objective: Teaching renal (patho)physiology presents a particular didactic challenge, as understanding the link between filtration, secretion and reabsorption processes and the measurementbased clearance concept places high demands on conceptual understanding. Traditional practical approaches using students own samples are limited by interindividual variability, restricted reproducibility and a lack of pathological references.
Method: We present a practical concept for renal physiology in which students, working in small groups of 3–4 students, determine the glomerular filtration rate (GFR) via creatinine clearance (photometric Jaffé reaction) as well as the clearance and fractional excretion of potassium (ionselective electrode). Specially prepared model solutions are used, the composition of which mimics the urine and plasma of a healthy or a person with impaired kidney function. The task of the students is to correctly classify the samples, provide a pathophysiological explanation for their decision, and compare the results between the practical groups. In addition to performing the measurements, students are required to interpret renal function parameters in a clinically oriented context.
Results: The use of defined model samples offers several educational advantages: **(i) Reproducibility**: target results remain consistent across cohorts and laboratory sessions, allowing reliable comparison between student groups; **(ii) Realtime error analysis**: deviations from expected values reveal pipetting, calculation or allocation errors (e.g. sample mixups) immediately during the experiment and can be addressed directly with the lecturers as part of the learning process; **(iii) Enhanced understanding of renal pathophysiology**: the specific construction of pathological sample profiles (e.g. reduced GFR or altered tubular potassium handling) enables focused discussion of glomerular and tubular dysfunction and supports differential diagnostic reasoning.
Conclusion: Standardised model samples combine experimental work, methodological reflection and an understanding of pathophysiology in a reproducible, easily scalable practical format. The concept promotes active learning and facilitates the integration of physiological principles with pathophysiological reasoning. Moreover, this approach can be applied to other physiology courses.

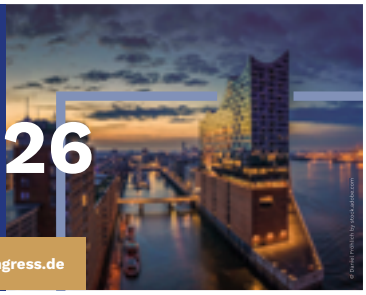

P21 Postergroup: Urine - Renal disease - inflammation

P2101

The murine ANO9 variant T595A causes renal defects and modulates immune responses in lymphocytes

Rainer Schreiber; Jiraporn Ousingsawat [1]; Karl Kunzelmann
Institut für Physiologie, Universität Regensburg, Regensburg, Germany; [1] Institut für Physiologie II, Universität Regensburg, Regensburg, Germany;

Objective: ANO9 is a phospholipid scramblase and probably also functions as a cation channel. Notably, an ANO9 variant (T604A in humans, T595A in mice) has been identified through metaanalysis of genomewide association studies as a strong promoter for chronic kidney disease (CKD).
Results: In murine kidneys, ANO9 is expressed in the apical membrane of proximal tubular epithelial cells. In ANO9 T595A knockin mice, tubular epithelial cells exhibit elevated expression of the T595A variant compared to cells from wildtype kidneys. Additionally, these mice show peritubular interstitial expansion and increased expression of TGFβ1 in tubular epithelial cells, suggesting renal inflammation. Furthermore, ANO9 T595A is expressed in murine CD3positive lymphocytes. When lymphocytes isolated from the lymph nodes of ANO9 T595A knockin and wildtype mice are cultured for 24 hours, activation with CD3/CD28 antibodies results in increased wholecell currents, enhanced Ca^{2+} signaling, and elevated IL2 release compared to wildtype lymphocytes. Experiments in Jurkat T lymphocytes indicate that ANO9 regulates RO2959sensitive storeoperated calcium entry (SOCE) via ORAI1 by activating plasma membrane Ca^{2+} ATPases (ATP2B1 and ATP2B4) through the PDZ domaincontaining protein discs large homolog 1 (DLG1).
Conclusion: These findings suggest that ANO9 modulates immune responses in both tubular epithelial cells and lymphocytes, with enhanced effects in cells expressing the ANO9 T595A variant. Further studies are needed to elucidate the mechanism underlying the activating effect of the ANO9 T595A variant on Ca^{2+} signaling, its role in immune regulation, and its contribution to chronic kidney disease.

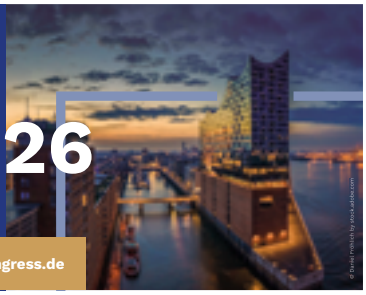

P21 Postergroup: Urine - Renal disease - inflammation

P2102

Phenotypic variability of urinederived stem cells and their antifibrotic effects in renal epithelial cells and UUO mice

Jasmine C. L. Atay; Anders Toftegaard Boysen; Rikke Nørregaard
Department of Clinical Medicine, Aarhus University Hospital, Aarhus, Denmark;

Objective: Chronic kidney disease (CKD) is characterized by persistent inflammation and fibrosis leading to progressive renal dysfunction. Urinederived stem cells (USCs) have shown therapeutic potential in kidney disease, but phenotypic heterogeneity may influence their functional properties. This study investigated whether distinct USC phenotypes differentially modulate renal inflammation and fibrosis.
Method: Distinct USC phenotypes derived from a single donor were classified as normal, swarmy, or tissuelike based on colony growth pattern. Surface marker expression (CD73, CD90, CD105, and CD146) was assessed by flow cytometry. Conditioned media (CM) from each phenotype was evaluated in HKC8 cells stimulated with tumor necrosis factor (TNF) α/interferon (IFN)γ or transforming growth factor (TGF)β (n=6 from two independent experiments). Based on the in vitro findings, the normal USC phenotype was selected for in vivo evaluation in a 7day unilateral ureteral obstruction (UUO) mouse model performed under inhaled sevoflurane anesthesia (n=78/group). USCs were delivered subcapsularly in a collagen matrix and renal inflammation, and fibrosis were evaluated by qPCR, western blotting, and immunohistochemistry.
Results: The tissuelike phenotype showed lower expression of all surface markers compared with normal and swarmy USCs, while normal and swarmy displayed similar marker profiles. CM from normal USCs showed the strongest antifibrotic effects, reducing expression of fibronectin (FN1), collagen type I alpha 1 (COL1a1) and alphasmooth muscle actin (αSMA). Swarming and mixed showed less pronounced effects. In UUO mice, treatment with normal USCs was associated with reduced FN protein levels by western blotting, although no clear differences were observed at the gene expression level or by αSMA or FN immunofluorescence staining. CD68positive cells were detected in areas of USC transplantation, indicating localized cellular infiltration.
Conclusion: These findings demonstrate USC phenotypedependent antifibrotic effects in vitro and suggest that the normal phenotype may retain some antifibrotic potential in vivo.

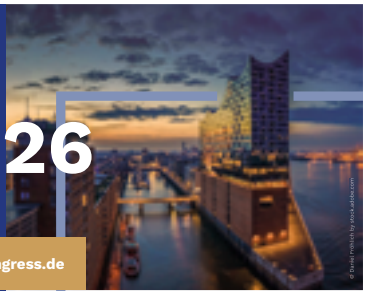

P21 Postergroup: Urine - Renal disease - inflammation

P2103

Chronic kidney injury by DOCAsalt in mice increases kidney collectin11

Marie Lykke Bach; Antonia Heinl; Camilla Enggaard; Mia Jensen; Sai Sindhu Thangaraj; Steffen Thiel; Per Svenningsen; Yaseelan Palarasah; Boye Lagerbon Jensen
Cardiovascular & Renal Research, Department of Molecular Medicin, University of Southern Denmark, Odense/DK; Inflammation, Molecular Medicine, University of Southern Denmark, Odense/DK; Biomedince, Aarhus Univeristy, Aarhus/DK;

Objective: Collectin kidney1 (CLK1) is kidneyproduced patternrecognition molecule that activates the lectin complement pathway and has been implicated in acute kidney injury. Whether CLK1 contributes to chronic proteinuric kidney injury remains unclear. We hypothesized that CLK1 is upregulated during chronic mineralocorticoidsaltinduced kidney injury and promotes complement activation, inflammation, and fibrosis.
Method: Male CLK1 wildtype (WT) and knockout (KO) mice were exposed to 21 days of DOCAsalt treatment following unilateral nephrectomy. Urine was collected longitudinally for assessment of albuminuria and KIM1. At termination, plasma and tissue were analyzed for CLK1, lectin pathway components, and markers of inflammation and fibrosis.
Results: DOCAsalt induced marked albuminuria, tubular injury, and hypertrophy of the remaining kidney in both genotypes. CLK1 mRNA and protein were strongly increased in WT kidneys and plasma but absent in KO mice. DOCAsalt elevated renal and urinary C3 and C3a, indicating intrarenal complement activation; tissue C3a generation was attenuated in KO mice. Plasma MBL and MASP3 increased in DOCAsalt mice, and CLK1 deficiency led to compensatory CLL1 upregulation. DOCAsalt increased inflammatory cytokines (TNF, IP10, MCP1, IL6) and fibrosis markers (Collagen I/III) in kidney tissue independently of genotype. IL6 levels in plasma and kidney were significantly reduced in CLK1 KO mice, despite similar degrees of albuminuria and structural injury.
Conclusion: Chronic DOCAsaltinduced kidney injury upregulates renal CLK1 and enhances complement activation, yet CLK1 is not required for the development of albuminuria, tubular injury, inflammation, or fibrosis. Our findings do not support a distinct pathogenic role for CLK1 in this form of kidney injury.

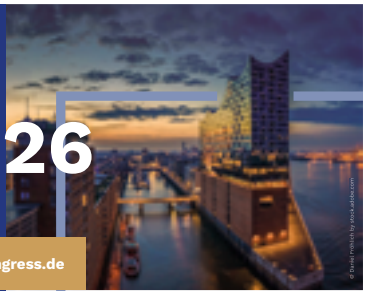

P21 Postergroup: Urine - Renal disease - inflammation

P2104

Urine composition in kidney transplant recipients and risk of developing urinary tract infections

Aimi D. K. Hamilton; Laura V. Sparsoe [1]; Lene U. P. Ludvigsen [2]; Bente Jespersen [2]; Helle A. Praetorius
Department of Biomedicine, Aarhus University, Aarhus, Denmark; [1] Department of Biomedicine, Aarhus University, Aarhus, Denmark; [2] Department of Renal Medicine, Aarhus University Hospital, Aarhus, Denmark;

Objective: The risk of urinary tract infection (UTI) is increased in kidney transplant recipients compared to the background population. Since bacterial survival in urine is dependent on urine composition, we investigated whether kidney transplant recipients have an altered urine composition compared to healthy age- and sexmatched controls and whether this affected bacterial survival and the subsequent risk of UTI.
Method: Kidney transplant recipients (n=50) delivered a urine sample on day 45 after transplantation and were followed for one year. Age- and sexmatched controls (n=50) delivered a urine sample on day of inclusion. Urine composition was assessed in part by measuring creatinine, osmolality, uromodulin and protein. In vitro growth of a uropathogenic *Escherichia coli* (UPEC) strain (RAR0001) was measured over 5h.
Results: Patient urine samples presented with a lower osmolality ($p<0.0001$), and lower concentrations of creatinine ($p=0.0001$) and uromodulin ($p<0.0001$), but higher concentrations of protein ($p=0.0204$) compared to controls. UPEC growth was significantly increased in urine from kidney transplant recipients compared to controls. This was particularly evident during the exponential growth phase, where the UPEC growth rate was nearly three times higher in recipient urine than in controls ($p<0.0001$). The UPEC growth rate was negatively correlated with urine osmolality ($r=0.2479$, $p=0.0143$) and uromodulin levels ($r=0.3747$, $p=0.0002$) but positively associated with protein levels ($r=0.5074$, $p<0.0001$). Furthermore, in a multivariate Cox regression analysis, low creatinine levels (HR=0.97 (0.940.99), $p=0.0063$) and high protein levels (HR=1.09 (1.011.17), $p=0.0266$) in urine immediately after transplantation, were identified as risk factors for development of UTI in the first year posttransplant. Additionally, female sex increased the risk of UTI (HR=5.25 (1.3321.73), $p=0.0186$), whereas recipient age had no influence (HR=1.01 (0.971.06), $p=0.5686$).
Conclusion: Kidney transplant recipients produced more dilute urine with a high protein content when compared to age- and sexmatched controls. This urine composition was associated with an accelerated bacterial growth and an increased risk of developing UTI one year posttransplant. Further studies are warranted to investigate whether this applies to other patient groups with increased risk of UTI.

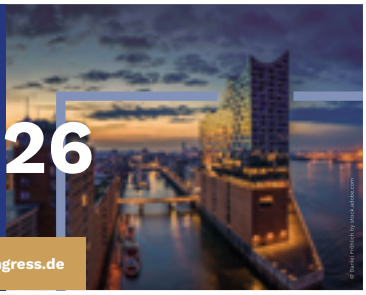

P21 Postergroup: Urine - Renal disease - inflammation

P2105

Targeting Alternative Pathway Complement Activation by C3b Inhibition in Experimental Proteinuric Kidney Disease

Christian Winding [#]; JeanClaude Kresse [#]; Michael Schou [*]; Fatih Demir; Sofie Dyreborg; Geraldine Mollet [1]; Nick Laursen [2]; Gregers Andersen [2]; Markus Rinschen; Henrik Bim [3 §]; Kathrin Weyer [§]
Department of Biomedicine, Aarhus University, Aarhus, Denmark; [1] Laboratory of Hereditary Kidney Diseases, Hôpital NeckerEnfants Malades, Paris DescartesSorbonne Paris Cité, Paris, France; [2] Molecular Biology and Genetics, Aarhus University, Aarhus, Denmark; [3] Department of Renal Medicine, Aarhus University, Aarhus, Denmark; [*] Presenting author; [#] Shared first authors, [§] Shared senior authors

Objective: Proteinuric kidney disease is characterized by aberrant glomerular filtration, tubular stress, inflammation, and progressive tubulointerstitial fibrosis. Activation of the alternative pathway (AP) of the complement system has been implicated in disease progression through amplification of local inflammatory responses. The nanobody EWEhC3Nb1 (EWE) binds complement factor C3b with high affinity and inhibits formation of the AP C3 convertase, representing a potential strategy to attenuate complementmediated kidney injury.
Method: Female podocin knockout mice with progressive proteinuric kidney disease were randomized to receive EWEhC3Nb1 (5 mg/mL) or PBS via subcutaneously implanted osmotic pumps under isoflurane anesthesia. Complement activation was assessed by mass spectrometrybased analysis of complement processing in plasma, urine, and kidney tissue. Kidney disease progression was evaluated by RTqPCR analysis of genes associated with immune activation, macrophage infiltration, tubular injury, and fibrosis.
Results: EWE administration achieved plasma and urinary concentrations sufficient to saturate C3b. Mass spectrometry analysis suggested reduced intrarenal complement activation and modulation of proteolytic processing associated with AP activation. Furthermore, EWE treatment was associated with reduced expression of markers related to inflammatory responses, macrophage infiltration, and fibrotic pathways, including reductions in NLRP3, MCP1, collagen 1a1, collagen 3a1, and fibronectin expression.
Conclusion: EWEmediated C3b inhibition was associated with reduced expression of genes linked to inflammatory and fibrotic pathways and provided evidence of complement inhibition in experimental proteinuric kidney disease. These findings support that complementtargeted therapy may exert renoprotective effects in proteinuric kidney disease.

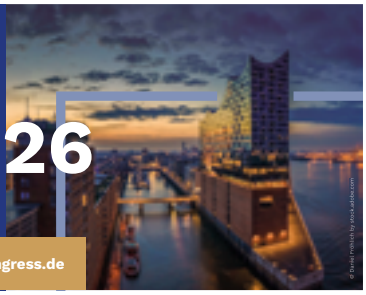

P21 Postergroup: Urine - Renal disease - inflammation

P2106
Role of ADCY10 in kidney fibrosis

Anupam Das; Antje Messer; Stephan Speier; Irakli Kopaliani; Claudia Goettsch Institut für Physiologie, Universitätsklinikum Carl Gustav Carus, Technische Universität Dresden, Dresden, Germany;

Objective: The early inflammatory phase of hypertensiondriven chronic kidney disease triggers the release of transforming growth factor beta 1 (TGFβ1), inducing kidney fibrosis via collagen deposition. Cyclic adenosine monophosphate (cAMP) is a regulator of fibrosis, which can either activate or inhibit profibrotic pathways. Soluble adenylyl cyclase (ADCY10) is a unique bicarbonate (HCO_3)/Ca2+activated enzyme that generates cAMP in distinct cellular microdomains, making it a potential target for understanding localized intracellular signalling pathways that affect fibrosis.
Method: Human kidney pericytes were stimulated with 10 ng/ml TGFβ1 for 48 hours. LRE1 (20 µM) was used as a pharmacological inhibitor of ADCY10. Hypertension was induced in ADCY10deficient mice ($ADCY10^{-/-}$) and wildtype littermates ($ADCY10^{+/+}$) by angiotensin II infusion (2mg/kg/day) for 14 days using osmotic minipumps.
Results: LRE1 reduced TGFβ1mediated induction of collagen1A1 (50%, p=0.0005) and fibronectin (50%, p=0.04) protein expression in cultured pericytes. Immunohistochemistry showed similar results. Activation of the cAMP effector protein Epac had no effect on the LRE1mediated reduction of collagen 1A1 and fibronectin. Activation of ADCY10 by HCO_3^- had no effect on collagen 1A1 expression. Additionally, LRE1 abolished the TGFβ1dependent inhibition of AMPK phosphorylation (pAMPK) (p=0.0013). In the model of ANGIIinduced hypertension, $ADCY10^{-/-}$ mice showed altered kidney fibrosis as assessed by Sirius red/Fast green, as well as collagen protein expression compared to WT littermates. Further, $ADCY10^{-/-}$ showed a 2fold increase in pAMPK (p=0.01).
Conclusion: This study shows a novel regulatory mechanism of kidney fibrosis in vitro involving ADCY10. The hypertension model supported the activation of an ADCY10mediated antifibrotic pathway via pAMPK.

P21 Postergroup: Urine - Renal disease - inflammation

P2107

Mapping Residues of GadoliniumBased Contrast Agents in the Rat Kidney

Luis Hummel; Janina Boyken [1]; Thomas Gladytz [2]; Axel Treu [3]; Ehsan Tasbihi [2]; Thoralf Niendorf [4]; Hubertus Pietsch [1]; Erdmann Seeliger
Institut für Vegetative Physiologie, Campus Charité Mitte, Charité - Universitätsmedizin Berlin, Berlin, Germany; [1] MR & CT Contrast Media Research, Bayer AG, Berlin, Germany; [2] Berlin Ultrahigh Field Facility (B.U.F.F.), MaxDelbrückCenter for Molecular Medicine in the Helmholtz Association (MDC), Berlin, Germany; [3] Bioanalytics, Bayer AG, Wuppertal, Germany; [4] ECRCKooperation von MDC und Charité, Experimental and Clinical Research Center, Berlin, Germany;

Objective: Gadoliniumbased contrast agents (GBCA) are routinely used to enhance magnetic resonance imaging (MRI). In recent years, GBCA residues were detected in multiple organs, with the kidney as primary organ of excretion being expectedly exposed to the highest GBCA concentrations. This study aimed to map the intricate spatial distribution of GBCA residues in rat kidneys at an early and a late time point.
Method: Rats received one of six marketed GBCA (three macrocyclic, three linear; cumulative dose 4.8 mmol Gd/kg) or saline and were sacrificed at day 5 or week 14 post administration (n=5 per GBCA and time point). In whole renal tissue slices, the distribution of elemental Gadolinium (Gd) was determined by laser ablation inductively coupled plasma mass spectrometry (LAICPMS) and assessed using a newly developed multilayered sub-segmentation. Matrixassisted laser desorption ionization mass spectrometry imaging (MALDIM-SI) was used to map intact GBCA chelates.
Results: At day 5, Gd was predominantly localized in the renal cortex across all GBCA, with 10- to 100fold lower medullary levels. Distribution patterns corresponded well with those of intact GBCA chelates. At week 14, Gd levels had decreased by one to two orders of magnitude, with the highest remaining Gd detected following the linear GBCA gadodiamide. Gd distribution patterns from linear GBCA showed Gd remaining predominantly in the cortex, while Gd from macrocyclic GBCA was highest in the medulla. Several GBCA exhibited a prominent ring of high Gd presence at the transition zone between outer and inner medulla, following a concentric ellipsoidal pattern similar to the renal capsule. At this late time point, intact chelates were only detectable following macrocyclic GBCA, with distribution patterns that matched those of elemental Gd.
Conclusion: GBCA residues in the kidney exhibited distinct distribution patterns, which changed during their elimination. While day 5 showed predominantly cortical presence, at week 14 the considerably lower levels of GBCA residues in cortex and medulla became more comparable. Macrocyclic GBCA showed more thorough elimination and continued to remain largely intact, likely due to the highly stable chelates. The observed retention patterns suggest that renal microanatomy as well as local physicochemical conditions play critical roles in GBCA retention, and provide a foundation for future investigations into retention mechanisms.

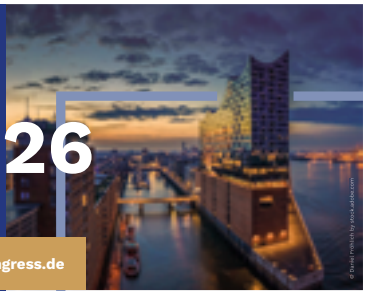

P21 Postergroup: Urine - Renal disease - inflammation

P2108

Functional transcriptomic analysis of the transcription factor WT1 in mice urogenital development

Florian Zantow; Holger Scholz; Karin Michaela Kirschner
Institut für Translatioinal Physiologie, Campus Charité Mitte, Charité - Universitätsmedizin Berlin, Berlin, Germany;

Objective: The Wilms tumour 1 (WT1) gene encodes a critical transcription factor involved in urogenital development. In murine models, a somatic WT1 knockout results in embryonic lethality, whereas human mutations are frequently linked to early childhood nephroblastomas. Given that the regulatory networks governed by WT1 during urogenital morphogenesis remain only partially elucidated, this research examines organspecific gene expression changes following a WT1 knockdown in XX/XY gonadal and renal primordia in mice.
Method: To investigate organspecific developmental influence of WT1, paired XX and XY gonadal primordia and the kidney primordia were isolated from wildtype E12.5 mice embryos and cultured individually in ex vivo hangingdrop organ cultures. A 48hour WT1 knockdown was induced using WT1specific vivo morpholinos, while contralateral organs served as controls treated with mismatch morpholinos. After confirming knockdown efficiency via immunoblotting, transcriptomic changes were mapped using mRNA sequencing on the Illumina HiSeq 2500 platform, and the raw FASTQ data were preprocessed and aligned.
Results: Initial bioinformatic analyses of the dataset were performed using OverRepresentation Analysis (ORA). Further analyses, including Gene Set Enrichment Analysis (GSEA) as well as pathway and network analyses, are planned to identify WT1dependent, organspecific signaling pathways in XX and XY gonads during embryonic development and to uncover potential sexindependent regulatory mechanisms.
Conclusion: The findings of this study are expected to expand the current understanding of WT1mediated regulation of organ development and may provide a foundation for future diagnostic and therapeutic approaches targeting WT1associated malignancies.

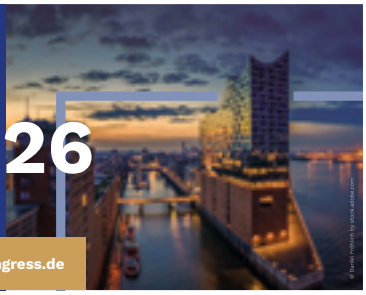

P21 Postergroup: Urine - Renal disease - inflammation

P2109

Utilising urinederived stem cells as a therapeutic platform for kidney disease

Anders Toftegaard Boysen; Natasja Patricia Simonsen; Rikke Nørregaard [1] Department of clinical medicine, Institute of Health, Skejby University Hospital, Skejby, Denmark; [1] Department of Clinical Medicine, Aarhus University, Aarhus, Denmark;

Objective: Chronic kidney disease (CKD) is characterised by persistent inflammation and fibrosis, leading to progressive renal dysfunction. Mesenchymal stem cells (MSCs) have been shown to hold great potential in ameliorating multiple pathological conditions, including CKD, yet sampling can be invasive, and the tissue source reflects their differentiation potentials. Urinederived stem cells (USCs) have recently gained attention as they can be isolated from urine and may originate from the kidneys. This study investigated the therapeutic potential of genetically engineered USCs expressing the antiinflammatory cytokine interleukin10 (IL10).
Method: Human USCs were isolated and characterised by flow cytometry. As a proofofconcept, USCs were engineered to express IL10 to increase potency and minimise donortodonor variance. IL10 secretion was validated using ELISA. The antifibrotic effects were evaluated in human proximal tubule cells and human precisioncut kidney slides (hPCKS). Key fibrotic markers were investigated using qPCR and WB. Regenerative potential was evaluated in human renal fibroblasts using a scratch assay. In all the assays, IL10engineered USCs were compared to nonengineered native USCs.
Results: Isolated USCs were positive for canonical MSC markers while lacking negative lineage markers. IL10engineered USCs demonstrated stable IL10 production and showed enhanced antifibrotic effects in both proximal tubule cells and hPCKS when compared to native USCs. Similarly, IL10expressing USCs significantly improved wound closure and regenerative responses in scratch assays.
Conclusion: USCs are a unique, noninvasive, robust, and easily genetically manipulated MSC source with strong therapeutic potential for kidney disease. Engineering USCs to express IL10 further enhances their antifibrotic and regenerative properties, supporting their potential use as an autologous cellbased therapy for CKD.

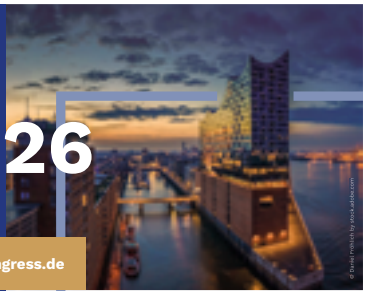

P21 Postergroup: Urine - Renal disease - inflammation

P2110

Genetic and structural adaptation of the kidney to extreme habitat in naked molerat (Heterocephalus glaber)

Antonia Lucrezia Bellingkrodt; Daniel Mendéz Aranda [1]; Dorothee Günzel [2]; Robert Labes [3]; Mingzhen Su [4]; Susanne Holtze [5]; Thomas Hildebrandt [5]; Gary L Lewin [1]; Sebastian Bachmann [4] Institut für Zell- und Neurobiology, Charité Universitätsmedizin Berlin, Berlin, Germany; [1] Molecular Physiology of Somatic Sensation, Max Delbrück Center for Molekular Medicine, Berlin, Germany; [2] Klinische Physiologie, Campus Benjamin Franklin, Charité - Universitätsmedizin Berlin, Berlin, Germany; [3] Institut für Translatioinal Physiologie, Campus Charité Mitte, Charité - Universitätsmedizin Berlin, Berlin, Germany; [4] Institut für Vegetative Anatomie, Campus Charité Mitte, Charité - Universitätsmedizin Berlin, Berlin, Germany; [5] Leibnitz Institute for Zoo and Wildlife Research, Berlin, Germany;

Objective: The naked molerat (Heterocephalus glaber) is a subterranean troglobiont from subSaharan Africa. It has extreme longevity, feeds on underground roots and bulbs, does not drink, and may activate fructosedriven glycolysis for ATP generation and metabolic water production. It has a maximum urine concentration capacity of 1500 mOsm/kg H_2O. We explored its renal architecture with focus on the loop of Henle and evaluated gene expressional profiles compared to laboratory rodents.
Method: Naked molerats of both sexes were anesthetized, sacrificed and the kidneys either immersionfixed or perfusionfixed via the heart for histology and immunohistochemistry. For transcriptome analysis kidneys were removed and stored frozen until use.
Results: The kidney parenchyma revealed rodenttype zonation into cortex, outer, and inner stripe of outer medulla (OSOM, ISOM), and inner zone/papilla (IZ). Zonal proportions, however, differed markedly with IS measuring 51% (rat: 17%) and IZ 26% (rat: 56%) along corticopapillary axis. Few longlooped AQP1positive descending thin limbs reached IZ to form bends with ascending thin limbs, while short loops with AQP1negative thin limbs formed bends with TAL variably at different levels of ISOM. TAL expressed uromodulin and NKCC2 throughout, but showed cell type heterogeneity for ROMK and Kir4.1 K+ channels and junctional claudin 10 and 16 expression along specific microdomains of TAL. Transcriptomics indicated energy metabolic pathways significantly distinct from rodent kidney.
Conclusion: Kidney epithelial morphology of the naked molerat displays features that significantly differ from laboratory rodents. In particular, organization of the loop of Henle is diverse, forming distinct TAL cell types and microdomains adapted to monovalent or divalent ion transport. Gene expression profiles confirm adaptations of the nephron with respect to lack of O_2, water, and homeothermy.

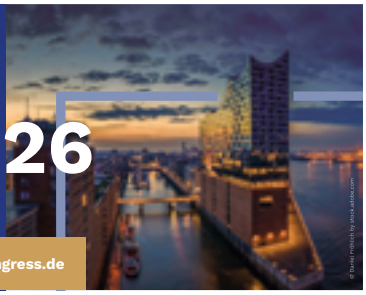

22 Postergroup: Urine - Tubular transport

P2201

The Physiology of Augmented Urine HCO_3^- Excretion During Respiratory Alkalosis

Jens Leipziger; Laura Woidemann Trans [1]; Benedikte Skjoldborg [1]; Hans Malte [2]; Christian Damsgaard ; Jesper Frank Andersen [3]; Peder Matzen Berg
Department of Biomedicine, University of Aarhus, Aarhus, Denmark; [1] Department of Biomedicine, Aarhus University, Aarhus, Denmark; Department of Biomedicine, Aarhus University, Aarhus, Denmark; Depart. of Biology, Zoophysiology, Aarhus Universität, Aarhus, Denmark; [3] Biomedicine, Physiology, Aarhus Universität, Aarhus, Denmark;

Objective: During respiratory alkalosis, the kidneys increase urinary HCO_3^- excretion to decrease blood pH. Increased HCO_3^- excretion is well demonstrated during highaltitude exposure, but the molecular mechanism underlying this renal response is unknown. Interestingly, augmentation of renal HCO_3^- excretion during metabolic alkalosis was recently shown to depend on pendrin and CFTR in the collecting duct CD βintercalated cells (βICs). Furthermore, secretin was shown to activate βICs via the secretin receptor. We hypothesized that βIC pendrin is necessary for renal pH compensation of respiratory alkalosis.
Method: Under anesthesia (i.p. ketaminexylazine), bladder catheterization experiments were conducted in mechanically ventilated pendrin wildtype (WT) and knockout (KO) mice to assess the renal response to hyperventilationinduced respiratory alkalosis. Additionally, intermittentlyclosedflow respirometry was performed to quantify the ventilatory response of pendrin WT and KO mice to hypoxia (12.5% O_2). Statistical differences were assessed using twoway ANOVA for repeated measures.
Results: Arterial blood gas analyses identified respiratory alkalosis during hyperventilation in both genotypes. A sharp increase in urine pH occurred shortly (i.e., 1015 minutes) after initiation of hyperventilation in WT mice. This effect was completely absent in pendrin KO mice. Furthermore, KO mice displayed a reduced hyperventilatory response and larger body temperature decreases during hypoxia in intermittentlyclosedflow respirometry. βIC function also requires CFTR and the secretin receptor. Both KO mouse models are currently being studied and we will also present these data.
Conclusion: Collecting duct βIC pendrin activation is obligatory for the ability to increase renal HCO_3^- excretion during respiratory alkalosis. Furthermore, renal compensation initiates immediately. Impaired βIC function impairs ventilatory compensation to hypoxia resulting in decreased metabolism and lower body temperature. This study provides insights to the key molecular mechanisms underlying pHregulation during acute respiratory alkalosis and their importance during acute hypoxia.

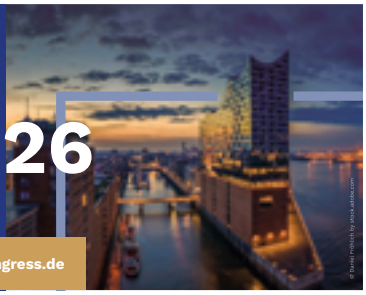

P22 Postergroup: Urine - Tubular transport

P2202

The parathyroid receptor 1 in the Thick Ascending Limb

Catarina Quintanova; Nina Himmerkus; Henrik Dimke [1]; Markus Bleich Physiologisches Institut, ChristianAlbrechtsUniversität Kiel, Kiel, Germany; [1] Cardiovascular and Renal Research, Dept. of Molecular Medicine, University of Southern Denmark, Odense, Denmark;

Objective: The parathyroid hormone receptor (PTH1R) is highly expressed in the kidney and bone. In the kidney, PTH plays a critical role in the regulation of calcium and phosphate homeostasis by maintaing serum calcium levels within a narrow range. One key action in kidney of PTH is to promote Ca^{2+} reabsorption in the thick ascending limb (TAL) and distal convoluted tubule (DCT). Recent studies have hypothesized the potential role of PTH1R in controlling paracellular calcium transport in the TAL by indirectly controlling the levels of claudin14, a tight junction (TJ) protein. Claudin14 expression is strictly localized in the TAL and its expression depends on high serum Ca^{2+} concentrations and interacts with claudin16/19 by reducing paracellular Ca^{2+} reabsorption. The TAL presents two major paracellular pathways, one mediated by claudin10 tight junctions (type α) that prefer Na^{+} and TJs with claudin16 and claudin19 which prefer Ca^{2+} and Mg^{2+} (type β). Based on our own previous research, we investigated the localization of PTH1R in different types of TAL cells and how the lack of PTH1R may influence claudin expression.
Method: Experiments were performed in male and female mice with cadherin 16kidney specific promotor (ksp) Cre PTH1R deletion (KO) and Crenegative littermates (WT). Immunofluorescence, protein expression, serum and urinary electrolyte determination were performed. TAL trans- and paracellular transport properties were assessed electrophysiologically in freshly isolated cortical TAL segments.
Results: PTH1R antibody staining confirmed the loss of PTH1R in the TAL of KO mice. The lack of PTH1R did not change transepithelial voltage. However, the transepithelial resistance was increased with a decrease in calculated equivalent short circuit current which may indicate a change in transcellular properties. Even though claudin14 was slightly increased in KO, there was no significant change in paracellular ion preference. The increased resistance translated in a change in calculated paracellular single ion permeabilities, however, on the background of unchanged permeability ratios for sodium, chloride, calcium or magnesium.
Conclusion: Under baseline conditions, the absence of PTH1R restricted to TAL did not lead to pronounced alterations in paracellular TAL transport properties of this segment. Further challenges are necessary to determine the effect of PTH1R in the local modulation of calcium handling in the TAL.

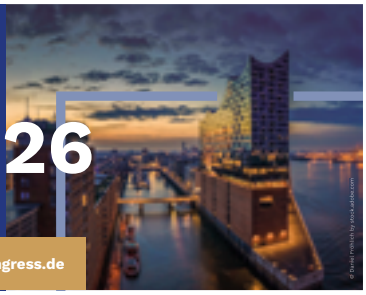

P22 Postergroup: Urine - Tubular transport

P2203

Genetic deletion of calcineurin Aβ does not increase renal sodium reabsorption via the sodium chloride cotransporter but leads to hypercalciuria

Turthushikh Damba; Henrik Dimke [1]; Kirsten Madsen; Marleen Kortenoeven
Cardiovascular and Renal Research, Molecular Medicine, University of Southern Denmark, Odense, Denmark; [1] Department of Molecular Medicine, University of Southern Denmark , Odense, Denmark;

Objective: Calcineurin inhibitors are widely used immunosuppressive drugs for preventing transplant rejection and treating autoimmune diseases but commonly cause hypertension and hypercalciuria. This hypertension has been attributed to increased renal sodium chloride reabsorption through activation of the thiazidesensitive sodium chloride cotransporter NCC. Dietary potassium lowers blood pressure by inducing NCC dephosphorylation, reducing its activity, which has been suggested to involve calcineurin. Calcineurin consists of a catalytic subunit A, CnA, which has three isoforms, and a regulatory subunit B. Their precise role in regulating NCC activity and renal electrolyte transport remains unclear. This study investigated the role of the catalytic subunit CnAβ, encoded by *Ppp3cb*, in renal sodium transport and NCC regulation.
Method: *Ppp3cb*deficient (KO) mice and wildtype (WT) littermates were studied in metabolic cages.
Results: KO and WT mice showed no differences in creatinine clearance or blood sodium, potassium or calcium levels. Urinary sodium and potassium excretion were also unchanged, suggesting that CnAβ does not contribute to increased sodium reabsorption during calcineurin inhibition. In contrast, urinary calcium excretion was markedly increased in *Ppp3cb* KO mice. Expression of total and phosphorylated (active) NCC did not differ between *Ppp3cb* KO and WT mice. Likewise, expression and phosphorylation of NKCC2 and expression or cleavage of ENaC were unchanged. To investigate if CnAβ is involved in potassium's effects on NCC dephosphorylation, mice received an oral gavage of potassium. No difference in the degree of NCC dephosphorylation was observed between WT and KO mice. *Ex vivo*, renal tubules were incubated in medium with different potassium concentrations for 30 min. High potassium reduced NCC phosphorylation and low potassium increased it similarly in renal tubules from both WT and KO mice. The calcineurin inhibitor tacrolimus increased NCC phosphorylation in both genotypes but did not block potassium's effect on NCC.
Conclusion: In conclusion, genetic deletion of CnAβ results in hypercalciuria, but CnAβ does not play a major role in the regulation of NCC or renal sodium handling. Tacrolimusinduced NCC phosphorylation appears independent of CnAβ, and might instead be mediated via CnAα., the only other isoform expressed in kidney. Since tacrolimus did not block the effect of potassium on NCC phosphorylation, this effect on NCC may be independent of calcineurin.

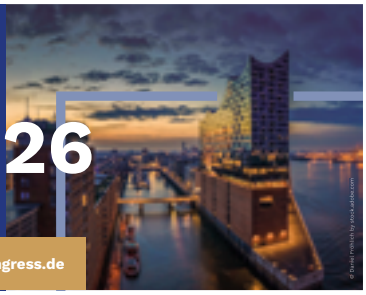

P22 Postergroup: Urine - Tubular transport

P2204

Localization and Modification of the Proteins Claudin7 and EpCAM in the Mouse Renal Collecting Duct

Yuanyuyue Huang; Sarah Mittmann; Anna Marie Seebohm; Nina Himmerkus; Catarina Quintanova; LauraSophie Beier; Markus Bleich
Physiologisches Institut, ChristianAlbrechtsUniversität Kiel, Kiel, Germany;

Objective: Claudin7 is one of the tight junction (TJ) protein members involved in the regulation of paracellular transport processes and is present in both the TJ and at basolateral side of mouse renal collecting duct (CD). Recent work in the MDCK II cell line has shown that claudin7 forms a protein complex with Epithelial Cell Adhesion Molecule (EpCAM) and being stored at the basolateral side of CD. It was hypothesized that enzymatic cleavage of EpCAM releases claudin7 and thereby participates in the rapid repair of TJs. As its roles in normal tissues become increasingly recognized, EpCAM is emerging as a putative novel important molecular target with significant prognostic, diagnostic, and therapeutic potential. Nevertheless, its function in renal CD is not fully understood yet. Based on previous research, we hypothesize that the EpCAMclaudin7 complex is involved in tight junction regulation in the renal CD. Here we investigate protein abundance and localization within the different cell types of CD and the effects of enzymatic cleavage of the complex.
Method: Segments were isolated enzymatically from C57BL/6 mouse kidneys. Protein expression, modification, and localization were analyzed by confocal microscopy of immunofluorescence and by Western blot, respectively. A- and Btype intercalated cells were distinguished by staining for the anion exchanger AE1 and H^+ATPase. Enzymatic cleavage of the EpCAM and claudin7 was tested by *in vitro* incubation with trypsin.
Results: After a detailed examination of the expression pattern in CD, we found that both claudin7 and EpCAM are expressed in the CD, where both are localized in the basolateral membrane and at the tight junction. While our findings indicate a differential distribution among the CD cell populations, with claudin7 being more prominent in principal cells and EpCAM showing a stronger signal in intercalated cells, they also showed a marked degree of colocalization. Trypsin (25µg/ml) cleaved EpCAM, but did not cleave claudin7. However, cleavage of EpCAM did not qualitatively change the localization of claudin7 and did not enhance the localization of claudin7 at the tight junction.
Conclusion: Our data from the renal CD indicates a more complex situation for the EpCAMclaudin7 expression and interaction compared to cell culture. In the native CD, their relationship might be affected by additional factors. Further studies will focus on probing additional contributors of the native tissue.

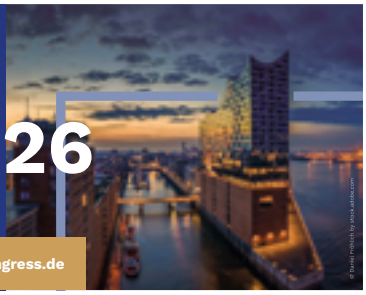

P22 Postergroup: Urine - Tubular transport

P2205

Spatial and Temporal Expression of the CalciumSensing Receptor in Renal and Extrarenal Tissues

Milos Bogdanovic; Henrik Dimke
Cardiovascular and Renal Research Unit, Institute of Molecular Medicine, University of Southern Denmark, Odense, Denmark;

Objective: The CalciumSensing Receptor (CASR) maintains calcium balance by regulating parathyroid hormone secretion and renal divalent cation transport. Although CASR is highly expressed in the thick ascending limb (TAL), its nephron distribution and temporal renal expression profile remain incompletely defined.
Method: To determine CASR localization, transgenic mice expressing EGFP under the *Casr* promoter and *Casr*^{tm1b} LacZ reporter mice were analyzed. CASR antibody specificity was validated using various *Casr* knockout mouse lines and evaluated on human kidney tissue. Mice were euthanized under 1.5% Isoflurane inhalation. Transgenic mouse kidneys were analyzed for EGFP, CASR, and betagalactosidase expression, while human kidney tissue was immunostained for CASR. Localization was assessed using selected nephron segmentspecific markers.
Results: In transgenic mice, EGFP expression was observed in known CASRexpressing sites, including the parathyroid and thyroid glands, pancreatic islets, and parts of the gastrointestinal tract. In the kidney, EGFP fluorescence was strongest in TAL segments of the cortex and outer stripe of the outer medulla, with lower expression in NCCpositive distal tubules and some Aquaporin2positive collecting ducts. No signal was detected in proximal tubules or the inner medulla. Renal expression patterns in postnatal day 7 and day 21 mice resembled those of adult animals. A highcalcium diet increased urinary calcium excretion but did not alter renal CASR or EGFP expression patterns. In *Casr*^{tm1b} kidneys, betagalactosidase activity was strongest in the TAL. Renal CASR expression patterns in human kidney tissue were similar to those observed in mice, although Pendrin colocalization with CASR was detected only in mice.
Conclusion: These findings define the spatial and temporal renal expression profile of CASR in mice and humans, demonstrating that nephron segmentspecific localization is established early postnatally and remains stable during hypercalcemic conditions.

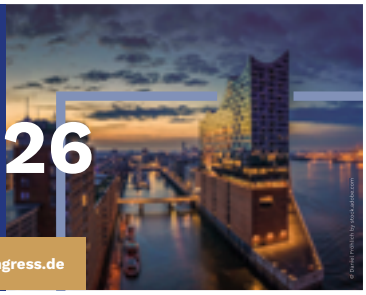

P22 Postergroup: Urine - Tubular transport

P2206

Effects of Parathyroid Hormone and Vitamin DInduced Hypercalcemia on Renal Calcium Handling and Metabolic Changes

Emmy Storm Petersen; Henrik Dimke
Cardiovascular and Renal Research Unit, Institute of Molecular Medicine, University of Southern Denmark, Odense, Denmark;

Objective: The calciumsensing receptor (CASR), expressed predominantly in the parathyroid glands and kidneys, plays a central role in systemic calcium homeostasis. In the parathyroid glands, CASR regulates parathyroid hormone (PTH) release. Increased PTH activates vitamin D, both raising blood calcium levels. The present study investigates how hypercalcemia induced by the PTH fragment teriparatide or the vitamin D analog dihydrotachysterol (DHT) differentially affects renal calcium transport.
Method: For all animal experiments 1.5% Isoflurane inhalation was used as anesthesia. Blood and urinary electrolytes were analyzed using an ABL835 FLEX analyzer or ion chromatography, respectively. Gene and protein expression were assessed by qPCR and immunohistochemistry.
Results: C57BL/6 mice received PTH and DHT for 3 days. Both treatments significantly elevated blood calcium concentrations compared with controls (control 1.3 ± 0.01 mM, DHT 2.1 ± 0.07 mM, PTH 1.9 ± 0.05 mM). However, urinary calcium excretion was only significantly elevated in DHTtreated mice. DHT treatment markedly induced renal expression of the CASRregulated claudin14 gene compared with PTH treatment. In contrast, extensive renal calcifications were observed exclusively in PTHtreated mice, predominantly located outside the collecting system.
PTH additionally induced metabolic acidosis, evidenced by a lower blood pH and decreased HCO_3^- concentrations. To assess the contribution of metabolic acidosis to renal calcifications, mice received $NaHCO_3^-$ supplementation with PTH treatment. PTH markedly elevated blood calcium concentrations despite $NaHCO_3^-$ supplementation (untreated 1.27 ± 0.00 mM, $NaHCO_3$ 1.26 ± 0.02 mM, PTH and $NaHCO_3$ 2.83 ± 0.22 mM) and prevented development of metabolic acidosis. Furthermore, PTH and $NaHCO_3^-$ treatment did not significantly increase claudin14 gene expression compared to untreated and $NaHCO_3^-$ treated alone. Although $NaHCO_3$ supplementation reduced renal calcifications, it did not prevent their development.
Conclusion: In conclusion, although PTH and DHT similarly induce hypercalcemia, they exert markedly different effects on renal calcium handling and associated metabolic changes. The data suggests that PTHinduced metabolic acidosis may contribute to renal calcification independently of hypercalciuria. Ongoing studies examining urinary pH, bicarbonate excretion, and renal phosphoproteomics aim to further elucidate the underlying mechanisms.

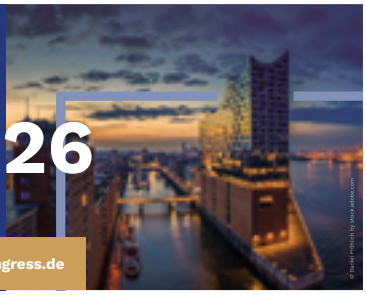

P22 Postergroup: Urine - Tubular transport

P2207
Reliable identification of nephron segments on kidney slides on cellular level

Jennifer König; Luca Scarsella; Stephanie Probst; Bettina Scharner; Vladimir T. Todorov [1] Physiology and Pathophysiology, University Witten/Herdecke, Witten, Germany; [1] Zentrum für Biomedizinische Ausbildung und Forschung (ZBAF), Lehrstuhl für Physiologie, Pathophysiologie und Toxikologie, Universität Witten/Herdecke, Witten, Germany;

Objective: Identification of nephron segments is essential for the spatial analysis of renal structure and function, both in murine and human kidney. Using kidney sections for visualization of these segments provides a powerful fundament to investigate pathological changes based on single cell or cell population analysis. Still, this task remains challenging due to lack of reliable antibodies. This study aims to establish an RNAprobe based panel for detection of defined nephron segments. We focus on proximal tubule segments, macula densa and terminal collecting duct on a single cell basis.
Method: Kidney sections were utilized for in situ hybridization by RNAscope™ technique. Segment specific RNA probes were selected to label distinct nephron segments as following:

Nephron segment	Subsegment	RNA probe
Proximal Tubule		Cubilin
	S1+S2	SGLT2 + SGLT1
	S3	SGLT1/SGLT5 + GLUT5
Loop of Henle		
	TAL	NKCC2
	TDL	UT A
Macula Densa		NKCC2 + NOS1
Collecting duct	Terminal region	UT A

Images were microscopically visualized using a Keyence BX810, with appropriate wavelength filters. For every kidney 1/3 of the slice or at least 1 mm² was selected for analysis. Subsegment specific cell populations were classified and analyzed with individually configurated pipelines by CellProfiler™ software.

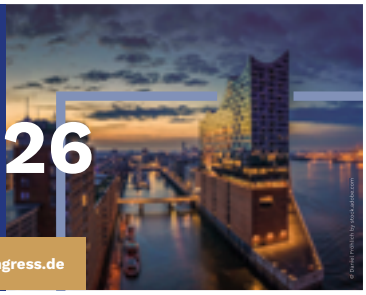

P2207

Reliable identification of nephron segments on kidney slides on cellular level

Results: RNAscope™ staining showed clear marker patterns in murine and human kidney sections. Cubilin identifed proximal tubules. Within the proximal tubule, SGLT2/GLUT2 marked mainly S1/S2 segments, while SGLT1 and SGLT5/GLUT5 were used for S3related regions. NKCC2 marked the thick ascending limb. The combination of NOS1 and NKCC2 was used to identify the macula densa. A panUTA probe detected urea transporterassociated regions, with terminal collecting duct signals interpreted as UTA1/UTA3isoform and outer medullary signals as UTA2 in the thin descending limb. Representative images show the localisation of these probe signals in the kidney tissue. In addition, CellProfiler™ analysis displays quantified percentages of cell populations positive for SGLT2 and SGLT1.

Conclusion: The established probe panel enables the reproducible spatial identification of single cells on murine and human kidney slides. It serves as the basis for cell specific analysis in experiments addressing further questions, such as pathological changes in tubular transport processes, e.g. related to diabetes or metabolic syndrome. Visualizing several probes on one slide allows the identification of cell populations with named marker RNA probes and can be extended by mRNAtargets of interest. Furthermore, the combination of mRNAvisualization and antibody staining covers analysis at the protein level.

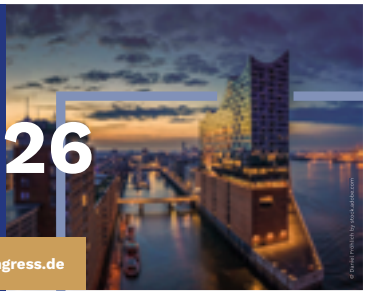

P22 Postergroup: Urine - Tubular transport

P2208

Engineering a genetically encoded phosphate sensor in human cells

Maysam Mansouri; Laurine Lang; Carsten A. Wagner
Physiologisches Institut, UniversitätsSpital Zürich, Universität Zürich, Zürich, Switzerland;

Objective: Phosphate homeostasis is tightly regulated through coordinated intestinal absorption, cellular uptake, bone storage, and renal excretion to maintain serum phosphate concentrations within a narrow physiological range. This process is orchestrated by a complex network of hormones, growth factors, receptors, and transporters. Dysregulated phosphate metabolism, particularly hyperphosphatemia, is strongly associated with chronic kidney disease and contributes to severe complications, including vascular calcification, cardiovascular dysfunction, and progressive renal damage. Therefore, technologies capable of sensing pathological phosphate levels and triggering timely therapeutic responses are highly relevant for precision medicine.
Method: Here, we present a genetically engineered phosphate sensor in human cells, termed GEPS, that enables phosphate sensing within pathological concentration ranges and drives proportional production of clinically relevant therapeutic proteins.
The GEPS is composed of a calciumsensing receptor (CaSR) rewired to a synthetic promoter containing regulatory elements, including binding sites for the master regulators NFAT, SRE, and CREB, which control the expression of the target transgene.
Results: We developed two circuit configurations. In the GEPSoff format, engineered HEK cells express luciferase as a reporter gene under physiological calcium levels, whereas elevated phosphate concentrations suppress luciferase expression. We demonstrated that GEPSoff can detect phosphate concentrations in the range of 1.5 to 3 mM. Conversely, in the GEPSon format, incorporation of the transcriptional repressor KRAB enables luciferase expression exclusively under pathological phosphate concentrations. Therefore, GEPSon design establishes an autonomous closedloop feedback system that activates therapeutic protein production under hyperphosphatemic conditions and switches off expression once phosphate levels return to the physiological range.
Conclusion: GEPS provides a versatile platform for gene- and cellbased therapies, enabling autonomous disease management through realtime phosphate sensing and contextdependent therapeutic protein delivery.

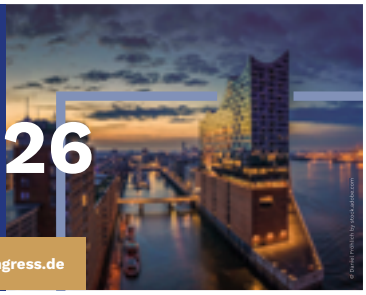

P22 Postergroup: Urine - Tubular transport

P2209

The potassium channel ROMK in the renal distal convoluted tubule is critical for the rapid adaptation of the kidney to an oral potassium load

Anna Moser; Twinkle Vohra; Dominique Loffing
Molekulare Anatomie, Insitut für Anatomie, Universität Zürich, Zürich, Switzerland;

Objective: The kidney maintains potassium (K^+) homeostasis by adjusting urinary K^+ excretion to dietary intake. A key mediator of renal K^+ secretion is the renal outer medullary K^+ channel (ROMK) which is expressed in the thick ascending limb (TAL), distal convoluted tubule (DCT), connecting tubule (CNT), and collecting duct (CD). While the role of ROMK in TAL, CNT and CD has been well characterized, its regulation and functional significance in the DCT remain poorly understood.

Method: Wildtype mice were fed either a control or highK^+ diet for varying durations (3 hours and 2 days). Nephron segments (TAL, DCT, CNT, CD) were isolated by freehand microdissection to analyse ROMK mRNA and protein abundance, as well as its complex glycosylation which serves as a marker of functionally mature ROMK. Moreover, a novel mouse model with inducible, DCTspecific ROMK deletion (ROMK^{flox}) was generated to investigate the role of ROMK in the DCT. Furthermore, isolated DCTs were incubated *ex vivo* under low- or highK^+ conditions to assess direct effects of extracellular K^+ on ROMK.

NCC^{creERT2}

Results: In control mice, complexglycosylated ROMK was most strongly expressed in the TAL, but clearly less abundant in the DCT, CNT, CD. In contrast, mice on highK^+ diet developed a significant increase of complexglycosylated ROMK in the DCT. Consistently, mice with DCTspecific ROMK deletion showed a transient defect in renal K^+ secretion with hyperkalemia following acute K^+ loading. Notably, ex vivo incubation of DCTs in highK^+ conditions (40 minutes, 3 hours and 6 hours) did not increase levels of complexglycosylated ROMK.

Conclusion: Shortterm dietary K^+ loading upregulates ROMK particularly in the DCT. This upregulation in the DCT appears to play an important role in the shortterm regulation of K^+ homeostasis and may occur independently of changes in extracellular K^+ concentration.

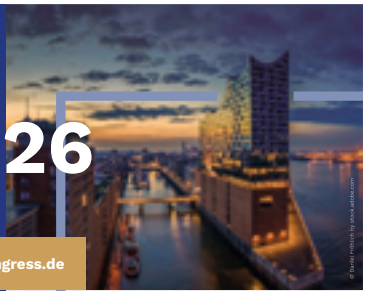

P22 Postergroup: Urine - Tubular transport

P2210
Kidney segmentspecific effects of low potassium intake

Adrienne Assmus; Qi Wu; Louise Nyrup Odgaard; Xiang Zheng; Robert Fenton
Department of Biomedicine, Aarhus University, Aarhus, Denmark;

Objective: Modern diets are typically high in sodium, widely recognized to increase blood pressure (BP), but also by low potassium (K^+) intake, also linked to higher BP. Previous studies have shown that the ability of low K^+ to increase BP is almost fully accounted for by an increase in abundance and activity of the thiazidesensitive sodium chloride cotransporter (NCC) in the kidney distal convoluted tubule (DCT). However, low potassium also affects other characteristics of the DCT as well as other tubule segments, both in morphology and function, with implications for longterm kidney health and homeostasis. Due to the heterogeneity of the kidney structure, many segmentspecific changes are undetectable when analysing whole organ samples. This study aims to increase our understanding of the effects of low K^+ intake on the molecular landscape of specific kidney tubules.
Hypothesis: Low K^+ intake underlies segmentspecific remodelling processes and molecular changes that are only observable by isolating these segments.
Method: Male C57Bl/6J mice are fed with low K^+ diet (KCl, 0.2% K^+, n=6) vs. control K^+ diet (1% K^+, n=6) for 5 days. Kidneys are perfusionfixed and collected on day 5, and paraffin embedded. Sections are then prepared for IHC with the following antibodies: megalin for PT, NKCC2 for TAL, NCC for DCT, and Aqp2 for CD; these sections are then processed with a laser microdissection microscope (LMD, Leica), and the tubule segments collected separately based on positive staining. All samples are then processed for mass spectrometry analysis.
Results: Mice on low K^+ diet showed the expected increase in NCC and pNCC (active form), and decreased αENaC expression. Tail cuff plethysmography showed increased BP, and mice had reduced urine volume and urinary K^+ excretion. Plasma K^+ was slightly decreased. Mass spectrometry analysis of the samples is ongoing, but preliminary data shows: 1) 2824 proteins were identified from the PT, and 16.1% changed with low K^+; 1777 IDs from the TAL, 3.4% changed; 2402 IDs from the DCT, 3.8% changed; and 2522 IDs from the CD, with 7.8% changed. 2) Changes in expression are segmentspecific, with almost no overlap in changed proteins between PT, TAL, DCT, and CD. 3) Both PT and DCT show downregulation of NADHrelated pathways, which is linked to kidney injury and CKD. PT shows upregulation of cytoskeletal markers, in line with low K^+ structural remodelling. The CD shows upregulation of catalytic activity markers.
Conclusion: Perspectives: Analysis and validation of specific pathways affected by low K^+ are ongoing. The choice to use low K^+ (0.2%) instead of more extreme and widely used K^+ depleted diet is deliberate as we aim to understand the effects of the human modern diet.

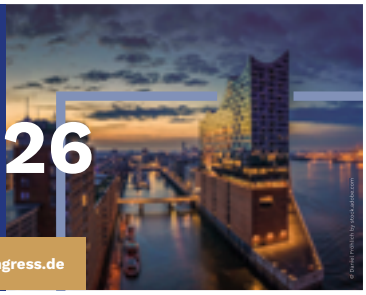

P22 Postergroup: Urine - Tubular transport

P2211

Synthetic inhibitory peptides reduce ENaCmediated sodium transport in murine cortical collecting duct cells

Franziska Schreiber; Alicia Kißler; Christoph Korbmacher; Alexandr V. Ilyaskin; Florian Sure Institut für Zelluläre und Molekulare Physiologie, FriedrichAlexanderUniversität ErlangenNürnberg, Erlangen, Germany;

Objective: The epithelial sodium channel (ENaC) is essential for renal sodium homeostasis and longterm blood pressure regulation. A unique feature of ENaC is its proteolytic activation, involving the removal of autoinhibitory tracts from the channel's α- and γsubunits. Previously, it was demonstrated that synthetic peptides (α8, γ11) corresponding to key sequences of these autoinhibitory tracts inhibit ENaC activity. Here, we explored the potential of using these synthetic inhibitory peptides to inhibit ENaCmediated sodium in murine cortical collecting duct cells.

Method: In *Xenopus laevis* oocytes heterologously expressing wildtype or mutant human ENaC, wholecell currents were measured using the twoelectrode voltageclamp (TEVC) technique. In addition, we performed shortcircuit current (I_{SC}) measurements on murine cortical collecting duct ($mCCD_{cl1}$) cells.

Results: In TEVC measurements, we confirmed that α8 and γ11 decreased ENaCmediated wholecell currents in a concentrationdependent manner (IC_{50} of α8: ~70 µM, of γ11: ~35 µM). Molecular dynamics simulations predicted critical residues mediating inhibition by α8 and γ11 (αPhe226, αTrp251, αHis255, αTyr447; γPhe204, γTrp229, γHis233, γTyr425). Sitedirected mutagenesis of these residues to alanine reduced or abolished ENaCinhibition by α8 or γ11. Proteolytic removal of the endogenous γautoinhibitory peptide by chymotrypsin decreased α8's potency to inhibit ENaC (IC_{50} increased to >300 µM).

In shortcircuit current (I_{SC}) measurements on murine cortical collecting duct ($mCCD_{cl1}$) cells, significantly higher concentrations of α8 were required to achieve ENaC inhibition compared to γ11 (IC_{50} γ11: ~5 µM; α8: ~190 µM; 18≤n≤26). This is probably due to the removal of the γautoinhibitory tract by endogenous proteases. In addition to inhibiting baseline ENaCmediated I_{SC}, both peptides reduced the stimulatory effect of aldosterone on I_{SC} (+15.4±2.2 µA/cm² with α8; +14.0±2.9 µA/cm² with γ11; +25.8±4.2 µA/cm² in vehicle controls; $p<0.05$, Student's *t*test, 14≤n≤18).

Conclusion: In conclusion, drugs mimicking the effect of the endogenous autoinhibitory tracts may provide a novel therapeutic strategy to reduce ENaC activity and enhance renal sodium excretion.

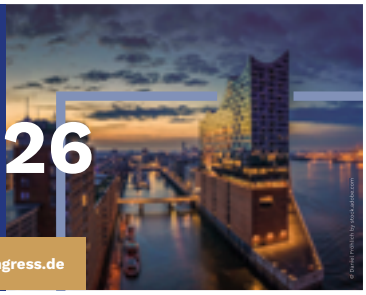

P22 Postergroup: Urine - Tubular transport

P2212

Aldosteroneidentified targets for optimal sodium and potassium supplementation in intestinal failure

Mads Vaarby Sorensen; Georg Lamprecht[1]; Jens Georg Leipziger; Peder Matzen Berg; Robert Förster[2]
Department of Biomedicine, University of Aarhus, Aarhus, Denmark; [1] Abteilung für Gastroenterologie, Zentrum für Innere Medizin, Universitätsmedizin Rostock, Rostock, Germany; [2] Division of Gastroenterology, Hepatology and Nutritional Medicine, Department of Internal Medicine, Rostock University Medical Center, Rostock, Germany;

Objective: Parenteral support (PS) is a lifesaving organ replacement therapy for patients with intestinal failure (IF). However, practical strategies to optimize PS Na^+ and K^+ remain poorly defined. We investigated whether renin and aldosterone reflect suboptimal electrolyte supplementation and could help guide physiologically optimal Na^+ and K^+ supplementation in patients with IF.
Method: Realworld monitoring data from IF patients receiving longterm PS were analyzed using for associations between parenteral Na^+ and K^+ supplementation, urinary Na^+ and K^+ excretion, and plasma renin and aldosterone in IF patients with a jejunostomy (SBJ) or with colon in continuity (SBCiC).
Results: In 618 visits from 110 patients, elevated aldosterone levels occurred frequently and were more common in SBJ (OR for hyperaldosteronism: 5.2; 95% CI 1.5 to 17.8). Even after adjusting for Na^+ and volume depletion, SBJ had significantly higher aldosterone levels (2.1fold higher; 95% CI 1.5 to 2.9; $p < 0.001$) than SBCiC. Urinary K^+ excretion increased with greater K^+ infusion and was significantly higher in SBJ than SBCiC (adjusted difference: 28 mmol/d; 95% CI 9 to 47; $p < 0.01$).
Conclusion: Aldosterone not only reflects Na^+ depletion but is also stimulated to excrete overzealous intravenous K^+ supplementation in patients with IF. Targeting a urinary Na^+ concentration of >20 mmol/L and a urinary Na^+ and K^+ ratio of >1 can help to guide physiologically optimal Na^+ and K^+ support in IF.

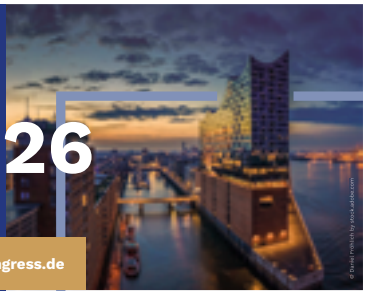

P22 Postergroup: Urine - Tubular transport

P2213

Reduced expression of magnesium transport proteins in the distal convoluted tubule of *Clcnkb*deficient mice may explain urinary magnesium wasting in classical Bartter syndrome

Henrik Dimke; Milos Bogdanovic; Ida Appel; Karsten Skjødt; ErnstMartin Fuchtbauer [1]; Kirsten Madsen; Lars Lund; Régine Chambrey [2]; Dominique Eladari [3]; R Todd Alexander [4]; Christian A. Hübner [5]; Christopher Hennings [5]; Marleen Kortenoeven Cardiovascular and Renal Research Unit, Institute of Molecular Medicine, University of Southern Denmark, Odense, Denmark; [1] Department of Molecular Biology and Genetics, Aarhus University, Aarhus, Denmark; [2] Paris Cardiovascular Research Center (PARCC), Paris, France; [3] University of Picardie Jules Verne, Amiens, France; [4] Membrane Protein Disease Research Group, The University of Alberta, Edmonton, Canada; [5] Institut für Humangenetik, Universitätsklinikum Jena, FriedrichSchiller Universität Jena, Jena, Germany;

Objective: The kidney thick ascending limb (TAL) plays a key role in the transport of sodium, chloride, potassium, calcium, and magnesium. Bartter syndrome is a hypokalemic, saltlosing tubulopathy caused by impaired TAL function. Pathogenic variants in *SLC12A1* or *KCNJ1* cause antenatal Bartter and variants in *CLCNKB* result classical Bartter syndrome. Although all variants impair TAL electrolyte transport, their effects on mineral handling differ. In contrast to antenatal forms, classical Bartter syndrome is frequently associated with hypomagnesemia, a feature also found in Gitelman syndrome resulting from pathogenic variants in *SLC12A3*. The mechanisms underlying these distinct clinical phenotypes remain poorly understood. Therefore, the purpose of the present study was to investigate how classical Bartter syndrome differentially affects renal mineral transport pathways.
Method: *Clcnkb* and *Slc12a3*deficient mice as well as human kidneys were investigated. Protein abundance and localization of electrolyte and mineral transporters were assessed by immunohistochemistry. Gene expression was determined in *Clcnkb*deficient mice.
Results: In human kidney, both ClCK channels and their essential subunit Barttin were found in TAL, distal convoluted tubule (DCT), and collecting system. *Clcnkb*deficient mice showed complete ablation of *Clcnkb* and extensive reductions in markers of DCT volume. Furthermore, DCT magnesium channels and select basolateral magnesium transporters were markedly reduced in *Clcnkb*deficient mice, similar to *Slc12a3*deficient mice. In contrast, the calcium transport machinery remained largely unaltered.
Conclusion: ClCK channels are expressed in both the TAL and DCT in mouse and human kidneys. Ablation of *Clcnkb* in mice leads to atrophy of the early DCT and subsequent reductions in TRPM magnesium channels, providing a possible explanation as to why hypomagnesemia is frequently observed in classical Bartter.

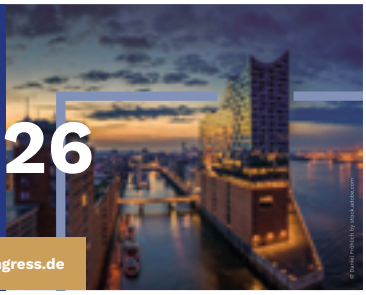

P22 Postergroup: Urine - Tubular transport

P2214

Barttin is upregulated under hypertonic cell culture conditions in mpkCCD cells and its functional deletion is associated with phenotypic changes

Moritz Pernecker; Shobika Karuppusamy; Vladimir T. Todorov; Bayram Edemir
Zentrum für Biomedizinische Ausbildung und Forschung (ZBAF), Lehrstuhl für Physiologie, Pathophysiologie und Toxikologie, Universität Witten/Herdecke, Witten, Germany;

Objective: The osmotic gradient in the kidney between cortex and medulla is driving force for urine concentration due to water absorption from collecting duct. In mouse renal collecting duct (mpkCCD) cells, the gene *Bsnd*, encoding Barttin, is upregulated in response to hyperosmolarity. Barttin is required for the physiological function of chloride channel *Clcnka*, encoding ClCKa, in the nephron, and its dysfunction is linked to Bartter syndrome IV, which is associated with impaired salt reabsorption. Interestingly, *Clcnka* gene expression is also upregulated under hyperosmotic conditions. The functional consequences of hypertonicity induced Barttin expression in mpkCCD cells are not fully understand. Here, we induced functional deletion of Barttin in mpkCCD cells and analysed the impact on cellular function.
Method: To investigate the function of Barttin, we used CRISPR/Cas9 technology to generate a functional knockout of *Bsnd* in mpkCCD cells. Deletion of Barttin protein expression was validated by Sanger sequencing and Western Blot. We cultured Barttin knockout (KO) cells and control (SCR) cells, under isotonic (300 mosmol/kg) and adapted hypertonic (600 mosmol/kg) conditions. Functional analysis usings livecell imaging was performed to monitor cell proliferation and migration. Furthermore, NGS was performed to screen for differences in gene expression, associated with loss of Barttin function.
Results: CRISPR/Cas9 induced efficient Barttin KO that was validated on DNA and protein level. The cells' grow properties depended on the osmolarity and genotype. In the case of hyperosmolarity, cells showed a lower proliferation. Interestingly, proliferation of Barttin deficient cells decreased in comparison to SCR cells at all osmolarities. Furthermore, Barttin loss was associated with a significant deregulation of 2,126 genes under isotonic and 1,841 genes under hypertonic conditions. This includes genes coding for ion channels, like the upregulation of the potassium channel *Kcnj16* (Kir5.1) only under hypertonic conditions and chloride channel *Clc1n* (ClC1) regardless of osmolarity.
Conclusion: Our results show that the absence of Barttin affects cell proliferation in mpkCCD cells independently of the osmotic environment. Furthermore, loss of Barttin expression induced the expression of ion transporter genes. Further research is needed to understand how Barttin expression functionally impacts ion transport under hypertonic cell culture conditions and how this gets impaired in Barttin deficient cells.

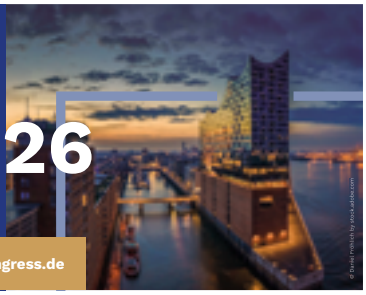

P23 Postergroup: The heart of the matter - drilling into genes & function

P2301
Cardiac effects of Swiprosin1/EFHD2

Wulf Gebhardt; Rolf Schreckenberg; Klaus Dieter Schlüter
Physiologisches Institut, Justus Liebig Universität Gießen, Gießen, Germany;

Objective: In the postischemic myocardium, immunocompetent cells initiate repair processes, which remove damaged cardiomyocytes and replace them with connective tissue. Beyond that, cardiomyocytes have the potential to reorganize their contractile apparatus. This process depends among others on the activity of Swiprosin1/EFHD2, a socalled Actinorganizing molecule. This study aims to investigate the influence of Swiprosin1 on the functional, structural, and metabolic remodelling of the postinfarct heart.
Method: The potential effects of Swiprosin1 on postischemic regain of function and postischemic tissue/structural maintenance after ischemia and reperfusion will be studied in two models of ascending complexity. This translational approach aims to investigate the effects of siRNAinduced Swiprosin1 knockdown as well as plasmidbased overexpression initially in human AC16 cardiomyocytes, and subsequently validate them in salineperfused hearts *ex vivo* from Swiprosin1 knockout mice.
Results: RTqPCR data verified effective a siRNAinduced knockdown of Swiprosin1 expressiom in cultured AC16 cells to below 50% compared to scrambled siRNA controls (n=3; $p<0.05$). PhalloidinFactin staining showed disruption of actin filament organization in response to both Swiprosin1 knockdown, and increased organization under Swiprosin1 overexpression (n=2). MitoSOX mitochondrial superoxide staining revealed decreased superoxide production following Swiprosin1 knockdown, and increased production after Swiprosin1 overexpression (n=3). Swiprosin1 knockdown was also found to reduce mitochondrial membrane potential as determined via MitoHealth dye, Hoechst33342 (n=3).
Conclusion: The observed influence of Swiprosin1 expression on cardiomyocytes further supports existing data suggesting an important role in cardiac remodelling.

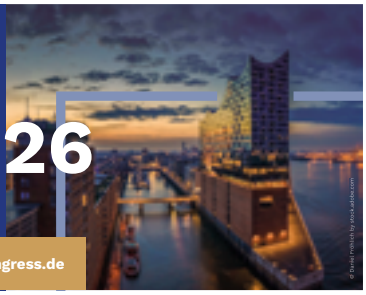

P23 Postergroup: The heart of the matter - drilling into genes & function

P2302

Investigation of Effects of Optogenetic G_q Pathway Activation on Ca^{2+} Signalling in Cardiac Cells

Dragana Stefanovska; Jonas Heer; Josef Madl; Yusuke Sakai [1]; Robert Lucas [1]; Peter Kohl; Franziska SchneiderWarme
Institute for Experimental Cardiovascular Medicine, Medical Faculty and Medical Center, University of Freiburg, Freiburg, Germany; [1] Division of Neuroscience and Centre for Biological Timing, School of Biological Sciences, Faculty of Biology Medicine and Health, University of Manchester, Manchester, United Kingdom;

Objective: Dysregulation of the G_q signalling cascade can contribute to cardiac hypertrophy, fibrosis, and arrhythmias through altered Ca^{2+} signalling. Optogenetics is a technique that involves expressing genetically engineered light sensitive proteins to control and monitor function of isolated cells, tissue, organs, and entire organisms in response to light stimulation. Compared to pharmacology, light activated proteins enable precise spatiotemporal and celltype specific signalling control. Human opsin 5 (hOPN5), a bistable UV lightsensitive opsin, has recently been shown to specifically activate the G_q signalling pathway, and has been employed to optically modulate heart function. Because of relatively low tissue penetration of UV light, we test the application of a modified version of hOPN5 (in the following as $hOPN5_{vis}$ provided by Yusuke Sakai and Robert Lucas; University of Manchester, UK), postulated to have a redshifted activation spectrum. We aim to assess the utility of this mutant to disentangle principles of G_q signalling for control of heart function.
Method: We first tested effects of $hOPN5_{vis}$ activation on intracellular Ca^{2+} dynamics in HEK293T cells, by using the fluorescent indicator Cal630 AM excited at 620 nm. To assess GPCR activation, visible light pulses at varying wavelengths were delivered using the FRAP configuration of a Leica DMi8 confocal microscope. To evaluate the functionality of $hOPN5_{vis}$ in more physiological systems we applied adenoviral transduction of hiPSCderived cardiomyocytes (CM) and transfected primary cardiac fibroblasts (cFB).
Results: Initial characterisation confirmed robust expression of $hOPN5_{vis}$ in HEK293T cells. Optical stimulation with 470 nm light revealed a lightintensitydependent titration of the Ca^{2+} response. Intracellular Ca^{2+} amplitude increased proportionally with light intensity. The ON response was rapid, with peak Ca^{2+} signals occurring 3.5 s after light onset, while the OFF response showed recovery to baseline within 36.7 s following the peak, demonstrating precise control of G_q pathway activation. Activation at different wavelength revealed peak Ca^{2+} response amplitudes at 490 nm. Similar to experiments in HEK cells, an increase in intracellular Ca^{2+} concentration was reliably induced in $hOPN5_{vis}$expressing cFB. Preliminary experiments in hiPSCCM indicated a lightinduced slowing in the spontaneous beating frequency. Further experiments are ongoing to validate the initial observation, and to assess effects on amplitudes of Ca^{2+} transients upon photostimulation.
Conclusion: In conclusion, $hOPN5_{vis}$ represents a promising tool that can be applied to precisely trigger the G_q signalling pathway and to study its downstream effects across cell systems. Future work will further explore its utility in cFB and CM, with the aim of obtaining a better understanding of effects of physiological G_q pathway activation, and to compare them to effects in diseased cells or cells obtained from aged animals.

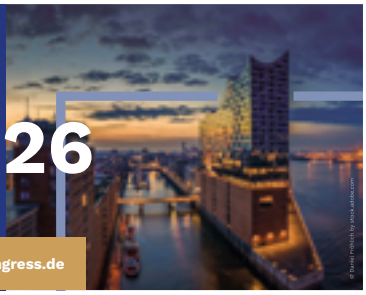

P23 Postergroup: The heart of the matter - drilling into genes & function

P2303

Impact of Acute Lipid Accumulation on Titin Phosphorylation and Subcellular Organization in rat Cardiomyocytes

Lena Großmann; Mahmoud Amer Kabouh; Katharina Kotulski; Max Anstötz [1]; Michael Singer; Martina Krüger
HerzKreislaufPhysiologie, Heinrich Heine Universität Düsseldorf, Düsseldorf, Germany; [1] Anatomie 2, Medizinische Fakultät, HeinrichHeineUniversität, Düsseldorf, Germany;

Objective: Obesity and diabetes are primary risk factors for cardiac dysfunction, yet the link between lipid accumulation and myocardial stiffness and cardiac dysfunction remains incompletely understood. This study investigates the effects of acute lipid droplet (LD) accumulation on titin, the giant muscle protein responsible for sarcomere elasticity, and the ultrastructural integrity of cardiomyocytes.
Method: Isolated adult rat cardiomyocytes were incubated for 4 hours with fatty acids (Oleate, Palmitate, or a combination) to induce LD formation, verified via HCS LipidTOX™ staining. Western blotting was performed to determine relative phosphorylation of titin's stiffnessregulating regions (N2B, PEVK) immediately after fatty acid treatment and 20 hours postremoval. Additionally, immunofluorescence microscopy was used to analyze sarcomere and cytoskeletal organization (αactinin, Filamin C, αtubulin, Connexin43 and Caveolin3).
Results: Microscopic analysis confirmed LD accumuluation in cardiomyoctes from all treatment groups. Sarcomeric organization and distribution of Connexin43, Filamin C, and αtubulin were preserved at all treatment regimes. In contrast, Caveolin3 expression increased, suggesting an early disruption of caveolae organization. Western blot data showed that relative titin phosphorylation (N2B/PEVK) was not significantly altered at either time point, but treated groups exhibited high standard deviations.
Conclusion: Acute 4hour lipid loading in rat cardiomyocytes does not significantly affect titinphosphorylation or sarcomere integrity at either time poin. However, early changes in caveolae organization may represent a key mechanism linking lipid accumulation to impaired cardiomyocyte function, contributing to the development of lipidinduced cardiac dysfunction.

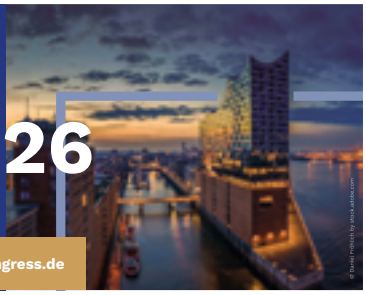

P23 Postergroup: The heart of the matter - drilling into genes & function

P2304

Loss of the E3 ubiquitin ligase Siah2 confers right ventricular cardioprotection

Maike Elisabeth Schneider; Nicole Molenda; Ling Li; Daniela Scherf[1]; Simone Kraut [1]; Bernd Niemann[2]; Norbert Weissmann[3]; M. Lienhard Schmitz[4]; Susanne Rohrbach
Institut für Physiologie, Justus Liebig Universität Gießen, Gießen, Germany; [1] Department of Medicine II – Internal Medicine with a Focus on Pneumology, Gastroenterology, Nephrology, and Internal Medicine Intensive Care, University Hospital Giessen and Marburg, Gießen, Germany; [2] Klinik für Herz, Kinderherz- und Gefäßchirurgie, Standort Gießen, Universitätsklinikum GießenMarburg, Gießen, Germany; [3] Excellence Cluster Cardio Pulmonary Institute (CPI), Universities of Gießen and Marburg Lung Center (UGMLC), JustusLiebigUniversity Gießen, Gießen, Germany; [4] Institute of Biochemistry, JustusLiebigUniversity Gießen, Gießen, Germany;

Objective: Pulmonary arterial hypertension (PAH) is a chronic disease characterized by elevated blood pressure in the pulmonary circulation, which can lead to right ventricular hypertrophy (RVH), RV remodeling and eventual RV failure (RVF). Experimentally, RVH can be induced by mechanic obstruction of the RV outflow via pulmonary artery banding (PAB) or chronic hypoxia. One of the proteins regulating the hypoxic response is the ubiquitin E3 ligase Siah2 (seven in absentia 2), but it's impact in the development of RVH is still unknown.
Method: The role of Siah2 was investigated in Siah2$^{-/-}$ mice in a model of PABinduced RVH. Cardiac remodeling was characterized by echocardiography, hemodynamic measurements and histology. Isolated cardiomyocytes and fibroblasts from these mice were characterized *in vitro*. To understand the celltypespecific effects of Siah2, mice with a floxed Siah2 gene were crossed with mice carrying a Cre recombinase under the control of a celltypespecific promoter (Myh6Cre and Col1a2Cre mice). The cardiomyocytespecific or fibroblastspecific Siah2 knockout was induced in these mice via a 10day tamoxifen (20 mg/kg BW, i.p.) treatment. After successful knockout these mice will also undergo PAB surgery analogous to the mice with a global Siah2 knockout. Induction of Siah2 gene expression *in vitro* was analyzed in rat cardiac fibroblasts and cardiomyocytes under hypertrophic conditions induced by phenylephrine and/or hypoxia (1% O_2).
Results: Echocardiographic analyses demonstrated a better preservation of RV function (TAPSE, cardiac output) in Siah2$^{-/-}$ mice compared to WT mice after RV overload. In addition, Siah2$^{-/-}$ mice were largely protected from RV hypertrophy and RV fibrosis induced by PAB. No such changes were observed in the LV. Siah2$^{-/-}$ fibroblasts demonstrated decreased proliferation, migration and lower expression of profibrotic genes. The according RV cardiomyocytes displayed a decreased hypertrophy (cell size) and reduced mRNA expression of loadinduced genes such as BNP or betamyosin heavy chain. However, the contractile response of isolated cardiomyocytes was not altered compared to WT cells after PAB. *In vitro*, Siah2 expression was not increased under hypertrophic conditions alone, but a significant upregulation was observed in fibroblasts when combined with hypoxia. In addition, exposure to transforming growth factorbeta 1 (TGFβ1) under hypoxia also led to increased Siah2 expression in fibroblasts. These same conditions did not alter Siah2 expression in cardiomyocytes. A cardiomyocytespecific knockout efficiency of >75% was achieved in four out of five animals via the 10day tamoxifen (20 mg/kg BW, i.p.) treatment.
Conclusion: Siah2 promotes cardiac fibrosis and hypertrophy in response to RV overload induced by PAB. Celltypespecific KO models will help understanding the precise role of Siah2 in the RV and may provide novel therapeutic approaches for RVH.

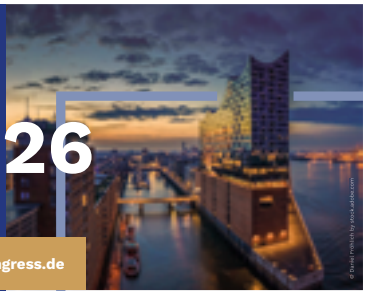

P23 Postergroup: The heart of the matter - drilling into genes & function

P2305

Angiocrine control of architectural cardiomyocytes governs mechanical integrity during ventricular compaction

SvenTore Janßen; Tram Anh Vu Nguyen; Claudia Carlantoni; Michael Spohn [1]; Danny Schreier; Ceren Saygi [1]; Marco Tarasco [2]; Lea Amina Kalayci [3]; Bente Siebels; Lukas Narjes [4]; Enrico Kittmann [5]; SaskiaLarissa JauchSpeer [5]; René Hägerling [3]; Reiner Mailer; Michael Orlich; Thomas Renné; Friederike Cuello [6]; Didier Stainier [7]; Manu Beerens; Maike Frye
Institut für Klinische Chemie und Laboratoriumsmedizin, Universitätsklinikum HamburgEppendorf, Hamburg, Germany; [1] Bioinformatics Core, Universitätsklinikum HamburgEppendorf, Hamburg, Germany; [2] Max Planck Institute for Heart and Lung Research - W. G. Kerckhoff Institute, Bad Nauheim, Germany; [3] Berlin Institute of Health, Charité - Universitätsmedizin Berlin, Berlin, Germany; [4] Department of Congenital and Pediatric Cardiac Surgery, Universitätsklinikum HamburgEppendorf, Hamburg, Germany; [5] Nephrologie/Rheumatologie und Endokrinologie/Diabetologie, III. Medizinische Klinik, Universitätsklinikum HamburgEppendorf, Hamburg, Germany; Institut für Klinische Chemie und Laboratoriumsmedizin, Universitätsklinikum HamburgEppendorf, Hamburg, Germany; [6] Institut für Experimentelle Pharmakologie und Toxikologie, Universitätsklinikum HamburgEppendorf, Hamburg, Germany; [7] Abt. III - Genetik der Entwicklung, MaxPlanckInstitut für Herz- und Lungenforschung, Bad Nauheim, Germany;

Objective: The embryonic myocardium has to withstand increasing hemodynamic and contractile loads despite the relatively low extracellular matrix (ECM) content of the developing heart. The mechanisms by which structural integrity is maintained during cardiac development while fibroblast support remains sparse are not understood.
Method: A *Pde2a*$^{flox;}$*Tie2*Cre mouse model was used to study the endothelialspecific role of phosphodiesterase 2A. Tissue stiffness measurements were conducted using a microscale nanoindentation setup. Spatial transcriptomics and singlecell RNA sequencing helped identifying unique expression patterns of ARCHCMs at singlecell resolution and localizing them within the myocardium of mice at different developmental stages. A coculturesystem of primary human coronary artery endothelial cells (HCAECs) and human induced pluripotent stem cellderived cardiomyocytes allowed us to study intercellular crosstalk exclusively via soluble proteins. The secretome of HCAECs was examined via mass spectrometry. Furthermore, bulk RNA sequencing, western blot and immunofluorescence were used to characterize both cells from in vitro experiments and in vivo tissues. ELISA was used to assess levels of cyclic nucleotides following PDE2A siRNAtreatment of HCAECs. Reanalizing publically available datasets allowed us to trace ARCHCM signatures.
Results: We identified a distinct cardiomyocyte population – which we termed architectural cardiomyocytes (ARCHCMs) - that combines ECM production with hemoglobin expression and localizes to mechanically critical regions of the developing myocardium. ARCHCMs expand during compaction and are selectively lost following Tie2lineage deletion of phosphodiesterase 2A (*Pde2a)*, which is accompanied by reduced myocardial tissue stiffness and ventricular noncompaction. Endothelialcardiomyocyte coculture experiments and angiocrine knockout models demonstrate that endothelial PDE2A regulates structural maturation of cardiomyocytes through coordinated angiocrine signaling rather than a single dominant factor. Reanalysis of mouse and zebrafish developmental and regeneration expression datasets, combined with cell state mapping in human heart failure, reveals enrichment of ARCHCM transcriptional signatures during cardiac remodeling, suggesting that this program is conserved during development and reactivated in regeneration and disease.
Conclusion: Together, our findings identify a Tie2lineageregulated cardiomyocyte specialization that acts as an intrinsic structural support mechanism for myocardial structural integrity during cardiac remodeling.

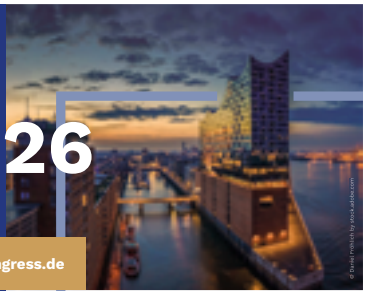

P23 Postergroup: The heart of the matter - drilling into genes & function

P2306

PLNR14del aggregation correlates with mutated mRNA fraction in cardiomyocytes

Judith Montag; Renee Maas [1]; Joost Sluijter [1]; Linda Van Laake [1]
Medical School Berlin, Berlin, Germany; [1] Department of Cardiology, Circulatory Health Laboratory, University Medical Center Utrecht, Utrecht, The Netherlands;

Objective: Phospholamban cardiomyopathy is an inherited cardiac disorder, caused by mutations in the *PLN* gene, encoding Phospholamban (PLB). PLB regulates relaxation of cardiomyocytes by inhibiting SERCA, which transports calcium from the cytoplasm to the sarcoplasmic reticulum. Mutations in PLN cause severe arrhythmogenic cardiomyopathies. One common mutation in the Netherlands is R14del (c.40_42delAGA), which is associated with altered calcium transients and formation of PLNaggregates in cardiomyocytes. It has been assumed that these aggregates affect cardiomyocyte function. In heterozygous patient tissue, as well as a heterozygous R14del mouse model, it can be observed that formation of aggregates does not affect all cardiomyocytes. Mouse models indicate that aggregation increases over time. Underlying triggers for aggregate formation have not been elucidated yet.
Method: We hypothesized that cardiomyocytes with aggregates show higher fractions of R14del mRNA. To test this, we used cryosections of four severely affected PLN R14del patients and isolated cardiomyocytes with and without aggregates. These cardiomyocytes were subjected to RTqPCR with allelespecific probes to quantify fraction of mutant and wildtype mRNA. Bulk tissue analysis was performed in comparison.
Results: Whereas bulk tissue and cardiomyocytes without aggregates show equal fractions of R14del and WT mRNA, we can show increased levels of R14del in cardiomyocytes with aggregates of up to 80%. Currently, we analyze cardiac tissue from heterozygous PLN R14del mice, in order to test whether this finding is also mimicked in the mouse model and to further assess, whether this is already detectable at early – preclinical - time points.
Conclusion: Our findings indicate PLN expression imbalance among individual cardiomyocytes. This might lead to functional heterogeneity among the cardiomyocytes which could contribute to the observed arrhythmias in PLN R14del patients. Thus, reduction of the aggregates may prove an interesting target for therapeutic interventions.

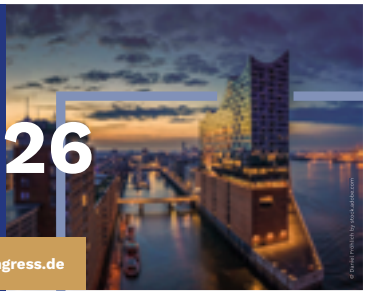

P23 Postergroup: The heart of the matter - drilling into genes & function

P2307

Gene transfer into human ventricular slices for optogenetic stimulation

Chaodi Cheng; Aida GarridoCharles; Kolja Schirge; Kathrin Kusch [1]; Thomas Mager [1]; George Kensah; Bernhard C. Danner [2]; Viacheslav O. Nikolaev [3]; Ahmed Wagdi; Malte Tiburcy [4]; Tobias Bruegmann
Institute of Cardiovascular Physiology, University Medical Center Goettingen, Göttingen, Germany; [1] Institute for Auditory Neuroscience and InnerEarLab, University Medical Center Goettingen, Göttingen, Germany; [2] Department of Cardiothoracic and Vascular Surgery, University Medical Center Goettingen, Göttingen, Germany; [3] Institute of Experimental Cardiovascular Research, University Medical Center HamburgEppendorf, Hamburg, Germany; [4] Institute of Pharmacology and Toxicology, University Medical Center Goettingen, Göttingen, Germany;

Objective: AAVmediated channelrhodopsin2 (ChR2) expression enables optogenetic pacing of cardiomyocytes *in vitro* and *in vivo in animal models, but extending this approach to human tissue has been challenging.* Human ventricular slices are a promising *ex vivo* model. However, sufficient gene transfer for optogenetic stimulation has not been demonstrated so far, with the challenge to obtain enough expression to overcome the electrotonic sink. Herein, we aimed to establish AAVmediated ChR2 gene transfer in human ventricular slices and to quantitatively relate transduction efficiency to functional optogenetic responsiveness.
Method: Human left ventricular tissue from failing hearts (N = 3) was cut into 300 µm thin slices with a vibratome and spanned into biomimetic cultivation setups (InVitroSys, Germany) for longterm culture with continuous electrical stimulation (bipolar, 3 ms, 0.5 Hz, 50 mA) and force measurements. 2.5×10^{11} or 7.5×10^{11} AAV2/9 particles (numbers indicate genome copies) expressing ChR2 in fusion with mCherry under the control of the CAG promoter were added to the chamber (lowdose AAV: n = 10 slices; highdose AAV: n =7 slices) between day 742 of culture. Optical pacing was tested with defined light intensities at 0.3 Hz. Optical pacing was evaluated and compared with electrical stimulation. Expression was quantified after tissue clearing by confocal imaging.
Results: Lightinduced contractions emerged at day 10 posttransduction, reaching functional plateau by day 30 in both groups. Optical pacing was achieved in 90% and 100% of the slices in lowdose and highdose groups, respectively, yielding comparable rheobase (0.5 ± 0.3 mW/mm² in both groups), chronaxie (11.4 ± 1.9 ms vs. 8.3 ± 0.6 ms) values and pacing thresholds (1.4 ± 0.4 mW/mm² vs. 0.6 ± 0.5 mW/mm² at 100 ms pulse width). Optical stimulation allowed pacing at frequencies up to 1.3 ± 0.2 Hz which was significantly lower compared to electrical stimulation (paired Student's ttest: p = 0.0008). Continuous illumination induced excitation block in ~30% of the slices in lowdose AAV group. Notably, correlating optical pacing thresholds with transduction efficiency revealed a minimal transduction rate of ~1015% required for reliable optical pacing.
Conclusion: By integrating longterm cultivation and AAVmediated gene transfer, we demonstrate a scalable framework for efficient gene transfer to screen for optimized AAV capsids as well as channelrhodopsin variants in intact adult human heart tissue.

P23 Postergroup: The heart of the matter - drilling into genes & function

P2308
Myo18Aγ and Myo18B play nonredundant roles in the organization of cardiac sarcomeres

Pim R. R. van Gorp; Juang Zhang; Cindy I. Bart; Sven O. Dekker; Arti A. Ramkisoensing; Daniël A. Pijnappels; Hailiang Mei; Antoine A. F. de Vries; Peter J. Hanley [1]; Markus Horsthemke [1] Leiden, The Netherlands; [1] Faculty of Medicine, Institute for Molecular Medicine, Health and Medical University Potsdam, Potsdam, Germany;

Objective: Class 18 myosins are encoded by *Myo18a* and *Myo18b*, both of which are highly expressed in the developing heart. Deletion of either gene in mice is embryonic lethal, indicating essential roles in cardiac development. Whereas *Myo18b* encodes a single protein, *Myo18a* encodes three isoforms (α, β and γ). Myo18Aγ localizes to sarcomeric Abands, similar to Myo18B, whereas Myo18Aα localizes to actin stress fibers. To investigate their roles in sarcomerogenesis, we used conditionally immortalized rat atrial myocytes (iAMs), neonatal rat ventricular myocytes (NRVMs), and isoformspecific knockout mouse models.
Method: RNASeq, immunofluorescence imaging, Western blotting and shRNAmediated knockdown were used to analyze expression patterns and sarcomere organization during cardiac differentiation. Viral vectors encoding tagged Myo18Aγ constructs were used to identify mechanisms of Aband targeting. Isoformspecific knockout mice were analyzed by echocardiography, magnetic resonance imaging, and transmission electron microscopy.
Results: Expression of Myo18Aγ and Myo18B increased during cardiac differentiation and decreased during dedifferentiation, whereas Myo18Aα expression modestly decreased. Myo18A redistributed from a perinuclear localization to Abands during differentiation, whereas Myo18B associated with Abands early during sarcomerogenesis. Analysis of truncated Myo18Aγ constructs identified amino acids 19–82 as essential for Aband targeting. In NRVMs, depletion of either Myo18Aγ or Myo18B disrupted myofibrillar organization, and neither protein compensated for loss of the other. Cardiac phenotyping revealed no obvious abnormalities in the isoformspecific knockout mouse models.
Conclusion: Myo18Aγ and Myo18B serve distinct, nonredundant roles in sarcomerogenesis and are required for sarcomeric organization. In contrast, Myo18Aα, Myo18Aβ and the Nterminus of Myo18Aγ are dispensable for embryonic development and postnatal cardiac structure and function.

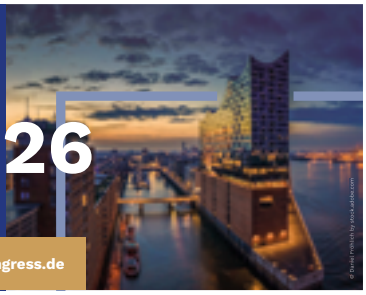

P23 Postergroup: The heart of the matter - drilling into genes & function

P2309

Impact of mutations associated with clonal hematopoiesis of indeterminate potential (CHIP) on human induced pluripotent stem cell (hiPSC)derived macrophages and their effects on cardiovascular cells

Christos Triantafyllou; Sarah Rieck; Bernd K. Fleischmann
Institute of Physiology I, University Hospital Bonn, Bonn, Germany;

Objective: Lossoffunction mutations associated with CHIP correlate with an increased risk of cardiovascular diseases, with *DNMT3A* and *TET2* being the most commonly affected genes. While the underlying pathomechanisms remain poorly understood, proinflammatory pathways in macrophages are assumed to play an important role.
Method: We differentiated and characterized hiPSCderived macrophages (hMacs) and compared them to human monocytederived macrophages (hMDMs) regarding molecular and functional aspects. To investigate the effect of CHIPcorrelated mutations on macrophages, we generated *DNMT3A* and *TET2* KO hiPSC lines and analyzed their hMac phenotypes, as well as their impact on cardiovascular cells.
Results: Flow cytometric analysis of macrophage surface markers revealed high expression in hMacs (96.8 ± 0.7% CD45+, 84.4 ± 3.9% CD14+, 91.6 ± 1.9% CD11b+), confirming the reproducibility of the differentiation. High similarity between hMacs and hMDMs was observed for both inflammasome activation and phagocytic ability via ASC speck formation and amyloidbeta uptake. Bulk RNASeq revealed enriched cell adhesion and division in hMacs and antigen presentation in hMDMs, presumably resulting from distinct developmental origins. For both generated KO hiPSC lines, we successfully confirmed pluripotency (94.3 ± 2.4% TRA160+) and differentiation potential (99.5 ± 0.2% TBXT+, 97.7 ± 1.6% SOX17+, 98.15 ± 0.8% PAX6+). Polarization into proinflammatory M1 macrophages was confirmed through increased expression levels of M1 markers (CD40, CD80, and CD86) and proinflammatory markers (*IL6*, *TNF*, *ICAM1*, and *CCL2*) using flow cytometry and qPCR. *TET2* KO M1 hMacs showed increased mRNA expression of *IL6*, suggesting the promotion of a proinflammatory phenotype.
Conclusion: Our results confirm the reproducible differentiation of hMacs, which are functionally similar to hMDMs, and the stable generation of *DNMT3A* and *TET2* KO hiPSC lines. The absence of DNMT3A and TET2 in hMacs appears to promote a proinflammatory phenotype, while their effects on cardiovascular cells will be addressed in coculture experiments.

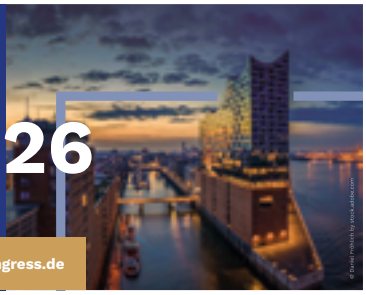

P24 Postergroup: Chloride Channels & Transporters

P2401

TMEM16Adependent Ca^{2+}activated Clchannels regulate vascular smooth muscle contraction by modulating Ca^{2+} entry and Ca^{2+} sensitivity

Marlon Gernemann; Line Mathilde Brostrup Hansen; Vladimir V. Matchkov
Department of Biomedicine, Aarhus University, Aarhus, Denmark;

Objective: Previous studies investigating the role of the TMEM16Adependent Ca^{2+}activated Clchannel in cerebrovascular contractility have reported impaired autoregulation in mice with this channel knocked down in the vascular wall. However, the physiological significance of TMEM16A channels remains controversial.
In the present study, we investigated Ca^{2+} dynamics and contractile responses to adrenergic stimulation in mouse tail arteries of wildtype (WT) mice and tamoxifeninducible smoothmusclecellspecific TMEM16A knockout (KO) mice. We hypothesized that the contribution of TMEM16A to agonistinduced contraction depends on transmural pressure.
Method: Tail arteries from WT and TMEM16AKO male mice were mounted in a pressuremyograph under noflow conditions at transmural pressures of 40, 60, or 100 mmHg. The vascular wall was loaded with the Ca^{2+}sensitive dye, FURA2/AM and alternately excited at 340 and 380 nm. Fluorescence emission at 515 nm was recorded using a fluorescent microscope and stored with Felix32 software (v.1.2, Photon Technology). Responses to cumulative concentrations of noradrenaline were assessed as changes in external diameter and in the 340/380 nm fluorescence ratio, used as an index of intracellular Ca^{2+} levels.
Results: TMEM16AKO tail arteries exhibited reduced sensitivity to noradrenaline compared to WT arteries at transmural pressures of 40 and 60 mmHg; however, this difference was absent at 100 mmHg. At 100 mmHg, TMEM16AKO arteries showed a reduced basal tone, whereas agonistinduced contraction was potentiated relative to WT arteries. Intracellular Ca^{2+} responses were greater in WT than in TMEM16AKO, particularly at 100 mmHg. These findings suggest that Ca^{2+} sensitivity increases in TMEM16AKO arteries as transmural pressure rises.
Conclusion: TMEM16Adependent Ca^{2+}activated Cl- channels play an important role in the contractile function of smooth muscle cells in mouse tail arteries by amplifying voltage-dependent Ca^{2+} influx while inversely regulating Ca^{2+}sensitivity. Further studies are required to elucidate the mechanism linking TMEM16A to modulation of smooth muscle Ca^{2+}sensitivity.

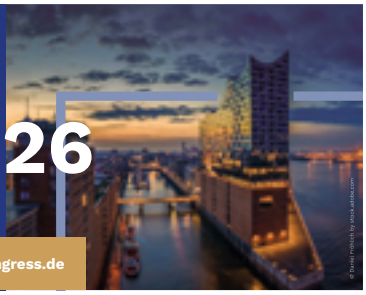

P24 Postergroup: Chloride Channels & Transporters

P2402

Expression of chloride channels in brain cancers and effects of CLIC1 on galvanotaxis of patientderived glioblastoma cells

Katrin Gärtner; Falko Lange; Anne Einsle; Katrin Porath; Tina Sellmann; Claudia Maletzki [1]; Thomas M. Freiman [2]; Rüdiger Köhling; Timo Kirschstein
OscarLangendorffInstitute of Physiology, Rostock University Medical Center, Rostock, Germany; [1] Hematology, Oncology, Palliative Medicine, Rostock University Medical Center, Rostock, Germany; [2] Department of Neurosurgery, Rostock University Medical Center, Rostock, Germany;

Objective: Chloride ion channels play a crucial role in maintaining intracellular and extracellular ion homeostasis, volume regulation, and, thus, proliferation, migration, and cell cycle control. These functions might be particularly important in brain tumors due to the cranial restriction. Their significance in the pathophysiology of glioblastomas, the most aggressive brain tumors with a very poor prognosis, is still poorly understood. This study aimed to systematically characterize chloride channel expression across different brain tumors entities and to assess the functional impact of CLIC1 on glioblastoma cell behavior.
Method: In our study, we systematically analyzed the expression of chloride channels in tissues of three different brain cancer entities, including glioblastoma, meningioma, and brain metastasis obtained from surgical resections. Tumorfree cortical tissues served as a reference. Additionally, basic clinical data and patient survival after tumor resection were determined. *In vitro*, expression patterns of chloride channels were monitored in patientderived lowpassage cell lines derived from glioblastoma and brain metastasis. To assess the effect of CLIC1 on proliferation, induction of apoptosis, and migration in the electrical field, ion channel function was perturbed employing IAA94.
Results: We identified a heterogeneous expression pattern of chloride channels among the different tumor entities. Moreover, among the investigated ion channels, CLCN3 and CLIC1 were found to be the highest expressed candidates. Interestingly, PACC1, a newly identified chloride channel, was poorly expressed in the brain metastasis and meningioma cohorts. Those findings were, in part, preserved in the *in vitro* tumor models. Inhibition of CLIC1 had only a minor effect on the proliferation of glioblastoma cells. In the direct current electrical field, glioblastoma cells presented a preferential anodal migration. Exposing the cells to IAA94 may diminish the directed migration.
Conclusion: Our results suggest that chloride channels exhibit a heterogeneous expression pattern across different brain tumor entities, with CLCN3 and CLIC1 showing the highest expression. Abundantly expressed CLIC1 appears to be important for the directional migration of glioblastoma cells in the electrical field.

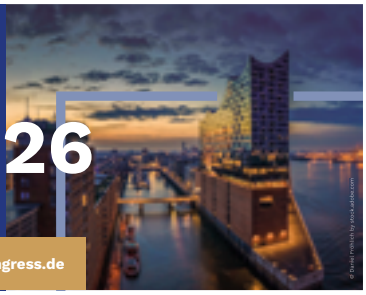

P24 Postergroup: Chloride Channels & Transporters

P2403

The chloride intracellular channel 1 (CLIC1) is essential for microglial morphodynamics and neuroinflammation

Ali Rifat; Tom Bickel [1]; Linus Alschäfscky [1]; Julia Onken [2]; Andranik Ivanov [3]; Giulia Albertini [4]; Bart De Strooper [4]; Jörg Rolf Paul Geiger; Christian Madry Institut für Neurophysiologie, Charité - Universitätsmedizin Berlin, Berlin, Germany; [1] Institute of Neurophysiology, Charité - Universitätsmedizin Berlin, Berlin, Germany; [2] Department of Neurosurgery, Charité - Universitätsmedizin Berlin, Berlin, Germany; [3] Core Unit Bioinformatics, Berlin Institute of Health, Charité – Universitätsmedizin Berlin, Berlin, Germany; [4] Department of Neurosciences, KU Leuven, Leuven, Belgium;

Objective: Microglia are the brain's innate immune cells and essential for maintaining brain homeostasis. The ability of microglia to react effectively to physiological and pathophysiological challenges depends on their morphodynamic versatility and inflammatory response, yet the molecular determinants, particularly ion channels and receptors, remain poorly understood. Given the implication of chloridedependent signaling in peripheral immune cell function, we aimed to investigate the role of chloride channels in mouse and human brain tissue.

Method: We combined singlecell RNA sequencing, RNAscope in situ hybridization, immunohistochemistry, live multiphoton imaging and patchclamp electrophysiology. These methods were combined with pharmacological and genetic interventions for target validation and mechanistic analyses. Acute mouse brain slices and human temporal lobe resections as well as human stem cell–derived microglia xenografted into mouse brains were used to assess microglial morphology, surveillance dynamics and electrophysiological properties.

Results: We identified CLIC1 as the most highly expressed Cl- channel in mouse and human microglia, and showed that it is essential for maintaining their physiological surveillance in the brain parenchyma. Mechanistic analyses identified that morphodynamic control by CLIC1 is independent of cellular Cl- homeostasis and involves interactions with ezrinradixinmoesin (ERM) proteins. Consistent with an influence on the actin cytoskeleton, CLIC1 and ERM regulated actindependent microglial dynamics. We also found that inhibiting CLIC1 strongly suppressed the NLRP3 inflammasomedependent release of IL1β from mouse and human brain microglia.

Conclusion: CLIC1 is a central regulator of microglial morphodynamics and inflammatory signaling. Rather than functioning as a classical ion channel, CLIC1 acts via chlorideindependent mechanisms linked to actin cytoskeleton remodeling and ERMassociated pathways. Given its exclusive expression in microglia controlling NLRP3dependent IL1β release, blockade of CLIC1 could have important therapeutic implications, since NLRP3 is a major driver of inflammation and neurodegenerative conditions such as Alzheimer's disease.

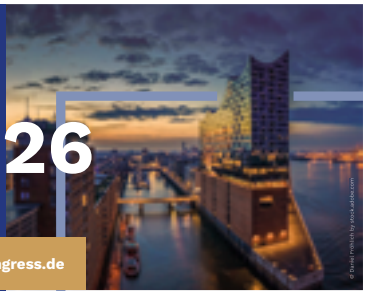

P24 Postergroup: Chloride Channels & Transporters

P2405

TMEM9s as molecular regulators of endosomal chloride/proton exchangers and their role in preventing diseaseassociated hyperactivity

Sumanta Kar; Rosa PlanellsCases; Viktoriia Vorobeva; Franziska Schmitt; Uwe Schulte [1]; Marina Schrecker [2]; Richard Hite [2]; Bernd Fakler [1]; Thomas J. Jentsch LeibnizForschungsinstitut für Molekulare Pharmakologie, MaxDelbrückCentrum für Molekulare Medizin, Berlin, Germany; [1] Institut für Physiologie, Universität Freiburg, Freiburg, Germany; [2] Structural Biology Program, Sloan Kettering Institute, Memorial Sloan Kettering Cancer Center (MSK) - NCI, New York, United States;

Objective: Endosomal activity fundamentally relies on their ionic balance, with increasing recognition of the critical role of luminal chloride (Cl) alongside protons (H^+). This balance is maintained by five distinct CLC chloride/proton exchangers in the endolysosomal system, each essential for cellular health, as their dysfunction (gain of function/ loss of function) results in severe disease. Though several members of CLC family had accessory ßsubunits, but there was no known subunits of endosomal ClC3, ClC4 and ClC5.
Method: Here, we have identified TMEM9A and TMEM9B as essential βsubunits for ClC3, ClC4, and ClC5. These transmembrane proteins are required not only for the stability and trafficking of their associated CLC transporters but also for regulating their activity. Our study combined highresolution complexome profiling and animal studies to identify Tmem9s study their physiological importance. We further performed functional assays through electrophysiology, vesiclegeneration assay in mammalian cells and flow cytometry.
Results: Mice lacking both TMEM9 and TMEM9B (T9s) exhibit dramatically reduced levels of these CLCs and fail to survive, highlighting their physiological necessity. In addition to their trafficking role, TMEM9 proteins strongly inhibit CLC ion transport. We found that these T9s express in wide range of tissues, and any alteration in their expression, affects the expression and function of ClC3, 4 and 5. This tonic inhibition serves as a protective mechanism, preventing excessive Cl^- accumulation and endosomal swelling. In mammalian cells, these T9s rescue the endoplasmic reticulum expression of CLC5. We studied functional regulation of these accessory subunits and identified two independent motifs, first one is trafficking regulatory motis, pACmotif. This pAC motif in T9s are absolute necessary for the endocytosis/ recycling of the ClCs. The inhibitory effect depends on a conserved Cterminal domain in T9s that interacts with multiple sites on the CLCs. Through our CryoEM structural analysis, we have identified how TMEM9 is inhibiting ClC3 function by occluding the cytosolic chloride entry pathway. Furthermore, the phosphoinositide PI(3,5)P2 was found to stabilize the TMEM9–ClC3 complex and is essential for maintaining effective inhibition of ClC3 activity.
Conclusion: Our study shows controlled inhibition of ClC transporters is essential for maintaining physiological function. And any loss of regulation can contribute to disease. Importantly, diseasecausing mutations in CLC genes often weaken this inhibition, leading to pathological gainoffunction through unregulated ion transport. These findings highlight the necessity of tightly controlled CLC activity and call for a revision of existing models of endosomal ion regulation, emphasizing the importance of regulatory suppression alongside trafficking activity.

16-19 September 2026 — Hamburg, Germany
Physiology with Flow: Set Sail!
PHYSIOLOGY in FOCUS 2026
The joint ANNUAL MEETING OF THE GERMAN PHYSIOLOGICAL SOCIETY
and the SCANDINAVIAN PHYSIOLOGICAL SOCIETY
www.dpg-congress.de

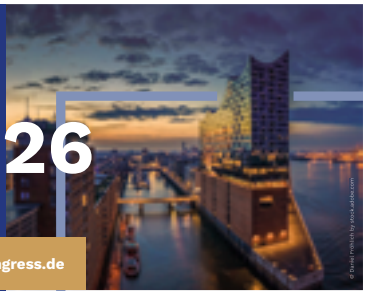

P24 Postergroup: Chloride Channels & Transporters

P2406
Cardiogenic lung edema is mediated by WNK1SPAK/OSR1NKCC1 signaling

Jie Yang; Juliana Falivene; Sarah Weidenfeld; Rose Deschler; Isabelle Langner; Tim Wendt; Gefei Li; Jana Grune; Wolfgang Kübler
Institut für Physiologie, Campus Charité Mitte, Charité - Universitätsmedizin Berlin, Berlin, Germany;

Objective: Cardiogenic lung edema is a common complication of leftsided heart failure with considerable morbidity and mortality and commonly viewed as the result of passive fluid filtration across an intact alveolocapillary barrier. In previous work, however, we identified a critical role for the furosemidesensitive Na?K?2Cl? cotransporter 1 (NKCC1) as driver of alveolar ion and fluid secretion by supplying basolateral Cl- influx and facilitating apical Cl- secretion in alveolar epithelial cells. Yet, how hydrostatic pressure modulates NKCC1 activity remains unclear. This study aimed to determine whether activation of the WNK1–SPAK/OSR1 signaling pathway regulates NKCC1 activation in cardiogenic edema.
Method: Hydrostatic edema was induced in isolated perfused lungs (IPL) of C57BL/6J mice by increasing left atrial pressure (P_{LA}) from 2.5 to 7 cmH2O. Lung wettodry (W/D) weight ratio, protein expression and phosphorylation were analyzed. Pathway analysis was performed using pharmacologic inhibitors targeting NKCC1 (furosemide), WNK1 (WNK463), and SPAK/OSR1(closantel, rafoxanide), or genetic knockout models including global *Nkcc1*$^{+/-}$, *Wnk1*$^{+/-}$, *Spak*$^{-/-}$, *Osr1*$^{-/-}$ and epithelial specific *Nkcc1* (*Nkx2.1*$^{\Delta NKCC1}$) deficient mice. *In vivo*, cardiogenic edema was assessed in mice following left anterior descending (LAD) coronary artery ligation.

Results: P_{LA} elevation increased lung W/D ratio and Nkcc1 phosphorylation in IPL of WT mice. Nkcc1 inhibition or global as well as epithelial specific *Nkcc1* deletion reduced edema formation. Wnk1 inhibition or genetic heterozygous deletion of *Wnk1* decreased Nkcc1 phosphorylation and fluid accumulation. Spak/Osr1 phosphorylation increased under hydrostatic stress but this response was attenuated in *Wnk1*deficient lungs. Both pharmacological inhibition and genetic deletion of *Spak/Osr1* attenuated cardiogenic edema and Nkcc1 activation. *In vivo*, *Nkcc1*deficient mice had less pulmonary edema following LAD ligation.
Conclusion: Cardiogenic edema is the result of active cellular signalling rather than passive fluid filtration. Specifically, activation of WNK1 with subsequent phosphorylation of the downstream kinases SPAK and OSR1 drives alveolar fluid secretion via NKCC1. These results provide a novel extrarenal mechanism of action for the wellestablished antiedematous effects of loop diuretics in the treatment of cardiogenic pulmonary edema and point towards WNK1, SPAK/OSR1 and NKCC1 as novel promising therapeutic targets.

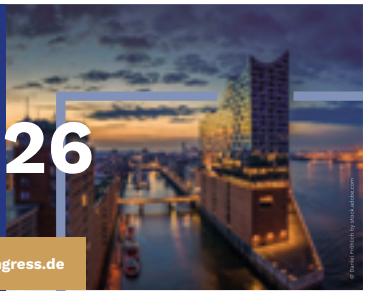

P24 Postergroup: Chloride Channels & Transporters

P2407

Cadmium complexation with glutathione: new insights into cellular uptake mechanisms

Nadiya Romanova; Daniel Hebrok; Andreas Mix [1]; Travis Issler [2]; Elmar J. Prenner [2]; WingKee Lee
Physiology and Pathophysiology of Cells and Membranes, Medical Faculty, Bielefeld University, Bielefeld, Germany; [1] Inorganic Chemistry and Structural Chemistry, Faculty of Chemistry, Bielefeld University, Bielefeld, Germany; [2] Department of Biological Sciences, University of Calgary, Calgary, Canada;

Objective: Cadmium (Cd) accumulates in proximal tubule cells (PTCs) and drives chronic nephrotoxicity. Cd complexes with glutathione (GSH), but CdGSH uptake into PTCs is unclarified. We hypothesized that CdGSH is cleaved by brush border γglutamyltransferases (GGT) yielding glutamate and cysteinylglycine, followed by dipeptidase hydrolysis to cysteine and glycine, resulting in Cdthiol species (GlyCysCdCysGly and CysCdCys), which could fulfil amino acid transporter (AAT) constraints rather than intact polar CdGSH. Candidate routes include xCT/SLC7A11, EAAT3/SLC1A1, B^0AT1/B^0AT3, and LAT1/LAT2.
Method: Renal PTC lines (WKPT, HPCT, HK2, SA7K) were exposed to ionic Cd or freshly preformed CdGSH (1:2). Toxicity was quantified by MTT assays, oxidative stress by DHR123 oxidation to Rh^+ fluorescence (60180 min) and lipid peroxidation by C11BODIPY581/591. GGT1/5 expression was quantified by qPCR. Extracellular processing and amino acid transport were probed with GGT inhibitor acivicin (5 µM), cystine or asparagine (02 mM), the xCT inhibitor erastin (00.5 µM) and pH adjustment (6.58.5). CdGSH coordination was evaluated by NMR.
Results: GSH complexation rightshifted the EC_{50} 11 µM for Cd (MTT, 24 h) by sixfold across four PTC lines. In WKPT cells, Cd (50 µM) increased ROS to 270% and 177% of control at 60 and 180 min, respectively, and lipid ROS to 270% at 60 min, whereas equimolar CdGSH caused weaker responses in ROS (109115%) and lipid peroxidation (156%). GGT1 mRNA predominated modestly in HPCT cells (2.8fold) and 20100 fold in WKPT, HK2 and SA7K cells. Acivicin and cystine partially reversed CdGSH toxicity, but not that of Cd^{2+}, consistent with extracellular CdGSH processing. Erastin reduced WKPT viability and flattened the CdGSH response, supporting functional coupling to xCT/SLC7A11dependent cystine transport and GSHredox homeostasis. Neither asparagine nor pH shift altered CdGSH or Cdinduced toxicity, arguing against asparaginesensitive AATs. NMR analyses predict predominant linear GlyCysCdCysGly and CysCdCys species, sterically compatible with cystine AATs.
Conclusion: GSH ligation attenuates Cdinduced ROS generation and cytotoxicity but does not abolish Cd toxicity in renal PTCs. GGTdependent processing of CdGSH generates transportcompetent Cdthiol metabolites that enter cells through cystinesensitive AATs, potentially by xCT/SLC7A11.

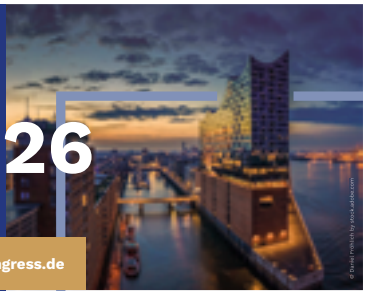

P24 Postergroup: Chloride Channels & Transporters

P2408

NaKCl cotransporter (NKCC) mediates vesicular salt transport relevant for mineralization in a marine model organism

Smilla Tetzlaff; Marian Hu
Physiologisches Institut, Christian
Albrechts

Objective: The NaKClcotransporter (NKCC) plays a crucial role in salt resorption and urine concentration in mammalian kidneys as well as in bone forming osteoblasts. Interestingly, in a marine model animal, the sea urchin larva NKCC is also enriched in mineralizing cells (PMCs) that generate the calcitic endoskeleton. PMCs endocytose seawater to absorb calcium ions that are delivered to the skeleton. Therefore, in this process large amounts of sodium chloride must be removed from the endocytotic vesicle and the cell to concentrate calcium ions to produce the CaCO3 skeleton. We investigated the role of the NaKCl cotransporter (NKCC) in promoting the removal of sodium and chloride ions from endocytotic, seawaterfilled vesicles.
Method: First, using antibody stainings in combination with endocytosis markers we investigated the subcellular localization of NKCC. Furthermore, we used the loopdiuretic azosemide to inhibit NKCC and investigated the impact on skeleton formation. Additionally, we used the cell impermeable sodium dye, corona green, to determine the sodium concentration within endocytotic vesicles of PMCs when the inhibitor is present. Finally, we used calcein quenching to determine water contents of endocytotic vesicles.
Results: The antibody staining revealed the presence of NKCC within endocytosed vesicles of PMCs and their syncytium. When NKCC is inhibited with azosemide the larvae show impaired skeletogenesis and calcium deposition into the skeleton. Additionally, PMCs treated with azosemide had significantly higher fluorescence intensities compared to control larvae indicating higher sodium concentrations in endocytosed vesicles under NKCC inhibition. Calcein quenching additionally revealed that inhibition of NKCC was accompanied by higher calcein fluorescence indicating vesicular water retention.
Conclusion: Our findings point towards a novel role of the NKCC to mediate salt transport in endocytotic vesicles of mineralizing cells. This export of salt from endocytotic vesicles can provide the osmotic driving force to remove water from these vesicles and thereby concentrates the remaining ions that are necessary to precipitate CaCO3. Extensive endocytosis of extracellular fluids and mineral exocytosis are a general feature associated with invertebrate and vertebrate mineralizing cells, therefore a detailed mechanistic understanding of osmolyte and water transport represents an important task to better understand the conserved physiology of mineralizing cells.

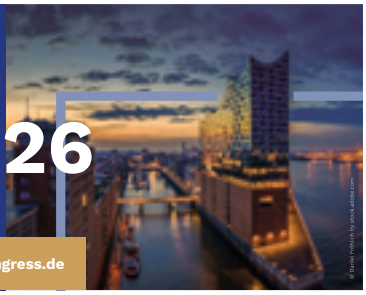

P24 Postergroup: Chloride Channels & Transporters

P2409

Beyond ion channel rescue: wtCFTR mRNA reprograms epithelial homeostasis in cystic fibrosis airway epithelia

Roshani Narayan Singh; WolfMichael Weber; Heymut Omran; Joerg GrosseOnnebrink Allgemeine Pädiatrie, Klinik für Kinder- und Jugendmedizin, Westfälische WilhelmsUniversität Münster, Münster, Germany;

Objective: Cystic fibrosis (CF) is caused by pathogenic variants in the CFTR gene, with ~10– 15% of patients lacking effective CFTR modulator therapy. Wildtype CFTR mRNA (wtCFTRmRNA) delivery represents a promising variantindependent strategy, but its capacity to restore epithelial function and to induce broader transcriptomic remodelling of the CF airway epithelium has not been systematically characterised.

Method: Primary human nasal epithelial cells from CF patients and healthy controls were differentiated at air–liquid interface. CF cultures were treated apically with chitosan nanoparticledelivered wtCFTRmRNA. Transepithelial ion transport was assessed using a modified Multi Transepithelial Current Clamp (MTECC) Ussing chamber system. Apical CFTR localisation was evaluated by immunofluorescence. Bulk RNA sequencing was performed on treated and matched untreated CF cultures to assess therapyassociated transcriptomic changes.

Results: cAMPmediated conductance (ΔG_t) increased from −0.012 ± 0.03 mS/cm² to 0.293 ± 0.038 mS/cm² (N=15), coinciding with the recovery and restoration of apical CFTR localisation. Bulk RNAseq revealed 5,583 differentially expressed genes (p_adj < 0.05) with clear separation of treated and untreated samples by principal component analysis. Treatment upregulated ionocyte markers (FOXi1, BSND), ciliogenesis regulators (FOXJ1, DNAH5), and secretory cell genes, while ER stress (HSPA6/7) and NFκBassociated inflammatory mediators (CXCL8, TNF, IL1B) were attenuated. No therapyassociated toxicity was detected.

Conclusion: Chitosanmediated wtCFTRmRNA delivery restores functional CFTR activity and induces broad transcriptomic remodelling of CF airway epithelia, suggesting effects on epithelial homeostasis extending beyond ion transport correction. Singlecell resolution analysis of an expanded cohort is underway.

P24 Postergroup: Chloride Channels & Transporters

P2410

Investigations of the binding of small molecule modulators of TMEM175 channels

Zizhuo Lu; Sönke Cordeiro; Thomas Baukrowitz; Han Sun [1]
Physiologisches Institut, ChristianAlbrechtsUniversität Kiel, Kiel, Germany; [1]
LeibnizForschungsinstitut für Molekulare Pharmakologie im Forschungsverbund Berlin e.V. (FMP), Berlin, Germany;

Objective: TMEM175 is an ion channel localized to endosomal and lysosomal membranes. It is primarily characterized as a K+ channel but also exhibits proton permeability, thereby contributing to lysosomal pH regulation. Lossoffunction variants of TMEM175 have been linked to Parkinson's disease, likely through impaired lysosomal proteolysis and the consequent accumulation of toxic proteins in dopaminergic neurons of the substantia nigra. In contrast, gainoffunction TMEM175 variants have been reported to exert neuroprotective effects. Collectively, these findings suggest that pharmacological activation of TMEM175 represents a promising therapeutic strategy for Parkinson's disease. Though some compounds have been reported to activate TMEM175 none of them seems to be selective for TMEM175 channels. In addition, the molecular mechanisms underlying TMEM175 activation remain poorly understood. A recently published study elucidated the cryoEM structure of human TMEM175 and proposed docking models for small molecules activating TMEM175 channels (Zhu et al. 2025). We aimed to identify binding sites for additional compounds that we discovered to activate TMEM175 channels. Building on these structural and pharmacological studies, the present work aims to define the binding sites of small molecule activators on TMEM175 and to elucidate the structural mechanisms underlying TMEM175 activation.
Method: We conducted our own docking studies with DCPIB, a compound that was also tested by Zhu et al. Our dockings revealed an alternative binding site for DCPIB at the cytoplasmic entrance of the channel pore, highlighting unresolved structural questions regarding small molecule–TMEM175 interactions. To determine where the interaction between DCPIB and the channel actually occurs, we mutated the relevant amino acids using sitedirected mutagenesis. We then characterized these mutated channels in patchclamp studies to assess their affinity for various small molecules.
Results: Our control measurements with mutations proposed to be involved in DCPIB binding by the cryoEM study are clearly contradictory to results published by Zhu et al. Instead, we were able to identify a residue at the cytoplasmatic entrance of the channel pore that significantly reduced the binding affinity of various small molecule activators, including DCPIB.
Conclusion: In this study, we identified a residue at the cytoplasmic entrance of the TMEM175 channel pore that significantly reduces the binding affinity of multiple smallmolecule activators, including DCPIB. This finding establishes the cytoplasmic pore region as a key site for pharmacological modulation of TMEM175. Defining this residue provides a structural basis for the rational optimization of selective TMEM175targeted therapeutics for Parkinson's disease.

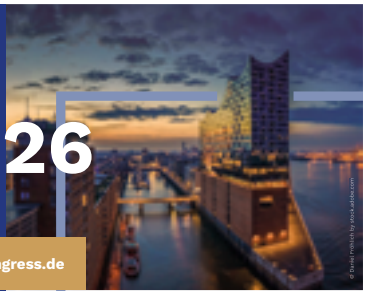

P24 Postergroup: Chloride Channels & Transporters

P2411

PAK1 deficiency reduces pharmacologically induced epithelial secretion in mouse colon tissue

Saeed Khomeijani Farahani; Martin Grunau; P. J. Hanley [1]; Ulla G. Knaus [2]; Ervice Vidal Pouokam Kamgné
Department of Human Medicine, Institute of Translational Medicine for Health Care Systems (ITM), MSB Medicalschool Berlin, Berlin, Germany; [1] Department of Human Medicine, IMM Institute for Molecular Medicine, HMU Health and Medical University, Potsdam, Germany; [2] School of Medicine, University College Dublin, Dublin, Ireland;

Objective: PAK1 is a cytoskeletonregulating kinase, but whether loss of PAK1 affects epithelial ion transport in colon tissue is still not clear. We therefore tested whether PAK1 deficiency changes pharmacologically induced secretion in mouse colon.
Method: Proximal and distal colon tissues from control and PAK1deficient mice were mounted in Ussing chambers under standard Parsons solution. Shortcircuit current responses were measured after pharmacological stimulation with carbachol and forskolin. Bumetanide was added after stimulation to estimate the NKCC1dependent component of the activated secretory current. Mouse tissues were obtained from animals maintained under approved procedures according to institutional regulations and EU Directive 2010/63/EU. Data are given as difference to the baseline just prior to administration of the drug and shown as mean ± SEM in $\mu A/cm^2$ and were compared by twotailed Welch's ttest.
Results: In proximal colon, carbacholinduced current was lower in PAK1deficient tissue than in control tissue (26.25 ± 7.91, n=12 vs. 14.09 ± 5.43, n=7; p=0.10). Forskolininduced current was also reduced (61.53 ± 17.07, n=14 vs. 36.56 ± 11.56, n=11; p=0.13), and the bumetanidesensitive component was smaller (−30.83 ± 8.90, n=12 vs. −12.84 ± 5.69, n=8; p=0.05). In distal colon, the differences were more pronounced. Carbachol responses were reduced from 71.68 ± 19.16 in controls to 37.40 ± 5.53 in PAK1deficient tissue (n=15 vs. 10; p=0.01). Forskolin responses were reduced from 138.71 ± 40.04 to 78.42 ± 24.80 (n=13 vs. 11; p=0.03), and bumetanidesensitive currents were reduced from −76.19 ± 21.99 to −30.27 ± 11.50 (n=13 vs. 10; p=0.005).
Conclusion: These data suggest that PAK1 deficiency reduces epithelial secretory capacity in mouse colon, especially in the distal segment. Since both cAMPdependent and Ca^{2+}dependent responses were reduced, the effect is unlikely to reflect only one single channel. Rather, PAK1 may support the organization or activity of the epithelial secretory machinery through cytoskeletondependent mechanisms. Followup pharmacology and ion-substitution experiments will test CFTR dependence, basolateral Na^+dependent Cl? loading and possible bicarbonate contribution.

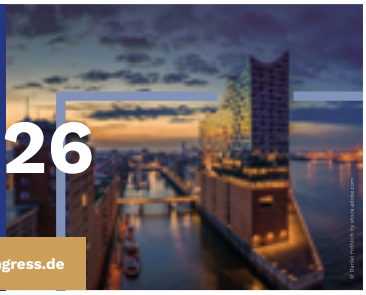

P24 Postergroup: Chloride Channels & Transporters

P2412

Sodium/hydrogen exchanger 2 (NHE2) deficiency enhances motility and epithelialmesenchymal transition (EMT) in intestinal epithelial cells

Ju Wang; Anna Seidler; Anurak Singh; Christian Stock; Ursula Seidler; Katerina Nikolovska
Department of Gastroenterology, Hepatology, Infectious Diseases and Endocrinology, Hannover Medical School, Hannover, Germany;

Objective: Epithelial cell migration is essential for intestinal homeostasis and regeneration. Migration is initiated as epithelial cells exit the stem cell compartment and enter the transitamplifying zone, followed by directional movement toward the crypt surface during their differentiation. As Na^+/H^+ exchanger isoform 2 (NHE2) shows maximal activity in the region where migration begins, we hypothesized that NHE2 might be involved in epithelial cell migration.

Method: Colonocyte migration was analyzed in wildtype (wt) and nhe2$^{-/-}$ mice using bromodeoxyuridine (BrdU) labeling. All experiments were performed using nhe2$^{-/-}$ and wt littermates, congenic on the FVB/N background, killed by cervical dislocation after light isoflurane anesthesia. In parallel, a 2D colonic organoid woundhealing model was established to assess restitution velocity, intracellular pH (pH_i) regulation, and epithelialmesenchymal transition (EMT)associated changes.

Results: BrdU tracing demonstrated significantly accelerated migration of colonocytes along the crypt axis in nhe2$^{-/-}$mice compared with wt littermates. Increased migration was associated with reduced expression of the adherens junction protein Ecadherin and the tight junction protein ZO1 in the midcrypt region, indicating impaired junctional organization during differentiation. Consistently, nhe2$^{-/-}$ colonocytes showed enhanced restitution velocity *in vitro*. Whereas wt colonocytes migrated collectively as epithelial sheets, nhe2$^{-/-}$ cells exhibited loss of epithelial morphology, increased detachment from the monolayer, and singlecell migration. Cells at the wound edge displayed reduced Ecadherin and occludin, but increased vimentin expression, consistent with EMTlike remodeling. Migratory nhe2$^{-/-}$ colonocytes also exhibited reduced pH_i despite increased NHE activity, which was abolished by pharmacological inhibition of NHE1. NHE8 expression was absent at the wound front of nhe2$^{-/-}$cultures.

Conclusion: These findings identify NHE2 as a key regulator of epithelial junctional integrity, pH_i homeostasis, and coordinated epithelial migration during intestinal renewal.

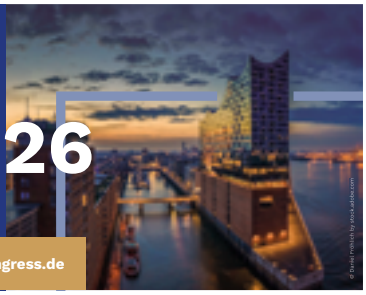

P24 Postergroup: Chloride Channels & Transporters

P2413

Dynamic regulation of SLC26A9 observed in excised membranes from *Xenopus laevis* oocytes

Jurek Loho
Department of Neurophysiology, Institute of Physiology and Pathophysiology, Phillips Universität Marburg, Cölbe, Germany;

Objective: In epithelial cells of the lung and stomach, the membrane transport protein Solute Carrier Family 26 Member A9 (SLC26A9) functions as an electrogenic Cl- channel, playing a crucial role in airway surface hydration and gastric acid production. The SLC26A9 protein contains a STAS intervening sequence (IVS) and a Cterminus (CT), whose removal enhances surface localisation and transport activity, respectively, resulting in a at least fourfold increase in transport rates. Preliminary experiments yielded findings suggesting that SLC26A9 may be regulated through phosphorylation, a mechanism that has not yet been described for any member of the SLC26 family. The purpose of this study is to further investigate this potentially novel regulatory mechanism of SLC26A9.
Method: Electrophysiologically detectable transport currents were used to identify electrogenic transport modes by altering the concentration gradient and genetically modifying SLC26A9. These currents were recorded from excised giant patches of oocyte membrane obtained from oocytes injected with a GFPtagged RNA vector containing different SLC26A9 constructs. Insideout and outsideout configurations were used to investigate differences in the extracellular and intracellular accessibility of SLC26A9 by adjusting the Cl- concentration gradient to isolate Cl- transport currents.
Results: Insideout recordings produced large, stable currents, whereas outsideout recordings exhibited strong and rapid rundown of SLC26A9mediated currents. This rundown could be prevented by applying Mg^{2+}+ATP to the intracellular side of the patch. Furthermore, truncation of the Cterminus of SLC26A9 abolished the rundown observed in outsideout recordings.
Mutation of three predicted phosphorylation sites within the Cterminus, substituting serine residues with alanine, resulted in a complete loss of SLC26A9induced currents.
Conclusion: These findings indicate that the observed rundown reflects a dynamic regulatory mechanism of SLC26A9 that has not previously been described for any member of the SLC26 family. The experiments strongly suggest that SLC26A9 is dynamically regulated through phosphorylation within the Cterminus. Further experiments will be required to elucidate the underlying molecular mechanism.

P24 Postergroup: Chloride Channels & Transporters

P2414

Levetiracetam targets Ncbe in mouse choroid plexus and alters cerebrospinal fluid secretion and pH

Laura Oellegaard Johnsen; Lasse Messell Desdorf [1]; Nicoline Staerke Jensen [1]; Jeppe Praetorius; Helle Hasager Damkier
Department of Biomedicine, Aarhus University, Aarhus, Denmark; [1] Department of Chemistry, Aarhus University, Aarhus, Denmark;

Objective: The Na^+dependent Cl/HCO_3^- exchanger Ncbe (*Slc4a10*) is a major basolateral HCO_3 uptake pathway in the choroid plexus and contributes to both cerebrospinal fluid (CSF) secretion and pH regulation. The antiepileptic drug levetiracetam (LEV) has previously been suggested to inhibit Na^+dependent HCO_3^- transport in hippocampal neurons. We therefore investigated whether LEV directly affects Ncbe activity and thereby alters CSF physiology.
Method: Ncbe and NBCn1 activity were assessed in transfected NIH3T3 cells by measuring Na^+dependent pH_i recovery after NH_4Clinduced acidification. In freshly isolated mouse choroid plexus epithelial cells, total Na^+dependent base import was assessed using the same approach. In male mice anaesthetized with ketamine/xylazine (80/10 mg kg^1 i.p.) CSF secretion was determined by ventriculocisternal perfusion, CSF pH by intraventricular microelectrode measurements, and transporter abundance by semiquantitative immunoblotting.
Results: LEV (0.5 mM) inhibited Ncbemediated transport by 57% in Ncbeexpressing NIH3T3 cells (unpaired ttest, n = 9, p = 0.007) but did not affect NBCn1mediated transport. In isolated choroid plexus epithelial cells, LEV reduced Na^+dependent pH_i recovery by 42% (oneway ANOVA, n = 5–6, p = 0.02), comparable to DIDS inhibition, and combined LEV + DIDS produced no additional effect. Semiquantitative immunoblotting of choroid plexus tissue (n = 5 treated, 8–9 controls) showed reduced abundance of Ncbe and NBCe2, whereas AQP1 abundance increased after 5 days of LEV treatment. CSF pH decreased after 5 days of LEV treatment from 6.95 ± 0.02 to 6.91 ± 0.03 (mean ± SD, n = 5, unpaired ttest, p = 0.031). Despite these inhibitory effects and with no change in initial ventricular CSF volume, CSF secretion rate increased by 141% versus control (twoway ANOVA, n = 5, p = 0.013).
Conclusion: These findings identify Ncbe as a direct pharmacological target of LEV in the choroid plexus and show that inhibition of basolateral HCO_3^- transport alters both CSF acidbase balance and CSF secretion.

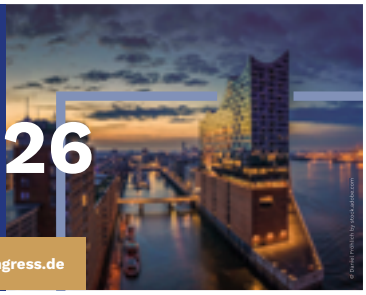

P25 Postergroup: Cardiac Function - essential knowledge

P2501

Impact of Cardiomyocytes Monoamine Oxidase B during Hypoxia/Reoxygenation

Beatrice Mantuano; Claudia Penna [1]; Pasquale Pagliaro [1]; Rainer Schulz; Jacqueline Heger
Fachbereich Medizin, Physiologisches Institut, JustusLiebigUniversität Gießen, Gießen, Germany; [1] Department Clinical and Biological Sciences, Università Degli Studi di Torino, Orbassano, Italy;

Objective: Ischemiareperfusion injury (IRI) is a multifactorial pathological condition in which excessive reactive oxygen species (ROS) production plays a central role in cardiomyocyte damage. Monoamine oxidase B (MAOB) is a mitochondrial protein that degrades biogenic amines, thereby producing ROS. Cardiomyocytespecific MAOB deletion protected against I/R. To gain a better understanding of the underlying protective mechanisms, we focus now on isolated adult cardiomyocytes

Method: Cardiomyocytes were isolated from adult mice and cultured either under normoxic conditions (pH 6.8, 37°C, 5% CO_2) or under hypoxic (glucosefree buffer, pH 6.2, 37°C, <1% O_2, 5% CO_2, 95 % N_2) and reoxygenation (pH 6.8, 37°C, 5% CO2) conditions. Necrotic cells were assessed using propidium iodide. Cardiomyocyte length, width and area were evaluated by phase contrast microscopy.

Results: Under normoxic conditions stimulation of cardiomyocytes with 250 µM phenethylamine (PEA, MAOB substrate) for five hours increased the number of necrotic cells and decreased cell length which could both be reversed by preincubation of cells for one hour with the selective MAOB inhibitor selegiline (1 µM). At 1 uM, the inhibitor alone had no effect, whereas a higher dose led to cell death. After 180 minutes of hypoxia and two hours of reoxygenation, cell necrosis was increased and both, cell width and length were decreased compared to control. PEA further significantly aggravated the hypoxia/reoxygenation damage. All effects were significantly reduced by selegiline (1µM).

Conclusion: MAOBderived ROS promoted necrotic cardiomyocyte death and structural damage. Pretreatment with low dose selegiline(1uM) confers significant cardioprotection

P25 Postergroup: Cardiac Function - essential knowledge

P2502

Sex Matters: Divergent Cardiac Remodelling After Myocardial Infarction

Jeanette Eresch; Daniel Ohrenberg; Alicia Watson; Adhi Shree Raya Asunama; Aya Abouissa; Julio Cordero [1]; Felix A. Trogisch; Volker Ast [2]; Jörg Heineke
Cardiovascular Physiology, European Center of Angioscience, Medical Faculty Mannheim, University Heidelberg, Mannheim, Germany; [1] Cardiovascular Genomics and Epigenomics, European Center of Angioscience, Medical Faculty Mannheim, University Heidelberg, Mannheim, Germany; [2] Next Generation Sequencing Core Facility, Clinical Chemistry, Medical Faculty Mannheim, University Heidelberg, Mannheim, Germany;

Objective: After myocardial infarction (MI), the subsequent loss of cardiomyocytes leads to remodelling processes and fibrotic scar formation. Sex differences critically influence cardiac repair following MI. In mouse models of MI, female mice had better cardiac outcomes and a lower risk of cardiac rupture compared to males. Similarly female MI patients demonstrate better systolic function and exhibiting a reduced propensity to contract heart failure over time when compared with male patient. These effects are attributed to the cardioprotective role of estrogen, whereas testosterone promotes adverse remodelling. However, the underlying mechanisms remain unclear. This study aims to further elucidate sexdependent cardiac remodelling after MI.
Method: To investigate cardiac remodelling after MI we used wildtype male and female littermates of a phenotypical unaffected mouse line in a minimalinvasive myocardial infarction model. MI was induced via ultrasoundguided coagulation of the left anterior descending artery (LAD) and confirmed by absence of distal blood flow, akinesia and ECG changes. Sham mice were subjected to the same procedure without occlusion. Echocardiography and histological analyses were conducted at multiple time points after MI and sham surgery. RNA bulk sequencing was performed from remote and scar tissue of infarcted mice 2 weeks after MI.
Results: Echocardiography revealed sexspecific disparities in scar and LV remodelling. Female mice exhibited early on cardiac protection, evident by preserved ejection fraction (EF) and attenuated LV dilatation. Male mice exhibited decline in EF and increased LV dilatation over time following infarction. Initial decline in global longitudinal strain (GLS) is evident in both sexes but preserved in females, while further declines in males. No difference could be seen in scar size and decline of synchronous wall movement. Females showed lower levels of LV remote fibrosis and a more inflammatory transcriptome, but downregulated extracellular matrix organisation in the scar tissue compared to males.
Conclusion: In conclusion, our findings reveal clear differences in post infarction cardiac remodelling between the sexes, with a clear cardioprotective phenotype in females. These findings highlight important sexdependent mechanisms in cardiac repair and may contribute to the development of more targeted therapeutic strategies after myocardial infarction.

P25 Postergroup: Cardiac Function - essential knowledge

P2503

Transient contractile unloading protects cardiac living slices prepared from ischemic porcine and rabbit myocardium

Thomas Seidel; Andreas Dendorfer [1]; Petra Kameritsch [1]
Innere Medizin, Infektiologie, Arztpraxis Weimar, Weimar, Germany; [1] WalterBrendelCentre of Experimental Medicine, Institute of Surgical Research, LMU Klinikum Großhadern, Munich, Germany;

Objective: Myocardial ischemiareperfusion injury can be mitigated by specific conditions of postischemic recovery. Suppression of active contraction and stabilization of the cytoskeleton may be protective by reducing mechanical damage and metabolic demands. Here, we utilized the ischemic and hypothermic stress inherent to the preparation and culture start of precision-cut myocardial slices as a model of ischemia and reperfusion, and tested the effects of actin and myosin inhibition on their contractile function and longterm survival in biomimetic culture.
Method: Hearts were obtained from slaughterhouse pigs or sacrificed rabbits (510 min warm, and 34 h cold ischemia). Living myocardial slices (300µm thickness) of pigs and rabbits were mounted in biomimetic culture chambers and incubated with various combinations of 2,3butanedione monoxime (B), mavacamten (M) and cytochalasin D (C) or vehicle for 2 h. Diastolic tension and twitch force were registered continuously.
Results: Under control conditions, porcine heart slices developed an initial tonic contracture of 14.4±1.5mN and did not respond to electrical stimulation. Combined treatment with two of the inhibitors (M+B, M+C) tended to reduce contracture and occasionally reestablished excitability. Only the combination of all three chemicals significantly reduced contracture to 5.5±0.9mN and, after washout, enabled paced contractions at 570±115µN for a total period of 23±5h. In rabbit myocardium, control slices also developed irreversible contracture (14.5±1.7 mN) and never responded to electrical stimulation. B and B+C reduced contracture to 9.4±1.1 and 4.1±0.5 mN, respectively, while B+M+C even caused slight relaxation (1.4±0.2mN). Treated rabbit slices responded to electrical stimulation, and, after 24 h, developed a twitch force of 1.3±0.3mN (B), 2.3±0.3mN (B+C) and 6.3±1.0 mN (B+M+C) for 57 days.
Conclusion: Reversible pharmacological inhibition of actinmyosin interaction may prevent contracture and fatal damage in pig and rabbit heart tissue exposed to warm and cold ischemia.

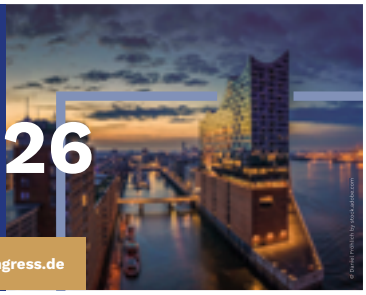

P25 Postergroup: Cardiac Function - essential knowledge

P2504

Impact of DUSP1 on the progression of right ventricular failure in rats

Ling Li; Bernd Niemann 1; Elisabeth Dominik 2; Maike Elisabeth Schneider; Jan Luca Zimmermann; Liane Moana Jurida 3; Michael Kracht 3; Susanne Rohrbach
Institut für Physiologie, Justus Liebig Universität Gießen, Gießen, Germany; 1 Klinik für Herz-, Kinderherz- und Gefäßchirurgie, Standort Gießen, Universitätsklinikum Gießen-Marburg, Gießen, Germany; 2 Cardiac and Vascular Surgery, University Hospital Gießen, Gießen, Germany; 3 Rudolf Buchheim Institute of Pharmacology, Justus Liebig University Gießen, Gießen, Germany;

Objective: Pressure overload can lead to right ventricular (RV) compensated hypertrophy followed by maladaptive cardiac remodelling, and heart failure. To identify molecular signatures and mechanisms of heart failure (HF) specific to the RV, we established animal models, which show two clearly distinguishable, slowly developing stages of disease (compensated and decompensated) in response to pulmonary artery banding (PAB) in rats. In cardiomyocytes from these rats, we identified a number of genes that are specifically deregulated in the RV, in particular a cluster of dualspecificity phosphatases (DUSPs). DUSPs act as important regulators of hypertrophic signalling pathways through the dephosphorylation of cardiac extracellular signalregulated kinase (ERK), p38 mitogenactivated protein kinase (MAPK), and cJun Nterminal kinase (JNK). In the present study, the role of DUSP1 was investigated in a model of chroniv RV pressure overload through AAVmediated overexpression of DUSP1 in cardiomyocytes.
Method: PAB surgery was performed in weanling rats to induce either compensatory RV hypertrophy (RVH, 7 weeks postsurgery) or RV failure (RVF, 22 weeks postsurgery). Adenoassociated virus 9 (AAV9) injection ($5x10^{12}$GC/kg) at 1 and 15 weeks after PAB or sham surgery maintained an approximate fivefold increase in DUSP1 or GFP (control) protein expression throughout the study.
Results: At 7 weeks after surgery, cardiac function did not differ between groups. However, at the stage of RVF, in PAB animals with DUSP1 overexpression, RV function was improved, as indicated by TAPSE and RV fractional area change (RV FAC), despite a similar degree of RV hypertrophy. In addition, these animals showed reduced cardiac BNP expression (PCR and Western blot) and lower BNP release (ELISA), together with a pronounced attenuation of cardiac inflammation as assessed by cytokine array analysis. Conversely, chronic DUSP1 overexpression in shamoperated animals (22 weeks after surgery) induced a moderate deterioration of both RV and LV function, as well as impaired mitochondrial morphology. DUSP1 overexpression was associated with increased macrophage- and neutrophilrelated inflammatory gene expression (Arg1, Cxcr1, CD11b) and enhanced neutrophil infiltration (Ly6G histology) in the RV of these animals, compared with GFPoverexpressing sham controls.
Conclusion: While chronic DUSP1 overexpression decelerates the progression toward right ventricular failure under pressure overload, its effects differ markedly between pathological stress (PAB) and baseline conditions. In shamoperated animals, representing a nonoverloaded physiological baseline, DUSP1 overexpression may disrupt intrinsic cardiac homeostatic signaling. Dysregulated MAPK activity, particularly involving the p38 MAPK and ERK pathways in our animals, which regulate cardiomyocyte stress resilience and immunometabolic crosstalk, may thereby contribute to a maladaptive shift in basal cardiac function.

16-19 September 2026 — Hamburg, Germany
Physiology with Flow: Set Sail!
PHYSIOLOGY in FOCUS 2026
The joint ANNUAL MEETING OF THE GERMAN PHYSIOLOGICAL SOCIETY
and the SCANDINAVIAN PHYSIOLOGICAL SOCIETY
www.dpg-congress.de

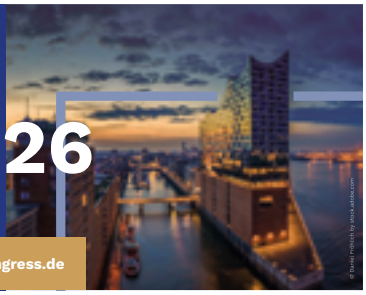

P25 Postergroup: Cardiac Function - essential knowledge

P2505

Endothelial cellderived SMOC1 deficiency, limits cardiac remodelling after myocardial infarction

Fatima Hacer Kurtoglu Babayev; Fredy Delgado Lagos; Bardia Amirmiran; Beate Fisslthaler; Ralf P. Brandes [1]; Mauro Siragusa; Ingrid Fleming
Institute for Vascular Signalling, Goethe University Frankfurt am Main, Frankfurt a. M., Germany; [1] Institut für Kardiovaskuläre Physiologie, Universitätsklinikum, Johann Wolfgang GoetheUniversität, Frankfurt a. M., Germany;

Objective: Endothelialtomesenchymal transition (EndMT) describes a transforming growth factor (TGF) β) process in which endothelial cells acquire mesenchymal features. The switch is activated after myocardial infarction (MI) and EndMT cells participate in cardiac tissue repair, impact on infarct size and contribute to fibrosis and adverse remodelling. We screened available single cell sequencing datasets for TGFb regulated genes activated after acute MI in mice. A cluster of endothelial cells expressing mesenchymal markers expressed secreted modular calcium binding protein 1 (SMOC1), which was previously reported to bind to the TGFb accessory receptor; endoglin.
Method: In cultured human endothelial cells, EndMT induction (IL1β, TGFβ2) upregulated SMOC1. SMOC1 silencing via siRNA enhanced EndMT markers (smooth muscle actin, endoglin, S100A4) and reduced endothelial cell phenotypic markers such as VEcadherin. Also, the TGFb2induced phosphorylation of SMAD2, was attenuated in SMOC1deficient cells indicating that TGFb2 signalling was regulated. The addition of recombinant SMOC1 largely prevented these changes and had a marked impact on endothelial cell gene expression e.g. increased VEcadherin. To assess the impact of endothelial cellderived SMOC1 in vivo VEcadherincre and $SMOC1^{fl/fl}$ mice were crossed to generate animals lacking SMOC1 in endothelial cells. These $SMOC1^{DEC}$ mice were then subjected to MI using a minimally invasive surgical approach.
Results: Functional analyses after MI revealed a continual worsening of cardiac function in the $SMOC1^{DEC}$ mice compared to their wildtype littermates with markedly increased end diastolic volume (WT: 72.6 ± 7.5 µL vs. SMOC1: 134.8 ± 14.4 µL) and substantially reduced ejection fraction (WT: 26.3 ± 2.6 % vs. SMOC1: 10.6 ± 1.09 %) after 14 days. Histological analysis (Masson's trichrome staining) revealed extensive infarct area expansion in hearts from $SMOC1^{\Delta EC}$ mice, together with the development of ventricular aneurysms. The latter were not observed in wildtype littermates.
Conclusion: These findings identify a critical role for SMOC1 in regulating EndMT and limiting cardiac inflammation and structural remodelling after infarction.

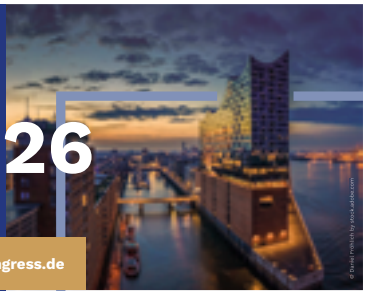

P25 Postergroup: Cardiac Function - essential knowledge

P2506

Lipid droplet accumulation alters force generation and fractional shortening in ex vivo models of murine cardiomyocytes and cardiac tissue

Michael Singer; Katharina Kotulski; Constanze Zieschang; Parisa Pourfarrokh; Katharina Bottermann [1]; Martina Krüger
HerzKreislaufPhysiologie, Heinrich Heine Universität Düsseldorf, Düsseldorf, Germany; [1] Institute of Pharmacology, University Hospital, Heinrich Heine University Düsseldorf, Düsseldorf, Germany;

Objective: Excess free fatty acids, as observed in obesity and type 2 diabetes, contribute to cardiovascular disease, yet their immediate mechanical consequences in cardiomyocytes remain poorly understood. We investigated how shortterm fatty acid exposure affects lipid droplet formation, unloaded shortening, and force generation in murine cardiomyocytes and cardiac tissue slices.
Method: Primary ventricular cardiomyocytes were isolated from adult wildtype mice and treated for 2 h with palmitate/oleate (OP). Cardiac tissue slices from wildtype mice were exposed to OP for 1.5 h. Lipid droplet formation was assessed by immunofluorescence microscopy using HCS LipidTOX, phalloidin, and αactinin staining. Cardiomyocytes were stimulated at 1 Hz to quantify sarcomere fractional shortening and maximum isometric force development. Active force generation in cardiac slices was measured using a Muscle Strip System.
Results: OP treatment induced pronounced lipid droplet accumulation in isolated cardiomyocytes. Under isometric conditions, maximum force development of OPtreated cardiomyocytes was reduced by 39 ± 23% compared with BSAtreated controls. Consistently, OP exposure reduced active force development in cardiac slices by approximately 30% within the first 15 min compared with BSA controls, indicating impaired force generation at singlecell and tissue level. In contrast, OPtreated cardiomyocytes displayed a 4060% increase in fractional shortening compared with BSAtreated controls. Together with previous findings from our group showing unaltered Ca^{2+} homeostasis after OP treatment, these data suggest a dissociation between unloaded shortening and forcegenerating capacity after acute lipid loading.

Conclusion: Shortterm fatty acid exposure induces rapid lipid droplet accumulation and impairs isometric force generation in isolated cardiomyocytes and cardiac tissue slices. The concomitant increase in fractional shortening indicates that unloaded shortening does not necessarily reflect contractile force under lipidloaded conditions. Ongoing experiments will determine whether changes in passive tension, force transmission, or cellular loadbearing properties contribute to this dissociation.

P25 Postergroup: Cardiac Function - essential knowledge

P2507

Acute ventricular stretch and Angiotensin II increase contractility and excitability in an explanted mouse heart model

Judith Sofie Langen; Philipp Sasse
Institute of Physiology I, University of Bonn, Bonn, Germany;

Objective: Chronic stretch and increased Angiotensin II levels are known to induce cardiac remodeling which increases the probability of cardiac arrythmia, however, little is known about their acute effects. Several acute pathological situations such as pulmonary embolism, myocardial infarction or the following reperfusion are associated with increased ventricular stretch and the onset of ventricular arrhythmia, which can be aggravated by Angiotensin II receptor signaling.
Method: To determine the effect of acute ventricular stretch and angiotensin II on cardiac contractility and excitability in Langendorffperfused mouse hearts, we introduced a small trocar (25gauge, 0.53 mm) usually used in ophthalmic surgery to the apex of the left ventricle. The trocar was connected to a force transducer to measure contractions and to a pressure control valve to modify cardiac enddiastolic pressure. To quantify cardiac excitability, we determined the pacing threshold using precise lightinduced current injection in mouse hearts expressing the lightgated cation channel channelrhodopsin2.
Results: Stepwise increase of the enddiastolic pressure up to 20 cmH_2O increased the contractility amplitude up to 324.8±67.4% (mean±SEM) reflecting the FrankStarling mechanism (N=9 hearts). Moreover, perfusion of hearts with Angiotensin II led to an increase in contractility amplitude by 8.0±1.2% (N=6). Importantly, increasing the enddiastolic pressure reduced pacing thresholds reflecting an increased cardiac excitability. Quantitatively, we found a dosedependent decrease in pacing threshold of 0.8±0.4%, 2.4±0.5%, 2.9±0.5% and 5.0±1% induced by an enddiastolic pressure of 5, 10, 15 and 20 cmH_20, respectively (N=9). Similarly, application of Angiotensin II also decreased pacing threshold by 5.3±1.8% (N=5) suggesting that Angiotensin II receptor signaling contributes to increased cardiac excitability.
Conclusion: To conclude, we found an acute stretch- and Angiotensin IIinduced increase in cardiac contractility and excitability indicating a higher vulnerability to extra beats which can trigger cardiac arrhythmia.

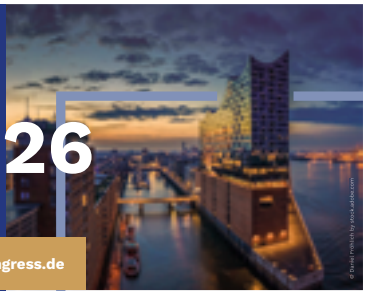

P25 Postergroup: Cardiac Function - essential knowledge

P2508

Proenkephalin (PENK) as a Modulator of Cardiac Hypertrophy and Right Ventricular Failure

Jan Luca Zimmermann; Jannis Völker; Ling Li; Liane Moana Jurida [1]; Bernd Niemann [2]; Michael Kracht [1]; Susanne Rohrbach
Institut für Physiologie, Justus Liebig Universität Gießen, Gießen, Germany; [1] Rudolf Buchheim Institute of Pharmacology, Justus Liebig University Gießen, Gießen, Germany; [2] Klinik für Herz, Kinderherz- und Gefäßchirurgie, Standort Gießen, Universitätsklinikum GießenMarburg, Gießen, Germany;

Objective: Despite anatomical and functional similarities between the left (LV) and right ventricles, their molecular responses to pressure overload differ significantly and the mechanisms driving progressive right ventricular failure remain poorly understood. Through the systematic comparison of RV and LV cardiomyocytes from rat models with slowly progressive RV failure (pulmonary artery banding, PAB) and LV failure (aortic banding, AOB), as well as by integrating these data with transcriptomic datasets from patients with chronic thromboembolic pulmonary hypertension (CTEPH), we were able to identify a central gene/protein signature for right heart failure (RHF). Among the most highly regulated genes within this signature was proenkephalin (PENK), the precursor of the endogenous opioid peptides enkephalins. Clinically, increased circulating PENK levels correlate with the degree of heart failure and mortality, identifying PENK as a candidate regulator of maladaptive cardiac remodeling.
Method: Rat PAB and AOB models were established representing compensated and decompensated stages of pressure overload. Gene expressions were analyzed using PolyA RNA sequencing, qPCR and Western blot (WB). FISH was used to localize PENK mRNA at the cellular level in cardiac tissue. For in vitro studies, adult cardiomyocytes and cardiac fibroblasts from rats were stimulated with phenylephrine (PE) ± propranolol or prazosin, TGFβ and angiotensin II. Gene expression was analyzed by RTqPCR, protein expression was confirmed by WB and cardiomyocyte morphology was quantified by measuring the cell surface area.
Results: RNAsequencing and proteomic analyses of PAB and AOB rat models identified a 113gene RHF core signature, shared across RVspecific gene sets and 95 CTEPH patient datasets. PENK was significantly upregulated in the RV of PAB rats at both hypertrophic and failing stages. In CTEPH patients, PENK mRNA correlated negatively with physical performance, linking higher PENK expression to worse RV function. FISH confirmed that PENK is mainly expressed in cardiomyocytes. Noradrenaline and endothelin1 were identified as inducers of PENK, and enkephalin impaired contractile function in isolated cardiomyocytes. Similarly, PE upregulated PENK and BNP mRNA in cardiomyocytes, with PENK protein confirmed by Western blot, while TGFβ was the dominant inducer of PENK and αSMA in cardiac fibroblasts.
Conclusion: These results identify PENK as a key mediator of right ventricular remodeling under pathological stress. Celltypespecific Penk knockout mice in the PAB model will enable a causal analysis of its role in right heart failure.

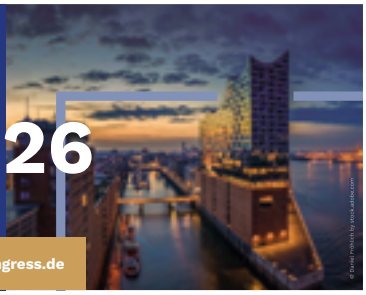

P25 Postergroup: Cardiac Function - essential knowledge

P2509
Obstructive apneas immediately impact atrial hemodynamics and arrhythmias

Lisa A. Gottlieb; Kathar Friederichs; Klaus Fuglsang Kofoed; Dominik Linz; Thomas Jespersen
Department of Biomedical Sciences, University of Copenhagen, Copenhagen, Denmark;

Objective: Obstructive sleep apnea (OSA) and atrial fibrillation (AF) often coexist. OSA causes intrathoracic pressure fluctuations, which act as mechanical stimuli to the thinwalled atria. Atrial stretching facilitates AF.
To provide a comprehensive mapping of how onset and release of obstructive apnea impact atrial arrhythmia occurrence and biatrial hemodynamics in an animal model.
Method: We simulated obstructive apnea by administrating intermittent negative upper airway pressure (60 mbar) for 75 seconds in anesthetized, spontaneously breathing pigs. We quantified atrial premature complexes on electrocardiography. We assessed atrial hemodynamics by intraatrial pressures and repetitive dynamic multislice computer tomography scans (n = 84) at baseline, during apnea and upon release.
Results: Atrial premature complexes were most frequent during the release period after apnea (0.16±0.27 arrhythmias/second vs. 0.04 ± 0.08 at baseline, $p < 0.010$; pigs = 27). During apnea release, right atrial volume was 30% and left atrial volume 32% larger than at baseline (pigs = 5; $p < 0.05$ baseline vs. release). Right atrial pressure increased from 5 ± 4 mmHg at baseline to 9 ± 6 mmHg in apnea release ($p < 0.05$). In particularly in the right atrium, the estimated atrial transmural pressure was higher during and upon apnea release, leading to higher estimated wall tension.
Conclusion: Release of an obstructive apnea associates with marked changes in atrial hemodynamics and arrhythmia burden in a porcine model. This has implications for understanding diseasemechanisms for OSArelated AF in humans.

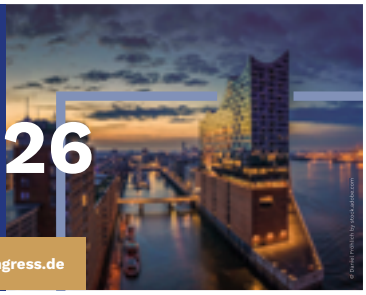

P25 Postergroup: Cardiac Function - essential knowledge

P2510

Therapeutic Gq protein inhibition improves right ventricular function under pressure overload from pulmonary artery banding

Amanda Ridder; Alexander Seidinger; Anna Klinke [1]; Volker Rudolph [2]; Daniela Wenzel
Systemphysiologie, Institut für Physiologie, RuhrUniversität Bochum, Bochum, Germany; [1] Klinik und Poliklinik für Kardiologie, Pneumologie, Angiologie und internistische Intensivmedizin, Klinik III für Innere Medizin, Universität zu Köln, Köln, Germany; [2] Clinic for General and Interventional Cardiology/ Angiology, Agnes Wittenborg Institute for Translational Cardiovascular Research, Herz- und Diabeteszentrum NRW, Bad Oeynhausen, Germany;

Objective: Our earlier data demonstrated that pharmacological Gq inhibition by FR900359 (FR) alleviates Sugen5416/HXinduced pulmonary hypertension (PH) and reduces vascular remodeling as well as right heart hypertrophy. To examine the role of Gq proteins in right ventricular function and remodeling in detail, in the current study we analyzed the effect of FR in a murine pressure overload model of pulmonary artery banding (PAB).
Method: Mice were subjected to chronic right ventricular pressure overload by PAB (70% constriction of the pulmonary artery) under inhalational anesthesia (1.52% isoflurane). After two weeks of disease progression, animals received daily intraperitoneal applications of solvent or FR for additional two weeks as a therapeutic intervention. Cardiac function was assessed by pressurevolume catheterization under 1% isoflurane. Right heart remodeling and hypertrophy were examined by histology.
Results: FR reduced right ventricular systolic pressure increase induced by PAB (DMSOSHAM: 21.69 ± 1.81 mmHg, n=10, DMSOPAB: 44.09 ± 7.02 mmHg, n=10, FRPAB: 25.73 ± 2.80 mmHg, n=10, p<0.001 FRPAB vs DMSOPAB) and decreased the slope of the end-systolic- and enddiastolicpressurevolumerelationships (ESPVR and EDPVR) to normal SHAM values. Compared with SHAM controls, PAB mice showed an impaired ventricula-rarterial coupling efficiency, which was improved by FR treatment (Ees/Ea: DMSOSHAM: 0.74 ± 0.09, n=10, DMSOPAB: 0.51 ± 0.07, n=10, FRPAB: 0.68 ± 0.12, n=10, p<0.001 FRPAB vs DMSOPAB). Morphometry demonstrated elevated right heart hypertrophy and fibrosis in PAB compared to SHAM, these increases were attenuated by FR.
Conclusion: These data suggest that pharmacological Gq inhibition is a promising therapeutic approach to improve right ventricular function under conditions of chronic pressure overload.

P26 Postergroup: Renal disease - oxygen/metabolism

P2601

Transcriptional Changes of O_2Sensing ADORGS Pathway Components in Mouse and Human Kidneys Under Normoxia, Hypoxia and Renal Fibrosis

Katharina AnnaElisabeth Broeker; Bettina Katharina Mariana Firmke; AnnaLena Forst [1]; Christoph Daniel [2]; Gunnar Schley [3] Lehrstuhl Physiologie I, Institut für Physiologie, Universität Regensburg, Regensburg, Germany; [1] Lehrstuhl für Medizinische Zellbiologie, Institut für Physiologie, Universität Regensburg, Regensburg, Germany; [2] Institut für Nephropathologie, Universitätsklinikum, FriedrichAlexanderUniversität ErlangenNürnberg, Erlangen, Germany; [3] Medizinische Klinik 4, Nephrologie und Hypertensiologie, Universitätsklinikum, FriedrichAlexanderUniversität ErlangenNürnberg, Erlangen, Germany;

Objective: The oxygendependent ADO–RGS (2aminoethanethiol dioxygenase–regulator of Gprotein signaling) pathway has recently emerged as a potential contributor to hypoxia adaptation by modulating G protein–coupled signaling, alongside the hypoxiainducible factor pathway. The kidney is particularly vulnerable to hypoxic injury, a major driver of chronic kidney disease (CKD), yet the localization of ADO and its RGS substrates across renal cell types remains unclear.
Method: This study investigated the expression of *Ado*, *Rgs4*, *Rgs5*, and *Rgs16* in archived kidney tissue of wildtype mice under normoxic, hypoxemic, and fibrotic conditions using RNAscope *insitu* hybridization and RTqPCR. Murine data were compared with human kidney biopsies from patients with acute or chronic kidney disease.
Results: Ado expression was uniform across kidney regions, cell types, and conditions. *Rgs4* showed mainly vascular expression at baseline but was induced under anemia in cortical and outer medullary fibroblasts alongside erythropoietin, and upregulated in fibroblasts and tubular cells in fibrotic lesions. *Rgs5* was primarily vascular at baseline, increased in medullary fibroblasts and *vasa recta* under hypoxia, and displayed moderate fibroblast induction with *denovo* tubular expression under fibrosis. *Rgs16* was mainly detected in PDGFRβ$^+$ interstitial cells in fibrotic kidneys. In human biopsies, *RGS4* upregulation was confirmed in fibrotic regions, whereas *RGS5* remained vascular.
Conclusion: Overall, the study identifies previously unrecognized *Rgs*expressing cell populations and reveals conditiondependent expression patterns of *Rgs4*, *Rgs5*, and *Rgs16*, particularly in fibroblasts and tubular epithelial cells, while *Ado* remains constant. These findings provide a foundation for future studies on cell type–specific roles of ADO–RGS signaling in kidney physiology and disease.

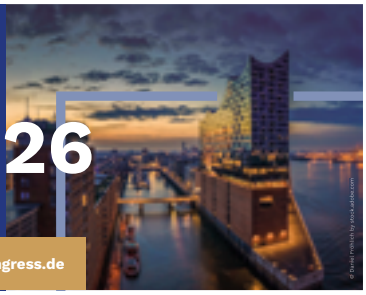

P26 Postergroup: Renal disease - oxygen/metabolism

P2602

StretchInduced Pulmonary Endothelial EV Release Promotes Ventilatorinduced Kidney Injury

Julia Naujox; Sara M. ExojoRamírez[1]; Juliana Roeder; Sergio A. EsquivelRuiz[2]; Fabian Schumacher[3]; Burkhard Kleuser[4]; Guillermo M. Albaiceta[1]; Laura AmadoRodríguez[1]; Wolfgang M. Kübler; Laura Michalick
Institut of Physiology, CharitéUniversitätsmedizin Berlin, corporate member of the Freie Universität Berlin and Humboldt Universität zu Berlin, Berlin, Germany; [1] Centro de Investigación Biomédica en Red (CIBER)Enfermedades Respiratorias, Madrid, Spain; [2] Departamento de Farmacología de la Universidad de Granada, Granada, Spain; [3] Pharmakologie und Toxikologie, FU Berlin, Berlin, Germany; [4] Institut für Pharmazie, Freie Universität Berlin, Berlin, Germany;

Objective: Ventilatorinduced kidney injury (VIKI) is a frequent complication in patients receiving mechanical ventilation (MV), yet mechanisms underlying this adverse lungkidney crosstalk remain largely unclear. Pulmonary endothelial overdistension activates mechanosensitive pathways that promote extracellular vesicle (EV) release into the circulation, potentially delivering injurious cargos to the glomerular endothelium. We therefore hypothesize that EVs released from ventilated lungs may induce renal dysfunction.
Results: *In vivo*, mice were subjected to 2h MV with either high (HV_T = 20 ml/kg bw) or lungprotective tidal volume (LV_T = 7 ml/kg bw). Nanoparticle tracking analysis (NTA) revealed increased circulating EV levels after HV_T compared to LV_T. Renal injury after HV_T was evident as elevated plasma urea and creatinine levels, increased glomerular tuft area, immune cell infiltration and podocyte effacement. Parallel analyses of plasma samples from cardiac surgical patients exposed to either continuous positive airway pressure (CPAP) during cardiopulmonary bypass (n=13), MV for 1h (n=6), MV for 8h (n=16), or MV with cardiopulmonary edema (CPE, n=25) revealed higher plasma EV concentrations in MV patients compared to CPAP controls. Circulating EV concentrations correlated positively with driving pressure, plateau pressure, and strain. Flow cytometry identified increased levels of $CD31^+$ endothelialderived EVs in plasma from CPE patients compared to the 1h MV group. *In vitro,* cyclic stretch (CS, 18% elongation) of pulmonary microvascular endothelial cells (HPMECs) increased EV release (100200 nm in size) compared to static controls. Pathogenic potential of EVs was assessed as change in human renal glomerular endothelial cell (HRGEC) barrier function using Electric Cell Impedance Sensing (ECIS®). EVs released by 18% CS HPMECs reduced HRGEC barrier function relative to equal amounts of EVs released from static cells.
Conclusion: MV triggers the release of pathogenic EVs from lung endothelial cells, which disseminate via the systemic circulation and induce renal dysfunction. Endothelialderived EVs may serve as potential biomarkers and therapeutic targets for monitoring and mitigating VIKI.

P26 Postergroup: Renal disease - oxygen/metabolism

P2603

Propofol and sevoflurane anesthesia acutely mediate different transcriptional effects in the porcine kidney

Carley Fowler; Bahareh Razmand; Phi Hung Nguyen [1]; Kelly A. Hyndman [1]; Stephanie Franzén
Surgical Sciences, Uppsala University, Uppsala, Sweden; [1] Medicine, University of Alabama, Birmingham, United States;

Objective: Volatile anesthetics are shown to impair renal function through reduced renal blood flow and oxygen delivery. Also, volatiles have been associated with a higher incidence of acute kidney injury. It remains unclear how volatiles mediate acute subcellular changes in the kidney. Therefore, we investigated renal transcriptomics in an experimental pig model with intravenous or volatile anesthesia.
Method: Renal tissue from pigs anesthetized with different anesthetics was used for RNA sequencing. Anesthesia, propofol (10 mg/kg/h) and sevoflurane (0.9 minimal alveolar concentration), was maintained for four hours before the renal tissue was harvested and snap frozen. 23 samples were analyzed: 9 cortex (6 propofol, 3 sevoflurane) and 14 medulla (7 propofol, 7 sevoflurane). Reads were mapped to the pig genome Sus scrofa (Sscrofa11.1) using the STAR program. Differentially expressed genes (DEGs) were identified across anesthesia type and kidney region using DESeq2. OverRepresentation Analysis was used for pathway enrichment analysis via the ClusterProfiler package.
Results: Comparing propofol vs sevoflurane revealed 104 DEGs. Regional analysis showed 1 unannotated gene in the cortex. In the medulla, 42 DEGs were significantly different between anesthesia groups. Propofol mediated upregulation in medullary metabolismassociated genes (*Gatm*). Sevoflurane upregulated medullary expression of the glutamate transporter (*Slc1a2)* and genes associated with hypoxia (ApoD, *Hif3a*). Genes with greater expression in propofol were enriched in cell cycle (GO:0022402) and chromosome segregation (GO:0007059) pathways.
Conclusion: Propofol and sevoflurane anesthesia mediate different transcriptomic outcomes in the kidney. In the medulla, propofol upregulates genes involved in metabolism and mitosis, and sevoflurane upregulates synaptic transporters and genes associated with hypoxia and oxidative stress.

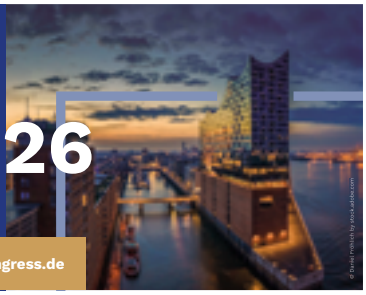

P26 Postergroup: Renal disease - oxygen/metabolism

P2604
MRIPHYSIOLNIRS: An Integrated Platform To Study Kidney Oxygenation

Thomas Gladytz; Kathleen Cantow [1]; Jason M. Millward; Sonia Waiczies; Dirk Grosenick [2]; Erdmann Seeliger [3]
Berlin Ultrahigh Field Facility (B.U.F.F.), Max Delbrück Center for Molecular Medicine in the Helmholtz Association, Berlin, Germany; [1] Integrative Nierenphysiologie, Institut für Translationale Physiologie, Charité - Universitätsmedizin Berlin, Berlin, Germany; [2] PhysikalischTechnischeBundesanstalt, Berlin, Germany; [3] Institut für Vegetative Physiologie, Campus Charité Mitte, Charité - Universitätsmedizin Berlin, Berlin, Germany;

Objective: Oxygen deprivation is extraordinarily important to pathophysiology in the kidneys. A clinically applicable diagnostic tool to measure kidney oxygenation is urgently needed. The gold standard for measuring tissue oxygenation is invasive physiological probes that provide absolute values of tissue pO_2 (PHYSIOL). Blood Oxygen LevelDependent Magnetic Resonance Imaging (BOLDMRI) provides surrogate parameters of renal oxygenation – T_2* and T_2 – noninvasively. However, the relationship between the surrogates T_2* and T_2 and the true tissue oxygenation pO_2 is influenced by several confounders. These include the tubular volume fraction (TVF) and the blood volume fraction (BVF), measurable by MRI, and deoxyhemoglobin concentration (deoxyHb), measurable by NearInfrared Spectroscopy (NIRS). We developed a reference framework for MRIbased oxygenation parameters by establishing MRIPHYSIOLNIRS: a platform to obtain data from these three modalities from the same rat kidney in vivo. We validated this approach using shortlasting aortic occlusion and hyperoxia, and analyzed correlations among the multimodal parameters.
Method: Rats (n=25) were anesthetized with urethane (1.2 g/kg i.p.) during surgery and MRI examinations. Experiments were approved by Berlin authorities; the animals were treated and euthanized humanely.
The multimodal data were obtained while the rats were in a 9.4 T scanner.
Results: Upon aortic occlusion, pO_2, T_2*, T_2, TVF and BVF decreased, while deoxyHb increased. Upon hyperoxia, pO_2, T_2* and T_2 increased, while BVF and deoxyHb decreased. These results are consistent with data previously obtained in singlemode studies, demonstrating successful integration of the MRIPHYSIOLNIRS platform. The correlation analyses revealed that T_2*, T_2 changes during aortic occlusion, hyperoxia and recovery are essentially driven by tissue oxygenation. The influence of the confounders was substantially stronger during aortic occlusion than during hyperoxia.
Conclusion: The quantitative effects of the confounders on the relationship between the surrogate parameters and true oxygenation vary considerably, depending on the (patho) physiological condition. Future work must include multiple clinically relevant scenarios. The MRIPHYSIOLNIRS platform lays the groundwork for future clinical applications aimed at improving the diagnosis and early detection of kidney disease, highlighting the potential for MRI oximetry to become established as a standalone system for measuring tissue oxygenation.

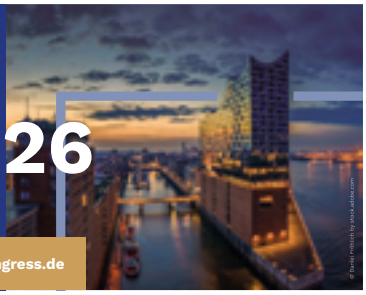

P26 Postergroup: Renal disease - oxygen/metabolism

P2605

Evaluation of renal injury in rat models of dietinduced MASLD and cholestatic liver disease

Sandra M. Hansen; Mariana M. Oliveira [1]; Mélanie Tremblay [1]; Rajeshwar P. Mookerjee [2]; Karen L. Thomsen; Christopher Rose [1]; Rikke Nørregaard; Henricus A. M. Mutsaers Department of Clinical Medicine, Aarhus University Hospital, Aarhus, Denmark; [1] Centre de Recherche du Centre Hospitalier de l'Université de Montréal, Montréal, Canada; [2] Institute for Liver and Digestive Health, University College London, London, United Kingdom;

Objective: Chronic kidney disease (CKD) is twice as common in patients with metabolic dysfunction–associated steatotic liver disease (MASLD) as in the general population, suggesting that hepatic injury may contribute to renal dysfunction. However, the underlying pathophysiological mechanisms remain unclear. Here, we evaluate the presence of renal injury in two animal models of liver disease, namely rats with bile duct ligation (BDL)induced cholestasis and rats with highfat diet (HFD)–induced MASLD, in order to gain more insight into the link between liver and kidney disease.
Method: Male Sprague Dawley rats were assigned to one of the following groups: BDL for 2.5 (n=8) or 5 weeks (n = 4), sham surgery for 2.5 (n=6) or 5 weeks (n=6), HFD for 8 (n=9), 12 (n=9), or 16 weeks (n=9), or chow diet for 16 weeks (n=15). Transcutaneous glomerular filtration rate (tGFR) was assessed in chow- and HFDfed rats at baseline and endpoint. Rats undergoing surgery or tGFR measurements were anaesthetized with 4% sevoflurane (inhalation) and maintained at 2%. At study completion, animals were sacrificed, and blood, urine, liver, and kidney tissues were collected for analysis.
Results: Plasma biomarkers, including ALT (n=412, p<0.001), AST (n=412, p=0.003), and albumin (n=412, p<0.001), confirmed pronounced liver injury in both 2.5- and 5week BDL rats. These parameters remained largely unchanged in rats fed a HFD for up to 16 weeks, consistent with the literature; however, Oil Red O staining confirmed hepatic steatosis in the HFD rats (n=46). In 5week BDL rats, renal tissue showed increased mRNA expression of inflammatory (*Il6*: n=124, p=0.014; *Il1β*: n=124, p=0.001) and fibrotic markers (*Tgfβ*: n=412, p=0.032; *Acta2*: n=412, p<0.001), accompanied by elevated fibronectin protein levels (n=412, p=0.002). Immunohistochemistry demonstrated increased fibronectin expression in both glomeruli and interstitium (n=24). In contrast, 16week HFD rats exhibited increased tGFR (n=915, p=0.012) consistent with glomerular hyperfiltration and elevated *Havcr1* mRNA levels (n=915, p<0.001), indicating proximal tubular stress, without changes in the mRNA levels of inflammatory and fibrotic markers. Histological and immunofluorescence analyses revealed focal microvesicular lipid accumulation and increased glomerular fibronectin staining (n=46). All data were tested for normality, and statistical analyses were performed using oneway ANOVA or Kruskal–Wallis tests as appropriate.
Conclusion: Collectively, these results demonstrate kidney injury in both BDLinduced cirrhosis and HFDinduced MASLD rats, with more tubular injury and inflammation observed in the BDL model. Plasma metabolomic analysis and snRNA sequencing of renal tissue are currently being performed to elucidate the pathophysiological mechanisms underlying the observed renal injury, which may ultimately help guide the development of therapeutic strategies to mitigate CKD risk in patients with liver disease.

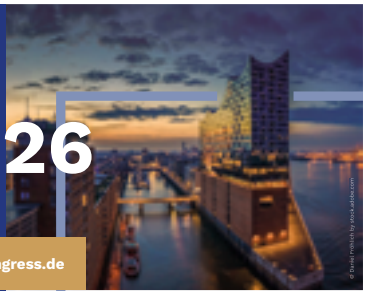

P26 Postergroup: Renal disease - oxygen/metabolism

P2606

Beyond Glucose Transport: OffTarget Effects of SGLT2 Inhibitors Reveal Mitochondrial and Transporter Remodeling in Kidney Disease

Anja M. Billing; Young Chul Kim [1]; Elina Kovalenko; Vera Christine Wulfmeyer; Volker Vallon [1]; Markus M. Rinschen
Department of Biomedicine, Aarhus University, Aarhus, Denmark; [1] University of California San Diego, San Diego, United States;

Objective: We investigated the offtarget molecular effects of SGLT2 inhibitors in kidney disease and metabolic dysfunction, aiming to identify SGLT2independent pathways that may contribute to their cardiorenal protective effects.
Method: To identify offtarget effects, we performed integrated proteomic and metabolomic profiling using LC–MS/MS in SGLT2 knockout (SGLT2KO) and wildtype mice across four conditions: healthy, diabetes, obesity, and nephropathy. Disease models included Western dietinduced obesity, Akitadriven type 1 diabetes, and aristolochic acidinduced nephropathy. Crossspecies validation was achieved by comparing murine data with plasma and urine profiles from individuals with familial renal glucosuria (genetic SGLT2 deficiency) and SGLT2i-treated patients with and without chronic kidney disease. Direct protein–drug interactions were assessed using thermal proteome profiling in kidney tissue, complemented by shortterm pharmacological studies in a microfluidic system. Proteomics was performed labelfree on an Exploris 480 platform, and targeted metabolomics on a triplequadrupole LC–MS.
Results: We generated a comprehensive multimodel atlas of SGLT2dependent and independent effects. SGLT2KO signatures were conserved between mice and humans, validating translational relevance. Notably, SGLT2i induced substantial offtarget remodeling of renal transport processes, with the strongest effects observed in nephropathy. Chronic kidney disease was characterized by pronounced mitochondrial dysfunction, which was partially rescued by SGLT2i independently of SGLT2. Thermal proteome profiling identified direct binding to multiple solute carrier (SLC) transporters and components of the mitochondrial respiratory chain.
Conclusion: SGLT2 inhibitors exert significant SGLT2independent effects in the kidney, targeting SLC transporters and mitochondrial pathways. Modulation of mitochondrial function may contribute to their cardiorenal protective phenotype. These findings expand the mechanistic framework of SGLT2i and highlight novel targets for therapeutic intervention.

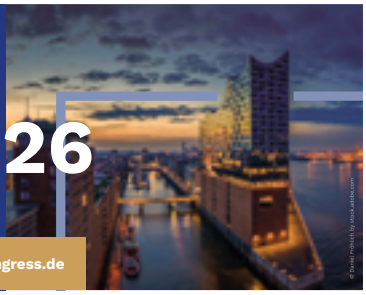

P26 Postergroup: Renal disease - oxygen/metabolism

P2607

Protein Degradation Pathway Remodeling in Diabetic Nephropathy: Implications for SGLT2i Renoprotection

Man Wang; Lukas Blume; Johannes Brand; Stephanie Zielinski; Elena Tasika; Batuhan Dogan; Shuya Liu [1]; Yu Zhao [2]; Tobias B. Huber [1]; Thorsten Wiech [3]; Sophie Wolfgramm [4]; Elke Krüger [4]; Desiree Loreth; Wiebke Sachs; Catherine MeyerSchwesinger Institut für Zelluläre und Integrative Physiologie, Zentrum für Experimentelle Medizin, Universitätsklinikum HamburgEppendorf, Hamburg, Germany; [1] Nephrologie/Rheumatologie und Endokrinologie/Diabetologie, III. Medizinische Klinik, Universitätsklinikum HamburgEppendorf, Hamburg, Germany; [2] Sektion für Translationale Immunologie, III. Medizinische Klinik, Universitätsklinikum HamburgEppendorf, Hamburg, Germany; [3] Institut für Pathologie, Sektion Nephropathologie, Zentrum für Diagnostik, Universitätsklinikum HamburgEppendorf, Hamburg, Germany; [4] Institut für Medizinische Biochemie und Molekularbiologie, Universitätsmedizin Greifswald, Greifswald, Germany;

Objective: Chronic hyperglycemia in diabetes damages proteins, increasing the demand for efficient protein degradation. Intracellular protein degradation is primarily mediated by the ubiquitin proteasome system (UPS) and autophagosomal lysosomal pathway (ALP). However, how these pathways are altered in diabetic nephropathy (DN) remains poorly understood. This study aimed to characterize UPS and ALP alterations during DN progression and to investigate whether modulation of these pathways contributes to the renoprotective effects of sodiumglucose cotransporter 2 inhibitors (SGLT2i).
Method: BTBR *ob*/*ob* mice, a model of type 2 diabetic nephropathy, were used. Glomeruli, kidney cortex, liver, and heart tissues were collected at early (8 weeks) and late (20 weeks) disease stages to provide an organ- and compartmentspecific analysis of UPS and ALP function by assessing the activity, abundance, and composition of key components.
Results: BTBR *ob/ob* mice showed a kidneyspecific impaired proteasome functionality, with a proteasome subtype distribution that was shifted towards an elevated immunoproteasome abundance. Proteasome impairment correlated with worsening albuminuria. In contrast, lysosomal activity and abundance were enhanced. These alterations displayed strong celltype specificity, with prominent proteasome changes in glomerular endothelial cells and marked lysosomal upregulation in mesangial cells. Importantly, SGLT2i treatment from 8 to 20 weeks of age attenuated immunoproteasome induction but did not restore proteasome activity in BTBR *ob*/*ob* kidneys.
Conclusion: DN is characterized by cell typespecific alterations in protein degradation pathways. The renoprotective effects of SGLT2i may be partly related to reduced immunoproteasome induction. However, the persistence of proteasome dysfunction despite SGLT2i suggests that restoration of proteasome activity may represent an additional therapeutic strategy in DN.

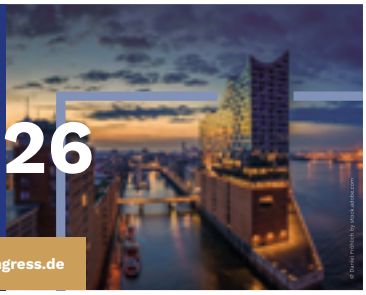

P26 Postergroup: Renal disease - oxygen/metabolism

P2608

Deficiency of the prostaglandin EP4 receptor exacerbates kidney injury and profibrotic remodelling in experimental diabetic kidney disease

Louise Nyrup Odgaard; Mariavittoria d´Acierno; Lena Kjær Rosenbæk; Ina Maria Schießl; Isabela B. Binotti A. de Araujo; Xiang Zheng; Anna Louise Venning Grandjean; Ewout Hoorn [1]; Robert Fenton
Department of Biomedicin, Aarhus University, Aarhus, Denmark; [1] Internal Medicine, Nephrology and Transplantation, Erasmus Medical Center, Rotterdam, The Netherlands;

Objective: Diabetic kidney disease (DKD) is a leading cause of chronic kidney disease and is characterized by progressive renal dysfunction, tubular injury, inflammation, and fibrosis. Tubular epithelial cells are increasingly recognized as active contributors to disease progression through maladaptive inflammatory and repair responses. The prostaglandin E2 receptor 4 (EP4) is expressed in tubular epithelial cells and has been implicated in the regulation of inflammatory and fibrotic pathways; however, its role in DKD remains incompletely understood. The aim of this study was to investigate tubular EP4 signaling in the development and progression of experimental diabetic kidney disease.
Method: Doxycyclineinduced (Pax8Cre system) tubulespecific EP4 knockout mice ($EP4^{/}$) and littermate controls ($EP4^{+/+}$) were rendered diabetic by streptozotocin (STZ) treatment. Mice were followed for 16 weeks after STZ induction. Blood glucose was monitored throughout the study. Twentyfourhour urines were collected using metabolic cages, and renal function was assessed by urinary and plasma biochemical measurements. Glomerular filtration rate (GFR) was assessed using transdermal monitoring. Renal injury, inflammation, and fibrotic remodeling were evaluated by histological analysis and renal gene expression profiling.
Results: STZ treatment promoted features of diabetic kidney disease in both genotypes. Tubular EP4 deficiency ($EP4^{/}$) aggravated the renal injury response compared with controls. Diabetic $EP4^{/-}$ mice had higher expression of inflammatory mediators, including IL1β and COX2, together with increased expression of tubular injury markers including KIM1 and LCN2. Profibrotic responses were also enhanced in $EP4^{/-}$ mice, with increased expression of αSMA and extracellular matrixrelated genes. Histological analysis of collagen using sirius red demonstrated significantly greater renal fibrosis in diabetic $EP4^{/-}$ mice. The sirius redpositive area increased by approximately 50% in STZtreated $EP4^{-/-}$ mice compared with vehicle $EP4^{-/-}$ controls (p=0.041, twoway ANOVA) and was approximately twofold higher than STZtreated $EP4^{+/+}$ mice (p=0.004, twoway ANOVA). Kidney function parameters remained relatively stable, but creatinine clearance normalized to body weight was significantly reduced in $EP4^{/}$mice compared with $EP4^{+/+}$ mice (p=0.035, twoway ANOVA), while transdermal GFR measurements were unchanged between groups.
Conclusion: Loss of tubular EP4 promoted kidney collagen deposition despite relatively preserved glomerular filtration. Therefore, tubular EP4 signaling appears to have a protective role in DKD progression by limiting inflammatory activation, tubular injury, and profibrotic remodeling. These data suggest that tubular EP4 signaling contributes to early renal adaptation during diabetic injury and may represent a potential therapeutic target in DKD.

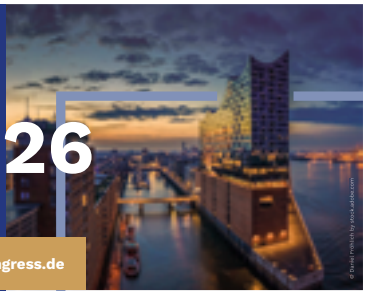

P26 Postergroup: Renal disease - oxygen/metabolism

P2609

Tissuespecific lipid remodeling revealed by integrative singlecell transcriptome and spatial lipidome analysis in MIDY pigs

Aisha Nadukkandy; Chunping Song [1]; Lei Cheng [1]; Sowmiya Kalaiselvan [1]; Camilla Brandt [1]; Simone Renner [2]; Helene Andersen [1]; Agnete Schou [1]; Line Petersen [3]; Thomass Voss [3]; Toke Bek [3]; Lolita Dokshokova [1]; Ibrahim Alzaim [1]; Joanna Kalucka [1]; Ian Mills [1]; Niels Jessen [4]; Martin Thomsen [1]; Eckard Wolf [2]; Yonglun Luo; Lin Lin [1] Department of Clinical Medicine, Aarhus University, Aarhus, Denmark; [1] Department of Biomedicine, Aarhus University, Aarhus, Denmark; [2] Center for Innovative Medical Models, Ludwig Maximilians University, München, Germany; [3] Department of Ophthalmology, Aarhus University, Aarhus, Germany; [4] Steno Diabetes Center, Aarhus University, Aarhus, Denmark;

Objective: Insulindeficient diabetes drives systemic metabolic complications, yet the cellular and spatial mechanisms underlying the observed pathophysiology remain poorly characterized. Existing studies are largely restricted to singleorgan analysis using rodent models, limiting translational insights into coordinated systemic adaptations during diabetes. In this study, we used the Mutant INSgeneinduced Diabetes of Youth (MIDY) pigs, a clinically relevant largeanimal model of insulindeficient diabetes, to investigate multiorgan molecular remodeling across metabolically active tissues using samples from the Munich MIDY Pig Biobank.

Method: Singlenuclei RNA sequencing was performed on approximately 70,000 nuclei isolated from four tissues (liver, kidney [cortex and medulla], and skeletal muscle) from MIDY pigs (n=3) and wildtype controls (n=3). To spatially resolve the metabolic alterations observed, transcriptomic data were integrated with matrixassisted laser desorption/ionization mass spectrometry imaging (MALDIMSI)based spatial lipidomics. Crossspecies comparisons to human diabetes samples were also performed to assess the conservation of identified signaling pathways.

Results: MIDY mutation induced distinct tissuespecific metabolic alterations across all tissues investigated. In the kidney, transcriptional reprogramming displayed regional specificity, particularly in the Loop of Henle and endothelial cells (ECs), with medullary ECs adopting a stressinduced procalcifying transcriptional state. In the liver, hepatocytes exhibited the strongest transcriptional response, characterized by disruption of lipid homeostasis and the accumulation of multiple lipid species. In skeletal muscle, increased lipid utilization was accompanied by transcriptional reprogramming in major cell types, such as Type II Myonuclei, suggesting adaptations to altered substrate availability.

Cellcell interaction analysis further revealed global upregulation of Semaphorin signaling pathways in the MIDY pigs. Notably, SEMA3A levels were also significantly elevated ($p = 0.0164$) in human type I diabetes plasma samples when compared to their agematched controls, indicating the translational relevance of these findings.

Conclusion: We generated the first multiorgan snRNA sequencing atlas of MIDY pigs, revealing tissuespecific metabolic adaptations to insulindeficient diabetes and providing mechanistic insights into systemic diabetic complications.

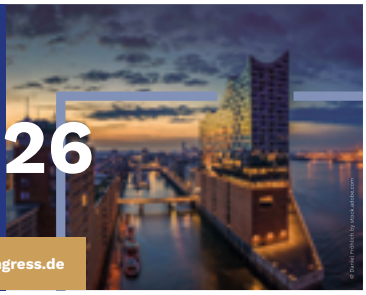

P26 Postergroup: Renal disease - oxygen/metabolism

P2610

In vivo effects of acute inhibition of sodiumglucose cotransporter 2 on tubuloglomerular feedback hemodynamics in diabetic rat model

Oleg Zhukov; Teddy Groves [1]; NielsHenrik HolsteinRathlou [2]; Dmitry D. Postnov [3]; Charlotte Mehlin Sørensen [2]; Olga Sosnovtseva Biomedical Sciences, Copenhagen University, Copenhagen, Denmark; [1] BRIGHT, Technical University of Denmark, Lyngby, Denmark; [2] Biomedical Sciences, Copenhagen University, Copenhagen, Denmark; [3] Center of Functionally Integrative Neuroscience, Aarhus University, Aarhus, Denmark;

Objective: Tubuloglomerular feedback (TGF) is a dynamic autoregulatory mechanism that plays a central role in diabetic hyperfiltration, and the renoprotective effects of sodium–glucose cotransporter 2 inhibitors. Current understanding of these mechanisms is largely based on steadystate TGF responses, and less is known about TGF dynamics, including TGFdriven oscillations of renal blood flow. We aim to characterize in vivo TGFdriven blood flow dynamics across multiple vascular–nephron units in diabetes and following sodium–glucose cotransporter 2 inhibition.
Method: We combined in vivo blood flow imaging, biochemical systemic analyzes, and computational modeling to study TGFdriven renal hemodynamics in Zucker diabetic fatty (ZDF) rats and lean controls (ZL) of both sexes at two stages of diabetes progression. Empagliflozin, a sodium–glucose cotransporter 2 inhibitor, was administered as an intravenous bolus to assess its effects on TGF hemodynamics.
Results: Empagliflozin decreased renal blood flow within several minutes postinjection, consistent with afferent vasoconstriction via TGF activation following sodium–glucose cotransporter 2 inhibition. This decrease in flow was attenuated in ZDF rats, possibly because elevated glucose levels competitively reduced the efficacy of empagliflozin. Both ZL and ZDF rats showed TGFdriven blood flow oscillations (10–40 mHz), suggesting that in ZDF rats, the TGF gain remained high enough for oscillations to occur despite hyperglycemia. Empagliflozin transiently inhibited the TGF oscillations followed by a possible restoration of oscillatory activity at a higher frequency.
Conclusion: These findings suggest that TGFdriven renal autoregulatory dynamics remain detectable in ZDF diabetes in vivo, and that sodium–glucose cotransporter 2 inhibition may perturb these dynamics. Our further analysis will investigate whether this perturbation is influenced by rat genotype, age, and sex.

P26 Postergroup: Renal disease - oxygen/metabolism

P2611

Hypoxia and Glucose Metabolism Shape Renal EPO and SGLT2 Expression in ObesityAssociated Kidney Stress

Nico Schmidt; Rallia Velliou [1]; Michelle Maaß; Vladimir T. Todorov; Timm Schreiber
Zentrum für Biomedizinische Ausbildung und Forschung (ZBAF), Lehrstuhl für Physiologie, Pathophysiologie und Toxikologie, Universität Witten/Herdecke, Witten, Germany; [1] Department of Physiology, Medical School, National and Kapodistrian University of Athens, Athens, Greece;

Objective: Renal epoproducing (REP) cells play a central role in systemic oxygen homeostasis, whereas sodiumglucose cotransporter 2 (SGLT2) is essential for renal glucose reabsorption in the proximal tubule. Changes in EPO and SGLT2 expression in metabolic diseases, such as obesity and diabetes mellitus, are associated with alterations in renal oxygen consumption, glucose metabolism, and hypoxia signalling pathways. However, the complex interactions between these factors have not yet been sufficiently investigated in the context of metabolic diseases. Therefore, this project investigates renal EPO and SGLT2 expression using tissuebased analyses and supplements these with cell culturebased models.

Method: Kidney sections from mice on a normal diet (ND) and a highfat diet (HFD) are examined using in situ hybridization to characterize the quantitative and spatial expression of EPO and SGLT2.In addition, tubular HK2 and EPOproducing FAIK cells were used to model metabolic and hypoxic conditions in vitro. The cells were cultured under low- and highglucose conditions and examined under normoxia or after hypoxic treatment. Additionally, vitamin D treatment was performed under both conditions as there is evidence of direct vitamin D receptormediated regulation in the EPO gene. The expression of EPO and SGLT2 was analysed using molecular biological methods and compared across different experimental conditions.

Results: Initial analyses revealed distinct localization patterns of EPO and SGLT2 in the renal tissue. While SGLT2 is expressed in proximal tubule structures, EPO expression is found in interstitial REP cell populations. Furthermore, metabolically differentiated analysis showed an increase in the expression of SGLT2 and EPO mRNA under HFD conditions.
In cell culturebased models, initial results suggest that glucose availability, hypoxic stimulation, and vitamin D treatment influence the expression of EPO and SGLT2. A dosedependent upregulation of EPO mRNA synthesis by vitamin D was demonstrated in the FAIK cell line. Further analyses of the interactions between metabolic and hypoxic signalling pathways are currently underway.

Conclusion: This study combined tissuebased and cell culturebased approaches to investigate the interaction between hypoxia signalling pathways and glucoserelated mechanisms in the kidney. The findings may contribute to a better understanding of renal metabolic adaptation and the regulation of EPO and SGLT2 under diabetic and hypoxic conditions.

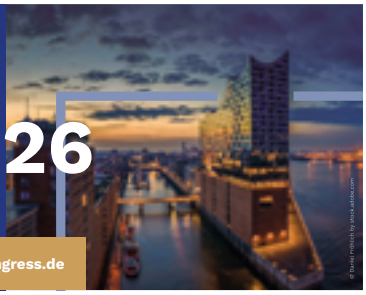

P26 Postergroup: Renal disease - oxygen/metabolism

P2612

The role of *Drosophila* nephrocytes on fly physiology in hyperglycemia

Karl K. Alornyo; Tobias B. Huber; Sybille Köhler
III. Department of Medicine, University Medical Center Hamburg Eppendorf, Hamburg, Germany;

Objective: Nephrocytes, the *Drosophila* homologue of mammalian podocytes, filter the hemolymph and secrete factors that influence distant organs, implicating them in systemic interorgan communication. We investigated the impact of nephrocyte absence on fly physiology under normal and metabolic stress conditions.
Method: We used *dKlf15* mutant flies, which lack nephrocytes, and Oregon R wildtype controls under normal diet and highsucrose diet (HSD). Functional (lifespan, climbing, Smurf assay), cellular (FITCalbumin uptake), and omics (hemolymph proteomics, bulk RNAseq of brain, gut, and heart/nephrocytes) approaches were applied.
Results: *dKlf15* mutants showed reduced lifespan, impaired locomotion, and accelerated gut barrier dysfunction on normal diet. HSD further reduced lifespan and elevated glucose, trehalose, and triglyceride levels in both genotypes. Notably, HSD improved climbing performance in mutants relative to controls, while accelerating gut injury in both strains. Oregon R flies developed HSDinduced nephrocyte filtration defects without morphological changes. Proteomics revealed conserved HSDassociated pathway alterations, including downregulation of immune and cytoskeletal processes and upregulation of metabolic and stress pathways. Transcriptomics identified distinct diet- and genotypedependent signatures across tissues.
Conclusion: Nephrocyte depletion reduces susceptibility to HSDinduced locomotor and gut phenotypes, underscoring nephrocytes as key regulators of systemic physiology under metabolic stress.

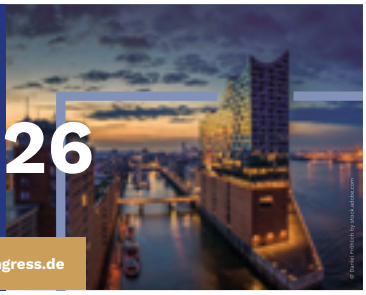

List of authors

Abbasi, Zeinab P09-01
Abdellatif, Mahmoud P13-01
Abdollahnia, Mohammad-Taha P12-05
Abeßer, Marco OC-12-03
Ablieh, Alia OC-02-02
Abouissa, Aya P25-02
Abplanalp, Wesley P03-03
Abreu, Sara Andreia Rodrigues P12-06
Adamzik, Michael OC-11-05
Adler, Marie P01-02
Agergaard, Jakob OC-08-03
Aguzzi, Adriano OC-12-02
Ahnert, Peter P03-12
Akhmedov, Alexander P13-02
Al Heialy, Saba OC-02-01
Albaiceta, Guillermo M. P26-02
Albertini, Giulia P24-03
Albinus, Ditte Mai Myrup P12-06
Alcicek, Fatih Celal P03-03, P16-09
Aldana, Blanca P08-07
Alesutan, Ioana OC-13-04, P02-10, P05-09, P17-07
Alexander, R Todd P22-13
Alexanderson, Helene P10-05
Alimy, Assil-Ramin P11-13
Alkner, Björn OC-01-06
Alle, Henrik OC-10-01, P18-03, P19-08, P19-15
Al-Masri, Sima OC-05-01
Alnajjar, Abdullah P04-04
Alornyo, Karl K. P01-14, P26-12
Alrø, Peter Nørrelund P03-11
Alschäfscky, Linus P24-03
Altayeva, Asli P02-09
Altmeppen, Hermann Clemens OC-12-02
Alzaim, Ibrahim P26-09
Alzheimer, Christian P19-01, P19-12
Amado-Rodríguez, Laura P26-02
Amer Kabouh, Mahmoud P23-03
Amirmiran, Bardia P25-05
Amrute-Nayak, Mamta OC-01-02, P04-07
Anan, Yaman OC-07-06
Andersen, Ask OC-11-04
Andersen, Gregers P21-05
Andersen, Helene P26-09
Andersen, Jesper Frank OC-03-02, P05-07
Andersen, Nicoline R. OC-01-04, OC-04-06, OC-08-03, P07-09
Andersen, Ove P03-09
Andersen, Pernille OC-04-06
Andersson, Daniel P10-03, P10-05
Andreasson, Kristofer M P10-05
Andresen, Maria Hovmann P03-04
Andriske, Michael P02-07
Anstötz, Max P23-03
Antczak, Philipp OC-03-03
Antony, Anson OC-13-04, P02-10
Appel, Ida P22-13
Apró, William P17-11
Arcuri, Edoardo OC-10-02
Arkan, Nick P01-02, P01-08
Armbruster, Annika P06-01, P06-08, P06-10
Asghariastanehei, Bita P09-02
Assmus, Adrienne P22-10
Ast, Volker P25-02
Asunama, Adhi Shree Raya P25-02
Atay, Jasmine C. L. P05-08, P21-02

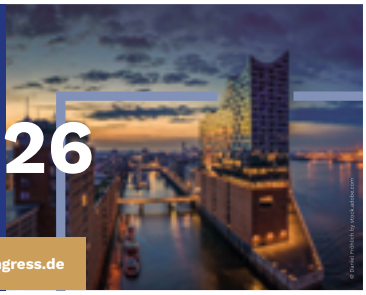

Aufenacker, Zino P08-08, P19-07
Auvinen, Juha P01-07, P11-05
Ayala-Torres, Carlos P11-11
Aygün, Talita P03-08
Azemi, Bardha P05-02, P09-12

B Thomsen, Morten P13-06
B. Binotti A. de Araujo, Isabela P26-08
Babenhauserheide, Anna P18-01, P18-10
Babes, Alexandru OC-07-04, OC-12-06
Babes, Ramona OC-12-06
Bach, Marie Lykke P21-03
Bachmann, Sebastian P21-10
Bader, Almke OC-04-01, OC-04-03
Baeta, Henrique P10-11
Bahiraii, Sheyda P02-10, P05-09
Bähring, Robert P18-01, P18-04, P18-07, P18-10, P18-13
Bakhareva, Alisa P19-16
Baksi, Arka OC-14-04, P16-11
Balzer, Felix OC-13-01
Bangsbo, Jens OC-01-04
Bär, Julia OC-12-02
Baranowsky, Anke P11-09, P11-13
Barbakadze, Salome P14-12
Bart, Cindy I. P23-08
Bashir, Faiza P11-03
Bastrup, Joakim A. P03-07
Battelino, Tadej P03-01
Bauer, Christiane K. P18-04, P18-10
Baukrowitz, Thomas OC-06-01, P09-08, P18-09, P18-11, P24-10
Baumgaertner, Ulf OC-10-02
Bayer, Marie Elisabeth P04-06
Bayer, Wibke P06-09
Becerra Moreno, Laura Johanna P01-10
Becker, Edgar OC-01-02
Becker, Jan Carl OC-15-05
Becker, Peggy OC-11-02
Becker, Roland OC-11-01
Beerens, Manu P23-05
Behrendt, Marc P09-07
Behrendt, Marc P09-01
Beier, Laura-Sophie P09-15, P22-04
Bek, Toke P26-09
Bellingkrodt, Antonia Lucrezia P21-10
Bencsik, Péter P04-05
Bengtsen, Mads P04-08
Benkerdagh, Chaimae P18-11
Benndorf, Klaus OC-06-02, P09-05, P18-08
Benson, Sven OC-15-02
Bentzen, Bo OC-09-05
Berdiev, Bakhrom K. OC-02-01
Berg, Peder Matzen OC-03-02, OC-05-05, P05-04, P05-07, P22-01, P22-12
Bergman, Bryan C. OC-08-03
Bergmeier, Marie P11-14
Bertelli, Sara OC-06-04
Bertelsen, Mads Frost P12-06
Bertog, Marko OC-07-06
Beule, Dieter OC-09-06
Beutner, Dirk P11-08
Biasini, Emiliano OC-12-02
Bickel, Tom P24-03
Bier, Jasmina OC-01-03
Billing, Anja M. P26-06
Binzen, Uta P20-03
Birdir, Cahit P03-08

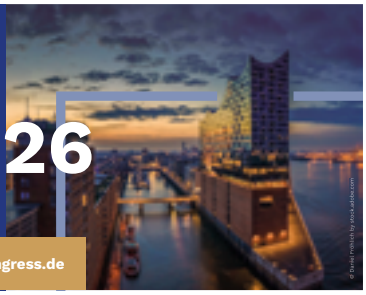

Birke, Anne P04-09
Birn, Henrik OC-13-03, P05-07, P21-05
Bischofberger, Josef P08-01
Bisen, Rajeshwari P18-05
Bishop, Christopher Allen P17-06
Bistrup, Claus OC-05-04
Bitzenhofer, Sebastian H. P07-10, P07-13
Bivoleanu, Ramona-Andreea P09-09
Blanchet, Clement OC-12-02
Bleich, Markus P22-02, P22-04
Blum, Kerstin OC-10-04
Blume, Lukas OC-04-05, P01-06, P01-13, P26-07
Boas, David P07-05
Bock, Theresa P13-01
Böckenhauer, Detlef P05-01
Bode, Steffanie P14-12
Boehm, Johannes P08-13
Boes, Mette Boye OC-05-04
Boettcher-Dierks, Vincent P01-08
Bogdanovic, Milos P22-05, P22-13
Böger, Rainer H. P06-05, P15-06
Bohlen, Lucas P12-02
Bonetti, Alessandro P04-01
Boras, Zdenko P03-05
Borchardt, André Atef P03-12
Borgmann, Hendrik OC-11-01
Borgmeyer, Maximilian P08-08
Both, Martin P12-05, P19-11
Böttcher-Dierks, Vincent P01-02, P01-05
Bottermann, Katharina P17-09, P25-06
Bouchard, Michelle P01-14
Bourdin, Mathilde P09-02
Bouron, Alexandre P14-05
Boyken, Janina P21-07
Boysen, Anders Toftegaard P21-02, P21-09
Bozyil, Ahmed Sait P17-01
Brand, Johannes P01-05, P26-07
Brandenberger, Christina OC-02-01
Brandes, Ralf P. P03-03, P04-01, P04-03, P04-06, P04-10, P16-09, P16-12, P17-12, P25-05
Brandt, Camilla P26-09
Brandt, Katharina OC-01-02
Brandt, Sören P08-10
Braun, Jessica L. OC-08-03
Braun, Maximilian P04-06
Braun, Rebecca OC-04-05
Braun, Stefan P10-02
Braun, Thomas P16-05
Brechmann, Noah P11-07
Brendel, Heike P03-08
Brendel, Josephine OC-09-06
Brinkmeier, Heinrich OC-01-05, P09-13
Broeker, Katharina Anna-Elisabeth OC-08-05, P26-01
Bruegmann, Tobias P23-07
Brügmann, Tobias P02-05, P11-08
Brunetti, Andrea P12-09
Brunsch, Dave OC-15-04
Bruusgaard, Jo C. P04-08
Buchberger, Christina P09-06
Bucher, Michael P02-08
Buck, Maike P11-13
Budde, Thomas P08-12
Budeus, Bettina P15-01
Bulk, Emma Etmar P14-03
Büttner, Tamara P06-09, P11-07
Butz, Frederike P14-02

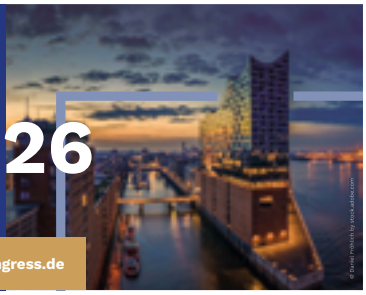

Buus, Niels Henrik P05-07

C. C. Girardi, Adriana OC-05-06
C. Danner, Bernhard P23-07
CabreraOrefic, Alfredo P16-12
Calabresi, Peter A. OC-01-03
Calloe, Kirstine P12-06
Cambet, Yves P09-02
Canavier, Carmen P18-06
Cantow, Kathleen P26-04
Cantutan, Berk OC-03-03
Cao, Ye P17-10
Caragea, Violeta Maria OC-07-04, P09-09
Carlantoni, Claudia P23-05
Carls, Esther OC-09-03
Carlström, Mattias P10-05
Carpentier, Gilles P09-15
Carr, Richard P09-01
Carrel, Monique OC-05-02
Carstens, Earl P09-09
Castebou, Cyril P09-02
Castro-Marsal, Júlia P09-04, P09-07
Catão D. Braga, Gabriela OC-05-06
Cejka, Daniel OC-13-04, P05-09
Celik, Funda P11-09
Chakraborty, Rahul P16-06
Chambrey, Régine P22-13
Chan, Shing Hei Darren OC-11-06
Chavakis, Triantafyllos OC-14-04
Chen, Yipeng OC-03-06, P01-11
Chen, Ying OC-04-02
Cheng, Chaodi P23-07
Cheng, Jingyuan OC-04-01
Cheng, Lei P26-09
Chernoff, Jonathan OC-08-02
Cheung, Stephen P15-04
Chitroceanu, Alexandra Maria OC-02-01
Cho, Woolyn P15-10
Choi, Yoon Young OC-09-04
Chouchani, Edward T. P17-13
Choudhary, Shalini P01-07, P11-05
Christensen, Birgitte Mønster P05-06
Christensen, Maria Vestergaard P03-09
Chung, Charles P10-01
Cicek, Suna P06-09
Ciechanska, Dominika P14-03, P14-12
Claußen, Maike P19-14
Connes, Philippe P09-02
Conradi, Lena-Christin P02-05
Conway, James OC-08-06
Cordeiro, Sönke P09-08, P18-14, P24-10
Cordero, Julio P25-02
Costantino, Sarah P13-02
Cragg, Stephanie P18-06
Cuello, Friederike P23-05
Cui, Minying P10-04
Curin Serbec, Vladka OC-12-02

D. K. Hamilton, Aimi P21-04
d´Acierno, Mariavittoria P26-08
da Costa, Raul OC-04-01
da Rocha, Joana F. OC-01-03
Dam, Vibeke S. OC-05-03
Damba, Turthushikh P22-03
Damkier, Helle Hasager OC-07-02, P24-14
Damsgaard, Christian P22-01
Daniel, Christoph P26-01
Das, Anupam OC-14-04, P21-06

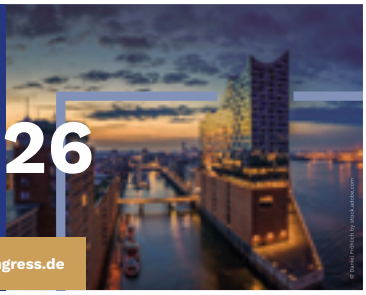

Dastmalchi, Maryam P10-05
Daum, Nils OC-13-01
Davies, Ben P05-01
de Borst, Martin H. P05-03
de Groot, Bert P18-09
de Lima, Franciele P09-02
De Strooper, Bart P24-03
de Vega Gómez, Enrique OC-04-01, OC-04-03
de Vries, Antoine A. F. P23-08
Dechend, Ralf OC-02-01
Dehmer, Emelie P09-04
Dekker, Sven O. P23-08
Delos Reyes, Buena P11-07
Demaurex, Nicolas P09-02
Demir, Fatih OC-05-06, P01-13, P21-05
Dendorfer, Andreas P25-03
Dervas, Eva P12-06
Deschler, Rose P24-06
Desdorf, Lasse Messell OC-07-02, P24-14
Deshmukh, Atul S. OC-01-04
Dessauer, Carmen P12-09
Dettmer, Katja P05-01
Deußen, Andreas OC-11-02, OC-14-04
Diederich, Lena OC-06-03
Diefenbach, Andreas OC-12-04
Diehm, Johanna P06-10, P15-08
Dieplinger, Benjamin OC-13-04, P05-09
Dieter, Alexander P08-14, P20-03
Dimke, Henrik P05-10, P22-02, P22-03, P22-05, P22-06, P22-13
Ditiashova, Vladyslava P01-09
Dittmer, Ulf P06-09
Diyakov, Alexey OC-15-03
Dodon, Daria P19-09
Dogan, Batuhan P26-07
Dokshokova, Lolita P26-09
Dominguez Rieg, Jessica A. OC-05-01
Dominik, Elisabeth P25-04
Domocos, Dan OC-12-06
Door, Michaela OC-14-05
Dörre, Maximilian OC-15-04
Dorsch, Anna Daniela P06-03
Dovc, Klemen P03-01
Draguhn, Andreas P12-05
Drakhlis, Lika OC-14-02
Drenjancevic, Ines P03-05, P03-13, P03-14, P16-13
Drexler, Nils OC-06-03
Drieu La Rochelle, Julie OC-08-02
Drumm, Bernard P20-02
Dubik, Magdalena O P01-09
Dubourg, Virginie P04-02
Düfer, Martina P14-03
Duh, Maja P17-03
Duncan, Anna Louise OC-07-02
Dura, Miroslav OC-06-05
Dutzler, Raimund OC-06-04
Duvarci, Sevil P07-12, P08-11
Dyck, Birte OC-11-05
Dyreborg, Sofie P21-05

Ebert, Antje D P12-05
Ebert, Franziska P19-12
Eckardt, Kai-Uwe OC-13-01
Edelmann, Elke P19-03
Edelmann, Elke P07-11, P19-04
Edelmann, Frank OC-02-01
Edemir, Bayram OC-13-06, P22-14

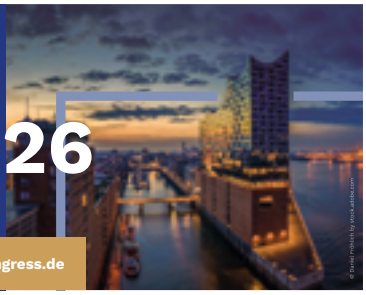

Edman, Sebastian P17-11
Efimov, Igor OC-09-02
Eftestøl, Einar P04-08
Egée, Stéphane P09-02
Egger, Margot OC-13-04, P05-09
Egger-Mackrodt, Richard P08-04
Egorov, Alexei V. P19-11
Ehmke, Heimo P13-08
Ehrhardt, Anja P06-09
Einsle, Anne P24-02
Eiring, Lisa OC-15-02
Eladari, Dominique P22-13
Elbenhardt Jensen, Thomas P17-13
Eller, Ruth S. OC-01-05
Ender, Anatoli P14-08
Endres, Thomas P07-11, P19-13
Engel, Daniel Robert OC-04-03
Engel, Jutta OC-10-04
Engel, Kristina OC-13-06
Enggaard, Camilla P21-03
Enghard, Philipp OC-13-01
Enke, Uta P09-05
Enzeroth, Raissa P09-07
Erappanakoppalu Veerabhadra, Jayashree P09-08
Erdogan, Cem OC-03-01, OC-13-01, OC-13-06, P03-10
Eresch, Jeanette P25-02
Erfinanda, Lasti OC-07-05
Ergasheva, Zhasmina P19-16
Eriksson, Gustaw OC-01-06
Ertas, Asude OC-01-03
Ertürk, Ali OC-04-02
Eschholz, Lena P08-14
Esquivel-Ruiz, Sergio A. P26-02
Euler, Gerhild P04-04
Evers, Lennart P02-05
Exojo-Ramírez, Sara M. P26-02

F. Jesus, Érika OC-05-06
Faber, Cornelius OC-14-05
Færgeman, Nils J. P17-13
Fähling, Michael OC-03-01, OC-13-01, OC-13-06
Faidel, David OC-02-01
Fakhreddine, Wassim P02-11
Fakler, Bernd P24-05
Falivene, Juliana P24-06
Falsig Pedersen, Stine P08-07
Fandrey, Joachim OC-02-03, OC-08-04, OC-15-02, P06-07, P06-09, P11-07, P11-12, P15-01, P15-07, P17-05
Fanutza, Tomas P08-08, P19-07
Feger, Martina P11-10
Fei, Lingyan OC-03-01
Felber, Julian OC-13-01
Feliciano, Raquel P03-09
Fels, Benedikt P16-07, P16-08
Fenton, Robert P22-10, P26-08
Ferdinandy, Péter P04-05
Fernández, Julián P13-07
Fernández-Fernández, José M. P09-02
Fertig, Niels P09-02
Fessen, Pauline P06-03
Filippi, Kerstin P10-11
Firmke, Bettina Katharina Mariana OC-08-05, P26-01
Fischer, Jens W. P17-09
Fischer, Philipp OC-10-04

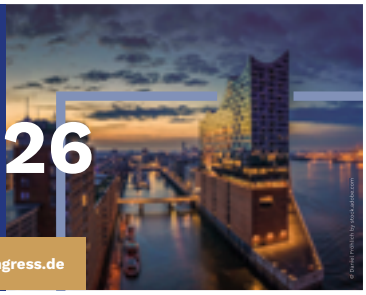

Fisslthaler, Beate P16-06, P25-05
Fleischmann, Bernd K. OC-09-03, OC-11-05, P10-11, P23-09
Fleming, Ingrid P02-04, P04-09, P16-06, P25-05
Fois, Giorgio P06-01, P06-08
Föller, Michael P11-10
Forné, Ignasi OC-04-03
Forst, Anna-Lena OC-08-05, P26-01
Förster, Robert P22-12
Fowler, Carley P26-03
Frahnert, Konrad S. OC-06-06
Frank, Emma OC-08-03
Frank Andersen, Jesper P22-01
Franke, Annika OC-14-02
Franssen, Caspar F. P16-07
Franz, Denise P07-01, P08-05
Franz, Kristina OC-02-01
Franzén, Stephanie P26-03
Freier, Marie P11-08
Freiman, Thomas M. P24-02
Freitag, Daniela P08-02
Frenz-Wiessner, Stephanie OC-04-01
Freundt, Johanna OC-09-01, OC-14-05
Frey, Norbert P12-05
Frick, Manfred P06-01, P06-06, P06-08, P06-10, P15-08
Friederichs, Kathar P25-09
Friese, Manuel A. OC-01-03
Frisdal, Angele P05-10
Fritz, Veronika P07-07
Fritzen, Andreas M OC-04-06
Frömbling, Sarah P01-02, P01-06, P14-05
Frömel, Timo P02-04
Fromm, Anja OC-12-04
Fromm, Michael OC-12-04
Frühauf, Alexander P03-08
Frye, Maike P23-05
Fuchtbauer, Ernst-Martin P22-13
Fuszard, Matthew OC-08-02

Gagnon, Dominique P15-04
Galler, Stefan P20-01
Gand, Luis OC-01-02
Gao, Jincheng OC-04-01, OC-04-03
Garaschuk, Olga P07-02, P19-09
Garrido-Charles, Aida P23-07
Gärtner, Katrin P24-02
Garumann, Johannes P16-06
Gastaldello, Stefano P10-05
Gatterer, Hannes P15-02
Gaudatis, Simonas P01-06
Gebauer, Cara P14-02
Gebhardt, Wulf P23-01
Geiger, Jörg Rolf Paul OC-10-01, P08-06, P18-03, P19-02, P19-08, P19-15, P24-03
Geiges, Linda P05-02, P09-12
Gejl, Kasper D. P10-09
Gekle, Michael P02-08
Geladas, Nickos P15-09
Gerevich, Zoltan P08-06, P19-02
Gernemann, Marlon P24-01
Ghadimi, Michael P02-05
Gharagozloo, Marjan OC-01-03
Ghezellou, Parviz P16-09
Ghodrat, Roohallah P17-08
Gibhardt, Christine S. P14-07
Gieselmann, Volkmar OC-11-05
Gillan, Jonathan L. OC-02-01

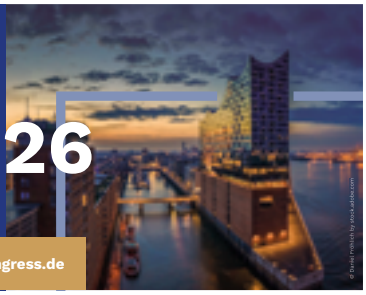

Ginsbach, Laura P03-12
Girardi, Adriana C. C. OC-05-01
Girdauskas, Evaldas P12-09
Gladytz, Thomas P21-07, P26-04
Glatzel, Markus OC-12-02
Gnielka, Felicitas E.M. P11-11
Gödecke, Axel P13-03
Goettsch, Claudia P21-06
Gohr, Olga P19-14
Gondin, Julien OC-01-02
Görlach, Agnes P11-02
Gorressen, Simone P17-09
Gorsek Sparove, Tina OC-01-06
Görtz, Gina-Eva OC-08-04
Gosak, Marko P17-03
Gottlieb, Lisa A. P25-09
Gottmann, Kurt P07-11
Gottschalk, Alexander OC-06-05
Graewert, Melissa OC-12-02
Graf-Riesen, Kathrin P10-11
Grandjean, Anna Louise Venning P26-08
Graumann, Johannes P04-09
Green, Benjamin B. OC-05-03
Greffrath, Wolfgang P20-03
Grey, Michael J. P09-15
Griffin, Caoimhin P02-13, P20-02
Grisk, Olaf OC-09-06, OC-11-01
Gritter, Martin P05-03
Grochowska, Katarzyna OC-12-02
Groetzner, Sarah P06-10
Grøndahl, Carsten P12-06
Grosenick, Dirk P26-04
Grosse-Onnebrink, Joerg P24-09
Grosser, Sabine OC-10-01, P19-08
Groß-Esser, Felix Niklas OC-07-03
Grossmann, Claudia P11-01, P16-03
Großmann, Lena P23-03
Groves, Teddy P26-10
Grunau, Martin P24-11
Gründer, Stefan OC-08-01, P11-15, P14-11
Grune, Jana OC-02-01, P24-06
Grünert, Tobias P19-02
Gudiksen, Anders OC-08-03
Guendel, Fabian OC-12-04
Gühmann, Martin OC-15-06
Guizouarn, Hélène P09-02
Gül, Zeynep Melis OC-04-04
Guldbrandsen, Halvor Osterby P12-01
Gundersen, Kristian P04-08
Günther, Stefan P04-06, P04-09, P16-06, P16-12
Günzel, Dorothee P05-05, P09-10, P09-14, P21-10
Gupta, Neha P02-13
Gustafsson, Thomas OC-01-06
Gutierrez, Eugenio Jimenez P03-04
Gutiérrez, José María P13-07

Haack, Alina P06-05
Haas, Rainer OC-04-02
Hach, Line Fleischer P03-09
Haddad, Bassam George OC-07-03
Hadler, Michael P19-15
Haertter, Daniel P10-11
Hägerling, René P23-05
Haley, Kaela OC-01-03
Halland, Nis P11-02
Halter, Rebecca Zoe OC-05-01

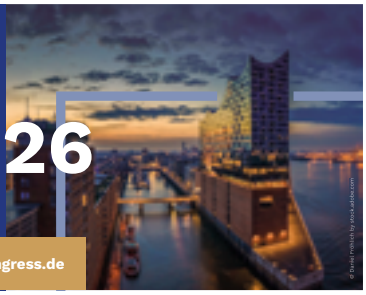

Hämälainen, Mari P01-07
Hamann, Eliott P13-06
Hamilton, Aimi OC-13-03
Hammer-Bahador, Niklas P08-04, P08-13
Hanley, Peter OC-08-02
Hanley, Peter J. P23-08 P24-11
Hannemann, Juliane P06-05, P15-06
Hansen, Camilla C. P07-09
Hansen, Line Mathilde Brostrup P07-05, P24-01
Hansen, Sandra M. P26-05
Hansen, Ulf-Peter OC-06-03
Harbaum, Lukas P04-04
Hardenberg, Jan-Hendrik B. OC-13-01
Harms, Frederike L. P18-04
Hartmann, Paulina OC-14-05
Hasan, Jian P09-13
Hasenberg, Mike P11-07
Hashmi, Mohammad Amiruddin OC-02-01
Hatje, Favian P01-13
Hauck, Sören P11-08
Havelund, Jesper P17-13
Hayslip, Natalie OC-05-01
Hazelton-Cavill, Paris OC-03-03, P01-12, P01-14
Hebar, Pia P17-09
Hebatullah, Laban OC-02-02
Hebrok, Daniel P24-07
Hecker, Markus OC-02-02, P02-03
Heckmann, Manfred OC-10-03, P19-10
Hedden, Maren P06-05
Heer, Jonas P12-03, P23-02
Heerdegen, Marco P07-01
Heeringa, Amarins N. P19-06
Heermann, Ralf P04-06
Hegelund Rasmussen, Katrine P13-06
Hegemann, Niklas OC-02-01
Hegemann, Peter OC-06-02
Heger, Jacqueline P25-01
Heineke, Jörg P25-02
Heinemann, Stefan H. OC-06-06
Heinen, Andre P13-03
Heinl, Antonia P21-03
Heinrich, Lara Maria Astrid P18-12
Heiter, Julia P11-06, P12-04
Hellal, Farida OC-04-02
Hellsten, Ylva OC-14-01, P13-06
Hengst, Clara M. P03-08
Hennig, Finn P14-05
Henning, Yoshiyuki OC-08-04, P06-07, P15-01
Hennings, Christopher P22-13
Henriquez-Olguin, Carlos P17-13
Hentsche, Carmen P16-11
Hepper, Ingrid OC-04-03
Herold, Kristina OC-03-05
Herzig, Karl-Heinz OC-12-05, P01-07, P11-04, P11-05
Hesse, Michael P10-11
Hessel, Anthony P10-01
Hetzel, Udo P12-06
Heuer, Alexa P14-12
Heuser, Arnd OC-09-06
Hildebrandt, Thomas P21-10
Hill, Cameron P10-01
Hille, Susanne OC-09-01, OC-14-05
Himmerkus, Nina P22-02, P22-04
Hinrichs, Gitte R. OC-05-04, P01-09
Hite, Richard P24-05

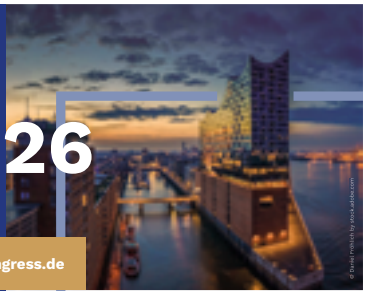

Hobson, Chad OC-05-03
Hoerr, Verena OC-14-05
Hoffmockel, Risto P03-06
Höger, Thomas P11-13
Hollywood, Mark P02-13
Holm, Oliver P13-06
Holstein-Rathlou, Niels-Henrik P26-10
Holtmeier, Richard OC-14-05
Holtze, Susanne P21-10
Honeycutt, Samuel E. OC-01-03
Hoorn, Ewout P05-03, P26-08
Horack, Alexander P02-01
Hörnschemeyer, Max P08-05
Horsthemke, Markus OC-08-02, P23-08
Hostrup, Morten OC-01-04
Hreha, Teri P01-09
Hu, Jiong P02-04
Hu, Marian P09-11, P18-14, P24-08
Hu, Poyi P06-04
Huang, Yuanyuyue P22-04
Huber, Tobias B. OC-03-03, P01-12, P01-14, P26-07, P26-12
Hubner, Norbert OC-09-06
Hübner, Christian A. P22-13
Huesgen, Pitter F. P10-11
Hülße, Sina P11-10
Hummel, Luis P21-07
Hussein, Rama OC-06-06
Huth, Lisa P. P12-04
Hutzfeldt, Arvid P01-13
Hyndman, Kelly A. P26-03
Hyttinen, Jari P14-09

Iaconianni, Pia P12-03
Ihalainen, Teemu O. P14-04, P14-09
Ikeotuonye, Chukwuanyinonso P02-07
Ilieva, Mirolyuba P05-08
Ilyaskin, Alexandr V. OC-07-06, P05-02, P09-12, P22-11
Imenez Silva, Pedro Henrique P05-03
Immler, Roland OC-04-02
Iodi Carstens, Mirela P09-09
Iqbal, Mohammed Ariff OC-01-03
Ishikawa-Ankerhold, Hellen OC-04-02
Isomäki, Märi P14-04
Issler, Travis P24-07
Itani, Nadja P04-05
Ivanov, Andranik P24-03
Ivaskevica, Karina OC-14-02

Jacobi, Robert OC-10-03, P19-10
Jaeschke, Lara OC-02-01
James, David E. OC-08-03
Jangsangthong, Wanchana OC-06-05, P12-08
Janßen, Sven-Tore P23-05
Janus, Franziska OC-12-04
Jaquet, Vincent P09-02
Jarvelin, Marjo-Riitta P01-07, P11-05
Jasarevic, Hena OC-09-02
Jasinski-Bergner, Simon OC-11-01
Jauch-Speer, Saskia-Larissa P23-05
Jeansson, Marie OC-13-02
Jensen, Boye Lagerbon OC-05-04, P21-03
Jensen, Iben Skov P01-09
Jensen, Jørgen Arendt P01-01
Jensen, Lars Jørn P03-09
Jensen, Mia P21-03
Jensen, Mathias D.H. P10-09

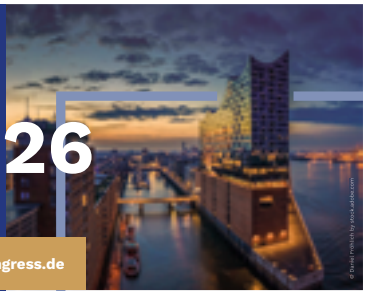

Jensen, Nicoline Staerke P24-14
Jensen, Rasmus P10-06
Jensen-Fangel, Søren P05-04
Jentsch, Thomas J. P24-05
Jeppesen, Majbritt P05-04
Jepps, Thomas OC-14-01, P03-07, P13-06
Jeschke, Udo OC-04-02
Jespersen, Bente P21-04
Jespersen, Thomas P25-09
Jessen, Niels P26-09
Jessen, Soeren OC-01-04
Jia, Huimin P02-02, P03-02
Jia, Longyuan P03-03, P16-09
Jimenez, Natalia Perez P01-01
Johnsen, Laura Oellegaard P24-14
Jokelainen, Jari P01-07, P11-05
Jolie, Theresa P14-06
Jonas, Wenke P17-10
Jones, Emily Aery P19-15
Jordy, Andreas B. OC-08-03
Jørgensen, Kasper S OC-04-06
Jørgensen, Sebastian B. P07-09
Joshi, Pooja OC-09-02
Jude, Baptiste P10-04
Jukic, Ivana P03-13, P03-14, P16-13
Jung, Johannes P14-01
Jurida, Liane Moana P25-04, P25-08
Jurisch, Victoria P03-03, P16-09

Kaestner, Lars P09-02
Kaira, Aayushi OC-08-06
Kaiser, Kira P07-06, P08-10
Kaiser, Toralf P03-12
Kakinuma, Hayato Yuuto OC-04-05
Kalaiselvan, Sowmiya P26-09
Kalayci, Lea Amina P23-05
Kalinski, Thomas OC-11-01
Kaloshi, Kevin P04-04
Kaltsoni, Iro P15-09
Kalucka, Joanna P26-09
Kameritsch, Petra P09-06, P25-03
Kampman, Olli P01-07
Kamps, Janine OC-12-02
Kang, Jiaming P07-03
Kann, Oliver P19-11
Kanta, Josephine Maria OC-04-06, P07-09
Kar, Sumanta P24-05
Karin, Kirschner P01-11
Karlsen, Anders OC-08-03
Kartalou, Georgia Ioanna P07-11
Karuppusamy, Shobika P22-14
Kasbary, Alexander P02-10
Kashefi, Ali P15-03
Kawabe, Hiroshi OC-08-06
Keine, Christian P19-06, P19-14
Keller, Anna Krarup OC-13-05
Kelterborn, Simon OC-02-05
Kempf, Sebastian P02-04
Kensah, George P23-07
Kercmar, Jasmina P17-03
Kern, Teresa P11-14
Ketterer, Barbara OC-13-04, P05-09
Khalifa, Asmaa P11-02
Khan, Bushra P04-07
Khan, Natasha Nadeem P08-11
Khanduri, Astha P04-03
Khedkar, Pratik Hemant OC-03-01, P03-10
Khodaie, Babak P19-04, P19-11

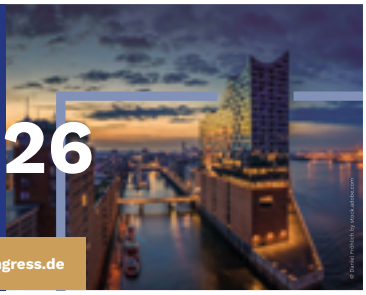

Khomeijani Farahani, Saeed P09-10, P24-11
Kibel, Aleksandar P03-14
Kick, Christina P14-03
Kiefer, Friedemann P14-12
Kiel, Annika P11-14
Kiens, Bente OC-04-06, OC-08-03, P17-13
Kikot'ová, Natalie P19-09
Kilauridze, Vakhtang P16-11
Kim, Young Chul P26-06
Kim-Hellmuth, Sarah OC-04-04
Kimura, Kenichi P10-11
Kind, Andreas OC-02-01
Kindig, Selina P06-08
Kindler, Stefan P18-01, P18-07, P18-13
Kirk, Jonathan OC-14-05
Kirschner, Karin Michaela OC-03-06, P03-10, P17-02, P21-08
Kirschstein, Timo P02-11, P24-02
Kirsten, Holger P03-12
Kißler, Alicia P22-11
Kittmann, Enrico P23-05
Kiukaanniemi, Sirkka Keinänen P01-07
Kiziltug, Mehmet OC-04-01
Kjær, Michael OC-08-03
Kjems, Jørgen P07-05
Kjølby, Mads OC-05-04
Klaassen, Sabine OC-09-06
Kläser, Eva P14-11
Klausch, Monique P07-11
Klein, Christoph OC-04-01
Kleinert, Maximilian P17-06, P17-10
Kleinsang, Fiona P06-05
Klemmer, Anna P09-03
Kleta, Robert P05-01
Kleuser, Burkhard P26-02
Klinke, Anna OC-14-03, P25-10
Klose, Verena OC-15-04
Klotz, Annika J. OC-09-01, OC-14-03, OC-14-05
Klotzsche von-Annelm, Anne P16-11
Kluge, Josephine OC-15-04
Klüssendorf, Malte OC-06-04, P09-03
Knauf, Felix P05-01
Knaus, Ulla G. OC-08-02, P24-11
Knipp, Sabine P02-10
Knosalla, Christoph OC-02-01, P02-02, P03-02, P06-04
Knowlton, Christopher P18-06
Knyrim, Maria OC-14-04
Kocana, Ceren OC-02-01
Koch, Josephine P16-07
Koch, Jochim P12-04
Koch, Oliver P14-03
Koch, Philipp P17-02
Kochina, Evgeniya P09-14
Koch-Nolte, Friedrich OC-03-04
Kofoed, Klaus Fuglsang P25-09
Kohl, Peter P12-03, P23-02
Köhler, Conny P16-03
Köhler, Sybille OC-03-03, P01-12, P01-14, P26-12
Köhling, Rüdiger P02-01, P02-11, P07-01, P08-05, P24-02
Koivumäki, Jussi P12-10
Kolb, Philipp P06-06, P06-10, P15-08
Koll, Nora P15-07
Kolobaric, Nikolina P03-13, P03-14, P16-13
Komoltsev, Ilia OC-10-06
König, Jennifer P22-07
Kononenko, Natalia P07-07

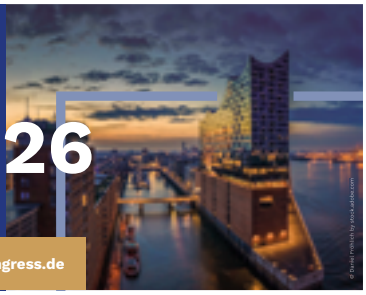

Konze, Sarah OC-14-02
Koos, Björn OC-11-05
Kopaliani, Irakli OC-11-02, OC-14-04, P16-11, P21-06
Korbmacher, Christoph OC-07-06, P05-02, P09-12, P22-11
Korff, Thomas OC-02-02, P03-06
Kornblum, Cornelia P10-11
Korotkova, Tatiana OC-10-06, P19-16
Kortenoeven, Marleen P22-03, P22-13
Koser, Franziska OC-14-05, P13-01
Koskolou, Maria P15-09
Kostenis, Evi OC-11-05
Kostritskaia, Yulia P09-03
Kosub, Christopher P01-06
Kotulski, Katharina P23-03, P25-06
Kovac, Valerija OC-12-02
Kovalchuk, Yury P07-02, P19-09
Kovalenko, Elina P13-04, P26-06
Kowalski, Kathrin P13-07
Kracht, Michael P25-04, P25-08
Kraeker, Kristin OC-02-01
Kraft, Theresia OC-01-02, OC-14-02, P04-07, P10-10, P13-07
Kralemann-Köhler, Angela P11-14
Kralj, Lana P17-03
Kramer, Edgar OC-08-06
Kraus, Pauline OC-10-02
Kraut, Simone P23-04
Krautwald, Mirjam OC-01-05, P09-13
Kravtsova, Olha OC-11-03
Kresse, Jean-Claude P21-05
Kretzler, Lucie OC-02-01
Kretzschmar, Tom OC-02-02
Kreutz, Julian P04-04
Krishnacoumar, Brenda OC-02-03, P06-09
Krishnasamy, Nadashree P03-12
Kristensen, Lasse Sommer P07-05
Križancic Bombek, Lidija P17-03
Krug, Susanne OC-12-04, P11-11
Krüger, Agnes Yasmine P04-06, P16-12
Krüger, Chiara-Sophie P07-04
Krüger, Elke OC-04-05, P26-07
Krüger, Marcus P13-01
Krüger, Martina OC-06-05, P23-03, P25-06
Kübler, Wolfgang OC-02-01, OC-02-06, P02-02, P03-02, P03-12, P06-02, P06-04, P24-06, P26-02
Kucherenko, Mariya M. OC-02-01, P02-02, P03-02, P06-04
Kuhn, Alexandra OC-14-06
Kuhn, Michaela OC-12-03
Kühnisch, Jirko OC-09-06, OC-11-01
Kühs, Samuel P14-11
Kulow, Vera Anna OC-03-01, OC-13-01, OC-13-06
Künne, Carsten P04-09
Kunz, Wolfram S. P10-11
Kunze, Tamara P16-07
Kunzelmann, Karl P21-01
Kuon, Felix Maximilian P07-04, P12-07
Kuppusamy, Maithreyan P10-11
Kürstein, Franz OC-09-06
Kurt, Simone OC-10-04
Kurtoglu Babayev, Fatima Hacer P25-05
Kusch, Kathrin P23-07
Kusche, Kristina P16-07, P16-08
Kuspiel, Sven P14-11
Kwon, Andrew OC-04-04

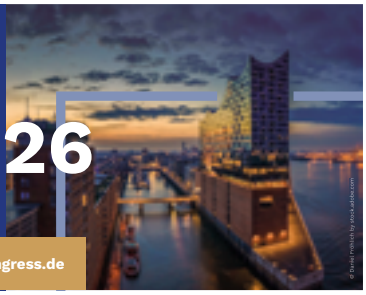

L. Martins, Flavia OC-05-06
Labes, Robert OC-03-01, OC-13-01, P21-10
Lackner, Helmut K. P05-09
Lagos, Fredy Delgado P25-05
Lahme, Karen OC-03-04, P01-04, P01-05, P01-06, P01-08, P01-10
Lam, Chun Kei P18-09
Lampert, Alina P01-06
Lamprecht, Georg P22-12
Landsberger, Martin P09-13
Landstorfer, Helena OC-02-05, P17-02
Lang, Laurine P22-08
Lange, Falko P02-11, P24-02
Langen, Judith Sofie OC-06-05, P25-07
Langner, Isabelle P24-06
Lanner, Johanna OC-01-06, P10-04
Lanner, Johanna T. P17-11
Lanzuolo, Chiara P04-07
Larsen, Steen OC-08-03
Lassé, Moritz OC-03-03, P01-12, P01-13
Lastinger, Julia P17-07
Laursen, Nick P21-05
Lauschke, Volker M P10-05
Lautala, Saara P14-06
Lebender, Leonard F OC-11-05
Lee, In-Fah M. OC-12-04
Lee, Rachel OC-05-03
Lee, Wing-Kee OC-12-01, P11-14, P24-07
Leffler, Andreas OC-12-06
Lehnart, Stephan E. OC-06-05
Lehr, Stefan P17-09
Lehto, Vesa-Pekka OC-12-05
Leijding, Cecilia P10-05
Leineweber, Pia OC-09-03
Leipziger, Jens Georg OC-03-02, OC-05-05, P05-04, P05-07, P22-01, P22-12
Leisegang, Matthias P04-01, P04-06, P04-09, P04-10, P16-12
Leistner, David M. P03-03
Leßmann, Volkmar P07-11, P19-04, P19-13
Lewin, Gary L P21-10
Li, Binjie OC-09-02
Li, Caihong OC-07-05
Li, Dan OC-09-04
Li, Gefei P24-06
Li, Housen OC-06-05
Li, Ling P23-04, P25-04, P25-08
Li, Mugeng OC-01-02
Li, Ni OC-09-04
Li, Qiuhua OC-02-01, P02-02, P03-02, P06-04
Li, Xueyu P01-06
Li, Xia OC-04-02, OC-04-04
Li, Yu OC-11-06
Li, Yong P12-09
Lichtenberger, Falk-Bach OC-03-01, P03-10
Lichtenfeld, Helena C. OC-01-03
Liebe, Franziska P09-10
Liekfeldt, Julia P09-13
Lifke, Marcus P15-06
Lin, Lin OC-13-05, P26-09
Linder, Monika I. OC-04-01
Lindholt, Jes Sanddal P03-11
Lindqvist, Cecilie B. P07-09
Link, Tanja P05-01
Linke, Wolfgang A. OC-09-01, OC-14-03, OC-14-05, P10-11, P13-01
Linz, Dominik P25-09
Lippmann, Kristina OC-10-03, P19-10
Lira, Mario P15-03

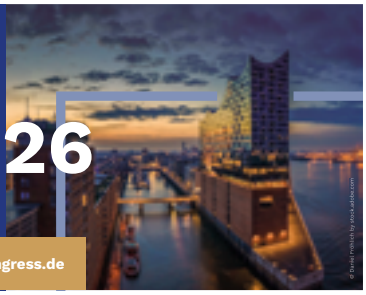

Littwitz-Salomon, Elisabeth P06-09
Liu, Shuya P26-07
Liu, Shaofei P03-02
Liu, Zihou OC-12-03
Lizé, Muriel P06-10
Lode, Holger P06-03
Loesslein, Anne OC-04-02
Loffing, Dominique OC-05-02, P22-09
Loffing, Johannes OC-05-02, P22-09
Login, Frédéric H. OC-05-03
Loho, Jurek P24-13
Lomonte, Bruno P13-07
Long, Jonathan Z. P07-09
Longo, Piersilvio OC-07-03
Lopes, Emanuel P18-06
Lopez, Melina P03-03
López Dávila, Alfredo J. OC-15-05, P13-07
Lorenz, Jürgen P07-04, P12-02, P12-07
Loreth, Desiree P01-02, P01-05, P01-06, P01-08, P14-05, P26-07
Löscher, Christine OC-14-05
Lu, Yingning P08-09
Lu, Zizhuo P24-10
Lubomirov, Lubomir OC-11-01, P02-07
Lucas, Robert P23-02
Luis Dias Casacão, Maria P16-04
Lund, Lars P22-13
Luo, Yonglun P26-09
Lupu, Loredana-Mirela P16-06
Lüttjohann, Annika P08-12
Lutze, Philipp P09-13

M. Kuebler, Wolfgang OC-07-05
Ma, Weikang P10-01
Maas, Renee P23-06
Maaß, Michelle P26-11
Machtens, Jan-Philipp OC-07-03
Madl, Josef P12-03, P23-02
Madry, Christian P08-06, P19-05, P24-03
Madsen, Kirsten P22-03, P22-13
Madsen, Mia Gebauer OC-13-05
Madsen, Nikolaj Horskær P03-11
Mager, Thomas P23-07
Magnus Wahlgren, Carl OC-01-06
Maier-Begandt, Daniela OC-04-01, OC-04-03
Mailer, Reiner P23-05
Mäkelä, Kari P01-07
Makridakis, Manousos P02-10
Malan, Daniela P12-08
Maletzki, Claudia P24-02
Malita, Alina P17-13
Malotka, Laetitia OC-13-01, OC-13-06
Malte, Hans P22-01
Malysa, Michael P04-04
Malyshkina, Anna P06-09, P15-01
Mamaj, Fjorarba P15-05
Mancini, Maicol P14-12
Mangazeev, Nicole P11-14
Manneck, David P09-10, P20-04
Mannell, Hanna P09-06
Manolache, Alexandra OC-07-04
Manolis, Athanasios P07-10, P07-13
Mansouri, Maysam P22-08
Mantke, René OC-11-01
Mantuano, Beatrice P25-01
Maraver, Antonio P14-12
Marincic Zagar, Ana P03-05, P16-13
Marks-Hultström, Amanda OC-13-02

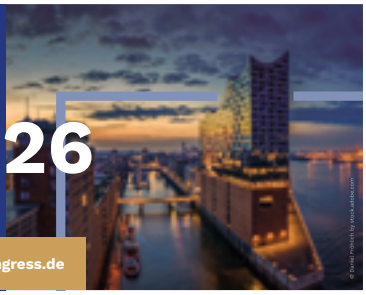

Marsch, Patrick M. P09-15
Marterstock, Michael OC-14-04
Martin, Marie P09-02
Märtin, Karla OC-02-04
Marullo, Anthony OC-01-01, P10-12
Marx, Jonas OC-03-05
Maslakova, Alina OC-11-02, OC-14-04, P16-11
Massa, Joana P14-03
Massberg, Steffen OC-04-02
Matamoros Angles, Andreu OC-12-02
Matchkov, Vladimir V. OC-11-04, P03-04, P07-05, P12-01, P13-04, P24-01
Mathilde Brostrup Hansen, Line OC-11-04
Matijass, Martin P10-11
Matschke, Johann OC-08-04
Matthey, Michaela OC-11-05
Mayer, Dirk P11-07
Mcdermott, Amy P01-01
McDonald, Fiona P16-04
McKie, Megan OC-09-05
Meades, Jessica OC-14-01
Meçi, Xheni OC-02-05, P17-02
Mederos y Schnitzler, Michael OC-11-02
Mei, Hailiang P23-08
Meibom, Emma OC-09-05
Meier, Elena P12-03
Meier-Rosar, Florian OC-03-05
Meis, Susanne P19-13
Meissner, Felix OC-04-01
Mejia, Felix P01-06
Melnikov, Alexandr OC-02-01, OC-02-06
Melnikova, Elizaveta OC-11-04
Melnikow, Alexander P03-12
Mendéz Aranda, Daniel P21-10
Mendez Otalvaro, Edward P18-09
Merrild, Camilla OC-13-05
Merza, Ornina P18-14
Messer, Antje P16-11, P21-06
Meurer, Thomas P18-10, P18-13
Meyer, Tobias N. P01-06, P01-08, P01-10, P01-13
Meyer-Schwesinger, Catherine OC-03-04, OC-04-05, P01-02, P01-04, P01-05, P01-06, P01-08, P01-10, P01-13, P01-14, P14-05, P26-07
Miao, Hongyu P06-06, P15-08
Michalick, Laura P06-02, P26-02
Mihaljevic, Dubravka P03-05
Mihaljevic, Justina P03-05
Mihaljevic, Zrinka P03-13, P03-14, P16-13
Mikhaylova, Marina OC-12-02
Mikicz, Vanessa P05-01
Milenkovic, Ivan P19-06, P19-14
Miliotis, Panagiotis P15-09
Mills, Ian P26-09
Millward, Jason M. P26-04
Mirtschink, Peter OC-14-04
Mitt, Karl OC-04-01
Mittag, Jennifer P03-08
Mitter, Gregor P05-09
Mittermaier, Franz Xaver OC-10-01, P19-08
Mittmann, Sarah P22-04
Mix, Andreas P24-07
Moberg, Marcus P17-11
Moesgaard, Lukas OC-01-04
Mohammadi, Behnam OC-12-02
Mohr, Timo OC-09-03
Molenda, Nicole P23-04
Molendijk, Jeffrey OC-08-03

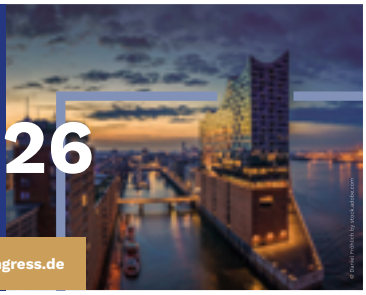

Molina, Christina E. P12-09
Moll, Amelie Johanna P11-11
Möller, Alexander OC-01-05
Møller, Jesper B P01-09
Møller, Lisbeth Liliendal Valbjørn OC-08-03
Mollet, Geraldine P21-05
Montag, Judith P23-06
Mookerjee, Rajeshwar P. P26-05
Morawietz, Henning P03-08
Moreira, Luis OC-01-03
Moreno-Justicia, Roger OC-01-04
Morhenn, Karoline P13-08
Moser, Anna OC-05-02, P22-09
Moss, Marcia L. P01-06
Mottaghy, Khosrow P15-03
Mrowka, Ralf OC-03-05, OC-06-06, OC-15-06
Müller, Bianca P16-11
Müller, Marion OC-14-03
Müller, Mario OC-03-05
Müller, Oliver J. OC-09-01, OC-14-05
Munk, Axel OC-06-05
Munsch, Thomas P19-04, P19-13
Murciano, Nicoletta P09-02
Murgia, Marta P10-05
Murko, Nastja P17-04
Murphy, Ben OC-01-01
Murphy, Matthew A. OC-01-03
Murphy, Ricardo P18-03
Musinszki, Marianne P18-09, P18-14
Mutsaers, Henricus A. M. OC-13-05, P26-05

Nader, Elie P09-02
Nadukkandy, Aisha OC-13-05, P26-09
Nair, Anagha G. OC-06-06
Naji, Mostafa Amin P01-01
Nangia, Shikha P09-15
Narjes, Lukas P23-05
Nasser-Grioua, Amel OC-01-02
Naujox, Julia P26-02
Nayak, Arnab OC-01-02, P04-07
Naz, Shagufta P11-03
Nazare, Marc P11-02
Neelsen, Lea C. P18-09
Negri, Samuele P07-10, P07-13
Nejsum, Lene Niemann OC-05-03, OC-13-05
Nelson, Niski P17-05
Neubauer, Veronika P06-08
Neumann, Katrin OC-04-05, P01-04, P01-08
Nevelchuk, Sonja P07-02
Neves Silva, Daniela OC-01-03
Newel, Doris P09-04
Newsom, Sean A. OC-08-03
Nguyen, Phi Hung P26-03
Nguyen, Tram Anh Vu P23-05
Nielsen, Heidi P08-07
Nielsen, Joachim OC-08-03, P10-03, P10-06, P10-09
Nielsen, Jens J. OC-01-04
Nielsen, Rikke OC-13-03
Nielsen, Sebastian P05-07
Niemann, Bernd P23-04, P25-04, P25-08
Niendorf, Thoralf P21-07, P26-04
Nikalexi, Eleni P08-12
Nikolaev, Viacheslav O. OC-12-03, P13-08, P23-07
Nikolovska, Katerina P24-12
Ning, Ruofei OC-11-04
Nissen, Ella P08-05

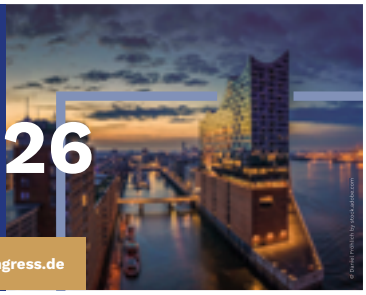

Nittka, Stefanie P20-03
Niu, Xiaochen OC-08-01
Nocke, Fabian P15-05
Nogueira Coelho, Jennifer OC-05-01
Noguera Hurtado, Héctor P14-01, P14-03
Nolte, Johannes P08-05
Nolze, Alexander P16-03
Nørregaard, Rikke OC-13-05, P05-08, P21-02, P21-09, P26-05
Nussbaum, Claudia OC-04-04
Nyborg, Esben OC-08-03
Nymark, Soile P14-04, P14-09
Nyrup Odgaard, Louise P22-10
Nyvad, Jakob P05-07

O. Crajoinas, Renato OC-05-06
O´Connell, Anna P16-04
O´Connor, Karen P16-04
O´Halloran, Ken OC-01-01, P10-12, P16-04
Obermayer, Benedikt OC-09-06
Oberwinkler, Johannes P09-04, P09-07
Odgaard, Louise Nyrup P26-08
Oechsler, Nina P13-02
Ogueboule, Zakarias OC-08-03
Ogwo, Anthony P18-09
Ohrenberg, Daniel P25-02
Oksche, Alexander OC-15-05
Olesen, Hanne Vebert P05-04
Olgunelma, Nicole P13-02
Oliveira, Mariana M. P26-05
Oliver, Dominik OC-07-03, P14-06, P18-05
Omran, Heymut P24-09
Onken, Julia P24-03
Oo, James P04-10, P17-12
Oppelt, Peter P17-07
Oprita, George OC-12-06
Orlich, Michael P23-05

Ørtenblad, Niels OC-08-03, P10-03, P10-06, P10-09

Ortner, Nadine P08-13
Osten, Felix OC-14-02
Osterhage, Valentin P06-05
Osthues, Jana P14-03
Oswald, Marleen Silke OC-02-04
Otenga, Felix Odhiambo P09-15
Otte, Jan V. OC-06-05
Ou, Hangjun P02-03
Ousingsawat, Jiraporn P21-01
Owald, David P14-08
Ozdede, Mehmet Ridvan P17-01

Padberg, Claudia P15-01
Paduraru, Adelina OC-12-06
Pagerols Raluy, Laia P11-06
Pagliaro, Pasquale P25-01
Palarasah, Yaseelan OC-05-04, P21-03
Pálfi, Katalin P04-10, P16-09, P17-12
Paneni, Francesco P13-02
Pankratova, Stanislava P05-08
Papadamakis, Athanasios P06-09
Pape, Hans-Christian P08-12
Paradies, Sandra P11-09, P11-13
Paradiž Leitgeb, Eva P17-03
Parahuleva, Mariana P04-04
Parker, Benjamin L. OC-08-03
Pasano, Joan M. M. P07-09

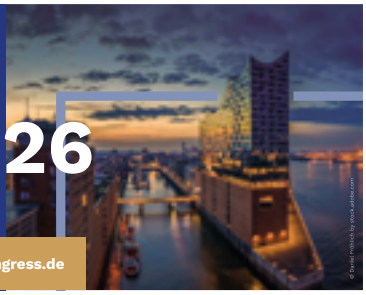

Pasch, Andreas OC-13-04, P05-09, P17-07
Patejdl, Robert OC-15-03, P02-05, P08-03
Paterson, David J. OC-09-04
Patzak, Andreas OC-03-01, P03-10
Pauli, Martin OC-10-03, OC-15-01, P19-10
Pavlidou, Nefeli P12-09
Pavlova, Elizaveta P03-10
Pedersen, Tina Myhre P12-01, P13-04
Penna, Claudia P25-01
Penttinen, Reetta P09-02
Perez, Anna P12-04
Perez Najar, Jose Eduardo P07-04
Pernecker, Moritz P22-14
Perret, Paul-Lennard OC-02-01, OC-02-06
Persikowski, Mia Joeli P11-06
Persson, Pontus B. OC-03-06
Pervaiz, Sumaira P09-03
Peters, Lisa P03-12
Petersen, Line P26-09
Pethö, Zoltan P18-02
Petrocelli, Jonathan J. P17-13
Petry, Andreas P11-02
Petzold, Anne OC-10-06, P19-16
Peusen, Bo OC-05-02
Peussa, Heidi P14-04, P14-09
Pham, T. C. Phung OC-08-03
Philipp, Karolin P11-01
Picard, Maxime P19-13
Pich, Andreas OC-01-02, P04-07
Piep, Birgit OC-14-02
Pietsch, Hubertus P21-07
Pijnappels, Daniël A. P23-08
Pilegaard, Henriette OC-08-03
Pinkenburg, Olaf P09-04, P09-07
Piontek, Jörg P11-11
Pippi, Josephine-Elisabeth OC-12-02
Plain, Allein P05-01
Plain Reyes, Allein P11-14
Planells-Cases, Rosa P24-05
Plomgaard, Peter P10-06
Podlacha, Magdalena P10-11
Pogoda, Kristin P09-06
Pollok, Katrin P05-01
Polozhentseva, Myroslava P19-09
Pombeiro Stein, Ines OC-12-06
Popp, Rüdiger P02-04
Popper, Bastian OC-04-01, OC-04-02
Porath, Katrin P02-11, P24-02
Postnov, Dmitry D. P07-05, P26-10
Potapenko, Tamara OC-12-03
Potocnik, Ivana P03-01
Potocnik, Nejka P03-01
Pouokam Kamgné, Ervice Vidal P24-11
Pourfarrokh, Parisa P25-06
Praetorius, Helle A. OC-13-03, P21-04
Praetorius, Jeppe OC-07-02, P05-05, P24-14
Prats, Clara OC-01-04
Prenner, Elmar J. P24-07
Priimägi, Arri P14-04
Probst, Stephanie P01-03, P22-07
Prost-Fingerle, Katrin OC-15-02
Prüser, Merten P12-05
Puig, Berta OC-12-02
Pusch, Michael OC-06-04

Qin, Lu P11-15
Quarch, Katja P16-03
Quintanova, Catarina P22-02, P22-04

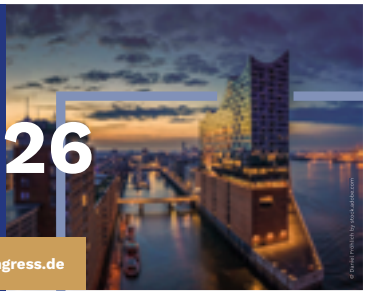

Quirós-Gutiérrez, Isabel P13-07

Raabe, Philipp OC-03-04
Rabe, Sindy P16-03
Raccuglia, Davide P14-08
Radulovic, Tamara P19-06
Rafea, Riham P16-06
Rahause, Sarah P08-05
Raich, Lukas OC-01-03
Raj, Nikita OC-04-02
Rajanathan, Rajkumar P12-01
Rakowski, Viktoria P11-15
Ralph, Jonathan P18-11
Ramkisoensing, Arti A. P23-08
Rasmussen, Line Jee Hartmann P03-09
Rasmussen, Mads OC-11-04
Rathje, Kristin P18-09
Raun, Steffen H. OC-08-03
Rausch, Niclas P17-06, P17-10
Rauschner, Mandy P04-02
Raza, Ghulam Shere OC-12-05, P01-07, P11-04, P11-05
Razazian, Mehdi P02-10, P05-09
Razmand, Bahareh P26-03
Rebers, Jan P12-03
Reichart, Gesine OC-15-03
Reichelt, Julia P01-06
Reichert, Andreas S. P17-08
Reichold, Markus P05-01
Reidick, Rebecca P01-04
Reiher, Nadine OC-03-05
Reimann, Jens P10-11
Reime, Sarah P04-02
Reimers, Lena-Marie OC-03-04, P01-06
Reimers, Sophie Claire OC-13-01
Reiss, Miriam P12-05
Reiter, Nina OC-04-03
Reitzner, Stefan M P10-05
Renigunta, Aparna P18-05
Renigunta, Vijayaram Kumar P18-05
Renné, Thomas P23-05
Renner, Simone P26-09
Reuter, Stefanie OC-03-05, OC-06-06, OC-15-06
Revuelta, David P12-09
Rewitz, Kim P17-13
Reynolds, Edwardo OC-02-01
Richter, Angelika P07-01
Richter, Erik A. OC-08-03, P07-09, P17-13
Richter, Franziska P07-01
Richter, Mathis OC-04-01
Ridder, Amanda P25-10
Riebeling, Johannes P02-05
Rieck, Sarah P23-09
Riecker, Achim P15-08
Rieg, Timo OC-05-01, OC-11-03
Riegel, Elisabeth P05-09
Riel, Elena B. P18-09
Riemann, Anne P04-02
Riemenschneider, Markus P12-07
Rifat, Ali P24-03
Rinschen, Markus M. OC-05-06, P01-13, P13-04, P21-05, P26-06
Rippe, Catarina P03-07
Ripphahn, Myriam OC-04-02
Rissiek, Björn OC-03-04, OC-12-02, P01-10
Rittik, Bhati P14-04, P14-09
Roche, Johanna P15-02

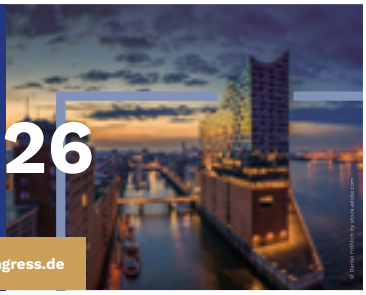

Rodrigez, Emanuel P03-12
Rodríguez-Urquirizar, Gorane P09-02
Roedel, Jan P07-03
Roeder, Juliana P26-02
Roeper, Jochen P08-02, P08-04, P08-09, P08-13, P18-06
Roggendorf, Clara P11-12
Rohlfs, Meino OC-04-01
Rohrbach, Susanne P23-04, P25-04, P25-08
Röhrdanz, Niels P07-06, P08-10
Rohweder, Arndt P02-10
Röja, Julia P17-11
Röll, Wilhelm OC-09-03
Romanova, Nadiya P24-07
Rong, Zhouyi OC-04-02
Rosa, Nicolas P09-02
Rose, Christopher P26-05
Rosenbæk, Lena Kjær P26-08
Rosenbaum, David P01-06
Rosendal Korshø, Anders OC-11-04
Rosenkranz, Sina Cathérine OC-01-03
Rosenthal, Rita P05-05
Rosti, Valentina P04-07
Rothämel, Paula OC-04-04
Rotmans, Joris I. P05-03
Rotordam, Maria Giustina GS-14-05, P09-02
Rott, Caroline P18-14
Röttger, Lars OC-12-02
Rousing, Amalie Quist P05-04
Rudolph, Volker P25-10
Rudolphi, Crissy F. P05-03
Rühl, Philipp OC-06-06
Ruhs, Stefanie P02-08, P16-03
Ruiz-Serrano, Amalia P13-02
Rukwied, Roman P09-01

Sach, Lara P08-07
Sachs, Wiebke P01-04, P01-05, P01-13, P26-07
Saez, Pablo P01-02
Safarzad, Mahdieh P02-04
Saftig, Paul P01-06
Sakai, Yusuke P23-02
Salazar, Manuela Gesell P13-02
Salinas-Hernandez, Ximena Icaria P08-11
Sandegaard, Samuel P05-05
Sandoval Flores, Lukas Daniel P11-09
Sang, Pengchao OC-02-01
Santana Kragelund, Fabiana P07-01, P08-05
Santarelli, Philina P04-07
Santos Alves, Estela P10-04
Saric, Sandra P03-13, P16-13
Sarkar, Rima P13-09
Sasse, Philipp OC-06-05, P12-08, P25-07
Sato, Miho OC-04-04
Sattler, Christian P09-05
Sattler, Christian P19-13
Sauer, Jonas-Frederic P08-06, P19-05
Sauter, Kathrin P07-10, P07-13
Saygi, Ceren P23-05
Scarsella, Luca P22-07
Schäfer, Daniel P11-07
Schäffler, Jonathan P05-01
Scharner, Bettina P01-03, P22-07
Schaubruch, Kirsten P04-06
Scheiermann, Christoph OC-04-04
Scherf, Daniela P23-04
Schewe, Marcus OC-07-01, P18-09, P18-11
Schiattarella, Gabriele G. OC-02-01

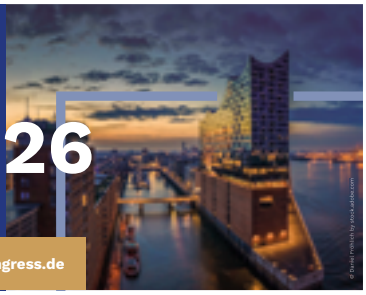

Schieffer, Bernhard P04-04
Schiemann, Thomas P07-04
Schießl, Ina Maria OC-13-06, P26-08
Schiffer, Miriam OC-09-03
Schiffer, Tomas A P10-05
Schild, Yves P06-09
Schimmelpfennig, Sandra P14-12
Schinke, Thorsten P11-13
Schiøtt, Birgit OC-07-02
Schirge, Kolja P23-07
Schlabs, Farina L. P17-13
Schlachter, Pius OC-01-03
Schley, Gunnar P26-01
Schlücker, Sebastian P11-07
Schlüter, Klaus-Dieter P04-05, P23-01
Schmalbruch, Johann OC-01-04
Schmauder, Ralf OC-06-02, P09-05
Schmelz, Martin P09-01
Schmid, Bettina OC-04-01, OC-04-03
Schmidinger, Barbara OC-04-02
Schmidt, Hartmut P19-10
Schmidt, Nico P26-11
Schmidt-Hieber, Christoph P09-05
Schmidt-Hutten, Lena P06-05
Schmitt, Franziska P24-05
Schmitz, M. Lienhard P23-04
Schneider, Alicia P02-12; P03-03
Schneider, Franziska P09-07
Schneider, Maike Elisabeth P23-04, P25-04
Schneider, Max Lennart P12-02
Schneider, Vivienne P11-12, P15-07
Schneider-Warme, Franziska P12-03, P23-02
Schneidmadel, Felix OC-03-05
Scholl, Ute P14-02
Scholz, Carsten C. OC-02-04, P06-03, P13-02
Scholz, Holger OC-02-05, P17-02, P21-08
Scholz, Tim P10-10
Schöneck, Kenneth P11-09, P11-13
Schönewald, Fabian P18-07
Schönherr, Roland OC-06-06
Schou, Agnete P26-09
Schou, Michael OC-13-05, P21-05
Schreckenberg, Rolf P04-05, P23-01
Schrecker, Marina P24-05
Schreiber, Franziska OC-07-06, P22-11
Schreiber, Rainer P21-01
Schreiber, Timm P26-11
Schreier, Danny P23-05
Schröder, Indra P18-08
Schröder, Katrin P15-10
Schroeder, Indra OC-06-03
Schröter Bonk, Julia Sophie OC-03-01, P03-10
Schubert, Annika OC-08-04, P15-01
Schubert, Rudolf P02-01, P02-09, P18-12
Schulte, Uwe P24-05
Schulte am Esch, Jan P11-14
Schulz, Friederike P18-09
Schulz, Marcel H. P04-01
Schulz, Rainer P04-04, P04-05, P25-01
Schulze, Jan-Ole P11-13
Schulzke, Jörg-Dieter OC-12-04
Schumacher, Fabian P26-02
Schumacher, Sina P01-03
Schwab, Albrecht P14-01, P14-03, P14-12, P18-02
Schwalbe, Harald P04-06
Schwarz, Alexander OC-12-02
Schweinitz, Andrea P09-05

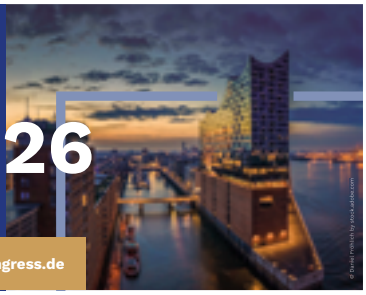

Schweizer, Michaela OC-01-03, OC-12-02
Schweizer, Patrick A P12-05
Schytz, Camilla T. P10-09
Sedej, Simon P13-01
Seebohm, Anna Marie P22-04
Seeger, Timon P12-05
Seeliger, Erdmann P21-07, P26-04
Seidel, Thomas OC-14-06, P25-03
Seidel, Thomas OC-09-02
Seidinger, Alexander OC-11-05, P25-10
Seidl, Karsten P11-07
Seidler, Anna P24-12
Seidler, Ursula P24-12
Seipold-Zimmermann, Lisa P01-06
Selescu, Tudor OC-07-04, P09-09
Sellmann, Tina P24-02
Semmler, Dominik P17-09
Sengupta, Shaon OC-04-04
Sergeant, Gerard P02-13
Serra, Selma A. P09-02
Seytter, Florian OC-04-04
Shafiq, Mohsin OC-12-02
Shahla, Hossein OC-15-05
Shalashova, Irina P06-10
Sharif, Saima P11-03
Sharma, Ravikant P11-04
Shi, Xian P09-15
Shorter, Emily OC-01-06, P10-04, P17-11
Shvadchak, Volodymyr P19-09
Siebecke, Katja P15-05
Siebels, Bente P23-05
Siebenmann, Christoph P15-02
Sielatchom Foyang, Maryl Brandy P09-14
Siemes, Devon OC-04-03
Sierla, Jonathan R. P11-06
Sigvardsen, Casper M. OC-04-06, P07-09, P17-13
Simm, Stefan P13-02
Simmons, Szandor OC-02-01, OC-02-06, P03-02, P03-12
Simonsen, Natasja P. P05-08, P21-09
Singer, Dominique P11-06, P12-04
Singer, Michael P23-03, P25-06
Singh, Anurak P24-12
Singh, Roshani Narayan P24-09
Siragusa, Mauro P04-09, P16-06, P25-05
Sîrbulescu, Ruxandra F. OC-01-03
Sirén, Anna-Leena OC-10-03, P19-10
Šišljagic, Dina P03-05
Sjøberg, Kim A. P17-13
Skands, Caroline KH P01-09
Skelin Klemen, Maša P17-03
Skjødt, Karsten P22-13
Skjoldborg, Benedikte OC-05-05, P22-01
Skov, Mathias OC-13-03
Slosarek, Ilka P09-10
Sluijter, Joost P23-06
Smith, Edward R. OC-13-04, P05-09
Smith, Nathaniel P18-11
Soares, Sabrina P09-01
Soattin, Luca OC-09-05
Sodum, Nalini OC-12-05
Soehngen, Fiona OC-14-02
Soehnlein, Oliver OC-04-01
Sohail, Azmat OC-13-04, P02-10, P05-09, P17-07
Solinski, Hans Jürgen P09-01

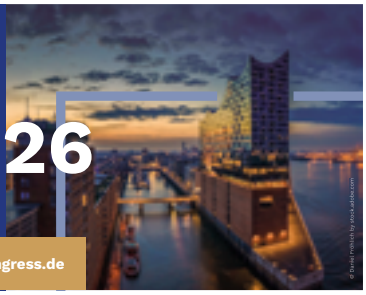

Solymosi, Philip D. OC-02-06
Somech, Raz OC-04-01
Somekh, Ido OC-04-01
Sommer, Till OC-03-05
Song, Chunping P26-09
Song, Feizhi OC-12-02
Soni, Ashnoor Kaur P01-05
Sørensen, Charlotte Mehlin P01-01, P26-10
Sørensen, Mads Vaarby P05-04, P05-07
Sørtvedt, Xabier P05-06
Sosnovtseva, Olga P26-10
Šošo Zdravkovic, Luna P08-06, P19-05
Soukara, Evangelia P15-09
Spallek, Moritz OC-12-01
Sparsø, Laura Vang OC-13-03
Speier, Stephan OC-11-02, OC-14-04, P16-11, P21-06
Sperandio, Markus OC-04-02, OC-04-04
Spiliotis, Konstantinos P07-01
Spinelli, Matteo P19-14
Spohn, Michael P23-05
Sporkova, Alexandra P02-03
Stæhr, Christian OC-11-04, P07-05
Stainier, Didier P23-05
Stange, Amanda Dyrholm OC-07-02
Staruschenko, Alexander OC-11-03
Stauber, Tobias OC-06-04, P09-03
Staudner, Tobias P05-02, P09-12
Stawarski, Michal P11-15, P14-11
Stefanovska, Dragana P23-02
Steil, Leif P13-02
Stein, Kimberley OC-09-01, OC-14-03
Steinberg-Shemer, Orna OC-04-01
Steinecke, Ceylan-Scarlett P19-03
Steiskal, Philip P19-02
Stener-Victorin, Elisabet OC-01-06
Stiene, Lennart P06-07
Stigloher, Christian OC-10-03, P19-10
Stock, Christian P24-12
Stocks, Ben OC-01-04
Stölting, Gabriel P14-02
Storm, Johan F. P18-03
Storm Petersen, Emmy P22-06
Stötzel, Julia P04-06
Stožer, Andraž P17-03
Strand, Martin F. P04-08
Strätz, Nicole P16-03
Ströbel, Philipp P11-08
Stubbe, Jane P03-11
Stumpff, Friederike P09-10, P09-14, P20-04
Stupin, Ana P03-13, P03-14, P16-13
Stupin, Marko P03-13, P16-13
Su, Mingzhen P21-10
Subramanian, Hariharan P13-08
Sudnitsyna, Julia OC-12-03
Sulcova, Dominika OC-10-02
Summer, Sabine OC-11-01
Sun, Han P18-11, P24-10
Sundberg, Carl Johann P10-05
Surala, Michael P08-06
Sure, Florian OC-07-06, P22-11
Süß, Anja P05-01
Svenningsen, Per OC-05-04, P01-09, P21-03
Swärd, Karl P03-07
Sylow, Lykke OC-01-04, OC-08-03
Syren, Pascal P12-05
Szabó, Ildikó P14-03

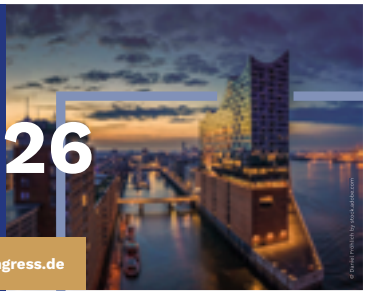

Szymanski, Witold P04-09, P16-06

Taghavi, Iman P01-01
Tahas, Stamatios Alan P12-06
Tahmasbi, Maryam OC-05-01
Tan, Yifan P01-13
Tarasco, Marco P23-05
Tasbihi, Ehsan P21-07
Tasika, Elena P01-04, P01-05, P01-13, P26-07
Tatematsu, Megumi OC-04-01
Tatzelt, Jörg OC-12-02
Tavares de Moraes, Bianca Portugal OC-04-02
Tavenier, Juliette P03-09
Taylor, Paul D. P03-08
Terlau, Jonas P08-12
Terpe, Philipp P02-08
Tersteegen, Anne P11-12
Tervonen, Aapo P14-09
Tetzlaff, Smilla P24-08
Tewari, Debanjan P09-05, P18-08
Thallmair, Sebastian P14-06
Thallmair, Veronika P14-06
Thangaraj, Sai Sindhu P21-03
Tharakan, Samuel Mathew OC-02-01
Tharaux, Pierre-Louis P01-13
Theisen, Simon OC-09-06
Theißen, Luisa P19-12
Thews, Oliver P04-02
Thiel, Steffen P21-03
Thiele, Moritz OC-13-01
Thies, Edda OC-12-02
Thoma, Emilia OC-10-01, P19-08
Thompson, Kilian P15-06
Thomsen, Karen L. P26-05
Thomsen, Martin P26-09
Thomsen, Morten B. P12-06
Thornbury, Keith P02-13
Tiburcy, Malte P23-07
Tiebl, Lisa P09-01
Tiffner, Adela OC-13-04, P02-10, P05-09
Timpe, Caspar Robert P12-08
Ting, Isaiah Joseph P16-08
Tirunagari, Praveenya P16-12
Todesca, Luca Matteo P14-03
Todorov, Vladimir T. P01-03, P02-07, P22-07, P22-14, P26-11
Toegel, Beatrice OC-13-04, P02-10, P05-09, P17-07
Tolj, Ivana P03-13, P16-13
Tornøe, Hannah Louise P12-06
Trampel, Katy A. OC-09-02
Tran, Huy P12-10, P14-04, P14-09
Trans, Laura Woidemann OC-05-05
Treebak, Jonas T. OC-01-04
Treiber, Nadja P19-12
Tremblay, Mélanie P26-05
Treskatsch, Sascha OC-13-01
Treu, Axel P21-07
Triantafyllou, Christos P23-09
Trogisch, Felix A. P25-02
Troschke-Meurer, Sascha P06-03
Tsamo Tetou, Arnold P09-14
Tschaikovski, Svetlana OC-11-01
Turner, Jerrold R. P09-15
Turner, Rachel P15-02
Tütüncü, Ecem P08-06, P19-02

U. P. Ludvigsen, Lene P21-04

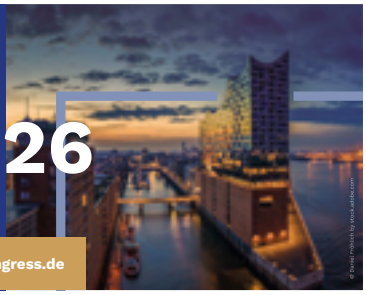

Uddin, Mohammed OC-02-01
Uhlig, Friederike P10-12
Ullmann, Pia P18-07
Unger, Andreas OC-14-05, P10-11
Untiet, Verena OC-10-05
Uplegger, Hela OC-12-02
Uršic, Dora P03-14
Uta, Petra P10-10

V. Sparsoe, Laura P21-04
Vaarby Sorensen, Mads P22-12
Vahldieck, Carl P16-07, P16-08
Vallon, Volker P26-06
van den Born, Jacob P16-07
van den Heuvel, Dominic OC-04-02
van den Munkhof, Hanna OC-10-06
van Gorp, Pim R. R. P23-08
Van Laake, Linda P23-06
van Megen, Wouter OC-05-02, P05-10
Veetil, Netra Nambiar P03-02
Velliou, Rallia P26-11
Verroest, Luca P01-07, P11-05
Vieira, Vanessa OC-01-03
Villar Ballesteros, Maria de Leyre P03-08
Vincetic, Ivo P03-13, P16-13
Vinetti, Giovanni P15-02
Vingborg, Anna P13-04
Virtanen, Paavo P12-10
Vitzthum, Helga OC-05-05, P01-06, P13-08
Vlahou, Antonia P02-10
Voelkl, Jakob OC-13-04, P02-10, P05-09, P17-07
Vogel, Elias OC-15-03
Vogel, Pascal P08-02, P08-09, P08-13
Vogt, Liffert P05-03
Vogt, Markus P02-05
Vohra, Twinkle P22-09
Voldstedlund, Christian T. P07-09, P17-13
Volk, Tilmann OC-09-02, OC-14-06
Völker, Jannis P25-08
Völker, Uwe P13-02
Volkova, Yulia L. P13-02
von der Ohe, Leonardo A. OC-02-01
von Walden, Ferdinand OC-01-06, P10-04
von Wedel, Dario OC-13-01
Vorobeva, Viktoriia P24-05
Voss, Thomass P26-09
Vuckovic, Marin P03-13
Vuerich, Roman P02-04

Wachsmuth, Lydia OC-14-05
Wacker, Eva P05-01
Wackerbarth, Lou Martha OC-04-02, OC-04-04
Wagdi, Ahmed P23-07
Wagner, Carsten A. P22-08
Wagner, Frauke P05-02, P09-12
Waiczies, Sonia P26-04
Walkenfort, Bernd P11-07
Walkowiak, Jaroslaw OC-12-05
Walsh, Emma C. P04-01
Walzog, Barbara OC-04-01, OC-04-03
Wang, Dan P19-14
Wang, Ju P24-12
Wang, Lu OC-06-04
Wang, Man P26-07
Wang, Peichun OC-11-06
Wang, Xiaoyan P06-09
Wang, Yu OC-11-06, P03-09

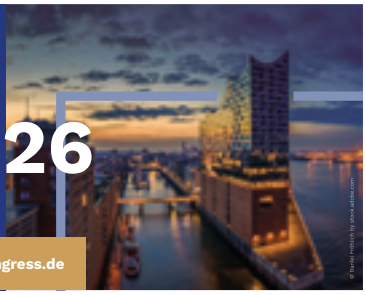

Warth, Richard P05-01
Warwick, Timothy P04-01, P03-03, P04-03, P04-06, P16-12
Watanabe, Shigeki P19-10
Watson, Alicia P25-02
Weber, Maruschka OC-15-04
Weber, Natalie P13-07
Weber, Wolf-Michael P24-09
Wedekind, Uta P01-13
Wegrzyn, Grzegorz P10-11
Wehle, Luise P18-03
Wei, Edward T. OC-07-04
Wei, Kuang-Yu P05-03
Wei, Xiang OC-04-01, OC-04-03
Weiberlen, Helia OC-08-06
Weidenfeld, Sarah P24-06
Weigand, Dominik OC-15-05
Weiß, Andreas P08-10, P19-03
Weißenberg, Gesa OC-08-04
Weissmann, Norbert P23-04
Wen, Xin P03-03, P16-09
Wendt, Tim P24-06
Wenzel, Daniela OC-09-01, OC-11-05, OC-14-03, P25-10
Werner, Franziska OC-12-03
Wespel, Susanne P06-10, P15-08
Westerhoff, Michelle P17-08
Weyer, Kathrin P21-05
White, James P. OC-01-03
Wiech, Thorsten P01-06, P01-13, P26-07
Wieers, Michiel L.A.J. P05-03
Wiegert, J. Simon P08-14, P20-03
Wiemann, Martin P10-11
Wiemuth, Dominik P11-15
Wiggenhorn, Amanda P07-09
Wilczak, Weronika P14-03, P18-02
Willbrand, Katrin OC-08-04
Winding, Christian P21-05
Winkler, Annika OC-02-01
Winning, Sandra OC-15-02, P06-09, P11-07, P11-12, P15-07
Wissing, Chantal OC-10-06
Witte, Kaya Elisa OC-12-01
Wittenmayer, Nina P08-08
Wittig, Ilka P04-06, P04-10, P16-09, P16-12
Witzenrath, Martin P03-12
Witzgall, Ralph P05-01
Wlodarczyk, Alina P14-06
Woidemann Trans, Laura OC-03-02, P22-01
Wojtaszewski, Jørgen F. P. P17-13
Wolf, Eckard P26-09
Wolfgramm, Sophie P26-07
Wölk, Sebastian P08-03
Woo, Marcel S. OC-01-03, OC-12-02
Wozny, Christian P08-08, P19-07
Wrann, Christiane D. OC-01-03
Wrobeln, Anna P17-05
Wu, Qi P22-10
Wulff, Peer P07-06, P08-10, P19-03
Wulfmeyer, Vera Christine P01-13, P26-06
Wünsch, Bernhard P14-03
Wurzel, Jana P16-09
Wyant, Gregory A. OC-01-03
Wyckelsma, Victoria L P10-05

Xanthopoulou, Emmanouella Michaela P10-04
Xiao, Haopeng P17-13
Xing, Zhanhua P04-10

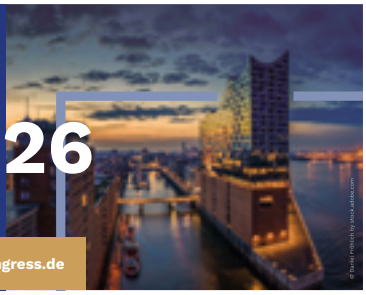

Xiong, Yueyue OC-01-03
Xu, Minze OC-03-01, OC-03-06, P01-11
Xu, Yu OC-11-06

Yacobovich, Joanne OC-04-01
Yalamarthi, Sai Sudha P11-08
Yamada, Takashi P10-05
Yang, Jie P24-06
Yang, Yue OC-03-05
Yonamine, Caio Y. OC-01-04
Yorgan, Timur Alexander P11-13

Zabri, Heba P17-09
Zach, Veronika OC-02-01
Zafiri, Daphne P07-12
Zantow, Florian P21-08
Zatschler, Birgit OC-11-02, P16-11
Zavialov, Vladimir P08-01
Zavvos, Athanasios P15-09
Zefi, Marina P10-10
Zehr, Simonida P04-01
Zehrer, Annette OC-04-01, OC-04-03
Zeidler, Judith P11-13
Zeng, Wangming OC-08-01
Zettner, Maximilian OC-10-03, P19-10
Zgierski-Johnston, Callum P12-03
Zhan, Yujiao OC-11-06
Zhang, Beijia P03-09
Zhang, Beijia OC-11-06
Zhang, Juang P23-08
Zhang, Qi OC-02-01
Zhang, Yongqiang P18-01
Zhang, Yaxin OC-01-05
Zhang, Yanhui P16-10
Zhao, Jia-Hao P13-07
Zhao, Yu P26-07
Zheng, Fang P19-01, P19-12
Zheng, Xiang P22-10, P26-08
Zhengye, Liu P10-04
Zhong, Yi P10-05
Zhou, Baoyu OC-01-02, P04-07
Zhou, Yinuo P04-10
Zhukov, Oleg P26-10
Zielinski, Stephanie P01-04, P01-05, P01-06, P01-13, P26-07
Zieschang, Constanze P25-06
Zimmermann, Jan Luca P25-04, P25-08
Zimmermann, Katharina P07-03, P09-09
Ziouziou, Tabea P18-06
Zipf, David P02-05
Zucker, Jennifer P07-11
Zurkan, Daniela OC-02-01
Zweigerdt, Robert OC-14-02